Author:
Perrett, Charlotte Averil

Title:
Factors affecting Salmonella invasion of epithelial cells

Factors affecting *Salmonella* invasion of epithelial cells

Charlotte Averil Perrett

A dissertation submitted to the University of Bristol in accordance with the requirements of the degree of Doctor of Philosophy in the Faculty of Medical and Veterinary Sciences

Department of Biochemistry

September 2007

Word count 76,330

THESIS CONTAINS CD/DVD

Abstract

Salmonella enterica are important zoonotic pathogens whose virulence depends upon their ability to enter and survive in host cells. The molecular mechanisms underlying *Salmonella enterica* serovar Typhimurium invasion of epithelial cells were investigated here using microscopy techniques, including confocal and electron microscopy and live cell imaging.

Salmonella produce autoinducer-2 (AI-2), a signalling molecule synthesised by LuxS, which is used by other bacterial species to co-ordinate gene expression with population density, a behaviour known as quorum sensing. It was investigated here whether *luxS* might affect the ability of *S.* Typhimurium to invade epithelial cells. No difference was found between *S.* Typhimurium SL1344 wild type and its isogenic *luxS*⁻ mutant with respect to the number and morphology of the membrane ruffles induced or their ability to invade epithelial cells. Initially the dynamics of the ruffling process appeared subtly altered in the *luxS*⁻ mutant so that ruffles were induced in a shorter time period after adhesion. However, this was not found to be a consistent phenotype, rather it was dependent on the consignment of MDCK cells. Furthermore, measuring, using fluorescent microscopy and flow cytometry, the expression of a single-copy green fluorescent protein fusion to the *prgH* (a SPI-1 gene) promoter indicated SPI-1 expression is similar between SL1344 wild type and *luxS*⁻. Thus, *luxS* does not appear to play a major role in regulating invasion of *Salmonella*, at least under the conditions used here.

Salmonella invasion protein A (SipA), *Salmonella* outer proteins E (SopE), SopE2 and SopB are translocated into host cells where they modulate the actin cytoskeleton to drive uptake of *Salmonella.* The role and importance of SipA remains controversial and contradictory data have been reported regarding its role in membrane ruffle formation. The hypothesis that the role of SipA in invasion may vary between *Salmonella* strains was investigated by examining the effect of SipA deletion in four *S.* Typhimurium strains, including those that possess or lack SopE. These studies confirmed SipA has no obvious effect on the number of ruffles formed during infection and reveal SipA optimises entry of most strains into MDCK cells. SipA⁻ SopE⁻ *Salmonella* strains were found to induce ruffles with markedly different morphology compared to that previously described for wild type and *sipA*⁻ mutants, including the presence of finger-like protrusions and numerous filopodia, both structures being highly dynamic when examined by live cell imaging. A similar phenotype was found for *sipA*⁻ *sopE2*⁻ and *sipA*⁻ *sopB*⁻ mutants. In describing a novel role for SipA in membrane ruffling induced by certain strains, it is revealed that SipA may play a key role in induction of invasion-competent membrane ruffles in strains where another effector is absent.

For my Mum and Dad

Acknowledgements

I would like to thank my supervisor Mark Jepson for sharing all his knowledge and experience with me, for his encouragement, patience and his friendship. I must also thank Mark and his wife Katy for the copious bottles of wine they have provided throughout my PhD, plus the honour of babysitting Harry and Matthew, without which I would never have become a babysitting legend! I would also like to thank Isabel Martinez-Argudo, Caroline Sands, Leann Clark and Alan Leard for their fun and friendship throughout my time in the lab. Thanks also go to Anjam Khan and Mike Karavolos who have provided advice and helpful discussions during my PhD.

I would also like to thank Tom Humphrey for giving me the opportunity to work in his laboratory, and for being so patient with me while I have been writing my thesis, and to all the members of his group for their support and encouragement.

Finally, to my wonderful Mum and Dad - thank you for allowing me to choose my own path in life, and for all the love and support you give me. Thanks also to my brother Tim, the rest of my family and all my friends who support and encourage me in all that I do.

Author's declaration

I declare that the work in this dissertation was carried out in accordance with the Regulations of the University of Bristol. The work is original, except where indicated by special reference in the text, and no part of this dissertation has been submitted for any other academic award.

Any views expressed in the dissertation are those of the author.

Signed: C. Perett Date: 21/09/07

Table of Contents

List of Figures

List of Tables

List of Abbreviations

aa	Amino acids
ABP	Actin binding protein
ADF	Actin depolymerisation factor
AHL	N-acyl homoserine lactone
AI-2	Autoinducer-2
AMC	Activated methyl cycle
ANOVA	Analysis of variance
ARP2/3	Actin related protein 2/3
ATP	Adenosine triphosphate
bp	Base pair(s)
CLSM	Confocal laser scanning microscopy
DAPI	4',6-diamidino-2-phenylindole
DC	Dendritic cell
DPD	4,5-dihydroxy-2,3-pentanedione
EPEC	Enteropathogenic *E. coli*
FITC	Fluorescin isothiocyanate
GAP	GTPase activating protein
GEF	Guanine nucleotide exchange factor
GDI	Guanine nucleotide dissociation inhibitor
GDP	Guanosine diphosphate
GFP	Green fluorescent protein
GTP	Guanosine triphosphate
HxA3	Hepoxilin A_3
IL-8	Interleukin-8
Ins(1,4,5,6)P_4	Inositol-1,4,5,6-tetrakisphosphate
Ins(1,3,4,5,6)P_5/InsP_5	Inositol-1,3,4,5,6-pentakisphosphate
InsP_6	Inositol hexakisphosphate
JNK	c-Jun amino-terminal kinase
LB	Luria Bertani broth
LEE	Locus of enterocyte effacement
Lsr	*luxS* regulated
MAP kinase	Mitogen activated protein kinase
MDCK	Madin-Darby Canine Kidney

MOI	Multiplicity of infection
OD_{600}	Optical density at 600nm
PBS	Phosphate buffered saline
PCR	Polymerase chain reaction
PEEC	Pathogen-elicited epithelial chemokine
PFA	Paraformaldehyde
PKC	Protein kinase C
PtdIns(3)P	Phosphatidylinositol-3-phosphate
PtdIns(5)P	Phosphatidylinositol-5-phosphate
PtdIns(4,5)P_2/PIP_2	Phosphatidylinositol-4, 5-bisphosphate
PtdIns(3,4,5)P_3	Phosphatidylinositol-3,4,5-triphosphate
PMN	Polymorphonuclear leukocyte
SCV	*Salmonella* containing vacuole
SDS-PAGE	SDS-polyacrylamide gel electrophoresis
SEM	Scanning electron microscopy
sem	Standard error of the mean
SGEF	SH3-containing guanine nucleotide exchange factor
Sip	*Salmonella* invasion protein
Sop	Salmonella outer protein
SPI	*Salmonella* pathogenicity island
SH3	Src homology 3
TEM	Transmission electron microscopy
TER	Transepithelial electrical resistance
TJ	Tight junction
TRITC	Tetramethyl rhodamine isothiocyanate
TTSS	Type three secretion system
VASP	Vasodilator-stimulated phosphoprotein
WASP	Wiskott-Aldrich syndrome protein
WAVE	WASP family verprolin-homologous
ZO-1	Zona occludens-1

Chapter One

Introduction

1.1. Classification and characteristics of *Salmonella*

Salmonellae belong to the Enterobacteriaceae; a grouping of enteric bacteria that includes pathogens from the genera *Escherichia*, *Shigella* and *Yersinia*. Members of the Enterobacteriaceae are non-sporulating, rod-shaped Gram-negative bacteria, with some, including the majority of *Salmonella* serovars, possessing peritrichous flagella to provide motility. Biochemically the Enterobacteriaceae are characterised as oxidase negative, catalase positive, facultative anaerobes, with an ability to ferment glucose, and reduce nitrate to nitrite. *Salmonella* is also identified by its ability to use citrate as a sole carbon source and to produce hydrogen sulphide.

The genus Salmonella comprises two species: *Salmonella bongori* and *Salmonella enterica*, although a third species, *Salmonella subterranean*, has been reported (Brenner *et al.*, 2000; Shelobolina *et al.*, 2004). Only *Salmonella enterica* is pathogenic, being an important zoonotic pathogen of humans and animals. *S. enterica* is divided into six subspecies, which together comprise over 2000 serovars according to the Kauffmann-White scheme (Popoff *et al.*, 2004). The serovars are distinguished on the basis of their somatic (O) antigen and the Phase 1 and Phase 2 flagellar (H) antigens. In *S. enterica* the two flagellar antigens refer to the flagellin subunit proteins FljB and FliC which can be alternately expressed by the organism. This process, known as flagellar phase variation, involves the inversion of approximately 1kb of DNA containing the promoter of *fljB*. In one orientation (referred to as ON), the promoter is situated directly upstream of the *fljBfljA* operon, allowing transcription of *fljB* and *fljA* to occur, while transcription of *fliC*, located elsewhere on the chromosome, is repressed by the *fljA* product. In the opposite orientation (referred to as OFF), *fljB* and *fljA* are not transcribed and thus *fliC* is expressed. The invertible DNA segment is flanked by 26bp inverted repeats (hix sites) and contains the *hin* gene,

encoding a recombinase that mediates reversible recombination reactions between these hix sites (For a review see van der Woude and Baumler, 2004). The antigenic formula for serovars Typhi, Paratyphi and Dublin also includes the virulence surface antigen (Vi), which only these serovars may possess.

As enteric bacteria, *Salmonella* predominantly inhabit the intestinal tract. *Salmonella* serovars can be host-restricted or have a broad host range. Host-restricted organisms are usually exclusively associated with one host species. For example *Salmonella enterica* serovar Typhi and serovars Paratyphi A, B and C only infect humans (Edsall *et al.*, 1960), while serovars Gallinarum and Abortusovis are constrained to poultry (Barrow *et al.*, 1994) and ovine (Pardon *et al.*, 1990) hosts respectively.

Organisms with a broad host range may be categorised as host-adapted or unrestricted (Uzzau *et al.*, 2000). Host-adapted serovars are usually associated with one particular host organism with infrequent infection of another species e.g. serovar Dublin which causes systemic disease in cattle but occasionally infects other species including humans (Taylor *et al.*, 1953). *Salmonella enterica* serovar Typhimurium infects a broad range of hosts including humans, mice, cattle, chickens and swine, so is often described as unrestricted or ubiquitous. However, the infection of different hosts by the same serovar does not necessarily produce the same disease state in each. *S.* Typhimurium causes enterocolitis in calves (Frost *et al.*, 1997), systemic disease and diarrhoea in chicks, with older chickens being asymptomatic carriers (Barrow *et al.*, 1987), and a systemic typhoid-like disease in mice (Carter and Collins, 1974). In humans, infection with *S.* Typhimurium commonly causes a self-limiting enterocolitis, although systemic disease may develop in immunocompromised individuals (Mastroeni *et al.*, 2003). This illustrates the importance of the *Salmonella* serovar and host species on the outcome of infection.

1.2. *Salmonella* as a human pathogen

Illness resulting from *Salmonella* infection has variable severity in humans, ranging from mild, self-limiting enterocolitis to systemic infection, and is dependent on the *Salmonella enterica* serovar and the immunological status of the host species; *Salmonella* infections are frequently more severe in infants, the elderly and the immunocompromised (Bodey *et al.*, 1986). *S.* Typhi causes typhoid (enteric) fever in humans; a systemic infection leading to sustained fever, severe headache, nausea, and loss of appetite, with additional symptoms of constipation or diarrhoea, enlargement of the spleen, and/or general malaise. Paratyphi A, B and C cause a similar clinical disease, although it is usually less severe. There are approximately 150 to 200 cases of typhoid reported each year in England and Wales, with a similar number of paratyphoid cases (Health Protection Agency, UK). However, worldwide the figure is much more significant. The World Health Organisation (WHO) has recently estimated that annually there are 21.7 million cases of typhoid, with 216,510 fatalities (Crump *et al.*, 2004). This gives a case fatality rate of 1%, although this can reach 10% in certain areas of Asia and Africa (WHO positional paper on Typhoid Vaccines, 2000).

Infection of humans by other serovars, but most commonly *S.* Typhimurium and *S.* Enteriditis, leads to self-limiting gastroenteritis, characterised by diarrhoea, abdominal cramps, fever, vomiting and malaise. Salmonellosis is a major cause of bacterial enteric disease in humans. In 2005, 11,447 cases of non-typhoidal Salmonellosis were reported in England and Wales (Health Protection Agency, UK) (Figure 1.1), and 35,836 cases in the United States (Centers for Disease Control and Prevention (CDC) Bacterial Foodborne and Diarrheal Disease National Case Surveillance Annual Report, 2005). These figures are likely to represent only a proportion of the cases that occur each year, due to mild infections not being presented for medical attention, stool samples not being retrieved for analysis, and failure to isolate a causative organism (Wheeler *et al.*, 1999). Indeed it has been estimated that in the United States 1.4 million cases of Salmonellosis occur annually, 40 times the number of cases reported (Mead *et*

al., 1999). The current global incidence of non-typhoidal *Salmonella* infections is not known. Although most countries have systems in place to report notifiable diseases, few have foodborne-disease surveillance programs. A past estimate calculated 1.3 billion cases of non-typhoidal Salmonellosis worldwide each year, with 3 million deaths (Pang *et al.*, 1995). As there has been a global trend for foodborne diseases including Salmonellosis to increase, it is likely the current figures are much higher.

The rise in foodborne diseases has led to increasing concern over the socio-economic impact of such infections, and calculations are being made to determine the potential costs of *Salmonella* infections. The United States of America Department of Agriculture Economic Research Service (ERS) suggest in the United States the cost per case of human Salmonellosis ranges from approximately US$40 for uncomplicated cases to US$4.6 million for cases ending with hospitalisation and death. The annual total cost for Salmonellosis in the United States alone is therefore approximately US$3 billion (ERS cost estimate, 2006). Thus, it is clear *Salmonella* infections represent both a major public health burden and a huge economic cost to society, hence, the importance of understanding *Salmonella* and its pathogenesis.

Figure 1.1 *Salmonella* in humans (excluding *S.* Typhi & *S.* Paratyphi). Faecal & lower gastrointestinal isolates reported to the Health Protection Agency, Centre for Infections, England and Wales, 1981 – 2006. http://www.hpa.org.uk/infections/topics_az/salmonella/data_human.htm

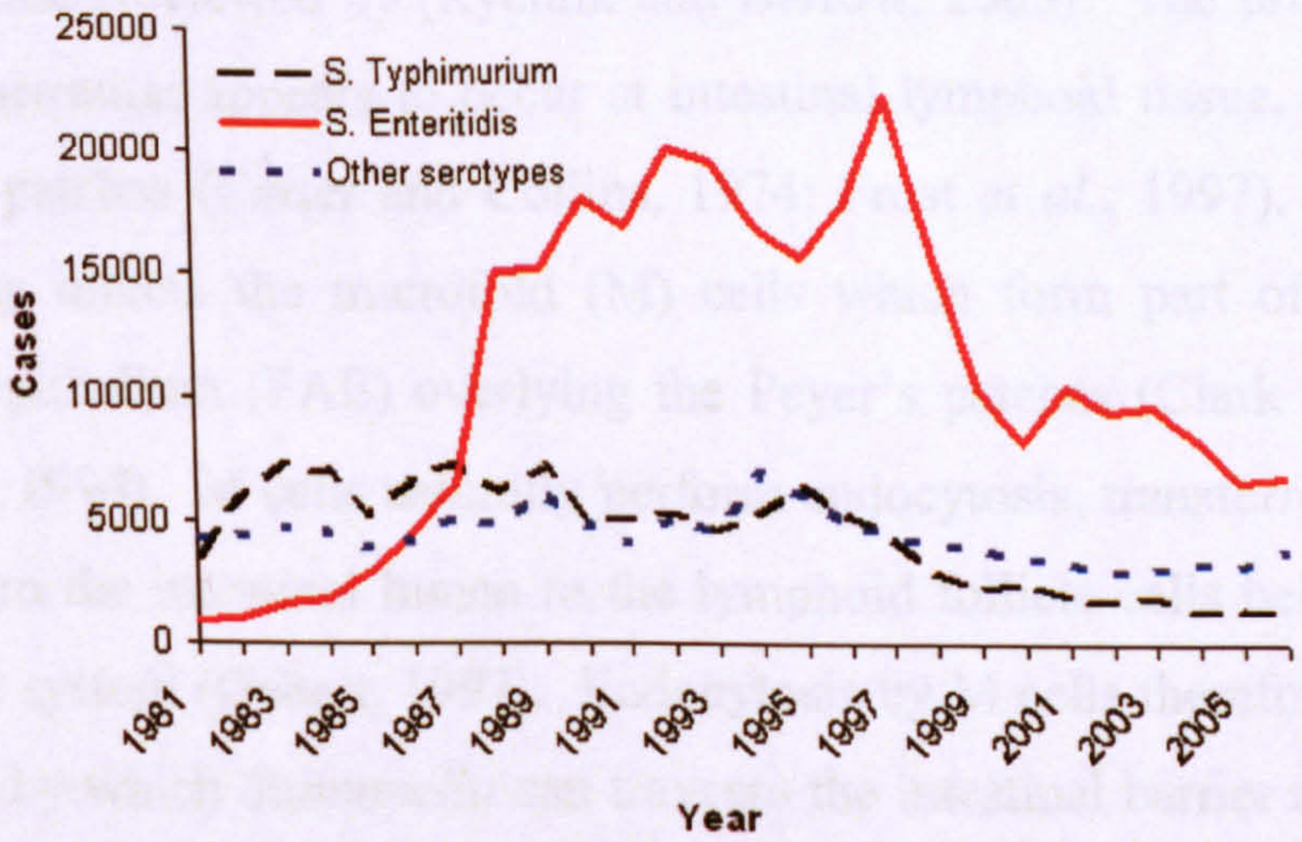

1.3. *Salmonella* - host interactions

1.3.1. Interactions with the host *in vivo*

Salmonella infections are usually acquired through the ingestion of contaminated food or water. Following ingestion, *Salmonella* enter the stomach, where gastric acidity provides an important defence against this organism since *Salmonella* is killed following exposure to a pH $\leq$ 3 (Lee *et al.*, 1995), and the average stomach pH in healthy volunteers under fasting conditions is approximately pH 2 (Verdu *et al.*, 1994). Reduction in gastric acidity (achlorhydria), for example from disease, use of antacids or use of drugs which inhibit acid secretion e.g. proton pump inhibitors, is therefore associated with increased *Salmonella* survival and reduced infectious dose (Collins, 1972). However, since Salmonellosis occurs with normal gastric function, other factors such as buffering of gastric acid, physical protection by food, or rapid emptying of the stomach may reduce protection provided by gastric acid (Giannella *et al.*, 1971; Waterman and Small, 1998). *Salmonella* has also evolved response mechanisms to facilitate survival in the stomach, for example the adaptive acid tolerance response (ATR), in which exposure to mildly acidic conditions promotes survival in subsequent highly acidic environments (Audia *et al.*, 2001; Foster, 1991).

Having left the stomach, *Salmonella* must survive changes in osmotic pressure, reduced oxygen concentration, the activities of bile, removal by peristalsis and competition from other bacteria to reach the distal ileum and the colon where it initiates disease (reviewed by (Rychlik and Barrow, 2005). The primary site of mucosal penetration appears to occur at intestinal lymphoid tissue, for example the Peyer's patches (Carter and Collins, 1974; Frost *et al.*, 1997). *Salmonella* preferentially infects the microfold (M) cells which form part of the follicle associated epithelium (FAE) overlying the Peyer's patches (Clark *et al.*, 1994; Jones *et al.*, 1994). M cells naturally perform endocytosis, transferring antigenic samples from the intestinal lumen to the lymphoid follicle cells below to prime the immune system (Gebert, 1997). Endocytosis by M cells therefore provides a mechanism by which *Salmonella* can traverse the intestinal barrier and modulate the host immune response (Figure 1.2).

Figure 1.2 Translocation of *Salmonella* across the intestinal epithelial barrier. Intestinal epithelial cells maintain a physical barrier against commensal flora, although specialized sites such as the follicle associated epithelium (FAE) allow constant sampling of the luminal flora through M cells. This property is used by *Salmonella* to cross the epithelial barrier where it becomes exposed to macrophages, dendritic cells (DCs) and B cells. To escape macrophage killing *Salmonella* remodel macrophage phagosomes, avoiding transition of the phagosome to a lysosome and creating an intracellular niche that allows efficient replication. This SPI-2-dependent process is an alternative to the SPI-1-dependent apoptotic killing of macrophages. *Salmonella* may enter epithelial cells through their basolateral pole in a TTSS/Sop-dependent manner. An alternative route of invasion involves inducing entry through the apical surface of epithelial cells. A third process of translocation may involve DCs crawling between epithelial cells or sending pseudopods to capture luminal bacteria and retract in a subepithelial position. Taken from Cossart and Sansonetti, 2004.

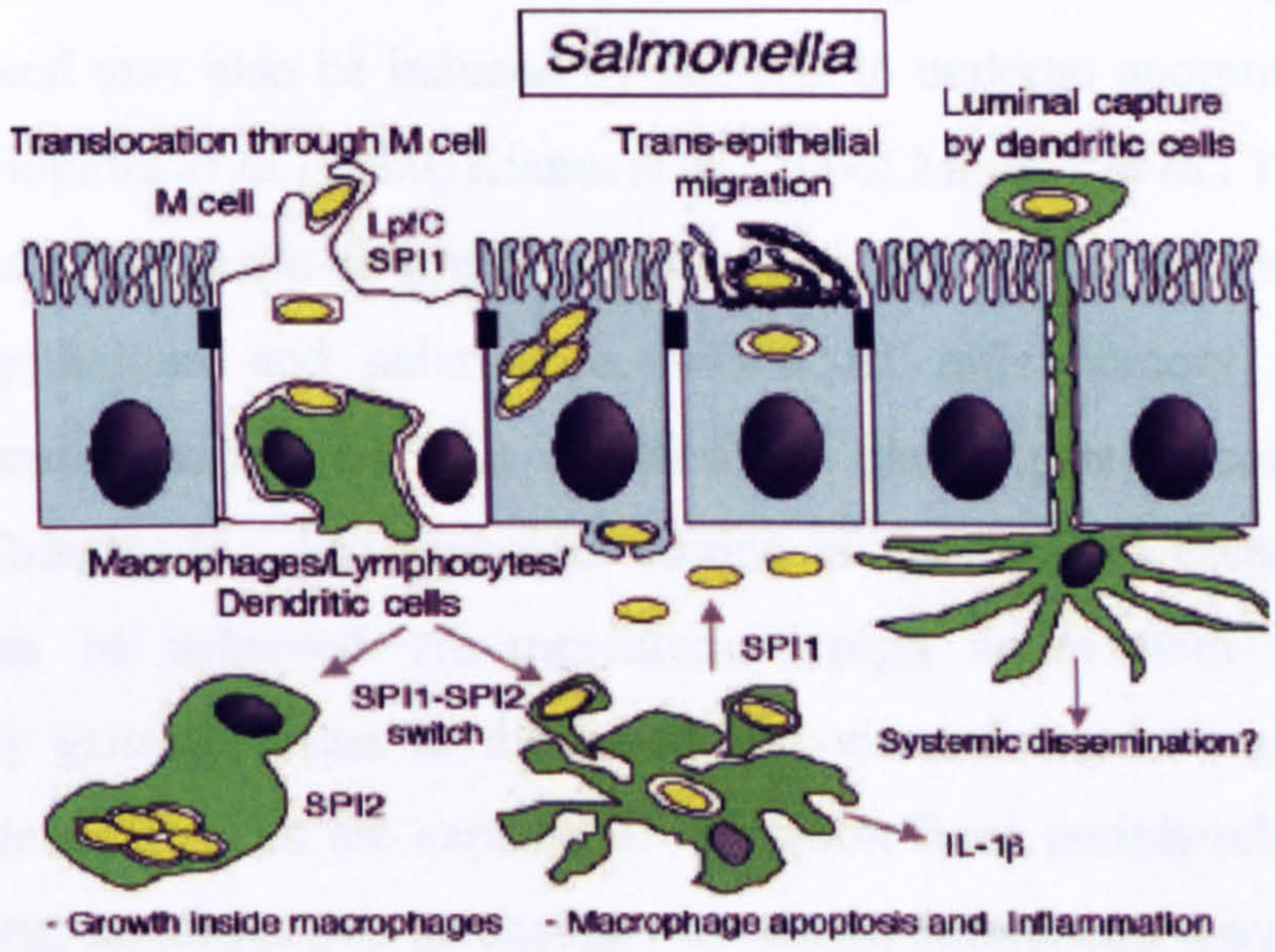

Invasion of M cells by *Salmonella* is accompanied by formation of structures resembling the membrane ruffles observed during infection of cultured epithelial cell lines (Clark *et al.*, 1994; Frost *et al.*, 1997; Jones *et al.*, 1994), and therefore indicates a role for *Salmonella* pathogenicity island-1 (SPI-1) in M cell invasion. However, while SPI-1 promotes invasion of murine M cells, it is not essential (Clark *et al.*, 1996; Clark *et al.*, 1998), indicating passive uptake or an alternative invasion mechanism may be important, and potentially that the mechanism of M cell invasion differs to invasion of other cells (Clark *et al.*, 1996; Jepson and Clark, 2001).

M cells are not an exclusive site of infection since *Salmonella* can also induce their uptake in enterocytes; invasion of villous epithelia being demonstrated in guinea pigs, rabbits and calves (Frost *et al.*, 1997; Takeuchi, 1967; Wallis *et al.*, 1986). However, attachment and invasion appears to occur faster at the M cell-covered domed villi than at the tips of absorptive villi (Frost *et al.*, 1997).

Invasion of epithelial cells is discussed in further detail below (1.3.2). Penetration of the intestinal barrier can also occur by *Salmonella* being shuttled across the epithelium by dendritic cells (DCs), which lie between adjacent enterocytes and have access to the intestinal lumen and the basolateral space (Rescigno *et al.*, 2001).

Having crossed the epithelial cell barrier, *Salmonella* comes into contact with macrophages and DCs in the submucosa. Both types of cell can phagocytose *Salmonella* and may also be induced by bacteria to undergo apoptosis (Chen *et al.*, 1996b; Hopkins *et al.*, 2000; Kiama *et al.*, 2006; Monack *et al.*, 1996). Since non-typhoidal *Salmonella* is usually restricted to the region encompassing the intestinal epithelium and submucosa, where an inflammatory response is instigated, macrophages and DCs are likely to play a part in controlling the spread of *Salmonella*. For typhoidal strains of *Salmonella*, escape from the intestine can be achieved via mesenteric lymph nodes with the bacteria subsequently gaining access to the blood and visceral organs e.g. spleen and liver. As dendritic cells are capable of migration from peripheral tissues they may represent an alternative mechanism by which *Salmonella* may disseminate and cause systemic disease (Vazquez-Torres and Fang, 2000). CD18 expressing phagocytes residing in the intestinal mucosa may also be responsible for systemic dissemination, transporting bacteria via blood to the spleen (Vazquez-Torres and Fang, 2000).

1.3.2. Interaction with epithelial cells

A characteristic of *Salmonella* infection is the uptake of the bacterium into non-phagocytic epithelial cells. Using transmission electron microscopy (TEM) to monitor *Salmonella* infection of guinea pig ileum epithelium over 48 hours, Takeuchi (1967) provided the earliest description of the invasion process in epithelial cells. *Salmonella* in close contact with the epithelial cell surface were shown to cause transient loss of microvilli and the production of a localised protrusion of the plasma membrane, a membrane 'ruffle', which surrounded the bacterium and brought it into the cell in a vacuole. Subsequently, the host cell architecture was regained and the cells appeared healthy. This invasion of the

epithelium was accompanied by inflammation and the association of *Salmonella* with polymorphonuclear leukocytes (PMNs) and macrophages in the lamina propria, Peyer's patches and submucosa. Such observations were repeated in other animal models e.g. rabbits and calves (Frost *et al.*, 1997; Giannella *et al.*, 1973; Wallis *et al.*, 1986; Watson *et al.*, 1995), thus it appears an early manifestation of the *Salmonella*-host interaction is attachment to and invasion of the intestinal epithelium by the bacteria, and subsequent inflammation of the lamina propria and lymph nodes.

The observations made in animal models have been repeated during invasion of cultured epithelial cells with *S. enterica* serovar Typhimurium. Therefore, *in vitro* tissue culture models have been used widely to elucidate the mechanisms employed by *Salmonella* to induce its uptake. The original *in vitro* models used either Caco-2 cells derived from human colonic carcinoma cells or Madin-Darby canine kidney (MDCK) cells, derived from dog kidney distal tubule cells. Both cell lines establish polarised monolayers when grown on porous membrane supports, providing a model for polarised intestinal epithelia. *Salmonella* invasion of these polarised cell lines was similar to the events recorded during *Salmonella* invasion in animals with loss of microvilli, the production of ruffles and the entrance of bacteria into *Salmonella* containing vacuoles (SCVs) (Finlay and Falkow, 1990; Finlay *et al.*, 1991; Francis *et al.*, 1993).

Non-polarised cells have also been used in *Salmonella* invasion assays, in particular the human cervical epithelial carcinoma cell line HeLa (Bakshi *et al.*, 2000; Finlay *et al.*, 1991; Giannella *et al.*, 1973), the human larynx epithelial carcinoma derived cell line HEp-2 (Hueck *et al.*, 1995), the human derived embryonic intestinal cell line Henle-407 (Galan and Curtiss, 1989; Hardt *et al.*, 1998a; Kaniga *et al.*, 1996) and African green monkey fibroblast-like COS cells (Patel and Galan, 2006; Stender *et al.*, 2000). *Salmonella* appears to use the same strategy to enter non-polarised and polarised epithelial cells i.e. the induction of membrane ruffles to engulf the bacterium. However, while the process of invasion appears similar in each cell line there may be differences in the mechanics. For example the Rho GTPases *Salmonella* stimulates to cause the actin rearrangements required for entry appear to be different between

polarised and non-polarised cells (Shi and Casanova, 2004). The importance of different bacterial proteins to invasion has also been shown to vary between cell lines and between polarised and non-polarised cells of the same cell line (Raffatellu *et al.*, 2005). This illustrates the need to test observations and hypotheses about molecular mechanisms of *Salmonella* invasion obtained from cell culture experiments in the context of the whole organism, in order to establish the relevance of such data to the disease process in a complex environment (Hurley and McCormick, 2003).

1.3.3. Intracellular survival of *Salmonella*

Immediately following invasion of host cells, individual *Salmonella* are found within *Salmonella*-containing vacuoles (SCVs). These discrete vacuoles undergo a series of stages of maturation, characterised by selective interactions with the host cell endocytic system, and which appear to deviate the SCV from the degradative endosomal pathway. In macrophages, maturation of the SCV may also prevent exposure to antimicrobial reactive oxygen species and reactive nitrogen species, the products of NADPH oxidase and inducible nitric oxide synthase (iNOS) (Chakravortty *et al.*, 2002; Gallois *et al.*, 2001; Vazquez-Torres *et al.*, 2000). Interaction of SCVs with the host cell endocytotic system begins with early endocytic markers, including early endosomal antigen-1 (EEA-1), the transferrin receptor (TfR) and Rab5, associating with the SCV membrane (Hashim *et al.*, 2000; Rathman *et al.*, 1997; Steele-Mortimer *et al.*, 1999). These early endocytic markers are rapidly replaced so that one hour post-infection the SCV membrane is associated with proteins characteristic of a late endosomal/lysosomal compartment, for example lysosomal glycoproteins (lgps), lysosome-associated membrane proteins (LAMPs) and v-ATPase, the latter responsible for endosomal acidification (Sato and Toyama, 1994; Steele-Mortimer *et al.*, 1999). SCVs also accumulate cholesterol, so that 12-20 hours post-infection SCVs represent a major site of cholesterol in the host cell (Catron *et al.*, 2002). Cholesterol is localised to lipid rafts in the SCV membrane, which are transient membrane platforms enriched in cholesterol and sphingolipids, implicated in cell processes such as membrane transport, signalling and protein sorting. Since, the SPI-2 effectors PipB and PipB2 have been shown to localise

to lipid rafts in the SCV membrane (Knodler *et al.*, 2003), it is likely lipid rafts represent an interface between intravacuolar *Salmonella* and the host cell.

Figure 1.3 Maturation of SCVs. Upon cell contact, the SPI-1 TTSS injects bacterial effectors that remodel the host actin cytoskeleton, triggering cell invasion. SPI-1 effectors also participate in the early stages of bacterial vacuole biogenesis and some persist in the host cell (and on the SCV membrane) long after bacterial uptake. Bacterial vacuoles transiently acquire early and recycling endosome markers such as early endosomal antigen 1 (EEA1), transferrin receptor (TfnR), Rab5 and Rab11. These proteins are then rapidly replaced by late endosomal markers, such as vacuolar ATPase (vATPase), lysosomal glycoproteins (lgps) and Rab7, which are maintained throughout infection. However, the late endosomal marker mannose 6-phosphate receptor (Man-6PR) is absent from the SCV, and the bacterial vacuoles seem to be mostly devoid of lysosomal enzymes, such as cathepsin D. SCV maturation is accompanied by centripetal movement along host cell MTs towards the MTOC, apparently powered by the dynein motor. In epithelial cells, SPI-2 phenotypes visible by light microscopy include the formation along MTs of tubular structures that extend from the SCV, called Sifs, and the appearance of microcolonies surrounded by Golgi membranes. SPI-2 effectors frequently localize to the SCVmembrane and to Sifs. Figure and legend from Ramsden *et al.*, 2007a.

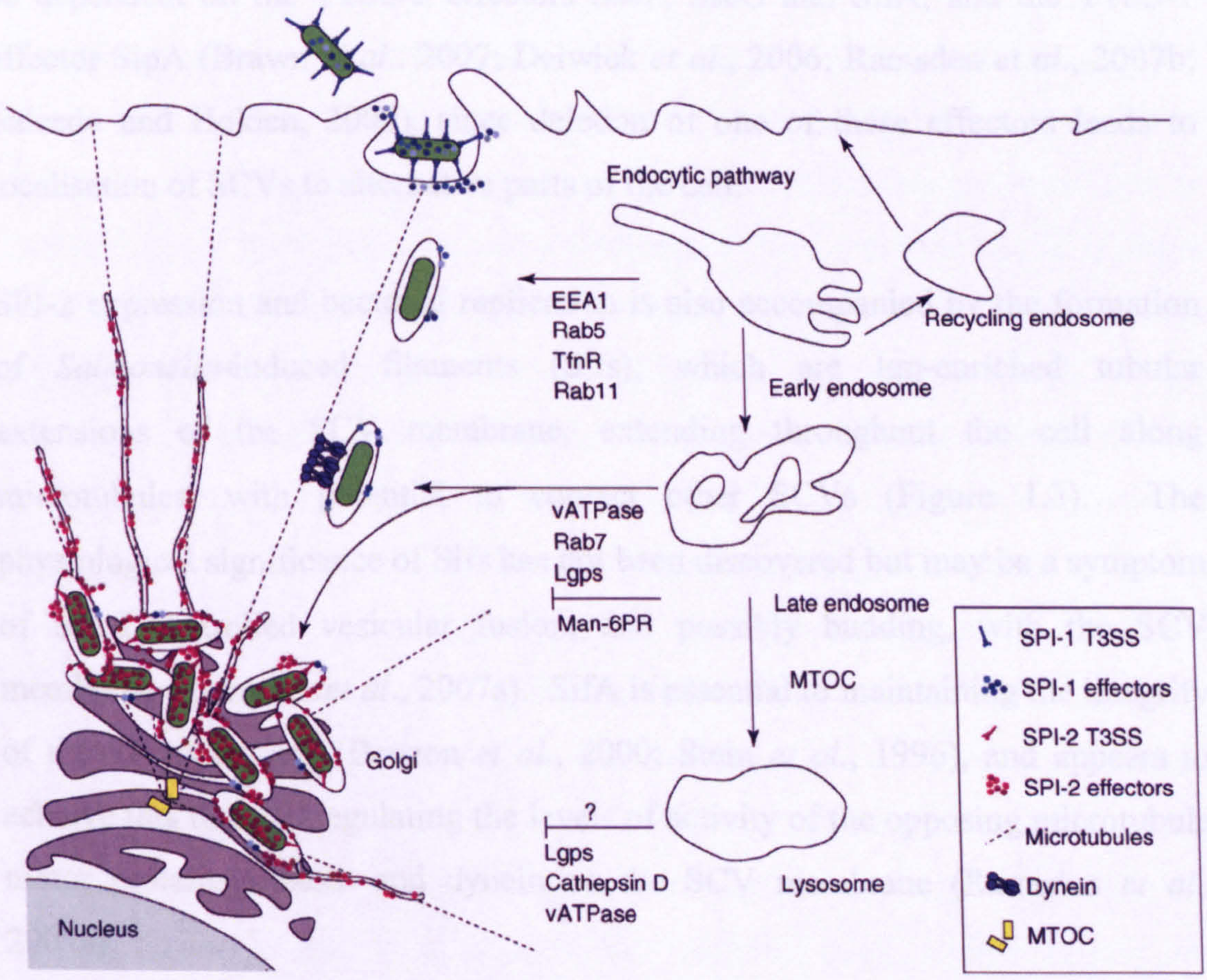

Maturation of SCVs is accompanied by their physical displacement along microtubules towards the microtubule-organising centre (MTOC) (Figure 1.3). The movement of SCVs along microtubules is dependent on the dynein-dynactin motor complex recruited by active Rab7 on the SCV membrane; Rab7 interacts with Rab-interacting lysosomal protein (RILP), which binds dynactin (Harrison *et al.*, 2004). Approximately 2 hours post-infection most vacuoles have been

shown to localise within 5μm of the MTOC (Ramsden *et al.*, 2007b). Migration to this cellular region may allow vesicular traffic to be intercepted providing nutrients to sustain bacterial replication and/or provide further membrane to maintain and expand the SCV, and therefore the intracellular niche of *Salmonella* (Ramsden et al., 2007a).

The SPI-2 TTSS becomes active at 3–4 hours post-invasion and translocation of SPI-2 effectors across the SCV promotes intravacuolar replication of *Salmonella.* This leads to the formation of microcolonies in the region of the MTOC and Golgi complex, close to the nucleus (Deiwick *et al.*, 2006; Ramsden *et al.*, 2007b; Salcedo and Holden, 2003). Retention of SCVs in this region appears to be dependent on the TTSS-2 effectors SseF, SseG and SifA, and the TTSS-1 effector SipA (Brawn *et al.*, 2007; Deiwick *et al.*, 2006; Ramsden *et al.*, 2007b; Salcedo and Holden, 2003), since deletion of one of these effectors leads to localisation of SCVs to alternative parts of the cell.

SPI-2 expression and bacterial replication is also accompanied by the formation of *Salmonella*-induced filaments (Sifs), which are lgp-enriched tubular extensions of the SCV membrane, extending throughout the cell along microtubules, with potential to contact other SCVs (Figure 1.3). The physiological significance of Sifs has not been discovered but may be a symptom of SPI-2-controlled vesicular fusion, and possibly budding, with the SCV membrane (Ramsden *et al.*, 2007a). SifA is essential to maintaining the integrity of the Sif membrane (Beuzon *et al.*, 2000; Stein *et al.*, 1996), and appears to achieve this through regulating the levels of activity of the opposing microtubule motor proteins kinesin and dynein on the SCV membrane (Ramsden *et al.*, 2007a).

While the cellular responses occurring after infection with wild type *Salmonella* are relatively well characterised, the *Salmonella* and host cell proteins involved in these processes are not. Currently, nineteen effectors translocated by TTSS-2 have been identified, but the roles of most are unknown and thus require further clarification alongside the role of TTSS-1 translocated effectors, some of which have also been implicated in the intracellular lifecycle of *Salmonella.*

1.4. The host response to *Salmonella* infection

Salmonella invasion of epithelial cells begins with adherence of the bacterium to the surface of the intestinal epithelium (Jones *et al.*, 1981). This is likely to be mediated through specific adhesins although no surface structures have yet been shown critical for infection. Since fimbriae are used for adhesion in other Gram-negative bacteria (reviewed in Soto and Hultgren, 1999), the presence of four known fimbrial systems in *Salmonella* suggests one or more of these systems may have a role in attachment to epithelial cells. However, the apparent redundancy of the fimbrial operons has so far made it difficult to determine the contribution of each fimbrial system to adherence (Darwin and Miller, 1999).

Once *Salmonella* is in close proximity with the apical membrane of the epithelial cell it stimulates a 'trigger mechanism of entry' (Cossart and Sansonetti, 2004; Swanson and Baer, 1995). Contact between the bacterium and host cell is mediated by a type three secretion system (TTSS) which delivers effector molecules into the cytoplasm of the epithelial cell to 'trigger' cytoskeleton rearrangements, producing membrane ruffles that allow endocytosis of the bacterium. *Salmonella* possess two known type three secretion systems (Galan, 1996; Shea *et al.*, 1996). It is the first of these, TTSS-1, encoded by *Salmonella* Pathogenicity Island 1 (SPI-1), which is employed to allow invasion, as shown by the lack of invasion of TTSS-1 mutants (Altmeyer *et al.*, 1993; Galan and Curtiss, 1989; Ginocchio *et al.*, 1992; Groisman and Ochman, 1993; Kaniga *et al.*, 1994). The membrane ruffles that are triggered by effector molecules translocated by TTSS-1 appear to occur through rearrangement of the actin cytoskeleton; treatment of cells with cytochalasins inhibits actin polymerisation and *Salmonella* invasion while microtubule inhibitors have no effect (Finlay and Falkow, 1988). The mechanisms by which *Salmonella* induces actin rearrangements are discussed below.

1.4.1. The actin cytoskeleton and its role in *Salmonella* invasion

Actin is the most abundant, and one of the most highly conserved, intracellular proteins in a eukaryotic cell. It exists as a 43kDa globular monomer known as

globular actin (G-actin), and when these monomers polymerise, as a filamentous polymer called F-actin. Two parallel F-actin strands twist around each other in a helical formation, giving rise to microfilaments measuring approximately 7nm in diameter (Figure 1.3). Microfilaments provide a framework to support and control the shape of a cell, and also have a role in cell translocation and participate in certain cell junctions, in cytoplasmic streaming and in contraction of the cell during cytokinesis.

Figure 1.4 The structure of actin monomers and filaments. A is a ribbon diagram of the structure of G-actin. G-actin is divided by a central cleft into two lobes and four subdomains, numbered I-IV. ATP and a magnesium ion (yellow circle) are shown binding at the bottom of this cleft. In B the structure of F-actin is shown. An electron micrograph of a negatively stained actin filament shows the filament appears alternately thinner and thicker, which is due to the twisting of two strands of beaded subunits around each other, shown in the lower diagram. (Figures taken from Molecular Cell Biology and Essential Cell Biology, 2004a)

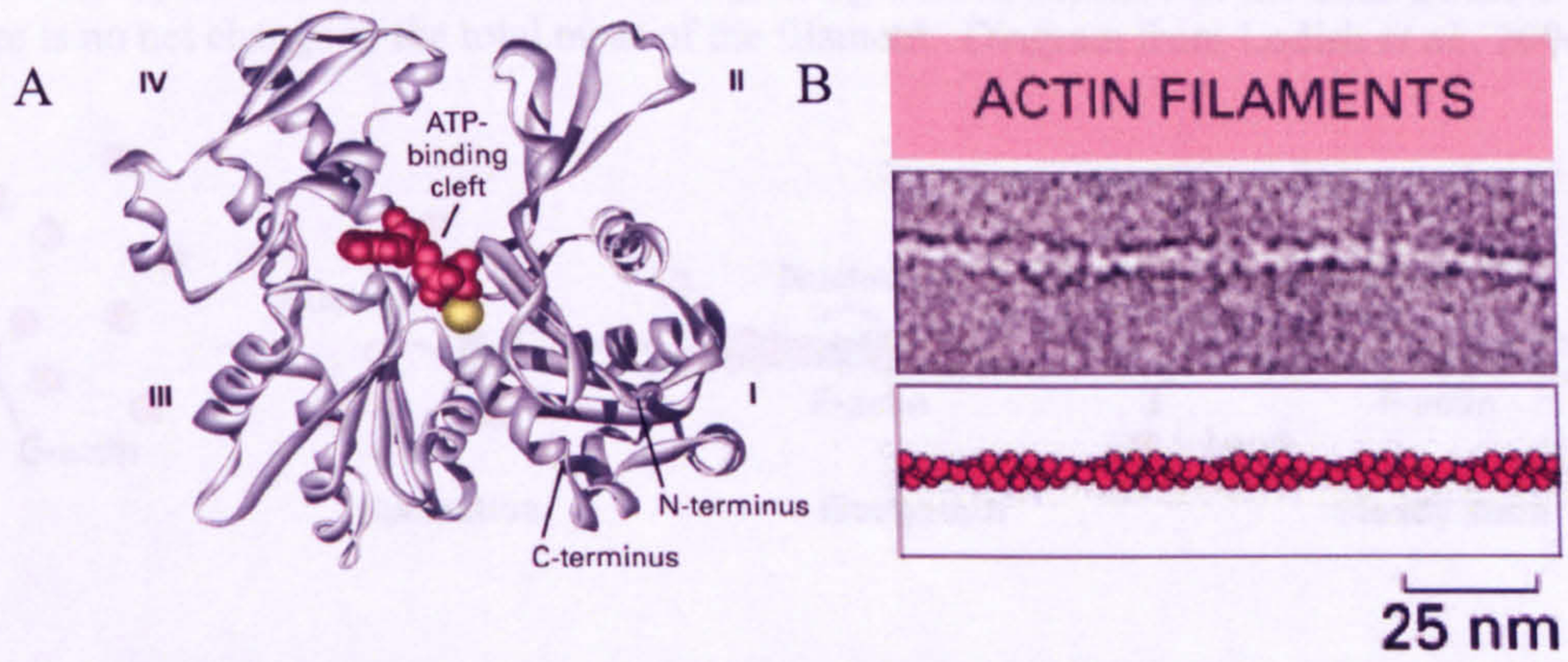

In vitro, monomers of ATP-G-actin, in the presence of magnesium, spontaneously polymerise to form F-actin but at low rates since three monomers are required to nucleate filament growth (Figure 1.4). Once the nuclei are formed they are rapidly elongated by addition of monomers to both ends of the filament. The monomers polymerise so the ATP-binding cleft of each subunit is orientated in the same direction, giving F-actin polarity; decoration of F-actin with myosin S1 fragments renders one end as pointed (-) and the other as barbed (+) when imaged by electron microscopy. ATP-G-actin preferentially binds to the barbed (+) end since the critical concentration (concentration of G-actin in equilibrium with F-actin) is lower at this end. Thus, G-actin is often rapidly added to the barbed end, while dissociating at the pointed end, which can lead to 'treadmilling'. This is where the filament length remains approximately constant

with new subunits travelling through the filament until they reach the end and dissociate (for a review of basic actin biochemistry Pollard and Borisy, 2003).

After GTP-G-actin is incorporated into a filament, the bound ATP is slowly hydrolysed to ADP with phosphate (Pi) being released. Thus, a filament is largely composed of ADP-F-actin with ATP-G-actin at either end. ATP hydrolysis is not essential for polymerisation. Instead this activity may reduce the binding strength between neighbouring monomers and destabilise the filament, thereby allowing monomers to dissociate (De la Cruz *et al.*, 2000).

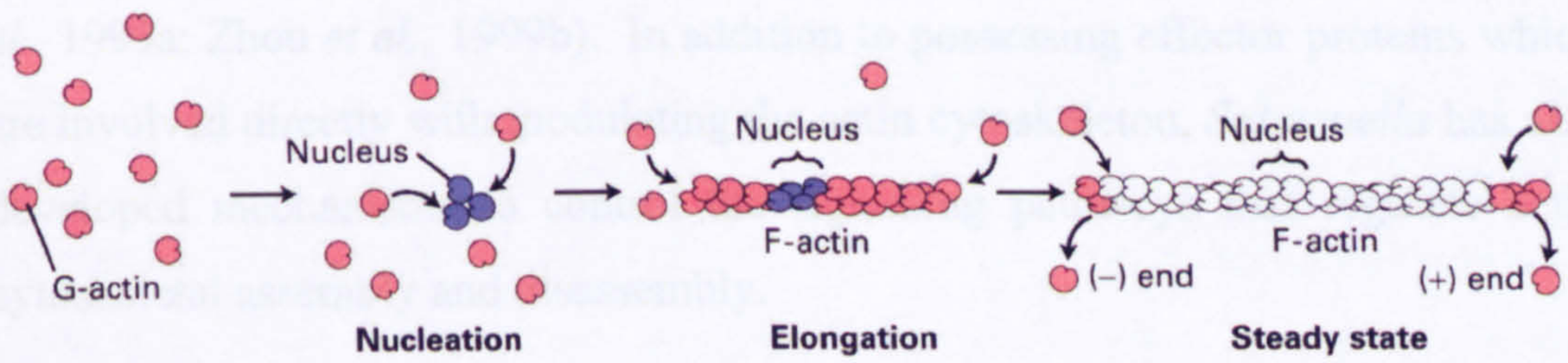

Figure 1.5 The phases of actin polymerisation *in vitro*. ATP-G-actin (peach) slowly forms a nucleus of actin (purple). The nucleus is rapidly elongated by addition of further monomers at both ends. The ATP-binding clefts (black triangles) all align in the same direction, giving F-actin its polarity. The ATP is slowly hydrolysed in the monomers so ADP-F-actin is formed (white). In the steady state G-actin monomers are exchanged with subunits at the ends of the F-actin but there is no net change in the total mass of the filament. Diagram from Lodish *et al.*, 2004.

There are a variety of actin-binding proteins (ABPs) which regulate the equilibrium between G-actin and F-actin, allowing the dynamism associated with the eukaryotic cell cytoskeleton. For actin polymerisation to continue, concentrations of ATP-G-actin must be maintained. This is one of the roles of profilin, which binds to ADP-G-actin and catalyses the exchange of ADP for ATP. Actin depolymerisation is achieved through proteins such as Actin depolymerisation factor (ADF)/cofilin, which bind F-actin and promote dissociation of ADP-actin from the F-actin minus end. Additionally ADF/cofilin can sever microfilaments to create new pointed ends for depolymerisation. However, this action also creates new barbed ends for polymerisation, thus ADF/cofilin can enhance Arp2/3 (actin related protein) complex-dependent actin polymerisation (DesMarais *et al.*, 2004). Gelsolin is one exception since after severing F-actin it caps the barbed ends so they are no longer free for

polymerisation (Zigmond, 2004). Other barb end-capping proteins are present in cells, such as CapZ, which through preventing the addition or loss of monomers at this filament end directs the extension of the microfilament, which is useful in driving membrane protrusions that may be required for translocation or particle uptake. Capping is not limited to the barbed ends, blockage of depolymerisation from pointed ends allowing maintenance of actin networks (Zigmond, 2004).

Since ABPs regulate the length and lifespan of F-actin, they are important regulators of the formation and dynamic properties of cellular protrusions, including those induced by *Salmonella*. *Salmonella* translocates two actin binding proteins into host cells via TTSS-1; *Salmonella* invasion protein A (SipA) and SipC. Together these ABPs enhance nucleation of actin polymerisation, increase the stability of F-actin, and promote bundling of F-actin at sites adjacent to the adhered bacterium (McGhie *et al.*, 2001, 2004; Zhou *et al.*, 1999a; Zhou *et al.*, 1999b). In addition to possessing effector proteins which are involved directly with modulating the actin cytoskeleton, *Salmonella* has also developed mechanisms to control the signalling pathways that regulate actin cytoskeletal assembly and disassembly.

1.4.2. Rho GTPases and their involvement in *Salmonella* invasion

An important group of proteins involved with signal transduction inside eukaryotic cells are the small GTPases. These are 20-25kDa monomeric proteins which bind guanosine triphosphate (GTP) and behave as molecular switches due to their alternation between a GDP-bound inactive form and a GTP-bound active form (Figure 1.5). Active GTPases bind numerous effector molecules that in turn stimulate signalling cascades promoting cellular responses such as cytoskeletal change, microtubule dynamics, vesicle trafficking, cell polarity and cell cycle progression. GTP-hydrolysis and liberation of phosphate inactivates the GTPases and subsequently 'switches off' these pathways.

Figure 1.6 Rho GTPase cycle. Guanine nucleotide exchange factors (GEFs) release guanosine diphosphate (GDP) from Rho GTPases promoting the binding of guanosine triphosphate (GTP) and activation of Rho GTPases. GTPase activating proteins (GAPs) stimulate the intrinsic GTPase activity of Rho GTPases and convert GTP-Rho GTPases to inactive GDP-GTPases. In resting cells Rho GTPases exist mostly in GDP-bound form and in complexes with Rho GDI in the cytosol. GDP dissociation inhibitor (GDI) inhibits the dissociation of GDP from Rho GTPases and thus prevents association of GDP-GTPase to the cell membrane. The GTP-bound form of Rho GTPases is associated with cell membranes.

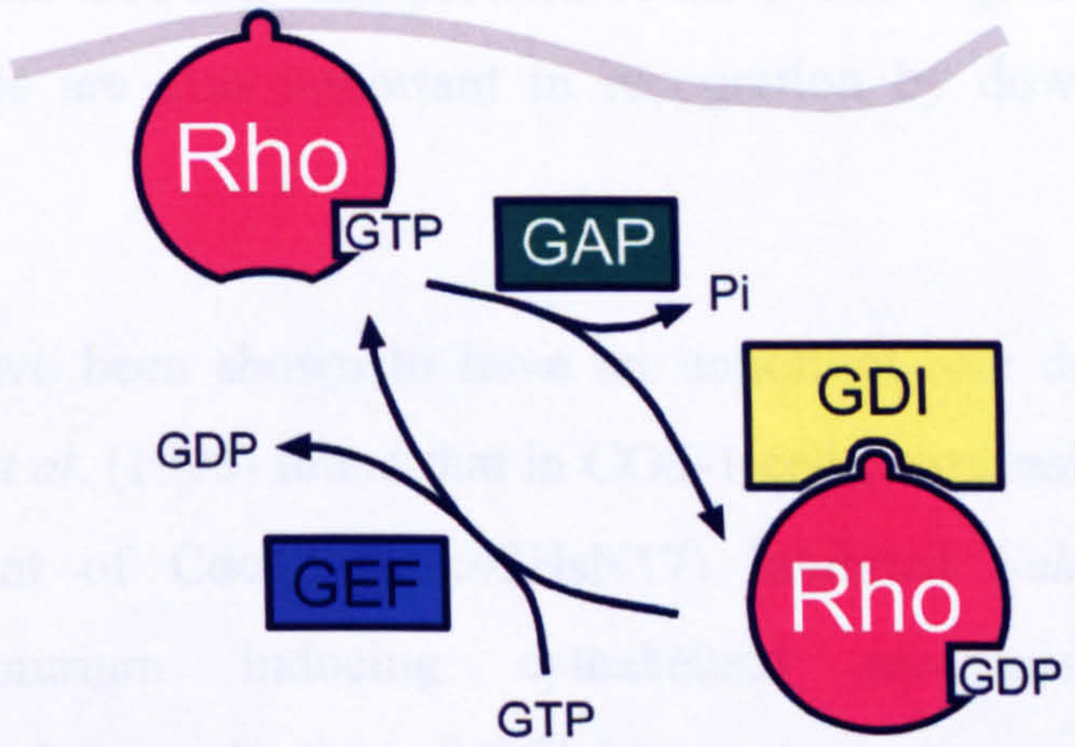

The Rho family of small GTPases interact with a number of proteins involved with regulation of the actin cytoskeleton. Cdc42, Rac1 and Rho are the most extensively characterised Rho GTPases with roles in regulating actin dynamics. Activation of Cdc42 stimulates the polymerisation of actin to create filopodia, activation of Rac induces formation of lamellipodia and membrane ruffles (Nobes and Hall, 1995; Ridley and Hall, 1992), while Rho regulates bundling of actin filaments into stress fibres and the formation of focal adhesion complexes (Paterson *et al.*, 1990).

The differences between the GDP- and GTP-bound forms of Rho GTPases are confined primarily to two regions of the protein referred to as switch I and switch II (Vetter and Wittinghofer, 2001). In the presence of Mg^{2+} these switch regions form a high-affinity binding pocket to stabilise the bound guanine nucleotide. GTP-GDP exchange is inherently very slow thus is regulated by guanine nucleotide exchange factors (GEFs), guanine nucleotide dissociation inhibitors (GDIs) and GTPase-activating proteins (GAPs) (Figure 1.5) (reviewed by Bos *et al.*, 2007). GEFs promote the exchange of GDP for GTP to activate Rho GTPases during signal transduction. GAPs promote the hydrolysis of the bound GTP molecules, transferring the GTPase back to the inactive state at the end of a

stimulation cycle, while GDIs inhibit GDP release from the Rho GTPase and shield the prenylated C-terminal, maintaining the Rho GTPases in an inactive state in the cytosol. This controls Rho GTPase cycling between the plasma membrane and cytosol. GEFs, GAPs and GDIs each induce their effect by altering the interaction of the guanine nucleotide with the switch I and II regions of their cognate Rho GTPase. The position of the switch regions in the GDP and GTP bound forms are also important in recognition by downstream effector proteins.

Rho GTPases have been shown to have an important role during *Salmonella* invasion. Chen *et al.* (1996) found that in COS-1 cells, expression of a dominant interfering mutant of Cdc42 (Cdc42HsN17) inhibited *Salmonella enterica* serovar Typhimurium inducing cytoskeletal reorganisation, bacterial internalisation, and the activation of JNK kinase, indicating a role for Cdc42 in *Salmonella* invasion and nuclear responses in host cells. The expression of a dominant interfering mutant of Rac1 (Rac1N17) in the same cells inhibited the bacteria-induced changes to a much lesser extent than Cdc42HsN17, indicating Rac1 is less important. However, in polarised MDCK II monolayers, Cdc42 has been shown to be dispensable and Rac1 required for internalisation at the apical membrane, with an uncharacterised SopE-dependent GTPase required for invasion at the basolateral surface (Criss *et al.*, 2001a; Criss and Casanova, 2003; Hobert *et al.*, 2002). Since both Cdc42 and Rac1 are activated during apical invasion of MDCK I cells which were not polarised (Tafazoli *et al.*, 2003), it appears the importance of specific GTPases during *Salmonella* invasion may be dependent upon whether cells are polarised rather than individual cell type.

Why are Rho GTPases important to bacterial invasion? With their ability to interact with large numbers of proteins and their role regulating essential host cell processes, Rho GTPases represent the interface between bacterial and host cell signalling pathways. Rho GTPases transmit signals from *Salmonella* effector proteins to downstream host effector proteins that allow *Salmonella* uptake into cells and the pathologies associated with Salmonellosis. Rac1 and Cdc42 have continually been implicated in the invasion of *Salmonella* (Chen *et al.*, 1996; Criss *et al.*, 2001; Criss and Casanova, 2003; Hobert *et al.*, 2002), and

Figure 1.6 shows signal-transduction pathways stimulated by these Rho GTPases that are likely to be involved with driving the production of membrane ruffles, and therefore invasion. Additionally, these Rho GTPases are involved in nuclear responses that lead to inflammation and the symptoms associated with gastroenteritis (1.4.3).

Figure 1.7 Signal transduction pathways induced by Rac and Cdc42 that lead to formation of actin-containing membrane protrusions (Adapted from Bishop and Hall, 2000).

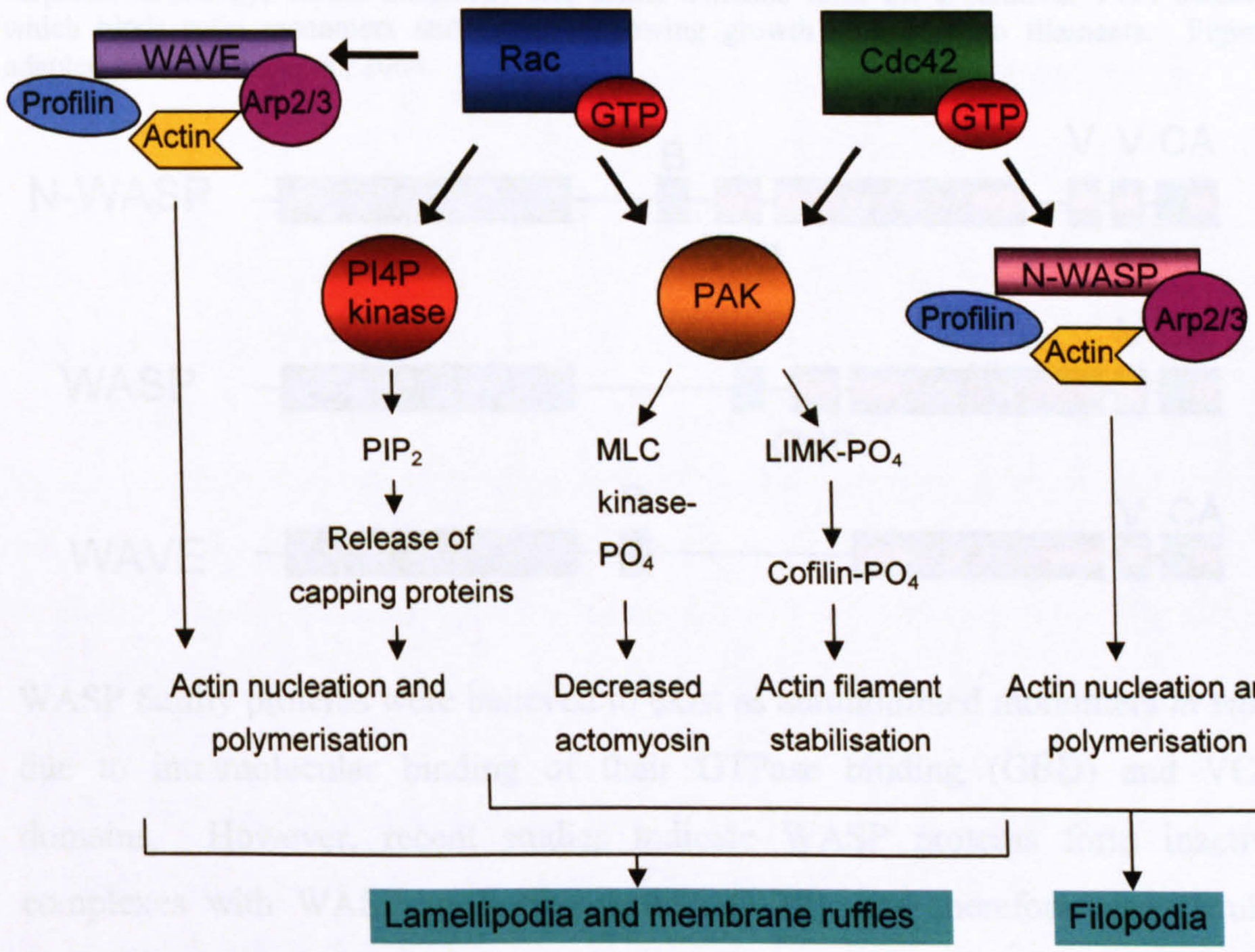

1.4.3. Downstream targets of Rho GTPases and their role in invasion

The rate-limiting step in actin polymerisation *in vitro* is the assembly of an actin nucleus. A family of regulatory proteins including Wiskott-Aldrich syndrome protein (WASP), neural (N)-WASP and WASP family verprolin-homologous (WAVE) proteins (the latter also termed suppressor of cAMP receptor (SCAR) proteins) function by relaying signalling from Cdc42 and Rac to Arp2/3. The conserved C-terminal VCA domain of the WASP and WAVE proteins enables these proteins to form a tripartite unit with G-actin and Arp2/3, leading to nucleation and formation of a branched filament network. The VCA domain is

composed of a verprolin homology domain (V) that binds an actin monomer, a linker region (C) and an acidic (A) region that associates with the Arp2/3 complex (Figure 1.7). The N-terminal of these proteins is more divergent, allowing targeting and regulation of the protein.

Figure 1.8 Modular domain organisation of WASP, N-WASP and WAVE proteins. WASP and N-WASP contain an N-terminal WASP homology 1 (WH1) domain, while the three WAVE isoforms possess a WAVE homology domain (WHD). B indicates a stretch of basic amino acids that are bound by PIP_2, GBD is the GTPase-binding domain that interacts with GTP-Cdc42, while PPPPP represents a proline-rich region that can bind SH3 domains and profilin. The verprolin homology, cofilin homology and acidic domains form the C-terminal VCA domain which binds actin monomers and Arp2/3, allowing growth of new actin filaments. Figure adapted from Stradal *et al.*, 2004.

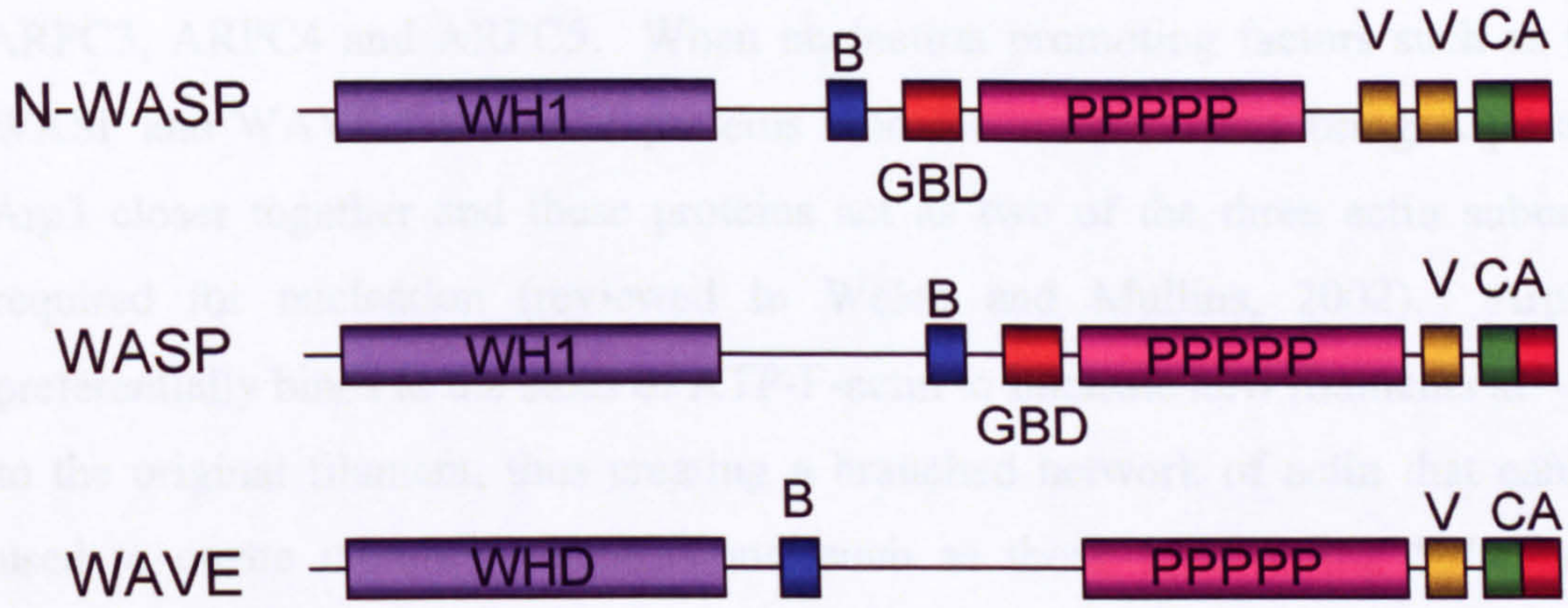

WASP family proteins were believed to exist as autoinhibited monomers *in vitro* due to intramolecular binding of their GTPase binding (GBD) and VCA domains. However, recent studies indicate WASP proteins form inactive complexes with WASP-interacting protein (WIP), and therefore also require Toca-1 (transducer of Cdc42 dependent actin assembly) for Cdc42 activation (reviewed in Stradal and Scita, 2006). In both cases co-operative binding of phosphatidylinositol-4, 5-bisphosphate (PtdIns(4,5)P_2 or PIP_2) and Cdc42 to the B and GBD regions respectively causes a conformational change releasing the VCA domain. This allows interaction of WASP with Arp2/3 to stimulate actin nucleation.

WAVE proteins are constitutively active *in vitro* but are kept inactive *in vivo* through association with four other proteins: Nap1, Sra1/PIR121, HSPC300 and Abi1. Sra-1 is a Rac effector and therefore believed to recruit the WAVE-containing complex to sites of Rac activation. It remains controversial whether

the binding of Rac-GTP causes dissociation of the complex to activate WAVE or whether a conformational change occurs to activate WAVE and allow binding of Arp2/3, although it is possible both may occur depending on the *in vivo* situation (Stradal & Scita, 2006). WAVE2 also binds activated Rac via the insulin receptor tyrosine kinase substrate p53 (IRSp53) (Miki *et al.*, 2000). However, while IRSp53/WAVE2 has been found to localise to sites of *Salmonella* invasion, only the association of WAVE2 with Abi1/Nap1/Sra1/HSPC300 is required for internalisation of *Salmonella* (Shi *et al.*, 2005).

The Arp2/3 complex is composed of 7 proteins; Arp2, Arp3, ARPC1, ARPC2, ARPC3, ARPC4 and ARPC5. When nucleation promoting factors such as the WASP and WAVE families of proteins bind the complex they bring Arp2 and Arp3 closer together and these proteins act as two of the three actin subunits required for nucleation (reviewed in Welch and Mullins, 2002). Arp2/3 preferentially binds to the sides of ATP-F-actin to nucleate new filaments at ~70° to the original filament, thus creating a branched network of actin that can be used to create membrane protrusions, such as those seen during *Salmonella* invasion (Figure 1.8). Indeed overexpression of the C-terminal VCA domain of Scar, which sequesters Arp2/3, inhibits *Salmonella* invasion by 80% at both apical and basolateral membranes of MDCK cells, indicating a requirement for Arp2/3 in *Salmonella* invasion (Criss and Casanova, 2003). However, Arp2/3-independent mechanisms are also required for actin assembly, as while dominant-interfering versions of N-WASP and WAVE in HeLa cells inhibit serovar Typhimurium invasion by a maximum of 50%, dominant-negative Cdc42 and Rac inhibit invasion by over 80% (Unsworth *et al.*, 2004). This Arp2/3-independent actin polymerisation may be performed by unidentified host cell proteins or by one or more of the effector proteins secreted by *Salmonella*.

Figure 1.9 Arp2/3 complex mediated actin nucleation. Arp2/3-complex-activating proteins, such as WASP and WAVE, close to the plasma membrane induce the binding of the Arp2/3 complex (blue) to the flank of existing filaments whilst simultaneously nucleating a new daughter filament. The presence of capping protein (orange) ensures that filaments at the leading edge remain short. ATP is hydrolysed to ADP in older filaments (shown by the transition of monomers from red to green). ATP hydrolysis and loss of the phosphate group from older monomers facilitates the release of Arp2/3 complex branches and the disassembly of F-actin to G-actin (Deeks and Hussey, 2005).

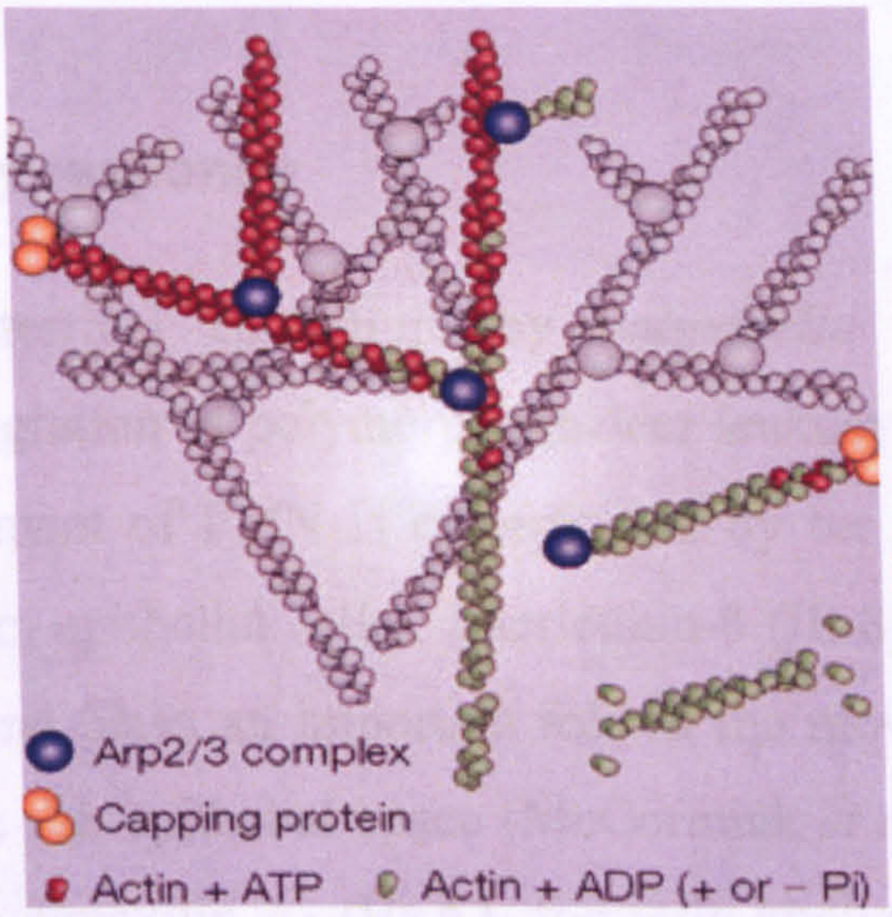

The use of Rho GTPases to modulate the activity of ADF/cofilin has also been shown important to *Salmonella* invasion. In the model proposed by Dai *et al.* (2004), the protein phosphatase Slingshot dephosphorylates ADF/cofilin immediately after translocation of effector proteins via TTSS-1. This activated ADF/cofilin stimulates F-actin depolymerisation providing new barbed ends and a pool of G-actin to facilitate the rapid actin polymerisation required for membrane ruffle production. This actin polymerisation is achieved through the activation of p21-activated kinase (PAK) by GTP-Rac. Activated PAK inhibits ADF/cofilin via LIM kinase (Dai *et al.*, 2004). The inactivation of ADF/cofilin allows stable microfilaments to be produced, leading to outward protrusion of the membrane and engulfment of the bacterium.

Recently, focal adhesion kinase (FAK) and p130Cas have been implicated in mediating *Salmonella* invasion in HeLa cells (Shi and Casanova, 2006). These proteins are commonly associated with focal adhesions; protein complexes that provide a physical linkage between integrins and the actin cytoskeleton, and transmit adhesion-dependent signals. Since β-integrins are not utilised by *Salmonella* for invasion (Shi and Casanova, 2006), it is not known how FAK and

p130Cas are recruited to *Salmonella* induced membrane ruffles. However, their role as scaffold proteins, with the observation that other focal adhesion proteins such as paxillin, vinculin, α-actinin and VASP are recruited to ruffles (Finlay *et al.*, 1991; Shi and Casanova, 2006), suggests focal adhesion proteins may also contribute to regulation of the actin cytoskeleton and *Salmonella* invasion.

1.4.4. Inflammatory response

Invasion of the intestinal epithelium by *Salmonella* is accompanied by inflammation and migration of polymorphonuclear leukocytes (PMN) across the epithelium. Recruitment of PMN is co-ordinated by the release of two PMN chemoattractants from epithelial cells. Interleukin-8 (IL-8) is secreted from the basolateral surface and plays an important role in the movement of PMN from the circulation to the sub-epithelial space (McCormick *et al.*, 1993; McCormick *et al.*, 1995a), while hepoxilin A_3 (HxA3, formerly known as pathogen-elicited epithelial chemoattractant (PEEC)) is secreted from the apical surface to elicit the final movement of PMN to the luminal surface (McCormick *et al.*, 1998; Mrsny *et al.*, 2004). Since the secretion of both chemoattractants is dependent on a functional SPI-1 TTSS (Gewirtz *et al.*, 1999; McCormick *et al.*, 1995a; McCormick *et al.*, 1995b; McCormick *et al.*, 1998), synthesis and secretion of these chemoattractants appears to be dependent upon the actions of *Salmonella* effector proteins.

SipA has been found necessary and sufficient for induction of PMN transmigration across polarised epithelial cell monolayers (Lee *et al.*, 2000), and research has been focused on elucidating the signalling pathways that connect SipA with HxA3 secretion. In the model proposed (Figure 1.9), apical SipA leads to the recruitment of ADP-ribosylation factor 6 (ARF6) and its exchange factor ARNO to the apical membrane. The subsequent activation of ARF6 by ARNO allows interaction between ARF6 and its effector phospholipase D (PLD), which in turn directs activation of protein kinase C alpha (PKCα), the release of HxA3 and movement of PMN to the apical surface (Criss *et al.*, 2001b; Lee *et al.*, 2000; Mrsny *et al.*, 2004; Silva *et al.*, 2004). The mechanism by which PKCα stimulates production and apical release of HxA3 is unclear.

Activation of phospholipase A_2 (PLA_2) by PKCα either directly or indirectly may allow release of arachidonic acid from membranes which can be converted to HxA3 by 12-lipoxygenase (12-LOX) (McCormick, 2007).

Figure 1.10 Model of SipA stimulated release of HxA3. Interaction of SipA with the apical membrane of polarised epithelial cells leads to recruitment of ARNO and activation of ARF6 at the apical membrane. This leads to an increase in phospholipase D (PLD) activity and local production of phosphatidic acid (PA) from phosphatidyl choline (PC). PA is metabolised to diacylglycerol (DAG) by PA phosphohydrolase (PAP). Generation of DAG (and potentially other signals) recruits PKC to the apical plasma membrane (PM). Activation of PKC leads to HxA3 production and apical secretion, which drives PMN transepithelial migration.

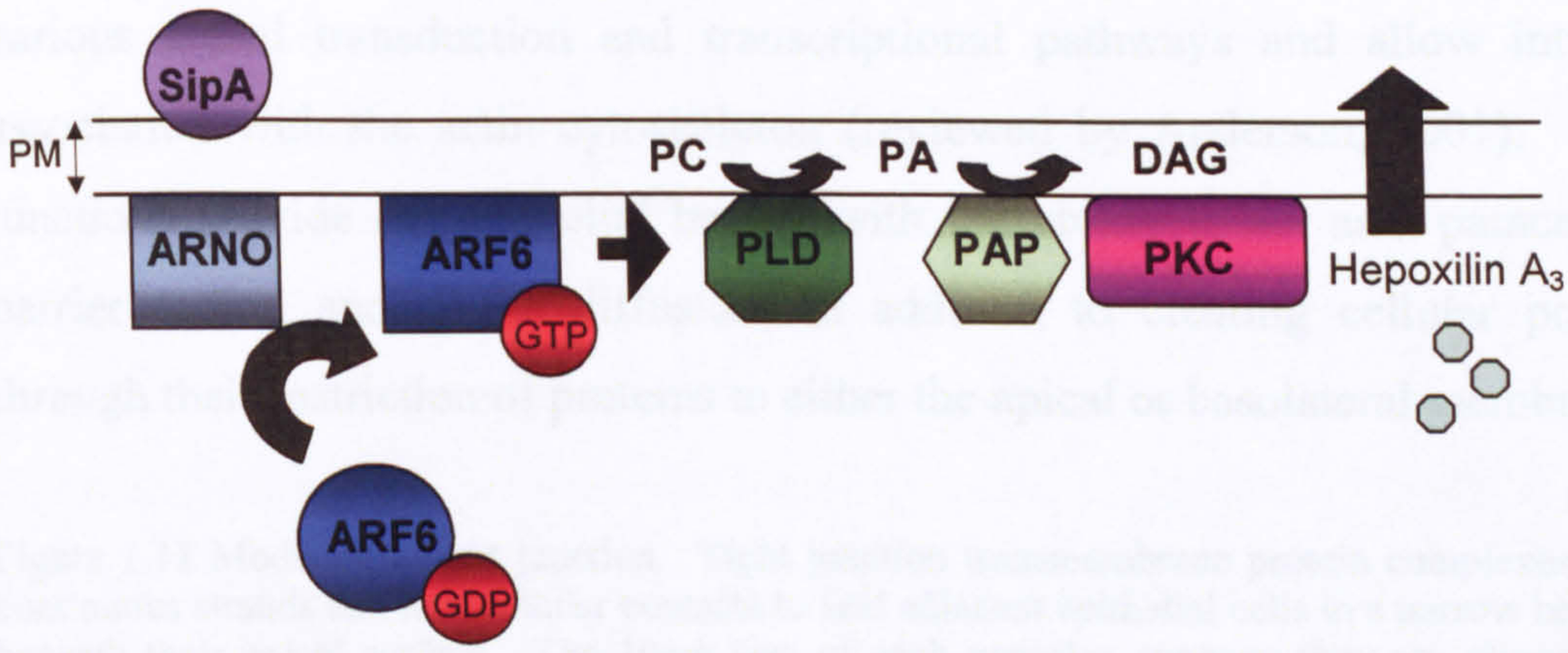

IL-8 secretion from the basolateral membrane also appears to be stimulated by *Salmonella* effector proteins. *Salmonella*-induced IL-8 secretion occurs through the activation of transcription factors NFκB and AP-1 (Gewirtz *et al.*, 1999; Hobbie *et al.*, 1997). Since activation of Cdc42 has been shown to stimulate activation of MAP kinases including JNK (Chen *et al.*, 1996a; Chen *et al.*, 1999; Hardt *et al.*, 1998a; Hobbie *et al.*, 1997), and these in turn activate the transcription factors NFκB and AP-1, it suggests effector proteins signalling through Rho GTPases may be important for IL-8 secretion. Indeed a *sopE sopE2* mutant has been shown to induce lower levels of IL-8 secretion from T84 cells than its parent (Huang *et al.*, 2004), and in a bovine ligated ileal loop model, SopE, SopE2 and SopB, alongside SipA, SopA and SopD, have been implicated in the inflammation and fluid accumulation responsible for the diarrhoea associated with *Salmonella* infection of calves (Zhang *et al.*, 2002). The mechanisms by which SopA and SopD lead to inflammation are not clear, although SopA requires its E3 ubiquitin ligase activity (Zhang *et al.*, 2006).

Salmonella infection causes the integrity of the epithelial monolayer to be lost, which is also likely to be important for the inflammation and production of diarrhoea induced by *Salmonella*. Intestinal epithelium cells are held together by a variety of intercellular junctions. Tight junctions are protein complexes circumscribing the cell near its apical surface and occluding space between adjacent cells (Figure 1.10). The interactions between transmembrane proteins such as occludin, claudin and junctional adhesion molecules (JAMs) hold adjacent cells together while scaffold proteins such as ZO-1 link junctions with various signal transduction and transcriptional pathways and allow intimate association with the actin cytoskeleton (reviewed by Anderson, 2001). Tight junctions provide the epithelial barrier with the ability to act as a paracellular barrier to ion and solute diffusion, in addition to creating cellular polarity through their restriction of proteins to either the apical or basolateral membrane.

Figure 1.11 Model of a tight junction. Tight junction transmembrane protein complexes create continuous strands and intercellular contacts to seal adjacent epithelial cells in a narrow band just beneath their apical surface. The 10nm size of each complex suggests they are oligomers of claudin monomers. Both claudins and occludin are homophilic cell-cell adhesion molecules, although some claudins can form heterophilic adhesions with other claudins. The extracellular contacts of these proteins create the aqueous spaces capable of size and ionic discrimination that allows the epithelium to act as a paracellular barrier. Diagram by Mariana Ruiz (http://commons.wikimedia.org/wiki/Image:Cellular_tight_junction.svg).

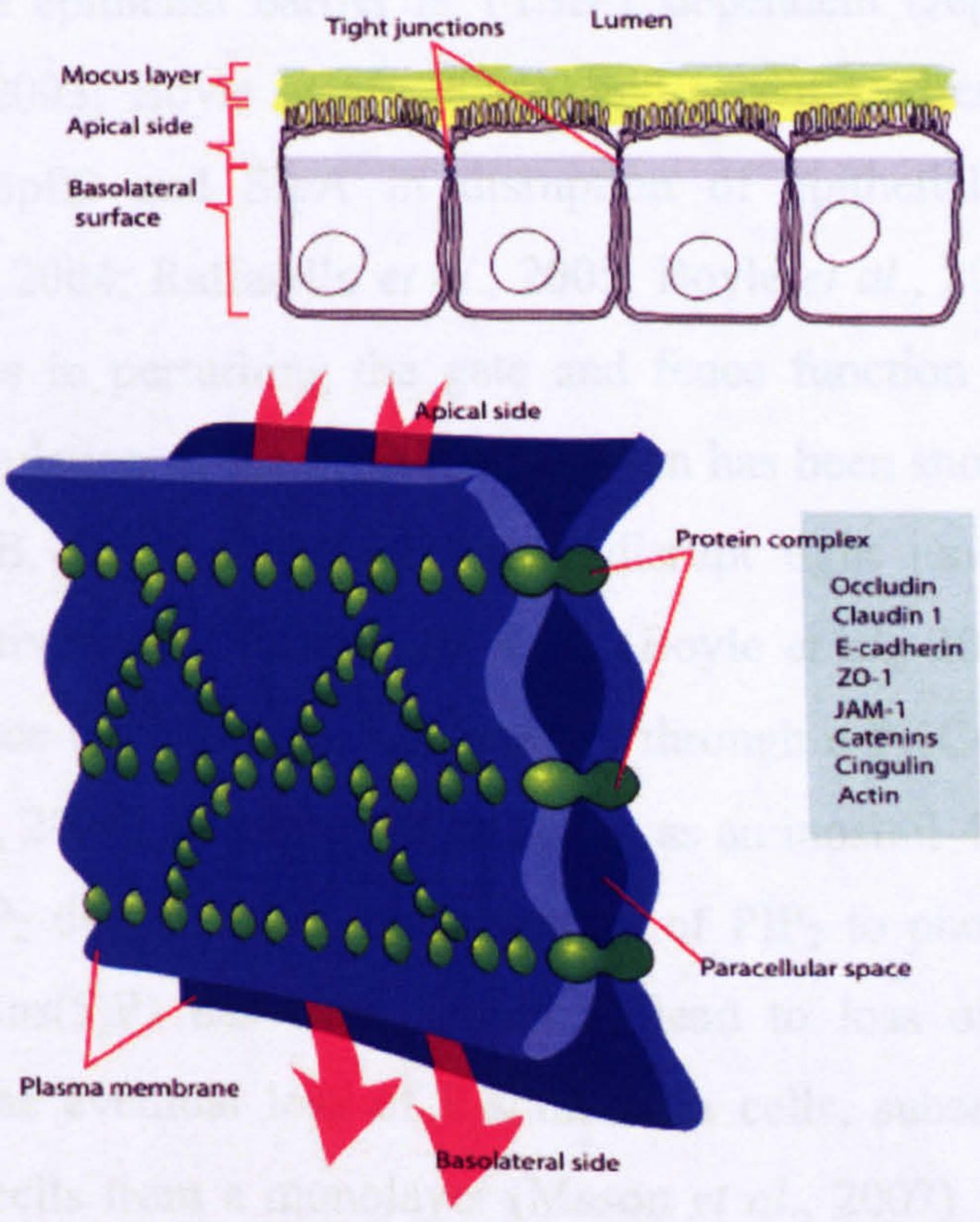

Transepithelial electrical resistance (TER) serves as an instantaneous measure of the integrity of the epithelial layer and particularly the permeability of tight junctions. *Salmonella* infection elicits a decrease in TER in polarised monolayers of MDCK (Finlay *et al.*, 1988; Jepson *et al.*, 1995; Jepson *et al.*, 2000), Caco-2 (Boyle *et al.*, 2006; Finlay and Falkow, 1990), and T84 (Kohler *et al.*, 2007; Raffatellu *et al.*, 2005) cells. The progressive reduction of TER concomitant with decreased cation permselectivity and increased paracellular permeability (Boyle *et al.*, 2006; Jepson *et al.*, 1995; Kohler *et al.*, 2007) does not appear to correlate with the contraction of the perijunctional actinomyosin ring that also occurs during *S.* Typhimurium infection (Jepson *et al.*, 2000). Thus, physical disruption of tight junctions by actinomyosin does not appear to be involved in modulation of tight junction permeability. Instead it has been proposed that *Salmonella* effector proteins alter distribution of some tight junction proteins to increase intestinal epithelial tight junction permeability. Indeed, ZO-1, occludin and claudin have been shown to be displaced from the membrane during *Salmonella* infection (Bertelsen *et al.*, 2004; Boyle *et al.*, 2006; Kohler *et al.*, 2007; Mason *et al.*, 2007) while concentrations of E-cadherin and ZO-2 increase at the membrane (Jepson *et al.*, 1995; Kohler *et al.*, 2007).

Disruption of the epithelial barrier is TTSS-1 dependent (Jepson *et al.*, 1996; Tafazoli *et al.*, 2003; Boyle *et al.*, 2006), and recent studies have implicated SopB, SopE, SopE2 and SipA in disruption of epithelial barrier function (Bertelsen *et al.*, 2004; Raffatellu *et al.*, 2005; Boyle *et al.*, 2006). Since a role for Rho GTPases in perturbing the gate and fence function of tight junctions through their regulation of the actin cytoskeleton has been shown (Braga, 2002), it suggests SopB, SopE and SopE2 may disrupt tight junction permeability through their activation of Cdc42 and Rac1 (Boyle *et al.*, 2006). SopB is also believed to reduce epithelial barrier function through a PKC-mediated pathway (Bertelsen *et al.*, 2004), and through its action as an inositol-4 phosphatase. The depletion of PIP_2 due to SopB hydrolysation of PIP_2 to phosphatidylinositol 5 phosphate (PtdIns(5)P) has been shown to lead to loss of ZO-1 from tight junctions and the eventual loss of F-actin from cells, subsequently leading to detachment of cells from a monolayer (Mason *et al.*, 2007). How SipA acts to reduce epithelia integrity has not yet been distinguished. Since a *sopB*$^-$ *sopE*$^-$

sopE2⁻ mutant does not reduce TER it indicates SipA is insufficient alone to achieve this effect. It is possible SipA functions with SopE and/or SopE2 to disrupt tight junctions, although it has also been shown that SipA and SopB can co-operate to reduce TER (Raffatellu *et al.*, 2005; Boyle *et al.*, 2006) suggesting SipA and SopB may act together.

As the integrity of the intestinal barrier is compromised, bacteria and PMN translocation are increased across the epithelium (Kohler *et al.*, 2007), possibly amplifying the immune response, especially since Toll-like receptors on the basolateral membrane may be exposed to pathogen-associated molecular patterns (PAMPs). Interaction of flagellin with Toll-like receptor 5 (TLR5) has been implicated in the induction of IL-8 (Gewirtz *et al.*, 2001a; Gewirtz *et al.*, 2001b). Interestingly SopE2 appears to contribute to the activation of three signalling pathways (ERK, p38 and NFκB) that are also activated by the flagellin-TLR5 interaction (Huang *et al.*, 2004), suggesting co-operativity between flagellin and effector proteins in inducing the inflammation and fluid secretion associated with *Salmonella* infection.

1.5. Genetic and molecular basis of interactions between *Salmonella* and host epithelial cells

At least 60 genes are required for *Salmonella* virulence (Groisman and Ochman, 1997), many of which are located within *Salmonella* Pathogenicity Islands (SPIs). SPIs have been defined as large gene cassettes within the *Salmonella* chromosome that are flanked by integration sites and encode determinants responsible for establishing specific interactions with the host and are required for bacterial virulence in the host (Marcus *et al.*, 2000). In some cases acquisition of a pathogenicity island enables a benign microorganism to become pathogenic. For example, a laboratory strain of *Escherichia coli* can become pathogenic by transforming it with a plasmid carrying the 35kb locus of enterocyte effacement (LEE), a pathogenicity island on the chromosome of enteropathogenic *E. coli* (EPEC) (McDaniel *et al.*, 1995). The acquisition of clusters of virulence genes is believed to occur through horizontal transfer from

bacteriophage or plasmids, suggesting an evolutionary route by which novel pathogens have emerged. The acquisition of pathogenicity islands by horizontal gene transfer is frequently reflected in the differing base composition between pathogenicity island regions and the bacterial chromosome, and the association with insertion sites such as tRNA genes (Hensel, 2004).

At present 17 SPIs been identified (Vernikos and Parkhill, 2006). Some of these SPIs are conserved throughout the genus *Salmonella*; others are specific to certain serovars. The most important of these pathogenicity islands are SPI-1, which encodes the genes for invasion of epithelial cells and induction of intestinal secretion and inflammatory responses, and SPI-2, which contains genes involved with intracellular replication and systemic infection.

1.5.1. S*almonella* Pathogenicity Island-1 (SPI-1)

SPI-1 maps to centisome 63 in the *S. enterica* serovar Typhimurium chromosome, and represents a 40kb insertion between genes that are consecutive in *E. coli* K12 (Mills *et al.*, 1995). While the GC content of the *Salmonella* chromosome is 52%, SPI-1 has a GC content of 42%, indicating its horizontal transfer from another organism (Groisman & Ochman, 1997). 29 genes are encoded by SPI-1 (Figure 1.11), including regulatory and structural genes for a type three-secretion system (TTSS-1), and secreted effector proteins and their chaperones. Thirteen of the SPI-1 genes are essential for an invasive phenotype (Groisman & Ochman, 1997).

Figure 1.12 Genetic organisation of SPI-1 region at centisome 63 in the *Salmonella* chromosome. Needle complex structural genes are indicated in blue; translocon genes are green; effector genes are in yellow; chaperone genes are purple; regulatory genes are red; genes of unknown function are white. Horizontal arrows indicate the direction of transcription of the corresponding open reading frames. Diagram from Ellermeier & Slauch, 2007.

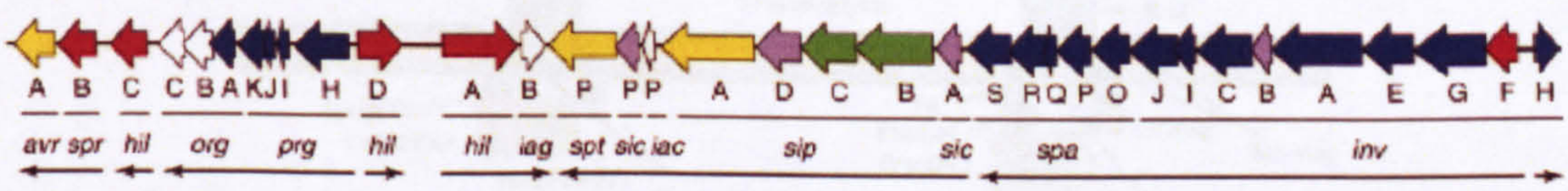

1.5.2. Type Three Secretion System-1 (TTSS-1)

Type three secretion systems (TTSS) are used by human, animal and plant bacterial pathogens to deliver bacterial effector molecules to the eukaryotic host cytoplasm (reviewed by Hueck, 1998). TTSS systems depend on external signals, usually contact with host cells, to stimulate secretion. The proteins translocated by a TTSS lack an N-terminal *sec* secretion signal and do not undergo N-terminal processing, thus secretion is *sec* independent. Some secreted proteins require specific chaperones for their secretion. TTSS are evolutionarily related to bacterial flagella and the supramolecular structure of the TTSS, termed the needle complex, is homologous to the flagella hook basal body complex (Figure 1.12). Like flagella, TTSS are temporally and spatially regulated to ensure the ~20 proteins that compose the TTSS are assembled in the correct order and deliver effector proteins at the correct time (Galan, 2001). In *Salmonella* the proteins composing TTSS-1 are encoded by the *inv-spa* gene cluster and the *prgHIJK-orgA* genes in SPI-1 (Figure 1.11).

Although the complete needle complex is sufficient for secretion of effector proteins, a translocase complex composed of SipB, SipC and SipD is required for transfer of these effectors across the host cell membrane (Collazo and Galan, 1997; Fu and Galan, 1998).

Figure 1.13 Schematic representation of the *Salmonella* SPI-1 (left) and flagellar (right) type III secretion system. Conserved secretion components are labelled with the serovar Typhimurium designations and *Yersinia* nomenclature (Plano *et al.*, 2001).

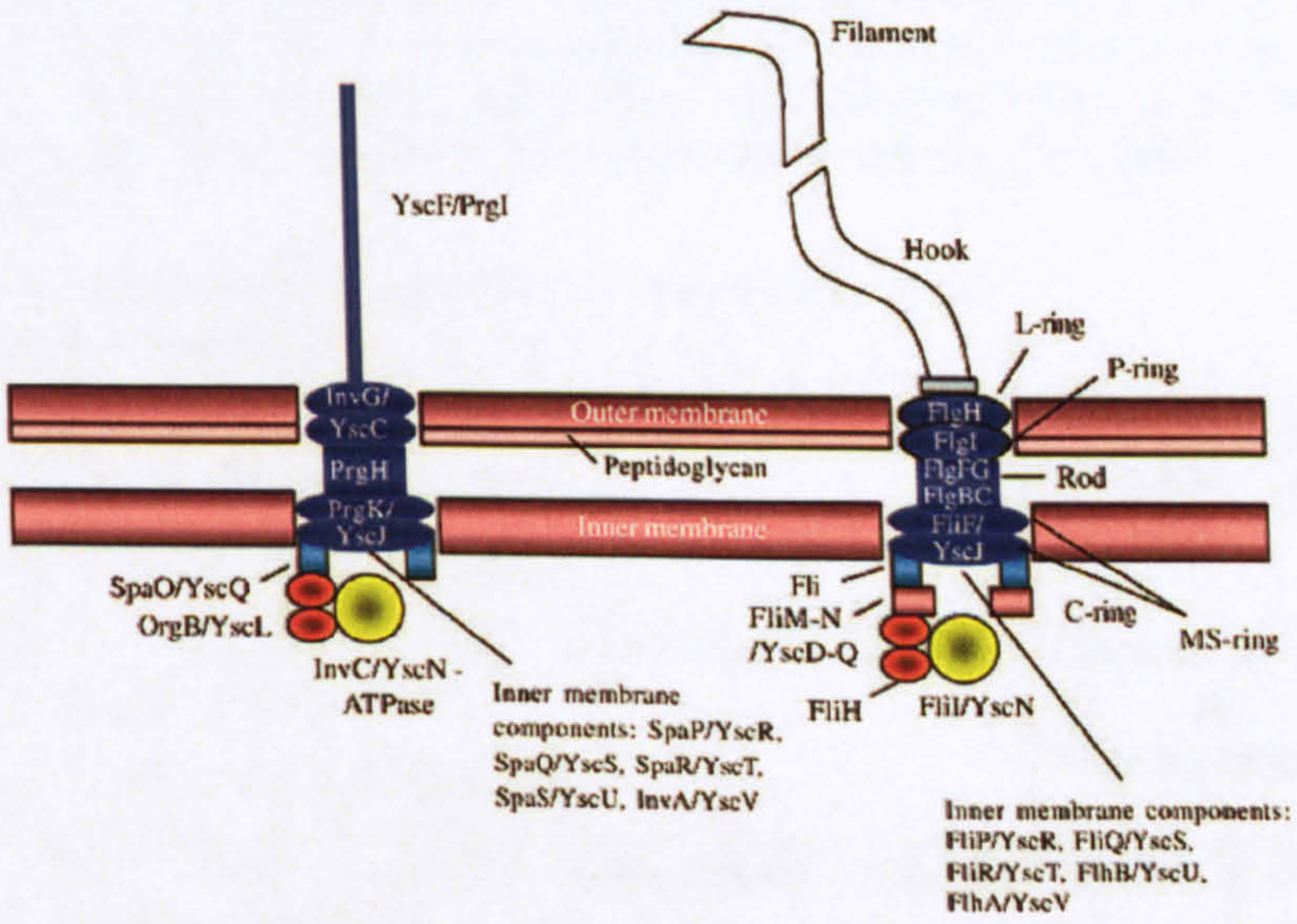

1.5.3.TTSS-1 secreted proteins

The proteins secreted via the SPI-1 secretion system fall into four functional categories (Fu and Galan, 1998). These include proteins which are required for protein secretion and/or the assembly of the needle complex, for example SpaO, InvJ, PrgI and PrgJ, proteins involved in the regulation of the secretion process, proteins required for protein translocation across the eukaryotic membrane and finally proteins with putative effector functions. Some secreted proteins may perform more than one function. For example, SipD is involved in regulating TTSS-1 secretion (Kaniga *et al.*, 1995a), and in allowing effector proteins to cross the host cell membrane (Collazo and Galan, 1997). Table 1.1 summarises the roles proposed for each of the polypeptides secreted by the SPI-1 TTSS to date. The effectors SipA, SopE, SopE2, SopB and SptP are the main concern of this study.

Table 1.1 The proposed roles for those *Salmonella* proteins secreted through the SPI-1 type three secretion system.

Secreted protein	Proposed Function	Reference
InvJ	Required for needle complex assembly and protein secretion; controls length of the needle component of TTSS-1 complex	Collazo *et al.*, 1995; Kubori *et al.*, 2000; Marlovits *et al.*, 2006
SpaO	Required for needle complex assembly and protein secretion	Collazo and Galan, 1996
PrgI	Component of the needle portion of the TTSS	Kubori *et al.*, 2000
PrgJ	Required for the assembly of the needle portion of the TTSS complex	Kimbrough&Miller.,2000; Sukhan *et al.*, 2001
SipA	Binds actin, diminishes its critical concentration, stabilises F-actin and increases the bundling activity of T-plastin. Inhibits ADF/cofilin and gelsolin-mediated actin depolymerisation. Potentiates activity of SipC Stimulates PMN migration by stimulating apical secretion of HxA3	Zhou *et al.*, 1999a, b; McGhie *et al.*, 2001, 2004; Lee *et al.*, 2000; Criss *et al.*, 2001
SipB	TTSS effector protein translocation through eukaryotic membranes Binds and activates caspase1	Collazo & Galan, 1997; Fu & Galan., 1999; Hersh *et al.*, 1999
SipC	TTSS effector protein translocation through eukaryotic membranes Actin nucleation and bundling	Collazo & Galan, 1997; Fu & Galan,1999; Hayward&Koronakis,1999
SipD	TTSS effector protein translocation through eukaryotic membranes	Collazo & Galan, 1997

SptP	GTPase activating protein (GAP) for Cdc42 and Rac and therefore antagonises SopE and SopE2. Also possesses tyrosine phosphatase activity. Both activities allow reversal of cellular changes stimulated by other *Salmonella* effectors	Kaniga *et al.*, 1996; Fu & Galan, 1998, 1999; Murli *et al.*, 2001
AvrA	Activates NF-κB transcription factor and augments apoptosis in human epithelial cells	Collier-Hyams *et al.*, 2002
SopE	Guanine nucleotide exchange factor (GEF) for Cdc42 and Rac; stimulates actin cytoskeleton rearrangements and nuclear responses	Hardt *et al.*, 1998a; Rudolph *et al.*, 1999
SopE2	GEF for Cdc42 and Rac; stimulates actin cytoskeleton rearrangements and nuclear responses	Bakshi *et al.*, 2000; Stender *et al.*, 2000
SopA	Contributes to invasion but mechanism unknown. Stimulates PMN transmigration and fluid accumulation that leads to enteritis, possibly through its E3 ubiquitin ligase activity	Raffatellu *et al.*, 2005; Wood *et al.*, 2000; Zhang *et al.*, 2002; Zhang *et al.*, 2006
SopB/SigD	Inositol phosphatase and promotes indirect activation of Rho GTPase activity; stimulates actin cytoskeleton reorganisation, nuclear responses and chloride secretion	Norris *et al.*, 1998; Zhou *et al.*, 2001; Patel & Galan, 2006
SopD	Promotes fluid accumulation in an intestinal loop model of infection	Jones *et al.*, 1998
SlrP	Required for mouse virulence: mechanism unknown	Tsolis *et al.*, 1999b
SspH1	Inhibits NFκB-dependent gene expression and therefore acts to suppress inflammatory responses	Haraga and Miller, 2003

1.5.4. *Salmonella* Invasion Protein A (SipA)

SipA is a 74kDa polypeptide of 684 residues, which exhibits significant homology to the Shigella IpaA virulence protein (Hueck *et al.*, 1995; Kaniga *et al.*, 1995b). As IpaA is encoded in an operon with identical arrangement to the *Salmonella sip* operon and secreted via a TTSS homologous to that encoded by SPI-1, it suggested SipA, like IpaA, was required for bacterial invasion.

Compared to SipB-D, the deletion of SipA has only a slight effect on the invasiveness of *Salmonella* (Kaniga *et al.*, 1995b). This has been explained in terms of SipA not having a role in the translocation of other effector proteins (Collazo and Galan, 1997). However, studies have shown that SipA optimises entry at early time points i.e. ≤ 15 minutes (Jepson *et al.*, 2001; Schlumberger *et al.*, 2007). This is suggested to be due to the role of SipA in enhancing actin rearrangements and membrane ruffling during *Salmonella* invasion (Zhou *et al.*, 1999a).

Upon translocation into host cells SipA quickly accumulates in small foci at the bacteria–host cell interface, reaching local concentrations sufficient for effective interactions with actin (Cain *et al.*, 2004; Higashide *et al.*, 2002; Schlumberger *et al.*, 2005). SipA binds to F-actin in a 1:1 ratio, and in addition to reducing the critical concentration of G-actin from 0.25μM to 0.02μM, which promotes filament assembly, SipA prevents depolymerisation of F-actin (Zhou *et al.*, 1999a). As total F-actin concentration does not appear to change in host cells, existing F-actin structures in the cell must be depolymerised before F-actin can be polymerised at sites of *Salmonella* entry, where SipA is found to localise (Higashide *et* al., 2002). Indeed, the more ordered binding of SipA to filaments it has polymerised suggests the main role of SipA in internalisation is polymerisation and stabilisation of new F-actin filaments rather than binding pre-polymerised filaments assembled by the cell (Galkin *et al.*, 2002).

The N-terminal of SipA includes a transport domain (amino acids (aa) 1–105) with a binding site for the type III secretion chaperone InvB (Bronstein *et al.*, 2000; Lilic *et al.*, 2006). Amino acids 446-685 in the carboxyl-terminal form an actin-binding domain that allows SipA to exert its actin-modulating function (Zhou *et al.*, 1999a). The crystal structure of SipA shows this C-terminus domain to be composed of 2 non-globular extensions attached to a core, globular domain. The non-globular extensions are responsible for polymerisation of actin molecules, while the globular domain allows binding to F-actin (Lilic *et al.*, 2003). This discovery, with the work of Galkin *et al.* (2002) confirmed the model of SipA binding to F-actin proposed by Mitra *et al.* (2000). In this model, SipA lies parallel to the actin filament axis, connecting subdomain 4 of one actin monomer with subdomain 1 of an actin subunit on the opposite long-pitch helical strand (Figure 1.13). This form of binding allows SipA to bind three to four actin monomers at once and suggests that SipA may be able to shift the equilibrium toward the trimeric actin nucleus, and explains its ability to decrease the actin critical concentration for filament assembly. It also explains why actin filaments become more rigid with the binding of SipA (Mitra *et al.*, 2000).

Figure 1.14 Structure and function of the SipA domain. A shows a schematic model for SipA non-globular "arm" tethering of actin protomers. The green portion of the "arms" is not observed in the crystal structure, and is therefore a hypothetical conformation to illustrate the model. B shows a schematic of the tethering arms model of SipA binding to F-actin. The actin filament is shown as two entwined polymers (one in orange, the other in green) of actin monomers (shown as spheres). SipA is drawn as a smaller blue sphere with two extended arms projecting from opposite sides of the molecule such that they contact actin monomers in opposing strands as was observed by electron microscopy (Lilic and Stebbins, 2004).

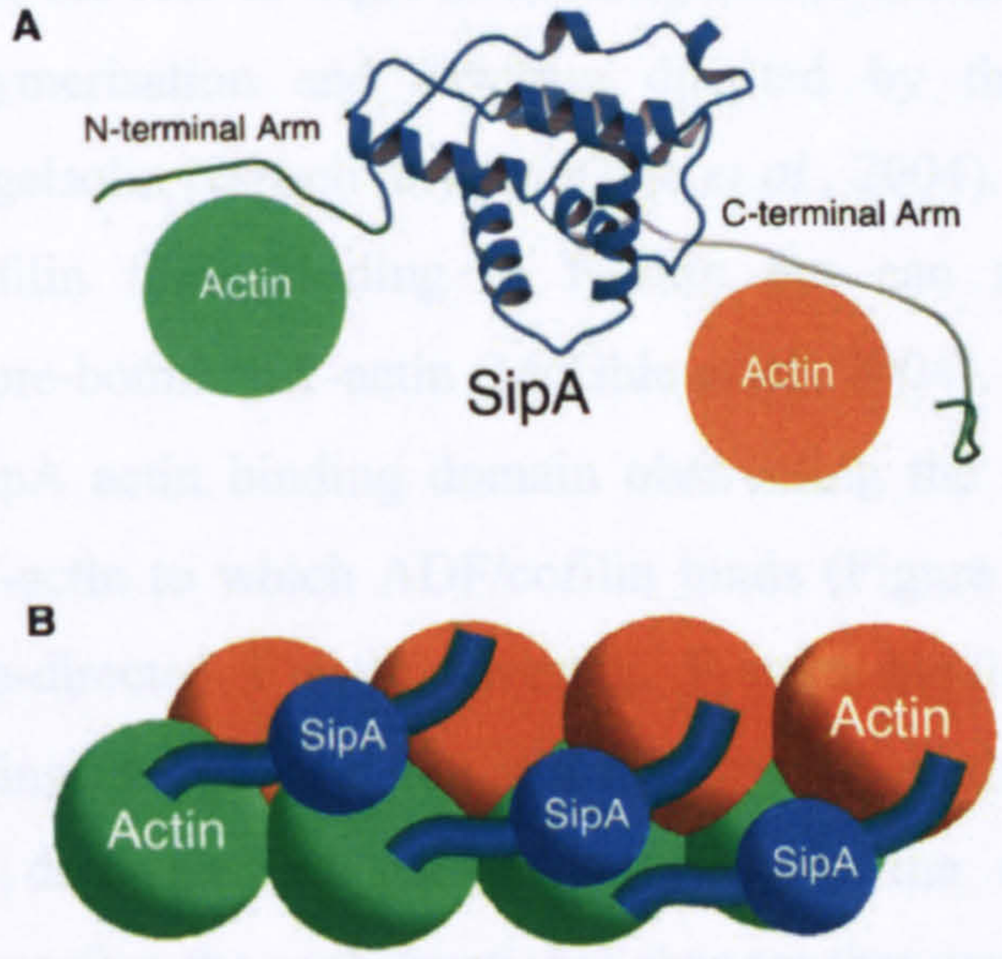

Recently two new functional domains, designated F1 and F2, have been discovered in the large central region (aa 105–446) of SipA (Schlumberger *et al.*, 2007). Domain F1, comprising aa 170–271, is required for initiation of SipA focus formation in the host cell membrane and appears to co-operate with the C-terminal actin binding domain to mediate bacterial invasion into host cells. The F2 domain (aa 280–394) enhances focal accumulation of SipA which has been proposed to occur through SipA-SipA binding since binding of SipA to actin is not required for SipA focus formation (Schlumberger *et al.*, 2007).

SipA is additionally able to modulate the actin cytoskeleton through its interaction with several bacterial and host cell proteins. SipC-mediated nucleation of actin polymerisation and F-actin bundling is potentiated by SipA, providing the first example of two bacterial effector proteins co-operating to subvert host cell function (McGhie *et al.*, 2001). SipA further increases actin bundling by stimulating T-plastin (fimbrin), a host cell actin binding protein (ABP) that cross-links F-actin into tight parallel bundles (Zhou *et al.*, 1999b). It would appear other *Salmonella* effector molecules that signal through Cdc42 lead

to T-plastin recruitment to the membrane, where its bundling activity may help to stabilise the ruffles. SipA actin rearrangements are believed to be independent of Cdc42, as shown by the ability of SipA to induce ruffling in cells expressing Cdc42HsN17, a dominant negative form of Cdc42 (Higashide *et al.*, 2002).

Further analysis of the role of SipA in actin dynamics has shown that SipA can block the depolymerisation and severing directed by the host cell ABPs ADF/cofilin and gelsolin respectively (McGhie *et al.*, 2004). SipA can not only exclude ADF/cofilin from binding to F-actin but can also displace these molecules when pre-bound to F-actin (McGhie *et al.*, 2004). This is proposed to be due to the SipA actin binding domain obstructing the subdomain-1 (SD1) binding site of F-actin to which ADF/cofilin binds (Figure 1.14). While SipA prevents gelsolin-directed F-actin severing, F-actin binding is not mutually exclusive indicating that gelsolin can still bind to SD1 in the presence of SipA. However, SipA does prevent gelsolin binding to the cleft between actin monomers and therefore the conformational changes that would induce severing.

Figure 1.15 Models of actin binding proteins (ABPs) bound to F-actin. Individual actin monomers are depicted as ovals, with the two-pitch helical strand indicated in blue and white. Left: SipA-C terminal (green) connects SD4 of one actin monomer with SD1 of another monomer on the opposite strand. Centre: ADF/cofilin (red) bound to F-actin alone (right strand) and in the presence of SipA (green) left strand. Bound SipA excludes ADF/cofilin from the SD1 binding site. Right: Gelsolin (purple) bound to F-actin alone (right strand) and in the presence of SipA (green) left strand. Gelsolin consists of two tandem-homologous halves (segments (S) 1–3 and 4–6). For clarity, S4–6 have been omitted from the opposing filament strand. S2 binds SD1, triggering S3 to enter the cleft. This initiates a conformational change allowing S1 to lodge between two monomers along the longitudinal axis and S4–6 to reach across the filament to engage a monomer on the other strand (not shown), facilitating filament severing. Bound SipA (green) allows S2 binding but excludes S3, allowing gelsolin to bind but not sever filaments. Adapted from McGhie *et al.*, 2004.

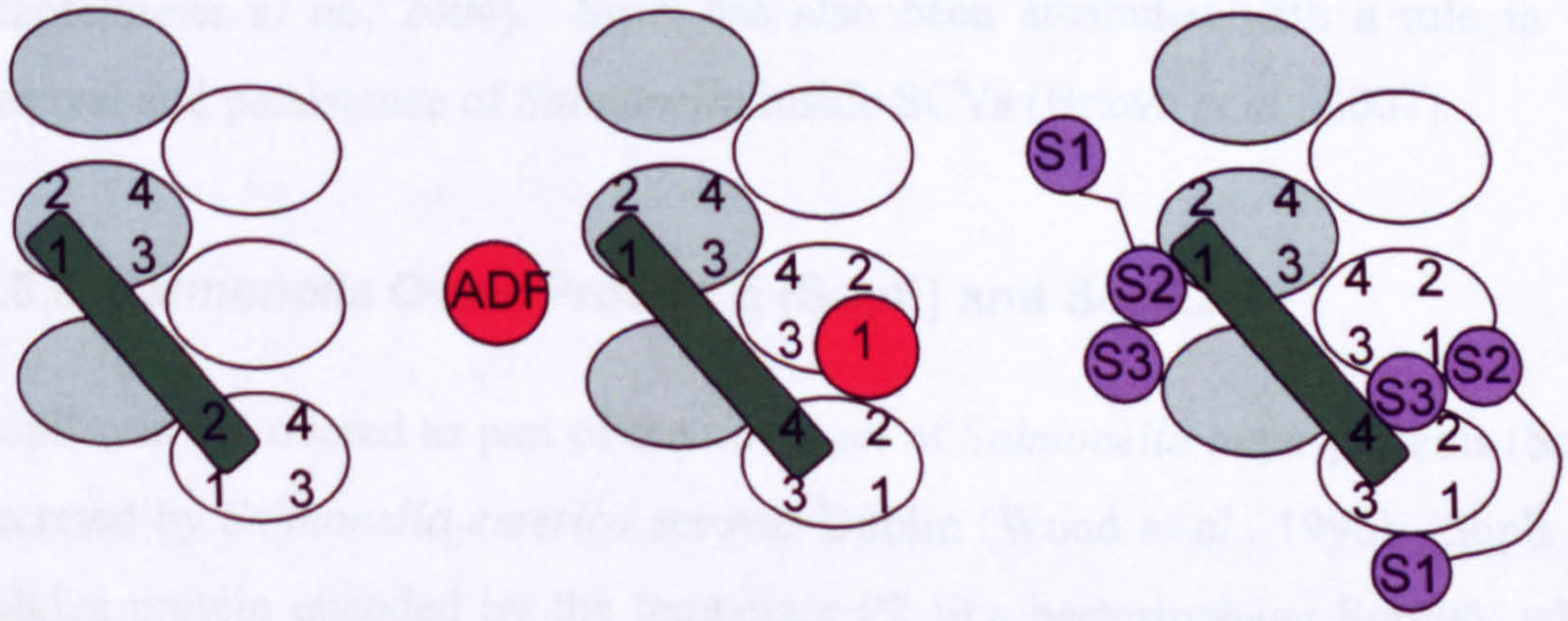

In addition to preventing gelsolin from severing F-actin, SipA can also reanneal gelsolin-capped actin filament fragments, although the mechanism by which this occurs is unknown (McGhie *et al.*, 2004). This again illustrates the importance of SipA in the actin reorganisation that leads to *Salmonella* invasion. It has also provided a model for the events that occur during invasion. SipB, SipC and SipD are secreted by the SPI-1 TTSS and insert into the target cell plasma membrane to allow translocation of *Salmonella* effector proteins to occur. Translocation of SipA stimulates SipC-driven actin nucleation and actin bundling, leading to rapid, localised reorganisation of the actin cytoskeleton, which is enhanced by the actions of SopE, SopE2 and SopB which stimulate Arp2/3. Meanwhile, SipA lowers the critical monomer concentration, stabilises F-actin and protects it from ADF/cofilin-depolymerisation and gelsolin severing, and reanneals gelsolin-capped F-actin fragments. This promotes the elongation of F-actin and the persistence of the pathogen-induced actin rearrangements, allowing time for the bacterium to enter the host cell. While SipA is responsible for stabilising actin, its activity must be regulated otherwise the ruffles produced during *Salmonella* invasion would not be able to support entry of the bacterium. This suggests there must be temporal and spatial regulation of SipA (Bourdet-Sicard and Van Nhieu, 1999) although a mechanism for this has not been determined.

In addition to its role in invasion, SipA is also advocated to elicit the production of chemoattractants that promote transepithelial PMN migration in a tissue culture model (Criss *et al.*, 2001b; Lee *et al.*, 2000; discussed in 1.4.4). This would explain the ability of SipA to induce inflammation and fluid accumulation in a bovine (Zhang *et al.*, 2002), and a streptomycin pre-treated mouse model (Hapfelmeier *et al.*, 2004). SipA has also been attributed with a role in the survival and persistence of *Salmonella* inside SCVs (Brawn *et al.*, 2007).

1.5.5. *Salmonella* Outer Protein E (SopE) and SopE2

SopE was discovered as part of the novel set of *Salmonella* outer proteins (Sops) secreted by *Salmonella enterica* serovar Dublin (Wood *et al.*, 1996). SopE is a 30kDa protein encoded by the temperate P2 like bacteriophage SopEΦ, which introduces SopE as an additional effector protein in *Salmonella* by lysogenic

conversion (Mirold *et al.*, 1999). As not all strains of *Salmonella* carry the *sopE* gene (Hardt *et al.*, 1998b; Mirold *et al.*, 1999; Mirold *et al.*, 2001a; Mirold *et al.*, 2001b), it was suggested SopE function was redundant or another protein similar to SopE existed. In 2000, SopE2 was found. SopE2 is a 30kDa protein with 69% homology to SopE at the amino acid level in serovar Typhimurium, but is found in all serovars of *Salmonella enterica* (Bakshi *et al.*, 2000; Stender *et al.*, 2000). It has therefore been proposed that at some point in evolution the *sopE* gene was duplicated in the *Salmonella* chromosome; providing *Salmonella* with one working copy and one additional copy that could be propagated to other species of *Salmonella* as a survival advantage (Bakshi *et al.*, 2000).

A *sopE* mutant exhibits reduced invasion compared to its wild type (Hardt *et al.*, 1998b; Wood *et al.*, 1996) indicating a role for SopE in *Salmonella* invasion. The discovery that expression of dominant negative forms of Cdc42Hs and Rac1 in COS-1 cells abrogates the cytoskeletal rearrangements induced by SopE revealed the role of SopE as a guanine exchange factor (GEF) for the Rho family of GTPases (Hardt *et al.*, 1998a). The same role was found to be performed by SopE2 (Stender *et al.*, 2000). However, while SopE activates both Cdc42 and Rac1, SopE2 only efficiently activates Cdc42 (Friebel *et al.*, 2001). Additionally, both are now also proposed to activate RhoG (Patel and Galan, 2006). Activation of these Rho GTPases by SopE and SopE2 leads to activation of host effectors involved with regulating the actin cytoskeleton and regulating gene expression via MAP kinase stimulated pathways (Hardt *et al.*, 1998a; Huang *et al.*, 2004; Patel and Galan, 2006). Transient transfection or microinjection of SopE or SopE2 into host cells is sufficient to activate Cdc42 and cause actin cytoskeleton rearrangements (Hardt *et al.*, 1998a; Stender *et al.*, 2000). Since similar observations were obtained using a fragment of SopE consisting of amino acids 78-240, this indicated the secretion and translocation signals of SopE are not required for activity and that the catalytic domain of SopE lies within amino acids 78-240 (Hardt *et al.*, 1998a).

X-ray crystallography has been used to determine the structure of the catalytic domain of SopE (Buchwald *et al.*, 2002) (Figure 1.15) and SopE2 (Williams *et al.*, 2004). $SopE_{78-240}$ and $SopE2_{69-240}$ are composed of six alpha helices arranged

in 2 three-helix bundles, arranged in a V-shape. The peptide segment, which connects the 2 bundles, contains a ^{166}GAGA^{169} motif which is the catalytic core. The ^{166}GAGA^{169} loop inserts itself between the switch I and II regions of Cdc42, pushing switch I away and pulling switch II towards the loop. Reorientation of the switch regions leads to removal of components important for binding of the guanine nucleotide. In switch I, this is extrusion of Phe28$_{Cdc42}$ from the nucleotide binding pocket, which then increases the nucleotide dissociation rate. In switch II the Mg^{2+} binding site is obstructed. This displacement of Mg^{2+} encourages nucleotide release, as the affinity of the binding site is reduced. The result is that SopE and SopE2 binding to a Rho GTPase increases the guanine nucleotide exchange 10^5 fold (Rudolph *et al.*, 1999).

Figure 1.16 A. Diagram of the structure of SopE, with helices as cylinders and the catalytic loop highlighted in red. B. Schematic representation of the Cdc42–SopE interaction with important interactions indicated. Hydrophobic contacts are in green, polar interactions in red. Arrowheads mark side chain and straight ends indicate main chain contributions. From Buchwald *et al.*, 2002.

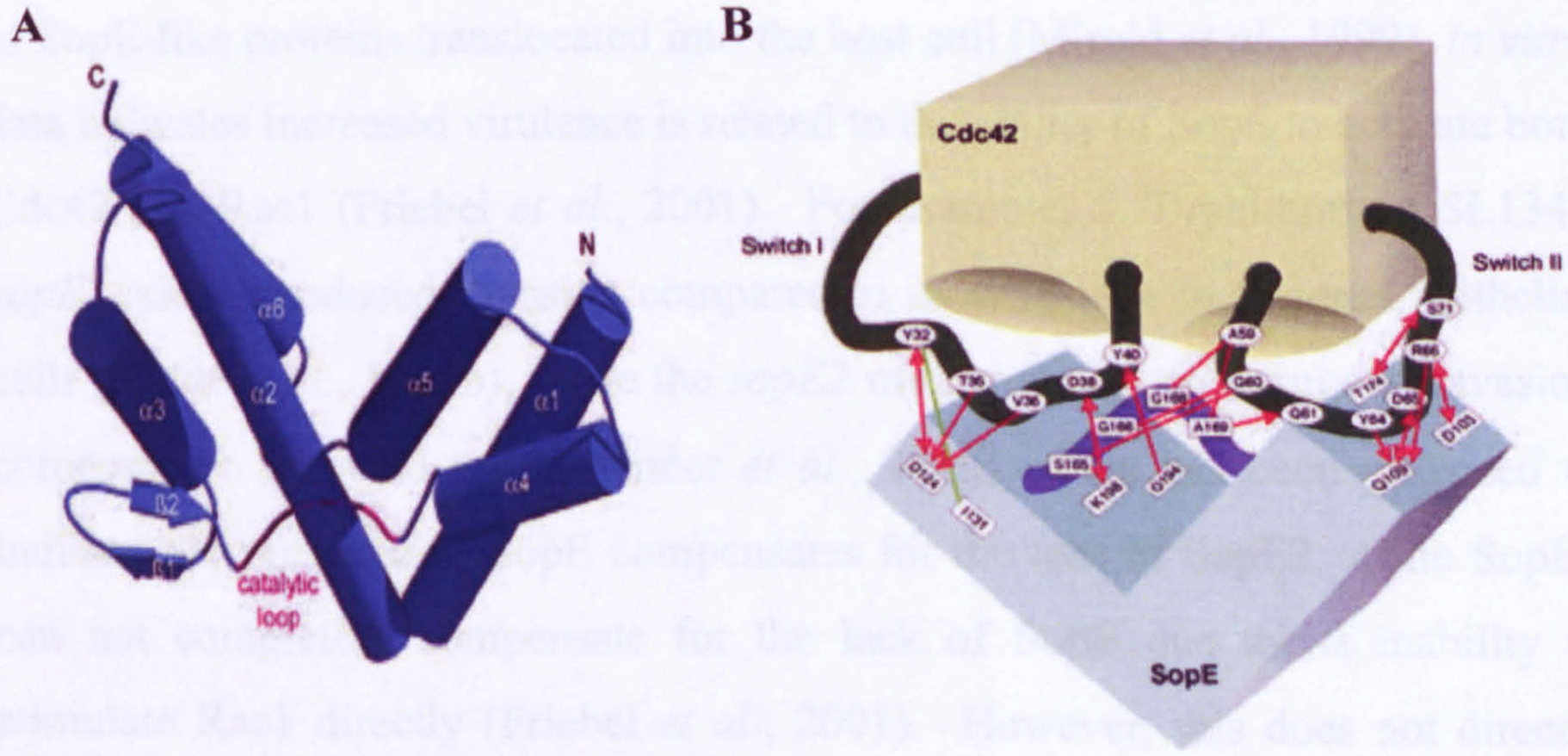

All eukaryotic GEFs known to act on Rho GTPases have a common sequence motif, the Dbl homology (DH) domain. SopE and SopE2 therefore represent a novel class of GEFs as despite a high α-helical structure, a feature of the Dbl domain, they share no sequence homology with these eukaryotic GEFs and have been shown to use a different fold and residues to stimulate guanine nucleotide exchange (Rudolph *et al.*, 1999; Buchwald *et al.*, 2002; Williams *et al.*, 2004). SopE and SopE2 also represent a novel class of bacterial effector since in contrast to similar bacterial effectors which introduce non-reversible modifications to their cellular targets, SopE and SopE2 precisely and reversibly

manipulate their targets by exhibiting structural and functional mimicry of host cell proteins (Patel *et al.*, 2005; Rudolph *et al.*, 1999). This is an important characteristic of *Salmonella* invasion and serves to ensure the subsequent phases of growth and replication can ensue post-invasion.

As mentioned above, SopE efficiently activates both Cdc42 and Rac1, while SopE2 activates Cdc42 (Friebel *et al.*, 2001). The differing targets of SopE and SopE2 may explain the use by *Salmonella* of two functionally similar effector proteins to stimulate invasion. It is also believed to increase the virulence of *Salmonella*. Strains expressing SopE are often associated with severe epidemics (Mirold *et al.*, 1999), and the lysogenic conversion of *S.* Typhimurium 14028 with SopEΦ increases the inflammatory response to *Salmonella* infection in a bovine ligated ileal loop model (Zhang *et al.*, 2002).

While improved epidemic virulence may be attributed to the higher concentration of SopE-like proteins translocated into the host cell (Mirold *et al.*, 1999), *in vitro* data indicates increased virulence is related to the ability of SopE to activate both Cdc42 and Rac1 (Friebel *et al.*, 2001). For example, *S.* Typhimurium SL1344 *sopE*⁻ exhibits reduced invasion compared to its wild type in cultured epithelial cells (Hardt *et al.*, 1998b), while the *sopE2* mutant shows no change in invasion compared to the wild type (Stender *et al.*, 2000). This has been proposed to indicate the presence of SopE compensates for the loss of SopE2, while SopE2 can not completely compensate for the lack of SopE due to its inability to stimulate Rac1 directly (Friebel *et al.*, 2001). However, this does not directly test whether the loss of signalling through Rac1 is responsible for these observations. It may be equally true that SopE and SopE2 interact in an additional manner and the subsequent absence of SopE terminates the interaction leading to reduced invasion.

In addition to a *sopE* mutant of *Salmonella enterica* serovar Typhimurium having reduced invasion efficiency, it has a reduced ability to hydrolyse inositol hexakisphosphate ($InsP_6$) and inositol-1,3,4,5,6-pentakisphosphate ($InsP_5$) (Zhou *et al.*, 2001). Since SopE lacks a phosphatase domain and transfection of epithelial cells with SopE did not lead to $InsP_5$ dephosphorylation or the

recruitment of a cellular inositol phosphate phosphatase to perform this function, it has been assumed that SopE promotes hydrolysis of $InsP_5$ alongside other *Salmonella* effector proteins (Deleu *et al.*, 2006). One of these is likely to be SopB which has already been shown to induce inositol phosphate fluxes in the host cell during *Salmonella* invasion (Norris *et al.*, 1998; Zhou *et al.*, 2001); however, it is currently unclear how SopB or another effector may aid this role of SopE.

Co-operativity between *Salmonella* proteins also extends to IL-8 secretion since the ability of SopE2 to regulate IL-8 production is influenced by flagellin (Huang *et al.*, 2004). Flagellin is required for efficient SopE2 translocation into host cells, with translocated SopE2 contributing to three signalling pathways (p38, ERK and NFκB) activated by the binding of flagellin to TLR5 to stimulate IL-8 production. A role for SopE2 in IL-8 induction provides one molecular mechanism by which SopE and SopE2 can induce intestinal inflammation and fluid accumulation observed during *Salmonella* infection (Zhang *et al.*, 2002; Hapfelmeier *et al.*, 2004).

1.5.6. SptP

SptP is a 60kDa protein composed of 544 amino acids (Kaniga *et al.*, 1996) that possesses two functional effector domains; an N-terminal domain (aa 107-290) that allows SptP to act as a GTPase-activating protein (GAP) antagonising the GEF activity of SopE and SopE2 (Fu and Galan, 1999; Kaniga *et al.*, 1996), and a C terminal domain (aa 340-513) that has tyrosine phosphatase activity and is homologous to YopH of *Yersinia* and to eukaryotic tyrosine phosphatases (Kaniga *et al.*, 1996). The N and C terminal domains independently lead to downregulation of the actin rearrangements that occur during *Salmonella* invasion (Fu and Galan, 1998), thereby preventing potential harm to the host cell through excessive cellular signalling, and ensures the intracellular niche of *Salmonella* is maintained (Galan and Zhou, 2000). Since the GAP activity of SptP specifically inactivates Cdc42 and Rac, and antagonises the actions of SopE, SopE2 and SopB, there must be correct temporal regulation of these effectors to enable successful invasion of *Salmonella*. The secretion and

translocation domains of these effector proteins appear to be responsible for this function. The N terminal domain of SopE targets SopE to rapid proteasome-mediated degradation, producing a much shorter half life than that of the SptP protein, and thus temporary activation of Rho GTPases (Kubori and Galan, 2003).

Figure 1.17 Proposed roles of SptP in the downregulation of the nuclear responses induced by *Salmonella*. A.. SopE, SopE2 and SopB activate Cdc42 and Rac which leads to their interaction with effectors involved with stimulating nuclear responses. One such effector is activated Cdc42 kinase (ACK) (Murli *et al.*, 2001). ACK stimulates the activity of the Ras GEF, GRF-1, by tyrosine phosphorylation and therefore may link activation of Cdc42 by *Salmonella* effectors to the activation of Ras-dependent signalling pathways leading to ERK activation. The GAP domain of SptP, by reversing the activation of Cdc42 and Rac, may therefore inhibit this ERK activation pathway. Additionally, the tyrosine phosphatase domain of SptP has been shown to prevent recruitment of Raf-1 to the plasma membrane by Ras-GTP (Lin *et al.*, 2003). B. The GAP domain of SptP also inhibits the phosphorylation and activation of Raf1 by Pak1 and Pak3 presumably through its inhibition of Cdc42 and/or Rac. Phosphorylation of Raf1 by Pak1 and 3 and Src results in complete activation of Raf. Activated Raf then phosphorylates MEK1/2, which phosphorylates extracellular-signal-regulated kinase (ERK) 1/2. ERK can enter the nucleus to control gene expression by phosphorylating transcription factors. During *Salmonella* infection this has been shown to induce IL-8 in epithelial cell and TNFα in macrophages, both of which are downregulated by SptP, in part by the mechanisms described above.

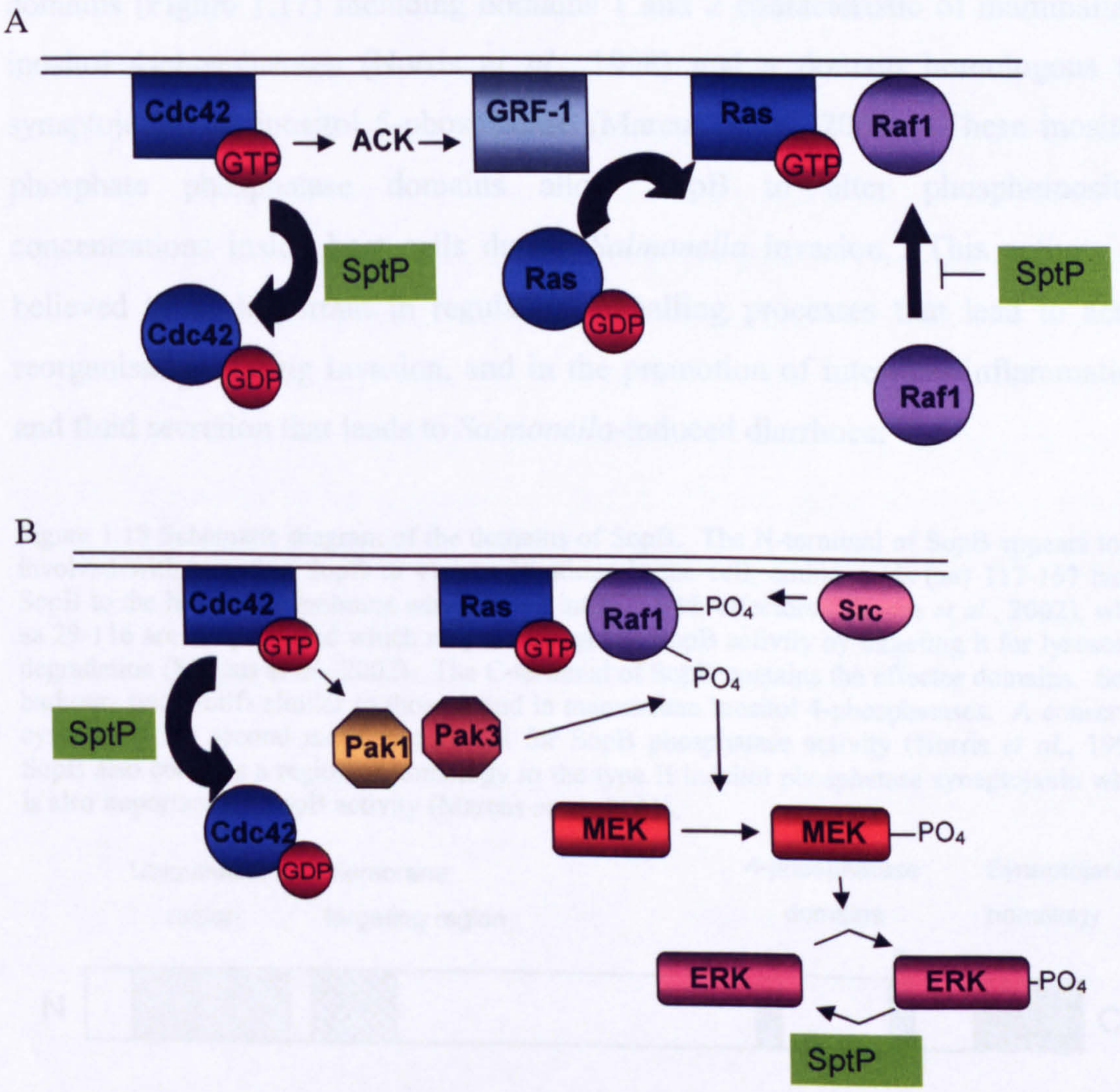

It has been proposed that since the two domains of SptP align co-linearly with the Rho GTPase so the phosphatase domain is held away from the Rho GTPase, the GAP domain may target the phosphatase domain to the membrane where it can interact with its substrates (Stebbins and Galan, 2000). The substrates of the tyrosine phosphatase domain are still being investigated although several have been found in a pathway that leads to IL-8 secretion (Figure 1.16) (Murli *et al.*, 2001; Lin *et al.*, 2003). This suggests the tyrosine phosphatase activity of SptP may be required for the downregulation of the nuclear responses that follow the stimulation of Cdc42 and Rac by *Salmonella* (Galan, 2001).

1.5.7. SopB

SopB, also known as SigD, is a 62kDa protein encoded by SPI-5 that is secreted and translocated through the SPI-1 TTSS (Galyov *et al.*, 1997; Hong and Miller, 1998; Wood *et al.*, 1998). SopB, like SptP, is composed of several functional domains (Figure 1.17) including domains 1 and 2 characteristic of mammalian inositol 4-phosphatases (Norris *et al.*, 1998) and a domain homologous to synaptojanin, an inositol 5-phosphatase (Marcus *et al.*, 2001). These inositol phosphate phosphatase domains allow SopB to alter phosphoinositol concentrations inside host cells during *Salmonella* invasion. This activity is believed to be important in regulating signalling processes that lead to actin reorganisation during invasion, and in the promotion of intestinal inflammation and fluid secretion that leads to *Salmonella*-induced diarrhoea.

Figure 1.18 Schematic diagram of the domains of SopB. The N-terminal of SopB appears to be involved with targeting SopB to various locations in the cell; amino acids (aa) 117-167 target SopB to the host cell membrane where it can interact with effectors (Marcus *et al.*, 2002), while aa 29-116 are ubiquitinated which may downregulate SopB activity by targeting it for lysosomal degradation (Marcus *et al.*, 2002). The C-terminal of SopB contains the effector domains. SopB harbours two motifs similar to those found in mammalian inositol 4-phosphatases. A conserved cysteine in the second motif is essential for SopB phosphatase activity (Norris *et al.*, 1998). SopB also contains a region of homology to the type II inositol phosphatase synaptojanin which is also important for SopB activity (Marcus *et al.*, 2001).

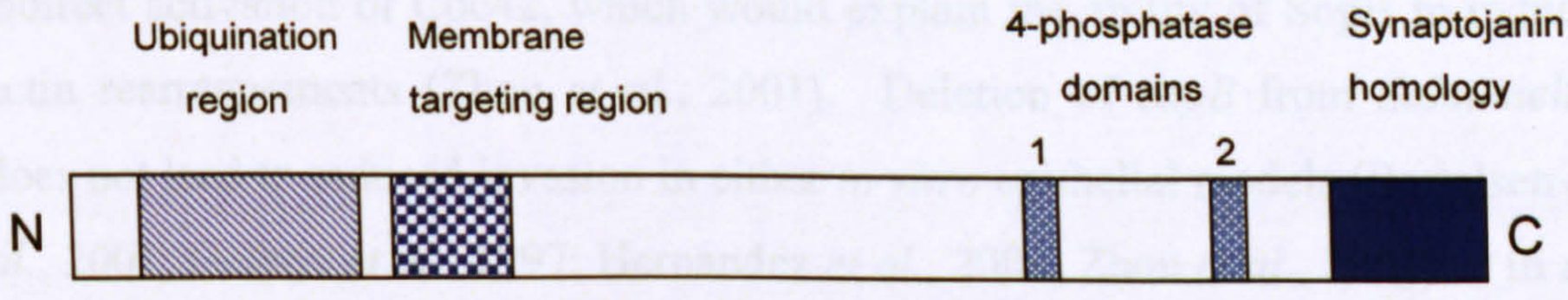

During *Salmonella* invasion the levels of cellular inositol hexakisphosphate ($InsP_6$) and inositol-1,3,4,5,6-pentakisphosphate ($Ins(1,3,4,5,6)P_5$) are depleted while there is initial accumulation of inositol-1,4,5,6-tetrakisphosphate ($Ins(1,4,5,6)P_4$) before its subsequent degradation to smaller inositol phosphates (Zhou *et al.*, 2001; Feng *et al.*, 2001). SopB has been shown responsible for these changes; acting as a specific 3-phosphatase upon $Ins(1,3,4,5,6)P_5$ both *in vitro* and *in vivo* to produce $Ins(1,4,5,6)P_4$ (Norris *et al.*, 1998; Zhou *et al.*, 2001). This increase in $Ins(1,4,5,6)P_4$ concentration is believed to have several roles in *Salmonella* pathogenesis.

$Ins(1,4,5,6)P_4$ can inhibit phosphatidylinositol 3-kinase (PI3K) signalling. Since PI3K signalling inhibits chloride secretion, a consequence of $Ins(1,4,5,6)P_4$ production by SopB may be indirect inhibition of chloride channel closure (Figure 1.18) and thus increased fluid secretion (Norris *et al.*, 1998; Bertelsen *et al.*, 2004). This would provide a molecular mechanism for the observation that SopB promotes fluid secretion in a bovine ligated ileal loop model (Galyov *et al.*, 1997; Jones *et al.*, 1998; Wood *et al.*, 1998; Zhang *et al.*, 2002). However, this model of SopB-induced fluid secretion has been challenged. Firstly, it has been found that oral infection with a *sopB* mutant does not reduce diarrhoea or mortality in calves (Tsolis *et al.*, 1999a) or reduce colitis in a streptomycin pre-treated mouse model (Hapfelmeier *et al.*, 2004). In the latter study, a strain in which additional effectors with a role in fluid secretion were removed was also studied, but no role for SopB in induction of colitis was found, demonstrating its role is not masked by the redundancy of other effector proteins. SopB expressed in epithelial cells has also been shown to reduce anion permeability, not increase it as this model would expect (Mason *et al.*, 2007). The role of SopB in enteropathogenesis therefore still requires further analysis.

Another proposed role of the phosphoinositide fluxes induced by SopB is indirect activation of Cdc42, which would explain the ability of SopB to induce actin rearrangements (Zhou *et al.*, 2001). Deletion of *sopB* from *Salmonella* does not lead to reduced invasion in either *in vitro* epithelial models (Bertelsen *et al.*, 2001; Galyov *et al.*, 1997; Hernandez *et al.*, 2004; Zhou *et al.*, 2001) or in an *in vivo* bovine model (Reis *et al.*, 2003) since SopE and SopE2 perform a similar

role and therefore mask the role of SopB. Deletion of both *sopE* and *sopE2* or the complementation of a *sopE⁻ sopE2⁻ sopB⁻* mutant with a plasmid expressing *sopB* has however shown SopB is important for invasion (Hapfelmeier *et al.*, 2004; Raffatellu *et al.*, 2005; Boyle *et al.*, 2006). It has been proposed that SopB stimulates cellular responses by activating SH3-containing guanine nucleotide exchange factor (SGEF), an exchange factor for the Rho GTPase, RhoG (Patel and Galan, 2006). Stimulation of an alternative GEF may allow SopB to activate Cdc42, and potentially stimulate nuclear responses leading to fluid secretion and the inflammatory response associated with the role of SopB during *Salmonella* infection of bovine ileal loops. How SopB activates GEFs is currently unknown but may involve phosphoinositide fluxes.

Figure 1.19 Proposed model of the mechanism of SopB antagonism of PI3K-mediated chloride secretion inhibition. In uninfected cells phosphatidylinositol 3-kinase (PI3K) is triggered by a wide range of growth factors and cytokines, including interaction of EGF with the EGF receptor. Activated PI3K phosphorylates PtdIns(4,5)P_2 to yield PtdIns(3,4,5)P_3. Calcium-mediated Cl^- secretion (CaMCS) is accompanied by basolateral K^+ efflux, which contributes to the driving force for Cl^- secretion and can be limiting for Cl^- secretion after elevation of $[Ca^{2+}]_i$ levels. PtdIns(3,4,5)P_3 can inhibit K^+ efflux and therefore can suppress CaMCS i.e. it is inhibitory. During *Salmonella* infection, SopB removes the phosphate from carbon 3 of Ins(1,3,4,5,6)P_5 (IP_5) to yield Ins(1,4,5,6)P_4 (IP_4). IP_4 inhibits the actions of PtdIns(3,4,5)P_3, possibly competing with PtdIns(3,4,5)P_3 for effector binding sites since IP_4 is a partial structural analogue of the PtdIns(3,4,5)P_3 head group. As a consequence, IP_4 could compete with phosphoinositide binding to pleckstrin homology domains of signalling proteins and inhibit the normal recruitment of signal transduction complexes to the plasma membrane. Additionally, SopB may dephosphorylate PtdIns(3,4,5)P_3 to PtdIns(4,5)P_2 reversing the action of PI3K and preventing PtdIns(3,4,5)P_3 inhibiting chloride secretion. Arrowheads depict stimulatory effects and capped lines designate inhibitory effects.

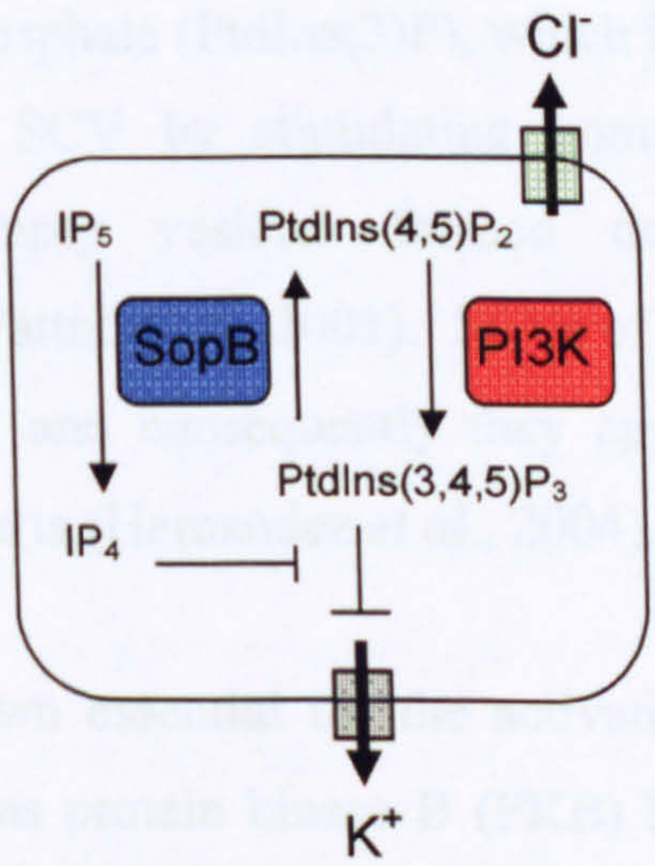

In addition to aiding bacterial uptake by stimulating cytoskeletal rearrangements, SopB also appears to have a role in formation of the *Salmonella*-containing

vacuole (SCV). SopB was demonstrated to be associated with the host cell membrane via hydrophobic interactions (Marcus *et al.*, 2001), proposed to enable it to deplete the phosphatidylinositol-4,5-bisphosphate (PtdIns(4,5)P_2) from the invaginating host cell membrane, allowing the SCV to seal and fission to occur (Terebiznik *et al.*, 2002). Recently SopB has been shown to exhibit 4' phosphatase activity, dephosphorylating PtdIns(4,5)P_2 to form phosphatidylinositol-5-phosphate or PtdIns(5)P (Mason *et al.*, 2007). This activity depletes PtdIns(4,5)P_2 from the membrane allowing SCV formation but has also been shown to reduce F-actin and disrupt ZO-1 architecture in cells which subsequently leads to the detachment of these cells from the monolayer (Mason *et al.*, 2007). This behaviour would explain the role of SopB in decreasing TER and disrupting the barrier function of cell monolayers during *Salmonella* invasion (Bertelsen *et al.*, 2004; Boyle *et al.*, 2006). It has therefore been proposed by the authors as a mechanism by which SopB may contribute to the inflammation and fluid secretion that leads to *Salmonella*-induced diarrhoea (Mason *et al.*, 2007). This may represent an alternative to the regulation of chloride secretion by SopB.

The phosphoinositide phosphatase activity of SopB may also be responsible for the maturation of SCVs into spacious phagosomes that allow bacterial replication. SCVs containing wild type bacteria have been shown to recruit phosphatidylinositol-3-phosphate (PtdIns(3)P), which is believed to contribute to the enlargement of the SCV by stimulating homotypic fusion with other PtdIns(3)P-containing empty vesicles formed during bacterial infection (Hernandez *et al.*, 2004; Pattni *et al.*, 2001). SCVs of a *sopB* mutant were found not to recruit PtdIns(3)P and consequently they appeared smaller than those containing wild type bacteria (Hernandez *et al.*, 2004).

SopB has also been shown essential for the activation of the serine-threonine kinase Akt, also known as protein kinase B (PKB) by *Salmonella* in epithelial cells (Steele-Mortimer *et al.*, 2000). Akt is recruited to the plasma membrane by phosphatidylinositol-3,4,5-triphosphate(PtdIns(3,4,5)P_3) and phosphatidylinositol -4,5-bisphosphate (PtdIns(4,5)P_2). It has been proposed that the 5' phosphatase activity of SopB converts PtdIns(3,4,5)P_3 into PtdIns(4,5)P_2, inducing a

conformational change in recruited Akt that allows its subsequent activation through phosphorylation of Thr308 and Ser473 by host proteins (Marcus *et al.*, 2001). The sustained activation of Akt by SopB has been shown to inhibit caspase-3 cleavage and therefore suppress apoptosis in epithelial cells (Knodler *et al.*, 2005). This suppression of apoptosis is likely to be important for *Salmonella* to establish a niche permissive for replication, and hence is another important role for SopB in pathogenesis.

1.6. Regulation of SPI-1

Since the ability of *Salmonella* to penetrate the intestinal monolayer is a key stage in pathogenesis, genes involved with invasion, including those encoded by SPI-1, are stringently controlled to ensure expression is timed to the point of infection most productive for invasion. SPI-1 is regulated by a number of transcriptional and post-transcriptional regulators, and by several environmental stimuli. The environmental stimuli include low oxygen tension (Jones and Falkow, 1994), high osmolarity and neutral pH (Bajaj *et al.*, 1996), which presumably act as cues for the arrival of the bacterium in the distal small intestine, the site favoured for invasion.

SPI-1 encodes several transcriptional regulators – hyper invasion locus (Hil) A, HilC, HilD and InvF (Figure 1.11). HilA is a transcriptional activator that belongs to the OmpR/ToxR family of DNA binding proteins and is the key regulator of SPI-1, directly binding to the promoters and activating expression of the *inv/spa* and *prg/org* operons. HilA also activates a second transcriptional regulator, InvF, which with the help of the chaperone SicA, induces expression of the *sip* operon and effector proteins located elsewhere in the chromosome e.g. *sopB* and *sopE* (Darwin and Miller, 2000, 2001). The use of InvF alongside HilA to control invasion genes has been proposed to allow increased production of specific proteins that might be needed in larger quantities for the invasion process e.g. effector proteins (Altier, 2005).

Expression of *hilA* is controlled by the combined action of HilC, HilD and RtsA. All three activators independently bind the *hilA* promoter and induce expression of *hilA* (Ellermeier and Slauch, 2003; Schechter and Lee, 2001). They can also independently activate expression of the *inv/spa* operon (Ellermeier & Slauch, 2003). This provides a further level of control to SPI-1 expression. HilC, HilD and RtsA also induce expression of *slrP*, encoding a TTSS effector of unknown function and *dsbA*, which encodes DsbA, a soluble periplasmic disulphide bond isomerase (Ellermeier & Slauch, 2003). A *dsbA* mutation blocks both secretion and translocation of SPI-1 TTSS effector proteins, indicating its requirement for TTSS-1 to function correctly. This observation may be a direct effect, for example lack of DsbA preventing assembly of the TTSS, or it could be an indirect effect, for example in the inability to form disulphide bonds in a non-SPI-1 protein required for assembly of TTSS-1 (Ellermeier and Slauch, 2004).

The invasion genes of SPI-1 are also subject to regulation outside of SPI-1, which includes regulation by global regulators that control functions other than invasion. This co-ordinate regulation has probably evolved as a means to stimulate invasion in response to regulatory cascades activated when the bacterium reaches the site productive for invasion. Typically, transcriptional regulation in response to environmental cues is mediated by two-component regulatory systems. These generally consist of a sensor kinase, often an integral membrane protein, which reversibly phosphorylates its response regulator in response to a specific environmental stimulus. Several two-component regulatory systems involved with SPI-1 regulation have been discovered. This includes EnvZ/OmpR, which controls SPI-1 expression by regulating *hilD* expression (Ellermeier *et al.*, 2005), and BarA/SirA. CsrA is a RNA binding protein that binds *hilD* mRNA preventing its translation and therefore inhibits SPI-1 expression as levels of *hilD* decrease. SirA induces the expression of two small RNA molecules *csrB* and *csrC*, which oppose the action of CsrA, indirectly leading to expression of HilD (Fortune *et al.*, 2006). The CpxAR two-component regulator is also believed to play a role in SPI-1 regulation. *In vitro* studies indicate Cpx regulates expression of *hilA* in response to pH (Nakayama *et al.*, 2003) and deletion of *cpxA* or constitutive expression of *cpxA* (*cpxA**) leads to reduced ability of *Salmonella* to colonise mice (Humphreys *et al.*, 2004).

Negative regulators of SPI-1 also exist, for example the PhoP/PhoQ two-component regulatory system which is a negative regulator of SPI-1 and a positive regulator of SPI-2, mediating the switch to an intracellular existence. PhoQ is a sensor kinase that phosphorylates the response regulator PhoP when Mg^{2+} is limiting. PhoP then aids the transcription of 25 different loci, many of which are essential for growth in a low Mg^{2+} environment, and several of which are responsible for virulence (Soncini *et al.*, 1996). Several of the gene loci activated by PhoP are also PmrA-dependent. PmrA is the response regulator of the PmrA/PmrB two-component system. The PhoP, PmrA dependent genes, including the *pmrCAB* operon, are induced not only by Mg^{2+} limitation, but the presence of a mildly acidic environment (Soncini and Groisman, 1996). Hence, *Salmonella* can use two two-component regulatory systems to modulate gene expression allowing certain gene loci to respond to a broader spectrum of environmental cues. This illustrates the complexity of invasion gene regulation and the importance of invasion to *Salmonella* pathogenesis.

Figure 1.20 Model of SPI-1 regulation. Blue arrows indicate activation of gene expression, while repression is shown as red lines with blunt ends. Solid lines represent direct transcriptional regulation. Short-dashed lines represent regulation where the mechanism is not known. Long-dashed lines represent post-translational effects. X represents an unknown intermediate through which Fur controls HilD post-transcriptionally. Diagram taken from Ellermeier & Slauch, 2007.

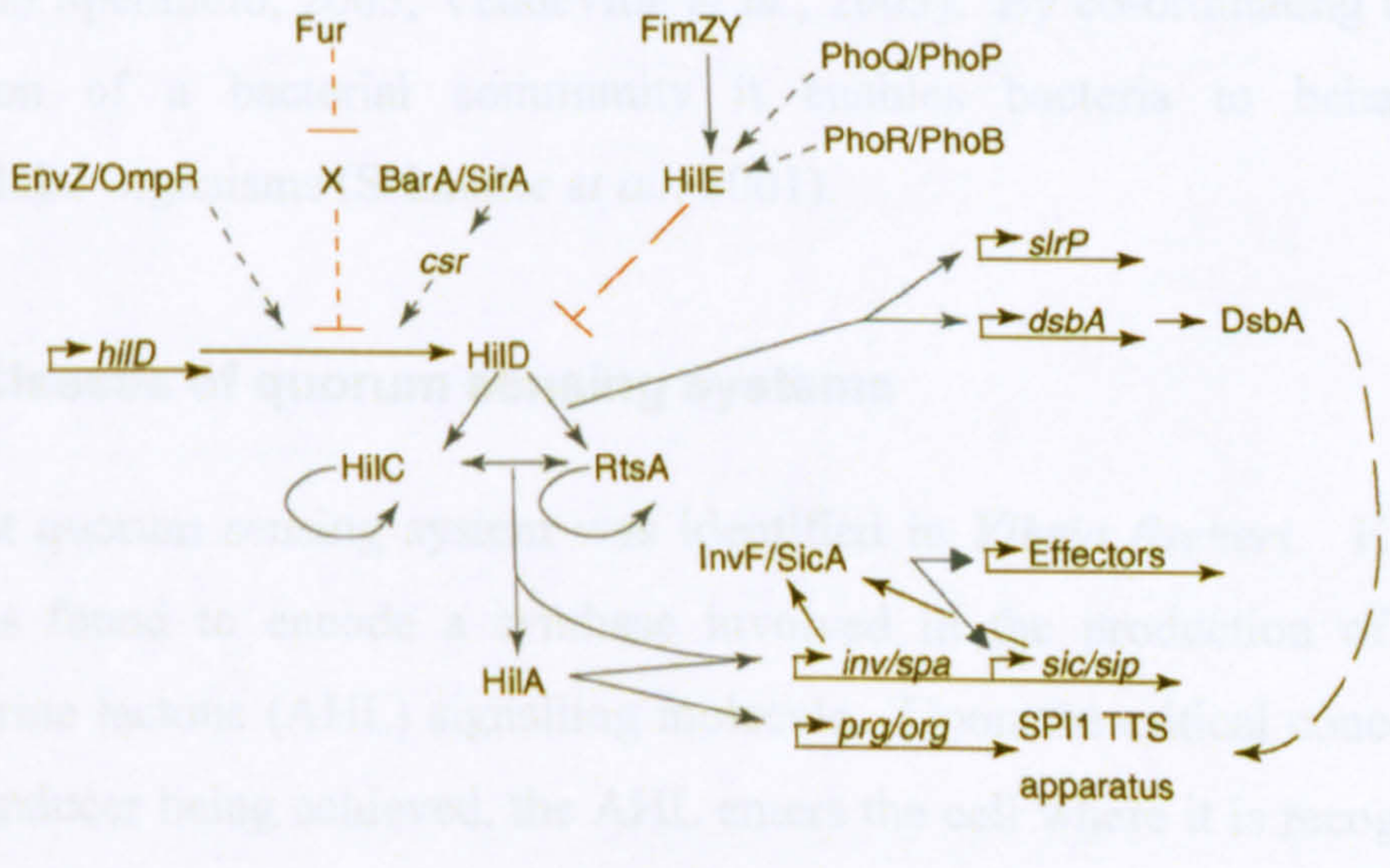

A model has now been proposed which links the two-component regulatory systems with the regulation of SPI-1 by *hilA* (Figure 1.19). In this model the various environmental signals sensed by the regulatory systems are integrated at the level of HilD synthesis. Production of HilD leads to transcriptional

activation of HilC and RtsA, which activate expression of themselves and each other, thereby amplifying the signal. HilD, HilC and RtsA lead to *hilA* activation and the subsequent activation of SPI-1 (Ellermeier and Slauch, 2007).

1.7. Quorum sensing

Quorum sensing is an intercellular signalling mechanism used by bacteria to regulate gene expression in response to changes in cell population density. Quorum sensing relies on the production of a small signalling molecule, often called an autoinducer, which is secreted by the bacteria during growth and accumulates extracellularly. The extracellular concentration of autoinducer increases as the size of the bacterial population increases. Once the population has reached a specific cell density, the critical concentration of the autoinducer will be exceeded, and can be detected by the bacteria. Detection of the autoinducer results in a signal transduction cascade that will lead to the regulation of transcription, and ultimately a change in population response. This response is usually one that is only productive when carried out simultaneously by many cells, and includes responses such as bioluminescence, antibiotic production, secretion of virulence factors and biofilm formation (reviewed by Kaper and Sperandio, 2005; Vendeville *et al.*, 2005). By co-ordinating the gene expression of a bacterial community it enables bacteria to behave like multicellular organisms (Schauder *et al.*, 2001).

1.7.1. Classes of quorum sensing systems

The first quorum sensing system was identified in *Vibrio fischeri*. *V. fischeri luxI* was found to encode a synthase involved in the production of an acyl homoserine lactone (AHL) signalling molecule. Upon the critical concentration of autoinducer being achieved, the AHL enters the cell where it is recognised by the N-terminus of LuxR and subsequently allows the LuxR C-terminus to act as a transcriptional activator of the *lux* operon and other target genes (Engebrecht *et al.*, 1983; Engebrecht and Silverman, 1984). Homologs of the LuxI/R system of *V. fischeri* are found in over 70 Gram-negative species (Henke and Bassler,

2004b) and thus this system is often described as the Gram-negative quorum sensing system. *Salmonella* possesses an incomplete LuxI/R quorum sensing system, having a receptor called SdiA (suppressor of division inhibition), but no synthase enzyme and subsequently no signal ligand (Michael *et al.*, 2001; Wang *et al.*, 1991). It is possible that SdiA detects the AHL produced by other bacterial species, using such detection as a cue that *Salmonella* has entered the intestine and/or as signal interception mechanism to modulate the behaviour of other species present in the environment (Ahmer, 2004).

Figure 1.21 The three classes of quorum sensing system. The three canonical quorum-sensing systems are: Gram-negative LuxI/R (left column), Gram-positive peptide-two component (middle column), and a hybrid system with features of both G^- and G^+ systems (right column). Representative autoinducers for each system are shown. Figure from Henke and Bassler, 2004a.

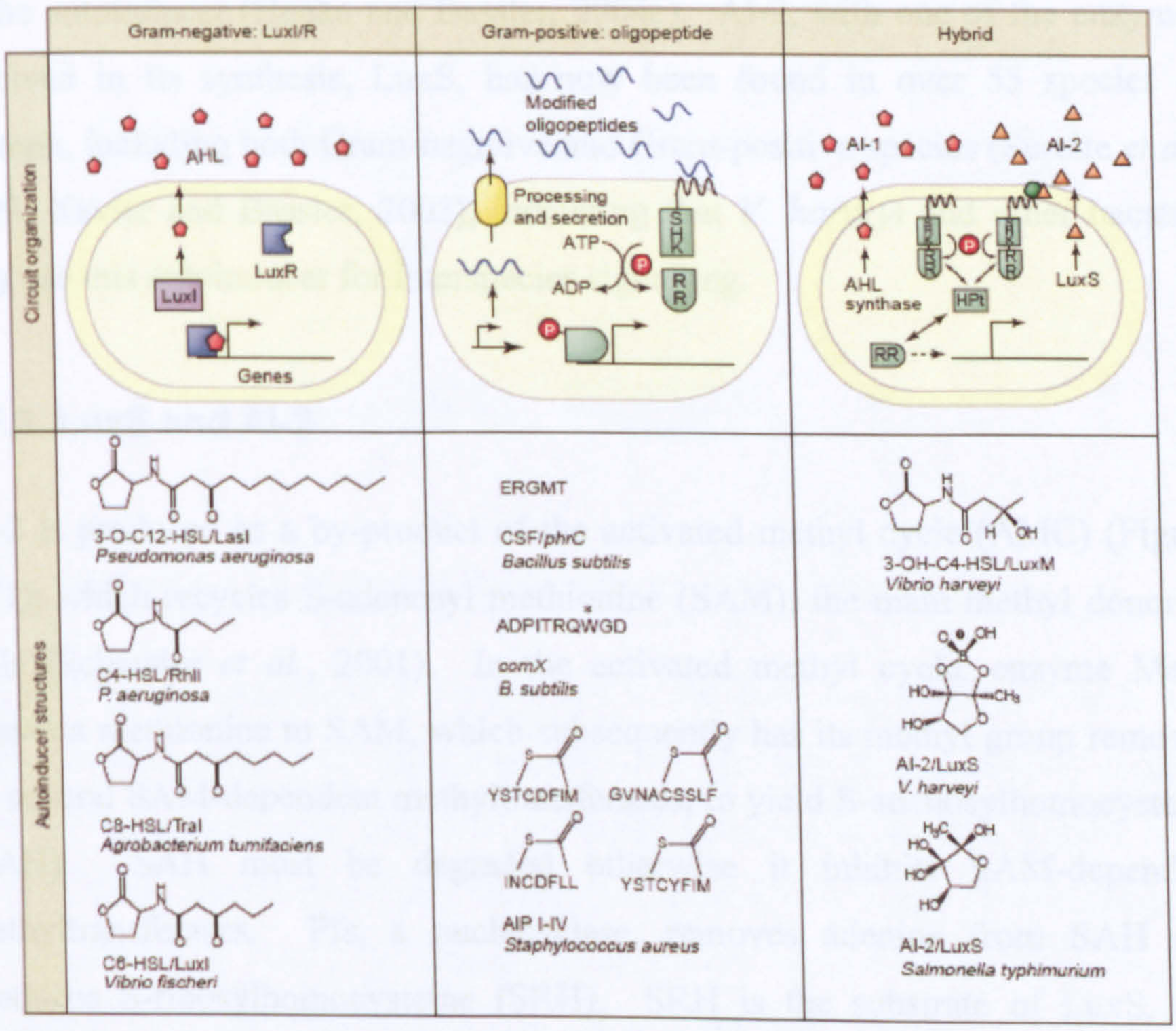

Since the discovery of the LuxI/R quorum sensing system, two further classes of quorum sensing systems have been identified (Figure 1.20). The second class of quorum sensing system is found in Gram-positive bacteria. The signals are synthesised as precursor peptides, which are processed and then secreted by an ATPase binding cassette (ABC) transporter. Detection of the signal peptides is

by two-component sensor kinase proteins that interact with cytoplasmic response regulator proteins in a phosphorelay cascade, leading to gene regulation (reviewed in Miller *et al.*, 2002).

The third quorum sensing system is termed the hybrid system and is exemplified by the quorum sensing system of *Vibrio harveyi*. *V. harveyi* possesses three independent quorum-sensing systems (Henke and Bassler, 2004c). The first is similar to the quorum sensing system of Gram-negative bacteria in that the autoinducer produced, AI-1, is a species-specific AHL that is used for intraspecies communication. The second quorum sensing system produces and detects autoinducer 2 (AI-2), a furanosyl borate diester (Chen *et al.*, 2002). A third system mimicking the Cqs system of *V. cholerae* also exists, using CAI-1 as the autoinducer (Henke and Bassler, 2004c). AI-2, with one of the enzymes involved in its synthesis, LuxS, has now been found in over 55 species of bacteria, including both Gram-negative and Gram-positive species (Surette *et al.*, 1999; Xavier and Bassler, 2003), indicating that *V. harveyi* and other bacteria may use this autoinducer for interspecies signalling.

1.7.2. LuxS and AI-2

AI-2 is produced as a by-product of the activated methyl cycle (AMC) (Figure 1.21), which recycles S-adenosyl methionine (SAM); the main methyl donor in cells (Schauder *et al.*, 2001). In the activated methyl cycle, enzyme MetK converts methionine to SAM, which subsequently has its methyl group removed by several SAM-dependent methyltransferases, to yield S-adenosylhomocysteine (SAH). SAH must be degraded otherwise it inhibits SAM-dependent methyltransferases. Pfs, a nucleosidase, removes adenine from SAH and produces S-ribosylhomocysteine (SRH). SRH is the substrate of LuxS, and results in the production of homocysteine and 4, 5-dihydroxy-2, 3-pentanedione (DPD). DPD is the precursor to all AI-2s. In *V. harveyi* DPD cyclises into a furanone ring, is hydrated, gains boron and loses water to become S-THMF-borate, a furanosyl borate diester (Chen *et al.*, 2002). In *S.* Typhimurium, AI-2 is a different derivative of DPD, R-THMF (Figure 1.21B), which lacks boron and has stereochemistry opposite to *V. harveyi* AI-2 (Miller *et al.*, 2004). Thus, what

has generically been termed 'AI-2' is actually a mixture of interconvertable molecules, more than one of which is important for interspecies signalling.

Figure 1.22 Biosynthesis of autoinducer-2 (AI-2). A. Metabolic pathway leading to DPD, the key product of the enzyme LuxS. B. Model showing proposed formation pathways for the AI-2 signaling molecules. *Vibrio harveyi* AI-2 (S-THMF-borate) is produced by the upper pathway and *S.* Typhimurium AI-2 (R-THMF) is produced by the lower pathway. Figure from Miller *et al.*, 2004.

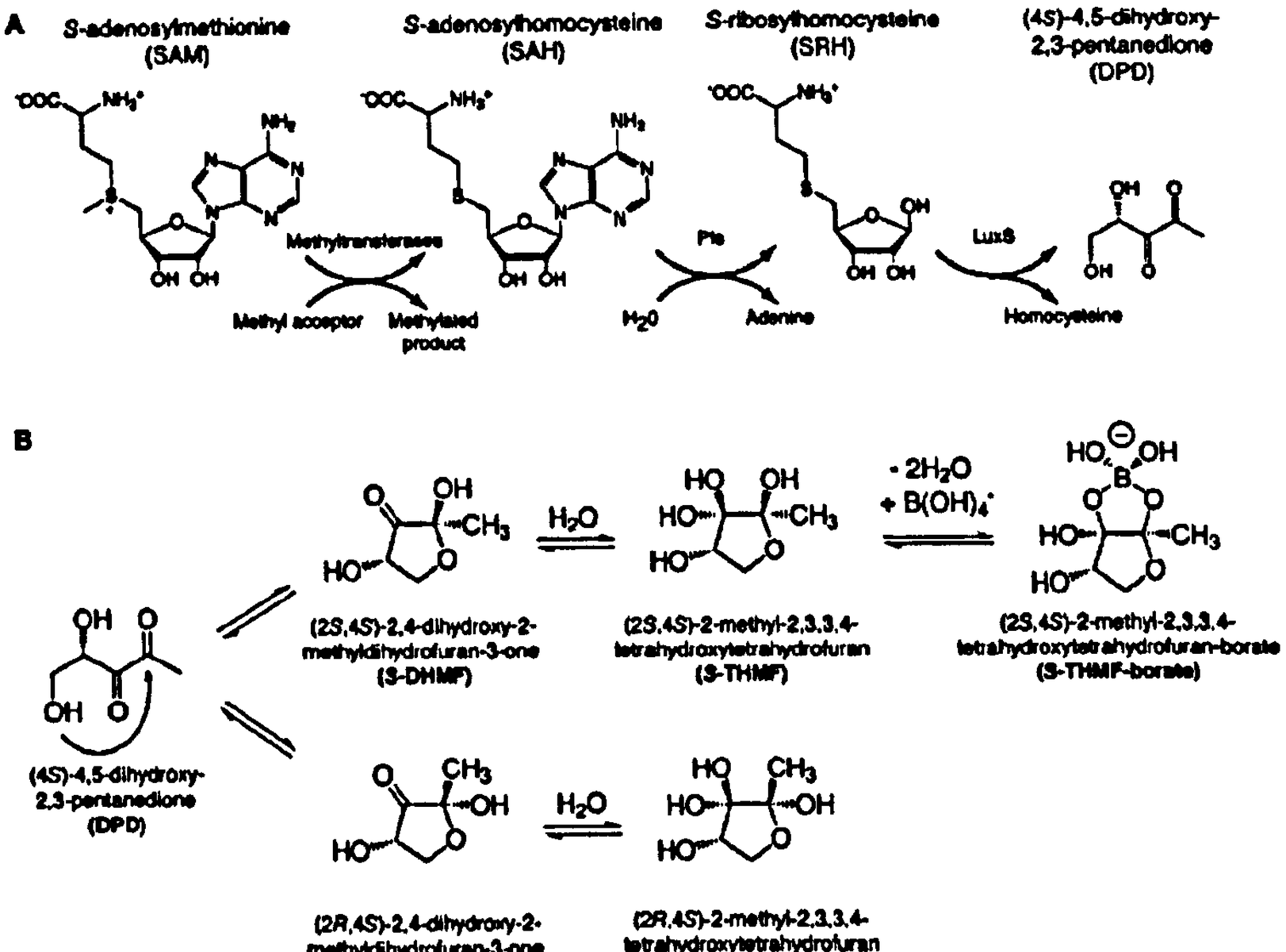

1.7.3. Detection of AI-2 and downstream signalling

In *Vibrio* spp., in particular *V. harveyi* and *V. cholerae*, the system by which AI-2 is detected has been well characterised. The *V. harveyi* AI-2 signalling cascade, which is homologous to that of *V. cholerae*, operates as follows (Figure 1.22). AI-2 diffuses into the periplasm where it can bind LuxP. LuxP upon binding AI-2 interacts with LuxQ, a hybrid sensor kinase which signals to LuxU, an integrator protein shared with the AI-1 detection pathway. LuxU is a phosphotransferase protein that relays the sensory information to the response regulator LuxO (Freeman and Bassler, 1999; Freeman *et al.*, 2000). Phospho-LuxO in conjunction with σ^{54} activates the expression of genes encoding five homologous small regulatory RNAs (sRNAs) (Lenz *et al.*, 2004; Lilley and Bassler, 2000). These sRNAs function in concert with the chaperone Hfq to

destabilize the mRNA encoding the master regulator of the quorum-sensing cascade, LuxR. Hfq fosters base pairing between the sRNA and the *luxR* mRNA, which promotes the degradation of both the sRNA and the mRNA. Under low cell density conditions the rate of synthesis of a sRNA is greater than synthesis of the target message. This means the sRNA will accumulate and the *luxR* mRNA will be reduced to negligible levels. One of the consequences of reduced levels of LuxR is no light production as the *luxCDABE* operon is not transcribed. By contrast, at high cell density the rate of synthesis of the *luxR* mRNA exceeds that of its regulatory sRNA, so the message accumulates, and light will be produced as LuxR binds the *luxCDABE* promoter and activates transcription. Control via sRNAs is hypothesized to enable an ultrasensitive (switch-like) response to the level of phospho-LuxO, and could be particularly suitable for 'all-or-none' behaviors such as quorum sensing (Henke and Bassler, 2004b).

In *Salmonella* and *E. coli* AI-2 uptake is mediated by an ABC transporter named Lsr (LuxS-regulated), which is homologous to the ribose ABC transporter (Taga *et al.*, 2001; Taga *et al.*, 2003; Xavier and Bassler, 2005). The Lsr transporter is expressed at low levels by cells, allowing uptake of AI-2 and therefore detection during growth. Once AI-2 has entered the cell LsrK phosphorylates the ring-open form of DPD at the C5 position and this phospho-DPD binds directly to the *lsr* operon repressor LsrR (Xavier *et al.*, 2007). Inhibition of LsrR allows greater transcription of the *lsr* operon and therefore a larger number of transporters in the cell membrane. This is why the extracellular concentration of AI-2 is found to fall after a peak at 4 hours of growth (Taga *et al.*, 2001; Taga *et al.*, 2003). LsrG cleaves phospho-DPD producing 2-phosphoglycolic acid (PG) (Xavier *et al.*, 2007). The role of the product of the *lsrF* gene remains unknown but may also be involved with modification of the signal molecule. The purpose for taking up AI-2 and modifying it after secretion is not clear. Perhaps transport of AI-2 into cells could terminate signalling, while modifications could generate a signal that can regulate further genes (Taga *et al.*, 2003).

Figure 1.23 Current schemes of AI-2 response. Response to AI-2 can follow one of the two currently identified routes. In one group of bacteria exemplified by *Salmonella* (shown on the left) AI-2 enters the bacterium through the Lsr transporter where it is phosphorylated to sequester it inside the cell. Phosphorylated AI-2 causes LsrR to relieve its repression of the *lsr* operon, allowing further AI-2 import. Phospho-AI-2 may also lead to expression of other target genes and/or undergo further processing. The alternative pathway of AI-2 response described for *Vibrio* spp. involves phosphorelay signal transduction as explained in the text. Figure from Vendeville *et al.*, 2005.

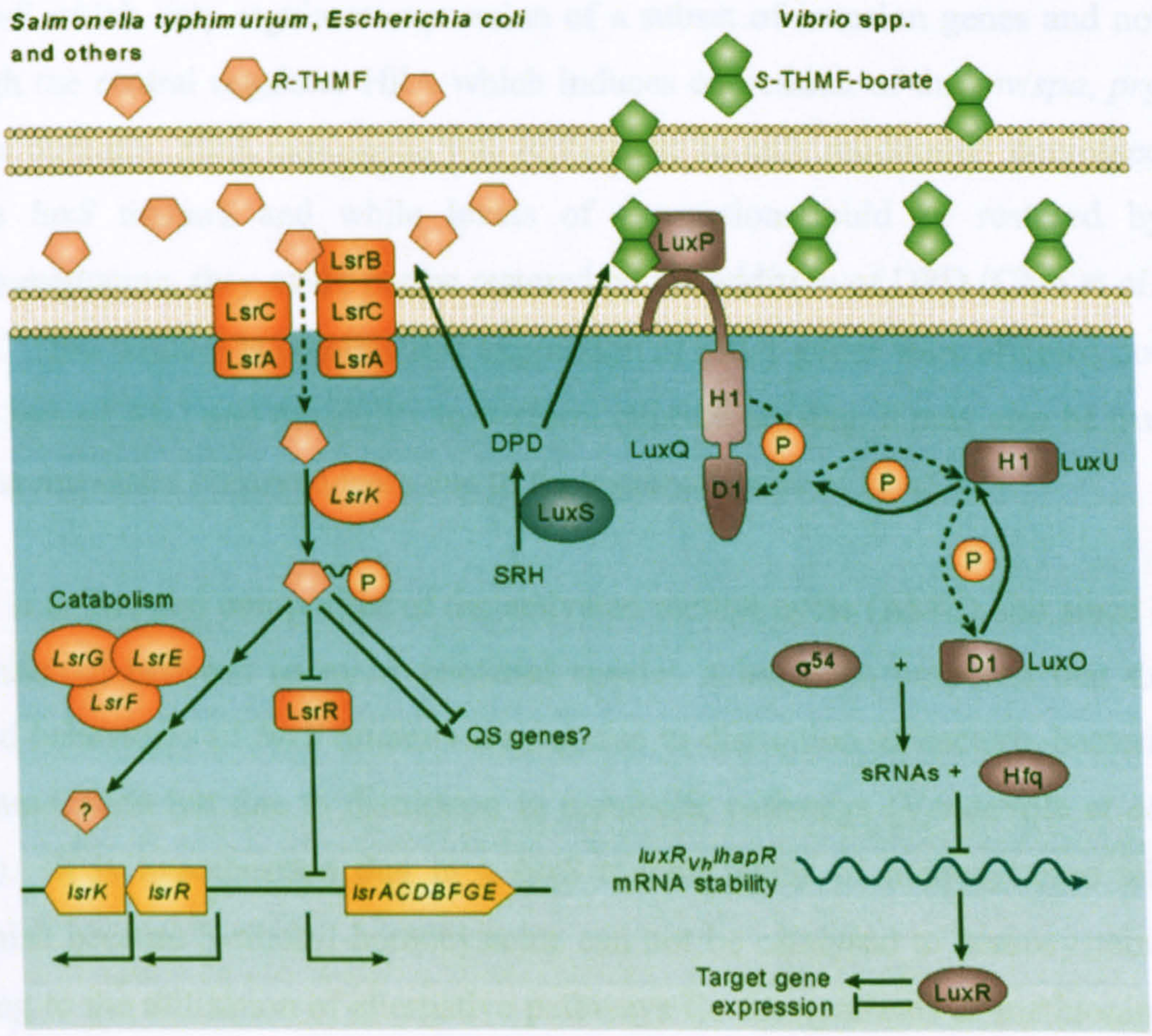

1.7.4. Role of AI-2

In addition to bioluminescence, *V. harveyi* and *V. cholerae* use quorum sensing to regulate virulence-associated traits, including expression of a type three secretion system (Hammer and Bassler, 2003; Henke and Bassler, 2004a, c). Since LuxS/AI-2 signalling is conserved amongst several Gram-negative bacteria (Surette *et al.*, 1999), quorum sensing could potentially also be important for the pathogenesis of *Salmonella*. Initially only the genes of the *luxS* regulated (*lsr*) operon were identified as being regulated by AI-2 in *Salmonella* (Taga *et al.*, 2001; Taga *et al.*, 2003). However, recently it has been reported that the *luxS* gene is required for expression of genes in SPI-1 and therefore may have a role in regulating the virulence of *Salmonella* (Choi *et al.*, 2007). A *S.* Typhimurium

luxS mutant exhibited reduced transcription of the *invF* gene and consequentially reduction in the transcription of the *sicA*, *sigD* and *sopE* genes whose expression is induced by InvF. The mutant was also reduced in its invasion of HEp2 cells and colonisation of a mouse model (Choi *et al.*, 2007). If *Salmonella* pathogenesis is linked to quorum sensing it appears odd that regulation occurs via InvF which only regulates expression of a subset of invasion genes and not through the central regulator HilA which induces expression of the *inv/spa*, *prg* and *sip* operons. HilA expression was reported to be only moderately decreased in the *luxS* mutant, and while levels of expression could be restored by complementation, they could not be restored by the addition of DPD (Choi *et al.*, 2007). Thus while it is possible that expression of SPI-1 genes were affected due to the lack of AI-2 and the ability to perform quorum sensing, it may also be true that the responses observed were due to the metabolic role of LuxS.

LuxS is an integral component of the activated methyl cycle (AMC) and since it is conserved between so many bacterial species it has been proposed that the altered behaviours of *luxS* mutants are not due to disruption of bacteria-bacteria communication but due to disruption in metabolic pathways (Vendeville *et al.*, 2005). It is hypothesised that in a *luxS* mutant levels of homocysteine will diminish because S-ribosyl-homocysteine can not be catalysed to homocysteine, leading to the utilisation of alternative pathways for the synthesis of methionine. A consequence of this is a change in the concentrations of other metabolites which may ultimately lead to changes in gene expression, explaining the difference in phenotype between wild type and its isogenic *luxS* mutant (Walters *et al.*, 2006). This would explain why in *S.* Typhimurium, *metE*, encoding methionine synthase which catalyses the formation of methionine from homocysteine and methyltetrahydrofolate, was one of the genes found to have altered expression in a *luxS* mutant (Taga *et al.*, 2001).

AI-2 production as a consequence of the role of LuxS in metabolism rather than a concerted effort to perform quorum sensing is proposed to be supported by two pieces of evidence. The first is the observation that the *luxS* gene is often found adjacent to other genes involved with metabolic reactions linked to the AMC e.g. in *Borrelia burgdorferi* where *luxS* is present in an operon with *pfs* and *metK*

(Schauder *et al.*, 2001). The second is the homology of the *Salmonella* and *E. coli* Lsr transporter to the transporters used for the uptake of sugars (Taga *et al.*, 2001). However, there is also evidence that suggests LuxS does not serve an essential metabolic role but another purpose. For example *luxS* mutants are relatively easy to create, they usually do not have growth defects in comparison to their wild type and in the case of *Salmonella*, AI-2 can not be used as a sole carbon source (Taga *et al.*, 2003).

The role of quorum sensing-mediated gene regulation is further complicated by discovery of AI-3. This novel autoinducer was discovered in EPEC and EHEC where it regulates expression of genes involved in virulence, including regulation of the LEE-encoded type three-secretion system, and flagella assembly (Sperandio *et al.*, 1999; Sperandio *et al.*, 2001; Sperandio *et al.*, 2003). Recently it has been shown that both AI-2 and AI-3 activity are also found in the supernatants of *Shigella* spp., *Salmonella* spp. and in normal flora bacteria such as commensal *E. coli* and *Enterobacter* (Walters *et al.*, 2006). Since catecholamine hormones such as epinephrine and norepinephrine appear to act as agonists of AI-3 in EHEC (Sperandio *et al.*, 2003), this indicates AI-3 may not only allow interspecies signalling among intestinal bacteria but interkingdom cross-signalling between bacteria and their host. Further research is required to understand the nature and the role of these interactions and elucidate whether *Salmonella* might use quorum sensing to regulate expression of virulence genes.

1.8. Using microscopy techniques to study invasion

Microscopy is any technique that produces visible images of structures or details too small to be seen by the human eye. Frequently it is simply defined as the use of a microscope. By obtaining images of *Salmonella* infection, in models ranging from whole animal and simple eukaryotic organisms to isolated cells, microscopy has aided elucidation of the sequence of events in the complex and highly dynamic interaction of *Salmonella* with its host.

A diverse range of microscopy methods have been applied to studying bacterial-host interactions. Wide field microscopy (WFM), also referred to as conventional light microscopy, is probably the most frequently used technique being relatively easy to use, flexible and allowing dynamic processes occurring in living cells to be studied. WFM in its simplest form involves a standard upright or inverted microscope (often with fluorescence capabilities) to which a camera e.g. a charge-coupled device (CCD) camera is added to enable simple image acquisition. The term 'wide-field' refers to the fact light is detected from different focal planes at the same time so the resulting images include both 'in-focus' and 'out-of-focus' light.

Confocal microscopy has also become a fairly standard research tool. Commonly, confocal laser scanning microscopy (CLSM) is used which usually builds up an image of fluorescence by scanning a laser point by point over a field of view. The emitted light follows a reverse path (is 'descanned') and passes through an aperture (pinhole) before detection by a detector, typically a photomultiplier tube (PMT) (Figure 1.23). In allowing light from only one plane of focus to reach the detector, the confocal aperture enables discrimination of objects at different depths of focus, effectively enhancing axial resolution and thereby giving CLSM its major advantage over WFM. Most CLSMs allow simultaneous detection of different fluorophores by selectively directing different wavelengths of emitted light to different detectors. The ability to rapidly switch between excitation wavelengths using an acousto-optic tuneable filter (AOTF) simplifies separation of fluorophore signals.

Figure 1.24 Principle of confocal microscopy. An objective focuses the laser illumination to a small spot on the sample. Reflected light from the illuminated part of the specimen is collected by the objective and reflected by a beam splitter (which removes any reflected laser light) towards a pinhole arranged in front of the detector. Information which does not originate from the focus level of the microscope objective is eliminated by this arrangement. In contrast, light from the focal plane is focused on the detector pinhole and registered by the detector. Diagram from http://fb6www.uni-paderborn.de/ag/ag-sol/fgruppe/mainframe/microscope_e.htm

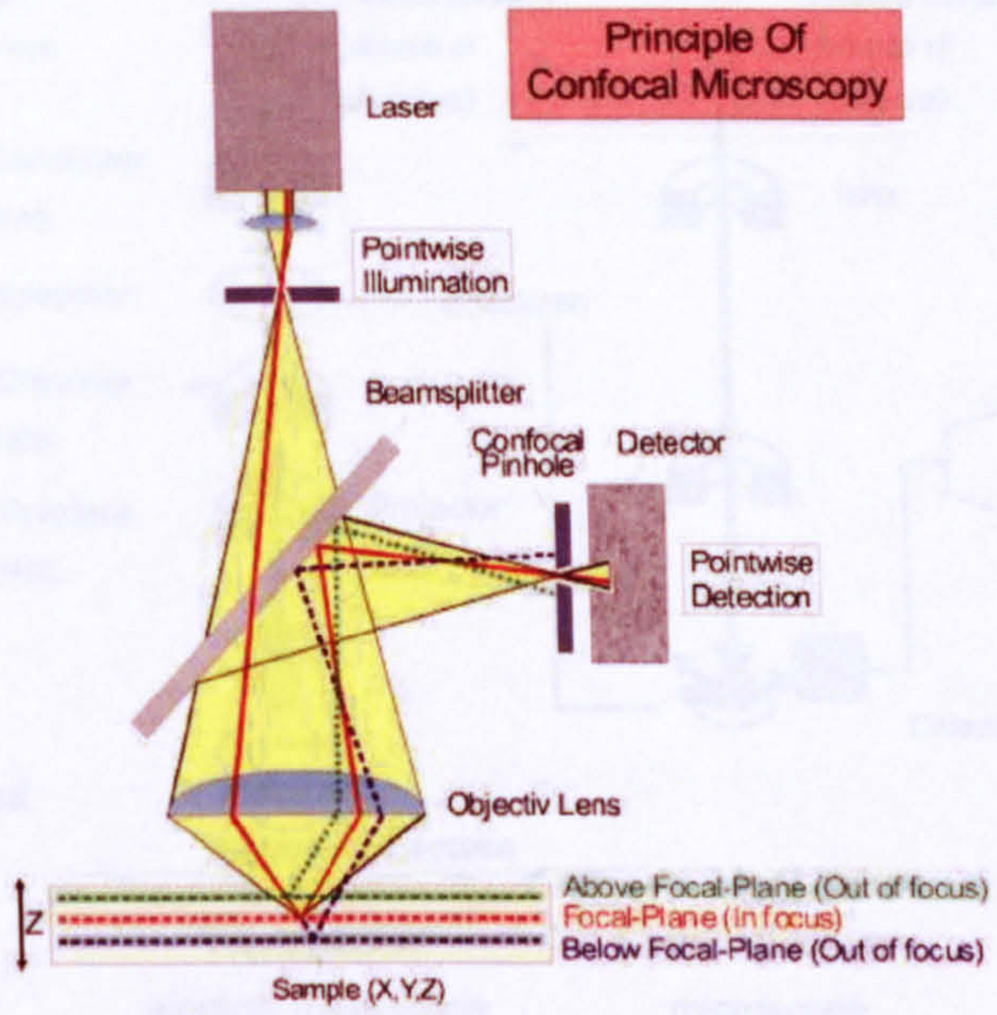

Alternative methods such as electron microscopy (EM) provide higher resolution. Electron microscopes function exactly as their optical counterparts except a focused beam of electrons is used instead of light to 'image' the specimen (Figure 1.24). In transmission electron microscopy (TEM) a beam of electrons is focused onto a specimen and the electrons that pass through the specimen without being scattered are focused to form a negative image of the specimen. Scanning Electron Microscope (SEM) differs by detecting low energy secondary electrons emitted from the surface of the specimen due to excitation by the primary electron beam. In SEM, the electron beam is rastered across the sample, with detectors building up a three-dimensional image of the specimen. EM is particularly useful for studying the morphology of bacterial surface structures. For example it has been used to examine the molecular architecture of the TTSS of *Salmonella* and other pathogens (Kubori *et al.*, 1998; Kubori *et al.*, 2000) and the expression of surface structures e.g. pili and flagella (Baumler and Heffron, 1995; Ramboarina *et al.*, 2005; Reed *et al.*, 1998).

Figure 1.25 Principal features of a light microscope, a transmission electron microscope and a scanning electron microscope. The different microscopes have a similar overall design. Differences however include the lenses which are made of glass in the light microscope and are electromagnets in the electron microscopes. Electron microscopes also require the specimen be placed in a vacuum to prevent the beam being disrupted due to electrons being scattered as they collide with air molecules. Figure adapted from Molecular Biology of the Cell, 3rd Edition (1994)

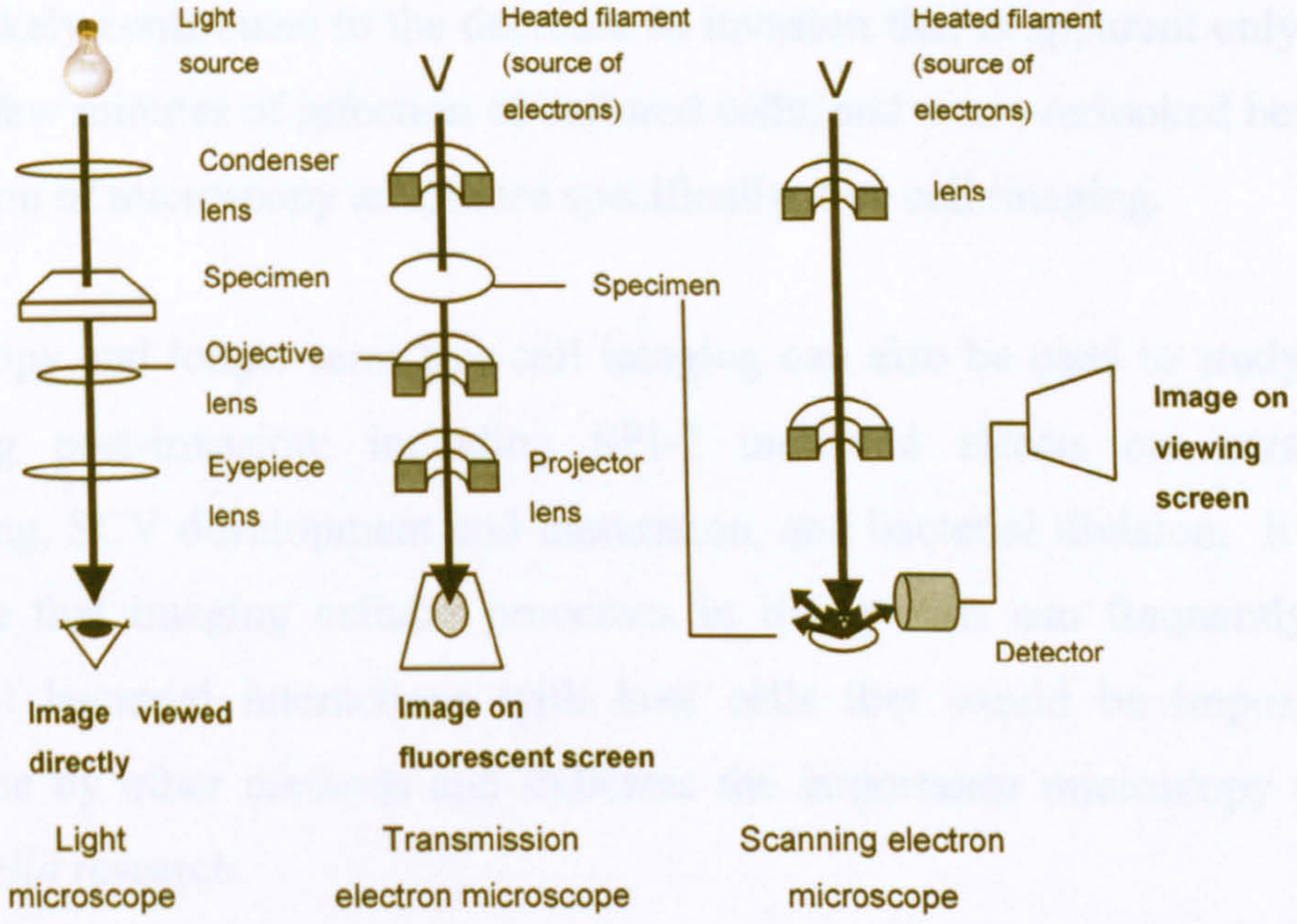

What has been the contribution of microscopy to *Salmonella* research? TEM studies of *Salmonella* invasion of epithelial cells in guinea pig ileum provided the first description of the invasion process including the major changes in epithelial cell morphology that are induced and the subsequent survival of the bacterium in SCVs (Takeuchi, 1967). Formation of *Salmonella*-induced membrane ruffles were studied extensively using TEM (Francis *et al.*, 1992; 1993) and SEM (Francis *et al.*, 1992; Jepson and Clark, 1998; Reed *et al.*, 1996; Reed *et al.*, 1998), with fluorescence labelling and light microscopy contributing towards determining how the redistribution of actin and various cytoskeletal proteins promoted formation of these ruffles (Finlay *et al.*, 1991; Jepson *et al.*, 1995; Jepson *et al.*, 2000; Zhou *et al.*, 1999a). Discovery of the SPI-1 TTSS turned attention to unravelling the roles of the various effector proteins in triggering cellular responses associated with bacterial pathogenesis, and these studies have also included the use of microscopy. For example, microscopy of living cells infected with *Salmonella* revealed the effects of SipA loss from *Salmonella*. Phase-contrast time-lapse microscopy showed that while *Salmonella sipA*

mutants induce ruffles over a time-course indistinguishable from wild type, after ruffle formation they differ in their location relative to the ruffle, frequently moving to the periphery of the ruffle rather than staying centrally located; a behaviour associated with delayed entry into the ruffle and frequent detachment of the bacterium from the cell (Jepson *et al.*, 2001). This phenotype of the *sipA* mutant likely contributes to the decrease in invasion that is apparent only within the first few minutes of infection of cultured cells, and was overlooked before the application of microscopy and, more specifically, live cell imaging.

Microscopy and longer-term live cell imaging can also be used to study events occurring post-invasion; including SPI-2 mediated effects on intracellular trafficking, SCV development and maturation, and bacterial division. It is clear therefore that imaging cellular processes in living cells can frequently reveal facets of bacterial interactions with host cells that would be impossible to determine by other methods and indicates the importance microscopy plays in *Salmonella* research.

1.9. Aims

Salmonella infections represent both a major public health burden and a huge economic cost to society. Research to understand *Salmonella* and its pathogenesis can potentially provide advances in the diagnosis, treatment, and prevention of diseases caused by this microorganism and therefore reduce this burden on society.

In this thesis the molecular mechanisms through which *Salmonella enterica* serovar Typhimurium regulates and induces its uptake into epithelial cells was investigated. Specifically, the aims of the project were to:

1. Examine whether *luxS* affects the ability of *S.* Typhimurium to invade epithelial cells.

2. Examine whether the role of SipA in invasion may vary between *Salmonella* strains, including those that possess or lack SopE.

Chapter Two

Materials and Methods

This chapter describes the general techniques used in this body of work. For particular techniques additional detail will be provided in the Materials and Methods section of the appropriate results chapter.

2.1. Materials

All chemicals unless otherwise stated were purchased from Sigma-Aldrich (Poole, Dorset, UK). The composition of solutions and buffers are given in Appendix II.

2.2. Bacteria

2.2.1. Bacterial strains

The bacteria examined in this thesis are all *Salmonella enterica* serovar Typhimurium. Each chapter contains a table listing the bacterial strains used in that particular piece of work, alongside their source, relevant genotype and antibiotic resistance.

2.2.2. Bacterial growth conditions

Using aseptic techniques 2ml of Luria Bertani (LB) Miller broth was inoculated with several colonies of *S.* Typhimurium grown on LB agar, and incubated overnight (approximately 16 hours) at 37°C as a static culture. 10mls of LB Miller broth were inoculated with 100µl of this static culture (1:100 dilution), and grown at 37°C for 3.5 hours at 100rpm in an orbital shaker (Stuart Scientific (now Barloworld Scientific), Staffordshire, UK). All mutants were grown in the appropriate antibiotic(s) at the following concentrations: chloramphenicol

15µg/ml, kanamycin 100µg/ml, carbenicillin 100µg/ml (Apollo Scientific Ltd., Stockport, UK), nalidixic acid 15µg/ml and tetracycline 15µg/ml.

All media and equipment were sterilised by autoclave, sprayed with 75% ethanol or flamed to white heat to maintain a sterile environment and prevent contamination.

2.2.3. Growth measurement of bacterial cultures

S. Typhimurium growth in LB Miller broth was measured by optical density at 600nm (OD_{600}). 1ml was removed from the bacterial culture and the optical density of the sample measured using a Sherwood Colorimeter (Sherwood Scientific Ltd., Cambridge, UK) with a 1cm light path. The reference absorbance of zero was set with LB Miller broth prior to use. The OD_{600} of cultures grown for 3.5 hours and used in the cell culture assays was ~ 0.34. If the OD_{600} of a culture varied greatly from this value, the cells of each culture were pelleted and resuspended in an appropriate volume of pre-warmed LB Miller broth.

2.2.4. Bacterial growth curves

2ml of LB Miller broth was inoculated with several colonies of *S.* Typhimurium grown on LB agar, and incubated overnight (approximately 16 hours) at 37°C as a static culture. 990µl of LB Miller broth was inoculated with 10µl of this static culture (1:100 dilution). The cultures were grown in 200µl volumes in a 100-well honeycomb plate at 37°C for 24 hours, using a Bioscreen plate reader (Thermo labsystems, UK). Optical density at 600nm was measured every 30 minutes after shaking. All assays were performed in triplicate on three separate occasions.

2.2.5. Maintenance of Bacterial Stocks

10ml of LB Miller broth was inoculated with several colonies of *S.* Typhimurium grown on LB agar, and incubated overnight (approximately 16 hours) at 37°C as

a static culture. The bacterial culture was diluted 1:1 with a sterile solution of 50% v/v glycerol in deionised water (a cryopreservation solution), and 1ml dispensed into 2ml cryovials. Cryovials were stored at -80°C.

To grow a bacterial strain from frozen, the cryovial was thawed rapidly, and 50µl removed to inoculate 10mls of LB Miller broth (+ antibiotics). This inoculum was incubated overnight at 37°C as a static culture, before streaking bacteria onto fresh LB Miller agar (+ antibiotics) and growing overnight at 37°C, from where it was stored at 4°C in a refrigerator.

2.3. Autoinducer 2 (AI-2) bioassay

2ml of LB Miller broth was inoculated with several colonies of *S.* Typhimurium grown on LB agar, and incubated overnight (approximately 16 hours) at 37°C as a static culture. The overnight culture was diluted 1:100 into fresh LB Miller broth (+ 0.5% glucose where stated) to a total volume of 30mls. Cultures were grown in a sealed 100ml conical flask incubated at 37°C, 100rpm in an orbital shaker. 1ml samples were removed from the flask at appropriate time points and passed through a 0.2µm syringe filter (Sartorius, Goettingen, Germany) into a 2ml cryovial tube (Simport Plastics, Quebec, Canada). The tube was snap frozen in liquid nitrogen and immediately stored at -80°C. The following day the samples were sent on dry ice to Dr Klaus Winzer (University of Nottingham) who assessed the AI-2 concentration.

AI-2 production was essentially analysed as described by Bassler *et al.* (1997) using 20µl AI-2 extract and 180µl 1: 5000 diluted overnight cultured *V. harveyi* biosensor BB170 in AB medium. Changes in bioluminescence upon addition of AI-2 were determined at 30°C every 30 min using an automated luminometer (VICTOR2, 1420 multilabel counter, Wallac). For a single experiment, the *V. harveyi* bioassay was performed at least in duplicate for each sample. Experiments were repeated on three separate occasions.

2.4. Molecular Biology

2.4.1. Creating mutants using the λ red system

Mutants of *S.* Typhimurium were created using the one step gene disruption technique of Datsenko and Wanner (2000). This technique uses the phage λ Red recombinase to integrate, by homologous recombination, a linear DNA fragment into the bacterial chromosome, thereby disrupting a chromosomal gene(s).

Generating PCR products homologous to the gene to be disrupted

To disrupt the gene of choice, primers were obtained from MWG based on sequences from http://www.falkow.stanford.edu/whatwedo/wanner. These primers have a 5' region of 40 nucleotides homologous to the gene chosen for disruption and are flanked by 20 nucleotides of sequence that can anneal to an antibiotic resistance cassette on a template plasmid. PCR using these primers amplifies the antibiotic resistance cassette from the plasmid, adding sequences to the 5' and 3' end of this cassette homologous to the regions flanking the gene of interest.

PCR was performed with Expand High Fidelity PCR system (Roche, Welwyn Garden City, UK) as described below (2.4.3.). 5 reactions were performed, with 5µl from each reaction being analysed by agarose gel electrophoresis to check the PCR was successful. The PCR reactions were then pooled into 2 microcentrifuge tubes and purified using a Qiagen® PCR purification kit (Qiagen, West Sussex, UK), with DNA being eluted in 50µl of sterile distilled water. To each 50µl volume of PCR product, 1µl *Dpn*I (Roche, Welwyn Garden City, UK), 6µl of the appropriate 10x buffer, and 3µl of sterile distilled water was added to make the final volume to 60µl. *Dpn*I degrades methylated DNA so will destroy the template DNA. The *Dpn*I digest was allowed to proceed for 2 hours at 37°C before the DNA was repurified using the Qiagen® PCR purification kit and eluted in 40µl water. 1µl of this DNA was compared in agarose gel electrophoresis with 6µl of a λ DNA/*Hin*dIII Fragment Marker (Invitrogen life technologies, Paisley, UK) to determine the concentration of the PCR product.

Transformation of the recipient strain with pKD46

Plasmid pKD46, which encodes λ Red recombinase under the control of the arabinose inducible pBAD promoter and has an ampicillin resistance cassette, was introduced into the recipient strain by electroporation as detailed below (2.4.11) with the following modification: cells were allowed to recover at 30°C and the selection plates were incubated overnight at 30°C as pKD46 is temperature sensitive.

Transforming the pKD46 transformant with the PCR product

2ml of LB Miller broth + 100µg/ml carbenicillin was inoculated with several colonies of pKD46 transformants grown on LB agar + 100µg/ml carbenicillin, and incubated overnight at 30°C as a static culture. Three conical flasks each holding 100mls of SOB medium + 100µg/ml carbenicillin were inoculated with 100µl of this static culture, and grown at 30°C, 100rpm in an orbital shaker. After 2 hours of growth, L-arabinose was added to a final concentration of 10mM, and growth was allowed to continue until an OD_{600} of ~ 0.6 was reached. The pKD46 transformants were then made electrocompetent.

Cultures were placed on ice for 20 minutes before the cells were pelleted at 4°C for 10 minutes at 3000 x g in a centrifuge. 2ml of ice-cold water was used to resuspend the pellet before adding a further 198mls of ice-cold water. Cells were pelleted again at 4°C for 10 minutes at 3000 x g and resuspended in 2mls of ice-cold water before 98mls of ice-cold water were added. Cells were pelleted and resuspended again in the same way into a final volume of 40mls. After the cells were pelleted again they were resuspended in a final volume of 150µl of ice-cold water.

15µl of purified PCR product was placed in each of three ice-cold microcentrifuge tubes to which 85µl of cells from one of the three cultures were added. This mixture was transferred to ice-cold 0.1cm electroporation cuvettes (Bio-Rad, Hercules, CA, USA). Electroporation was performed at 2.5kV, 200Ω, 25µFd using a Bio-Rad Micropulser™ electroporator (Bio-Rad, Hercules, CA, USA). Shocked cells were incubated in 1ml SOC media in a 37°C water bath for

60 minutes, and 100µl plated onto agar selecting for antibiotic resistant transformants. A further 100µl was plated after the bacteria were pelleted and resuspended in 200µl SOC media. The remaining 100µl was kept at room temperature, and if no colonies were obtained within 24 hours, spread on a selective agar plate. After this primary selection, mutants were colony-purified in selective media at 37°C and then tested for ampicillin sensitivity to test for the loss of pKD46.

2.4.2. P22 transduction

P22int-4 HT bacteriophage was provided by Dr C. M. A. Khan (University of Newcastle, UK). To produce the phage lysate, several colonies of the donor strain were inoculated into 10mls LB Miller broth containing the appropriate antibiotics. To this, 10µl of P22 phage were added and the culture grown overnight at 37°C, in an orbital shaker at 200rpm. A few drops of chloroform were added to the overnight culture before vigorous shaking to lyse the cells and release the phage. The culture was spun in a bench top centrifuge at 12,000 x g for 3 minutes to pellet the cell fragments. The supernatant was removed and filter sterilised using a 0.2µm syringe filter (Sartorius, Goettingen, Germany), with the lysate being stored at 4°C.

The recipient strain was grown overnight in 5ml LB Miller broth at 37°C and in an orbital shaker at 200rpm. 1ml of this culture was placed in a 1.5ml microcentrifuge tube and spun in a bench top centrifuge at 12000 x g for 1 minute with the pellet being resuspended in 100µl LB Miller broth. 10µl of the P22 lysate was added, and the tube incubated at room temperature for 30 minutes. A control to which no P22 lysate was added was also set up. 1ml of warm (37°C) LB Miller was added to the cells before incubation in a 37°C water bath for 30 minutes. The sample was spun in a bench top centrifuge at maximum speed for 1 minute and the pellet resuspended in 100µl LB Miller broth, before spreading onto an LB agar plate containing the relevant antibiotic(s) and incubated overnight at 37°C. Transductants were checked using PCR.

2.4.3. Polymerase Chain Reaction (PCR)

Where the product generated by PCR was used in gene deletion or cloning, PCR was performed with Expand High Fidelity PCR system (Roche, Welwyn Garden City, UK). Each reaction was set up as stated in Table 2.1 using 20-50ng of template, 40pmol of each primer, 0.2mM of each deoxynucleoside triphosphate (dNTP), 1.5mM $MgCl_2$ (included in the 10x buffer) and ~2.5 units of *Taq* polymerase.

Analytical reactions were performed with Taq DNA polymerase from Promega (Madison, USA). Where the bacterial chromosome was used as DNA template, a colony was picked from an agar plate using a 200µl pipette tip attached to a pipette and suspended in 50µl sterile distilled water in a microcentrifuge tube. This microcentrifuge tube was placed in a water bath at 100°C for 10 minutes before 5µl aliquots were used in the reactions. Each reaction was set up as stated in Table 2.2, using 40pmol of each primer, 0.2mM of each dNTP, 1.5mM $MgCl_2$ and ~1.25 units of *Taq* polymerase.

The PCR was performed in a PCR machine using the following programme, unless otherwise stated:

1 cycle:
95°C, 5 min

30 cycles:
95°C, 1 min (Denaturation)
55°C, 1 min (Annealing)
72°C, 1 min (Elongation)

1 cycle:
72°C, 10 min

Hold at 4°C

The annealing temperature was changed according to the primers used. For amplification of long PCR products i.e. 2.5kb or larger, an elongation temperature of 68°C and a time of 1 minute 30 seconds was typically used.

Table 2.1 PCR mix using Expand High Fidelity PCR system (Roche, UK). All volumes in µl. Primers were obtained from MWG-Biotech AG, Ebersberg, Germany and dNTPs were from Bioline Ltd, London, UK.

	Reaction	Control
10x buffer	5	5
dNTPS (50x)	1	1
Primer 1 (4pmol/µl)	5	5
Primer 2 (4pmol/µl)	5	5
Water	31.25	33.25
Taq polymerase (3.5units/µl)	0.75	0.75
Template DNA	2	-
Total volume	**50**	**50**

Table 2.2 PCR mix using Taq DNA polymerase from Promega (USA). All volumes are in µl. Primers were obtained from MWG-Biotech AG, Ebersberg, Germany and dNTPs were from Bioline Ltd, London, UK.

	Reaction	Control
10x buffer	5	5
$MgCl_2$ (25mM)	3	3
dNTPS (50x)	1	1
Primer 1 (4pmol/µl)	5	5
Primer 2 (4pmol/µl)	5	5
Water	25.75	30.75
Taq polymerase (3.5units/µl)	0.25	0.25
Template DNA	5	-
Total volume	**50**	**50**

2.4.4. Agarose gel electrophoresis

DNA electrophoresis was performed with a Mini-Sub Cell GT (Bio-Rad, Hercules, CA, USA). A 0.8% agarose solution was made in 1x TBE, with the solution being heated in a microwave until the agarose dissolved. The solution was cooled until it was hand hot and then poured into a gel tray which had been sealed at both ends with autoclave tape. Ethidium bromide was added to a final concentration of 0.2µg/ml and the comb inserted. The gel was left to solidify for ~20 minutes before it was placed in an electrophoresis chamber (Bio-Rad, Hercules, CA, USA). To prepare samples for electrophoresis, 1µl of 6x concentrate gel loading solution (Type I, Sigma Aldrich, Poole, Dorset, UK) was added for every 5µl of DNA solution. Typically 6µl of 1kb DNA ladder (Promega, Madison, WI, USA) or 12µl of DNA sample were loaded per well. Electrophoresis was performed in 1x TBE buffer using 60V for 1 hour, or until the dye markers had migrated an appropriate distance. The DNA was viewed under ultraviolet light using a Chromato Vue® C-62 UV Transilluminator (Ultraviolet products Inc., San Gabriel, CA, USA) and images were captured using an Olympus C-5060 digital camera (Olympus UK Ltd, London, UK) with AlphaDigiDoc™ RT Software for Windows (Alpha Innotech Corp, San Leandro, CA, USA). DNA digests were compared to bands of known molecular weight present in the 1kb DNA ladder.

2.4.5. Purification of DNA from an agarose gel

Upon viewing the gel under ultraviolet light, the band corresponding to the DNA of interest was excised from the gel using a sterile scalpel blade and purified using a QIAquick gel extraction kit (Qiagen, West Sussex, UK) according to the manufacturer's instructions. DNA was eluted in 50µl water.

2.4.6. Transformation and propagation of plasmid DNA

Plasmids were propagated in *E. coli* DH5α cells (Invitrogen Life Technologies, Paisley, UK). Transformation was performed by adding 3-5µl of plasmid DNA to 50µl of competent *E. coli* DH5α cells. The cells were incubated on ice for 30

minutes before being heat shocked at 42°C for 45 seconds and replaced on ice for a further 2 minutes. 400µl of pre-warmed (37°C) LB broth was then added and the cells incubated at 37°C for 1 hour in an orbital incubator. Clones were selected for ampicillin/carbenicillin resistance by plating 125µl of the cell suspension on LB agar plates containing 100µg/ml carbenicillin and incubating the plates overnight at 37°C. Large discrete colonies were selected and propagated in 5ml LB broth containing 100µg/ml carbenicillin at 37°C overnight in an orbital incubator. The following morning, plasmid DNA was extracted and digested with restriction enzymes, using the methods given below, to check the presence of the plasmid. Glycerol stocks were prepared from overnight cultures by mixing equal volumes of bacterial culture and 50% glycerol and placing 1ml aliquots into 2ml cryovials (Simport Plastics, Quebec, Canada) before storing at -80°C.

2.4.7. Purification of plasmid DNA by miniprep

Plasmid DNA was isolated using a QIAprep Spin Miniprep Kit (Qiagen, West Sussex, UK) according to the manufacturer's instructions with the following modifications. 1ml of a 5ml bacterial culture grown at 37°C, in a shaking incubator at 150rpm overnight, was placed in each of two 1.5ml microcentrifuge tubes and the cells pelleted by placing in a bench top centrifuge at 12,000 x g for 5 minutes. The cell pellet in one microcentrifuge tube was resuspended in 250µl of buffer P1 before this bacterial suspension was transferred to the second 1.5ml tube to resuspend the second pellet. The protocol then proceeded according to the manufacturer's instructions, with plasmid DNA being eluted from the QIAprep column using 50µl of sterile distilled water into a sterile 0.5ml microcentrifuge tube. The DNA concentration was determined by measuring the absorbance at 260nm in an Eppendorf Biophotometer (Eppendorf, Hamburg, Germany) using sterile water as a blank. Plasmid DNA was stored at -20°C.

2.4.8. Purification of plasmid DNA by midiprep

2ml of LB Miller broth was inoculated with several bacterial colonies grown on LB + antibiotic(s) agar, and incubated overnight at 37°C as a static culture. 100mls of LB Miller broth + antibiotic(s) were inoculated with 1ml of this static culture (1:100 dilution), and grown overnight at 37°C at 100rpm in an orbital shaker. Plasmid DNA was extracted from these cultures using a Qiagen Plasmid Midi Kit (Qiagen, West Sussex, UK) according to the manufacturer's instructions. Plasmid DNA was eluted from the QIAprep column using 100µl of sterile distilled water. The DNA concentration was determined by measuring the absorbance at 260nm in an Eppendorf Biophotometer (Eppendorf, Hamburg, Germany) using sterile water as a blank. Plasmid DNA was stored at -20°C.

2.4.9. Restriction digests

For preparative restriction digests, 1µg of DNA was used in the digest, with 20 units of restriction enzyme(s), a volume of an appropriate 10x buffer that was one-tenth of the final reaction volume, BSA at a final concentration of 1mg/ml and sterile distilled water to make the reaction up to the specified volume. The reaction was allowed to proceed for 2 hours at 37°C before using agarose gel electrophoresis to isolate the DNA.

For analytical digests of plasmids, the reaction mixtures typically contained 5µl of plasmid DNA isolated by a miniprep, 10 units of restriction enzyme(s), 2µl of an appropriate 10x buffer and 0.2µl 10mg/ml BSA, made up to a final volume of 20µl with sterile distilled water. The reaction was allowed to proceed for 1 hour at 37°C before addition of 4µl 6x DNA loading buffer. Agarose gel electrophoresis (2.4.4.) was performed to separate the digest products. The size of the products was determined by comparison with the bands of known molecular weights present in the 1kb DNA ladder (Promega, Madison, WI, USA).

2.4.10. Ligation of DNA

For cloning, DNA ligations were performed in 20-30µl reaction volumes containing equal amounts of vector and insert or a 3-fold excess of insert. 0.2-0.3µl T4 Ligase (New England Biolabs UK Ltd., Hertfordshire, UK), 2-3µl 10x Ligase buffer and sterile distilled water were added to make up the final volume. A control reaction without insert DNA was also performed to assess background re-ligation of vector. Reactions were allowed to proceed overnight at 15°C in a PCR machine. Ligation mixtures were used directly to transform competent *E. coli* DH5α cells as described above (2.4.6).

2.4.11. Transformation of *Salmonella* by electroporation

2ml of LB Miller broth was inoculated with several colonies of *S.* Typhimurium grown on LB agar, and incubated overnight (approximately 16 hours) at 37°C as a static culture. 10mls of LB Miller broth were inoculated with 100µl of this static culture, and grown at 37°C for 3.5 hours at 100rpm in an orbital shaker (Stuart Scientific (now Barloworld Scientific), Staffordshire, UK). The cells were then made electrocompetent. 1ml of the log phase culture was placed in each of 2 microcentrifuge tubes, and the cells pelleted by placing in a bench top centrifuge cooled to 4°C at 12,000 x g for 2 minutes. Cells were removed from the centrifuge and placed on ice. 1ml of ice-cold water was used to resuspend the cell pellet in one microcentrifuge tube and this bacterial suspension was used to resuspend the second pellet. The cells were pelleted at 4°C for 1 minute at 12,000 x g and then resuspended in 1ml ice-cold water. This procedure was repeated twice more with the final resuspension in 40µl ice-cold water. 1µg of DNA was added to the surface of the electrocompetent bacterial suspension. After gentle mixing with a pipette, the contents of the microcentrifuge tube were transferred to an ice-cold 0.2cm electroporation cuvette (Bio-Rad, Hercules, CA, USA). Electroporation was performed at 2.5kV, 200Ω, 25µFd using a Bio-Rad Micropulser™ electroporator (Bio-Rad, Hercules, CA, USA). Shocked cells were incubated in 1ml SOC media at 37°C for 30 minutes. 50 and 200µl were plated onto agar containing the appropriate antibiotic to select for transformants, and plates incubated overnight at 37°C.

2.5. Secreted Protein Analysis

2.5.1. Secreted Protein preparation

A single bacterial colony was picked from a plate and placed in 10mls LB Miller broth (+ antibiotic) and incubated overnight at room temperature as a static culture. The overnight culture was diluted 1:10 into fresh LB Miller broth to a total volume of 50mls, and grown for 4 hours at 37°C in a shaking incubator at 100rpm. The culture supernatant was then collected and filtered using 0.45µm syringe filters (Sartorius, Goettingen, Germany). The proteins were precipitated by adding trichloroacetic acid (TCA) to a final concentration of 10% and placing the supernatant on ice for 1 hour. The proteins were pelleted at 4°C for 15 minutes at 3000 x g, and resuspended in 300µl of 1% SDS before placing in a 2ml microcentrifuge tube. 1.5ml acetone was added and the proteins incubated at –20°C overnight. The proteins were then pelleted using a bench-top centrifuge at 4°C, maximum speed for 10 minutes, before they were made soluble in 20µl of 1x SDS-PAGE sample buffer. The sample was denatured by heating at 95°C for 10 minutes. Before loading onto a polyacrylamide gel for electrophoresis, the samples were vortexed and spun in a bench top centrifuge at maximum speed for 3 minutes to pellet any debris e.g. cell fragments.

2.5.2. SDS-Polyacrylamide gel electrophoresis (SDS-PAGE)

SDS-PAGE was performed using a Mini Protean III electrophoresis system (Bio-Rad, Hercules, CA, USA). Before use the glass plates were cleaned thoroughly using deionised water followed by 70% ethanol. A spacer plate and a short plate were placed in the casting stand. The resolving gel was prepared as stated in Table 2.3, with all components being added in the order given. TEMED was added last and after thorough mixing, the solution was poured between the plates leaving a ~2.5cm gap to the top of the small plate for the stacking gel. 0.1% SDS was placed over the resolving gel to prevent the top of the gel drying out while the gel solidified. Once the resolving gel had set, the 0.1% SDS was poured off and the gel rinsed with deionised water. Excess water was removed using filter paper (No. 1 filter paper, Whatman, Middlesex, UK). The stacking gel was then

made as shown in Table 2.4 and poured onto the resolving gel. The comb was added and the gel allowed to set. The gel plate was placed in the gel tank which was then filled with 1x SDS-PAGE running buffer. The comb was removed from the stacking gel and the wells rinsed using the running buffer. 10µl of the secreted protein samples and 3µl of a pre-stained protein molecular weight marker (Fermentas Life Sciences, Ontario, Canada) were loaded. Gels were subjected to electrophoresis at 30mA for 70 minutes or until the dye front had left the resolving gel.

Table 2.3 Solutions for preparing a resolving gel for SDS-PAGE. A 10% resolving gel was used. 30% Acrylamide/Bis-Acrylamide solution 37.5:1, ammonium persulphate and TEMED were all purchased from Bio-Rad (CA, USA).

Components	Volume of components (ml) per volume	
	5ml	10ml
Water	1.6	3.3
30% acrylamide mix	2.0	4.0
1.5M Tris pH 8.8	1.3	2.5
10% SDS	0.05	0.1
10% ammonium persulphate	0.05	0.1
TEMED	0.002	0.004

Table 2.4 Solutions for preparing a 5% stacking gel for SDS-PAGE.

Components	Volume of components (ml) per volume	
	2ml	3ml
Water	1.4	2.1
30% acrylamide mix	0.33	0.5
1.5M Tris pH 8.8	0.25	0.38
10% SDS	0.02	0.03
10% ammonium persulphate	0.02	0.03
TEMED	0.002	0.003

2.5.3. Coomassie Blue Staining

The acrylamide gel was placed in a Perspex box, covered with Coomassie Blue stain and left for 1 hour at room temperature on a rocking platform. The stain was removed and replaced with sterile distilled water. A piece of paper towel was placed at the end of the box to capture any dye that was removed during the de-staining procedure. The gel was left at room temperature on the rocking platform until excess Coomassie Blue had been removed. An image of the gel was taken using a Samsung Digimax A7 digital camera (Samsung UK Ltd., Chertsey, UK).

2.5.4. Western Blotting

A Bio-Rad Trans-Blot Transfer Cell was used to transfer the proteins from the polyacrylamide gel to nitrocellulose (Bio-Rad, Hercules, CA, USA). For each polyacrylamide gel, one Transblot® transfer medium pure nitrocellulose membrane and 2 transfer papers were pre-wetted in ice-cold SDS PAGE transfer buffer. A 'sandwich' of transfer paper, nitrocellulose, polyacrylamide gel and transfer paper was assembled with a 10ml pipette being rolled across the 'sandwich' to remove air bubbles. The 'sandwich' was placed between two sponges and inserted into the easy lock cassette which is placed in the electrophoretic blotting cell. A magnetic stirrer was placed in the bottom of the gel tank before the electrophoretic blotting cell and ice block was inserted. The tank was filled with ice-cold running buffer and placed on a magnetic stir plate. Transfer was performed at 100V for 60 minutes.

Transfer of proteins to the nitrocellulose was checked by incubating the membrane for 1-2 minutes with Ponceau stain (0.1% Ponceau in 5% acetic acid) at room temperature on a rocking platform. This also provided an opportunity to mark the positions of the lanes with a pencil and to cut the membrane into segments for incubation with different primary antibodies, thereby preventing cross-reaction. The Ponceau stain was removed by washing the membrane for 5 minutes with PBS on a rocking platform. The membrane was blocked with 5% milk protein, prepared in PBS, overnight at 4°C.

The membrane was incubated with a primary antibody diluted in PBS for 1 hour at room temperature on a rocking platform, followed by three 5 minute washes in PBS. The membrane was then incubated with a 1:2000 dilution of secondary alkaline phosphatase linked IgG antibody (Sigma, Poole, Dorset, UK) for 1 hour at room temperature on a rocking platform before three further 5 minute washes in PBS. Detection was performed using 1 tablet of Sigma Fast™ 5-bromo-4-chloro-3-indolyl phosphate/ nitro blue tetrazolium (BCIP/NBT) dissolved in 10mls sterile water. The membrane was placed in the detection reagent mixture and kept in the dark at room temperature until the membrane had developed (2-3 minutes). The membrane was then washed in PBS to stop the reaction, and once dry was scanned, using a HP Digital Flatbed Scanner 3770, to generate a computer image.

2.6. Cell culture

2.6.1. Cells

Four different cell lines were employed. The Madin-Darby canine kidney strain I cell line (MDCK I) (Barker and Simmons, 1981) was the principal cell line used for all the work performed. The majority of experiments conducted in Chapter 3 used MDCK strain I cells from passage 82, the passage number at which cells were acquired from Professor N. L. Simmons (University of Newcastle, UK). However, a change in phenotype of these cells led to their replacement with MDCK I cells (passage 92) donated by Dr D. Sheppard (Physiology Department, University of Bristol, UK), who had also obtained the MDCK I cells from Professor N. L. Simmons. MDCK strain two cells (MDCK II) (Barker and Simmons, 1981) (passage 125-127) were also supplied by Professor N. L. Simmons (University of Newcastle, UK).

The human cervical carcinoma HeLa cell line and the human intestinal Caco-2 cell line were also used. HeLa cells (passage 43) were obtained from the American Type Culture Collection (ATCC, Rockville, MD, USA), and the Caco-

2 cells (passage 4) were supplied by the European Collection of Cell Cultures (ECACC, Health Protection Agency, Porton Down, Salisbury, UK).

2.6.2. Growth and maintenance of cultured cells

Maintenance of all cultured cells was carried out in a class II vertical laminar flow hood (Microflow Pathfinder; Intermed, Hampshire, UK) using aseptic techniques to ensure sterility and avoid contamination of cells and growth media.

Cells were grown on disposable polystyrene flasks with screw tops with a volume of $75cm^2$ (Costar, Corning Life Sciences, Koolhovenlaan 1119NE Schiphol-Rijk, Netherlands) and maintained at 37°C in a humidified atmosphere of 5% CO_2.

MDCK I and MDCK II cells were grown in Eagle's Minimum Essential Medium (EMEM) supplemented with 10% (v/v) foetal calf serum, 1% (v/v) non-essential amino acids, 1% GlutaMAX and 100µg/ml kanamycin. HeLa cells were grown in Dulbecco's Modified Eagle's Medium (DMEM) supplemented with 10% (v/v) foetal calf serum, 1% (v/v) non-essential amino acids, 1% GlutaMAX, 0.1 mg/ml streptomycin and 100units/ml penicillin. Caco-2 cells were grown in DMEM supplemented with 10% (v/v) foetal calf serum, 1% (v/v) non-essential amino acids, 1% GlutaMAX and 12µg/ml gentamicin. The foetal calf serum was purchased from Biosera (East Sussex, UK); GlutaMAX was from GIBCO (Invitrogen Life Sciences, Paisley, UK).

The cells were passaged after reaching confluency, which was assessed by light microscopy. All media was pre-warmed to 37°C before passaging took place. The media was discarded and the cells washed three times with phosphate buffered saline (PBS). 5mls of 1x trypsin-EDTA was added and the cells returned to the humidified incubator until the cells became detached from the surface (in general this was 60 minutes for MDCK cells, 30 minutes for Caco-2 cells and 5 minutes for HeLa cells). The trypsin solution was deactivated by addition of 10mls of the appropriate culture media, and the solution passed through a cannulus 10-15 times to achieve a single cell suspension. New stock

flasks were seeded with approximately 4 million cells per flask (ratio of cells: media; 1:4), changing the media every 3-4 days.

For experiments in which the number of ruffles induced or the numbers of invaded bacteria were being quantified, MDCK or HeLa cells were seeded onto sterile 13mm coverslips (thickness no. 1; VWR international, Pennsylvania, USA). To seed cells onto coverslips, a single cell suspension was obtained as described above, and the number of cells determined using a haemocytometer (improved Neubauer double cell clear sight chamber, Weber Scientific International, West Sussex, UK). Cells were then diluted in cell culture media to give a final concentration of 0.66×10^5 cells/ml. The coverslips were placed in sterile 12-well tissue culture plates (Corning Life Sciences, Netherlands), and 1ml of the cell suspension added. The plates were then placed at 37°C in a humidified atmosphere of 5% CO_2 for 2-3 days.

For live cell imaging experiments, cells were seeded onto 22mm sterile coverslips (thickness no. 1; VWR international, Pennsylvania, USA) that had been placed in a 6-well tissue culture plate (Corning Life Sciences, Netherlands). Cells were diluted to a concentration of 1×10^5 cells/ml and 2mls of this cell suspension was added to the coverslips before placing in the humidified incubator for 3 days.

In experiments where MDCK cells were grown to form a fully polarised monolayer (Chapter 4), MDCK II cells were grown on Anocell permeable culture inserts of $0.5cm^2$ (10mm diameter, 0.02µm pore size; Anocell, Nunc, Roskilde, Denmark). Caco-2 cells were also used as polarised monolayers and were grown on polycarbonate tissue culture inserts (12mm diameter, 3µm pore size; Corning Life Sciences, Netherlands). In both cases, 1.5mls of the appropriate tissue culture media was placed in the wells of a sterile 12-well tissue culture plate, before the inserts were placed in the wells. A single cell suspension was made and cells seeded in the apical chamber of the insert at a density of $0.5 \times 10^6/cm^2$ in a volume of 500µl. The plates were maintained at 37°C in a humidified atmosphere of 5% CO_2 for 3-4 days for MDCK II

monolayers and 14 days for Caco-2 monolayers, with the apical and basolateral bathing media being changed every 3-4 days.

Before cells were used in an experiment, confluence was assessed using light microscopy, and for cells grown on tissue culture inserts, TER was measured across the monolayer using an electrical voltohmmeter (EVOM, World Precision Instruments, Hertfordshire, UK). The transepithelial electrical resistance was expected to exceed 200 $\Omega.cm^2$ for Caco-2 cells and 50 $\Omega.cm^2$ for MDCK II cells, otherwise the cells were discarded.

2.6.3. Maintenance of Cell Stocks

Confluent monolayers in cell culture flasks, free from contamination, were treated with trypsin as previously described, with 10mls of cell culture media added to terminate the effects of the trypsin, before a single cell suspension was made. The contents of the flask were placed in a 20ml universal tube (Sterilin, Staffordshire, UK), and the cells pelleted using a centrifuge operating at 100 x g for 3 minutes. The supernatant was decanted and the pellet resuspended in a solution which had been filter sterilised and was composed of 2mls foetal calf serum and 5mls of the cryopreservative, dimethyl sulphoxide (DMSO). 1ml aliquots were dispensed into 2ml cryovials (Simport Plastics, Quebec, Canada), and these were placed in a cryopreservation module, which was placed at -80°C to achieve slow and uniform cooling. After freezing overnight, the vials were removed from the module and transferred to liquid nitrogen (-196°C) for permanent storage.

To culture from frozen stocks, a vial of cells was removed from liquid nitrogen and thawed rapidly. The contents of the cryovial were removed and added to 10ml of culture medium that had been pre-warmed to 37°C, in a 20ml universal. To remove the DMSO which can be toxic to cells, the cells were pelleted using a centrifuge operating at 100 x g for 3 minutes, the supernatant removed and the cells resuspended in 10ml of fresh culture medium. This cell suspension was then placed in a 75cm^2 cell culture flask, to be cultured as described.

2.7. Infection of Cultured Epithelia

2.7.1. Modified Krebs Buffer

Before experimental infections of cultured cells took place, the cell culture media was removed and replaced with a modified Krebs buffer. This buffer was made in Milli-Q deionised water and had the following composition in mM: 137 NaCl, 5.4 KCl, 1 $MgSO_4$, 0.3 KH_2PO_4, 0.3 NaH_2PO_4, 2.4 $CaCl_2$, 10 glucose and 10 Tris. The pH was adjusted to pH 7.4 at 37°C with 0.5M HCl, and the media made sterile by autoclaving.

2.7.2. Bacterial Infection Assay for cells grown on coverslips

MDCK and HeLa cells grown on 13mm coverslips were removed from the 5% CO_2, 37°C incubator two to three days post-seeding, and the culture medium aspirated from the wells and replaced with 1ml pre-warmed modified Krebs buffer. This procedure was repeated twice more to wash the cells and remove waste products. The tissue culture plates were then placed in a 37°C incubator for 15 minutes, to allow the cells to equilibrate. Subsequently, 50µl of a serovar Typhimurium culture was added to each well (multiplicity of infection (MOI) of 100), the plate gently rocked to distribute the bacteria evenly in the well, and the plate incubated at 37°C for the required length of time.

2.7.3. Bacterial Infection Assay for cells grown on culture inserts

On the fourteenth day post-seeding for Caco-2 cells and the third-day post-seeding for MDCK II monolayers, the cell culture plates were removed from the incubator. The culture inserts were removed from the plate and placed in a new plate containing 1.5ml pre-warmed Krebs buffer. The bathing media was aspirated from the apical surface and replaced with 0.5ml of pre-warmed Krebs buffer. This step was repeated twice more before placing the cells in a 37°C incubator for 15 minutes, to allow equilibrium to be reached. 25µl of a serovar Typhimurium culture was added to the apical chamber (MOI of 100), the plate gently rocked to distribute the bacteria evenly in the well in which they were

placed, and the plate incubated at 37°C for the required length of time. Control monolayers were treated in the same manner but no bacteria were added. In experiments using polarised MDCK II cells TER was measured at specific time points.

2.7.4. Measuring transepithelial resistance (TER)

Transepithelial electrical resistance (TER) was measured across polarised, cultured MDCK II monolayers using a voltohmmeter (EVOM, World Precision Instruments, Hertfordshire, UK). The voltohmmeter has a voltmeter, ohmmeter and AC constant current source coupled to a pair of silver/silver chloride electrodes. This type of voltohmmeter allows the rapid measurement of epithelial integrity with minimum affect on the integrity of the cell monolayer.

To take a measurement, one of the electrodes is placed in the apical medium and the other (slightly longer) side is placed in the basolateral medium, ensuring neither electrode is touching the sides of the culture insert or well. A measurement is made by passing a constant current across the epithelium and the resistance offered by the monolayer is measured by the ohmmeter (resistance range 0-20kΩ). The TER measurement was corrected for the growth area of the culture insert to produce a TER value measured in $\Omega.cm^2$.

2.7.5. Gentamicin Protection Assay

A 12-well plate was seeded at a concentration of 0.66×10^5 cells/well. The plates were then placed at 37°C in a humidified atmosphere of 5% CO_2 for 2-3 days to establish confluent monolayers. Invasion of the monolayer was identical to that performed for 13mm coverslips (2.7.2). The gentamicin protection assay was carried out essentially as described by Steele-Mortimer *et al.*, 2002. Following incubation, the monolayers were washed 3 times in pre-warmed modified Krebs media to remove any non-cell associated bacteria. To remove any externally associated bacteria 1ml of pre-warmed modified Krebs medium containing 100μg/ml gentamicin was added to each well and incubated for a further 30 minutes at 37°C. Monolayers were then washed in PBS 3 times to

remove residual gentamicin and lysed by 10 minute incubation at room temperature in 1ml of 1% (v/v) Triton X-100 in PBS. The total number of viable bacteria per well was determined by serial dilution in PBS of the Triton X-100 lysed monolayer solution (10^{-2} to 10^{-5}) with plating of 100µl onto LB Miller plates (+ antibiotics) in duplicate. Plates were incubated overnight at 37°C and counts made the following day.

2.7.6. Analysis of membrane ruffling by immunocytochemical staining of F-actin

Upon completion of the infection period, each coverslip was removed from the well plate with forceps and washed, with moderate agitation, in a beaker of PBS to remove non-adherent bacteria. The coverslips were subsequently placed in a well of a 12-well plate filled with 1ml of 2% paraformaldehyde (PFA), and left to fix for 45 minutes at 4°C. The coverslips were washed in the beaker of PBS and placed in a well of a 12-well plate containing 1ml of 0.1% (v/v) Triton X-100 for 15 minutes to allow permeabilisation. The coverslips were washed again in PBS and placed in a well of 1ml PBS, before removal to an empty well. 50µl of goat anti-*Salmonella* CSA-1 antibody (Kirkegaard and Perry Laboratories Inc, Gaithersburg, MD, USA), diluted 1:200 in PBS, was applied to the coverslip and left for 45 minutes at room temperature. The lid of the cell culture plate was replaced to prevent drying. A little PBS was added to each coverslip to aid its removal from the well plate. Coverslips were then washed in PBS before incubation with 50µl fluorescin isothiocyanate (FITC)-conjugated rabbit anti-goat immunoglobulin (1:100 in PBS, Sigma-Aldrich, Poole, Dorset, UK) and tetramethyl rhodamine isothiocyanate (TRITC)-phalloidin (1:500 in PBS; Sigma-Aldrich, Poole, Dorset, UK) for 45 minutes. The lid was replaced to prevent drying, and the cell culture plate covered with foil to limit photobleaching. The coverslips were finally washed in PBS and mounted in Vectashield containing 4',6-diamidino-2-phenylindole (DAPI) (Vector Laboratories Inc., Burlingame, CA, USA) on glass slides (76 x 26mm; Menzel-Glazer, Braunschweig, Germany). Excess liquid was removed with tissue and the coverslip fixed in place with nail varnish.

Coverslips were examined using a Leica DM LB2 fluorescent upright microscope (Leica Microsystems, Mannheim, Germany). *Salmonella* (FITC-labelled) were viewed using a filter cube with a 450-490nm excitation filter and 515nm emission filter, actin and ruffles (TRITC-labelled) were viewed using a 515-560nm excitation filter and 590nm emission filter, and cell nuclei (DAPI-stained) were viewed using a UV filter cube with 340-380nm excitation and 425nm emission. Quantification of cells and membrane ruffles in 10 randomly selected areas of each coverslip was performed to produce a measure of the number of ruffles induced by each strain. The total number of cells counted per coverslip was 250 or greater. Images were collected using a Leica AOBS SP2 confocal imaging system equipped with an argon and green HeNe laser.

2.7.7. Immunocytochemical staining of F-actin in polarised cell monolayers

Upon completion of the infection period, the bacterial suspension at the apical surface of the monolayer was removed and discarded, and the culture insert washed in a beaker of PBS to remove non-adherent bacteria. The insert was subsequently placed in a well of a 12-well plate filled with 1.5ml of 2% paraformaldehyde (PFA), before 500µl of 2% PFA was added to the apical chamber. The cell monolayer was fixed for 45 minutes at 4°C, after which the insert was washed in a beaker of PBS and placed in a well of a 12-well plate containing 1.5ml of 0.1% (v/v) Triton X-100, with 500µl 0.1% (v/v) Triton X-100 being applied to the apical chamber. The cell monolayer was permeabilised for 15 minutes. The insert was then washed in PBS and placed in a well of 1.5ml PBS, with 500µl of PBS applied to the apical surface. The liquid in the apical chamber was subsequently discarded and the insert removed to an empty well. 100µl of goat anti-*Salmonella* CSA-1 antibody (Kirkegaard and Perry Laboratories Inc, Gaithersburg, MD, USA), diluted 1:200 in PBS, was applied to the apical surface of the monolayer and the insert left for 45 minutes at room temperature. The lid of the cell culture plate was replaced to prevent drying. The culture insert was again washed in PBS before incubation with 100µl FITC-conjugated rabbit anti-goat immunoglobulin (1:100 in PBS, Sigma-Aldrich, Poole, Dorset, UK) and TRITC-phalloidin (1:500 in PBS; Sigma-Aldrich, Poole,

Dorset, UK) for 45 minutes. The lid was replaced to prevent drying, and the cell culture plate covered with foil to limit photobleaching. The culture insert was washed in PBS and placed on a glass slide (76 x 26mm; Menzel-Glazer, Braunschweig, Germany). Forceps were used to carefully separate the filter from the plastic sides. Vectashield containing DAPI (Vector Laboratories Inc., Burlingame, CA, USA) was applied to the surface of the filter and a 22mm glass coverslip placed on top. Excess liquid was removed with tissue and the coverslip fixed in place with nail varnish. The inserts were analysed in the same manner as the coverslips (2.7.6.).

2.7.8. Differential antibody staining of adhered/invaded *Salmonella*

S. Typhimurium adherence and invasion were quantified using differential immunocytochemical staining. After the infection period, coverslips were washed thoroughly in PBS and fixed in 2% PFA at 4°C for 45 minutes. The monolayers were washed again in PBS before being incubated with 50µl of goat anti-*Salmonella* CSA-1 antibody (Kirkegaard and Perry Laboratories Inc, Gaithersburg, MD, USA), diluted 1:200 in PBS, for 45 minutes at room temperature. Coverslips were then washed in PBS before incubation with 50µl fluorescin isothiocyanate (FITC)-conjugated rabbit anti-goat immunoglobulin (1:100 in PBS, Sigma-Aldrich, Poole, Dorset, UK) for 45 minutes. The coverslips were then washed in PBS and placed in a well of a 12-well plate containing 1ml of 0.1% (v/v) Triton X-100 for 15 minutes to allow permeabilisation. The coverslips were washed in PBS and incubated a second time with the goat anti-*Salmonella* antibody (CSA-1) (1:200 PBS) for 45 minutes, after which they were washed in PBS and 50µl secondary rabbit anti-goat IgG antibody conjugated to tetramethyl rhodamine isothiocyanate (TRITC) (1:50 in PBS; Sigma-Aldrich, Poole, Dorset, UK) was added for 45 minutes. Coverslips were then washed in PBS and mounted in Vectashield containing DAPI (Vector Laboratories Inc., Burlingame, CA, USA) on glass slides (76 x 26mm; Menzel-Glazer, Braunschweig, Germany). Excess liquid was removed with tissue and the coverslip fixed in place with nail varnish.

Culture inserts were stained in a similar manner except 100µl of antibody was applied to the apical surface of the monolayer, and in the washing stages 1.5ml was placed in the well with 500µl applied to the apical chamber. Mounting was as described in 2.7.7.

To assess the level of invasion of each *Salmonella* strain, coverslips were examined using a Leica DM LB2 upright microscope (Leica Microsystems, Mannheim, Germany). Adhered *Salmonella* (FITC-labelled) were viewed using a filter cube with a 450-490nm excitation filter and 515nm emission filter, the total *Salmonella* population (TRITC-labelled) were viewed using a 515-560nm excitation filter and 590nm emission filter, and cell nuclei (DAPI-stained) were viewed using a UV filter cube with 340-380nm excitation and 425nm emission. Quantification of cells and membrane ruffles in 10 randomly selected areas of each coverslip was performed to produce a measure of the number of ruffles induced by each strain. The total number of cells counted per coverslip was 250 or greater.

2.8. Microscopy

2.8.1. Confocal Laser Scanning Microscopy

Images of TRITC-phalloidin (F-actin) and FITC immunostaining (*Salmonella*) were obtained by confocal laser-scanning microscopy using a Leica TCS SP2 AOBS confocal system (Leica Microsystems, Mannheim, Germany) attached to a Leica DM IRBE microscope with an Ar laser (488nm) and green HeNe laser (543nm) for excitation. An oil-objective lens (63x NA 1.4) was used, and imaging parameters were selected to optimise confocal resolution and standardised to allow direct comparison between images. Stacks of images at 0.5µm intervals were acquired and maximum projections of these created with Leica confocal software. Cytochemical staining for comparative studies was performed in the same experiment, and images were obtained using identical imaging parameters. Final images were composed using Adobe Photoshop 6.0 software.

2.8.2. Scanning Electron Microscopy

Post-infection, coverslips were washed thoroughly in PBS, to remove non-adherent *Salmonella*, and fixed overnight at 4°C in 2% glutaraldehyde in PBS. Following dehydration through graded ethanol solutions (20 minutes each in 25%, 50%, 75%, 100% absolute alcohol); 40µl of hexamethyldisilazine was added to the surface of the coverslip and allowed to evaporate (~2 hours) in a fume hood. The coverslips were attached to 12mm diameter aluminium SEM stubs (Agar Scientific, Essex, UK) using adhesive carbon tabs (Agar Scientific), and gold coated using a sputter coater. The specimens were examined using a Philips 501B SEM, and digital images captured using software generously provided by Dr A. Gebert (Gebert and Preiss, 1998).

2.8.3. Phase-contrast time-lapse microscopy

MDCK I cells were seeded on 22mm coverslips (2.5 x 10^4 cells per coverslip) and maintained at 37°C in a humidified atmosphere of 5% CO_2. 3-4 days post seeding the coverslip was washed twice with warm (37°C) modified Krebs buffer in its well before forceps were used to place the coverslip in the lid of a coverslip holder (Figure 2.1). The chamber was screwed onto the lid and 1ml of modified Krebs buffer placed in the well. The coverslip holder was then placed on the stage of a Leica DM IRB inverted epifluorescent microscope. The stage is enclosed within a microscope incubator which was switched on at least 30 minutes prior to the start of the experiment to allow the required temperature of 37°C to be achieved and stabilised. *S.* Typhimurium grown for 3.5 hours in LB Miller was added to the chamber of the coverslip holder at a MOI of approximately 50. Phase-contrast images were obtained with a 40x oil-immersion lens (NA 1.0). Improvision Openlab 4.0.3 software was used to automate the acquisition of images at each of three focal depths (1.5µm steps) at 10 second intervals over a 20 minute time course with a Hamamatsu ORCA ER cooled CCD camera.

A randomly selected field of view of 80µm x 105.5µm was scrutinised to determine the timing of images in which the initial attachment of each bacterium

occurred and the membrane ruffle first appeared. Data on the time interval between bacterial binding and induction of membrane ruffling was pooled from 3 experiments, which represents the study of 90 individual ruffles for each strain. All data are expressed as medians, with the range of values indicated. Significance of differences between median values was assessed using a Mann Whitney U test for two data sets, and a Kruskal Wallis test followed by Dunn's Multiple Comparison Test for three or more data sets. Significance was set at $P \leq 0.05$.

To create the movies presented in Appendix III, the Improvision Openlab 4.0.3 files were saved as LIF files and opened in Improvision Volocity 4 software. The files could then be exported into Windows and saved as an AVI file for use with Windows Media Player (Microsoft, Redmond, WA, USA).

Figure 2.1 Setting up the coverslip holder for live cell imaging. The coverslip holders used were made in the University of Bristol workshop. Panel a shows a 22mm coverslip (cell side up) being positioned centrally within the chamber base using forceps. Panel b shows the complete coverslip holder once the base has been screwed onto the lid and a seal formed between the coverslip and rubber O-ring in the underside of the upper part of the chamber. To the well is added 1ml of buffer, in this case modified Krebs buffer warmed to 37°C (panel c). Once on the microscope stage, log phase *Salmonella* are added to the well during image capture. (Perrett and Jepson, 2007)

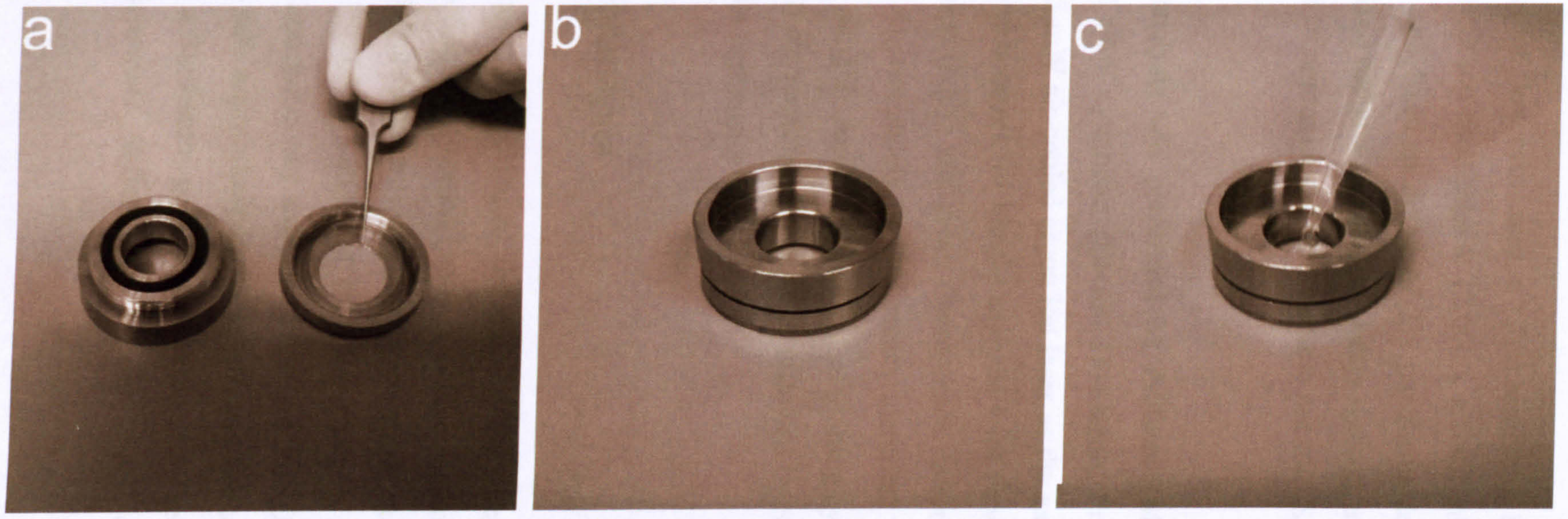

2.9. Flow cytometry

To prepare samples for flow cytometry, a 1.2ml sample of bacterial culture was pelleted using a bench top centrifuge at 12,000 x g for 5 minutes. The bacteria were resuspended and fixed in 500µl of 2% paraformaldehyde (PFA) for 15 minutes at 4°C. Fixed bacteria were subsequently washed, and diluted in PBS to obtain a maximum of approximately 10^7 bacteria per ml. Samples were kept at 4°C until analysis.

Flow cytometric analysis was performed by Professor Mick Bailey using a FACSVantage SE flow cytometer (Becton Dickinson, Franklin Lakes, N.J.) equipped with a 15-mW air-cooled argon ion laser as the excitation light source (488nm). Routine parameters for sample analysis were forward and side scatter (FSC and SSC, respectively) and green fluorescence detection (FITC) for cells containing GFP. Approximately 50,000 events identified as *Salmonella* cells were collected per sample. Analyses consisted of plotting cytograms of FSC and SSC to visualise all the particles in a sample, followed by SSC versus FITC for displaying total cells expressing GFP.

2.10. Statistical Analysis

Where the data is normally distributed, the results of an experiment are expressed as means ± standard error of means (sem) of 3 independent experiments. The PRISM Graphpad 3.0 software was used to apply statistical tests, with significance set at $P \leq 0.05$. An unpaired, two-way Student's t-test was performed with two data sets and a one-way analysis of variance (ANOVA) was performed with three or more data sets, followed by a Tukey post-hoc test when all samples were compared or a Bonferroni post-hoc test where only selected samples were compared, to determine differences between the various data sets.

Chapter Three

Investigation to determine whether the *luxS* gene is important in the invasion of epithelial cells by *Salmonella*

3.1. Introduction

Quorum sensing is an intercellular signalling mechanism used by bacteria to regulate gene expression in response to changes in cell population density. Quorum sensing relies on the production and secretion of a small signalling molecule during growth, so that as the size of a bacterial population grows there is a corresponding increase in the extracellular concentration of the autoinducer. Once the population has reached a specific cell density, the critical concentration of the autoinducer will be exceeded, and can then be detected by the bacteria. Detection of autoinducer results in activation of signalling pathways that lead to regulation of transcription, and ultimately modulation of population behaviour. This response is usually one that is only productive when carried out simultaneously by many cells, and includes responses such as bioluminescence, antibiotic production, production of virulence factors and biofilm formation (Davies *et al.*, 1998; Derzelle *et al.*, 2002; Engebrecht and Silverman, 1984; Miller *et al.*, 2002). By co-ordinating the gene expression of a bacterial community, quorum sensing enables bacteria to behave like multicellular organisms (Schauder *et al.*, 2001).

Quorum sensing systems have been classified into three groups based on the type of signalling molecule used. The first system is found in Gram-negative species, where an acyl homoserine lactone signal is used (Cao and Meighen, 1989; Eberhard *et al.*, 1981); the second is found in Gram-positive microorganisms where the signalling compound is usually a peptide (Kleerebezem *et al.*, 1997). The third system relies upon the production of an autoinducer-2 (AI-2) molecule by an AI synthase, encoded by the *luxS* gene (Surette *et al.*, 1999). Since the *luxS* gene has been found in over 55 species of bacteria, including both Gram-negative and Gram-positive species (Surette *et al.*, 1999; Xavier and Bassler,

2003), it has been suggested this autoinducer may be used for interspecies signalling, rather than the intraspecies communication associated with the other classes of quorum sensing. Hence, AI-2 may enable differential gene expression dependent on whether bacteria exist in pure culture or in a consortium (Bassler, 1999).

The *luxS* gene has been found in *Salmonella* (Surette *et al.*, 1999), with the AI-2 signal being identified as 2-methyl-2,3,3,4-tetrahydroxytetrahydrofuran (R-THMF) (Miller *et al.*, 2004; Schauder *et al.*, 2001). This is a derivative of 4, 5-dihydroxy-2, 3-pentanedione (DPD), a by-product of the activated methyl cycle (AMC) in which LuxS plays a role. Discovery of the *luxS* gene in *Salmonella* has led to the proposal that quorum sensing may be used by *Salmonella* to regulate gene expression. An initial screen for genes regulated by *luxS* in *Salmonella* identified those of the *luxS* regulated (*lsr*) operon (Taga *et al.*, 2001). The *lsr* operon encodes a transporter for AI-2, which is homologous to the ribose ABC transporter (Taga *et al.*, 2001). The transporter is expressed at low levels by cells, initially only allowing uptake of small quantities of AI-2, and therefore detection, during growth. AI-2 is sequestered inside the cell through phosphorylation by LsrK (Taga *et al.*, 2003; Xavier *et al.*, 2007). The phosphorylated product binds the *lsr* operon repressor LsrR, and prevents it binding to the *lsr* operon. Inhibition of LsrR allows greater transcription of the *lsr* operon, and therefore, a larger number of transporters in the cell membrane (Taga *et al.*, 2001). Thus, by the time AI-2 has exceeded its critical concentration there are enough transporters in the bacterial membrane to allow the bacteria to detect AI-2 in the environment and begin concerted uptake of the signalling molecule, which in later phases of growth may lead to termination of quorum sensing (Taga *et al.*, 2003).

Current work is focused on determining whether there are further genes in *Salmonella* which are regulated by AI-2, and whether quorum-sensing affects the behaviour of *Salmonella* in any way. The aim of the study reported here was to examine whether *luxS* affected the ability of *S.* Typhimurium to invade epithelial cells through comparison of a wild type *S.* Typhimurium strain and its isogenic

luxS deletion mutant in the ability to induce membrane ruffles and invade cultured epithelial cell lines.

3.2. Materials and Methods

3.2.1. Bacterial strains

The *S.* Typhimurium strains listed in Table 3.1 were grown as previously described in Chapter 2. Briefly, several colonies grown on LB agar were inoculated into 2mls LB Miller broth and grown overnight at 37°C as a static culture. From this culture, 100µl was used to inoculate 10mls LB Miller broth (+ 0.5% glucose where stated), and grown at 37°C for 3.5 hours with shaking at 100rpm in an orbital shaker. Where appropriate, antibiotics were used at the following concentrations; chloramphenicol 15µg/ml, kanamycin 50µg/ml, carbenicillin 100µg/ml.

3.2.2. Autoinducer 2 (AI-2) bioassay

300µl of an overnight static culture was used to inoculate 30mls of LB Miller broth (+ 0.5% glucose where stated) in a sealed 100ml conical flask, which was incubated at 37°C, in an orbital shaker at 100rpm. A 1ml sample was removed from the flask at 0, 1, 2, 3, 3.5, 4, 5, 5.5 and 6 hour time intervals and passed through a 0.22µm filter into a 1.5ml cryovial tube. The tube was snap frozen in liquid nitrogen and immediately stored at -80°C. The following day the samples were sent on dry ice to Dr Klaus Winzer (University of Nottingham) who assessed the AI-2 concentration.

AI-2 production was analysed as described by Bassler *et al.* (1997) using 20µl AI-2 extract and 180µl 1:5000 diluted overnight cultured *V. harveyi* biosensor BB170 in AB medium. Changes in bioluminescence upon addition of AI-2 were determined at 30°C every 30 minutes using an automated luminometer (VICTOR2, 1420 multilabel counter, Wallac). For a single experiment, the *V. harveyi* bioassay was performed at least in duplicate for each sample. Experiments were repeated on three separate occasions.

3.2.3. Cell culture

For experiments in which epithelial cells were infected with *Salmonella* and subsequently fixed and stained, MDCK strain I and HeLa cells were seeded on 13mm coverslips (2.5 x 10^4 cells per coverslip) and maintained at 37°C in a humidified atmosphere of 5% CO_2 for 3 days. Caco-2 cells were seeded at a density of 0.5x10^6/cm^2 on Transwell cell culture inserts (3μm pore size) and maintained at 37°C in a humidified atmosphere of 5% CO_2 for 14 days.

3.2.4. Infection of cultured cells

The culture media was replaced by modified Krebs buffer and cell monolayers kept at 37°C for 15 minutes to achieve equilibrium. *S.* Typhimurium was then added at a multiplicity of infection (MOI) of approximately 100, with monolayers being maintained at 37°C for 15 minutes.

3.2.5. Time-lapse phase-contrast microscopy

MDCK cells were seeded on 22mm coverslips (2.5 x 10^4 cells per coverslip) and maintained at 37°C in a humidified atmosphere of 5% CO_2. 3-4 days post seeding, the coverslips were transferred to modified Krebs buffer and placed in a temperature-controlled open perfusion system. *S.* Typhimurium grown for 3.5 hours in LB Miller or LB Miller + 0.5% glucose were added at a multiplicity of infection (MOI) of approximately 50, and phase-contrast images were obtained with a Leica DM IRB inverted microscope and 40x oil-immersion lens (NA 1.0). Improvision Openlab 4.0 software was used to automate the acquisition of images at each of three focal depths (1.5μm steps) at 10 second intervals over a 20 minute time course with a Hamamatsu ORCA ER cooled CCD camera.

A randomly selected field of view of 80μm x 105.5μm was scrutinised to determine the timing of images in which the initial attachment of each bacterium occurred and the membrane ruffle first appeared. Data on the time interval between bacterial binding and induction of membrane ruffling was pooled from at least 4 experiments, which represents the study of over 200 individual ruffles

for each strain. All data are expressed as medians, with the range of values indicated. Significance of differences between median values was assessed using a Mann Whitney U test for two data sets, and a Kruskal Wallis test followed by Dunn's Multiple Comparison Test for three or more data sets. Significance was set at $P \leq 0.05$.

3.2.6. Flow cytometry

For measurement of GFP in *Salmonella*, samples were taken after 3.5 or 6 hours of growth in LB at 37°C, and the bacteria pelleted using a bench top centrifuge at maximum speed. The bacteria were resuspended and fixed in 2% paraformaldehyde (PFA) for 15 minutes at 4°C. Fixed bacteria were subsequently washed, and diluted in PBS to obtain a maximum of approximately 10^7 particles per ml. Samples were kept in the dark at 4°C until analysis.

Flow cytometric analysis was performed by Professor Mick Bailey (University of Bristol) and was performed on a FACSVantage SE flow cytometer (Becton Dickinson, Franklin Lakes, N.J.) equipped with a 15-mW air-cooled argon ion laser as the excitation light source (488nm). SL1344 without the *gfp*$^+$ gene were used as negative controls, *rpsM*::*gfp*$^+$ mutants, which constitutively express GFP, were used as positive controls. Approximately 50,000 events identified as *Salmonella* cells were collected per sample. GFP fluorescence intensity values are presented as means for the populations.

Table 3.1 *Salmonella enterica* serovar Typhimurium strains used in this chapter

Bacterial strain	Relevant genotype	Antibiotic resistance	Source (Reference)
SL1344	Wild type	None	C. M. A. Khan
SL1344 *luxS*	SL1344 with inframe deletion within *luxS*	None	C. M. A. Khan
SL1344 *luxS* p*luxS*	SL1344 with inframe deletion within *luxS*, pBRSL*luxS*	Carbenicillin	C. M. A. Khan
JH3010	SL1344 with transcriptional gene fusion *prgH::gfp+*	Chloramphenicol	J. Hinton (Hautefort *et al.*, 2003)
SL1344 *luxS* *prgH::gfp+*	SL1344 with inframe deletion within *luxS* gene and with transcriptional gene fusion *prgH::gfp+*	Chloramphenicol	I. Martinez-Argudo
SL1344 *luxS* pBRSL*luxS* *prgH::gfp+*	SL1344 with inframe deletion within *luxS* gene and with transcriptional gene fusion *prgH::gfp+*, pBRSL*luxS*	Chloramphenicol & Carbenicillin	I. Martinez-Argudo
JH3016	SL1344 with transcriptional gene fusion *rpsM::gfp+*	Chloramphenicol	J. Hinton (Hautefort *et al.*, 2003)
SL1344 *luxS* *rpsM::gfp+*	SL1344 with inframe deletion within *luxS* gene and with transcriptional gene fusion *rpsM::gfp+*	Chloramphenicol	I. Martinez-Argudo
SL1344 *luxS* pBRSL*luxS* *rpsM::gfp+*	SL1344 with inframe deletion within *luxS* gene and with transcriptional gene fusion *rpsM::gfp+*, pBRSL*luxS*	Chloramphenicol & Carbenicillin	I. Martinez-Argudo
SL1344 ON	*hin*::*kan* (phase-locked ON); $FljB^+$	Kanamycin	C. M. A. Khan
SL1344 OFF	*hin*::*kan* (phase-locked OFF); $FliC^+$	Kanamycin	C. M. A. Khan

3.3.Results

3.3.1. The relationship between growth and AI-2 production

The parent and isogenic *luxS* deletion mutant of *S. enterica* serovar Typhimurium strain SL1344 were first compared for growth and autoinducer-2 (AI-2) production.

The growth of SL1344 wild type and the *luxS* deletion mutant (*luxS*) was measured in LB and LB containing 0.5% glucose at 37°C. Growth and AI-2 production was compared in the two types of media because it had previously been shown that the behaviour of *S.* Typhimurium strains LT2 and 14028, in regards to AI-2 production, was altered when grown in the presence of glucose. Growth in LB + 0.5% glucose leads to maximum extracellular concentrations of AI-2 (Surette and Bassler, 1998; Taga *et al.*, 2003). *S.* Typhimurium SL1344 was tested for a similar behaviour.

The timings of the growth phases of the wild type and *luxS* mutant were similar at 37°C, in both LB and LB + 0.5% glucose (Figure 3.1). The first 60 minutes of growth represents the lag phase of the culture. At this point there is only a small increase in the optical density at 600nm because, while cell mass increases as cells adapt to the new environment and grow, limited division takes place. The exponential phase, which sees a large increase in the optical density of the culture as cell density increases due to rapid division, occurs between 1 to 4 hours. The growth rate of the cultures during this phase is shown in Figure 3.1C. The presence of glucose in the growth medium is shown to increase the growth rate of both the parent and mutant; however, there is little difference in the growth rate between wild type and *luxS* in either media. By approximately 4 hours cells have entered the stationary phase of growth, characterised by small increments in OD_{600} readings as a constant cell density is reached. At this point the rate of cell division becomes proportional to the rate of cell death. The stationary phase is maintained until the end of the experiment at 8 hours.

Figure 3.1 Growth of *S.* Typhimurium SL1344 wild type and *luxS*. The growth curves of wild type (wt, ■) and *luxS* deletion mutant (Δ) in LB (A) and LB + 0.5% glucose (B) are shown with the corresponding growth rates for the parent and mutant strain during the exponential phase of growth (C). Results are the average of three independent experiments ± standard error of the mean (sem).

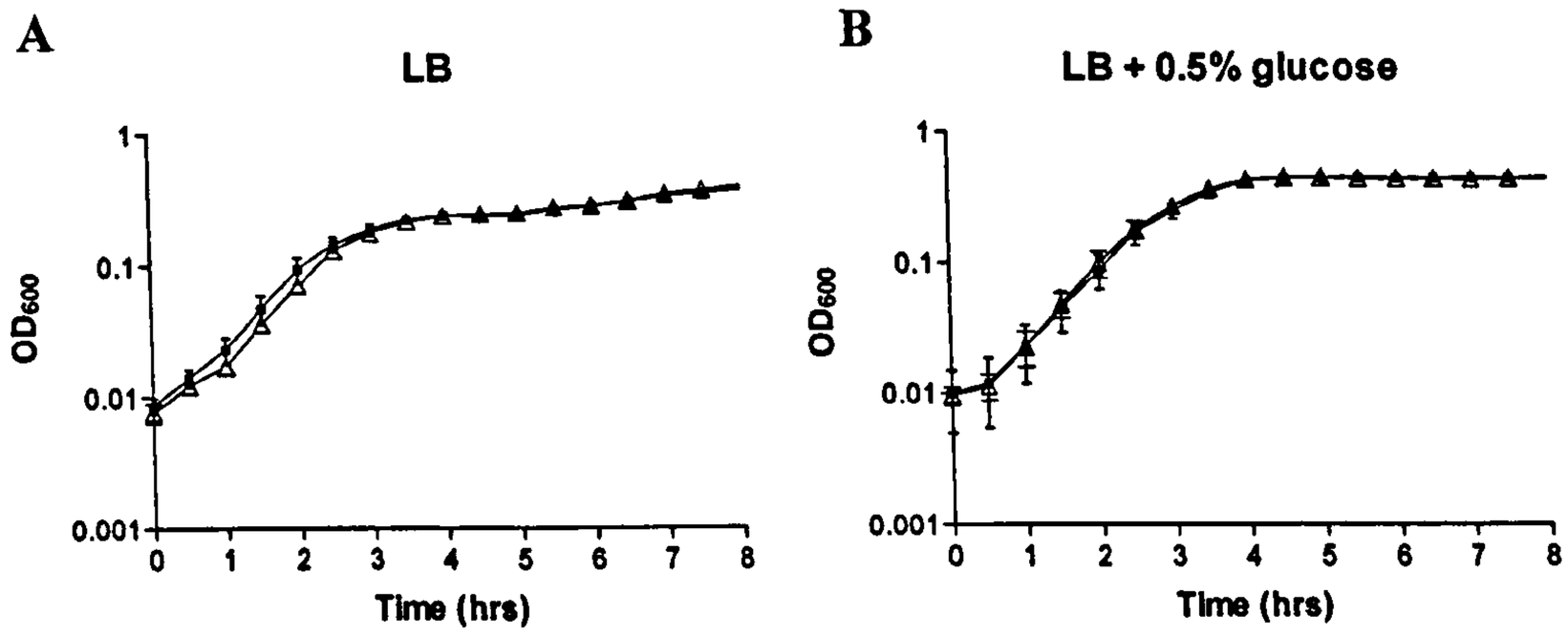

C

	Growth rate (hr^{-1})	
	LB	LB + 0.5% Glucose
wt	1.330 ± 0.052	1.446 ± 0.178
luxS⁻	1.314 ± 0.013	1.438 ± 0.041

Figure 3.2 Autoinducer-2 production by SL1344 wt and *luxS*. *S.* Typhimurium SL1344 wild type (■) and the *luxS* deletion mutant (Δ) were grown in LB (A) or LB + 0.5% glucose (B) at 37°C for 6 hours. At appropriate time points, samples were removed and the AI-2 concentration measured as described in Materials and Methods. Three independent experiments were performed with duplicate readings of the AI-2 concentration being taken. These results show the mean ± sem for one representative experiment.

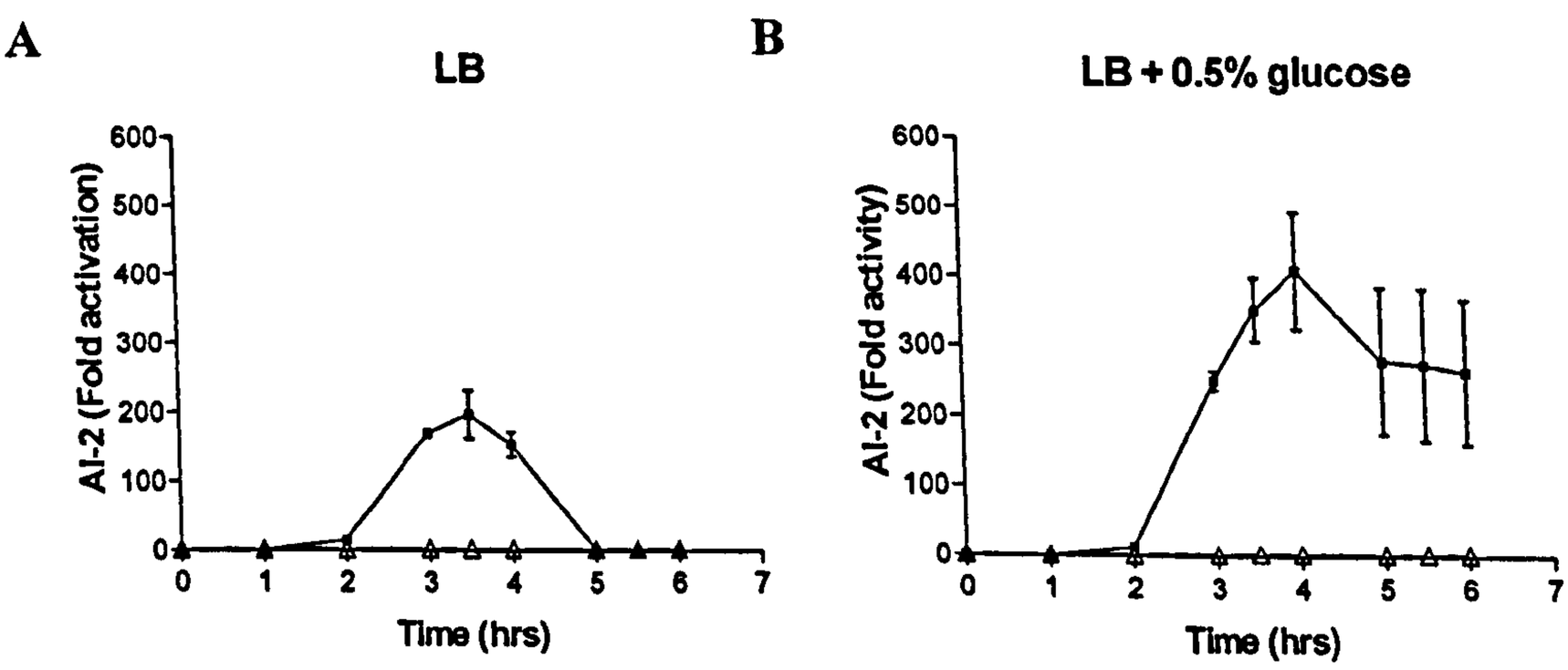

From the growth curves and growth rate data there was no indication of a difference in the growth of the parent and *luxS*⁻ mutant, therefore the presence of autoinducer-2 in the cell culture medium was determined over the growth curve. The parent strain and mutant were grown in LB or LB + 0.5% glucose for 6 hours. At specific time points, cell-free samples of the culture were prepared and stored at -80°C. A *Vibrio harveyi* bioassay performed by Dr K. Winzer at the University of Nottingham was used to quantify the amount of AI-2 present. Figure 3.2 shows the results of this assay.

For growth in LB (Figure 3.2A) there is no AI-2 present in the wild type culture for the first hour after sub-culturing which corresponds to the lag phase in the growth curve, where limited population growth occurs. As wild type bacteria enter the exponential phase of growth the concentration of AI-2 starts to increase until it reaches a peak between 3 and 3.5 hours, a time point in the mid to late exponential phase of growth. After the peak at 3 hours, the concentration of AI-2 in the wild type culture media decreases until at approximately 5 hours no AI-2 remains. A similar trend is seen for the wild type in LB + 0.5% glucose (Figure 3.2B). However, there are two differences. First, the maximum concentration of AI-2 is higher, which probably corresponds to the slightly higher growth rate seen in LB + 0.5% glucose (Figure 3.1C). Second, when the concentration of AI-2 decreases, it occurs at a much slower rate than when the wild type is grown in LB. This means by 6 hours the concentration of AI-2 is still relatively high; approximately the same concentration as the maximum concentration achieved for growth in LB.

In LB and LB + 0.5% glucose there is no AI-2 production by the *luxS* deletion mutant (Figure 3.2A and B). This was expected, as SL1344 *luxS*⁻ lacks AI-2 synthase, one of the enzymes required to synthesise the AI-2 signal. The behaviour of SL1344 wild type and the *luxS* mutant in regards to AI-2 production was analogous to that reported for strains LT2 and 14028 (Surrette & Bassler, 1998; Taga *et al.*, 2003).

3.3.2. Preliminary comparisons of ruffling and invasion of Madin-Darby Canine Kidney cells by SL1344 wild type and *luxS*⁻

An initial measurement of whether quorum sensing has an effect on the virulence of *Salmonella* was made by comparing the abilities of SL1344 wild type and the *luxS*⁻ mutant to invade and induce ruffling in Madin-Darby Canine Kidney (MDCK) cells. The ability to produce membrane ruffles was assessed using TRITC-phalloidin staining of actin, while invasion was quantified using differential immunocytochemical staining of adhered and total cell-associated *Salmonella* (Figure 3.3). 3.5 hour and 6 hour *Salmonella* cultures were selected for infection of the MDCK monolayer. A 3.5 hour culture represents *Salmonella* in the late log phase of growth (Figures 3.1), and is the point at which there is a relatively high concentration of autoinducer-2 in the wild type culture medium, while there is no AI-2 present in the *luxS*⁻ mutant culture (Figure 3.2). 6 hours represents *Salmonella* in the stationary phase of growth (Figure3.1), with little or no AI-2 present in either the wild type or *luxS*⁻ mutant culture (Figure 3.2).

For the 3.5 hour cultures, the *luxS*⁻ mutant seemed to have slightly greater ability to induce ruffling and invade cells after 15 minutes of infection compared with the SL1344 wild type (Figure 3.4). For example there is an average of 4.471 ± 1.014 *luxS*⁻ bacteria that have invaded per cell after a 15 minute infection, compared to 3.422 ± 0.849 wild type bacteria. However, the *luxS*⁻ mutant inducing higher levels of ruffling and invasion compared to the wild type was not observed in all experiments, and therefore no significant difference was found between the wild type and mutant. For 6 hour cultures there was no difference observed between wild type and *luxS*⁻, either in the number of ruffles per cell or the number of bacteria that invaded per cell. Thus it appeared the ruffling and invasion behaviour of wild type and the mutant did not differ significantly.

Figure 3.3 CLSM images of MDCK I monolayers infected with *S.* Typhimurium SL1344 for 15 minutes. A) FITC-labelled *Salmonella* and TRITC-phalloidin staining of actin allows the identification and quantification of the number of membrane ruffles. B) Differential immunocytochemical staining of *Salmonella* allows the identification of surface adhered (FITC) and total cell associated (TRITC) bacteria, from which the number of invaded bacteria (the bacteria that appear red in the overlay) can be quantified. Scale bar, 10μm.

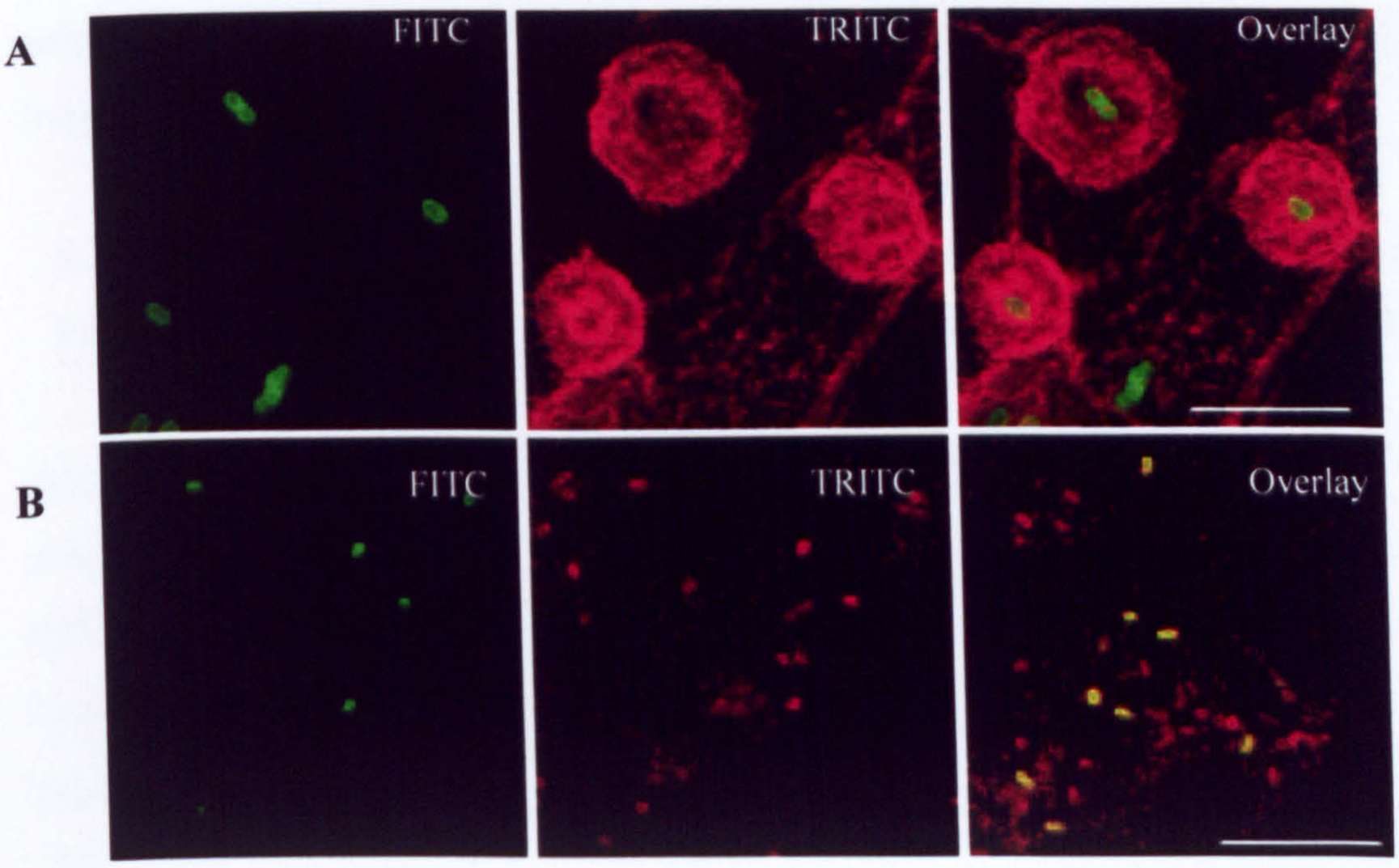

Figure 3.4 Comparison of the abilities of *S.* Typhimurium SL1344 wild type and the *luxS* mutant to A) induce ruffling in, and B) invade MDCK cells. Infection was for 15 minutes. *S.* Typhimurium invasion and associated membrane ruffles were counted in randomly selected microscope fields and expressed as numbers per MDCK cell. Results are the mean of five independent experiments ± standard error of the mean.

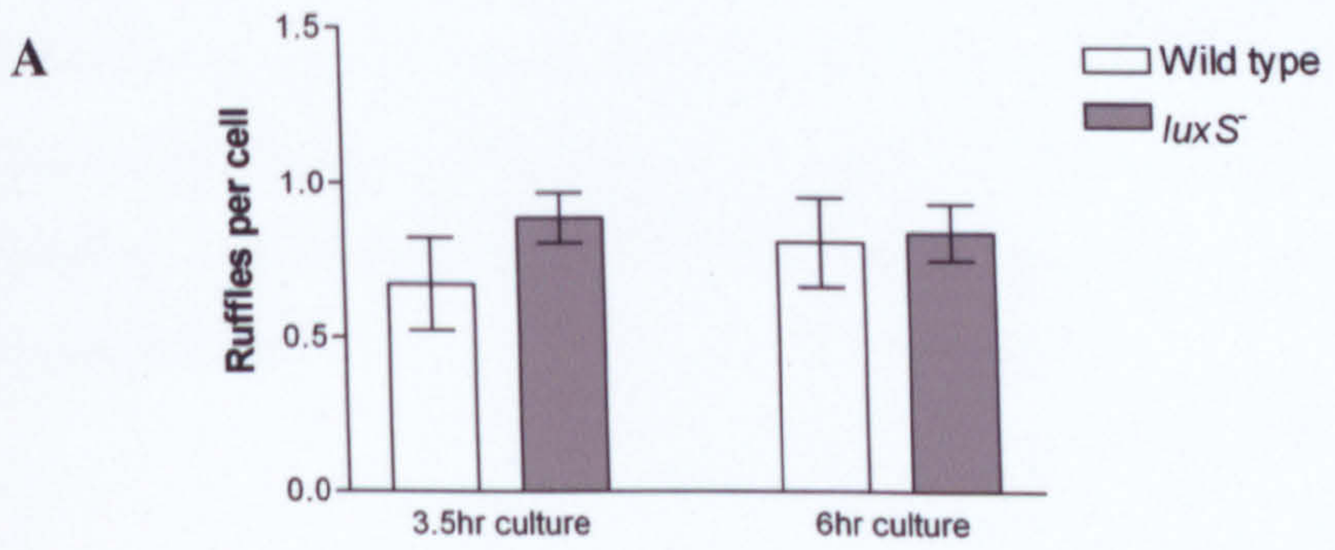

When comparing the 3.5 hour wild type culture against the 6 hour wild type culture for either the number of ruffles formed per cell, or the number of invaded bacteria per cell there was no significant difference. The same was true when comparing the 3.5 hour *luxS*⁻ culture against the 6 hour *luxS*⁻ culture. This indicates neither the growth phase of the bacteria nor the presence/absence of AI-2 significantly affects the frequency of ruffle induction or invasion.

3.3.3. Initial comparisons of the time course of membrane ruffle initiation by SL1344 wild type and its isogenic *luxS* mutant at 37°C

Despite the small difference in the number of ruffles induced or invasion at a single time point, it remained possible that the kinetics of ruffle induction might differ between wild type and the *luxS*⁻ mutant. Therefore time-lapse phase-contrast microscopy was also employed to compare the early interaction of the parent and mutant with MDCK cells. Appendix III contains examples of the movies generated using this technique, while Figure 3.5 shows the phase-contrast stills from a representative movie (Appendix III, movie A4) of a single bacterium interacting with MDCK cells: from adherence of the bacterium to the cell surface, to its invasion and the subsequent disappearance of the membrane ruffle. While Figure 3.5 shows the ruffle generated by a *luxS*⁻ bacterium, the process of ruffle generation appears very similar for the wild type and *luxS* mutant, with the bacterium maintaining a central position during the propagation and development of the ruffle, and with no noticeable difference in the size or morphology of the ruffles (Figure 3.6).

Figure 3.5 Use of time-lapse phase-contrast microscopy to examine membrane ruffle propagation and development. Phase-contrast images of a representative membrane ruffle generated by *S.* Typhimurium SL1344 (*luxS* deletion mutant) in MDCK I epithelial cells is shown. The movie from which the frames were taken is located in Appendix III (Movie A-4). Images were captured at 10 second intervals. Timestamps on each image indicate relative time compared to the first image in which this bacterium attached to cells (0s). Scale bar, 5μm.

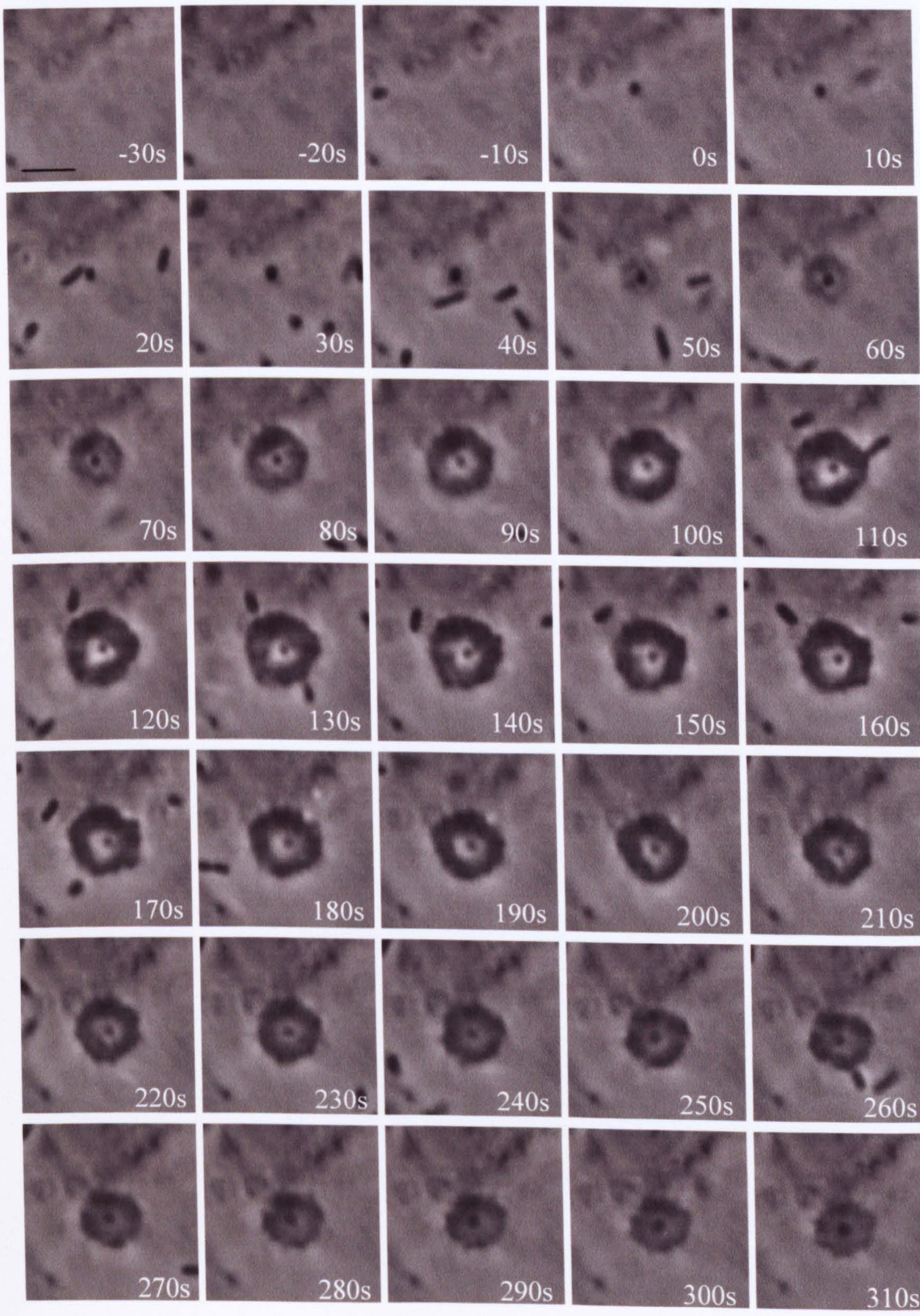

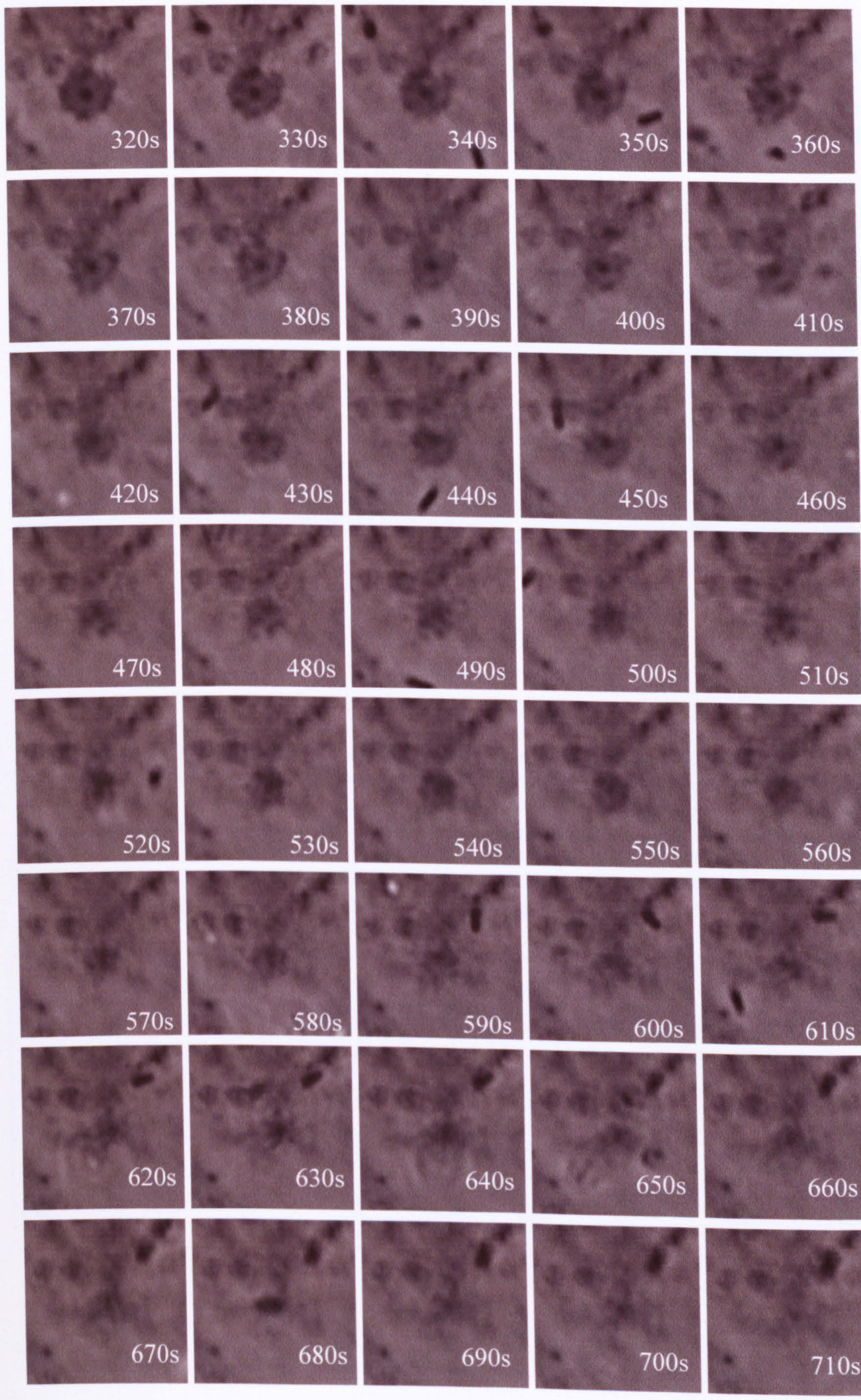
320s
330s
340s
350s
360s
370s
380s
390s
400s
410s
420s
430s
440s
450s
460s
470s
480s
490s
500s
510s
520s
530s
540s
550s
560s
570s
580s
590s
600s
610s
620s
630s
640s
650s
660s
670s
680s
690s
700s
710s

Figure 3.6 Phase-contrast images of representative membrane ruffles generated by *S.* Typhimurium SL1344 wild type (A) and *luxS* deletion mutant (B) in MDCK epithelial cells. Each image shows the maximum size achieved by the ruffle under observation. Each ruffle image was taken from a separate movie from three individual experiments. Note the central position of the bacterium in the ruffle and the circular nature of the ruffles. Scale bar 5μm.

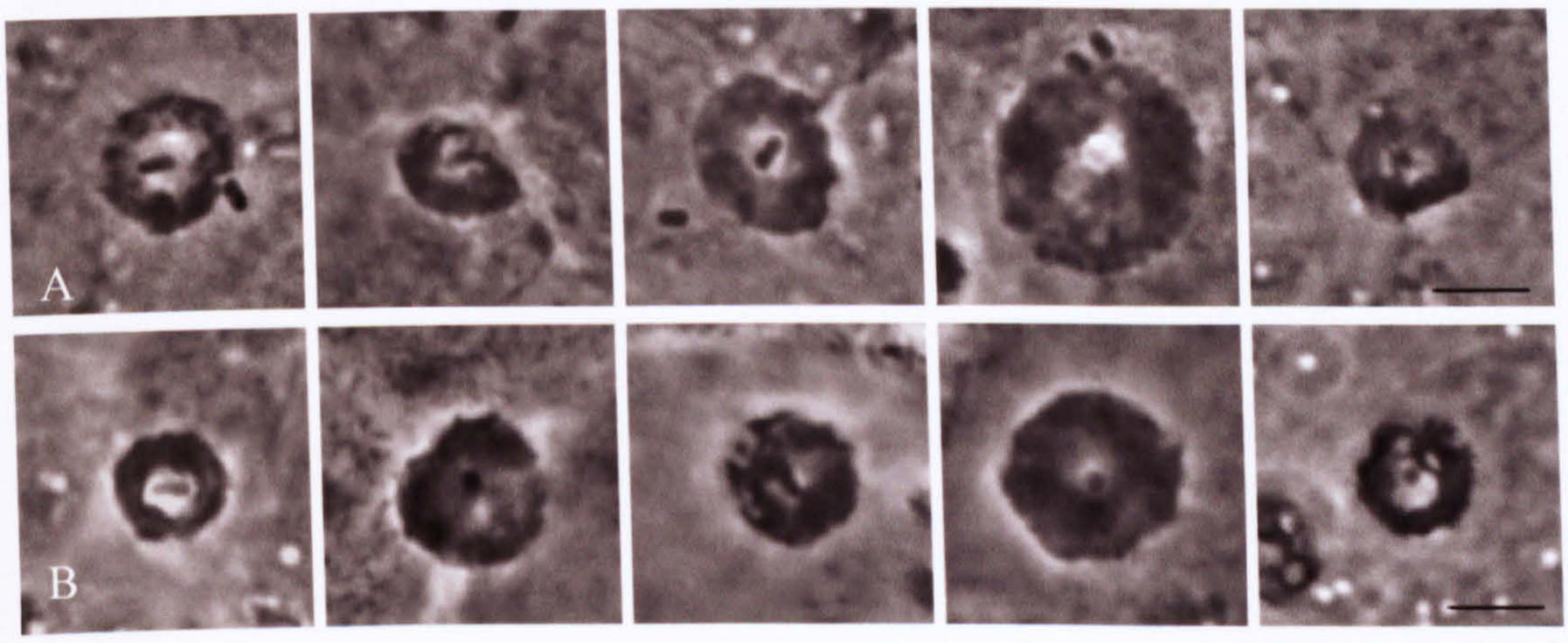

Table 3.2 Comparisons of the time taken for membrane ruffle initiation after bacterial adherence by wild type (wt) and *luxS*⁻ *S.* Typhimurium SL1344 grown for 3.5 hours in LB or LB + 0.5% glucose. The time interval between bacterial binding to MDCK cells and induction of membrane ruffling was obtained from phase-contrast video microscopy. Data expressed as medians with the number of productive bacterial-cell interactions analysed (n), and the minimum (min.) and maximum (max.) time intervals measured. Asterisk denotes a statistically significant difference between mutant and wild type assessed by the Mann Whitney U test, at a level of $P<0.001$.

	LB				**LB + 0.5% Glucose**			
	Ruffle induction time after adherence (s)				Ruffle induction time after adherence (s)			
	n	**Median**	Min.	Max.	n	**Median**	Min.	Max.
wt	508	**60**	10	780	226	**50**	10	540
luxS⁻	508	**40***	10	410	221	**30***	10	380

The precise dynamics of the process of ruffling for both wild type and *luxS*⁻ was quantified by measuring for all bacteria in a randomly selected field, the time interval between bacterial adherence to the cell surface and the induction of membrane ruffling. This data does not have a normal distribution, so the median time interval is used to compare the parent and mutant, with non-parametric statistical tests being applied to test for statistical differences.

When comparing 3.5 hour cultures of SL1344 wild type and the *luxS* deletion mutant in this way, the median time interval between bacterial binding and induction of membrane ruffling was 60 seconds for SL1344 wild type, compared to 40 seconds for *luxS*⁻ mutant (Table 3.2). This was a significant reduction in the time from adherence to membrane ruffling for the *luxS*⁻ mutant ($P<0.001$). A similar trend was found when the bacteria were grown in LB + 0.5% glucose ($P<0.001$), although for both wild type and mutant, growth in this media reduced the ruffle induction time after bacterial adhesion by 10 seconds (Table 3.2).

From the bacterial-cell interactions studied in Table 3.2, measurements were made of the numbers of bacteria inducing ruffling within a specific time period after adherence. The results are shown in Figure 3.7. For cultures grown in LB, ~60% of wild type bacteria induce ruffle formation within 60 seconds after adherence, while 75% of the *luxS*⁻ population has induced ruffling within this time interval. By two minutes 80% and 90% of the populations have induced ruffling respectively, and by 4 minutes (data not shown) nearly all the bacteria from either population are associated with ruffles. The trend seen in LB is similar to that for growth in LB + 0.5% glucose (Figure 3.7B). ~70% of wild type bacteria and 86% of the *luxS* deletion mutant have induced ruffle formation within 60 seconds of adherence, which rises to 91% and 95% respectively by 2 minutes (Figure 3.7B), and 99% for wild type and mutant by 4 minutes (data not shown). This data illustrates that the process of invasion occurs rapidly after adherence to the cell surface, is not affected greatly by the media in which growth occurs, and that for bacteria that do not produce AI-2, the bacterial population on average induce ruffles after adherence more rapidly, which accounts for the shorter median time interval between adherence and ruffle induction reported in Table 3.2.

Figure 3.7 Comparison of the proportion of SL1344 wild type and *luxS* deletion mutant bacteria inducing ruffle formation within 10 second time intervals after bacterial adherence to the cell surface. Data is for 3.5 hour cultures grown in LB (A) and LB + 0.5% glucose (B). Data from the experiments presented in Table 3.2 were pooled and the cumulative total of bacteria ruffling within each 10 second time period was calculated. These figures are expressed here as a proportion of the total population.

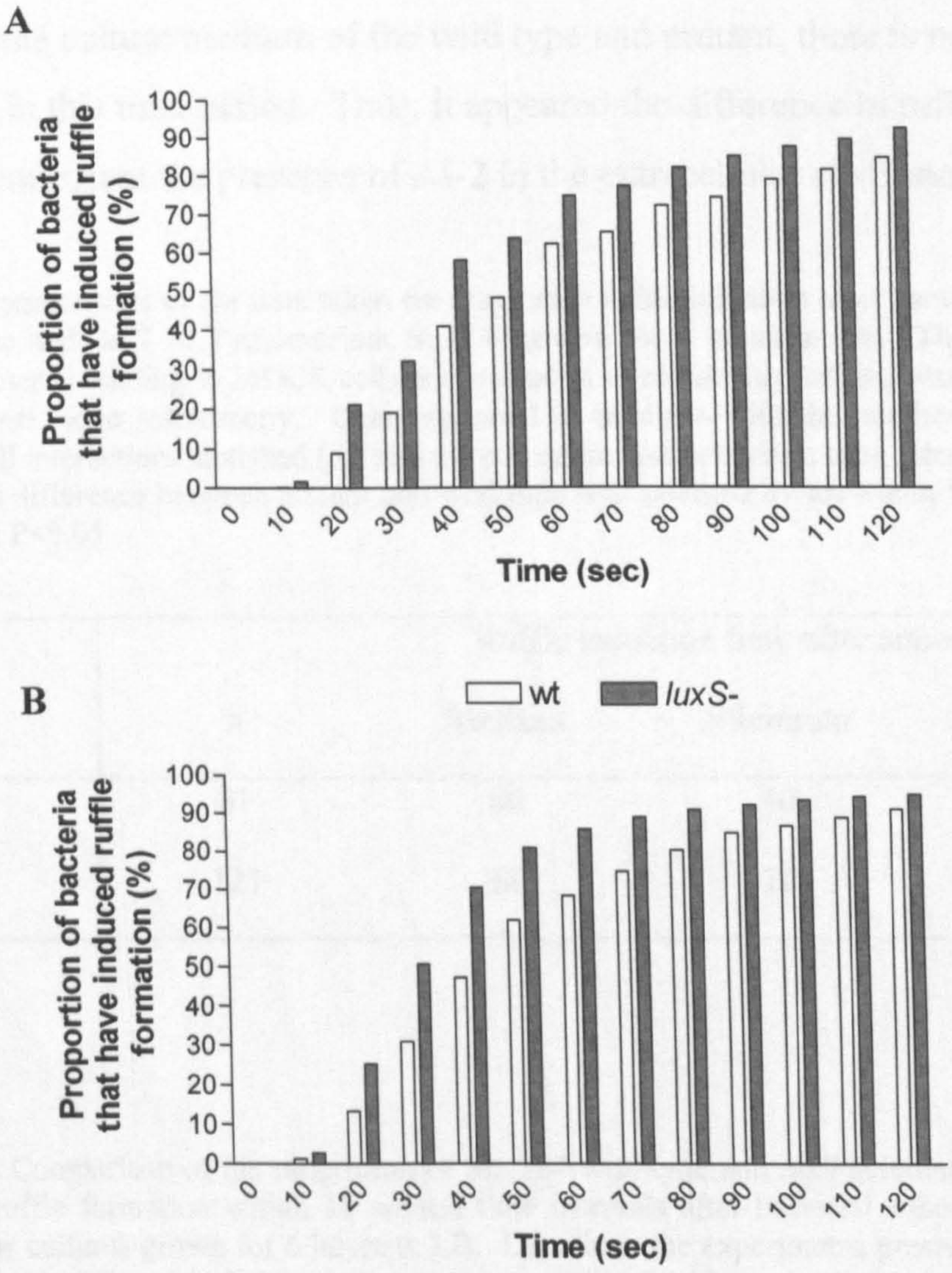

6 hour cultures grown in LB were also examined using phase-contrast time-lapse microscopy. Although the median time interval between bacterial binding and induction of membrane ruffling was 60 seconds for SL1344 wild type, compared to 50 seconds for the *luxS* mutant, no significant difference was found between the wild type and *luxS* mutant (Table 3.3). Certainly, when the wild type and mutants are compared for the proportion of bacteria that have induced ruffling within certain time periods after adhesion, the graphs produced are very similar, and indeed almost overlap (Figure 3.8).

The 6 hour data was interesting because at 3.5 hours when there was a relatively high concentration of AI-2 in the wild type culture and none present in the *luxS*⁻ culture, there was a significant difference in the median time it took to induce ruffling after adhesion, while at 6 hours where there is very little, if any, AI-2 present in the culture medium of the wild type and mutant, there is no significant difference in this time period. Thus, it appeared the difference in ruffle induction time was consistent the presence of AI-2 in the extracellular environment.

Table 3.3 Comparisons of the time taken for membrane ruffle initiation after bacterial adherence by wild type and *luxS*⁻ *S.* Typhimurium SL1344 grown for 6 hours in LB. The time interval between bacterial binding to MDCK cells and induction of membrane ruffling was obtained from phase-contrast video microscopy. Data expressed as medians with the number of productive bacterial-cell interactions analysed (n), and the minimum and maximum time intervals measured. A statistical difference between mutant and wild type was assessed by the Mann Whitney U test, at a level of $P<0.05$

	Ruffle induction time after adherence (s)			
	n	**Median**	Minimum	Maximum
wt	81	**60**	10	230
luxS⁻	121	**50**	10	340

Figure 3.8 Comparison of the proportion of SL1344 wild type and *luxS* deletion mutant bacteria inducing ruffle formation within 10 second time intervals after bacterial adherence to the cell surface, for cultures grown for 6 hours in LB. Data from the experiments presented in Table 3.3 were pooled and the cumulative total of bacteria ruffling within each 10 second time period was calculated. These figures are expressed here as a proportion of the total population.

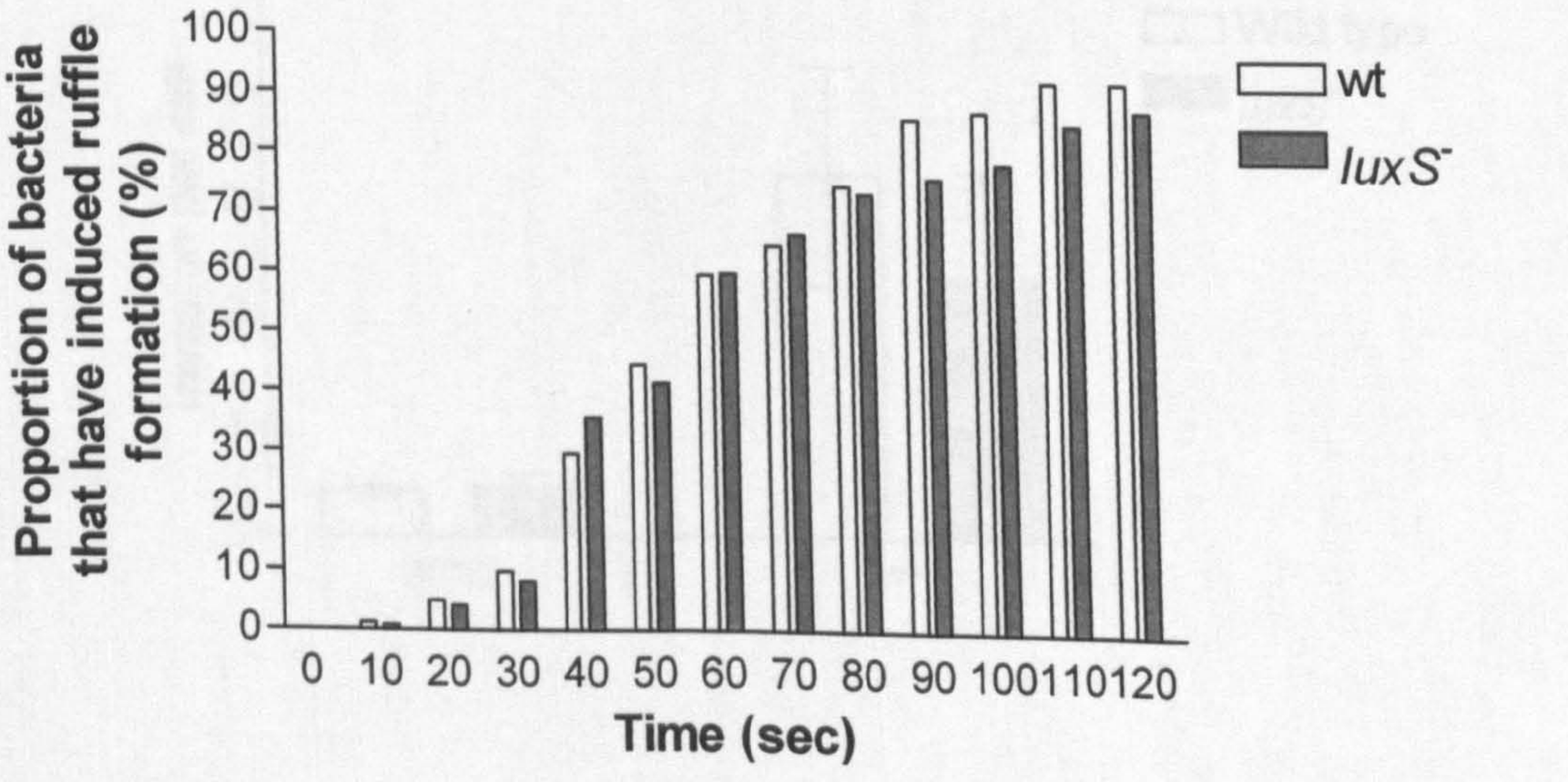

3.3.4. Comparisons of the time course of membrane ruffle initiation by SL1344 wild type and its isogenic *luxS* deletion mutant at 30°C

To investigate additional effects the lack of AI-2 production may have on *Salmonella* pathogenesis, it was decided to compare the invasion and ruffling behaviour of the wild type and *luxS*⁻ mutant at 30°C. The motivation for this investigation came from microarray data which suggested SPI-1 was upregulated in the *luxS* mutant at 30°C (Dr C. M. A. Khan, unpublished data). This indicated temperature may have an additional effect to quorum sensing on the regulation of pathogenicity.

Figure 3.9 Comparison of the abilities of SL1344 wild type and the *luxS*⁻ mutant to A) induce ruffling in, and B) invade MDCK cells at 30°C or 37°C. Infection was for 15 minutes. *S.* Typhimurium invasion and associated membrane ruffles were counted in randomly selected microscope fields and expressed as numbers per MDCK cell. Results are the mean of one experiment with four replicas ± standard error of the mean.

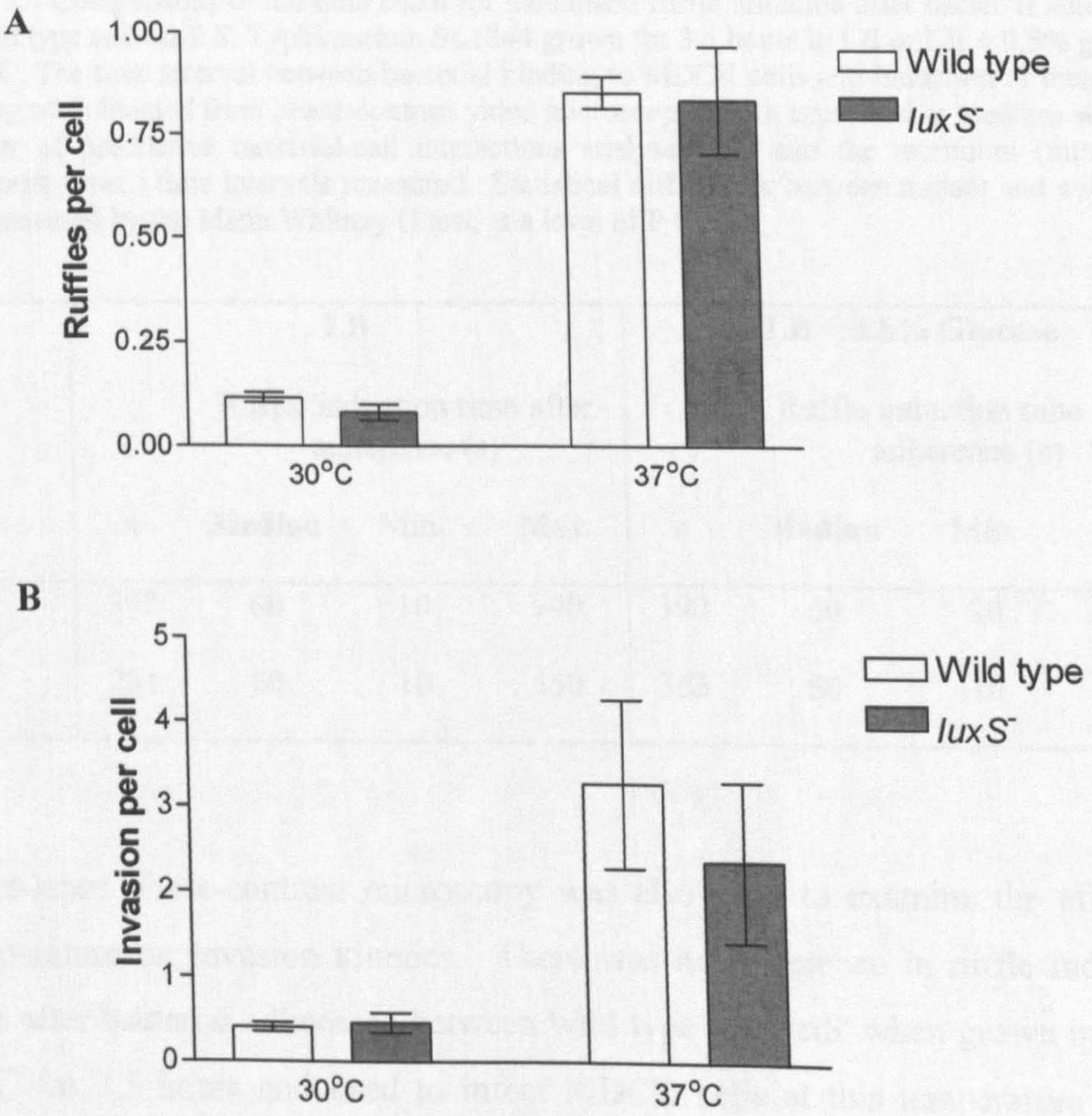

Initially, TRITC-phalloidin staining of actin and differential immunocytochemical staining of adhered and total cell-associated *Salmonella* were used to make comparisons between the wild type and *luxS*⁻ strain. In the same experiment, log phase cultures of both strains grown in LB at 30°C were used to infect MDCK cells for 15 minutes at 30°C, and log phase cultures grown at 37°C were used to infect MDCK cells for 15 minutes at 37°C (Figure 3.9). No difference was found in the number of ruffles per cell or the number of invaded bacteria per cell when comparing the SL1344 wild type with the *luxS* deletion mutant at either 30°C or 37°C. However, when comparing the behaviour of wild type at 30°C to wild type at 37°C there was a significant difference in the number of ruffles per cell and in the number of bacteria invaded per cell ($P<0.001$). The same was true when comparing the *luxS*⁻ mutant at 30°C and 37°C ($P<0.05$), and indicates the virulence of *Salmonella* is affected by temperature.

Table 3.4 Comparisons of the time taken for membrane ruffle initiation after bacterial adherence by wild type and *luxS*⁻ *S.* Typhimurium SL1344 grown for 3.5 hours in LB or LB + 0.5% glucose at 30°C. The time interval between bacterial binding to MDCK cells and induction of membrane ruffling was obtained from phase-contrast video microscopy. Data expressed as medians with the number of productive bacterial-cell interactions analysed (n), and the minimum (min.) and maximum (max.) time intervals measured. Statistical differences between mutant and wild type were assessed by the Mann Whitney U test, at a level of $P<0.05$.

	LB				**LB + 0.5% Glucose**			
	Ruffle induction time after adherence (s)				Ruffle induction time after adherence (s)			
	n	**Median**	Min.	Max.	n	**Median**	Min.	Max.
wt	302	**60**	10	940	390	**50**	20	670
luxS⁻	251	**60**	10	550	363	**50**	10	520

Time-lapse phase-contrast microscopy was also used to examine the effect of temperature on invasion kinetics. There was no difference in ruffle induction time after bacterial adherence between wild type and *luxS*⁻ when grown in LB at 30°C for 3.5 hours and used to infect MDCK cells at this temperature (Table 3.4). When the cultures used to infect MDCK cells were grown in LB + 0.5% glucose at 30°C, there was also no difference in the time interval between

adhesion and ruffle induction between wild type and *luxS*. As had been seen at 37°C, growth in the presence of glucose reduced the median time interval for ruffle induction by 10 seconds for both wild type and *luxS*. Together the immunocytochemical staining and time-lapse microscopy data suggest little difference between the SL1344 parent and its isogenic *luxS* deletion mutant in ruffle propagation and invasion at 30°C.

3.3.5. Comparisons of ruffling and invasion in three epithelial cell lines by SL1344 wild type, *luxS* and a *luxS* complemented mutant

To test whether the phenotypic differences that had been observed using time-lapse imaging was dependent on the absence of LuxS, a plasmid carrying the *luxS* gene was introduced into the mutant by Dr G. Moore (University of Newcastle). The complemented mutant (denoted *luxS* p*luxS*) was first compared to the wild type and mutant for ruffling and invasion ability in MDCK cells using the staining techniques previously described (Figure 3.10). The number of ruffles propagated by the wild type and *luxS* deletion mutant was similar to the numbers from preliminary experiments, with both producing approximately 1 ruffle per cell after 15 minutes infection. The complemented strain produced an equivalent number of ruffles, showing it behaved like the wild type and *luxS* mutant.

In regards to invasion, the mean number of *luxS* mutant bacteria invading cells during a 15 minute infection was slightly lower than the wild type and the complemented strain, but was shown not to be significantly different, again verifying the results from the initial analysis. To provide additional validation of the immunofluorescence technique of measuring invasion, a gentamicin protection assay was also used (Figure 3.10C). While the results of this assay also showed no difference between the three organisms, agreeing with previous observations, lower levels of bacteria (~50% less) were measured to have invaded. This may suggest gentamicin treatment was either penetrating cells or causing cell lysis leading internalised bacteria to be killed through exposure to gentamicin. Alternatively, the lower counts may be due to bacteria not recovering sufficiently from exposure to gentamicin and/or triton.

Overall these experiments served to show there was no difference in the number of ruffles generated or in the invasion rate of the parent strain compared to its isogenic mutant, and that carriage of the plasmid encoding *luxS* was not affecting virulence of the transcomplemented mutant.

Figure 3.10 Comparison of the abilities of SL1344 wild type, *luxS*⁻ mutant and *luxS*⁻ p*luxS* to induce ruffling in and invade MDCK cells. Infection was for 15 minutes. The ability to produce membrane ruffles was measured using TRITC-phalloidin staining of actin (A), while invasion was measured using differential immunocytochemical staining of adhered and total cell-associated *Salmonella* (B) and a gentamicin protection assay (C). ICS, immunocytochemical staining assay. Results are the mean of three independent experiments ± sem.

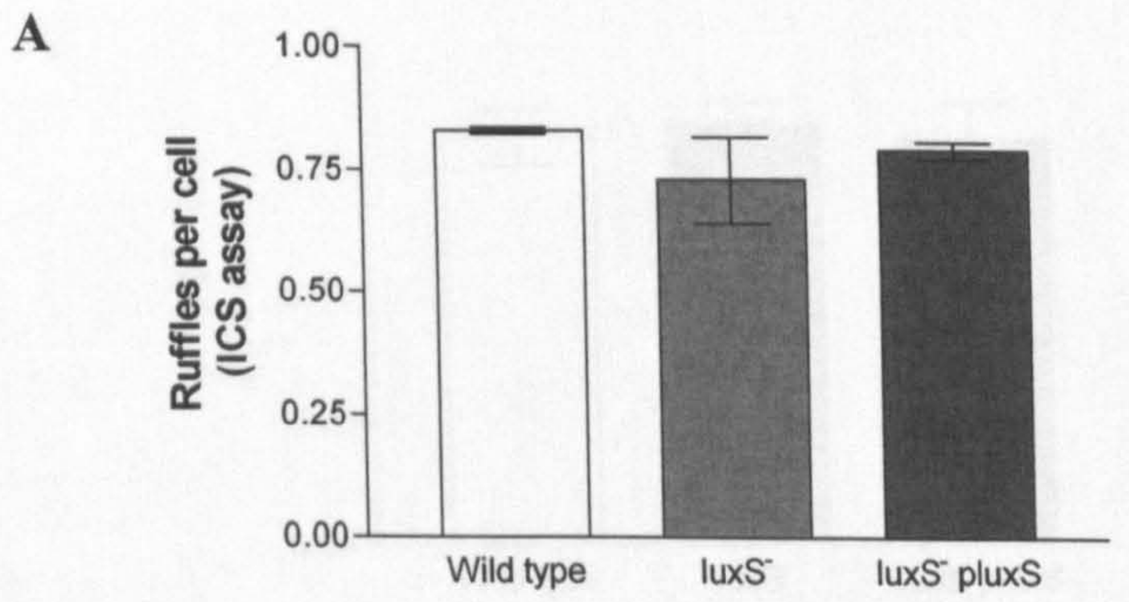

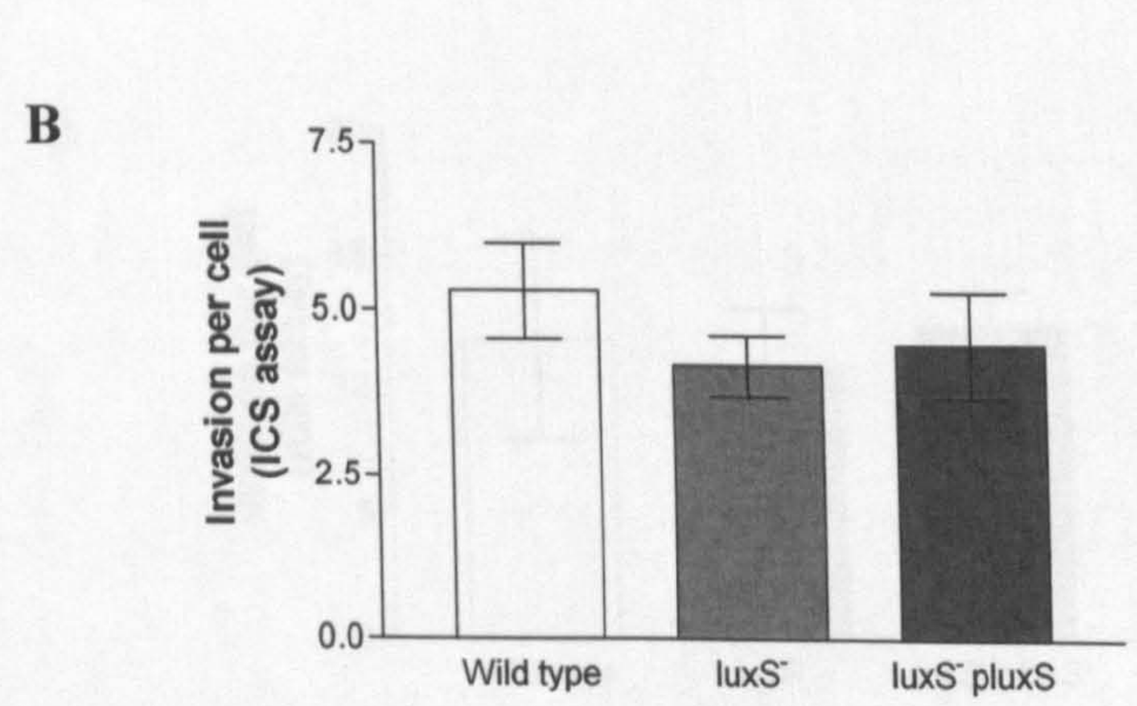

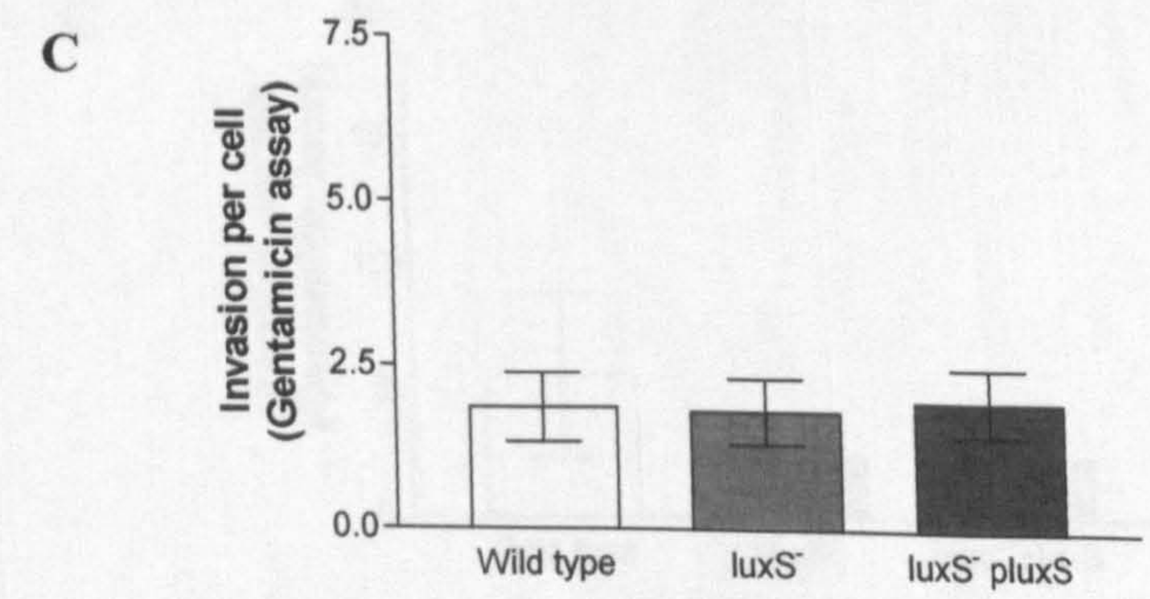

To confirm deletion of the *luxS* gene in *S.* Typhimurium does not affect its ability to form ruffles or invade these ruffles, these behaviours were measured in two additional epithelial cells lines; HeLa, a human cervical carcinoma cell line, and Caco-2, a human colon adenocarcinoma cell line.

Figure 3.11 Comparison of the abilities of SL1344 wild type, *luxS*⁻ mutant and *luxS*⁻ p*luxS* to induce ruffling in and invade HeLa cells. Infection was for 15 minutes. The ability to produce membrane ruffles was measured using TRITC-phalloidin staining of actin (A), while invasion was measured using differential immunocytochemical staining of adhered and total cell-associated *Salmonella* (B) and a gentamicin protection assay (C). ICS, immunocytochemical staining assay. Results are the mean of three independent experiments ± sem.

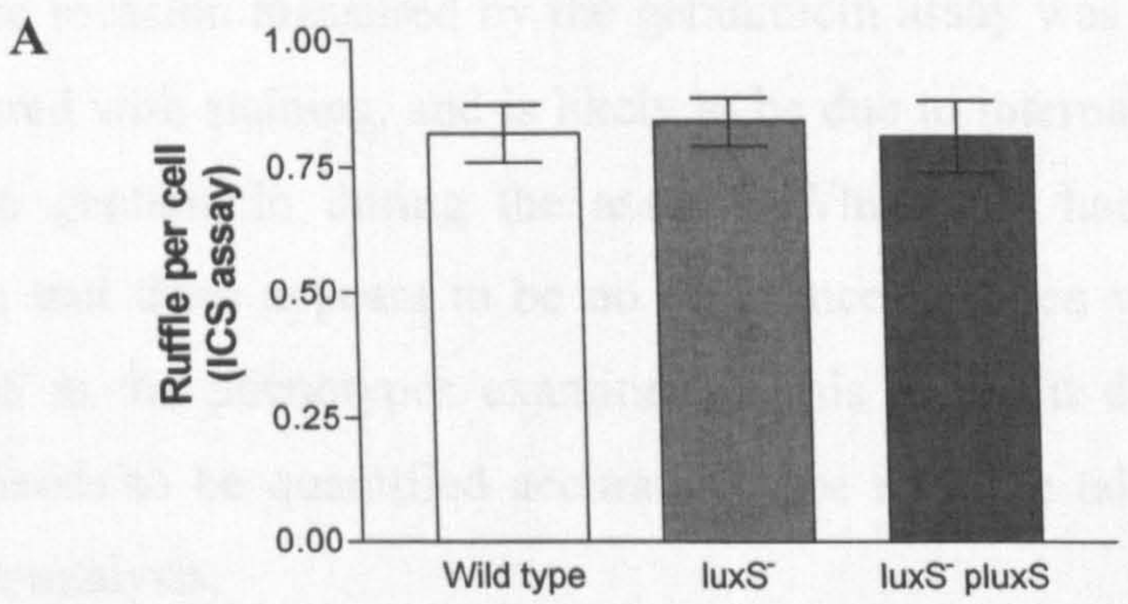

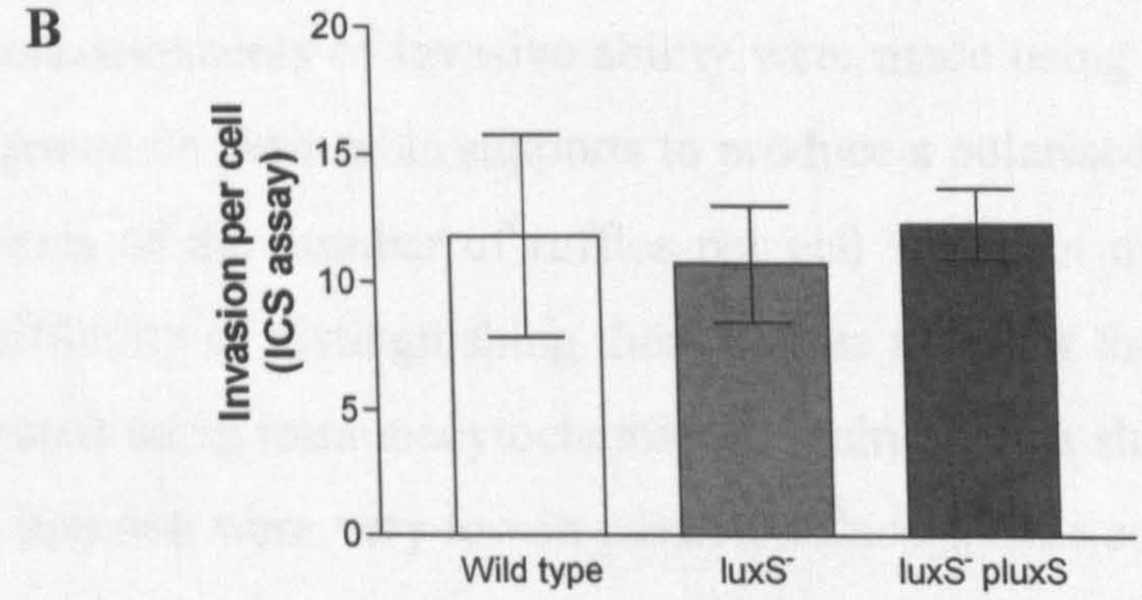

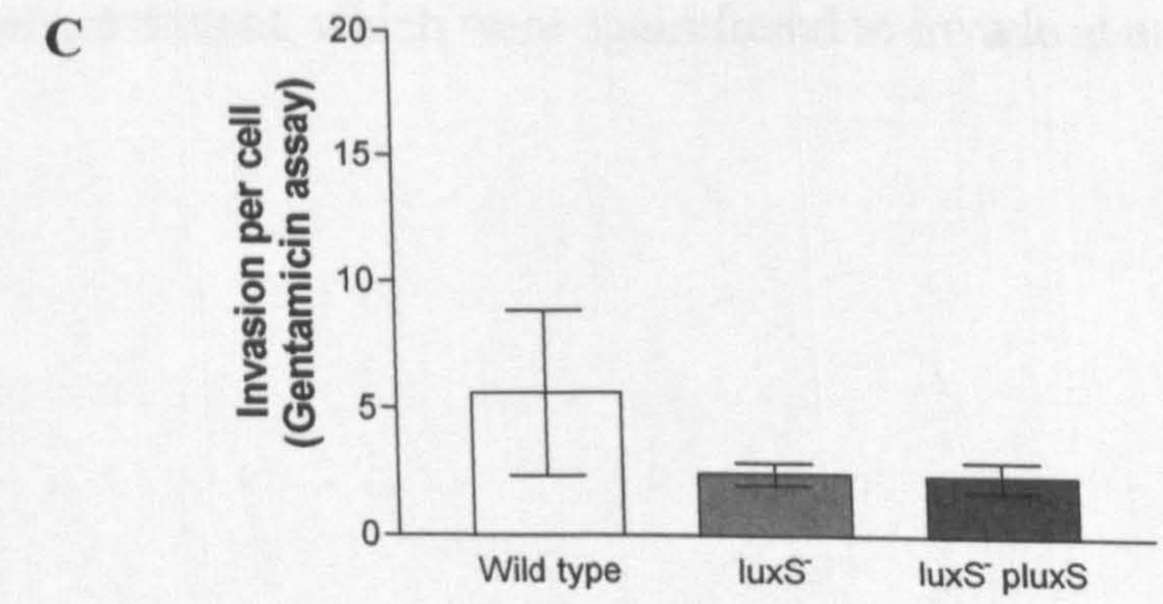

In the HeLa cell line (Figure 3.11) the number of ruffles produced per cell (~0.8) was similar to the number produced in the MDCK cell line, and again there was no difference between the wild type, *luxS*⁻ mutant and complemented strain. Invasion was analysed both by immunocytochemical staining and the gentamicin protection assay. The two methods gave very different measures of the number of bacteria that had invaded cells, for example with fluorescent microscopy the mean number of invaded *luxS*⁻ bacteria was 10.73 ± 2.25 per cell, but with the gentamicin protection assay there were only 2.45 ± 0.47 per cell. This disparity between the two methods had been noted when measuring invasion in MDCK cells, where invasion measured by the gentamicin assay was approximately half that measured with staining, and is likely to be due to internalised bacteria being exposed to gentamicin during the assay. While this had no effect on the conclusion that there appears to be no difference between wild type, *luxS*⁻ and *luxS*⁻ p*luxS* in the phenotypes examined in this study, it does indicate that if invasion needs to be quantified accurately care must be taken in choosing the method for analysis.

The final measurements of invasive ability were made using Caco-2 cells which had been grown on permeable supports to produce a polarised monolayer. While measurements of the number of ruffles per cell were not made because of the inherent difficulty of distinguishing these ruffles amongst the cells, the invasion was compared using immunocytochemical staining and is shown in Figure 3.12. Levels of invasion were very low in polarised Caco-2 cells compared to the other cell lines, with less than 0.3 bacteria per cell for the wild type, *luxS*⁻ mutant and complemented mutant, which were again found to invade at an equal rate.

Figure 3.12 Comparison of the abilities of SL1344 wild type, *luxS*⁻ mutant and *luxS*⁻ p*luxS* to invade Caco-2 cells. Infection was for 15 minutes. The ability to produce membrane ruffles was measured using TRITC-phalloidin staining of actin. Results are the mean of three independent experiments ± standard error of the mean.

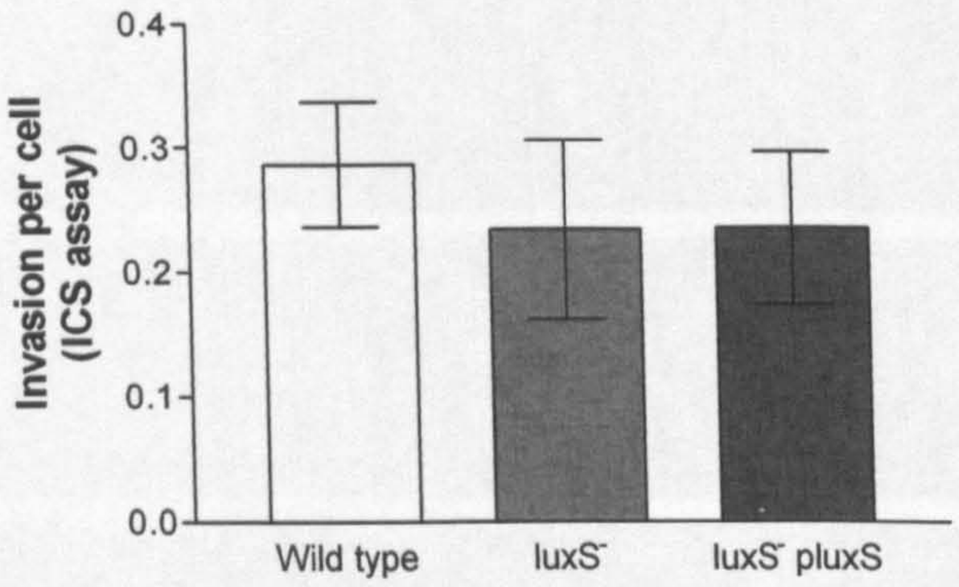

Confocal scanning microscopy was used to generate representative images of the ruffles propagated by the wild type, *luxS*⁻ mutant and complemented SL1344 in each cell line (Figure 3.13). There appear to be no real differences between the morphology of the ruffles and the position of the bacteria relative to the ruffles between wild type, *luxS*⁻ and the complemented strain. In MDCK cells and Caco-2 cells the ruffles generated by *Salmonella* are often circular in nature, while those in HeLa cells tend to be more spiky and diffuse. The HeLa ruffles more frequently have more than one bacterium associated with them. The differences in the appearance of the ruffles formed probably reflect the different nature of the epithelial cells, including their state of differentiation and polarity; HeLa cells do not polarise while MDCK cells polarise to some extent on coverslips, and Caco-2 cells fully polarise on permeable supports.

Together, the data investigating the ruffle propagation and invasion behaviour of the SL1344 parent, its isogenic *luxS* deletion mutant and plasmid complemented mutant in the three epithelial cells lines suggests lack of AI-2 production in *S.* Typhimurium SL1344 does not significantly affect its ability to invade epithelial cells.

Figure 3.13 Confocal microscope images of membrane ruffles induced by *S.* Typhimurium SL1344 wild type, *luxS*⁻, and *luxS*⁻ p*luxS* in MDCK (A), HeLa (B), and Caco-2 (C) cells. Each image shows a representative selection of TRITC-phalloidin –stained ruffles after a 15 minute infection. Each image is a single optical section. No difference in size or form is evident between populations of membrane ruffles induced by the strains. Scale bar, 5μm.

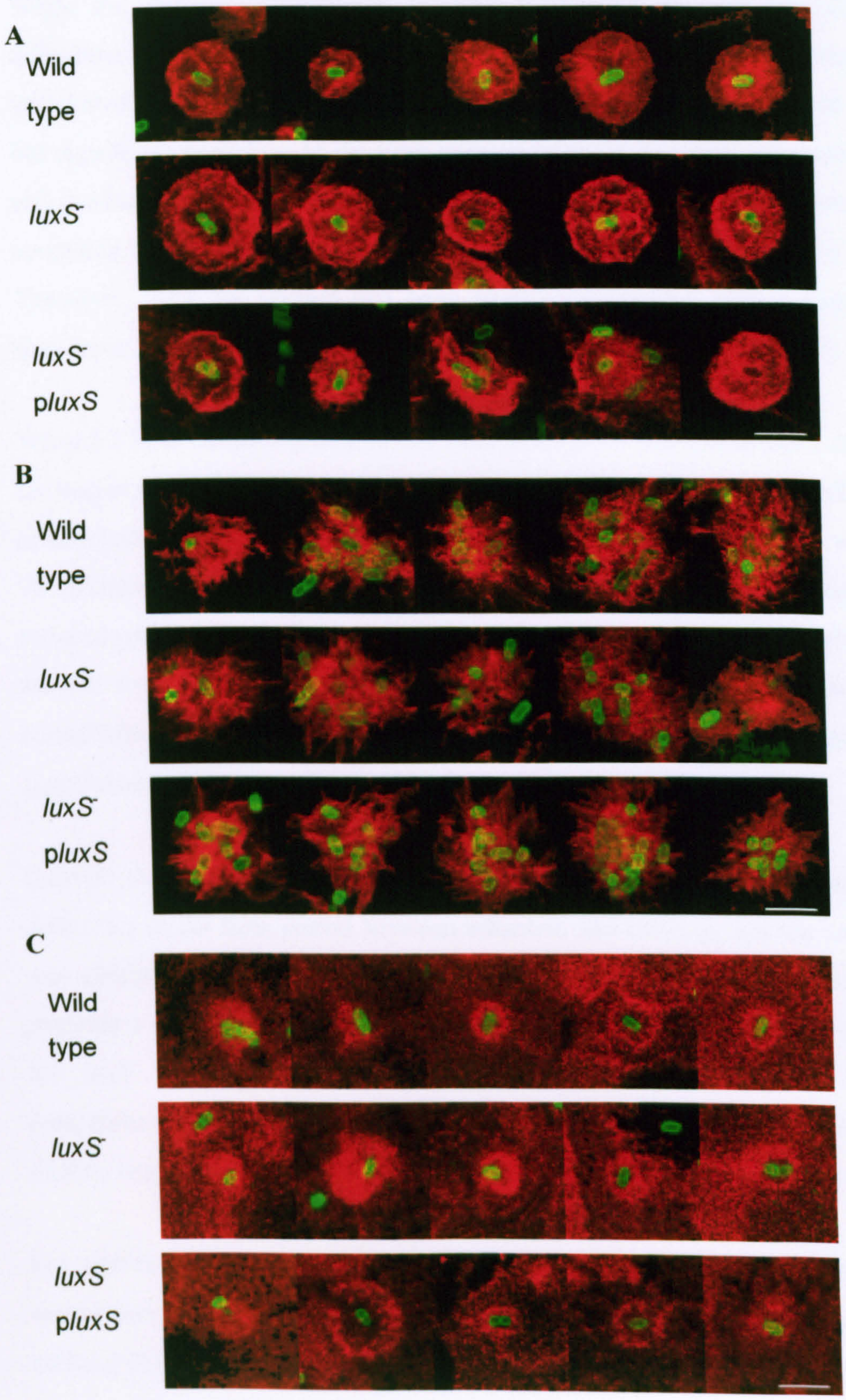

3.3.6. Comparisons of the time course of membrane ruffle initiation by SL1344 wild type, *luxS*⁻, and a *luxS*⁻ complemented mutant

While the immunocytochemical staining techniques had not identified any difference in the invasion capabilities of the wild type and *luxS*⁻ mutant, in the initial studies use of phase-contrast time-lapse microscopy had detected a subtle but significant reduction in the time interval between bacterial adherence to the cell surface and induction of ruffle formation for the *luxS* deletion mutant compared to wild type when grown for 3.5 hours in LB or LB + 0.5% glucose. Therefore, once the mutant had been transcomplemented with a plasmid the time-lapse imaging was repeated to confirm this observation (Table 3.5).

When 3.5 hour cultures grown in LB were analysed it was found that a difference no longer existed between the wild type and mutant. In fact the *luxS* deletion mutant had a median time interval that was 10 seconds greater than the wild type; 70 seconds compared to 60 seconds for the wild type, when previously it had induced ruffling faster (Table 3.5). Plasmid complementation produced the same median time interval as the wild type, showing the complemented mutant was comparable to the wild type, and like the wild type did not have a time interval significantly different to the *luxS* deletion mutant.

Cultures that had been grown for 6 hours in LB in the preliminary study had no difference in the time period between adhesion and ruffling, and the same result was obtained in this instance. The median time for a wild type bacterium to generate a ruffle after binding to the cell surface was again 60 seconds, and for the *luxS*⁻ mutant, 50 seconds (Table 3.5). The mutant that had been complemented had a median time interval of 70 seconds, so on average took slightly longer to induce ruffling, although this was not found to be significant.

For growth in LB + 0.5% glucose (Table 3.6), the wild type, *luxS*⁻ mutant and complemented strain all had a median time interval between adherence and ruffling of 50 seconds, and so as had been found for cultures grown in LB there was no difference between them. This result again conflicted with the findings of the initial study, where the *luxS* deletion mutant had a median value of 30

seconds compared to 50 seconds for the wild type, and had represented a statistically significant reduction.

Table 3.5 Comparisons of the time taken for membrane ruffle initiation after bacterial adherence by SL1344 wild type, *luxS*, and *luxS* p*luxS* for 3.5 hours and 6 hours growth in LB. The time interval between bacterial binding to MDCK cells and induction of membrane ruffling was obtained from phase-contrast video microscopy. Data expressed as medians with the number of productive bacterial-cell interactions analysed (n), and the minimum (min.) and maximum (max.) time intervals measured. Statistical differences assessed by the Kruskal Wallis test, and Dunn's Multiple Comparison Test at a level of $P<0.05$.

	LB 3.5 hours Ruffle induction time after adherence (s)				**LB 6 hours** Ruffle induction time after adherence (s)			
	n	**Median**	Min.	Max.	n	**Median**	Min.	Max.
wt	111	**60**	20	630	183	**60**	20	330
luxS	119	**70**	20	490	190	**50**	20	520
luxS p*luxS*	127	**60**	20	460	192	**70**	20	660

Table 3.6 Comparisons of the time taken for membrane ruffle initiation after bacterial adherence by SL1344 wild type, *luxS*, and *luxS* p*luxS* for 3.5 hour growth in LB+ 0.5% glucose. The time interval between bacterial binding to MDCK cells and induction of membrane ruffling was obtained from phase-contrast video microscopy. Data expressed as medians with the number of productive bacterial-cell interactions analysed (n), and the minimum (min.) and maximum (max.) time intervals measured. Statistical differences were assessed by the Kruskal Wallis test, followed by Dunn's Multiple Comparison Test at a level of $P<0.05$.

	Ruffle induction time after adherence (s)			
	n	**Median**	Minimum	Maximum
wt	87	**50**	10	230
luxS	86	**50**	10	250
luxS p*luxS*	91	**50**	20	280

3.3.7. Comparisons of the time course of membrane ruffle initiation by SL1344 wild type, *luxS*⁻, and a *luxS*⁻ complemented mutant in alternative MDCK cell lines

At this time it had been noted that the behaviour of the MDCK strain I cell line that was being used had changed. The morphology of the cells appeared altered, the cells had become more resistant to the trypsin used during sub-culturing, and the rate of growth had slowed. Although new cultures were set up from frozen stocks of these cells, the atypical behaviour persisted and experiments with these cells were terminated due to concerns of genetic drift. A new batch of MDCK strain I cells were therefore obtained and invasion of SL1344 wild type and its *luxS* deletion mutant was investigated using phase-contrast time-lapse microscopy to determine whether the cells were responsible for the different results between the initial and most recently acquired results.

In the new MDCK strain I cell line the median time interval between adherence and ruffling for wild type was 40 seconds compared to 50 seconds for the *luxS*⁻ mutant and complemented mutant. It should be noted that on this occasion the wild type induces ruffling faster than the *luxS*⁻ mutant; in the initial studies it was the *luxS*⁻ mutant which induced ruffling in a shorter time period.

Statistical tests found a significant difference to exist between the wild type and *luxS* deletion mutant. However, a statistical difference did not exist between the wild type and complemented mutant, although the latter had the same median as the *luxS*⁻ mutant, and therefore was also not statistically different from *luxS*⁻. Examining the proportions of bacteria inducing ruffling at each time point (Figure 3.14) it was found that while *luxS*⁻ p*luxS* did not differ from the wild type and *luxS*⁻ mutant in the proportion of its population that had induced ruffling at early time points i.e. ≤60 minutes, at later time points *luxS*⁻ p*luxS* had a reduced number of the population that had induced ruffling. For example, at 2 minutes 91.7% of wild type bacteria and 92.3% of *luxS*⁻ bacteria had induced ruffling compared to 84.4% of *luxS*⁻ p*luxS* bacteria. By 4 minutes (data not shown) the proportion of bacteria inducing ruffling was comparable between all three strains. This data indicates there is greater variation in ruffle induction times

post-adherence for *luxS*⁻ p*luxS* and is why no statistical significance is found between wild type and *luxS*⁻ p*luxS*, but is why there is a statistical significance between wild type and *luxS*⁻.

Table 3.7 Comparisons of the time taken for membrane ruffle initiation after bacterial adherence by SL1344 wild type, *luxS*⁻, and *luxS*⁻ p*luxS* grown for 3.5 hours in LB. The time interval between bacterial binding to MDCK cells and induction of membrane ruffling was obtained from phase-contrast video microscopy. Data expressed as medians with the number of productive bacterial-cell interactions analysed (n), and the minimum (min) and maximum (max) time intervals measured. Asterisk denotes a statistically significant difference between mutant and wild type assessed by the Kruskal Wallis test, followed by Dunn's Multiple Comparison Test at a level of $P<0.05$.

	Ruffle induction time after adherence (s)			
	n	**Median**	Minimum	Maximum
wt	180	**40**	10	520
luxS⁻	178	**50***	10	580
luxS⁻ p*luxS*	180	**50**	20	450

Figure 3.14 Comparison of the proportion of SL1344 wild type, *luxS* deletion mutant, and *luxS*⁻ p*luxS* bacteria inducing ruffle formation within 10 second time intervals after bacterial adherence to the surface of the new batch of MDCK cells. Cultures were grown for 6 hours in LB. Data from the experiments presented in Table 3.7 were pooled and the cumulative total of bacteria ruffling within each 10 second time period was calculated. These figures are expressed here as a proportion of the total population.

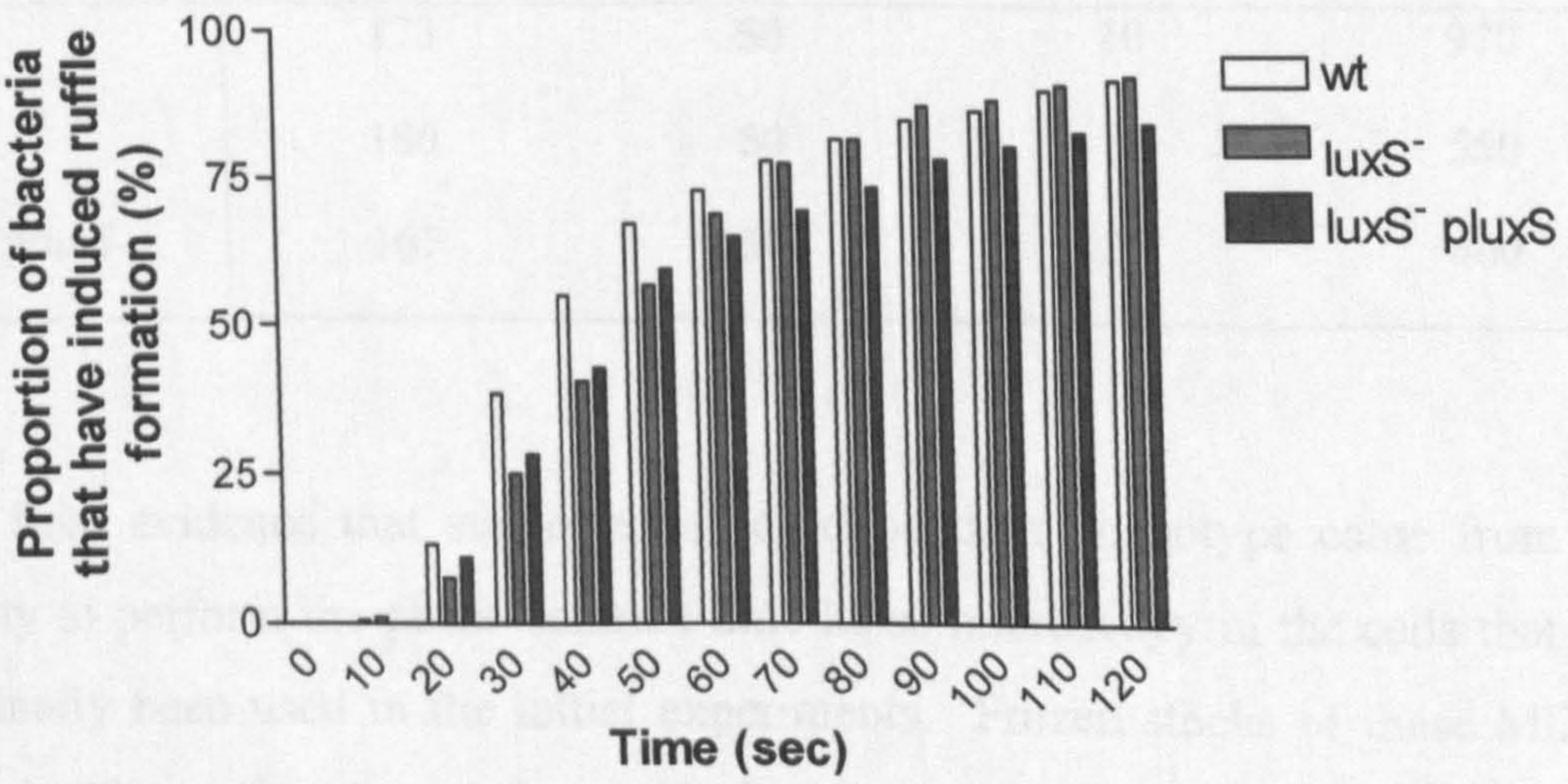

Since the data obtained in MDCK I cells when the complemented mutant had been tested alongside the wild type and *luxS*⁻ mutant (3.3.6) was similar to the data obtained in the new MDCK I cells, it suggested the difference in phenotype between wild type and the *luxS*⁻ mutant in the initial live-cell imaging experiments was due to the cells being used at that time. To further test whether the phenotype observed in the initial experiments was cell dependent, live cell imaging experiments were conducted using MDCK strain II cells.

The ruffles produced in MDCK strain II cells were morphologically similar to those generated in strain I cells, and ruffle development appeared to occur in the same manner. The median time interval for ruffle induction after adherence for wild type, the *luxS*⁻ mutant and the complemented mutant was identical at 50 seconds, indicating that loss of AI-2 production does not change the phenotype of SL1344 in regards to ruffle behaviour in this cell line.

Table 3.8 Comparisons of the time taken for membrane ruffle initiation after bacterial adherence to MDCK II cells by SL1344 wild type, *luxS*⁻, and *luxS*⁻ p*luxS* grown for 3.5 hours in LB. The time interval between bacterial binding to MDCK cells and induction of membrane ruffling was obtained from phase-contrast video microscopy. Data expressed as medians with the number of productive bacterial-cell interactions analysed (n), and the minimum and maximum time intervals measured. Significant difference between mutant and wild type assessed by the Kruskal Wallis test, followed by Dunn's Multiple Comparison Test at a level of $P<0.05$.

	Ruffle induction time after adherence (s)			
	n	**Median**	Minimum	Maximum
wt	173	**50**	10	970
luxS⁻	180	**50**	10	550
luxS⁻ p*luxS*	167	**50**	20	400

The final evidence that supported a cell-dependent phenotype came from the ability to perform the phase-contrast time-lapse microscopy in the cells that had originally been used in the initial experiments. Frozen stocks of these MDCK cells had been given to another research group who were then able to provide us with these cells. The results of experiments using the original cells (Table 3.9) showed once again that the *luxS* deletion mutant was significantly quicker in

inducing ruffle formation compared to the wild type. Dependence of this phenotypic difference on the absence of *luxS* was confirmed by plasmid complementation, which significantly increased the delay between adhesion and ruffle propagation back to wild type levels. Thus, although it is difficult to replicate the exact conditions of experiments performed in the initial study, it does appear that the SL1344 *luxS*⁻ phenotype observed was cell-dependent.

Table 3.9 Comparisons of the time taken for membrane ruffle initiation after bacterial adherence in the MDCK cells used in preliminary investigations by SL1344 wild type, *luxS*⁻, and *luxS*⁻ p*luxS* grown for 3.5 hours in LB. The time interval between bacterial binding to MDCK cells and induction of membrane ruffling was obtained from phase-contrast video microscopy. Data expressed as medians with the number of productive bacterial-cell interactions analysed (n), and the minimum and maximum time intervals measured. Asterisk denotes a statistically significant difference between mutant and wild type, and mutant and complemented assessed by the Kruskal Wallis test, followed by Dunn's Multiple Comparison Test at a level of $P<0.05$.

	Ruffle induction time after adherence (s)			
	n	**Median**	Minimum	Maximum
wt	240	**70**	10	690
luxS⁻	240	**50***	20	680
luxS⁻ p*luxS*	240	**70**	10	730

3.3.8. Comparing SPI-1 expression in SL1344 wild type, *luxS*⁻ deletion mutant, and a *luxS*⁻ complemented mutant

Alongside the use of time-lapse microscopy to decide whether there was a specific phenotype associated with a *luxS* gene deletion in regards to ruffling and invasion behaviour, the expression of *Salmonella* Pathogenicity Island-1 (SPI-1) was studied. As *Salmonella* require the expression of SPI-1 genes in order to invade epithelial cells, any difference between the wild type and *luxS*⁻ deletion mutant in the ability to induce ruffle formation may be associated with a change in the expression of SPI-1 genes in these strains. Initially, the proteins secreted by the SPI-1 type three secretion system (TTSS-1) in each of the strains were isolated from culture supernatants grown in LB at 37°C and analysed by SDS-PAGE and Western blotting. The data from these assays was qualitative since the total protein concentration of the samples was not measured and adjusted to

be equal to those of the other samples; instead these methods were used as a quick assessment of whether differences existed between the proteins secreted by wild type, *luxS*⁻ and *luxS*⁻ p*luxS*. From SDS-PAGE analysis, deletion of *luxS* did not appear to cause any change in the *S.* Typhimurium secreted protein profile; the same banding pattern was observed for wild type, *luxS*⁻ and *luxS*⁻ p*luxS*. Western blotting using SipA and SipC monoclonal antibodies (Figure 3.15) showed SipA and SipC were both secreted by wild type, *luxS*⁻ and the complemented mutant, indicating the *sip* operon was expressed in all three strains. It appeared therefore that deletion of *luxS* did not affect the ability of *S.* Typhimurium to synthesise and secrete those proteins required for epithelial invasion.

Figure 3.15 Western blot analysis of the secreted proteins of serovar Typhimurium SL1344 wild type (lane 1), *luxS*⁻ mutant (lane 2) and *luxS*⁻ p*luxS*, the transcomplemented mutant (lane 3). Culture supernatant proteins were prepared by precipitation with 10% trichloroacetic acid, separated by SDS-PAGE, transferred to a nitrocellulose membrane, and probed with anti-SipA and anti-SipC monoclonal antibodies.

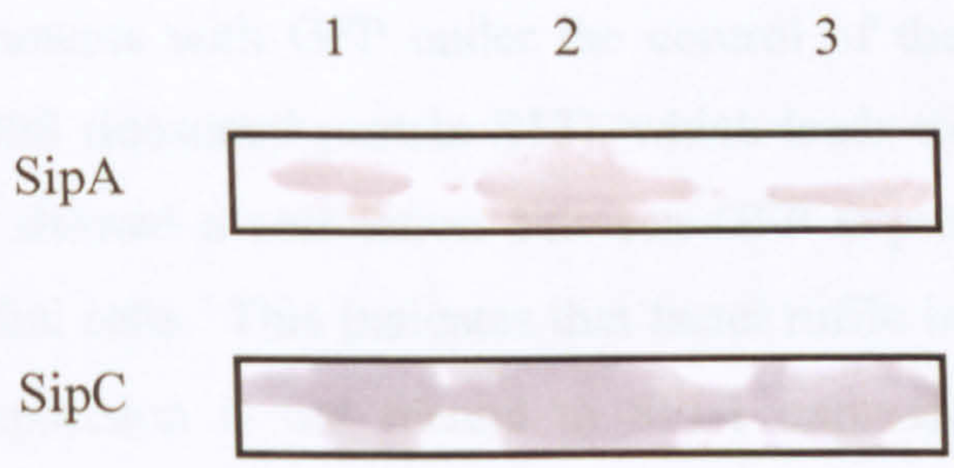

In addition to examining expression and secretion of TTSS-1 proteins, the expression of SPI-1 genes was examined in SL1344 wild type, *luxS*⁻ and the complemented mutant with *prgH* promoter::*gfp*⁺ fusions created by Dr I. Martinez–Argudo (University of Bristol). *prgH* is a gene in SPI-1 that encodes a structural component of the TTSS-1 apparatus, more specifically PrgH with PrgK forms the ring of TTSS-1 located in the inner membrane (Kimbrough and Miller, 2000; Kubori *et al.*, 1998). The *prgH* promoter may be used as a measure of SPI-1 expression (Altier *et al.*, 2000; Hautefort *et al.*, 2003), and in this case was fused with the gene *gfp*⁺, encoding a very bright form of GFP (Hautefort *et al.*, 2003). This gene fusion was inserted, using the λ red system, as a single copy in the *Salmonella* chromosome at the *putPA* locus, a site that does not affect virulence (Hautefort *et al.*, 2003).

To ensure the gene fusion had no effects on the virulence of the SL1344 wild type and *luxS*⁻ mutant, Dr I. Martinez–Argudo compared the number of ruffles per cell and the invasion per cell for a 15 minute infection in MDCK cells for wild type and the *luxS* deletion mutant with and without the *prgH*::*gfp*$^+$ fusion. The number of ruffles and invasion per cell were similar for all strains tested.

Several time-lapse microscopy experiments were also conducted with the GFP strains and led to some interesting observations. Only bacteria expressing GFP i.e. only those expressing SPI-1 interacted with MDCK cells and induced ruffling. This could suggest the SPI-1 TTSS complex may have a role in promoting initial adherence of *Salmonella* to cells, although alternatively there could be co-regulation of another factor with SPI-1 to promote adhesion. It also appeared that bacteria with higher levels of GFP expression induced ruffling quicker. Although this is consistent with higher *prgH* expression maximising invasion efficiency, an alternative mechanism may also underlie this observation. Further experiments with GFP under the control of the *rpsM* promoter (*rpsM* encodes the 30S ribosomal protein S13), which leads to constitutive expression of GFP, also showed a correlation between GFP expression and the ability to invade epithelial cells. This indicates that faster ruffle induction while related to high GFP expression is not related to SPI-1 expression and that potentially expression of GFP in *Salmonella* may have an unknown effect on processes inside the bacterium that manifest as a subtle change in virulence.

To determine if there were differences in the expression of SPI-1, fluorescence microscopy was used to measure the proportion of SL1344 *prgH*::*gfp*$^+$, SL1344 *luxS*⁻ *prgH*::*gfp*$^+$, and SL1344 *luxS*⁻ p*luxS prgH*::*gfp*$^+$ bacteria that expressed GFP after 3.5 hours growth in LB + 0.5% glucose. This growth media was used as glucose represses expression of the Lsr transporter (Taga *et al.*, 2003) leading to maximal concentrations of AI-2 in the culture media (Figure 3.2), and therefore amplifies the difference between the wild type and *luxS*⁻ mutant cultures, which may enhance the ability to observe differences. In these experiments 10 random fields of view were selected per strain and images taken from the phase-contrast and GFP fluorescence channels (Figure 3.16 A and B). The length of exposure was controlled to limit false-positive results for GFP expression. Comparison of

the number of bacteria in the GFP channel to the number of bacteria in the phase-contrast channel allowed quantification of the proportion of bacteria expressing GFP. Comparing the GFP expression of SL1344 *prgH*::*gfp*$^+$, SL1344 *luxS*$^-$ *prgH*::*gfp*$^+$, and SL1344 *luxS*$^-$ p*luxS prgH*::*gfp*$^+$ in this manner shows a difference did not exist. In all cases approximately 75% of the bacterial population were expressing GFP, and corresponds with other reports that only a subset of a *Salmonella* population expresses SPI-1 (Hautefort *et al.*, 2003).

The use of fluorescence microscopy to measure GFP expression has limitations, particularly in the number of bacteria that can be analysed this way and the risk of false-positives due to incorrect exposure times and the requirement for arbitrary thresholding. The difficulty in calibrating the threshold also makes it difficult to measure the relative GFP intensities of each bacterium, which would enable a comparison of not only how many bacteria in a population are expressing GFP, and therefore SPI-1, but a measure of how strongly these genes are being expressed and whether this differs between wild type and the *luxS*$^-$ deletion mutant. Therefore, to complement this work, flow cytometry was also employed allowing much larger numbers of bacteria to be examined and a more reliable quantitative assessment of the GFP intensity to be made.

Figure 3.16 Proportion of *S.* Typhimurium SL1344 *prgH::gfp*$^+$, *luxS*$^-$ *prgH::gfp*$^+$, and *luxS*$^-$ p*luxS* *prgH::gfp*$^+$ expressing GFP as determined by fluorescence microscopy. A shows SL1344 *prgH::gfp*$^+$ bacteria viewed by phase contrast, while B shows the same field of view when viewed by the GFP channel; note not all the bacteria viewed in A can be seen in B. Scale bar, 20μm. C shows the quantification of the number of bacteria observed that express GFP. Data represents the mean of two independent experiments in which ten individual fields of view were examined.

A

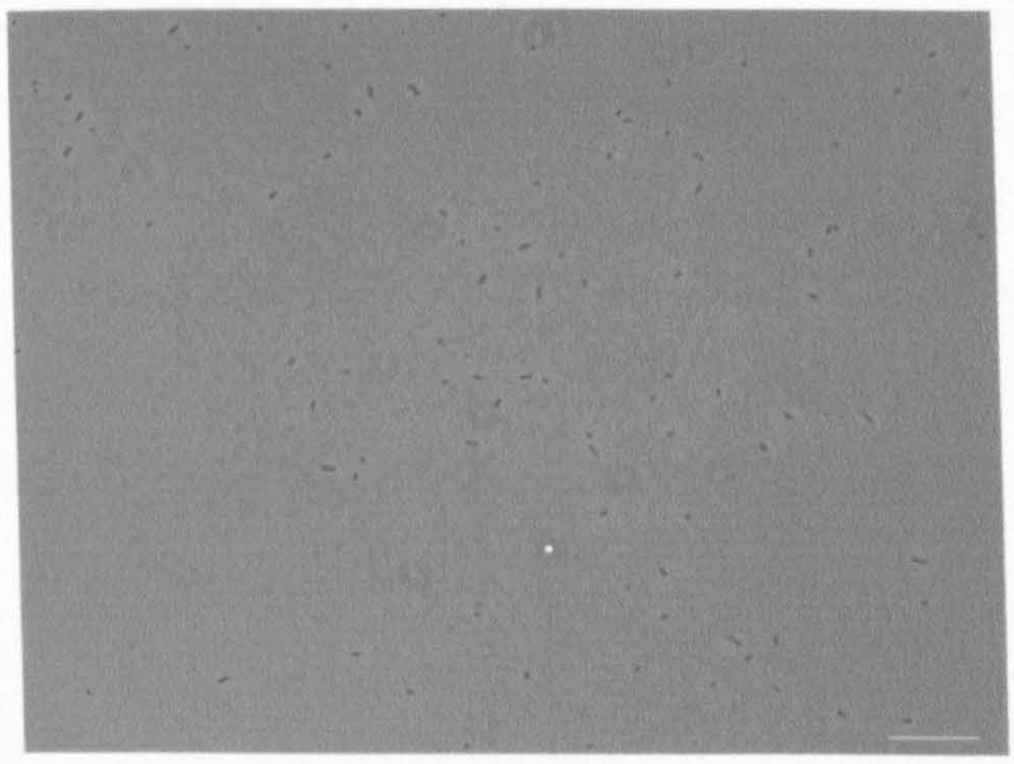

B

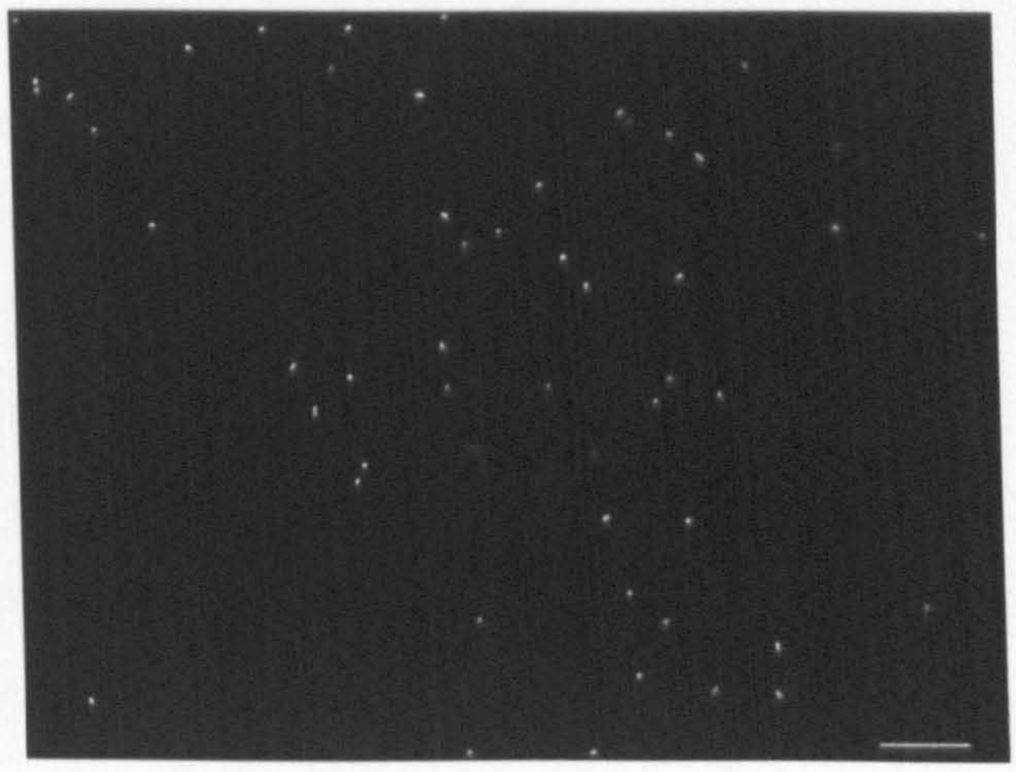

C

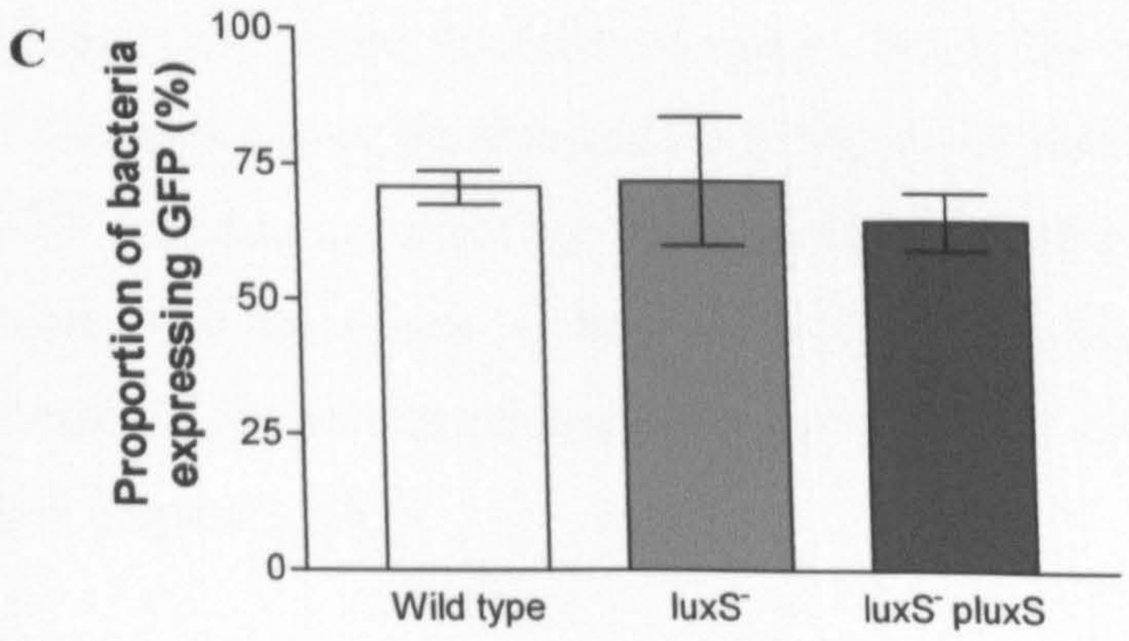

For the work using flow cytometry, the original wild type, *luxS*⁻ mutant and transcomplemented mutant were used as negative controls, since they lack the ability to produce GFP. The wild type, *luxS*⁻ mutant and transcomplemented mutant which had been created to carry the promoter fusion *rpsM*::*gfp*$^+$ in the *putPA* locus were used as positive controls. The *rpsM* gene encodes the 30S ribosomal protein S13, which is constitutively expressed, and thus fusing the *rpsM* promoter to *gfp*$^+$ gives constitutive expression of GFP. Bacteria were grown in LB to prevent catabolite repression of the Lsr transporter (Taga *et al.*, 2003). Thus, at 3.5 hours there will be a high concentration of autoinducer-2 in the wild type culture medium with no AI-2 present in the *luxS*⁻ mutant culture (Figure 3.2), while at 6 hours there will be little or no AI-2 present in either the wild type or *luxS*⁻ mutant culture (Figure 3.2).

Figure 3.17 shows representative histograms of the flow cytometry data, in which the GFP signal (y-axis) is plotted against the number of bacteria counted. For the bacteria that do not possess a single copy of *gfp*$^+$ inserted into the chromosome, nearly all the bacteria are found below the threshold intensity; a fluorescent intensity of 10^3 arbitrary units (Figure 3.17A). When the percentage of the population expressing GFP is therefore calculated for these strains, a value of ≤0.3% is typically obtained (Figure 3.18A and Figure 3.19A). The pattern of GFP expression is changed when examining the *Salmonella* containing the constitutive fusion (*rpsM*::*gfp*$^+$); nearly all the bacteria are found within a fairly narrow peak above the threshold value, showing they express GFP (Figure 3.17B). Approximately 99% of the population is therefore found to express GFP (Figure 3.18A and Figure 3.19A). When examining the inducible promoter (the *prgH*::*gfp*$^+$ fusion) the pattern is different again. While the majority of bacteria have a GFP intensity above the threshold (~70%), these bacteria have a broader range of GFP intensities, reflecting the inducible nature of GFP expression, which together with the subset of bacteria which have fluorescent intensities below the threshold, forms a much broader peak than seen when GFP expression is constitutive (Figure 3.17C).

Figure 3.17 Histograms of the flow cytometry data generated whilst determining the expression of SPI-1 in *S.* Typhimurium SL1344 using flow cytometry. Three independent experiments were performed, with the histograms for wt (A), wt *rpsM*::*gfp*$^+$ (B) and wt *prgH*::*gfp*$^+$ (C) from a single representative experiment being shown below.

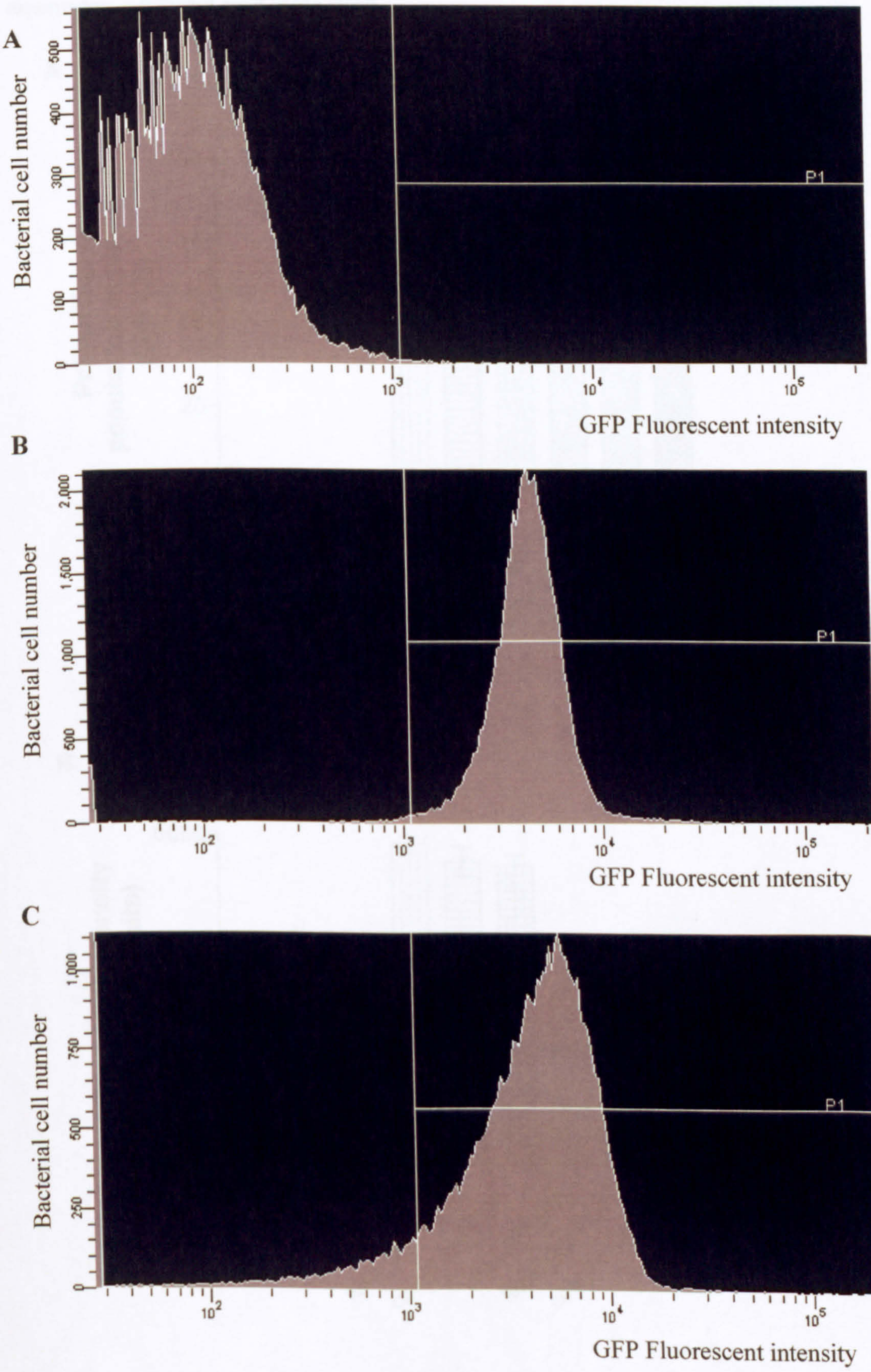

Figure 3.18 Determining the expression of SPI-1 in *S.* Typhimurium SL1344 grown for 3.5 hours using flow cytometry. Bacterial cultures were grown in LB. A. shows the proportion of each bacterial population measured that express GFP, while B. shows the mean intensity of the GFP. Compl refers to the transcomplemented mutant, *luxS*⁻ p*luxS*. Data represents three independent experiments ± standard error of the mean.

A

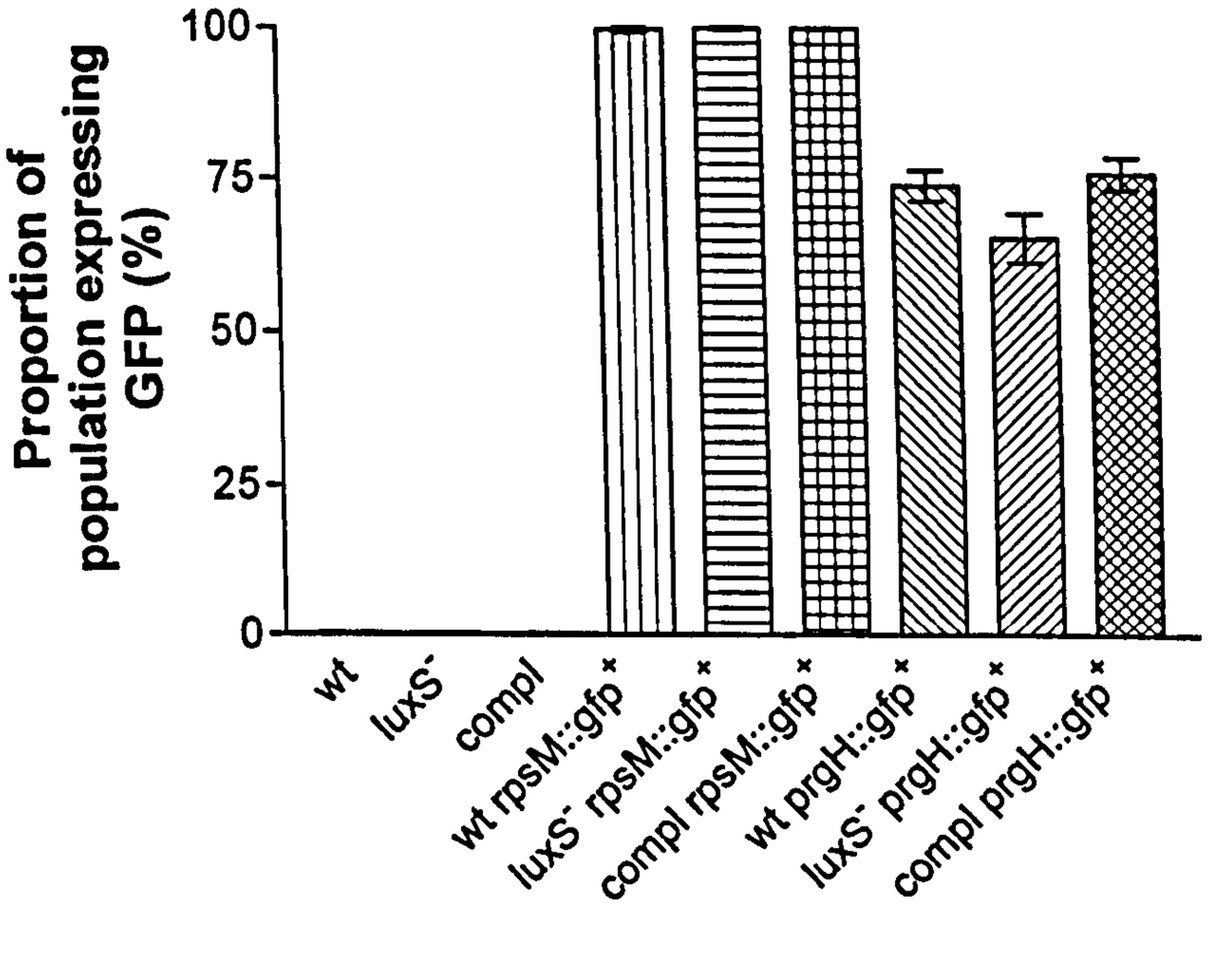

B

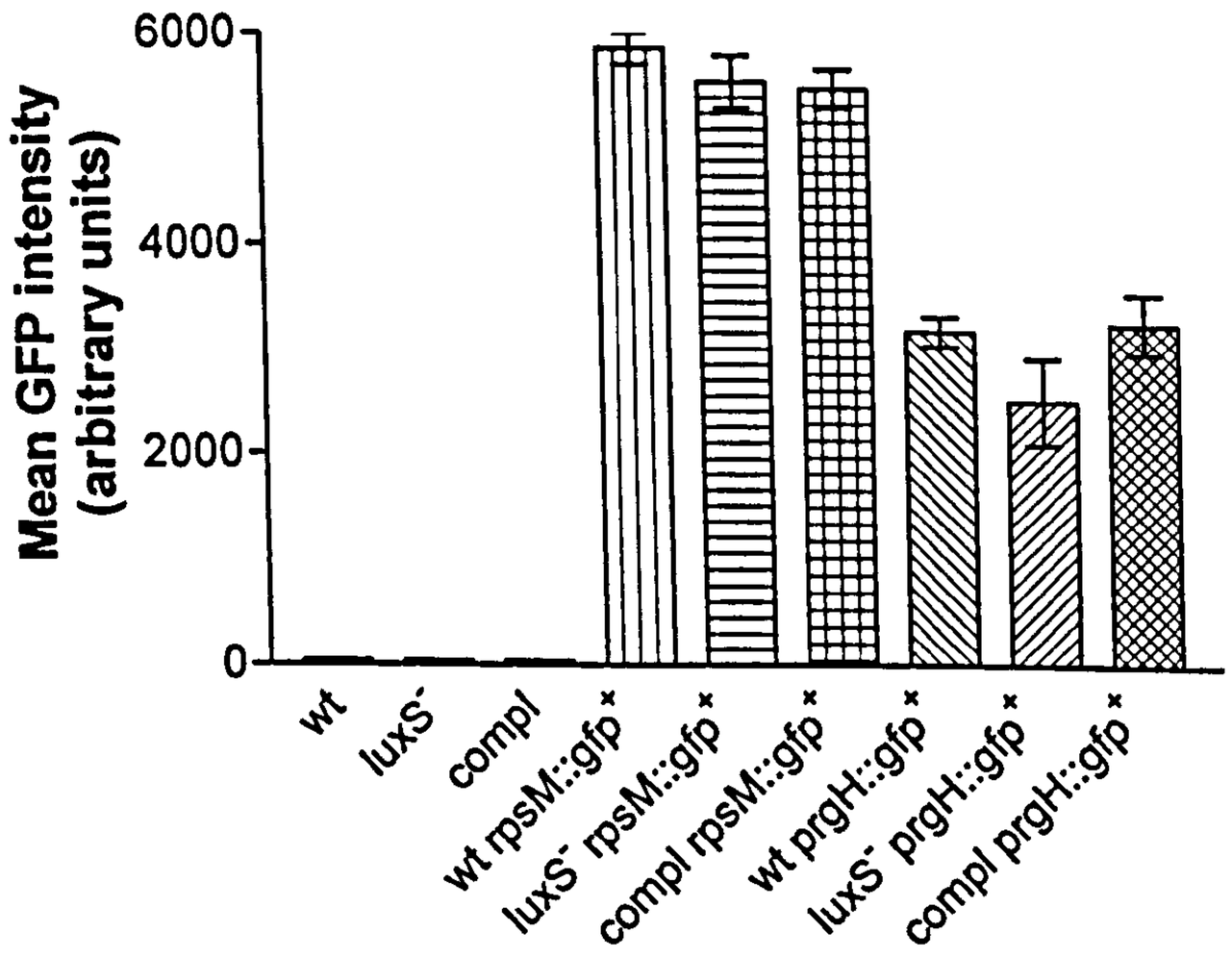

Figure 3.19 Determining the expression of SPI-1 in *S.* Typhimurium SL1344 grown for 6 hours using flow cytometry. Bacterial cultures grown in LB. A shows the proportion of each bacterial population measured that express GFP, while B shows the mean intensity of the GFP. Compl refers to the transcomplemented mutant, *luxS*˜ p*luxS*. Data represents three independent experiments ± standard error of the mean.

A

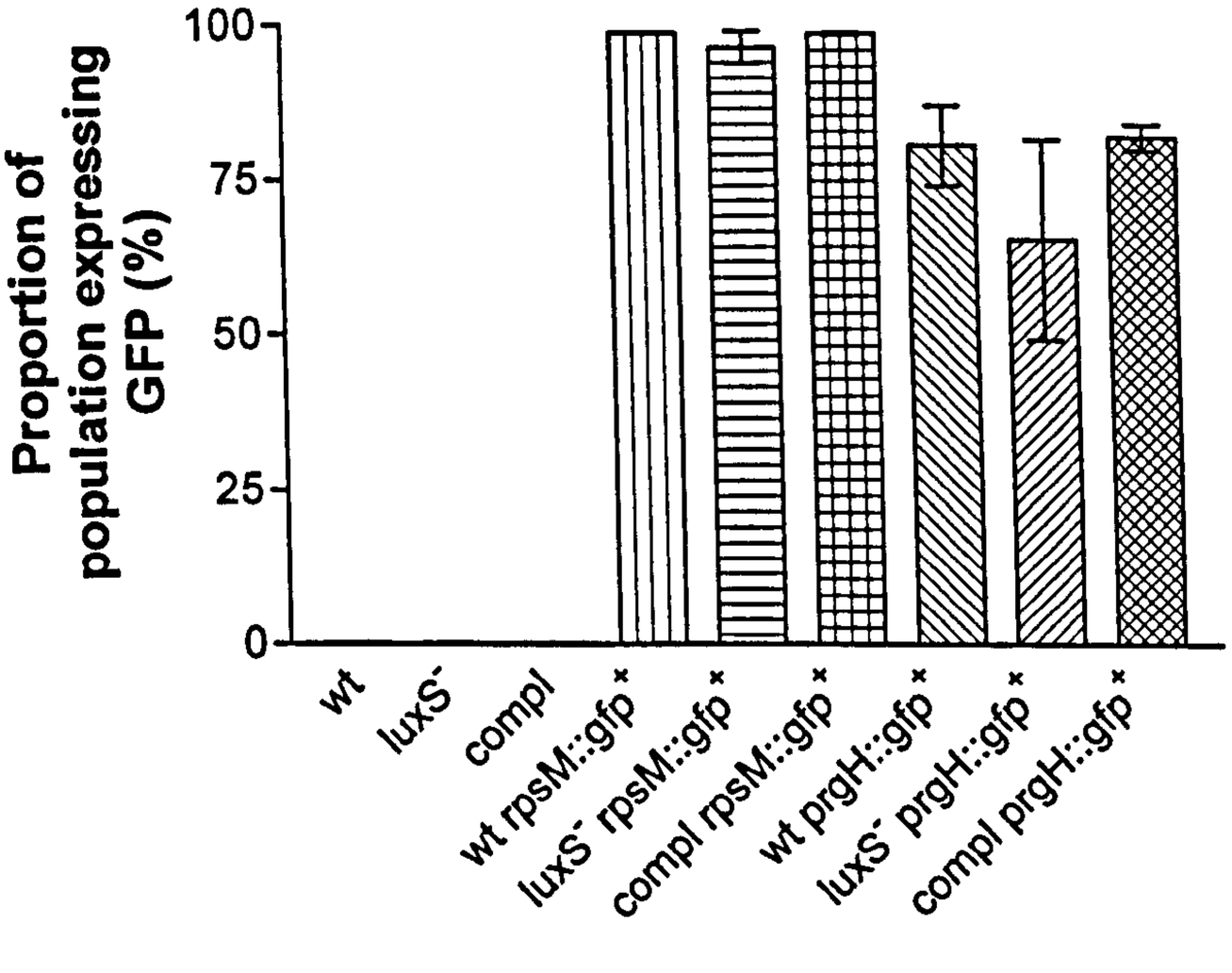

B

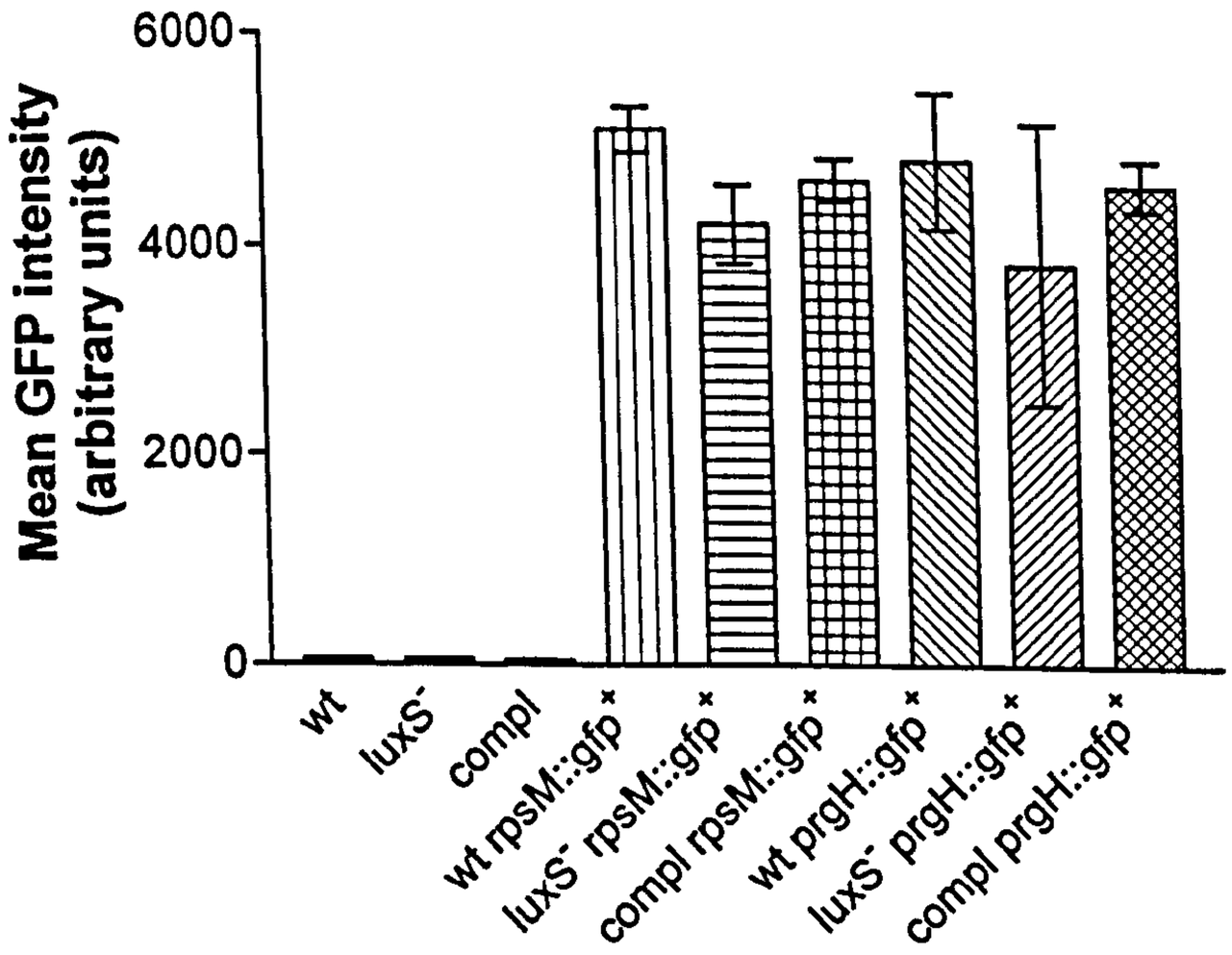

When examining the proportion of SL1344 *prgH*::*gfp*$^+$, *luxS*$^-$ *prgH*::*gfp*$^+$, and *luxS*$^-$ p*luxS prgH*::*gfp*$^+$ populations expressing GFP after 3.5 hours it was found *luxS*$^-$ *prgH*::*gfp*$^+$ had the lowest percentage of the population expressing GFP; a mean average of 65% compared to 74% for wild type and 76% for the complemented mutant (Figure 3.18A). However, this difference was not judged to be significant (P=0.113). It therefore appears the proportion of the population expressing GFP is found to be similar when performing analysis by fluorescent microscopy or flow cytometry.

The trend seen for GFP expression in 3.5 hour cultures of the *prgH*::*gfp*$^+$ strains was repeated for 6 hour cultures (Figure 3.19A). 65% of the *luxS*$^-$ *prgH*::*gfp*$^+$ population expressed GFP compared to ~80% of the SL1344 *prgH*::*gfp*$^+$ and *luxS*$^-$ p*luxS prgH*::*gfp*$^+$ populations. Again there was no significant difference (P=0.479), which is likely to be due to the large variation in the results of *luxS*$^-$ *prgH*::*gfp*$^+$ (Figure 1.19A).

The mean intensity of GFP expressed by all the strains was also measured during flow cytometry (Figures 3.18B and 3.19B). As expected the wild type, *luxS*$^-$ mutant and complemented mutant that did not possess GFP had very low intensities; approximately 44 arbitrary units for 3.5 hours growth and 60 units for 6 hours growth, and corresponds to background fluorescence. The constitutively expressing strains (*rpsM*::*gfp*$^+$) have mean intensity values close to 6000 units after 3.5 hours of growth (Figure 3.18B), with this value decreasing to ~5000 units for a 6 hour culture (Figure 3.18B). This decrease may indicate the presence of mechanisms in the cell that degrade GFP, which may be necessary as excess amounts of GFP can be toxic to cell (Wendland and Bumann, 2002). Alternatively the reduction in GFP intensity at 6 hours may be the result of processes such as cell division and cell maturation. The inducible GFP strains (*prgH*::*gfp*$^+$) have average intensity values of 3000 units after 3.5 hours of growth compared to approximately 4000 after 6 hours growth. This may represent increased expression of GFP at the 6 hour time point but may also represent an accumulation of GFP molecules over time to give a higher intensity at later time periods or again be due to maturation of the cells. The *luxS*$^-$ deletion mutant has a lower mean GFP intensity than either wild type or the

complemented mutant, which have similar values, but this is not statistically significant (P=0.236 at 3.5 hours, P=0.716 at 6 hours), and therefore is likely to reflect that a lower percentage of the mutant population expressed GFP.

Together the results of the fluorescent microscopy and flow cytometry experiments indicate that the expression of GFP is similar in the wild type and *luxS* mutant. Presuming that the number of copies of PrgH is therefore similar, this would indicate the parent and *luxS* mutant are likely to have comparable numbers of TTSS-1 and concentrations of effector proteins since *prgH* expression is regulated by HilA which also regulates the *spa*, *inv* and *sip* operons of SPI-1 (Bajaj *et al.*, 1995; Bajaj *et al.*, 1996). If SPI-1 expression is similar between wild type and the *luxS* mutant, the ability to form a ruffle and invade would not be expected to differ, supporting the data from both the immunocytochemical staining assays and live cell imaging analysis that failed to find a difference in invasion behaviour.

3.3.9. Comparisons of ruffling and invasion of MDCK cells by SL1344 wild type and flagella phase mutants

Comparison of phase variation rates between the *S.* Typhimurium SL1344 parent and isogenic *luxS* mutant had shown that in the wild type, flagella phase variation showed a bias towards expression of phase-2 flagella (composed of FljB), but in the *luxS* deletion mutant this bias was towards expression of phase-1 flagella (composed of FliC) (Dr C.M.A Khan, personal communication). To investigate whether flagella phase bias had an effect on invasion, phase-locked mutants of SL1344 that expressed only FljB (termed locked ON) or FliC (termed locked OFF) were compared to the parent for ability to form ruffles and invade MDCK cells.

The mutant locked into expression of FljB (ON) produced the greatest number of ruffles per cell (1.186±0.116), which was significantly greater than either wild type ($P<0.05$) or the mutant locked into expression of FliC (OFF) ($P<0.01$) (Figure 3.20A). The wild type and OFF mutant produced similar levels of ruffles and did not differ statistically. Despite producing more ruffles the mutant locked

into expression of FljB did not have an increased level of invasion; in fact it had the lowest invasion, although the levels of invasion were similar for the wild type and two locked mutants, and not considered significantly different (Figure 3.20B).

Figure 3.20 Comparison of the abilities of SL1344 wild type, ON and OFF mutants to induce ruffling in and invade MDCK cells. Infection was for 15 minutes. The ability to produce membrane ruffles was measured using TRITC-phalloidin staining of actin (A), while invasion was measured using differential immunocytochemical staining of adhered and total cell-associated *Salmonella* (B). Results are the mean of four independent experiments ± standard error of the mean. Asterisk denotes a statistically significant difference between ON mutant and wild type, and ON mutant and OFF mutant assessed by a One Way ANOVA, followed by Tukey's test, at a level of $P<0.05$, and $P<0.01$ respectively.

A

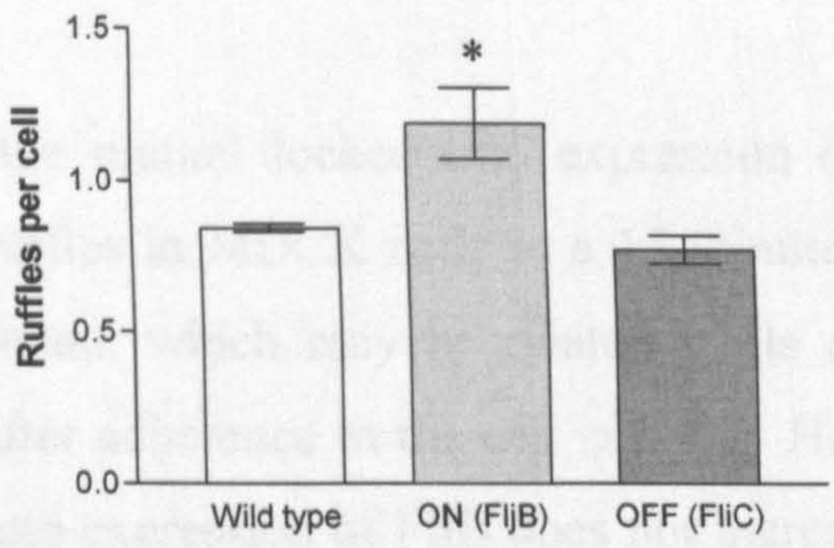

B

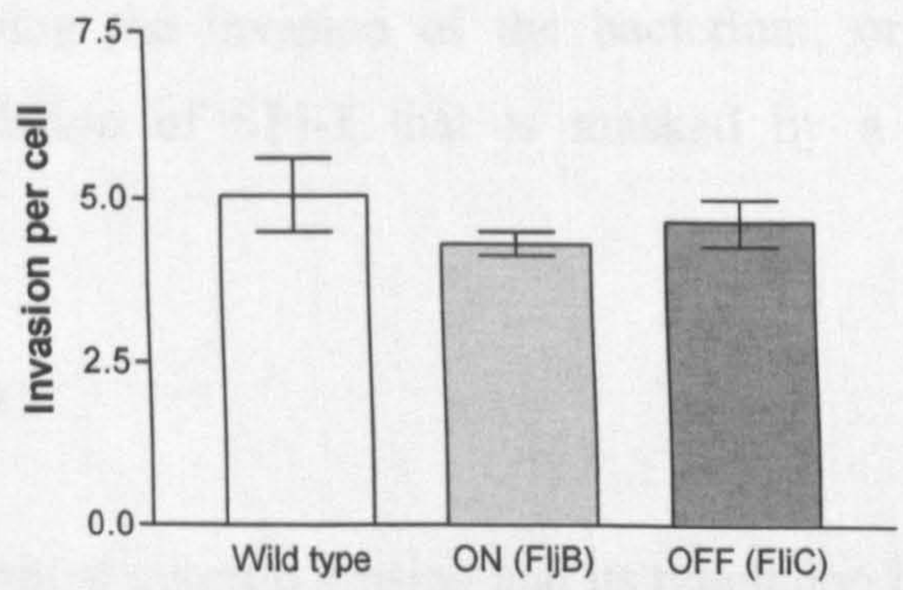

The ruffling kinetics of the phase locked mutants was subsequently compared to the wild type using phase-contrast time-lapse microscopy. The mutant locked into expression of FljB was found to significantly differ from both wild type and the mutant locked into expression of FliC ($P<0.05$ and $P<0.01$ respectively). The median time between adherence and ruffle induction was 40 seconds for the mutant locked into expression of FljB, compared to a median time interval of 50 seconds for the wild type and mutant locked into expression of FliC.

Table 3.10 Comparisons of the time taken for membrane ruffle initiation after bacterial adherence to MDCK I cells by SL1344 wild type, ON and OFF mutants grown for 3.5 hours in LB. The time interval between bacterial binding to MDCK cells and induction of membrane ruffling was obtained from phase-contrast video microscopy. Data expressed as medians with the number of productive bacterial-cell interactions analysed (n), and the minimum and maximum time intervals measured. Asterisk denotes significant difference between ON mutant and wild type, and ON mutant and OFF mutant assessed by the Kruskal Wallis test, followed by Dunn's Multiple Comparison Test at a level of $P<0.001$ and $P<0.05$, respectively.

	Ruffle induction time after adherence (s)			
	n	**Median**	Minimum	Maximum
Wild type	240	**50**	10	490
ON	240	**40***	10	570
OFF	240	**50**	10	340

Overall it appears the mutant locked into expression of FljB can produce a greater number of ruffles in MDCK cells in a 15 minute time period than wild type or an OFF mutant, which may be related to its ability to induce ruffle formation quicker after adherence to the cell surface. However, the invasion of the mutant locked into expression of FljB does not increase proportionally. The reason for this is not clear, perhaps the FljB flagella are not lost as easily as the FliC flagella delaying the invasion of the bacterium, or perhaps there is a difference in regulation of SPI-1 that is masked by a cell-type dependent adhesion effect.

3.4. Discussion

Since the first reports of quorum sensing and its regulation of bioluminescence in *Vibrio* spp. (Eberhard *et al.*, 1981; Engebrecht *et al.*, 1983; Engebrecht and Silverman, 1984), the ability to carry out quorum sensing has been shown to be wide-spread throughout the microbial kingdom and to modulate many different physiological processes (Bassler and Losick, 2006). *Salmonella* has been shown to possess the *luxS* gene and secrete autoinducer-2 (AI-2) (Surette and Bassler, 1998, 1999; Surette *et al.*, 1999), components of a quorum sensing system used by *Vibrio* spp. (Kuo *et al.*, 1994; Surette *et al.*, 1999). This has led to the

proposal that *Salmonella* may also regulate gene expression in response to population size (Surette & Bassler, 1998, 1999).

Initial screening of genes regulated by *luxS* in *Salmonella* identified only genes involved with the synthesis and detection of this molecule; *metE*, which encodes an enzyme with a role in the activated methyl cycle (AMC), the cycle from which AI-2 is a by-product, and those of the *luxS* regulated (*lsr*) operon, which encode a transporter for AI-2 and enzymes which modify this signal upon its entrance into cells (Taga *et al.*, 2001; Taga *et al.*, 2003; Xavier *et al.*, 2007). Recent work in this field has therefore focussed on elucidating whether other behaviours in *Salmonella* may be regulated by quorum sensing, and recently it was reported that the *luxS* gene is necessary for expression of a subset of genes in SPI-1 (Choi *et al.*, 2007). This potentially implicates quorum sensing in the regulation of *Salmonella* pathogenesis. The work documented in this chapter also examined whether *Salmonella* may use quorum sensing to regulate virulence; specifically examining the effect of deletion of *luxS* on the ability of *Salmonella* to stimulate its uptake into epithelial cells.

Initially, the growth and AI-2 production of *S.* Typhimurium SL1344 wild type and its isogenic *luxS* mutant were compared. The growth of both parent and mutant were indistinguishable, indicating loss of *luxS* does not affect processes required for the bacterium to grow and divide in an obvious manner, and therefore supports the argument that LuxS does not have an essential metabolic role. A debate currently exists over whether AI-2 is a true quorum sensing signalling molecule or simply a by-product of metabolic reactions of the AMC, secreted as a waste product. The evidence for the latter model has been largely circumstantial, for example finding the *luxS* gene adjacent to other genes with a metabolic function, and the Lsr transporter of *Salmonella* and *E. coli* having homology to other sugar uptake transporters (Vendeville *et al.*, 2005). However, recently a phenotype microarray screen of an *E. coli luxS* mutant treated with synthetic AI-2 found the majority of phenotypes gained by the mutant involved the ability to use different carbon, nitrogen, and phosphate sources (Walters *et al.*, 2006). It is unclear if the ability to use these compounds is a result of AI-2 being used as a metabolite or is a product of AI-2 signalling, but does illustrate

luxS is intimately linked to cellular metabolism and this role needs to be given consideration when deciding whether a behaviour is linked to quorum sensing.

The secretion pattern of AI-2 was very different between wild type and *luxS*. *luxS* encodes AI-2 synthase which produces the pre-cursor of AI-2, 4,5-dihydroxy-2,3-pentanedione (DPD) during the conversion of S-ribosylhomocysteine (SRH) to homocysteine as part of the activated methyl cycle (Schauder *et al.*, 2001). The loss of *luxS* prevents synthesis of AI-2, and so, as has been previously reported for *Salmonella* mutants (Surette *et al.*, 1999; Taga *et al.*, 2001; Brandl *et al.*, 2005), no AI-2 activity is found in the growth medium of the *luxS* mutant at any stage during growth. It should be noted that the assay measuring the presence of AI-2 does so indirectly; induction of luminescence in a *V. harveyi* reporter strain possessing only the AI-2 sensor indicates the presence of AI-2, while the amount of fluorescence induced indicates the relative concentration of AI-2 (Bassler *et al.*, 1997). This explains why AI-2 concentration is expressed as fold induction or activity.

The extracellular AI-2 activity profile over the growth curve for wild type SL1344 matched that previously reported for *S.* Typhimurium (Taga *et al.*, 2003; Choi *et al.*, 2007). AI-2 is detected in the culture supernatant once the bacteria have entered the exponential phase of growth, with AI-2 concentration continuing to increase until a maximal level is reached at ~3 hours for SL1344 (data shown here; Choi *et al.*, 2007), and 4 hours for strain 14028 (Taga *et al.*, 2003). The different timings of the AI-2 peak concentration between SL1344 and 14028 may reflect an inter-strain difference, although could also be the result of differences in the experimental protocol.

Since AI-2 is produced and secreted during growth, AI-2 will be present in a culture during the lag phase; however, because the level of growth is very low, the AI-2 concentration is likely to be below the level of detection. Low levels of AI-2 in the lag phase are well documented when measuring the fluorescent intensity of *Vibrio* spp. cultures (Kaplan and Greenberg, 1985; Miller *et al.*, 2002; Surette and Bassler, 1999). Immediately after sub-culturing, fluorescent intensity is relatively high since cells have the autoinducer bound; however as the

lag phase continues fluorescence intensity continually decreases as the initial signal is diluted. Fluorescent intensity of the *Vibrio* population only starts to increase during the exponential growth phase where the specific cell number to achieve the critical concentration of autoinducer is reached. Subsequently, a linear relationship between cell number and fluorescence develops as AI-2 provides a measure of cell density. Since, the kinetics of AI-2 production observed in *Salmonella* is similar to those reported in *Vibrio fischeri* (Kaplan & Greenberg, 1985), *Vibrio harveyi* (Surette & Bassler, 1999) and *Vibrio cholerae* (Miller *et al.*, 2002) all of which have been shown to use AI-2 for regulation of population-dependent behaviours, this suggests AI-2 can be considered a signalling molecule, implying *Salmonella* does have the ability to perform quorum sensing.

AI-2 concentration in the *Salmonella* culture supernatant decreases upon cells reaching the late log phase of growth, so that for growth in LB, no AI-2 remains by 6 hours (12 hours for *S.* Typhimurium 14028 (Taga *et al.*, 2003)). The decrease in AI-2 concentration is due to the transport of AI-2 into *Salmonella* by the Lsr transporter, composed of LsrA, LsrB, LsrC and LsrD (Taga *et al.*, 2001). AI-2 subsequently converts to a ring-open form of DPD, which is phosphorylated by LsrK sequestering 'AI-2' inside the cell (Taga *et al.*, 2001; Taga *et al.*, 2003; Xavier *et al.*, 2007). Phospho-DPD acts to inhibit LsrR, an inhibitor of *lsr* operon transcription, and therefore phospho-DPD acts indirectly to upregulate the *lsr* operon and hence the number of transporters on the cell surface which can take up AI-2 (Taga *et al.*, 2001). The *lsr* operon is subject to catabolite repression (Surette and Bassler, 1998; 1999; Taga *et al.*, 2003), and explains why, in the presence of glucose, while the AI-2 concentration does decrease, it occurs at a much slower rate than for growth in LB; the number of transporters in the bacterial membrane being less numerous.

It is not clear why *Salmonella* secretes AI-2 and then transports it back into the cell. One proposal has been that uptake of AI-2 provides a mechanism for switching off quorum sensing once the bacteria have reached the stationary phase of growth (Taga *et al.*, 2003). By taking up the AI-2 secreted, it may also allow *Salmonella* to recycle AI-2, providing an energetic advantage, especially as it

prevents any competitors in the environment obtaining this carbon source. However, a direct role in metabolism has not been indicated; *S.* Typhimurium can not grow in minimal medium containing AI-2 as the sole carbon source (Taga *et al.*, 2001). This also argues against the proposal that AI-2 is a metabolic waste compound excreted during exponential growth due to its toxicity, and is subsequently internalised at a later stage of growth when controlled amounts can be degraded (Winzer *et al.*, 2002). It has been suggested that the modifications to AI-2 made upon its import into the cell by LsrK, LsrG and possibly LsrF (Taga *et al.*, 2003; Xavier *et al.*, 2007) may allow it to act as a different signal, interacting with another sensory system in the bacterium (Taga *et al.*, 2003). Such a system may be responsible for switching off quorum sensing and/or it may have another effect on the cell. This effect is likely to be subtle since few genes have been found to change in their expression in a *luxS* mutant (Taga *et al.*, 2001; Choi *et al.*, 2007).

Examining the growth and AI-2 profiles of the parent and *luxS* mutant *S.* Typhimurium SL1344 ensured that any differences seen in the assays conducted were likely to be due to the presence/absence of AI-2, and that these results could be compared with previous work. To confirm a phenotypic difference between wild type and the *luxS* mutant was due to AI-2, 3.5 and 6 hour cultures were used to infect epithelial cells. 3.5 hours represents a time point when there is most difference between the wild type and *luxS* mutant cultures, with a high concentration of AI-2 present in the wild type supernatant and none in the mutant culture, while 6 hours represents a time when the two cultures are most similar, with no AI-2 present in either culture supernatant. Thus, if a phenotypic difference occurred for 3.5 hour cultures and was due to AI-2 production in the wild type it would be expected that at 6 hours this difference would not be present.

Initial experiments showed no difference between the SL1344 wild type and its isogenic *luxS* mutant when quantifying the number of ruffles propagated or the number of bacteria invaded per MDCK cell after a 15 minute infection with either a 3.5 or 6 hour culture. No difference was also found when comparing a 3.5 hour wild type culture with a 6 hour wild type culture or comparing a 3.5

hour *luxS* culture with a 6 hour *luxS* culture. At 3.5 hours *Salmonella* is in the late exponential phase of growth, while at 6 hours the bacteria are in the stationary phase of growth. It is widely accepted that for growth in liquid *Salmonella* starts synthesising TTSS-1 and secreting effector proteins during the late exponential phase of growth so that invasion is optimal during the transition into stationary phase (Kusters *et al.*, 1993; Lee and Falkow, 1990; Lundberg *et al.*, 1999). Subsequently, in the stationary phase the genes controlling invasion are downregulated leading to reduction in invasion (Lee & Falkow, 1990). Since *Salmonella* from the 6 hour cultures had been in the stationary phase a very short time this may explain why no difference was found between the 3.5 and 6 hour cultures in this study. Comparing the ability of 3.5 hour, 6 hours and a 12 hour culture to induce ruffles and invade may enable validation of this explanation.

While the growth phase of the bacteria was not a factor that influenced invasion of *Salmonella*, temperature was shown to be important. Comparing wild type infection at 30°C and 37°C or comparing a *luxS* mutant infection at 30°C and 37°C found the numbers of ruffles and the level of invasion in MDCK cells were significantly lower at 30°C. This trend was previously shown in HEp-2 cells (Small *et al.*, 1987). Since *Salmonella* outside a host organism will typically be exposed to temperatures at or below room temperature (≤22°C), 30°C could act as a cue to *Salmonella* that it has entered a host organism leading to expression of genes, including those in SPI-1, which will enable it to colonise the organism, explaining why invasion is observed at this temperature. A temperature of 37°C is indicative of being in the intestinal tract of a human host and so it can be conceived that at this temperature *Salmonella* further upregulates virulence mechanisms to increase the rate at which invasion can occur, and is why invasion at 37°C is higher than 30°C. This could potentially be tested by growing *Salmonella* at both temperatures and then performing the infection at 37°C.

Alternatively the difference in invasion may be related to growth phase. At 3.5 hours *Salmonella* grown at 37°C is in the late log phase while *Salmonella* grown at 30°C is still in the log phase. Since the ability to enter epithelial cells is affected by growth phase (Lee and Falkow, 1990; Kusters *et al.*, 1993) this could

explain the difference. Again testing this hypothesis could be achieved by repeating the experiment but using cultures in the same growth phase.

Microarray data had suggested at 30°C SPI-1 was upregulated in the *luxS* mutant (Dr C. M. A. Khan, unpublished data). It would therefore be expected that at 30°C the *luxS* deletion mutant would have increased invasion compared to the wild type because SPI-1 encodes TTSS-1 which is necessary for transfer of *Salmonella* effector molecules into host cells, and which cause the physiological changes required for *Salmonella* uptake (Altmeyer *et al.*, 1993; Collazo *et al.*, 1995; Galan and Curtiss, 1989; Ginocchio *et al.*, 1992; Groisman and Ochman, 1993; Kaniga *et al.*, 1994). This was not indicated by my experiments; quantifying the ruffles and invasion per cell for infection at 30°C found no difference between the wild type and *luxS*⁻ mutant. This suggests AI-2 does not have a role in regulating SPI-1 in response to temperature, although it could be possible that while SPI-1 expression is upregulated in the *luxS*⁻ mutant, post-transcriptional or post-translational modifications made by regulatory systems that ensure virulence mechanisms are only switched on and functional at the correct temperature i.e. temperatures indicative of a host environment, inhibit higher expression and increased pathogenesis.

Visualisation of the infection process using phase-contrast time-lapse microscopy confirmed the results of the immunocytochemical staining assays as there was found to be no obvious difference between wild type and the *luxS*⁻ mutant in the manner in which ruffles were propagated, or how the bacteria invaded cells. However, it was initially observed at the late log phase of growth that the *luxS*⁻ mutant was significantly quicker to induce the formation of a membrane ruffle after it had adhered to the surface of a cell, compared to the wild type. This was an important observation because simultaneous experiments using SL1344 wild type and various effector mutants did not find a difference in ruffle induction time. The reason for this subtle difference between wild type and the *luxS*⁻ mutant was not clear. To ensure the phenotypic difference was due to AI-2 production, all experiments were repeated with a *luxS*⁻ mutant carrying a copy of the *luxS* gene on a plasmid i.e. was transcomplemented. It was also planned to add an exogenous source of AI-2 to the *luxS* mutant culture to check this

response was related to quorum sensing. Apart from *Vibrio* spp. where the role of AI-2 in regulating the behaviour of the population has been well defined (Bassler *et al.*, 1994; Henke and Bassler, 2004a; Surette *et al.*, 1999), much of the evidence for AI-2-dependent behaviours in other microorganisms is largely circumstantial. Observation of a phenotypic change due to deletion of *luxS* and the subsequent restoration of the wild type phenotype by complementation of the mutant with a plasmid carrying *luxS*, only serves to illustrate the importance of *luxS*. Since *luxS* encodes an enzyme that is part of the AMC, a change in phenotype may only be the consequence of changes in metabolism. To be certain a phenotype is linked to AI-2 signalling it is necessary to complement the *luxS* mutant phenotype with AI-2. The addition of supernatant from a species which secretes AI-2, addition of DPD which spontaneously cyclises into AI-2 or the addition of synthetically derived AI-2 have all been used to confirm a phenotype is AI-2-dependent (Choi *et al.*, 2007; Taga *et al.*, 2001; Taga *et al.*, 2003).

The ruffling and invasion behaviour of the wild type, *luxS*⁻ mutant and complemented mutant was performed in three different epithelial cell lines: MDCK, HeLa and Caco-2. The use of multiple cell lines allowed investigation into whether a *luxS* deletion produces the same phenotype in all cell culture models, in addition to checking whether any phenotype was cell-dependent. In all three cell lines no difference was found between the wild type and *luxS*⁻ mutant, as had been indicated by the preliminary study. However, some general differences in *S.* Typhimurium behaviour were noted between the cell lines. Firstly, the morphology of ruffles in HeLa cells seemed to be distinct from the ruffles generated in MDCK and Caco-2 cells which are largely circular in nature, with one bacterium centrally positioned. In HeLa cells, the ruffles were more diffuse with no particular shape, regularly had actin spikes and frequently there was more than one bacterium associated with each ruffle. These disparities have been described previously (Finlay and Falkow, 1990; Mills and Finlay, 1994), and are likely to reflect differences in the nature of HeLa cells compared to MDCK and Caco-2 cells, particularly as the MDCK cells were partially polarised and the Caco-2 cells fully polarised.

The numerous bacteria associated with one ruffle may suggest either the formation of one ruffle pre-disposes that area of the membrane to further attachment of bacteria and/or induction of ruffling, or that one ruffle allows multiple bacteria to enter the cell. The latter case is more likely since it was observed here with time-lapse microscopy that, particularly in the later stages of an infection when a large proportion of the cell surface is involved with ruffle formation, bacteria are seen to enter the cells via pre-existing ruffles. Such observations have been made by other researchers (Francis *et al.*, 1992; Pattni *et al.*, 2001).

The larger number of bacteria associated with the HeLa cell ruffles is likely to explain why the number of bacteria invading per cell is approximately two times greater for HeLa cells than MDCK cells, despite the number of ruffles per cell for each cell line being similar. When measuring invasion, two different assays were used: the differential immunocytochemical staining of adhered and total cell-associated *Salmonella*, and the gentamicin protection assay. In both MDCK and HeLa cells the level of invasion was two fold less with the gentamicin protection assay. The results also tended to be much more variable on a day-to-day basis which has been previously reported, with the physiological states of the eukaryotic cells and bacteria being considered responsible for the observed variability (Elsinghorst, 1994). However, this is true of all assays using biological material, although perhaps the combined effects of using gentamicin and Triton X-100 in this assay make the outcome of the experiment more dependent on cell physiology. An additional problem with the gentamicin protection assay includes the potential for gentamicin to penetrate epithelial cells, leading to killing of internalised bacteria and hence lower estimations of invasion. This may be a particular concern when infecting with *Salmonella* because the macropinocytosis that accompanies *Salmonella*-induced membrane ruffling (Francis *et al.*, 1993; Mills and Finlay, 1994) increases the chance of gentamicin entering eukaryotic cells.

Insufficient permeabilisation of cells by Triton X-100 may also lead to the variation in results, as obviously if there is insufficient lysis of cells then a proportion of invaded bacteria will not be isolated for counting. The differential

immunocytochemical staining technique also relies on the use of Triton X-100 to enable the staining of invaded bacteria. However, because the cells and bacteria are subsequently visualised it is relatively easy to see whether sufficient permeabilisation has occurred for the counts to be accurate; equal numbers of adhered and total bacteria, or very faint staining of the internalised bacteria indicating this not to be the case. Such occurrences are infrequent, occurring approximately once every fifty experiments here.

Visualisation of the infection process is an important advantage of the immunocytochemical staining assay as it is easy to check the health of the eukaryotic cell monolayer and the confluency of the cells, both of which may affect the results obtained. As mentioned above, the permeabilisation of cells and staining of bacteria can also be checked and ensures human error is kept to a minimum by checking that bacteria were added to the well and in the correct number! This technique also has the advantage that since the numbers of adhered bacteria are measured in order to calculate the level of invasion, it is easier to detect any differences in adhesion with this method, compared to the gentamicin protection assay. The heterogeneity of invasion across the cell monolayer can also be determined which can reveal important facets of the invasion process. Of course while the differential immunocytochemical staining technique is preferred by our laboratory, it does have disadvantages, namely that it is a labour intensive method of quantifying bacterial invasion and is only valid if there is a suitable antibody that will bind an epitope from the bacterium under study, and under all circumstances.

When using the differential staining technique, Caco-2 cells were found to have a much lower rate of invasion than MDCK or HeLa cells (~0.3 bacteria per cell). A similar relationship between HeLa and Caco-2 cells has been described (Mills & Finlay, 1994), and is likely to reflect the fact Caco-2 cells were grown on permeable supports to obtain a polarised monolayer. Since Caco-2 cells are derived from human colon cells and may be used as polarised monolayers they are probably more indicative of the epithelial cells encountered by *Salmonella* in the gut, and therefore, the levels of invasion observed in the assay may be more indicative of events *in vivo*.

In order to further examine the subtle difference between wild type and the *luxS*⁻ mutant in ruffle induction time post-adherence, time-lapse microscopy experiments were performed with the wild type, *luxS*⁻ mutant and complemented mutant (*luxS*⁻ p*luxS*). It was demonstrated that the initial phenotypic difference between wild type and the *luxS*⁻ mutant in ruffle induction time after adherence was cell-dependent, and furthermore, limited to a particular subpopulation of MDCK strain I cells that may have undergone genetic drift. This demonstrates why it is important to measure a phenotypic difference in a variety of cell lines, to ensure that what is being measured is not an artefact of the cell line being used, and thus is biologically relevant. In this case by using alternative MDCK strain I cells and a MDCK strain II cell line it was shown there was no difference in the ruffling behaviour of the *luxS* deletion mutant against the wild type, just as the ruffling and invasion assays had predicted. The results presented here therefore suggest *luxS* does not affect invasion of *Salmonella* into epithelial cells. However, this is not to say quorum sensing has no role in *Salmonella* invasion. It is possible that the *in vitro* models used here were not suitable for detecting differences between the wild type and *luxS*⁻ mutant and/or they do not adequately represent conditions *in vivo*, preventing the effect of *luxS* on virulence being fully determined. Indeed the recent study by Choi *et al.* (2007) showed a *S.* Typhimurium SL1344 *luxS* mutant had lower invasion of HEp-2 cells and lower colonisation of the liver and spleen in a mouse model, suggesting *luxS* does play a role in regulation of virulence. It would indeed be interesting to repeat experiments using a 60 minute infection and include use of HEp-2 cells to see if this accounts for the difference between these two reports. However, it does highlight how many variables need to be considered when designing experiments to determine whether a particular gene is responsible for a change in behaviour.

To complement the work performed studying the relationship between *luxS* deletion and invasion behaviour, the expression of SPI-1 between the wild type and *luxS* deletion mutant was compared. SPI-1 encodes a type three secretion system (TTSS-1) and some of the effector proteins secreted through this structure that are essential to invasion (Galan & Curtiss III, 1989; Ginocchio *et al.*, 1992; Groisman & Ochman, 1993; Altmeyer *et al.*, 1993; Kaniga *et al.*, 1994, 1995; Collazo *et al.*, 1995; Hueck *et al.*, 1995). Therefore, if quorum sensing were to

play a role in regulating *Salmonella* invasion, a change in SPI-1 expression may be a possible consequence. *prgH* is a gene located in SPI-1 that encodes PrgH a structural component of the TTSS-1 apparatus (Kubori *et al.*, 1998; Kimbrough & Miller, 2000). By placing the gfp^+ gene which encodes a stable, bright variant of GFP (Scholz *et al.*, 2000), under the control of the *prgH* promoter, a measure of SPI-1 expression can be determined by reading the fluorescent intensity of the bacteria (Hautefort *et al.*, 2003). This type of reporter system has successfully been used to measure changes in gene expression during growth in media simulating various environmental conditions, monitor gene expression in macrophages, and monitor bacterial numbers during *in vivo* infection of a mouse (Hautefort *et al.*, 2003; Mansson *et al.*, 2007).

In regards to the mode of GFP fluorescence detection it was found that flow cytometry was the superior method, not only because it was more sensitive, allowing measurements of the GFP intensity of each bacterium to be made, but it also allowed much larger populations to be screened and was less laborious. However, fluorescent microscopy is still a useful tool, particularly in preliminary experiments. Initial information as to the success of inserting the gene fusion into the chromosome and any obvious differences between different bacterial populations can be made, in addition to allowing checks to be made that the correct protocol is being used to induce expression of SPI-1 and that fixatives do not affect GFP fluorescence.

When the SL1344 wild type and *luxS*⁻ mutant carrying a single copy of the *prgH*::gfp^+ fusion in their chromosome were compared by fluorescence microscopy and flow cytometry, a slight reduction was found in the proportion of the population expressing GFP, and therefore PrgH, in the *luxS*⁻ mutant, but this difference was not statistically significant. Flow cytometry also indicated the amount of PrgH expression per cell was slightly lower in the *luxS*⁻ mutant compared to the wild type but again was not statistically different. If PrgH is assumed to be characteristic of all SPI-1 genes, then this data suggests SPI-1 expression is similar between SL1344 wild type and *luxS*⁻. This conclusion is supported by the SDS-PAGE and Western blotting experiments where no difference was found in the profile of proteins secreted by TTSS-1. Since wild

type and *luxS*⁻ mutant have similar SPI-1 expression it is not surprising that the ability of both to induce membrane ruffles and invade epithelial cells was similar. Again this leads to the conclusion that *luxS* does not consistently play a role in regulating invasion in the *in vitro* models tested here.

The study by Choi *et al.* (2007) also examined the expression of SPI-1 genes, including *prgH*. The level of expression of these genes was inferred from real time PCR using mRNA as a template. *prgH* expression was two-fold lower in a *luxS* mutant compared to the wild type, but could be restored by complementation with a plasmid carrying a copy of *luxS*. These results mirror those observed here, although no consistent reduction in *prgH* expression was found. However, this may represent a difference in the methods used, especially since real time PCR only measures the level of transcription while measurements of fluorescence reflect transcription and translation.

DPD was unable to restore the expression of *prgH* in the *luxS* mutant when examined by real time PCR, which indicates quorum sensing does not regulate PrgH (Choi *et al.*, 2007), supporting the conclusions drawn from the work presented here. HilA, which induces PrgH expression, was also found not to be regulated by quorum sensing, suggesting that in addition to the *prg* operon the *inv/spa* operon will not have altered expression. This validates *prgH* as a suitable marker for the expression of the majority of SPI-1 genes. However, subsets of genes involved with SPI-1-mediated invasion do appear to rely on quorum sensing for their regulation, namely *invF* and InvF-regulated genes, leading to the suggestion that quorum sensing can modulate the virulence of *Salmonella* (Choi *et al.*, 2007). It also illustrates the limitation of an approach examining the expression of one gene as a marker for adjacent genes. A superior approach for my experiments may therefore have been be to monitor the expression of genes under different regulators, in this case choosing one gene regulated by HilA and one gene regulated by InvF.

Both fluorescence microscopy and flow cytometry identified ~70% of the wild type, *luxS*⁻ and *luxS*⁻ p*luxS* populations expressed GFP^+ from the *prgH* promoter. This compares well with the results of Hautefort *et al.* (2003) who reported 60-

80% of a population expressed the *prgH* gene at a given time and provided the first evidence of variation in gene expression between individual bacterial cells. Differential expression of *sipA*, a gene also located in SPI-1, has additionally been shown within a population (Schlumberger *et al.*, 2005). However, in this study only 26% of the bacterial population were found to express *sipA*. Since translational efficiency has been reported to determine the phenotypic variations observed between bacteria of a genetically identical population (Ozbudak *et al.*, 2002), differences between transcription and translation may therefore explain why *sipA* and *prgH* show differences in expression. Although *sipA* and *prgH* are both found in SPI-1 they are under the control of different promoters, and while HilA directly activates transcription of the *prgH* promoter, transcription of the *sip* operon is mediated indirectly by HilA through InvF (Bajaj *et al.*, 1995; Darwin and Miller, 1999, 2000). Thus *sipA* can have different expression compared to *prgH*, and could account for the differences observed between the studies. Alternatively, the difference may be the consequence of using an immunostaining technique to measure SipA concentrations in bacteria, which may be less sensitive than the chromosomal single copy GFP reporter.

Regardless of the differences in the level of SPI-1 gene expression detected by the two techniques, it does appear that it is not necessary for the full proportion of *Salmonella* to express SPI-1. The fact that multiple bacteria may enter through one membrane ruffle (shown here; Francis *et al.*, 1992; Pattni *et al.*, 2001) explains how it may be possible for the population to tolerate a proportion of the population not co-operating in a behaviour necessary for host colonisation. There may be further behaviours that also allow the population to cause disease with a subset of bacteria exhibiting different gene expression. This flexibility may allow the population sufficient numbers to overcome host defence mechanisms and cause infection, while maintaining population fitness.

The final set of experiments examined the ruffling and invasion ability of SL1344 that possessed either flagella only composed of FljB (termed locked ON, and represent phase II flagella) or only composed of FliC (termed locked OFF, and represent phase I flagella). The premise for this study was that in SL1344 wild type, flagella phase variation shows a bias towards expression of phase-2

flagella (composed of FljB), but in the *luxS*⁻ deletion mutant this bias is towards expression of phase-1 flagella (composed of FliC) (Dr C.M.A Khan, personal communication). Thus it was examined whether this might make a difference in the ability of *Salmonella* to invade epithelial cells.

Motility is known to be important in the invasion of cultured cells by *Salmonella* (Dibb-Fuller *et al.*, 1999; Jones *et al.*, 1992; Jones *et al.*, 1981; Khoramian-Falsafi *et al.*, 1990; La Ragione *et al.*, 2003; Van Asten *et al.*, 2000). However, it still remains unclear whether flagella are simply necessary to bring the bacterium toward the site of invasion or whether there is a direct requirement, for example in mediating contact of the bacterium with the epithelium to enable TTSS secretion, or as some form of effector during invasion (van Asten and van Dijk, 2005). Although flagella phase variation has been postulated to play a role in *Salmonella* pathogenesis by providing a mechanism for the bacteria to temporarily avoid cellular immunity (Fierer and Guiney, 2001; Ikeda *et al.*, 2001), the role of flagella phase variation in *Salmonella* invasion is unknown. In the only study where this has been investigated, a mutant locked into expression of FljB was found attenuated in mice while a mutant locked into expression of FliC was as virulent as wild type (Ikeda *et al.*, 2001). However, comparison in a bovine ileal loop model showed no difference between the locked mutants and the wild type, indicating while phase variation may influence the virulence of *Salmonella* in the murine typhoid infection model it does not play a role in enteropathogenesis (Ikeda *et al.*, 2001).

Examining the invasion of SL1344 phase-locked mutants in MDCK cells, it was found the mutant locked into expression of FljB induced ruffle formation quicker than both the wild type and the mutant locked into expression of FliC. This explains the observation that the mutant locked into expression of FljB propagated a greater number of ruffles, and may indicate that FljB provides better adhesion to the cell surface than FliC, enabling quicker or enhanced contact of TTSS-1 to the cell surface. It could be envisaged that the faster ruffle induction time of this mutant reflects more intimate contact of TTSS-1 with the cell so there is relatively little leakage and loss of effectors into the surrounding environment, and this full complement of effectors can drive ruffle propagation

faster. However, despite the increased ability to induce ruffling, the mutant locked into expression of FljB did not differ in the ability to invade cells from wild type and the mutant locked into expression of FliC. This may suggest that FljB is inhibitory to invasion, perhaps it takes longer for the FljB flagella to be shed, or alternatively that FliC mediates some process that enhances invasion. It may be interesting in the future to study these phase-locked mutants carrying a single copy of *prgH*::*gfp*$^+$ with phase-locked mutants expressing *prgH*::*gfp*$^+$ but which can not produce SPI-1 TTSS, or produce the TTSS but cannot secrete effector molecules, as it may clarify the role of SPI-1 in adhesion.

Since the wild type shows a bias towards expression of FljB and the *luxS*$^-$ deletion mutant shows a bias towards FliC, it could have been expected that the wild type would exhibit an increased ability to induce ruffling compared to *luxS*$^-$. Since this did not happen it suggests the effects of a *luxS* deletion on flagella phase variation does not have an obvious effect on invasion. However, it must be remembered that wild type and *luxS*$^-$ populations although biased towards the expression of one type of flagellin will have bacteria expressing the other flagellin and this may lead to a phenotype being masked. Therefore, it may be interesting to compare phase-locked *luxS* mutants to determine whether there is any effect of *luxS* on flagella and invasion.

In summary, it was found that in *S.* Typhimurium SL1344, deletion of *luxS* does not appear to affect the expression of *prgH*, and therefore probably does not affect the ability of the *luxS* mutant to form TTSS-1 or its ability to secrete the effector proteins required for invasion. As a consequence the behaviour of the *luxS*$^-$ mutant was similar to that of the wild type, with no consistent difference being exhibited in the time in which it takes to induce ruffle formation after adherence to a cell, in the number of ruffles that it can propagate and in the rate of invasion. Thus, I have found no evidence to suggest *luxS* affects invasion of *Salmonella* in the *in vitro* models used here, indicating quorum sensing is not involved with these specific virulence mechanisms.

Chapter Four

Investigation to determine whether the role of SipA in invasion may vary between S. Typhimurium strains

4.1. Introduction

An important stage in *Salmonella enterica* pathogenesis is the ability of the bacterium to enter and survive in host cells, including those that are not normally phagocytic e.g. intestinal epithelial cells. To enter such cells, *Salmonella* depends on a 40kb region of the chromosome, located at centisome 63, termed *Salmonella* pathogenicity island 1 (SPI-1) (Mills *et al.*, 1995; Collazo and Galan, 1997). Genes within SPI-1 encode the regulatory and structural proteins of a type III protein secretion system (TTSS-1), and several effector proteins and their chaperones (reviewed by Hueck, 1998; Ly and Casanova, 2007). These effector proteins, with others encoded elsewhere in the *Salmonella* chromosome, are translocated into the host cell cytoplasm by TTSS-1 (Galan, 2001), where they subvert the host cellular machinery, mediating uptake of *Salmonella* into the cell in a membrane 'ruffle' (Finlay *et al.*, 1991; Ginnochio *et al.*, 1992; Francis *et al.*, 1992). The ability to transfer bacterial proteins into host cells is central to pathogenesis. Mutations in genes encoding components of TTSS-1 virtually eliminate invasion of cultured epithelial cells as effector protein translocation is inhibited (Galan and Curtiss III, 1989; Ginocchio *et al.*, 1992; Groisman and Ochman, 1993; Altmeyer *et al.*, 1993; Kaniga *et al.*, 1994; Collazo *et al.*, 1995). Likewise, inactivation of the *Salmonella* invasion protein (Sip) genes *sipB*, *sipC* or *sipD*, which encode a translocon required for effector protein transfer across the host cell membrane, confers a profound defect in invasion of cultured cells (Hueck *et al.*, 1995; Kaniga *et al.*, 1995a; Kaniga *et al.*, 1995b).

The entrance of *Salmonella* into host cells is dependent upon the actin cytoskeleton since addition of cytochalasins which interfere with actin polymerisation prevent *Salmonella* invasion (Finlay and Falkow, 1988). The co-ordinated actions of six effector proteins (SipA, SipC, SopB/SigD, SopE, SopE2

and SptP) modulate the host cell actin cytoskeleton to drive internalisation of *Salmonella* (Hayward and Koronakis, 2002). *Salmonella* outer protein E (SopE) and SopE2 act as guanine nucleotide exchange factors (GEFs) for Rho GTPases, such as Cdc42, Rac1 and RhoG (Hardt *et al.*, 1998; Rudolph *et al.*, 1999; Stender *et al.*, 2000; Patel and Galan, 2006), while SopB indirectly activates Rho GTPases, possibly through the endogenous eukaryotic SH3-containing GEF (SGEF) (Patel and Galan, 2006). Activation of Rho GTPases leads to signalling events that promote actin polymerisation and the cytoskeletal rearrangements necessary for the membrane ruffling that drives *Salmonella* uptake. SptP, as a GTPase activating protein (GAP), is an antagonist of this pathway, downregulating the Rho GTPases and switching off actin polymerisation (Fu and Galan, 1999; Murli *et al.*, 2001). This allows *Salmonella* to terminate membrane ruffling; the host cell survives and regains its normal architecture, providing a suitable environment in which *Salmonella*, enclosed within a *Salmonella* containing vacuole (SCV), can replicate.

While SopE, SopE2 and SopB stimulate actin polymerisation, SipA and SipC as actin binding proteins (ABPs), control and localise the polymerisation to sites where bacteria have adhered. SipC possesses distinct C- and N- terminal domains which directly nucleate actin polymerisation and bundle filamentous actin (F-actin), respectively (Hayward and Koronakis, 1999; McGhie *et al.*, 2001). *In vitro* SipA stimulates these SipC activities (McGhie *et al.*, 2001), while also binding F-actin and promoting its formation by decreasing the critical concentration of globular actin (G-actin) required for polymerisation (Galkin *et al.*, 2002; Zhou *et al.*, 1999a). SipA also inhibits F-actin depolymerisation through excluding host ABPs, such as actin depolymerisation factor (ADF)/cofilin and gelsolin, from the sites on F-actin they require to initiate depolymerisation and severing (Zhou *et al.*, 1999a; McGhie *et al.*, 2004). Interactions with bacterial and host cell proteins by SipA enhances the strength of actin filaments; SipA stimulates F-actin bundling by SipC (McGhie *et al*, 2001), and cross-linking of F-actin into tight parallel bundles by T-plastin (fimbrin), a host cell ABP (Zhou *et al.*, 1999b). The multiple actions of SipA are likely to be responsible for the localised, stable F-actin filaments that support the membrane protrusions required for bacterial invasion, and explain why *sipA* null

mutants exhibit invasion defects at early time points (Zhou *et al.*, 1999a; Jepson *et al.*, 2001).

While SipA, SipC, SopB, SopE and SopE2 have all been shown to drive the internalisation of *Salmonella* (Bakshi *et al.*, 2000; Hueck *et al.*, 1995; Kaniga *et al.*, 1995a; Kaniga *et al.*, 1995b; Wood *et al.*, 1996), and their mechanisms of action are largely understood, the relative importance of each has been difficult to determine since these proteins show redundancy i.e. exhibit overlapping functions so that deletion of one may not significantly change bacterial phenotype, and masks the role of the deleted protein. The exact role and importance of SipA in particular remains controversial, with contradictory data reported regarding the role of SipA in membrane ruffle formation (Zhou *et al.*, 1999a; Jepson *et al.*, 2001; Higashide *et al.*, 2002). Furthermore, analysis of the role of SipA in the invasion of epithelial cells has only been performed in *S.* Typhimurium strain SL1344 (Kaniga *et al*, 1995b; Hueck *et al.*, 1995; Zhou *et al.*, 1999a, b; Jepson *et al.*, 2001; Higashide *et al.*, 2002), thus, it is not clear if SipA exhibits the same role in each *Salmonella* strain, a pertinent question considering SL1344 is one of only a small number of *Salmonella* strains that possess SopE (Hardt *et al.*, 1998b; Mirold *et al.*, 1999). The work presented here examines the hypothesis that the role of SipA in invasion may vary between *Salmonella* strains. The effect of SipA deletion in four serovar Typhimurium strains, including those that possess or lack SopE, is compared with respect to the number, morphology and dynamics of the membrane ruffles they induce, and their ability to invade cultured epithelial cells, using a range of microscopy techniques, including confocal and electron microscopy and live cell imaging. The role of SipA is also investigated in the absence of SopE2 and SopB to determine whether the role of SipA might be dependent upon the other effector proteins required for invasion.

4.2. Materials and Methods

4.2.1. Bacterial strains

The *S.* Typhimurium strains listed in Table 4.1 were grown as described in Chapter 2. Briefly, several colonies grown on LB agar were inoculated into 2mls LB Miller broth and grown overnight at 37°C as a static culture. From this culture, 100µl was used to inoculate 10mls LB Miller broth, which was grown at 37°C for 3.5 hours in a shaking incubator at 100rpm. Antibiotics were used at the following concentrations; carbenicillin 100µg/ml, chloramphenicol 15µg/ml, kanamycin 100µg/ml, tetracycline 50µg/ml.

4.2.2. Creating a *sipA* null mutant

This method is based on the one step gene disruption technique of Datsenko and Wanner, 2000. Briefly, primers 5'+P1-SipA and 3'+P2-SipA (Table 4.3) were obtained from MWG based on sequences from http://www.falkow.stanford.edu/whatwedo/wanner. A PCR using these primers amplified the chloramphenicol resistance cassette from plasmid pKD3, adding sequences to the 5' and 3' end of this cassette homologous to the regions flanking the *sipA* gene (Figure 4.1). PCR products were purified using a Qiagen® PCR purification kit, and then digested with *Dpn*I, repurified and suspended in 40µl water. The DNA concentration was determined by measuring the absorbance at 260nm using sterile water as a blank.

Plasmid pKD46, which encodes λ red recombinase under the control of the arabinose inducible pBAD promoter, was introduced into the parent strain containing the gene to be disrupted. pKD46 transformants were grown in LB with carbenicillin and 30mM L-arabinose at 37°C until an OD_{600} of ~ 0.6 was reached. The pKD46 transformants were made electrocompetent by concentrating 100-fold and washing three times with ice-cold water. Electroporation was performed using a Bio-Rad Micropulser™ electroporator, as recommended by the manufacturer, using 15µl of purified PCR product and 85µl of cells. Shocked cells were incubated in 1ml SOC media at 37°C for 60 min,

and 100µl plated onto agar selecting for chloramphenicol resistant (cm^R) transformants. A further 100µl was plated after the bacteria were pelleted and resuspended in 200µl SOC media. The remaining 100µl was kept at room temperature, and if no colonies were obtained within 24 hours, spread on the selective agar plates. After this primary selection, mutants were colony-purified in selective media at 37°C and then tested for ampicillin sensitivity to test for the loss of pKD46.

Figure 4.1 Schematic of the creation of a SL1344 *sipA*⁻ mutant using the λ Red system.

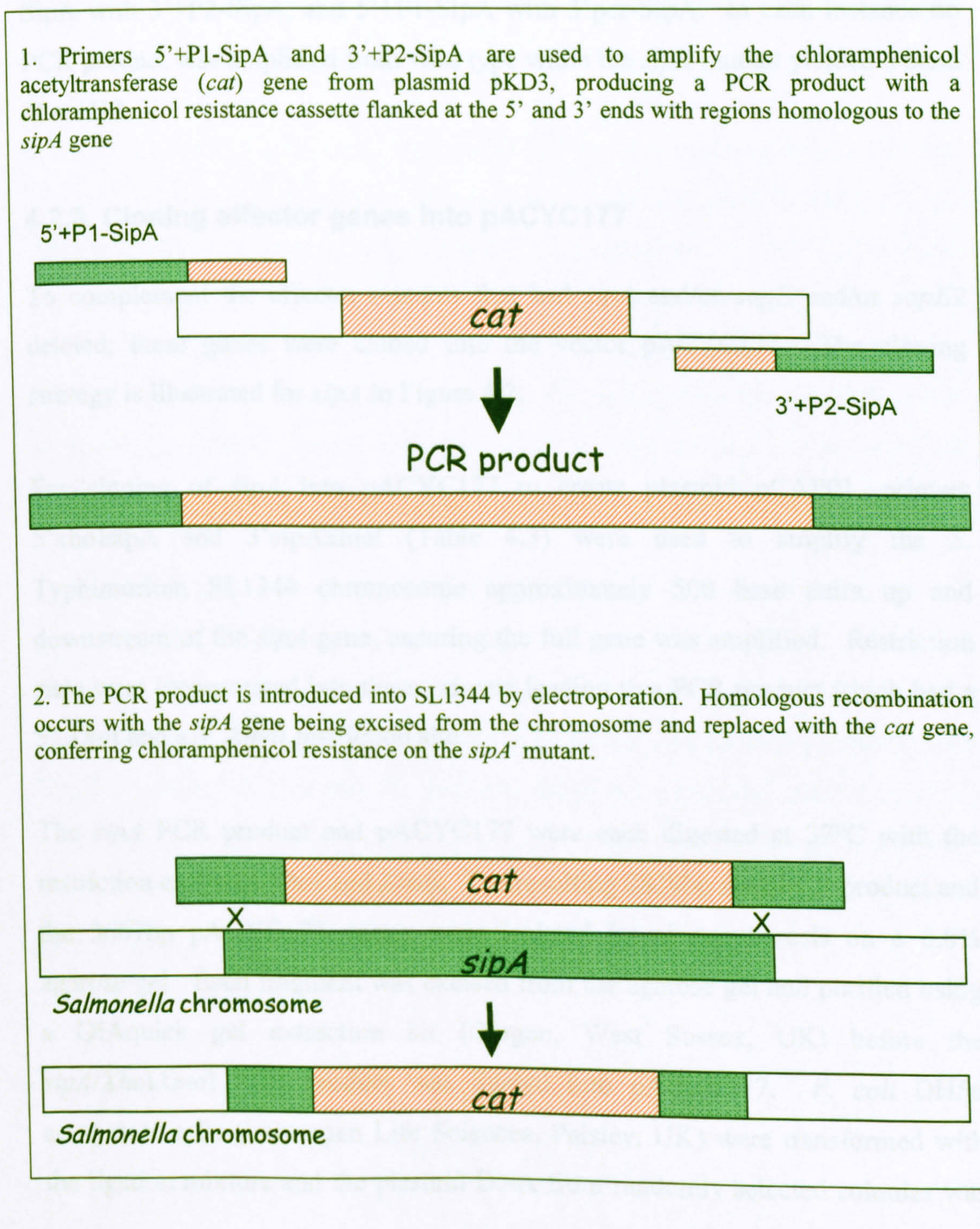

PCR verification was used to show that chloramphenicol resistant colonies were *sipA*⁻ mutants. A freshly isolated colony was suspended in 40µl water in a 0.5ml microcentrifuge tube, and subsequently incubated in boiling water for 10 minutes. 5µl aliquots were removed for use in separate 50µl PCRs. Primers 5'pcr-SipA and 3'pcr-SipA (Table 4.3) were used to amplify *sipA*. In the wild type this produced a PCR product of 2.5kb, and in the *sipA* null mutant a product of ~1kb. To check the presence of a deleted *sipA* gene in the mutant, PCR to amplify the chloramphenicol resistance gene was performed with primers 5'+P1-SipA and 3'+P2-SipA (Table 4.3), and by mixing the two primer sets e.g. 5'pcr-SipA with 3'+P2-SipA, and 5'+P1-SipA with 3'pcr-SipA. In each instance no PCR product was amplified from wild type while the *sipA* mutant yielded a band of a ~1kb.

4.2.3. Cloning effector genes into pACYC177

To complement the effector mutants that had *sipA* and/or *sopE* and/or *sopE2* deleted, these genes were cloned into the vector pACYC177. The cloning strategy is illustrated for *sipA* in Figure 4.2.

For cloning of *sipA* into pACYC177 to create plasmid pCAP01, primers 5'xhoIsipA and 3'sipAxmaI (Table 4.3) were used to amplify the *S.* Typhimurium SL1344 chromosome approximately 500 base pairs up and downstream of the *sipA* gene, ensuring the full gene was amplified. Restriction sites were incorporated into these primers leading to a PCR product which had a 5' *Xho*I and a 3' *Xma*I restriction site.

The *sipA* PCR product and pACYC177 were each digested at 37°C with the restriction enzymes *Xho*I and *Xma*I. The resulting 2839bp *sipA* PCR product and the 3667bp pACYC177 vector were isolated by electrophoresis on a 0.8% agarose gel. Each fragment was excised from the agarose gel and purified using a QIAquick gel extraction kit (Qiagen, West Sussex, UK) before the *sipA*/*Xho*I*Xma*I PCR product was ligated into pACYC177. *E. coli* DH5α competent cells (Invitrogen Life Sciences, Paisley, UK) were transformed with the ligation mixture and the plasmid DNA from randomly selected colonies was

purified by miniprep. Clones were analysed for the correct *sipA* orientation using different restriction digests. Digestion of correctly orientated *sipA* with *Xho*I and *Xma*I generated two DNA bands of 2839bp and 3667bp, while digestion with *Dra*I produced DNA bands of 3871bp, 1559bp, 692bp, 365bp and 19bp, and digestion with *BamH*I, bands of 2720bp and 3790bp.

Final confirmation that the *sipA* gene was present was provided by the MWG DNA sequencing service. Two individual sequencing reactions were performed; the first using the 5'pcr-SipA and 3'pcr-SipA primers, the second using the 5'xhoIsipA and 3'sipAxmaI primers (Table 4.3). Cells were then transformed with plasmid pCAP01 using electroporation.

For cloning of *sopE* and *sopE2* into pACYC177 to create plasmids pCAP03 and pCAP02 respectively, a similar approach was used. Primers 5'xhoIsopE and 3'sopEhindIII were used to amplify the *S.* Typhimurium SL1344 chromosome approximately 500 base pairs up- and downstream of the *sopE* gene, while primers 5'xhoIsopE2 and 3'sopE2hindIII were used to amplify the *sopE2* gene. Both PCR products had a 5' *Xho*I restriction site and a 3'*Hin*dIII recognition site, so restriction endonucleases *Xho*I and *Hin*dIII could be used to cut the PCR products and pACYC177 prior to ligation.

Clones were analysed for the correct *sopE* orientation with *Xho*I and *Hin*dIII generating two DNA bands of 3421bp and 1596bp, and also digestion with *Dra*I, producing DNA bands of 2323bp, 1980bp, 692bp and 19bp. Clones were analysed for the correct *sopE2* orientation with *Xho*I and *Hin*dIII generating two DNA bands of 3421bp and 1511bp, and digestion with *Dra*I producing DNA bands of 2271bp, 1523bp, 692bp, 427 and 19bp. Again, the plasmids were sequenced by MWG to confirm the presence of either *sopE* (pCAP03) or *sopE2* (pCAP02).

Figure 4.2 Schematic of pCAP01 creation

1. pACYC177 is chosen as the cloning vector due to its low copy number ~15 copies per cell.

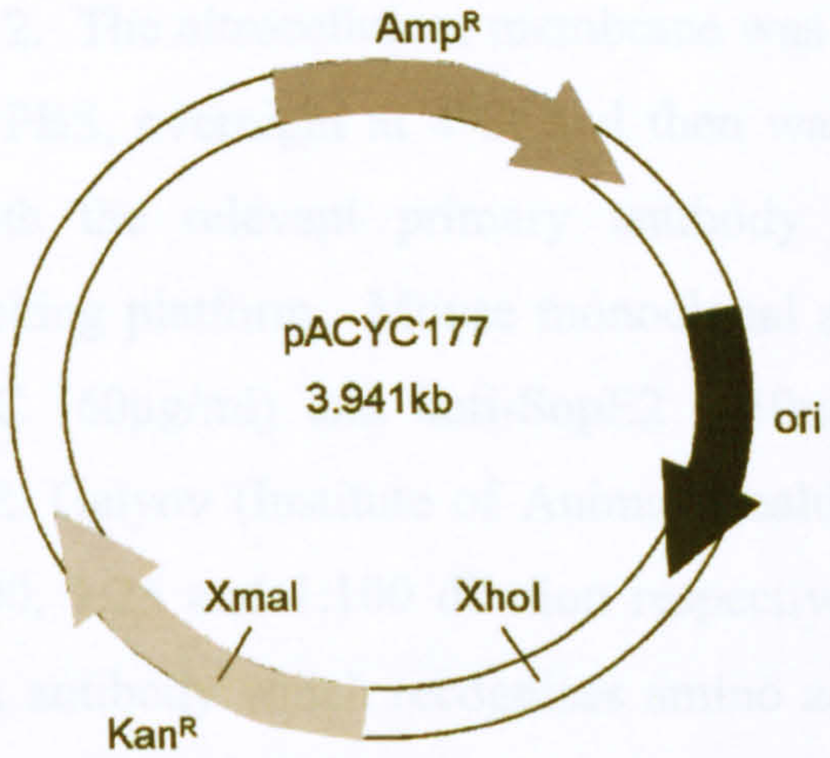

2. The cloning vector and a PCR product containing the *sipA* gene with ~500bp up- and downstream are cut with the restriction endonucleases *Xho*I and *Xma*I to yield sticky ends.

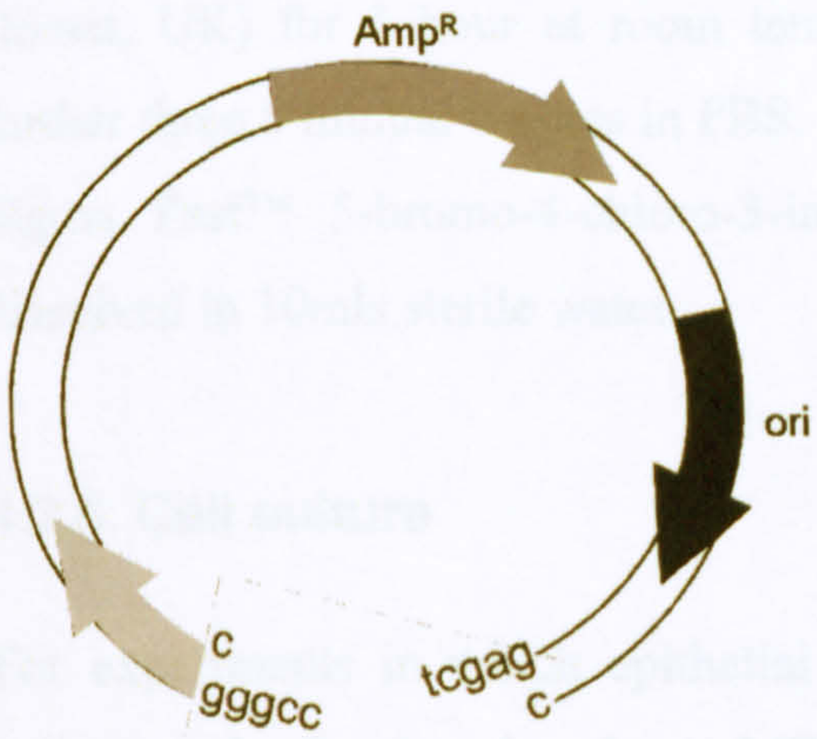

3. The cut vector and PCR product are ligated together to yield pCAP01.

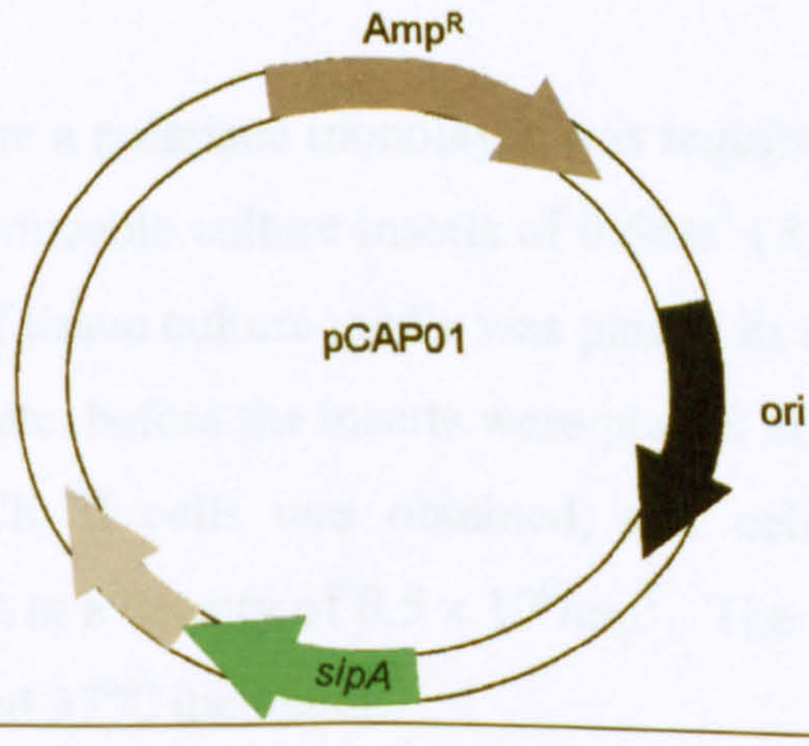

4.2.4. SDS-PAGE and Western blotting

SDS-PAGE and the transfer of proteins onto nitrocellulose were performed as described in Chapter 2. The nitrocellulose membrane was blocked with 5% milk protein, prepared in PBS, overnight at 4°C, and then washed with PBS before being incubated with the relevant primary antibody for 1 hour at room temperature on a rocking platform. Mouse monoclonal anti-SipA (MAB AA1; 500µg/ml), anti-SipC (60µg/ml) and anti-SopE2 (650µg/ml) antibodies were provided by Dr E. E. Galyov (Institute of Animal Health, Compton, UK), and were used at a 1:100, 1:25 and 1:100 dilution respectively. Polyclonal rabbit anti-SopE peptide A antibody which recognises amino acids 2-16 of SopE was provided by Dr C. M. A. Khan (University of Newcastle, UK), and was used 1:500. Incubation with the primary antibody was followed by three 5 minute washes in PBS. The membrane was then incubated with a 1:2000 dilution of secondary alkaline phosphatase linked IgG antibody (Sigma-Aldrich, Poole, Dorset, UK) for 1 hour at room temperature on a rocking platform before a further three 5 minute washes in PBS. Detection was performed using 1 tablet of Sigma Fast™ 5-bromo-4-chloro-3-indolyl phosphate/ nitro blue tetrazolium dissolved in 10mls sterile water.

4.2.5. Cell culture

For experiments in which epithelial cells were infected with *Salmonella* and subsequently fixed and stained, MDCK strain I cells were seeded on 13mm coverslips (2.5×10^4 cells per coverslip, unless otherwise stated) and maintained at 37°C in a humidified atmosphere of 5% CO_2 for 3 days.

For experiments where a polarised monolayer was required, MDCK II cells were grown on Anocell permeable culture inserts of $0.5cm^2$ (Anocell, Nunc, Roskilde, Denmark). 1.5mls of tissue culture media was placed in the wells of a sterile 12-well tissue culture plate, before the inserts were placed in the wells. A single cell suspension of MDCK II cells was obtained, and cells seeded in the upper chamber of the insert at a density of $0.5 \times 10^6/cm^2$. The plates were kept for 3-4 days in the humidified 37°C incubator.

4.2.6. Infection of cultured cells

The culture media was replaced by modified Krebs buffer and cell monolayers kept at 37°C for 15 minutes to achieve equilibrium. *S.* Typhimurium was then added at a multiplicity of infection (MOI) of approximately 100, unless otherwise stated, with monolayers being maintained at 37°C for 15 minutes, unless otherwise stated.

4.2.7. Statistics

Results are expressed as means ± standard error of the mean (sem). Statistical analysis was calculated using a two-tailed, unpaired Student t-test or where there were more than 2 samples, a One-Way ANOVA followed by a Tukey post-hoc test when all samples were compared or a Bonferroni post-hoc test where only selected samples were compared. Significance was set at a value of $P<0.05$ or less. The PRISM Graphpad 3.0 software was used to apply statistical tests.

Table 4.1 *Salmonella enterica* serovar Typhimurium strains used in this chapter

Bacterial strain	Relevant genotype	Antibiotic resistance	Source/Reference
SL1344 (2001)	Wild type	None	Hueck *et al.*, 1995
EE633	SL1344 *sipA*::lacZY4	tetracycline	Hueck *et al.*, 1995
SL1344	Wild type	None	C. M. A. Khan
SL1344 *sipA*⁻	SL1344 with inframe deletion within *sipA*	chloramphenicol	This study
SL1344 *sipA*⁻ pCAP01	SL1344 with inframe deletion within *sipA*, p*sipA*	chloramphenicol & carbenicillin	This study
SL1344 *sopE*⁻	SL1344 with inframe deletion within *sopE*	kanamycin	C. M. A. Khan
SL1344 *sopE*⁻ pCAP03	SL1344 with inframe deletion within *sopE*, p*sopE*	kanamycin & carbenicillin	This study
SL1344 *sipA*⁻ *sopE*⁻	SL1344 with inframe deletion within *sipA* and *sopE* genes	chloramphenicol & kanamycin	This study
SL1344 *sipA*⁻ *sopE*⁻ pCAP01	SL1344 with inframe deletion within *sipA* and *sopE* genes, p*sipA*	chloramphenicol, kanamycin & carbenicillin	This study
SL1344 *sipA*⁻ *sopE*⁻ pCAP03	SL1344 with inframe deletion within *sipA* and *sopE* genes, p*sopE*	chloramphenicol, kanamycin & carbenicillin	This study
SL1344 *sopE2*⁻	SL1344 with inframe deletion within *sopE2* gene	kanamycin	This study
SL1344 *sopE2*⁻ pCAP02	SL1344 with inframe deletion within *sopE2* gene, p*sopE2*	kanamycin & carbenicillin	This study
SL1344 *sipA*⁻ *sopE2*⁻	SL1344 with inframe deletion within *sipA* and *sopE2* genes	chloramphenicol & kanamycin	This study
SL1344 *sipA*⁻ *sopE2*⁻ pCAP01	SL1344 with inframe deletion within *sipA* and *sopE2* genes, p*sipA*	chloramphenicol, kanamycin & carbenicillin	This study
SL1344 *sipA*⁻ *sopE2*⁻ pCAP02	SL1344 with inframe deletion within *sipA* and *sopE2* genes, p*sopE2*	chloramphenicol, kanamycin & carbenicillin	This study
SL1344 *sopB*⁻	SL1344 with inframe deletion within *sopB* gene	None	O. Steele-Mortimer *et al.*, 2000

Table 1.1 cont'd

SL1344 *sopB*⁻ p*sopB*	SL1344 with inframe deletion within *sopB* gene, p*sopB*	carbenicillin	O. Steele-Mortimer *et al.*, 2000
SL1344 *sipA*⁻ *sopE*⁻ *sopB*⁻	SL1344 with inframe deletion within *sipA*, *sopE* and *sopB* genes	chloramphenicol & carbenicillin	This study
SL1344 *sptP*⁻	SL1344 with inframe deletion within *sptP*	kanamycin	This study
S1579/94	Wild type	None	R.M. La Ragione
S1579/94 *sipA*⁻	S1579/94 with inframe deletion within *sipA*	chloramphenicol	This study
S1579/94 *sipA*⁻ pCAP01	S1579/94 with inframe deletion within *sipA*, p*sipA*	chloramphenicol & carbenicillin	This study
S1579/94 *sopE*⁻	S1579/94 with inframe deletion within *sopE*	kanamycin	This study
S1579/94 *sopE*⁻ pCAP03	S1579/94 with inframe deletion within *sopE*, p*sopE*	kanamycin & carbenicillin	This study
S1579/94 *sipA*⁻ *sopE*⁻	S1579/94 with inframe deletion within *sipA* and *sopE* genes	chloramphenicol & kanamycin	This study
S1579/94 *sipA*⁻ *sopE*⁻ pCAP01	S1579/94 with inframe deletion within *sipA* and *sopE* genes, p*sipA*	chloramphenicol, kanamycin & carbenicillin	This study
S1579/94 *sipA*⁻ *sopE*⁻ pCAP03	S1579/94 with inframe deletion within *sipA* and *sopE* genes, p*sopE*	chloramphenicol, kanamycin & carbenicillin	This study
F98	Wild type	nalidixic acid	E.E. Galyov
F98 *sipA*⁻	F98 with inframe deletion within *sipA*	nalidixic acid & chloramphenicol	This study
F98 *sipA*⁻ pCAP01	F98 with inframe deletion within *sipA*, p*sipA*	nalidixic acid, chloramphenicol & carbenicillin	This study
12023	Wild type	None	D.W. Holden
12023 *sipA*⁻	12023 with inframe deletion within *sipA*	chloramphenicol	This study
12023 *sipA*⁻ pCAP01	12023 with inframe deletion within *sipA*, p*sipA*	chloramphenicol & carbenicillin	This study

Table 4.2 Plasmids used in this work

Plasmids	Relevant genotype	Source or reference
pKD46	λ red recombinase under the control of the arabinose inducible pBAD promoter, ampicillin resistance	Datsenko & Wanner, 2000
pKD3	cm^R	Datsenko & Wanner, 2000
pACYC177	Cloning vector; cb^R, kan^R	R. La Ragione
pCAP01	pACYC177 carrying *sipA*; cb^R	This study
pCAP02	pACYC177 carrying *sopE2*; cb^R	This study
pCAP03	pACYC177 carrying *sopE*; cb^R	This study

Table 4.3 Primers used in this study. Sequences underlined are priming sites that allow the primer to bind pKD3. Sequences in bold type are restriction sites.

Primer	Sequence	Engineered restriction endonuclease site
5'pcr-SipA	AGTAGCAGCCTGGAAACCGC	
3'pcr-SipA	GGTGATCACTTTTTTGACTC	
5'+P1-SipA	CAAAAGCTTCCTGCAAGGATAACAGAAGAGGATATTAATAGTGTAGGCTGGAGCTGCTTC	
3'+P2-SipA	TTGCTTCAATATCCATATTCATCGCATCTTTCCCGGTTAACATATGAATATCCTCCTTAG	
5'xhoIsipA	CCG**CTCGAG**TATAATCAAATAAACAGTAATACC	*Xho*I
3'sipAxmaI	TCC**CCCGGG**TGAACCGGGTACTACATGTGTGAT	*Xma*I
5'pcr-sopE	TAAAAGTATTCCTGCTATCT	
3'pcr-sopE	GATACTATTGGTTCATATTA	
5'xhoIsopE	CCG**CTCGAG**CAGTGCTGGTACAATATCGCCAC	XhoI
3'sopEhindIII	CAT**AAGCTT**ATACGCCTGAAGAGCTGGTTG	*Hin*dIII
5'pcr-sopE2	TGAAAGCAAGAAATATAAAC	
3'pcr-sopE2	TAGTTTCAGAAAATCTGCTA	
5'xhoIsopE2	CCG**CTCGAG**GATTACAGTGACGGAGAGGTTTG	*Xho*I
3'sopE2hindIII	CAT**AAGCTT**AGTGATCCTCAAGGCAAACCAG	*Hin*dIII
SptP5'pcr	TATCGCAGCTTGAGTCATTT	
SptP3'pcr	CGCCATTGGTCATAACCGAG	

4.3. Results

4.3.1. Determining the presence or absence of SopE in four *Salmonella enterica* serovar Typhimurium strains

To examine whether SipA has the same role in different strains of *S.* Typhimurium, and whether this role is influenced by the presence of SopE, four strains of *S.* Typhimurium were obtained; two, SL1344 and S1579/94, were reported to possess the SopE protein, and two, F98 and 12023, were believed to lack SopE. To check the *sopE* genotype of these strains, a polymerase chain reaction (PCR) was performed with primers 5'pcr_sopE and 3'pcr_sopE (Table 4.3), which amplify an 843 base pair (bp) fragment of the *sopE* gene. Figure 4.3 shows the results of agarose gel electrophoresis performed with the PCR products.

Figure 4.3 Determining the presence or absence of the *sopE* gene in *S.* Typhimurium strains. Primers 5'pcr_sopE and 3'pcr_sopE were used to amplify the *sopE* gene in two independent PCRs. Lane 1 is the 1kb marker. The presence of *sopE* in strains SL1344 (lanes 2 and 3) and S1579/94 (lane 6) was indicated by a PCR product of 843bp. No PCR product was produced for strains F98 (lane 5) and 12023 (lane 7) indicating the absence of *sopE* in these strains. SL1344 *sopE*⁻ (lane 4) produces a band at 1.6kb since the kanamycin resistance cassette inserted at the site of the *sopE* gene by homologous recombination is larger than the portion of the *sopE* gene removed.

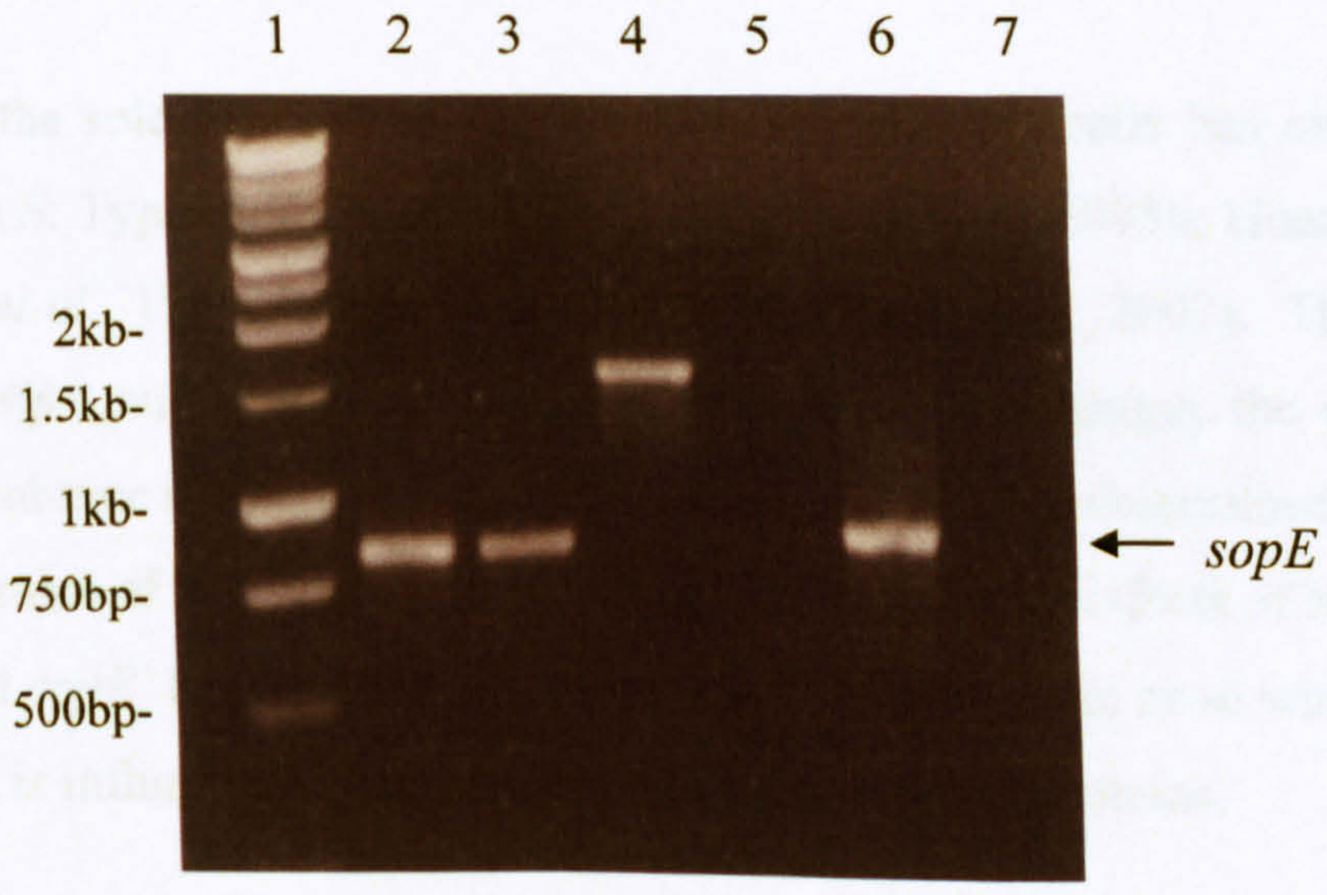

The size of the PCR product for *S.* Typhimurium strains SL1344 and S1579/94 lies between the 750bp and 1kb markers, suggesting it is the 843bp product expected when the *sopE* gene is amplified by primers 5'pcr_sopE and 3'pcr_sopE. This confirms strain SL1344 and strain S1579/94 possess the *sopE* gene. Reactions using DNA from strains F98 and 12023 repeatedly failed to produce a PCR product, confirming these serovar Typhimurium strains lack *sopE*. A SL1344 *sopE* null mutant (SL1344 *sopE*$^-$) produced a band at ~1.6kb, which corresponds to the extra nucleotides present due to insertion of a kanamycin resistance cassette in place of part of the *sopE* gene.

The results of the PCR were validated by looking for the presence of SopE in the supernatants of cultures grown until late log phase in LB at 37°C i.e. conditions that stimulate protein secretion through TTSS-1. Coomassie Blue staining of the acrylamide gel, in which the proteins were separated, did not provide enough resolution to identify the presence of SopE (Figure 4.4A); therefore a Western blot was performed using an anti-SopE monoclonal antibody (Figure 4.4B). Anti-SipA and anti-SipC monoclonal antibodies were used as positive controls to demonstrate the ability of TTSS-1 to secrete proteins. Figure 4.4B confirms that all 4 of the *S.* Typhimurium strains synthesise and secrete the effector proteins SipA and SipC, but only strains SL1344 and S1579/94 produce and secrete SopE, matching the results obtained from the PCR (Figure 4.3).

Analysis of the role of SipA in the invasion of epithelial cells has only been performed in *S.* Typhimurium strain SL1344 (Kaniga *et al*, 1995b; Hueck *et al.*, 1995; Zhou *et al.*, 1999; Jepson *et al.*, 2001; Higashide *et al.*, 2002). Therefore, by creating *sipA* null mutants in each of these wild type strains, the effect of SipA on membrane ruffling and invasion behaviour could be determined in three additional strains of *S.* Typhimurium. Moreover, comparing effects of SipA loss in *sopE*$^+$ and *sopE*$^-$ backgrounds allows inferences to be made as to whether the role of SipA is influenced by the presence of other effector proteins.

Figure 4.4 Analysis of the proteins secreted by four serovar Typhimurium strains into the culture supernatant. The protein samples from SL1344 (lane 1), S1579/94 (lane 2), F98 (lane 3) and 12023 (lane 4) were precipitated with 10% trichloroacetic acid, separated by SDS-PAGE and either stained with Coomassie Blue (A) or transferred to a nitrocellulose membrane, and probed with anti-SipA, anti-SipC and anti-SopE monoclonal antibodies (B). Positions and molecular weights of standard proteins are shown to the left in A.

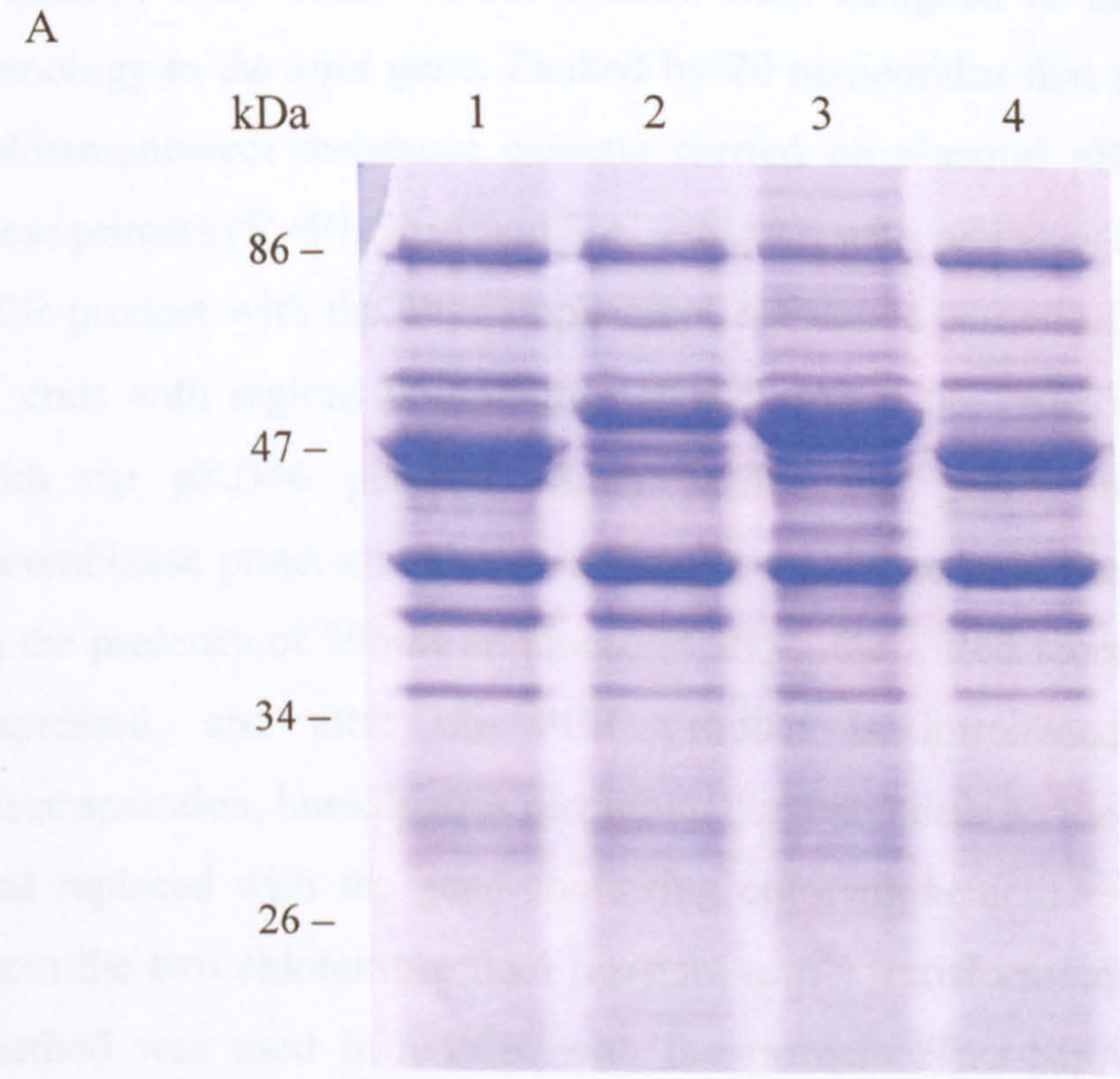

4.3.2. Creation of *sipA*⁻ mutants and transcomplemented mutants

Creation of *sipA*⁻ mutants

The λ Red system described by Datsenko and Wanner (2000) was used to obtain a SL1344 *sipA*⁻ strain. PCR primers were designed to have a 40 nucleotide homology to the *sipA* gene, flanked by 20 nucleotides that are homologous to a chloramphenicol resistance cassette carried on plasmid pKD3. A PCR using these primers (5'+P1-SipA and 3'+P2-SipA), with pKD3 as a template, yielded a PCR product with the chloramphenicol resistance cassette flanked at the 5' and 3' ends with regions homologous to the *sipA* gene. SL1344 was transformed with the pKD46 plasmid which carries the genes encoding the λ Red recombinase proteins under an inducible arabinose promoter. By growing cells in the presence of 30mM arabinose at 30°C, the λ Red recombinase proteins are expressed, and after the PCR product is introduced into SL1344 by electroporation, homologous recombination can occur so the *sipA* gene is excised and replaced with the gene conferring chloramphenicol resistance. The DNA from the two chloramphenicol resistant (cm^R) transformants obtained using this method was used in a PCR with the primers 5'pcr-SipA and 3'pcr-SipA to identify true SL1344 *sipA*⁻ mutants (Figure 4.5).

Figure 4.5 Testing *S.* Typhimurium SL1344 chloramphenicol resistant transformants for a *sipA*⁻ genotype. A *sipA*⁻ mutant (transformant 3.1; lanes 4, 6, 8 and 10) produced a PCR product of ~1kb with each of the primer sets used: 5'pcr-SipA and 3'pcr-SipA (lanes 2 – 4), 5'+P1-SipA and 3'+P2-SipA (lanes 5 and 6), 5'pcr-SipA and 3'+P2-SipA (lanes 7 and 8), and 5'+P1-SipA and 3'pcr-SipA (lanes 9 and 10). Wild type (lanes 2, 5, 7, and 9) only yielded a PCR product of 2.2kb with the 5'pcr-SipA and 3'pcr-SipA primers. Lane 3 represents a chloramphenicol resistant transformant (1.1) which yields a wild type copy of the *sipA* gene. Lane 1 is the marker ladder.

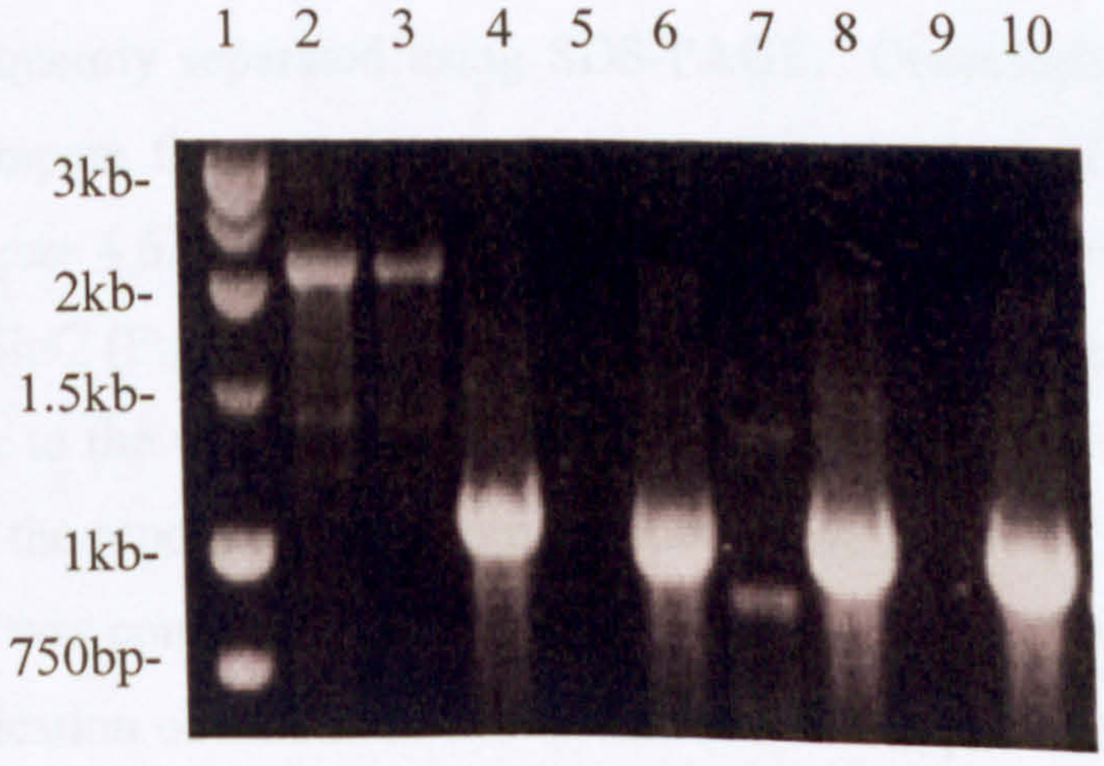

The presence of the wild type *sipA* gene leads to the amplification of a 2.178kb fragment by the 5'pcr-SipA and 3'pcr-SipA primers (lane 2, Figure 4.5). Since chloramphenicol resistant transformant 1.1 produced a PCR product identical in size to that from the wild type, it could be concluded this was not a *sipA* deletion mutant (lane 3, Figure 4.5). The successful replacement of the *sipA* gene with the chloramphenicol resistant cassette led to a smaller PCR product of ~1kb, and indicated that transformant 3.1 was a *sipA* deletion mutant. This was confirmed by performing 3 further PCRs with the primer sets; 5'+P1-SipA and 3'+P2-SipA (lanes 5 and 6), 5'pcr-SipA and 3'+P2-SipA together (lanes 7 and 8), and 5'+P1-SipA and 3'pcr-SipA (lanes 9 and 10). Each of these reactions uses a primer that recognises the chloramphenicol resistance gene, and therefore, a product is only obtained in the *sipA* mutant. Thus, as Figure 4.5 shows, a PCR product of ~1kb is again obtained using DNA from transformant 3.1 as a template (lanes 6, 8 and 10), while no product is yielded from the wild type DNA (lanes 5, 7 and 9). It should be noted that use of the primer 3'+P2-SipA with wild type DNA led to the production of several different products (lane 2 and lane 7), and is due to non-specific binding of the primer at the annealing temperature used.

Confident that transformant 3.1 was a *sipA* deletion mutant, P22 phage was used to transfer this gene knockout back into SL1344 wild type thereby eliminating any additional mutations that were acquired during the creation of the *sipA*$^-$ mutant using the λ red system. PCR using the combinations of primers mentioned above were used to test the cm^R transductants for the absence of *sipA*, and once a suitable transformant was identified, the secreted proteins of the wild type and the *sipA* mutant were isolated from late log phase cultures. The proteins were subsequently separated using SDS-PAGE. Coomassie Blue staining was used to compare the complete protein secretion pattern of the wild type and mutant (Figure 4.6A), while a Western blot was used to confirm the presence of SipA and SipC (Figure 4.6B). The secretion profile of the *sipA* deletion mutant was similar to the wild type apart from the absence of a band at ~86kDa, which pertains to the reported size of SipA (Hueck *et al.*, 1995; Kaniga *et al.*, 1995b). This result was confirmed by the Western blot; the anti-SipA antibody leading to the identification of a band at ~86kDa in the wild type, with no band present in the *sipA*$^-$ mutant.

Figure 4.6 Secreted protein profile of *S.* Typhimurium SL1344 wild type and *sipA*⁻ mutant. The protein samples from wild type (lane 1) and *sipA*⁻ (lane 2) were precipitated with 10% trichloroacetic acid, separated by SDS-PAGE and either stained with Coomassie Blue (A) or transferred to a nitrocellulose membrane and probed with anti-SipA and anti-SipC monoclonal antibodies (B). Positions and molecular weights of standard proteins are shown to the left in figure A.

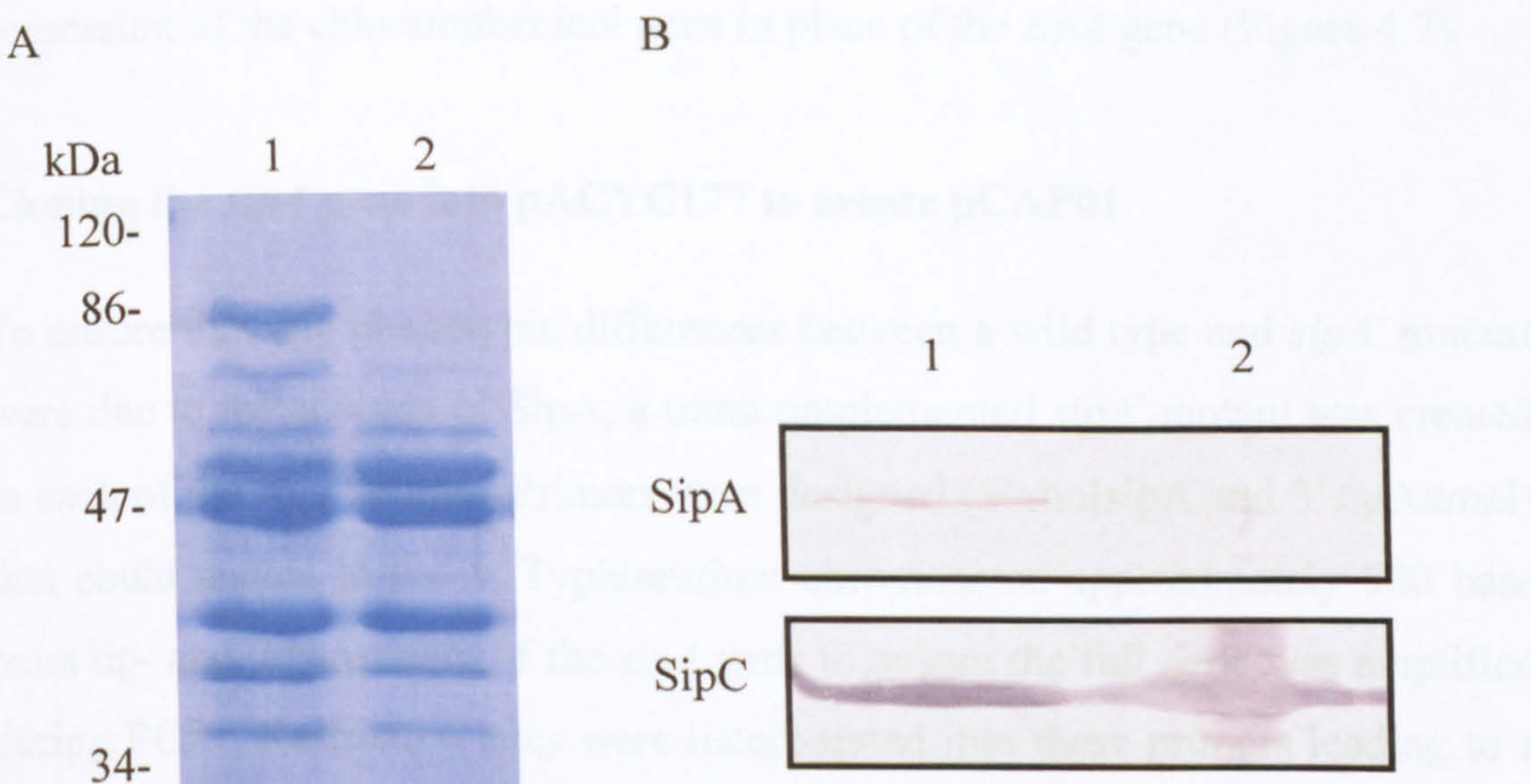

Figure 4.7 Testing *S.* Typhimurium chloramphenicol resistant transformants for a *sipA*⁻ genotype. Primers 5'pcr-SipA and 3'pcr-SipA were used to identify cm^R transductants where the chloramphenicol gene had inserted into the *sipA* gene. Wild types produce a PCR product of 2.2kb, while *sipA*⁻ transductants produce a product of 1kb. *S.* Typhimurium strain F98 wild type (lane 1) and two cm^R *sipA*⁻ mutants (lanes 2 and 3) are shown in A. 12023 wild type (lane 2) and *sipA*⁻ transformant (lane 3), and S1579/94 wild type (lane 4) and *sipA*⁻ transformant (lane 5) are shown in B. Lane 4 in A and lane 1 in B contain a 1kb ladder.

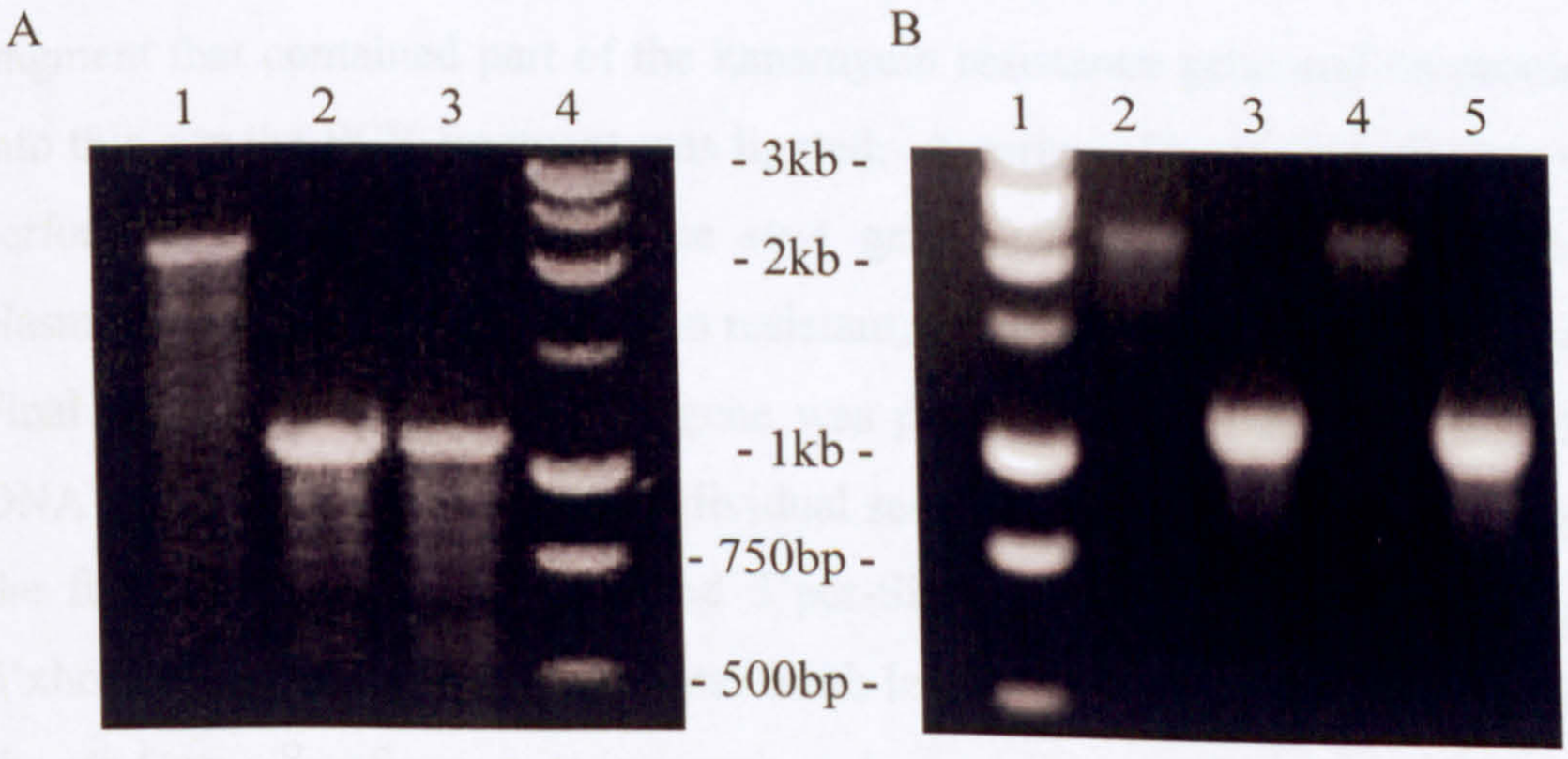

P22 transduction was subsequently used to transfer the mutated *sipA* gene from SL1344 into the other serovar Typhimurium strains; S1579/94, F98 and 12023, thus creating *sipA* null mutants in each strain. Chloramphenicol resistant transductants were screened using PCR as described before to test for the possession of the chloramphenicol gene in place of the *sipA* gene (Figure 4.7).

Cloning the *sipA* gene into pACYC177 to create pCAP01

To ensure that any phenotypic differences between a wild type and *sipA*⁻ mutant were due to the absence of SipA, a transcomplemented *sipA*⁻ mutant was created in each of the four strains. Primers were designed (5'xhoIsipA and 3'sipAxmaI) that could anneal to the *S.* Typhimurium chromosome approximately 500 base pairs up- and downstream of the *sipA* gene to ensure the full gene was amplified during PCR. Restriction sites were incorporated into these primers leading to a PCR product which had a 5' *Xho*I restriction site and a 3' *Xma*I recognition site. The PCR product (insert) and plasmid pACYC177 (vector) were sequentially cut with restriction enzymes *Xho*I and *Xma*I, before the insert was ligated into plasmid pACYC177, to yield plasmid pCAP01. pACYC177 is a low copy number plasmid (~15 copies per cell) that possesses ampicillin resistance genes and kanamycin resistance genes. A low copy number plasmid was used to reduce any metabolic burden the presence of a plasmid may have, and to achieve levels of expression of *sipA* similar to that from the chromosome.

Digestion of pACYC177 with *Xho*I and *Xma*I led to the removal of a 274bp fragment that contained part of the kanamycin resistance gene and its promoter. Into this site the PCR fragment was ligated. A series of restriction digests were performed to identify whether the *sipA* gene had inserted correctly into the plasmids isolated from carbenicillin resistant, kanamycin sensitive transformants. Final confirmation that the *sipA* gene was present was provided by the MWG DNA sequencing service. Two individual sequencing reactions were performed; the first using the 5'pcr-SipA and 3'pcr-SipA primers, the second using the 5'xhoIsipA and 3'sipAxmaI primers. Both led to the amplification of a region of the *sipA* gene, confirming its presence and correct orientation in pCAP01. This

plasmid was introduced into the *sipA*⁻ mutants of each strain to complement *in trans*.

Figure 4.8 Comparing the SipA profile of wild type, *sipA*⁻ and *sipA*⁻ pCAP01 serovar Typhimurium strains SL1344 (A), S1579/94 strains (B), F98 and 12023 (C). Lane 1 corresponds to the wild type, lane 2 to the *sipA*⁻ mutant and 3 to *sipA*⁻ pCAP01. Culture supernatant proteins were prepared by precipitation with 10% trichloroacetic acid, separated by SDS-PAGE, transferred to a nitrocellulose membrane, and probed with anti-SipA and anti-SipC monoclonal antibodies.

A

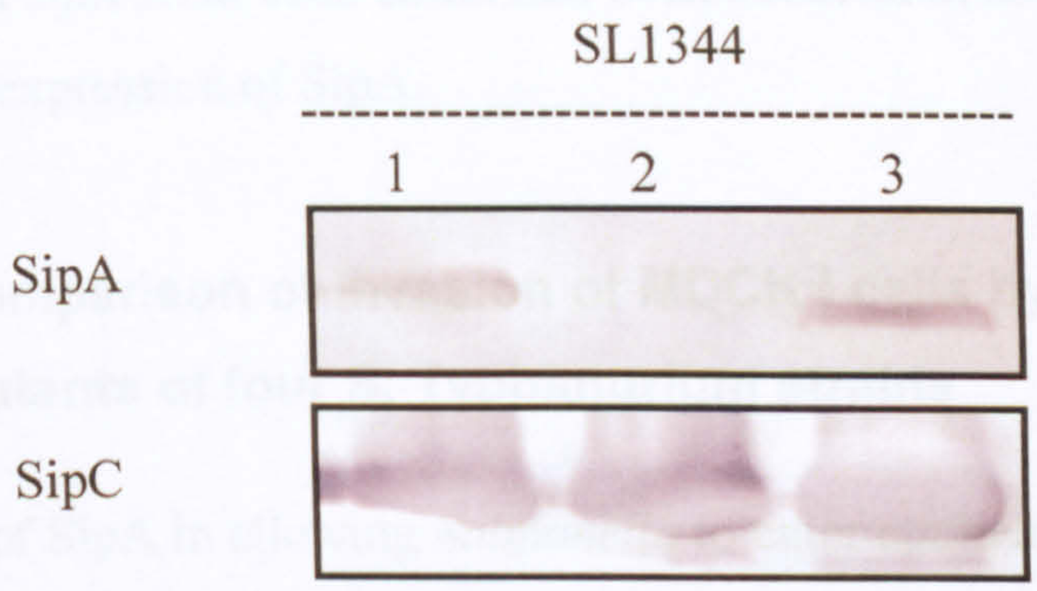

B

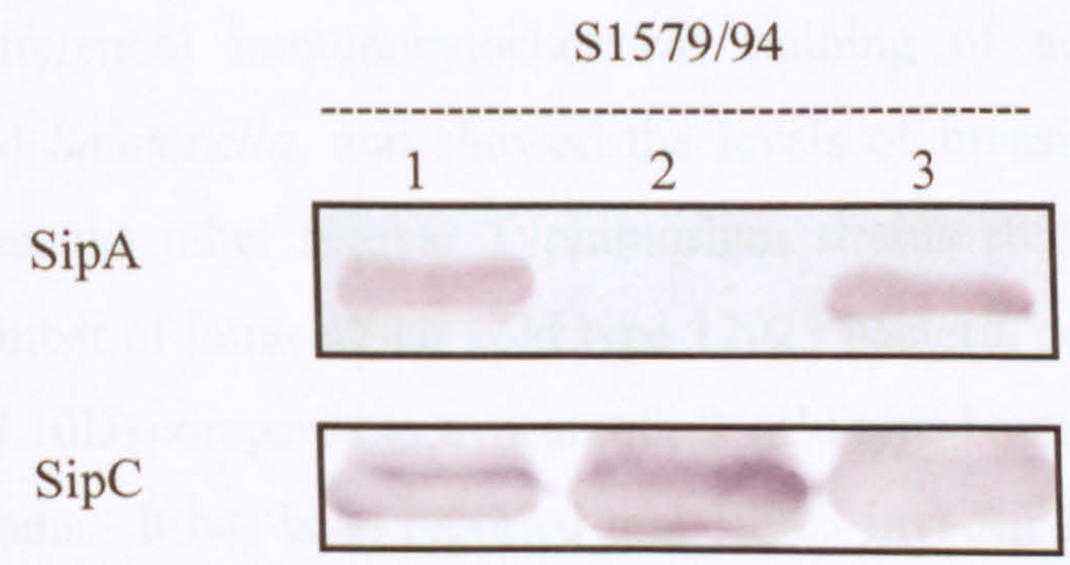

C

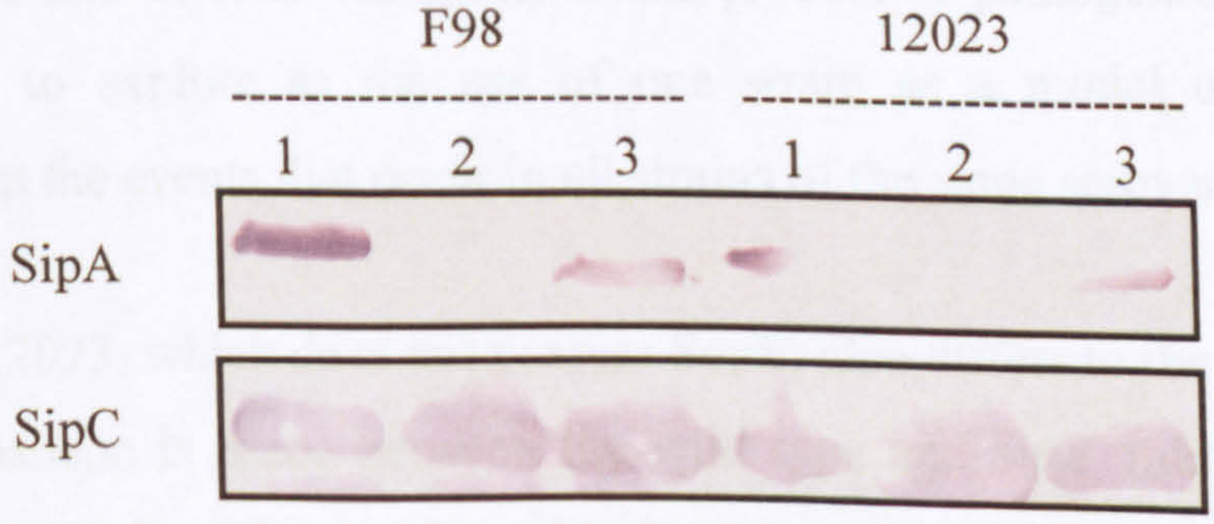

To check the expression of *sipA* from the plasmid the proteins secreted by the wild type, *sipA*⁻ and *sipA*⁻ pCAP01 of each strain were analysed using a Western blot performed with anti-SipA and anti-SipC monoclonal antibodies (Figure 4.8). SipC was present in the secreted proteins of every strain tested, indicating secretion of effector proteins through TTSS-1 had occurred. SipA was only present in wild type and the transcomplemented mutant strains, indicating the deletion of *sipA* from each strain had been successful, as had the use of pCAP01 to restore expression of SipA.

4.3.3. Comparison of invasion of MDCK I cells by the wild type and *sipA*⁻ mutants of four S. Typhimurium strains

The role of SipA in allowing *Salmonella* to enter epithelial cells was examined in each of the four *S.* Typhimurium strains by comparing the abilities of each set of wild type, *sipA*⁻ mutant and transcomplemented mutant (*sipA*⁻ pCAP01) to invade Madin-Darby Canine Kidney (MDCK) strain I cells. Invasion was measured using differential immunocytochemical staining of adhered and total cell-associated *Salmonella*, and showed the levels of invasion of strain 12023 are lower than the other serovar Typhimurium strains studied. For example, the mean number of intracellular wild type 12023 bacteria per cell was 0.60 ± 0.159 (Figure 4.10D) compared to a mean of ~3 wild type bacteria per cell for the other three strains. It has been reported that 12023 invades HeLa cells at low levels (Unsworth *et al.*, 2004), and therefore, it seems likely that 12023 invades most cultured cells at low levels, perhaps indicating fundamental differences between this strain and other strains of *S.* Typhimurium. That within serovar Typhimurium there is variability in the process of pathogenesis is an important concept to explore as the use of one strain as a model organism may not represent the events that occur in all strains of the same serovar.

Strain 12023, which does not possess SopE, also differs to the other strains when a comparison is made between the wild type and *sipA*⁻ mutant. In 12023 the *sipA*⁻ mutant has slightly higher levels of invasion compared to the wild type but

is not statistically different (Figure 4.9D). In strains SL1344 and S1579/94 which possess SopE, and F98 which lacks SopE, the *sipA*⁻ mutant shows a significant decrease in invasion when compared to its wild type, corresponding to an approximately 2.5-fold reduction in SL1344 ($P<0.05$) and S1579/94 ($P<0.01$), with a 5-fold reduction in F98 ($P<0.01$). pCAP01 led to a significant reversal of the invasion defect in these *sipA*⁻ mutants (Figure 4.9), indicating the differences in invasion of the wild type and *sipA*⁻ mutant are due to the absence of SipA alone. It appears the effect of SipA on *Salmonella* invasion is not dependent on SopE since *sipA* deletion from F98, which lacks SopE, leads to the biggest reduction in invasion of all the strains studied, while in 12023, which also lacks SopE, there is no affect on invasion.

Figure 4.9 Comparing the ability to invade MDCK cells by wild type, *sipA*⁻ and *sipA*⁻ pCAP01 serovar Typhimurium strains SL1344 (A), S1579/94 (B), F98 (C) and 12023 (D). SL1344 and S1579/94 possess SopE, while F98 and 12023 do not. Infection was for 15 minutes, with the ability to enter cells being measured using differential staining of adhered bacteria. Results for are the mean of three (SL1344 and 12023) or four (S1579/94 and F98) independent experiments ± standard error of the mean. Asterisks denote a statistical difference when using a one way ANOVA with a Tukey post test at a level of $P<0.05$. The variance between the F98 strains was not homogenous and therefore data was square root transformed before being analysed with a one-way ANOVA.

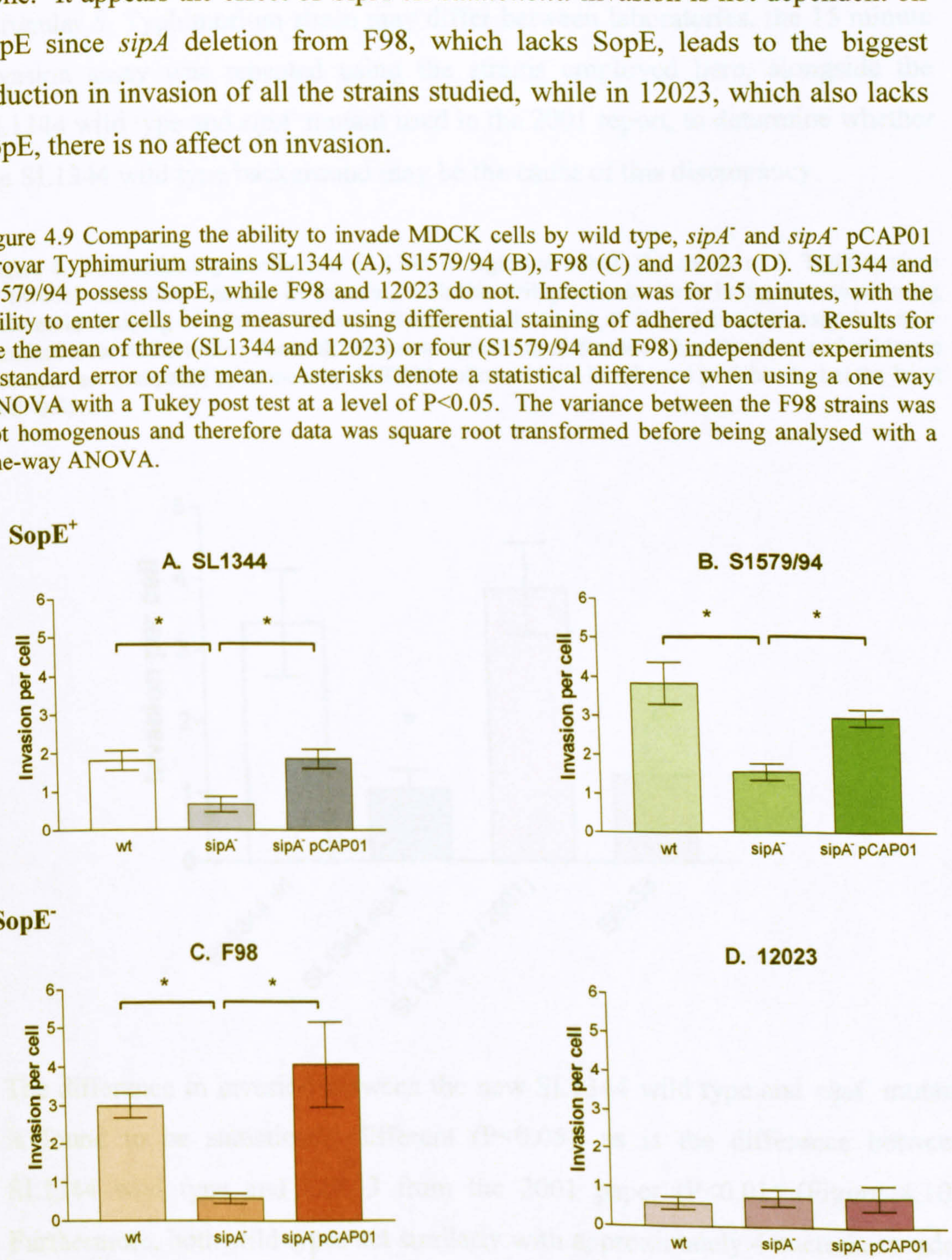

4.3.4. Differences in invasion between wild type and its isogenic *sipA*⁻ mutant are not dependent on MOI or cell density

The invasion of the SL1344 *sipA*⁻ mutant created using the λ red system was significantly lower than the wild type in MDCK cells after a 15 minute infection. However, this did not correlate with the results of Jepson *et al*., 2001, who found no difference between their SL1344 wild type and its isogenic *sipA*⁻ mutant (EE633; Hueck *et al*., 1995) after a 15 minute infection in MDCK cells. Since a particular *S*. Typhimurium strain may differ between laboratories, the 15 minute invasion assay was repeated using the strains employed here, alongside the SL1344 wild type and *sipA*⁻ mutant used in the 2001 report, to determine whether the SL1344 wild type background may be the cause of this discrepancy.

Figure 4.10 Determining whether the SL1344 background affects the ability of *S*. Typhimurium to invade. Infection was for 15 minutes, with the ability to enter cells being measured using differential staining of adhered bacteria. Results are the mean of six independent experiments ± standard error of the mean. Asterisk denotes a significant difference when the means of wild type and *sipA*⁻ are compared by a one way ANOVA followed by a Bonferroni post-hoc test at the level of $P<0.05$.

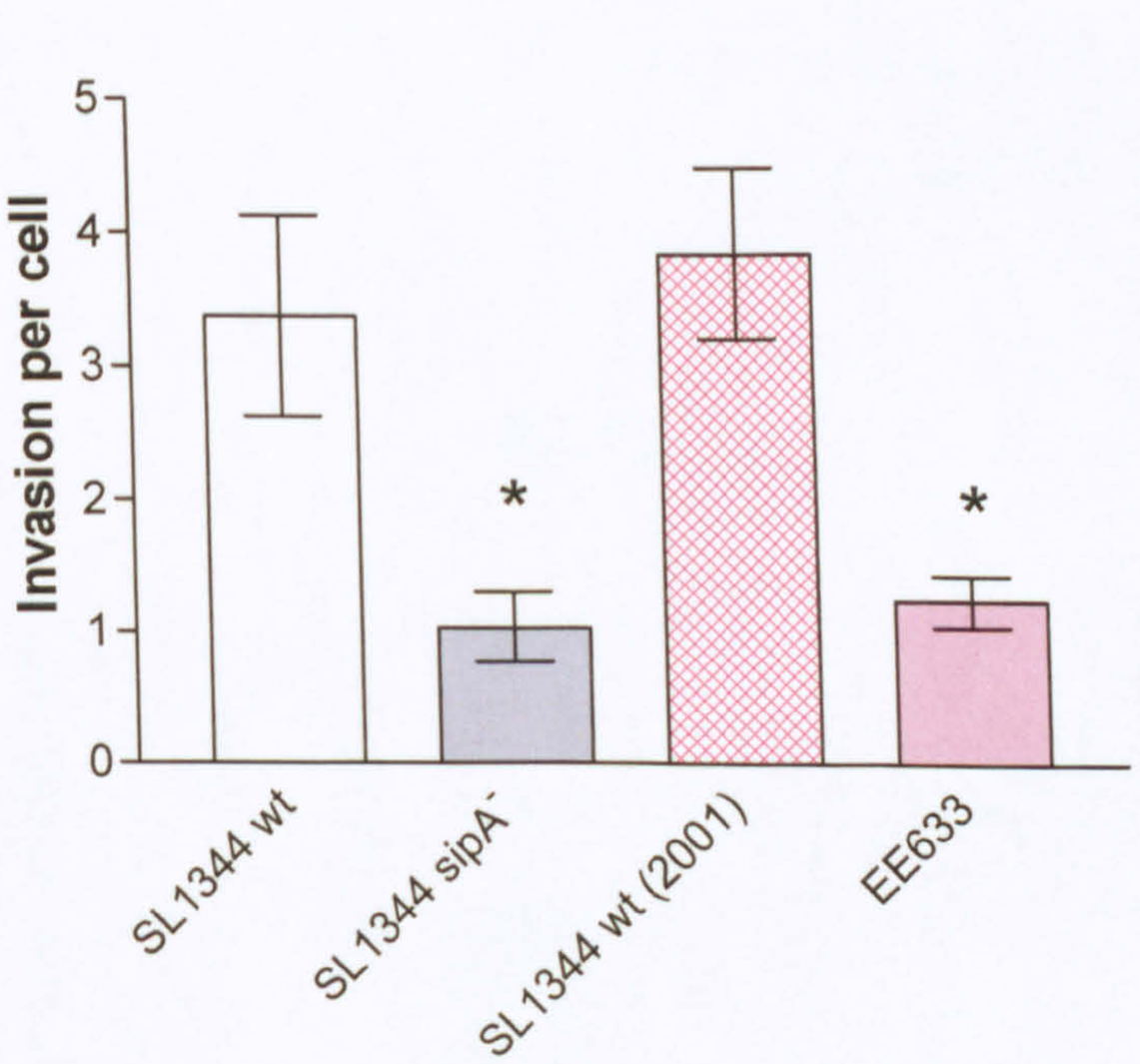

The difference in invasion between the new SL1344 wild type and *sipA*⁻ mutant is found to be statistically different ($P<0.05$), as is the difference between SL1344 wild type and EE633 from the 2001 paper ($P<0.01$) (Figure 4.10). Furthermore, both wild types act similarly with approximately 4 bacteria invaded per cell, and both *sipA* null mutants act similarly with 1 bacterium per cell. It

therefore appears loss of SipA from SL1344 does cause reduction in invasion, and establishes the difference between the two studies is not due to a difference in wild type.

Since the difference in results between the two studies is not due to a strain difference, and the protocol used in both sets of experiments was the same, it was decided to address whether a difference in the strain of MDCK cells used could be the cause; MDCK strain II cells being used by Jepson *et al.*, (2001) while MDCK strain I cells are used here. In MDCK I and MDCK II cells a similar number of bacteria were internalised (Figure 4.11), with both wild types having comparable levels of invasion to each other, and having significantly higher levels of invasion than either *sipA*⁻ mutant. This indicates the behaviour of *S.* Typhimurium SL1344 is the same in both sets of cells. MDCK cell strain was therefore not the cause of the different observations between the results reported here and those of Jepson *et al.*

Figure 4.11 Determining whether the strain of MDCK cells affects the ability of *S.* Typhimurium SL1344 to invade. Infection was for 15 minutes in MDCK I (A) or MDCK strain II cells (B). The ability to enter cells was measured using differential staining of adhered bacteria. Results are the mean of three independent experiments ± standard error of the mean. Asterisk denotes a significant difference when means are compared by a one-way ANOVA followed by a Bonferroni post-hoc test at the level of $P<0.05$.

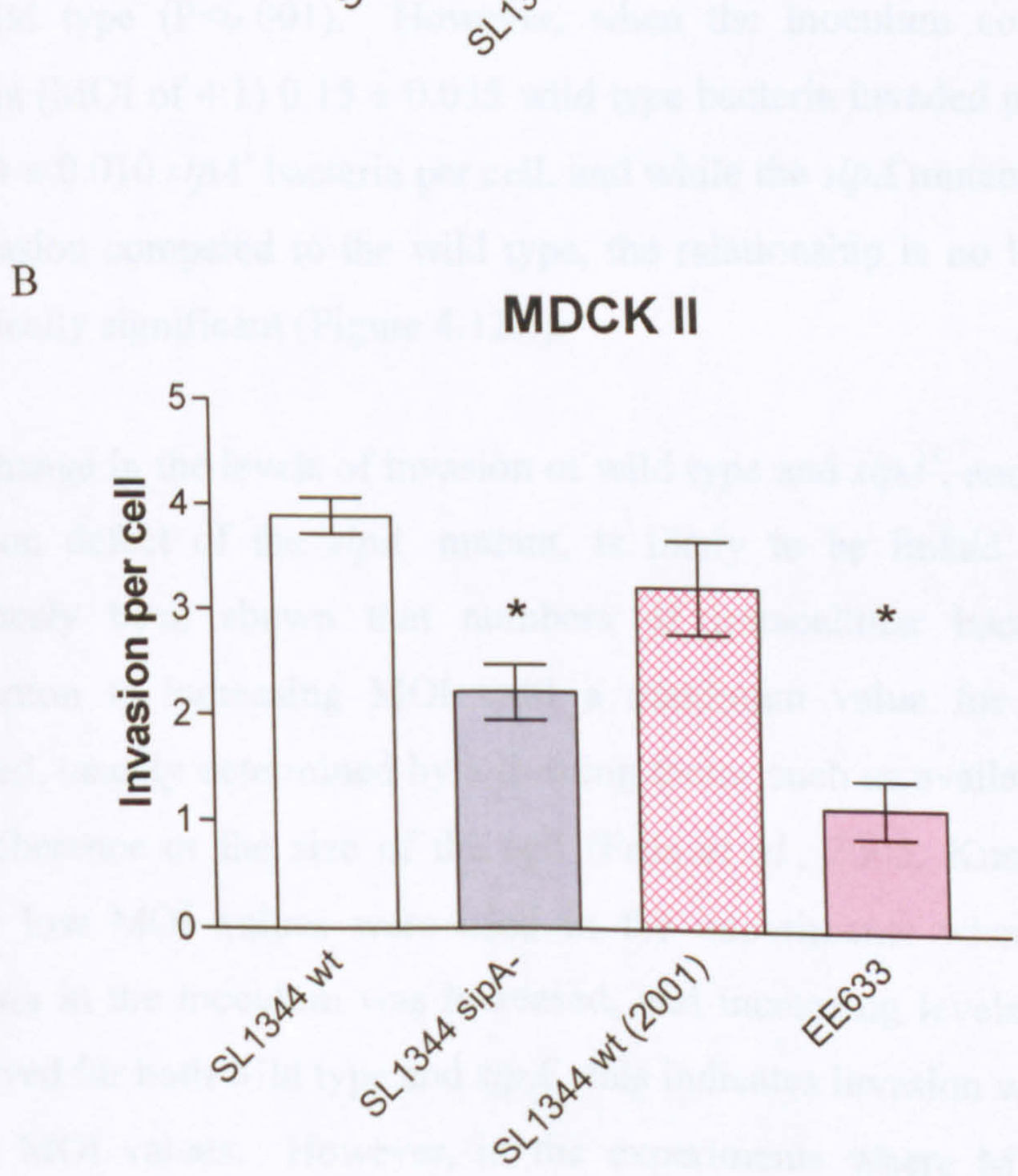

The final variable that was investigated as a possible cause of the discrepancy between the two studies was multiplicity of infection (MOI). The effect of MOI on invasion was examined in two ways; firstly by varying the density of MDCK cells but keeping the number of bacteria in the inoculum the same, and secondly by fixing the cell density but varying the number of bacteria in the inoculum, without changing the size of the inoculum (Figure 4.12).

At each of the three MDCK cell densities studied, the level of wild type invasion remains constant at ~4 bacteria per cell, as does the invasion of SL1344 *sipA*$^-$, which is ~1 bacterium per cell (Figure 4.12A). Thus, reduction in invasion by the *sipA*$^-$ mutant is found statistically significant ($P<0.05$) in each case. This consistency in the invasion levels of both wild type and *sipA*$^-$ was not observed when the numbers of bacteria in the inoculum were changed; consequentially the extent of the invasion defect of the *sipA*$^-$ mutant varied (Figure 4.12B). For example when the inoculum contained 2.5×10^8 bacteria (MOI of 100:1) approximately 4 wild type bacteria invade a cell compared to just 1 *sipA*$^-$ bacterium which represents a significant reduction in *sipA*$^-$ invasion compared to the wild type ($P<0.001$). However, when the inoculum contained 1×10^7 bacteria (MOI of 4:1) 0.15 ± 0.035 wild type bacteria invaded per cell compared to 0.04 ± 0.010 *sipA*$^-$ bacteria per cell, and while the *sipA*$^-$mutant has a lower rate of invasion compared to the wild type, the relationship is no longer considered statistically significant (Figure 4.12B).

The change in the levels of invasion of wild type and *sipA*$^-$, and the extent of the invasion defect of the *sipA*$^-$ mutant, is likely to be linked to MOI. It has previously been shown that numbers of intracellular bacteria increase in proportion to increasing MOI until a maximum value for internalisation is reached, usually determined by a limiting factor such as availability of receptors for adherence or the size of the cell (Friis *et al.*, 2005; Kusters *et al.*, 1993). Since low MOI values were used in the experiments where the number of bacteria in the inoculum was increased, and increasing levels of invasion were observed for both wild type and *sipA*$^-$, this indicates invasion was not saturated at these MOI values. However, in the experiments where MDCK density was varied, the MOI values were much higher and since the level of invasion was

constant for both wild type and *sipA*⁻, this suggests invasion saturation had occurred. Since the minimum MOI to achieve the maximum levels of invasion was 100 this indicates saturation occurs at MOI ≥100.

Figure 4.12 Examining the effect of multiplicity of infection on invasion of MDCK cells by *S.* Typhimurium SL1344. MDCK cell density (A) or the number of bacteria added (B) was used to change the MOI and examine the effect on the invasion difference between SL1344 wild type and *sipA*⁻. Infection was for 15 minutes, with the ability to enter cells being measured using differential staining of adhered bacteria. Results are the mean of two independent experiments ± standard error of the mean. Asterisk denotes a significant difference when means are compared by a two-way ANOVA followed by a Bonferroni post-hoc test at the level of $P<0.05$.

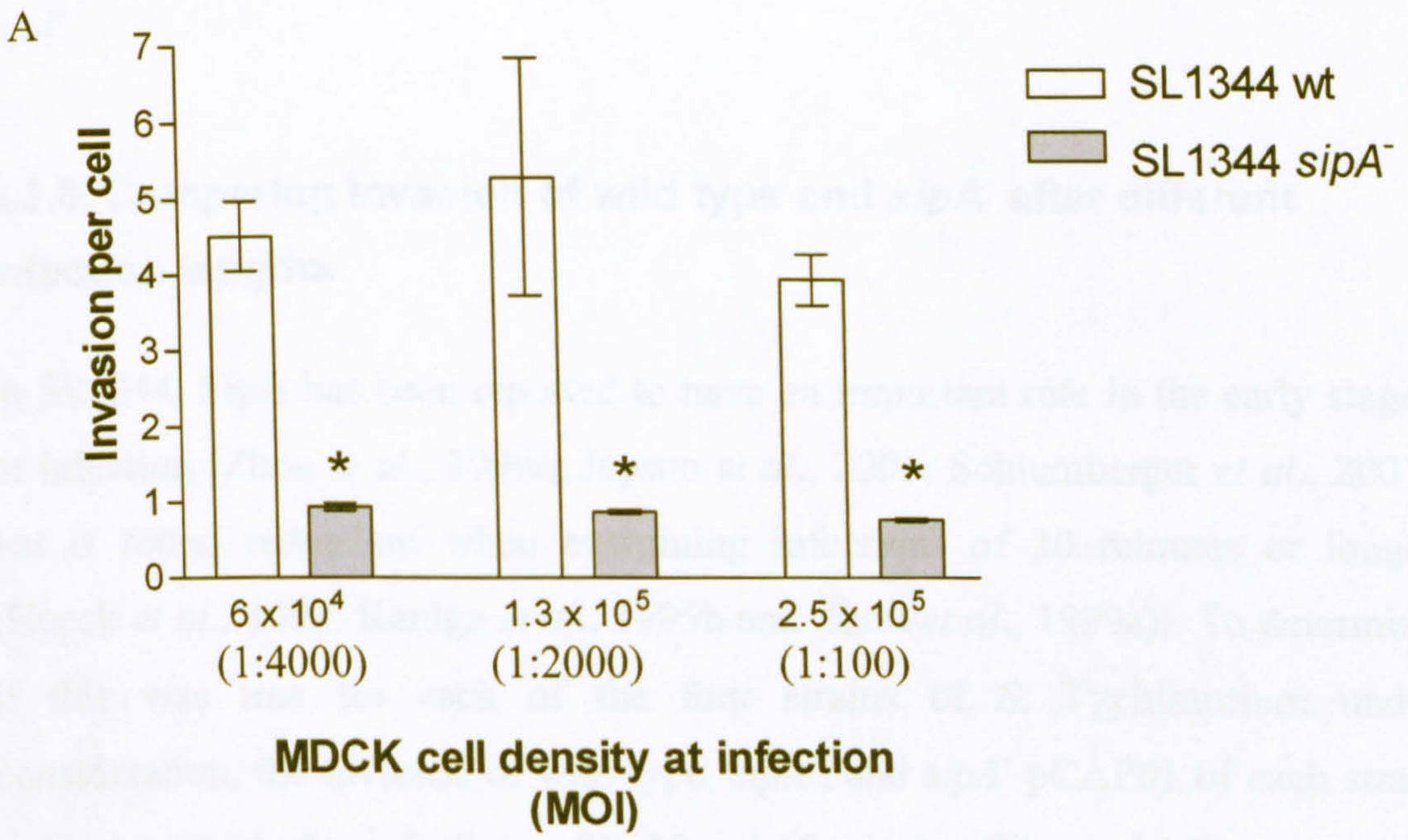

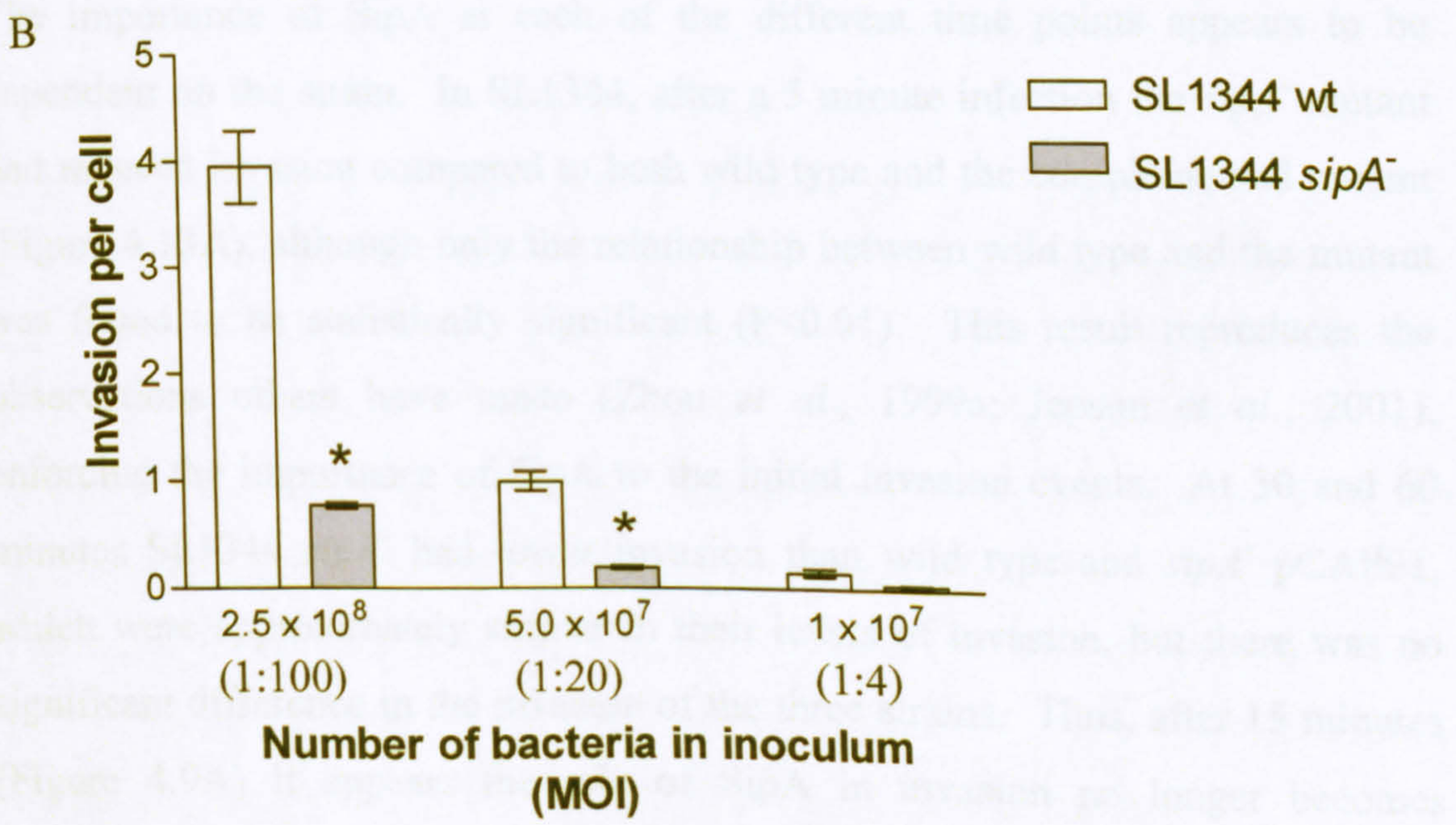

The MOI used by Jepson *et al.*, 2001, was reported to be ~100, and as shown here, even if it was higher or lower, a difference between the SL1344 wild type and *sipA*⁻ mutant created here would still be seen, indicating the *sipA*⁻ mutant does have an invasion defect at 15 minutes. However, an explanation as to why the results of this study differ from those of Jepson *et al.*, 2001 was not found. It appears differences in the way the *sipA*⁻ mutants were created, the epithelial cell strain used or the multiplicity of infection are not responsible, suggesting either there is some difference in protocol that is not apparent, or perhaps there has been a change in the properties of MDCK cells that affects internalisation of *sipA*⁻.

4.3.5. Comparing invasion of wild type and *sipA*⁻ after different infection lengths

In SL1344, SipA has been reported to have an important role in the early stages of infection (Zhou *et al.*, 1999a; Jepson *et al.*, 2001; Schlumberger *et al.*, 2007) but is found redundant when examining infections of 30 minutes or longer (Hueck *et al.*, 1995; Kaniga *et al.*, 1995b and Zhou *et al.*, 1999a). To determine if this was true for each of the four strains of *S.* Typhimurium under consideration, the invasion of wild type, *sipA*⁻, and *sipA*⁻ pCAP01 of each strain were compared after infections of 5, 30 and 60 minutes (Figure 4.13).

The importance of SipA at each of the different time points appears to be dependent on the strain. In SL1344, after a 5 minute infection the *sipA*⁻ mutant had reduced invasion compared to both wild type and the complemented mutant (Figure 4.13A), although only the relationship between wild type and the mutant was found to be statistically significant ($P<0.01$). This result reproduces the observations others have made (Zhou *et al.*, 1999a; Jepson *et al.*, 2001), enforcing the importance of SipA to the initial invasion events. At 30 and 60 minutes SL1344 *sipA*⁻ had lower invasion than wild type and *sipA*⁻ pCAP01, which were approximately similar in their levels of invasion, but there was no significant difference in the invasion of the three strains. Thus, after 15 minutes (Figure 4.9A) it appears the role of SipA in invasion no longer becomes important, matching similar reports by Higashide *et al.* (2002) who found no

difference at 20 minutes, Zhou *et al.* (1999a) who found no difference by 30 minutes and Hueck *et al.* (1995) who observed no difference after 1 hour.

S1579/94 is the second strain examined that possesses SopE, and the behaviour of S1579/94 wild type, *sipA*⁻ and *sipA*⁻ pCAP01 mirrors that of SL1344 wild type, *sipA*⁻ and *sipA*⁻ pCAP01, both in the level of invasion and the relationship between each i.e. the wild type and the complemented mutant have higher levels of invasion compared to *sipA*⁻ at each time point (Figure 4.13A and B). Thus, the role of SipA in invasion appears similar in the two strains of *S.* Typhimurium possessing SopE.

SipA being the cause of the invasion defect in S1579/94 could be disputed since the pCAP01 plasmid carrying a copy of the *sipA* gene did not fully complement the *sipA*⁻ phenotype. At 15 (Figure 4.9B), 30 and 60 minutes the relationship between wild type and *sipA*⁻ is statistically significant ($P<0.05$), but only at 15 minutes does the complemented mutant have significantly greater invasion than *sipA*⁻. In part this is probably due to the high level of variation in some of the results but also the stringency of the statistical test (a one-way ANOVA) applied; for example if a less rigorous test such as the students t-test is conducted, significant differences are found between *sipA*⁻ and *sipA*⁻ pCAP01 e.g. at 30 minutes. While the inability of pCAP01 to fully restore wild type levels of invasion to the *sipA*⁻ mutant is most evident in S1579/94, it is also seen in the other serovar Typhimurium strains examined. Complementation of a mutant by expressing a functional copy of the deleted gene from a plasmid often does not fully complement the mutant phenotype due to the pleiotropic effects plasmid maintenance or copy number artefacts may have on the bacterium (Knodler *et al.*, 2005; Abromaitis *et al.*, 2005; Birnbaum and Bailey, 1991). It is therefore felt the failure to obtain wild type levels of invasion by *sipA*⁻ pCAP01 indicates a different level of expression of SipA from the plasmid compared to the chromosome, rather than implying SipA is not the sole cause of this defect. An additional factor supporting SipA as the sole cause of the invasion defect is the fact on certain occasions the complemented mutant can have invasion levels statistically different to *sipA*⁻ e.g. F98 *sipA*⁻ pCAP01 at 60 minutes.

Figure 4.13 Comparing the ability to invade MDCK cells by wild type, *sipA*⁻ and *sipA*⁻ pCAP01 serovar Typhimurium strains SL1344 (A), S1579/94 (B), F98 (C) and 12023 (D) after infections of 5, 30 and 60 minutes. Results are the mean of three (S1579/94 and 12023) or four (SL1344 and F98) independent experiments ± standard error of the mean. Asterisks shows a significant difference when compared using a one way ANOVA followed by a Tukey post test at a level of $P<0.05$.

A. SL1344 (SopE⁺)

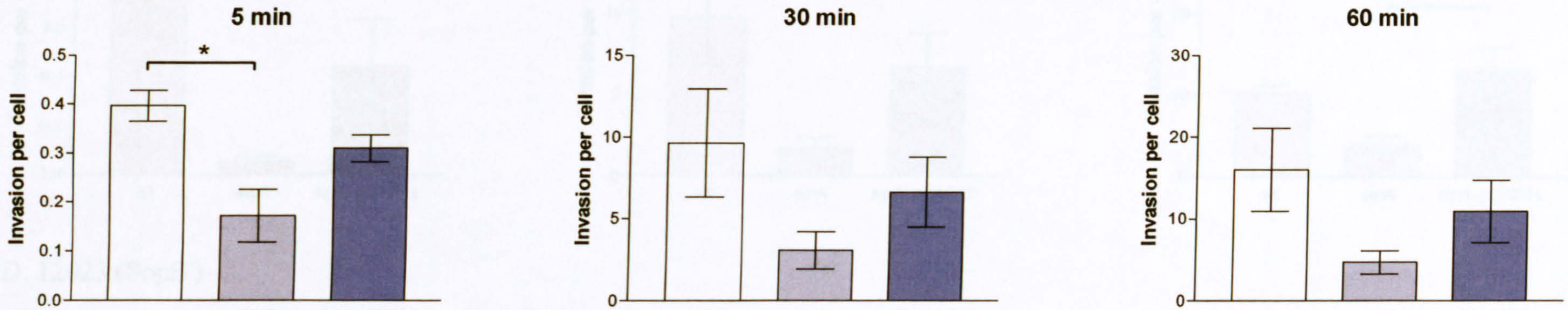

B. S1579/94 (SopE⁺)

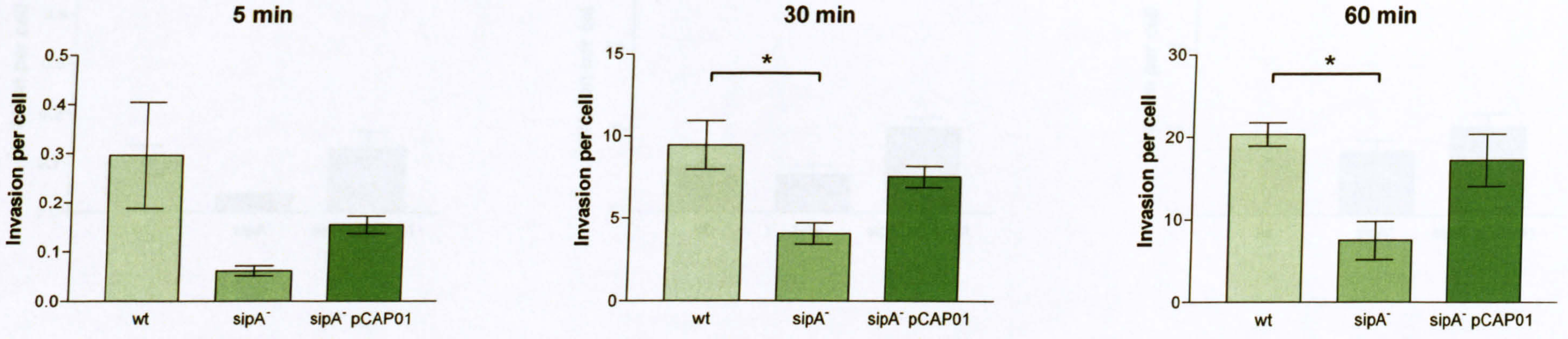

C. F98 (SopE$^-$)

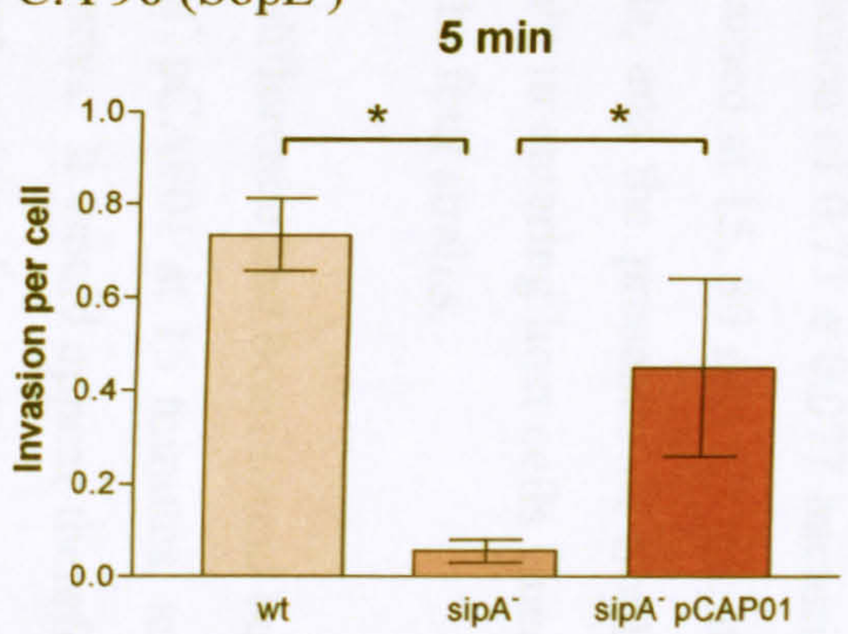

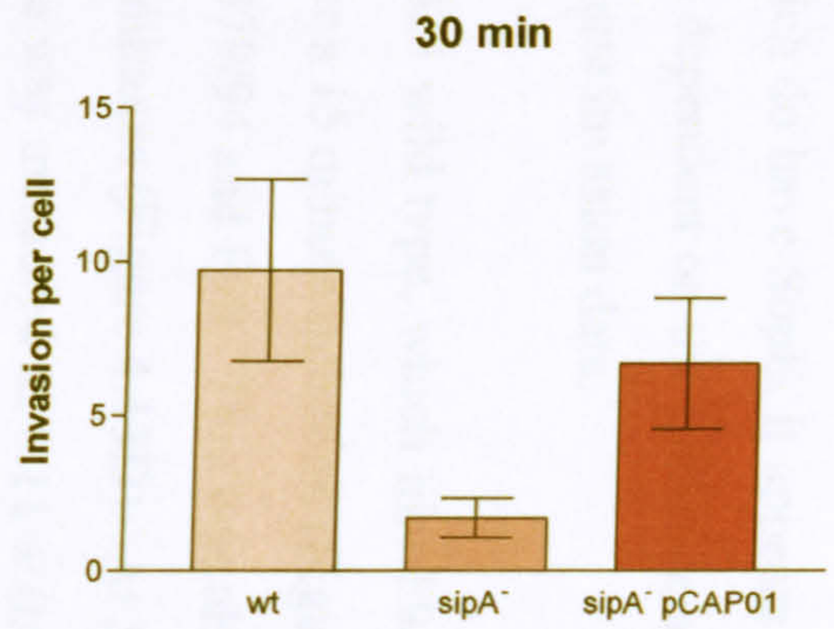

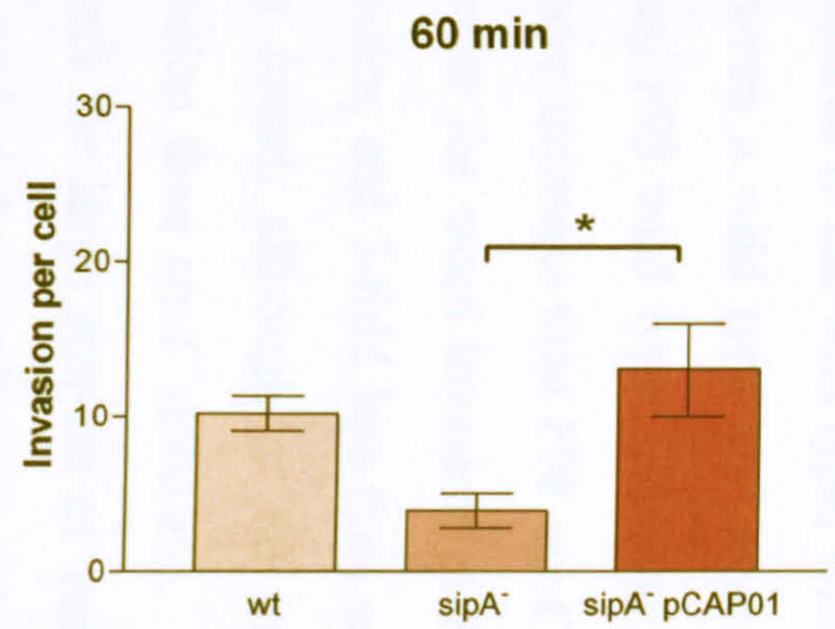

D. 12023 (SopE$^-$)

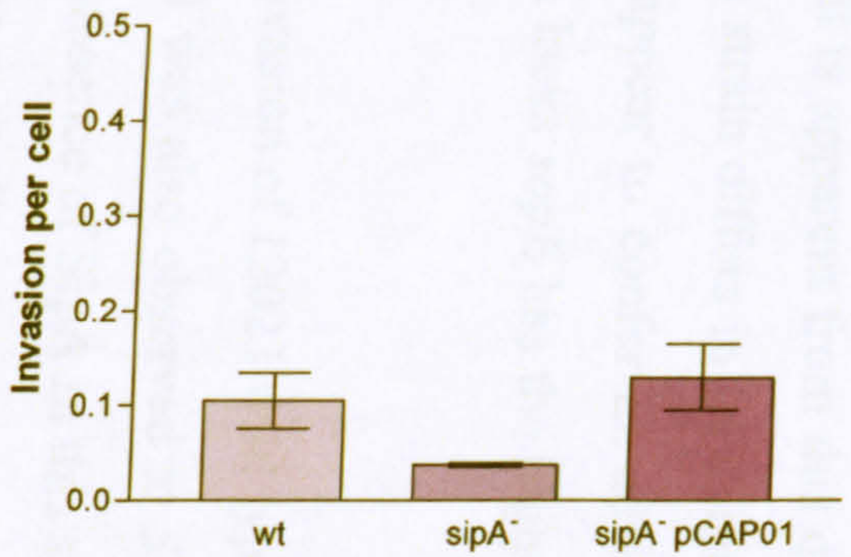

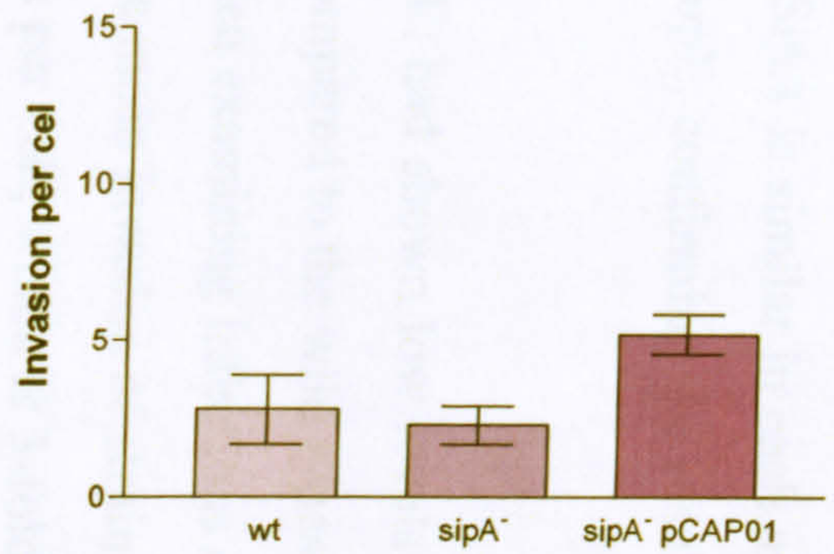

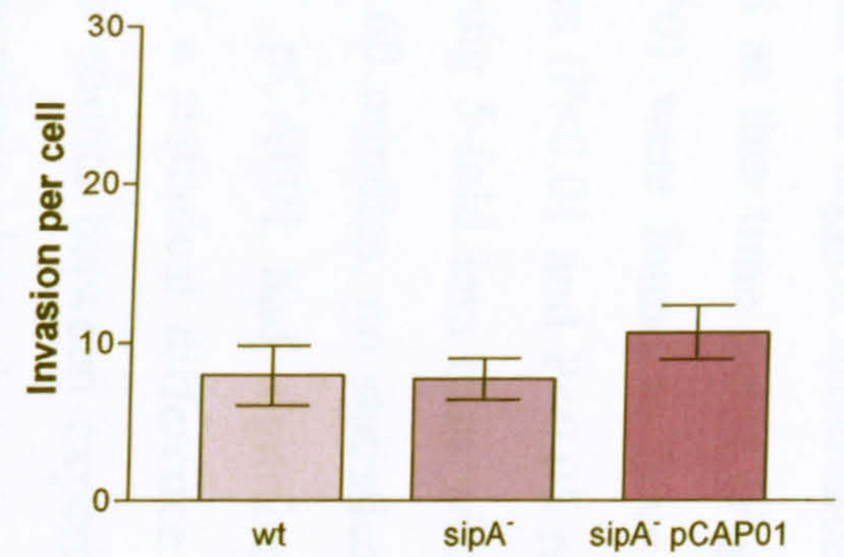

At 5 minutes the F98 *sipA*⁻ mutant exhibited a 10-fold decrease in invasion compared to the wild type, which represented the biggest difference in invasion between a wild type and *sipA* null mutant at this time point (Figure 4.13C). Thus, F98 wild type and also *sipA*⁻ pCAP01 were found to have statistically greater invasion than F98 *sipA*⁻ at 5 minutes ($P<0.01$ and $P<0.05$ respectively). Despite the mean invasion of F98 *sipA*⁻ being 5-fold less than wild type at 30 minutes, and 3-fold less than wild type by 60 minutes, no statistical difference was found, although at 60 minutes *sipA*⁻ pCAP01 had significantly higher invasion than *sipA*⁻ ($P<0.05$). The lack of a statistical difference is likely to reflect the large amount of variation in the counts between experiments since examining the results of each set of experiments show there is a consistent reduction in invasion of the *sipA*⁻ mutant. Since the results of F98, a strain that does not have the *sopE* gene, replicates the results of SL1344 and S1579/94 which do have SopE, it appears the role of SipA is similar in each and therefore not dependent on the presence/absence of SopE, confirming the results of the 15 minute invasion data.

12023 wild type, which like F98 lacks SopE, had shown low levels of invasion after a 15 minute infection (Figure 4.9D), compared to the wild types of SL1344, S1579/94 and F98. This was also found when examining infections of 5, 30 and 60 minutes (Figure 4.13D). At 5 minutes the mean invasion of strain 12023 wild type was measured as 0.11 ± 0.029 bacteria per cell, which is 3-fold lower than S1579/94, which had the third lowest rate of invasion at 0.30 ± 0.108. SL1344 after 5 minutes had invasion of 0.40 ± 0.031 bacteria per cell and F98 a mean invasion of 0.73 ± 0.077 bacteria per cell. It is apparent from this data and that obtained at 15, 30 and 60 minutes that each strain differs in its ability to invade cells, and the presence of SopE does not appear to confer an advantage on a strain in entering host cells since F98 which lacks *sopE* has the highest invasion of the four strains.

No difference had been found between the invasion of 12023 wild type, *sipA*⁻ and *sipA*⁻ pCAP01 at 15 minutes, and this trend was also observed at 5, 30 and 60 minutes. It would appear therefore that the absence of SipA in this strain has no effect on invasion. The use of 12023 in these studies therefore illustrates that

invasion can vary between *S.* Typhimurium strains and may suggest subtle differences in the mechanisms used by each strain to gain access to cells and thus in its virulence. The results additionally suggest that absence of SipA and SopE together do not necessarily lead to a greater invasion defect since despite the very marked effect on F98 this was not apparent in 12023.

4.3.6. Comparison of the ability to induce ruffling in MDCK I cells by the wild type and *sipA*⁻ mutants of four S. Typhimurium strains

In addition to measuring the ability of each strain and its *sipA*⁻ mutant to enter MDCK cells, the ability to induce the formation of membrane ruffles was measured using TRITC-phalloidin staining of actin. The number of ruffles induced per cell was similar for strains SL1344, S1579/94 and F98; ~0.8 ruffles per cell. *S.* Typhimurium strain 12023 consistently produced less ruffles than the other strains, with an average of 0.40 ± 0.044 ruffles per cell induced by 12023 wild type; significantly less than each of the other wild types. The reduced number of ruffles may explain the reduced level of invasion seen with this strain (Figure 4.9D). No statistical difference was observed between the wild type and *sipA*⁻ mutant in each of the four strains of *S.* Typhimurium when comparing the number of ruffles produced per cell after a 15 minute infection ($P>0.05$; Figure 4.14). There was also no statistical difference between wild type and *sipA*⁻ pCAP01 or *sipA*⁻ and *sipA*⁻ pCAP01 in SL1344, S1579/94, F98 or 12023. Overall it appears that in the four strains examined, the absence of SipA does not affect the ability of any serovar Typhimurium strain to induce ruffling, and is not influenced by the presence or absence of SopE.

Figure 4.14 Comparing the ability to induce ruffles in MDCK cells by wild type, *sipA*⁻ and *sipA*⁻ pCAP01 serovar Typhimurium strains SL1344 (A), S1579/94 (B), F98 (C) and 12023 (D). SL1344 and S1579/94 possess SopE, while F98 and 12023 do not. Infection was for 15 minutes, with the ability to induce ruffle formation being measured using TRITC-phalloidin staining of actin. Results are the mean of three independent experiments ± standard error of the mean.

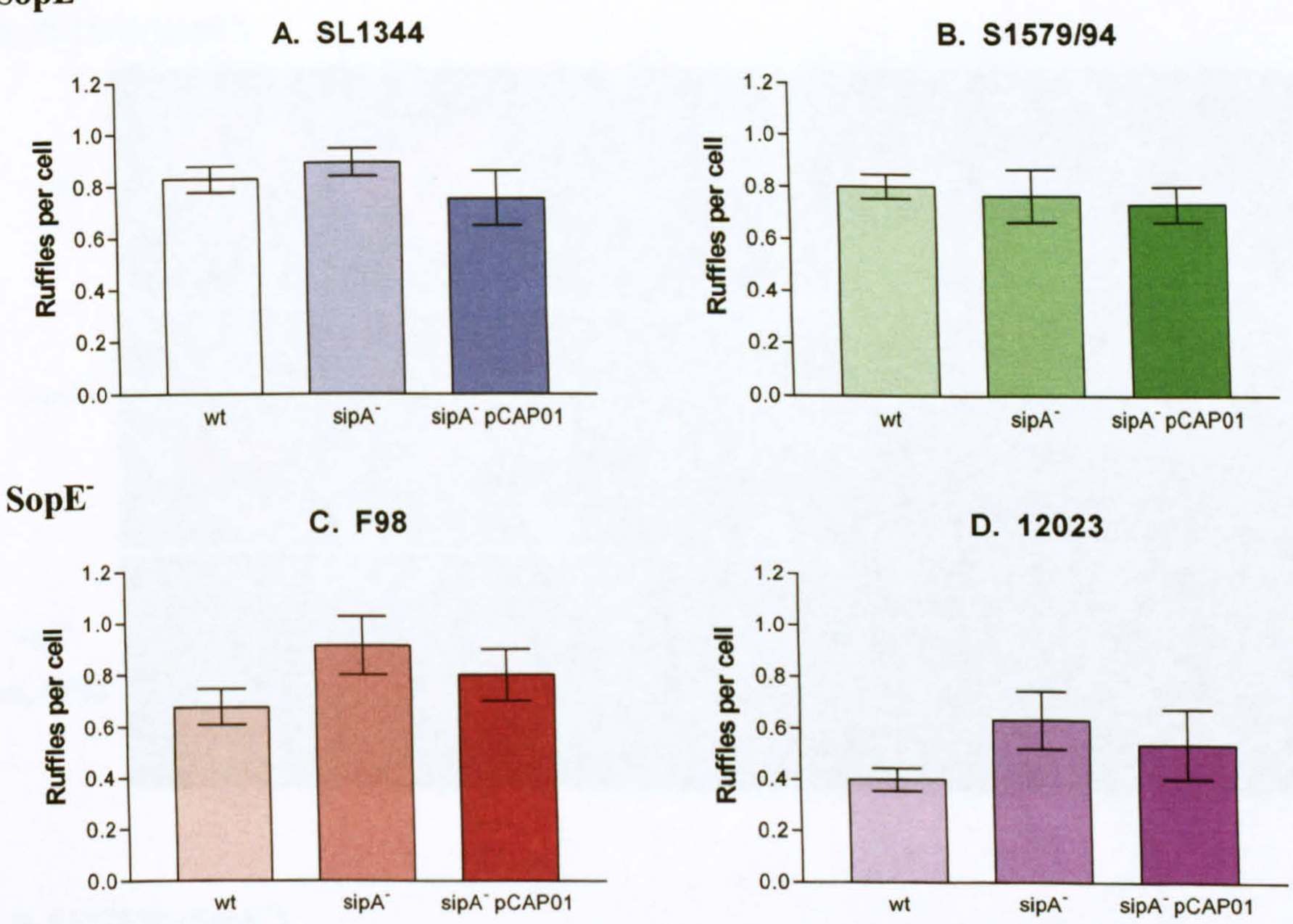

4.3.7. Imaging the morphology of the ruffles induced by the wild type and *sipA*⁻ mutants of the four *S.* Typhimurium strains

The staining of actin in MDCK cells with TRITC-phalloidin allowed the morphology of the ruffles induced by each wild type and *sipA*⁻ mutant to be analysed by Confocal Laser Scanning Microscopy (CLSM) (Figure 1.15). The ruffles induced by the wild type of each strain appear similar, with a circular ruffle forming around the bacterium which sits centrally. However, there appears to be a difference in the size of the ruffle induced. Wild type F98 and 12023, which naturally lack SopE, produce ruffles that appear smaller in diameter than ruffles produced by wild type SL1344 and S1579/94, which both possess SopE. Since CSLM provides an image of the monolayer at one point in time, the ruffles observed will be in all phases of propagation, and therefore it was not felt possible to accurately quantify this difference.

Figure 4.15 CLSM images showing the morphology of membrane ruffles induced by wild type and its isogenic *sipA*⁻ mutant in four *S.* Typhimurium strains. Each image shows a representative selection of images of TRITC-phalloidin stained MDCK cells infected for 15 minutes with SL1344 (A), S1579/94 (B), F98 (C) or 12023 (D) bacteria stained with FITC. Each image is presented as a projected series of optical sessions showing membrane ruffles in their entirety. Scale bar 10μm

A. SL1344 (SopE⁺)

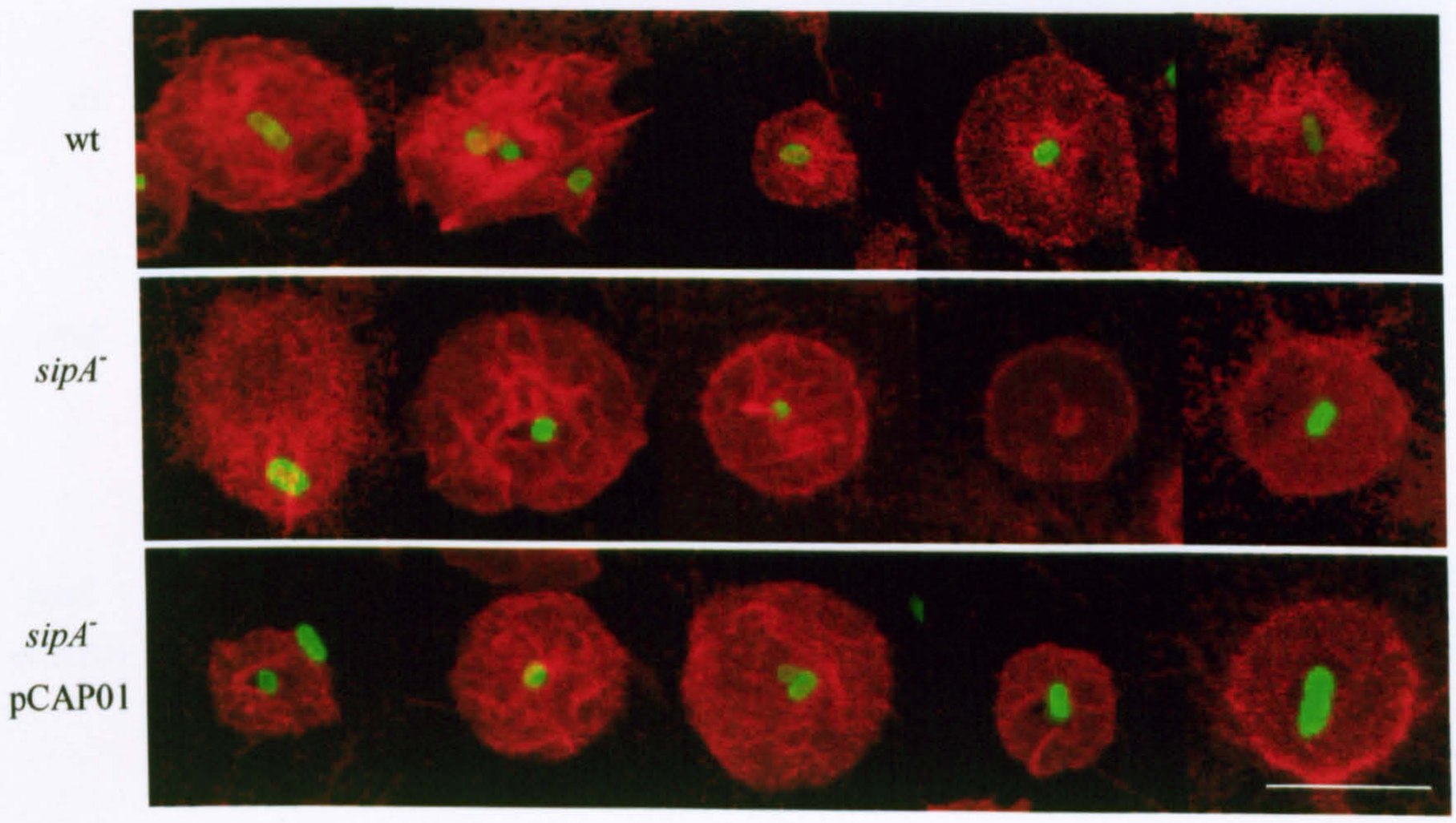

B. S1579/94 (SopE⁺)

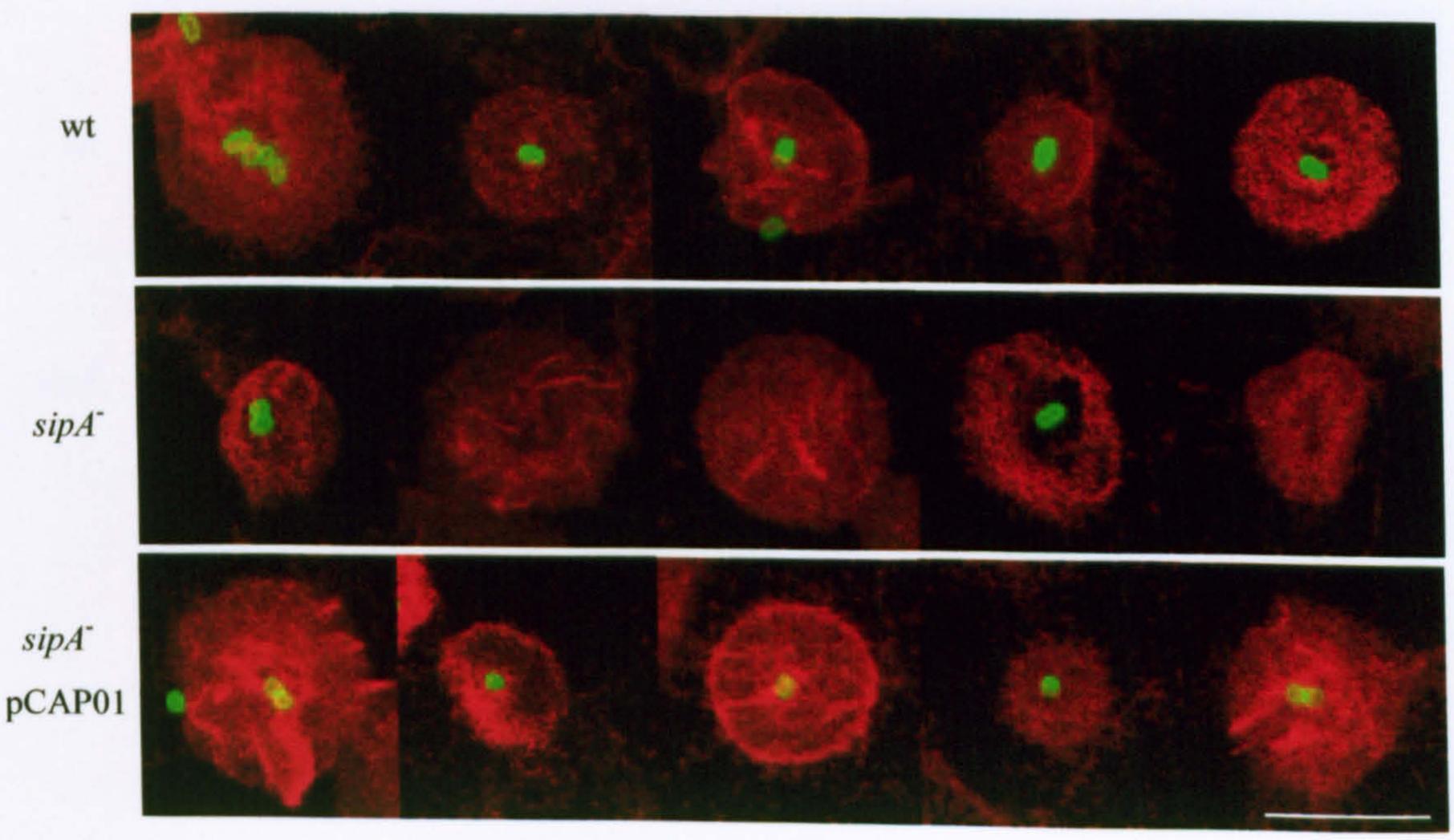

C. F98 (SopE$^-$)

wt

sipA$^-$

sipA$^-$
pCAP01

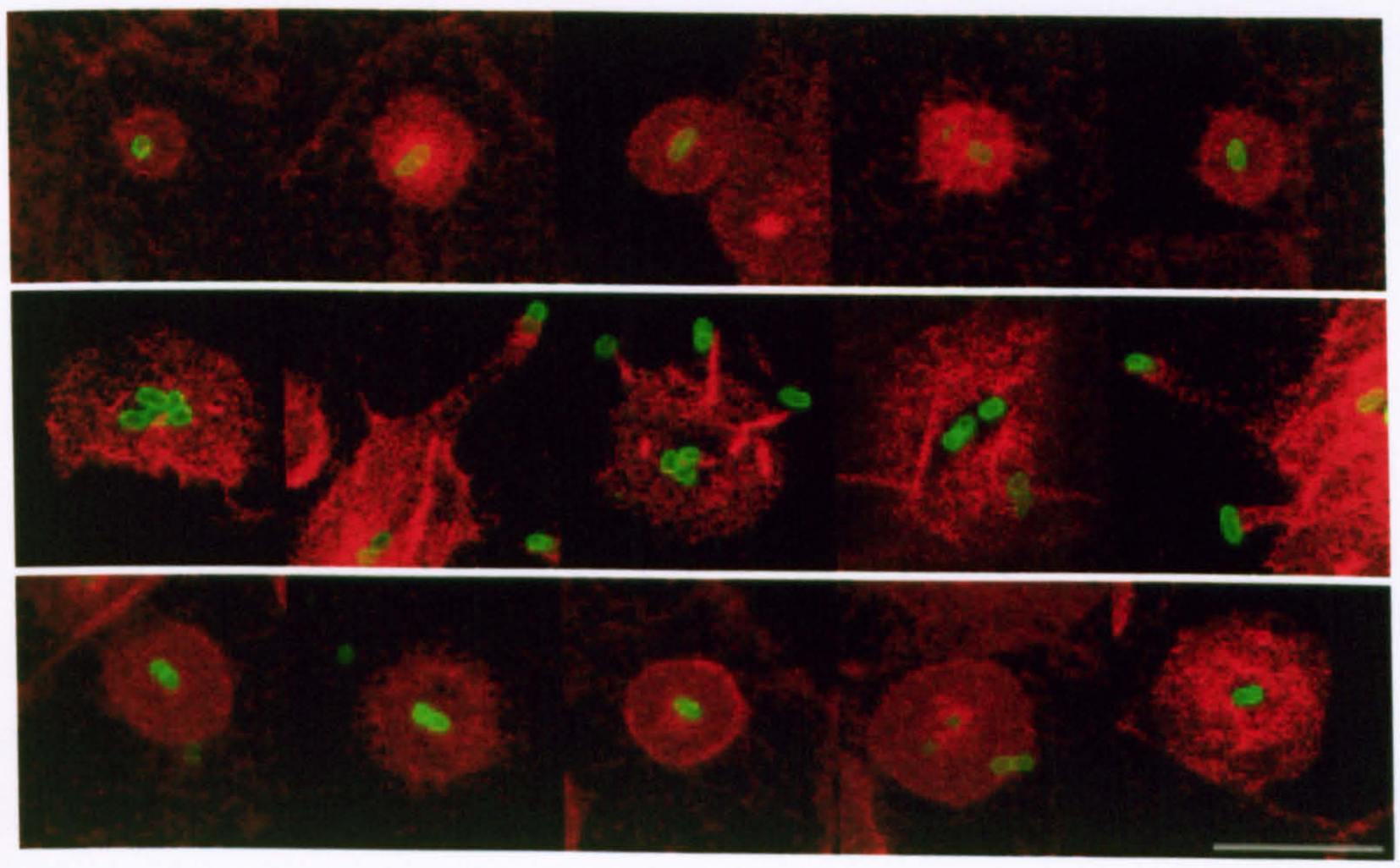

D. 12023 (SopE$^-$)

wt

sipA$^-$

sipA$^-$
pCAP01

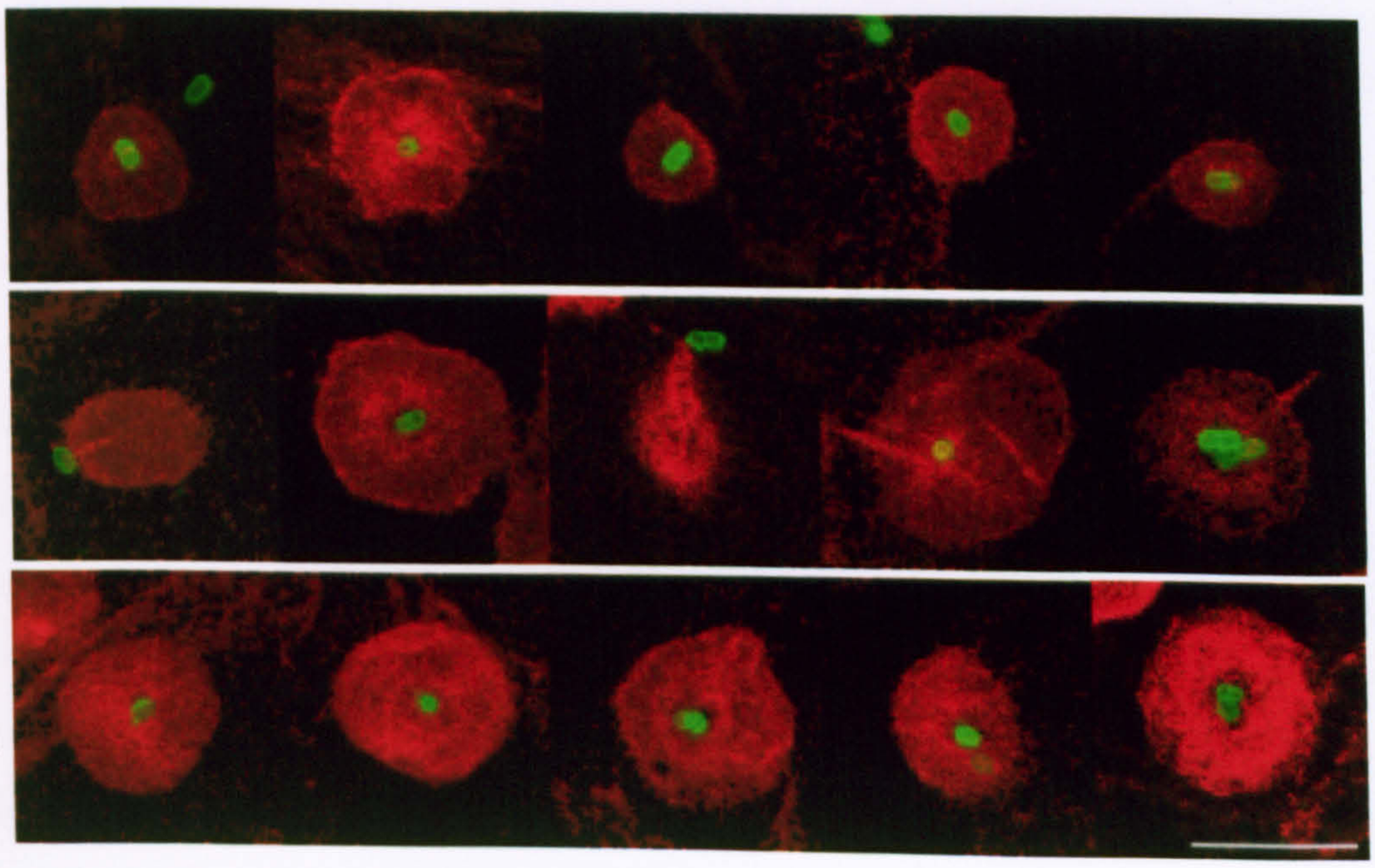

In SL1344 and S1579/94 the actin distribution of the wild type, *sipA*⁻ and *sipA*⁻ pCAP01 ruffles appear very similar, producing ruffles of similar size with a circular morphology. However, a difference is observed in the location of the bacterium in relation to the ruffle; in wild type and *sipA*⁻ pCAP01, the bacterium consistently lies in the centre of the ruffle, while in the *sipA*⁻ mutant the bacterium is located at the edge of a number of ruffles, and a larger number of ruffles appear to have no bacterium associated with the ruffle at all. This matches the observations made by Jepson *et al.* (2001) who found during ruffle formation, *sipA*⁻ bacteria are frequently pushed to the edge of the ruffle, where they may then move towards the centre to invade the cell, or may detach with the ability to induce a new ruffle. A larger number of ruffles without bacteria were observed compared to ruffles where the bacteria were displaced to the outskirts of the ruffle; however, this may be an artefact of the staining protocol, as the cells are subject to several washings and this is likely to dislodge the bacteria from the ruffle if they are not firmly attached, which seems likely if the bacterium is in transit as the ruffle propagates. This was one reason for analysing ruffle induction and propagation using time-lapse microscopy (4.3.11).

When examining strains F98 and 12023 it was observed that the morphology of a small number of ruffles of the *sipA*⁻ mutant are very distinct, not only from the wild type of any of the strains, but the *sipA*⁻ ruffles of SL1344 and S1579/94. Amongst the ruffles induced by F98 and 12023 *sipA*⁻, there appeared to be ruffles with a greater number of filopodia-like structures, giving the ruffles a 'spiky' appearance. Furthermore, some ruffles possessed finger-like projections, which protruded from the ruffle and on occasion had an associated bacterium, often attached at the end of the structure (Figure 4.15C and D). The presence of pCAP01 restored the wild type ruffle morphology phenotype in ~95% of the mutant bacteria, indicating that this dramatic change in morphology was due to the absence of SipA from a *sopE*⁻ strain. Thus, it appears the absence of SipA and SopE leads to a dramatic change in ruffle morphology, which has not been reported before.

The ruffles induced by the *sipA*⁻ mutants of F98 and 12023, like those of the SL1344 and S1579/94 *sipA*⁻ mutants, also had bacteria located at the periphery of

the ruffle rather than the centre, or lacked bacteria associating with the ruffle at all. Therefore, it was decided to quantify the proportion of ruffles with no associated bacteria, in order to determine whether this defect was dependent on SipA, and whether it was affected by the presence or absence of SopE. Comparison of the four wild types shows each has ~3-5% of ruffles without bacteria and as there is no significant difference between the wild types, it indicates SopE has no role in this phenotype (Figure 4.16). Indeed lack of bacteria associated with these ruffles is likely to be a consequence of the washing steps in the staining protocol.

The percentage of ruffles without bacteria is ~4-fold greater in each strain when *sipA* is deleted, however, only in F98 and 12023 where SopE is also absent is this difference statistically significant ($P<0.01$ and $P<0.001$ respectively). The loss of SipA leading to an increase in the number of ruffles that have no bacterium associated with them corresponds to the microscopy observations, where during ruffle propagation *sipA*$^-$ bacteria are pushed to the periphery of the ruffle and may subsequently detach. This detachment leads to a higher proportion of ruffles without bacteria, and thus, while the number of ruffles induced by the *sipA*$^-$ mutant is no different to the wild type, this explains why the rate of invasion is reduced. It is interesting to note that while 12023 *sipA*$^-$ has a significantly higher proportion of ruffles without bacteria compared to its wild type, the invasion of the *sipA*$^-$ mutant does not differ to its wild type (Figure 4.9D). The reason for this anomaly is not clear, but may be a consequence of the very small number of ruffles induced by this strain, or suggest there is a delay before 12023 can enter through the centre of the ruffle it has induced, so that while the 12023 bacterium is located in the centre of the ruffle it is not entering any faster than the *sipA*$^-$ mutant which has been pushed to the outskirts of the ruffle. Additionally there may be another trait of 12023 which masks the effect of SipA absence.

Figure 4.16 Quantifying the number of ruffles induced by serovar Typhimurium strains SL1344, S1579/94, F98 and 12023 that do not have bacteria associated with them. The wild type, *sipA*⁻ and *sipA*⁻ pCAP01 of each strain are compared. Infection was for 15 minutes, with ruffles being identified using TRITC-phalloidin staining of actin. Results are the mean of three independent experiments ± standard error of the mean. Asterisk denotes a significant difference when compared using a one-way ANOVA with a Bonferroni post-test at the level of $P<0.05$.

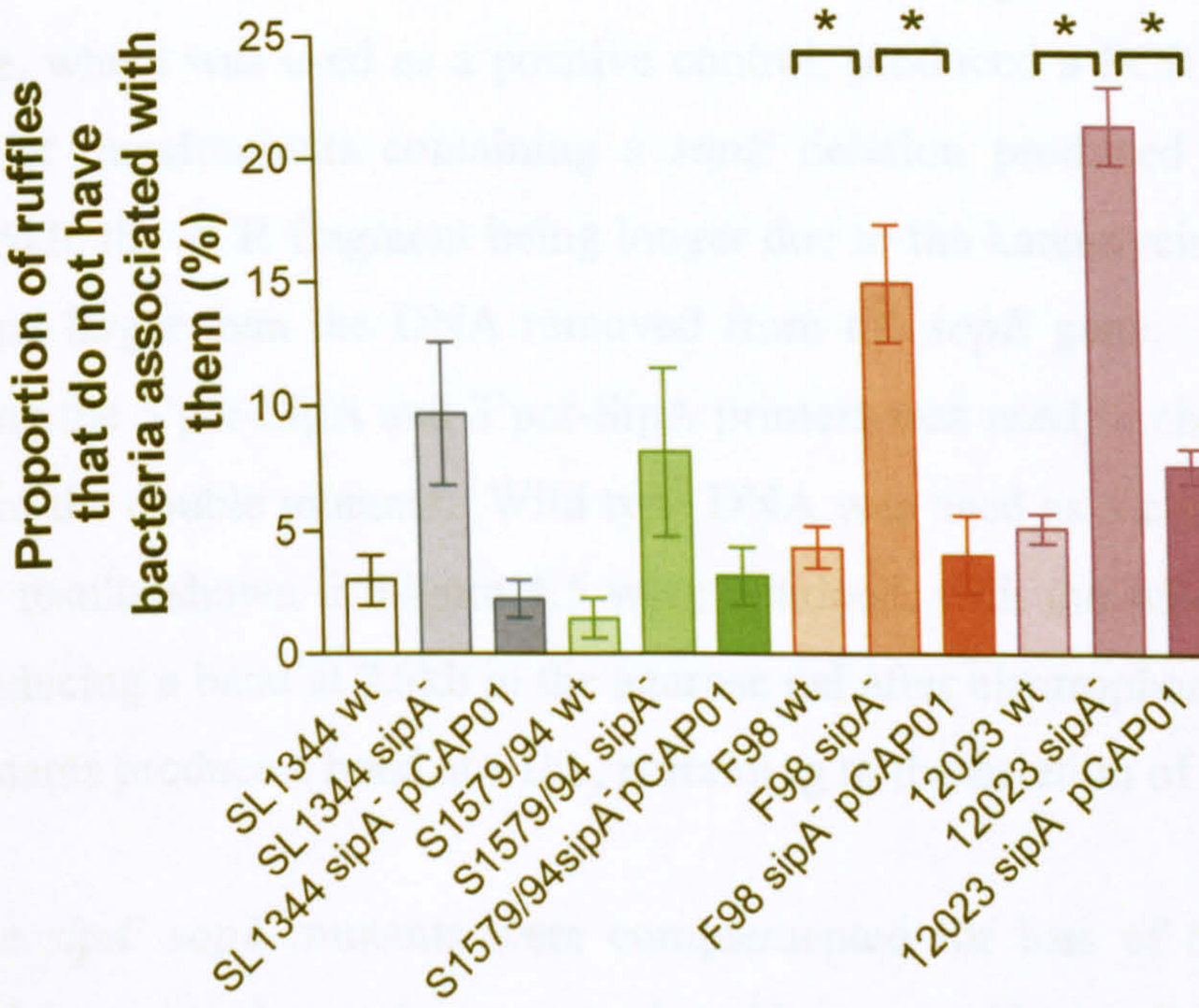

4.3.8. Creating SL1344 and S1579/94 *sopE*⁻ and *sopE*⁻ *sipA*⁻ mutants

Since in strains F98 and 12023, which naturally lack SopE, the deletion of SipA leads to a dramatic change in ruffle morphology, it was decided to investigate whether a similar observation was found when the *sipA* and *sopE* genes were inactivated from strains SL1344 and S1579/94, which possess SopE. A SL1344 *sopE*⁻ mutant had been obtained from Dr C. M. A. Khan (University of Newcastle) to act as a control when analysing the *sopE* genotype of each of the four *S.* Typhimurium strains (Figure 4.3). The *sopE*⁻ mutant had been created in the same manner as the *sipA*⁻ mutants i.e. using the λ red recombinase system, on this occasion inserting a kanamycin cassette in place of the *sopE* gene. The *sipA* deletion was transferred into SL1344 *sopE*⁻ by phage transduction, creating double mutant SL1344 *sipA*⁻ *sopE*⁻. Phage transduction was also used to transfer the *sopE*⁻ deletion from SL1344 *sopE*⁻ into S1579/94 wild type, creating S1579/94 *sopE*⁻, and into S1579/94 *sipA*⁻ to create S1579/94 *sipA*⁻ *sopE*⁻.

Once kanamycin resistant transformants in the case of S1579/94 *sopE*$^-$, and kanamycin and chloramphenicol resistant transformants in the case of the SL1344 and S1579/94 *sipA*$^-$ *sopE*$^-$ mutants, had been isolated, PCR using the 5'pcr_sopE and 3'pcr_sopE primers (Table 4.3) was used to check whether *sopE* had successfully been deleted. As was shown in Figure 4.3, DNA from the wild type, which was used as a positive control, produced a PCR product of ~1.6kb, whilst transformants containing a *sopE* deletion produced a PCR product of ~2.5kb, the PCR fragment being longer due to the kanamycin resistance cassette being larger than the DNA removed from the *sopE* gene. An additional PCR using the 5'pcr-SipA and 3'pcr-SipA primers was used to check the loss of *sipA* from the double mutants. Wild type DNA was used as a control and a repeat of the results shown in Figure 4.5 were obtained, with the wild type PCR product producing a band at 2.5kb in the agarose gel after electrophoresis, while the *sipA*$^-$ mutants produce a band at ~1kb, pertaining to the deletion of *sipA*.

The *sipA*$^-$ *sopE*$^-$ mutants were complemented for loss of SipA with pCAP01, which carries the *sipA* gene. A plasmid carrying the *sopE* gene (pCAP03) was also created in order to complement the loss of SopE in the *sopE*$^-$ and *sipA*$^-$ *sopE*$^-$ mutants. To create pCAP03, the *sopE* gene plus ~500bp up- and downstream of the gene were amplified from SL1344 wild type DNA in a PCR using primers 5'xhoIsopE and 3'sopEhindIII to produce a PCR product with a 5' *Xho*I restriction site and a 3' *Hin*dIII recognition site. This PCR fragment and plasmid pACYC177 were cut with *Xho*I and *Hin*dIII. A 520bp fragment containing part of the kanamycin resistance cassette was removed from pACYC177 during this restriction digest, and into this site the PCR fragment was ligated. *E. coli* DH5α was electroporated in the presence of the ligation reaction and colonies screened for a carbenicillin resistant, kanamycin sensitive phenotype, which indicated the presence of a plasmid which may contain the *sopE* gene. Clones were analysed for the presence of the *sopE* gene using a restriction digest with *Xho*I and *Hin*dIII. Digestion of correctly orientated *sopE* generated two DNA bands of 3400bp and 1590bp respectively. The presence of the *sopE* gene was finally confirmed by two sequencing reactions performed by the MWG DNA sequencing service; one using the 5'pcr_sopE and 3'pcr_sopE primers, the second using the 5'xhoIsopE and 3'sopEhindIII primers. Upon this confirmation

electroporation was used to transform SL1344 *sopE*⁻, SL1344 *sipA*⁻ *sopE*⁻, S1579/94 *sopE*⁻ and S1579/94 *sipA*⁻ *sopE*⁻ with plasmid pCAP03.

Once the complete set of SL1344 and S1579/94 *sipA* and *sopE* single and double mutants had been created and complemented, the secreted proteins from each, after growth in LB at 37°C for 4 hours, were collected and SDS-PAGE performed. A Western blot was then performed using anti-SipA, anti-SipC and anti-SopE antibodies to compare their protein secretion profile (Figure 4.17). All the mutants possessed SipC in their supernatant indicating TTSS-1 was functional, and the SL1344 and S1579/94 *sipA*⁻ *sopE*⁻ mutants lacked SipA unless they had been complemented with pCAP01. Likewise, the SL1344 and S1579/94 *sopE*⁻ and *sipA*⁻ *sopE*⁻ mutants lacked SopE unless they had been complemented with plasmid pCAP03 (Figure 4.17).

Figure 4.17 Comparing the SipA and SopE profile of wild type and various mutants of *S.* Typhimurium strains SL1344 (A), S1579/94 (B), F98 and 12023 (C). Lanes correspond to wild type (1), *sipA*⁻ (2), *sipA*⁻ pCAP01 (3), *sopE*⁻ (4), *sopE*⁻ pCAP03 (5) *sopE*⁻*sipA*⁻ (6), *sopE*⁻*sipA*⁻ pCAP01 (7) and *sopE*⁻*sipA*⁻ pCAP03 (8). Culture supernatant proteins were prepared by precipitation with 10% trichloroacetic acid, separated by SDS-PAGE, transferred to a nitrocellulose membrane, and probed with anti-SipA, anti-SipC and anti-SopE monoclonal antibodies.

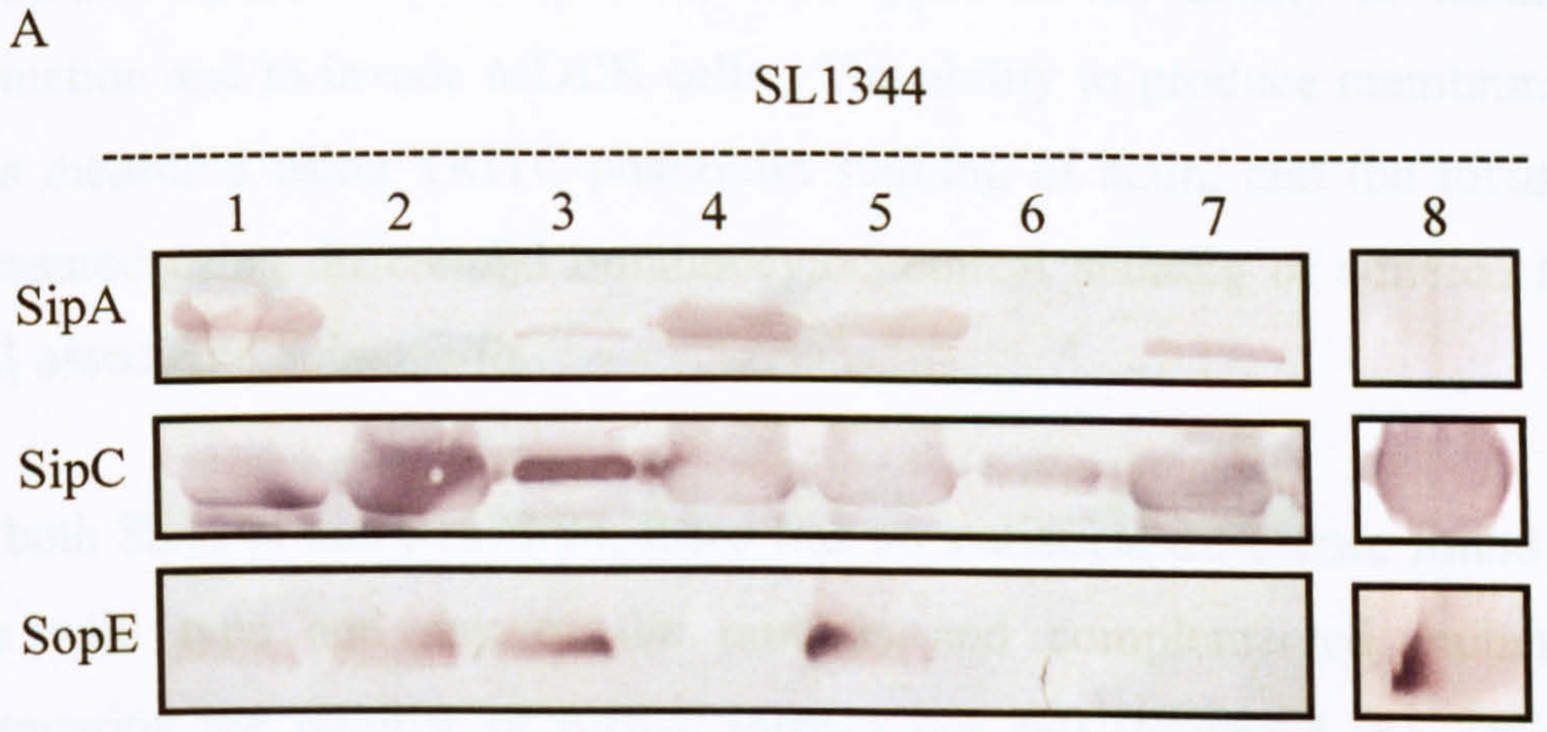

4.3.9. Examining the effect on ruffle induction and invasion that occur with loss of SipA and/or SopE from S. Typhimurium strains

The *sipA*⁻, *sopE*⁻ and *sipA*⁻ *sopE*⁻ mutants of SL1344 and S1579/94 were compared against their respective wild types in the ability to induce ruffle formation and to invade MDCK cells. The ability to produce membrane ruffles was measured using TRITC-phalloidin staining of actin, and the invasion was measured using differential immunocytochemical staining of adhered and total cell-associated *Salmonella*.

In both SL1344 and S1579/94, there was no statistical difference found between the wild type and any of the mutants and complemented mutants when comparing the number of ruffles formed per cell (Figure 4.18). It therefore appears that neither the absence of SopE nor the absence of SipA and SopE together affects the process of ruffle formation. However, it was noted that in SL1344, the *sipA*⁻ *sopE*⁻ mutant did produce greater number of ruffles than either the wild type or the single mutants. Since this behaviour is not seen with the S1579/94 double mutant (Figure 4.18B) or with the F98 and 12023 *sipA*⁻ mutants (Figure 4.14C and D) and does not represent a significant difference compared to the wild type, it is unlikely to represent an important difference.

While the ability to propagate ruffles was not affected by the absence of one or more of the effector proteins, this was not true for the process of invasion. Figure 4.19A shows the invasion per cell for SL1344. On average 3.35 ± 0.299 wild type bacteria entered each cell, and this number was significantly reduced when either *sipA* or *sopE* were deleted, or they were both absent. The *sipA*⁻ mutant had invasion 2.5 times lower than the wild type, which is similar to the data shown in Figure 4.9A, where the reduction was 3-fold. The 2-fold reduction in invasion of the SL1344 *sopE*⁻ mutant corresponds to data already published. For example Hardt *et al.* (1998b) saw a 1.6-fold decrease after 20 minutes of infection, and Stender *et al.* (2000) report a two- to threefold reduction after infection of COS-7 cells for 45 minutes. Thus, like SipA, SopE contributes to efficient entry of host cells.

Figure 4.18 Comparing the ability to induce ruffles in MDCK cells by serovar Typhimurium strains SL1344 and S1579/94. Infection was for 15 minutes, with the ability to induce ruffle formation being measured using TRITC-phalloidin staining of actin. Results are the mean of three independent experiments ± standard error of the mean. Statistical differences were measured using a one-way ANOVA, followed by a Tukey post-test, at a level of $P<0.05$.

A. SL1344

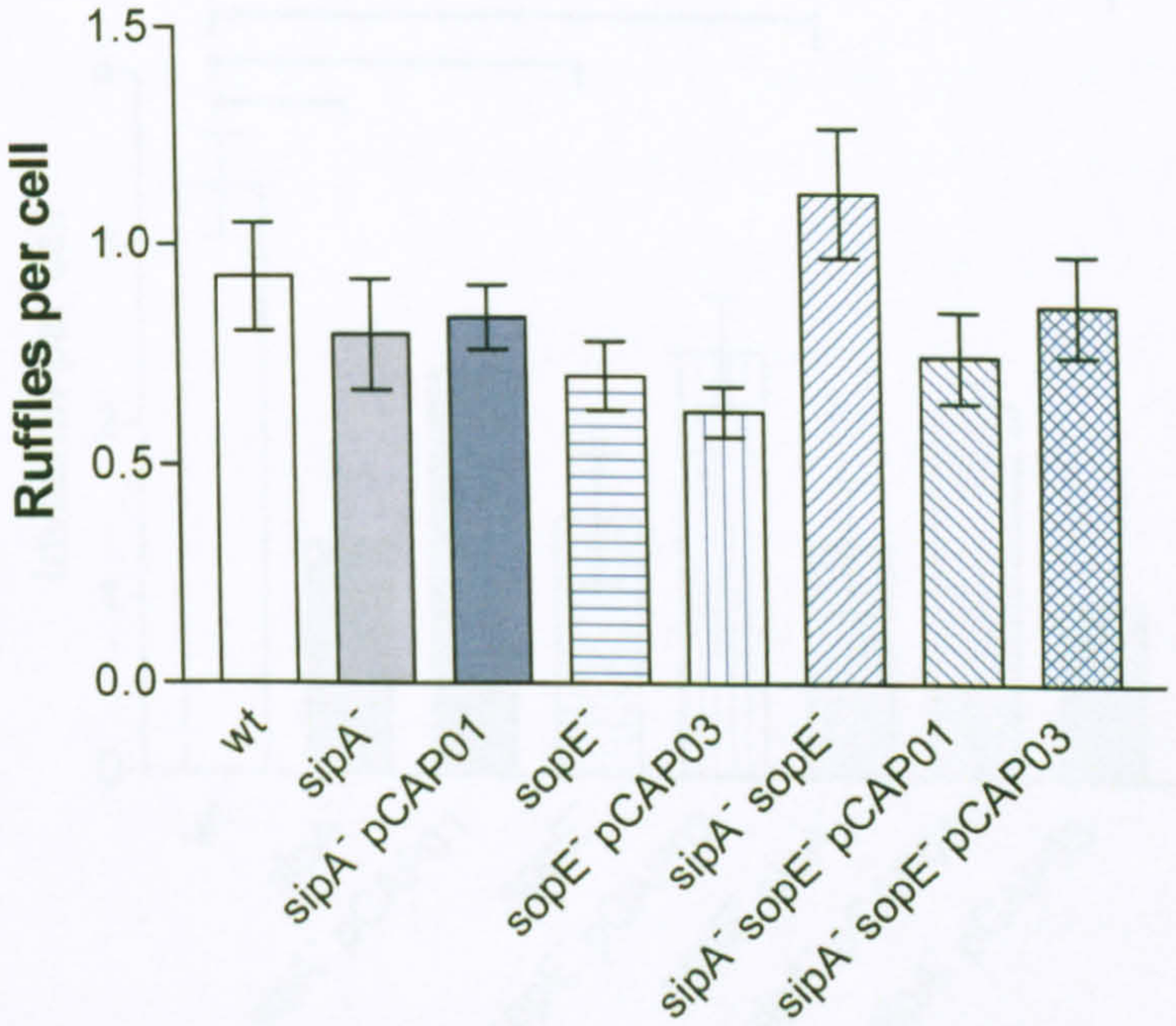

B. S1579/94

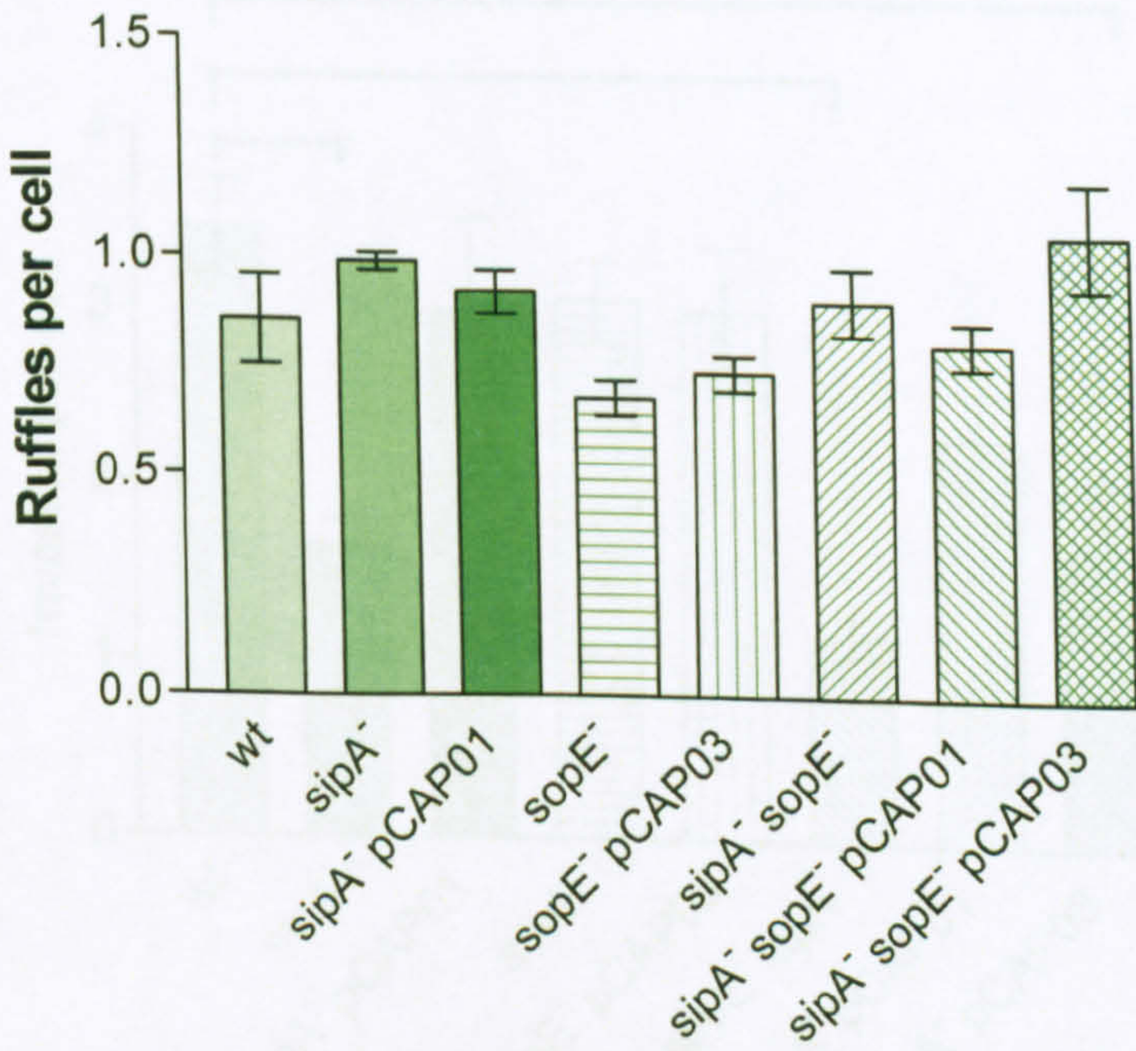

Figure 4.19 Comparing the ability to invade MDCK cells by effector mutants of serovar Typhimurium strains SL1344 and S1579/94. Infection was for 15 minutes, with the ability to induce ruffle formation being measured using TRITC-phalloidin staining of actin. Results are the mean of four independent experiments ± standard error of the mean. Asterisk denotes a statistical difference when compared to the wild type in a one way ANOVA with a Tukey post-test at the level of $P<0.05$.

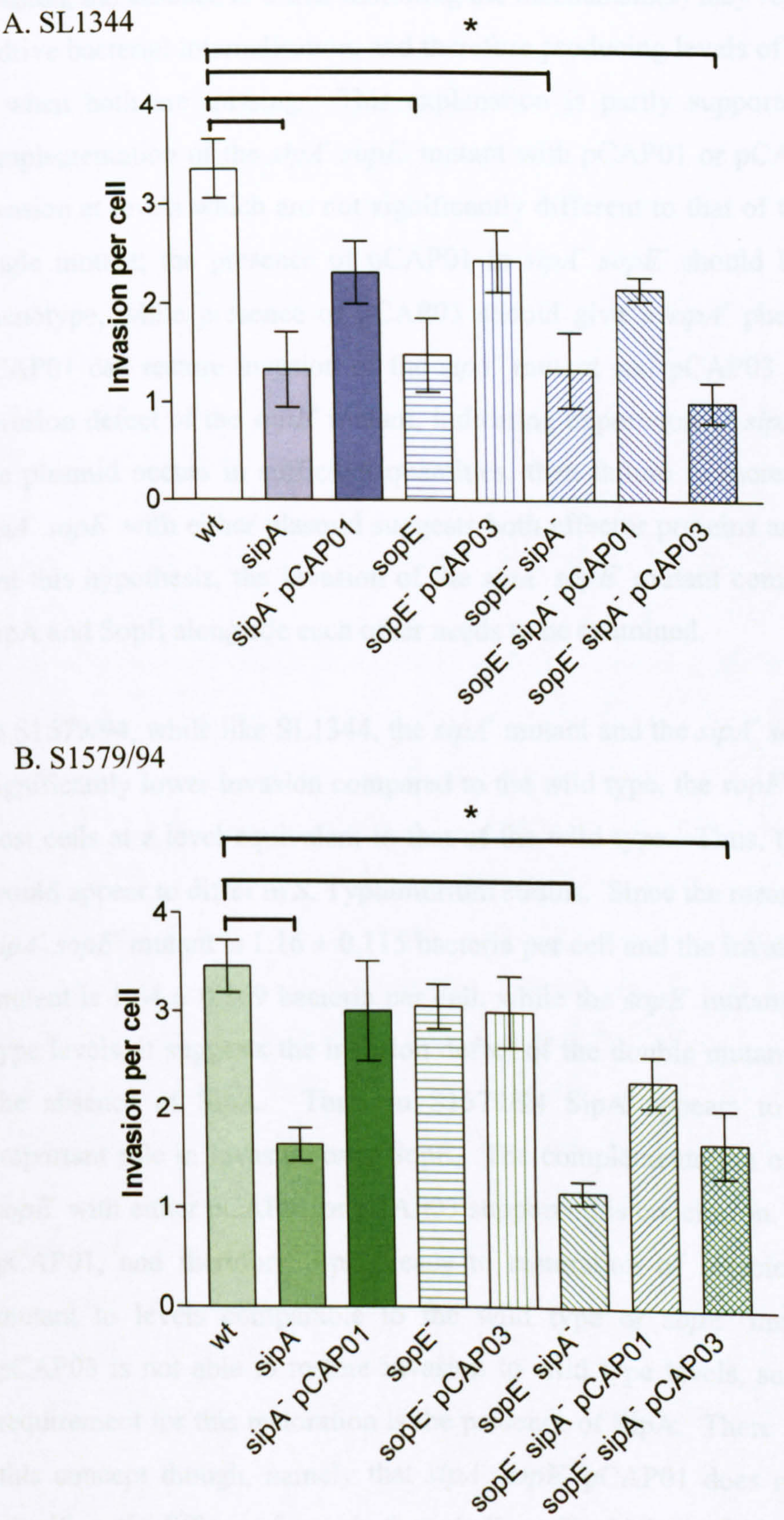

In SL1344, the level of invasion when the *sipA* and *sopE* genes are both inactivated remains similar to that of the single mutants, and indeed there was no significant difference found between either of the single mutants and *sipA⁻ sopE⁻* (Figure 4.19). This may potentially indicate SipA and SopE act together during invasion, the absence of either inhibiting the mechanism(s) they regulate together to drive bacterial internalisation, and therefore producing levels of invasion equal to when both are missing. This explanation is partly supported by the fact complementation of the *sipA⁻ sopE⁻* mutant with pCAP01 or pCAP03 maintains invasion at levels which are not significantly different to that of their equivalent single mutant; the presence of pCAP01 in *sipA⁻ sopE⁻* should lead to a *sopE⁻* phenotype, while presence of pCAP03 should give a *sipA⁻* phenotype. Since pCAP01 can restore invasion of the *sipA⁻* mutant and pCAP03 can restore the invasion defect of the *sopE⁻* mutant, indicating expression of *sipA* or *sopE* from the plasmid occurs in sufficient quantities, then failure to increase invasion of *sipA⁻ sopE⁻* with either plasmid suggests both effector proteins are required. To test this hypothesis, the invasion of the *sipA⁻ sopE⁻* mutant complemented with SipA and SopE alongside each other needs to be examined.

In S1579/94, while like SL1344, the *sipA⁻* mutant and the *sipA⁻ sopE⁻* mutant had significantly lower invasion compared to the wild type, the *sopE⁻* mutant entered host cells at a level equivalent to that of the wild type. Thus, the role of SopE would appear to differ in *S.* Typhimurium strains. Since the mean invasion of the *sipA⁻ sopE⁻* mutant is 1.16 ± 0.115 bacteria per cell and the invasion for the *sipA⁻* mutant is 1.64 ± 0.169 bacteria per cell, while the *sopE⁻* mutant invades at wild type levels, it suggests the invasion defect of the double mutant it due solely to the absence of SipA. Thus, in S1579/94 SipA appears to have the more important role in invasion over SopE. The complementation of S1579/94 *sipA⁻ sopE⁻* with either pCAP01 or pCAP03 supports this conclusion. The presence of pCAP01, and therefore SipA, leads to restoration of invasion in the double mutant to levels comparable to the wild type or *sopE⁻* mutant. However, pCAP03 is not able to restore invasion to wild type levels, suggesting the sole requirement for this restoration is the presence of SipA. There is a problem with this concept though, namely that *sipA⁻ sopE⁻* pCAP01 does not have invasion significantly different from *sipA⁻* or *sipA⁻ sopE⁻* which would be expected if SipA

was the only cause of the invasion defect. This could therefore still point to some role for SopE in S1579/94, but illustrates that effector proteins may have different levels of importance in different *Salmonella* strains. This may in part explain why different research groups observe different effects in the behaviour of an effector mutant.

4.3.10. Examining the morphology of ruffles induced by strains of S. Typhimurium lacking SipA and/or SopE

The morphology of the ruffles induced by the *sipA*$^-$, *sopE*$^-$ and *sipA*$^-$ *sopE*$^-$ mutants of SL1344 and S1579/94 were compared against their respective wild types using CLSM to determine whether the changes observed in the *sipA*$^-$ mutants of F98 and 12023 could be replicated in the *sipA*$^-$ *sopE*$^-$ mutants of SL1344 and S1579/94.

As had been observed before (Figure 4.15A and B), the ruffles induced by the wild type of SL1344 and S1579/94 appeared similar with a roughly circular ruffle forming around the bacterium, which sits centrally. Examining the *sopE*$^-$ mutants of SL1344 and S1579/94 revealed these mutants produce smaller ruffles than the wild type, while complementation of this mutant with pCAP03 increased the ruffle size to diameters surpassing those of the wild type ruffles (Figure 4.20). The ruffles of F98 wild type and 12023 wild type, both strains of which naturally lack SopE, had also been observed to produce small ruffles (Figure 4.15C and D), and thus it does appear that absence of SopE limits ruffle size, without affecting ruffle morphology. This supports the observations reported by Stender *et al.* (2000) using SEM. Using actin staining, they and Hardt *et al.* (1998a) also reported the actin cytoskeleton rearrangements induced by SL1344 *sopE*$^-$ as being less extensive/localised than those induced by wild type. This is not observed here; the actin is clearly focused in the *sopE*$^-$ induced ruffles, with very little in the surrounding vicinity (Figure 4.20A and B). The difference in the cultured cell line used for these other studies, Henle-407 and COS-7, compared with MDCK I cells here, could account for this difference.

Figure 4.20 CLSM images showing the morphology of membrane ruffles induced by wild type and effector mutants of SL1344 and S1579/94. Each image shows a representative selection of images of TRITC-phalloidin stained MDCK cells infected for 15 minutes. Bacteria are stained with FITC. The wild type, *sipA*⁻ and *sipA*⁻ pCAP01 images are those shown in Figure 4.15 but included here for comparison. Each image is presented as a projected series of optical sessions showing membrane ruffles in their entirety. Scale bar 10µm

A. SL1344

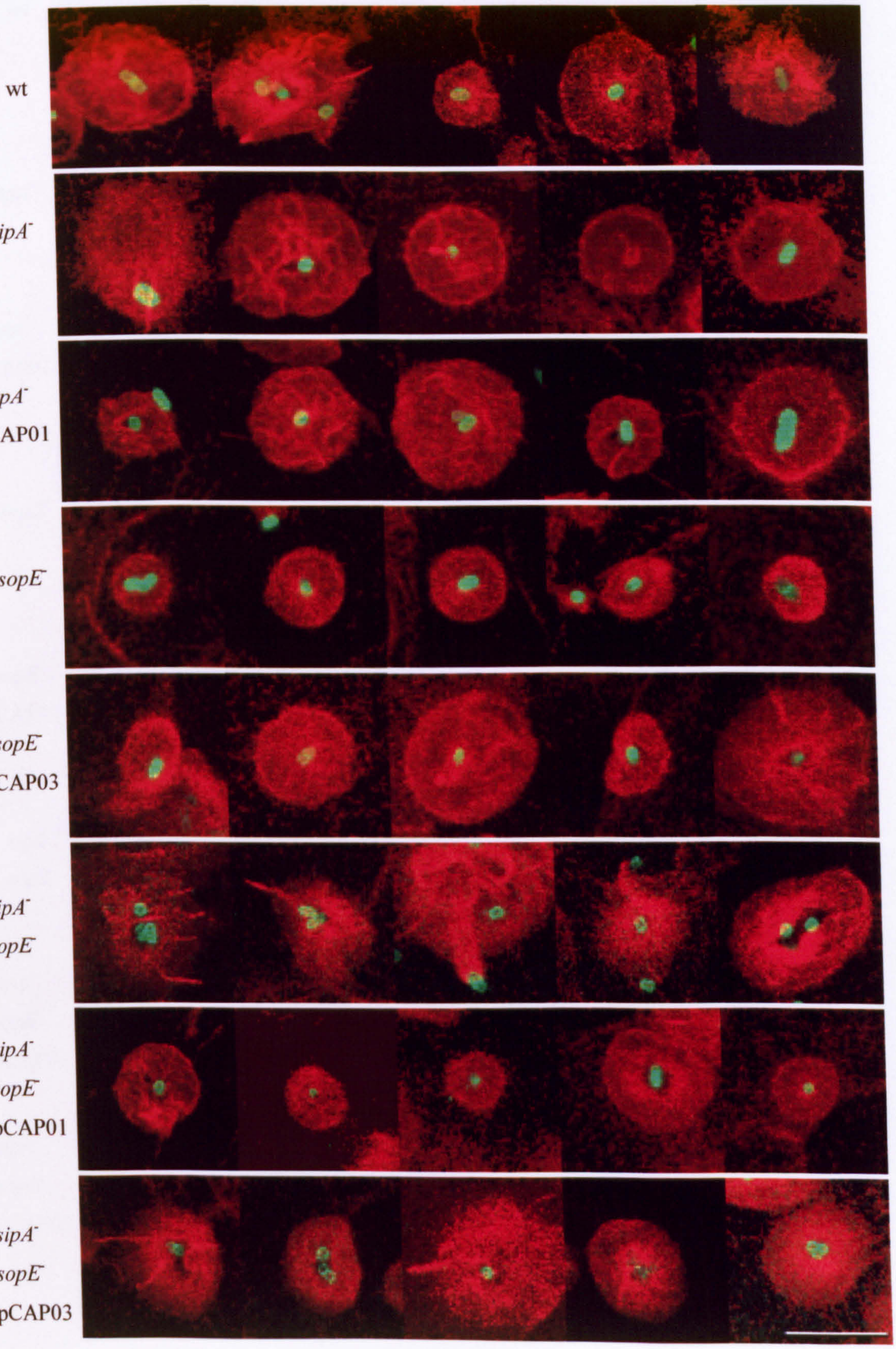

B. S1579/94

wt

sipA⁻

sipA⁻
pCAP01

sopE⁻

sopE⁻
pCAP03

sipA⁻
sopE⁻

sipA⁻
sopE⁻
pCAP01

sipA⁻
sopE⁻
pCAP03

The SL1344 and S1579/94 *sipA*⁻ *sopE*⁻ mutants produced ruffles like those of the F98 and 12023 *sipA*⁻ mutants. The ruffles produced were more 'spiky' due to the presence of large numbers of filopodia, and many possessed the finger-like projections that had been found associated with the F98 and 12023 *sipA*⁻ mutant ruffles (Figure 4.15). Thus, it appears the absence of SipA and SopE does lead to a dramatic change in ruffle morphology. The presence of pCAP01 in *sipA*⁻ *sopE*⁻ fully restores the wild type ruffle morphology phenotype, while pCAP03 partially restores the wild type phenotype, indicating it is the loss of SipA and SopE together that is responsible for the morphological change. Transcomplementation of *sopE*⁻ with pCAP03 led to the production of ruffles which were often much larger than those of the wild type, suggesting an over-expression of SopE. Since pCAP03 in *sipA*⁻ *sopE*⁻ could only partially restore the wild type morphology it may indicate the ratio of SipA to SopE is important for correct ruffle propagation.

Several features of the ruffles were quantified to provide more substantial evidence of the differences that exist between the ruffles induced by each strain and its mutants. Figure 4.21 examines the proportion of ruffles that exhibit finger-like protrusions. This phenotype seems to be clearly associated with the absence of SipA and SopE since in *sopE*⁻ strains (natural or *sopE*⁻ mutants), inactivation of *sipA* significantly increases (5-16-fold) the proportion of ruffles with fingers. Complementation with pCAP01 carrying the *sipA* gene restores levels back to that of the wild type in all four strains indicating loss of both effector proteins is responsible for this phenotype. This is also supported by the failure of the *sipA*⁻ single mutant, or a *sopE*⁻ single mutant in the SL1344 and S1579/94 strains, to increase the proportion of ruffles with fingers (Figure 4.21).

Figure 4.21 Quantifying the proportion of ruffles which have one or more finger-like protrusions in serovar Typhimurium strains SL1344, S1579/94, F98 and 12023. The wild type, *sipA*⁻ and *sipA*⁻ pCAP01 of each strain are compared in A, while the *sopE*⁻ and *sipA*⁻ *sopE*⁻ mutant are compared in strains SL1344 (B) and S1579/94 (C). Infection was for 15 minutes, with ruffles being identified using TRITC-phalloidin staining of actin. Results are the mean of three independent experiments ± standard error of the mean. Asterisk denote a significant difference when compared using a one-way ANOVA with a Bonferroni post-test at the level of $P<0.05$.

A

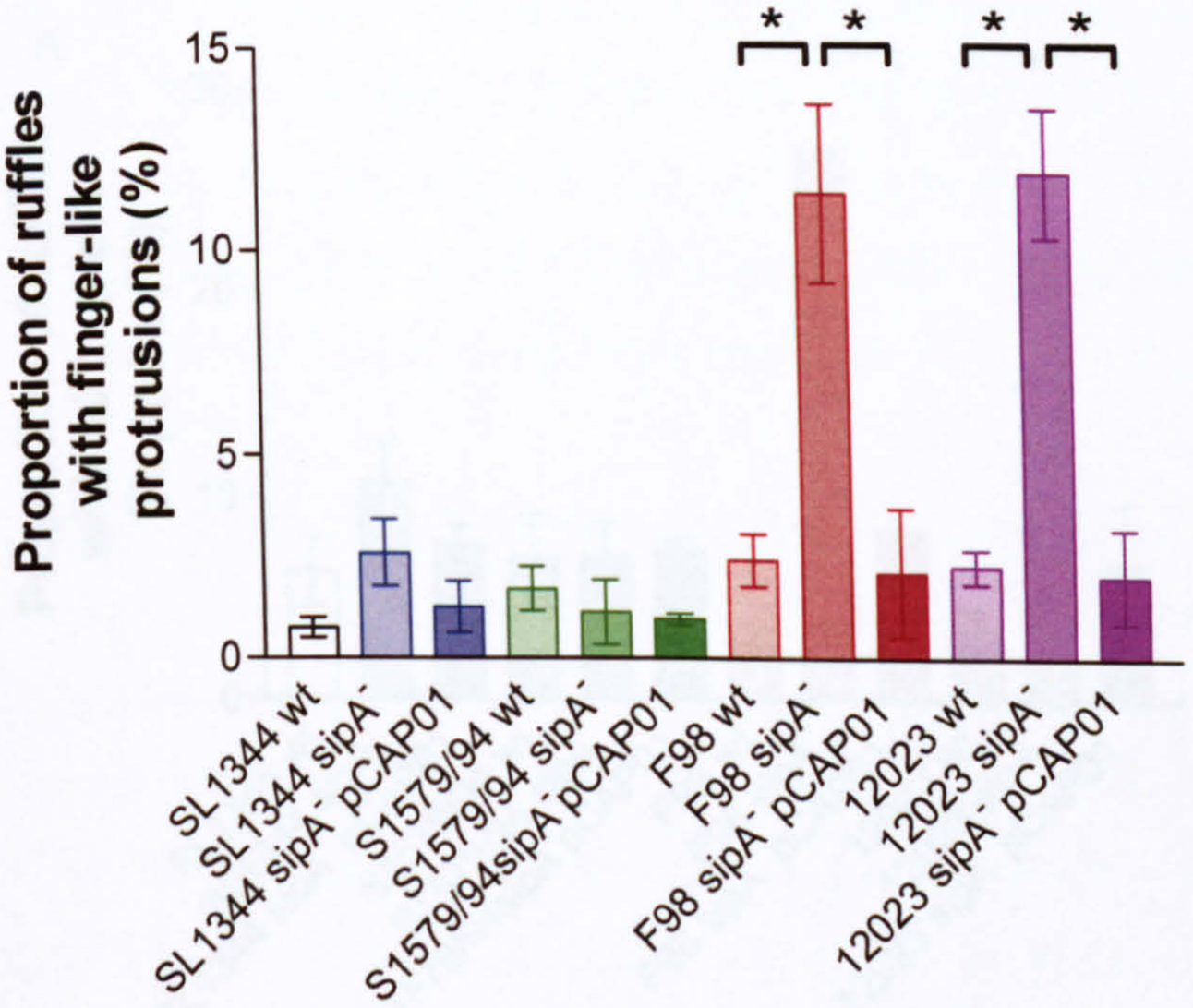

B

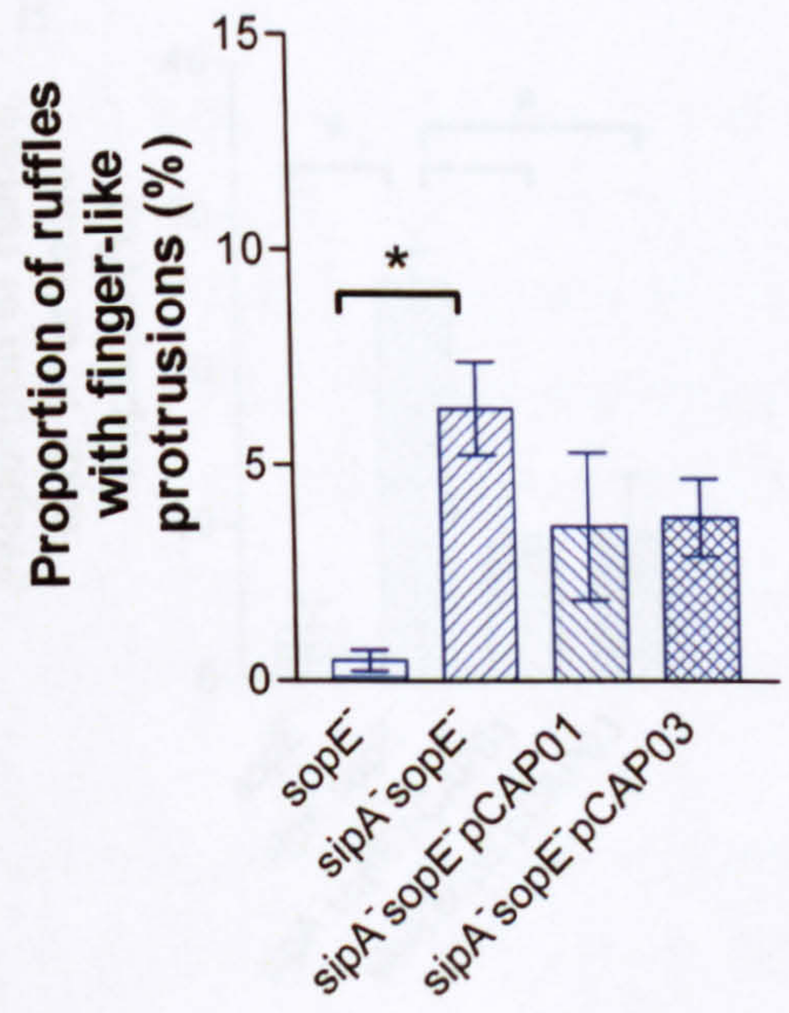

C

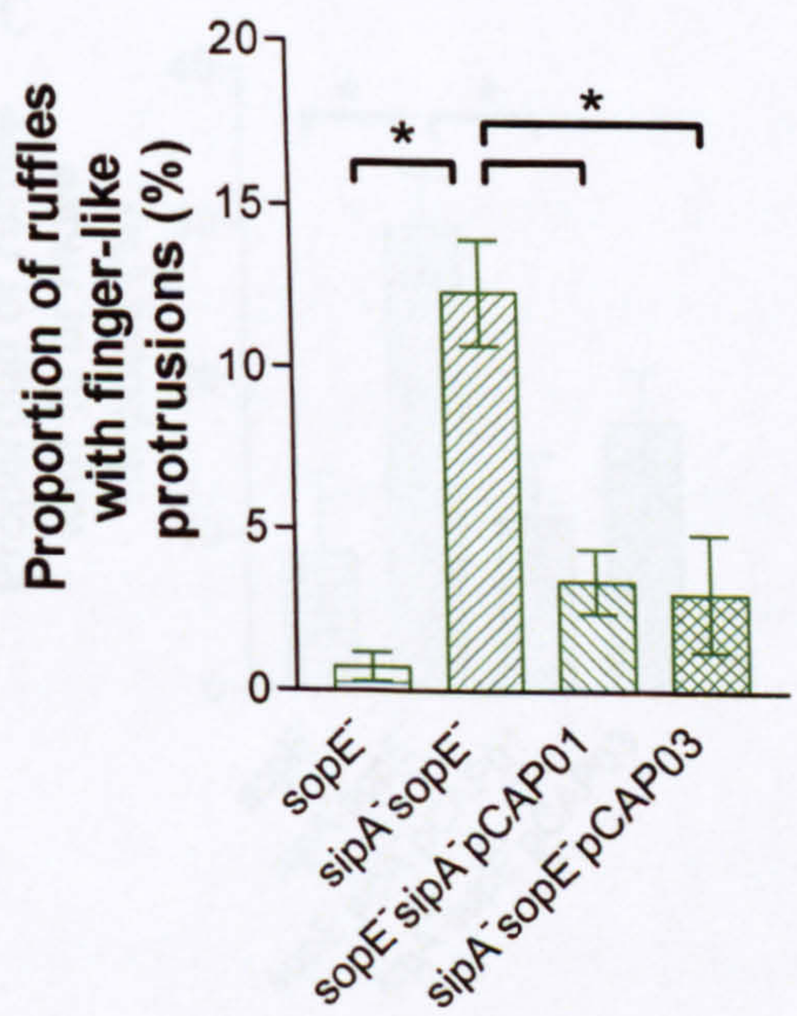

Figure 4.22 Quantifying the number of ruffles with ≥10 filopodia in serovar Typhimurium strains SL1344, S1579/94, F98 and 12023. The wild type, *sipA*⁻ and *sipA*⁻ pCAP01 of each strain are compared in A, while the *sopE*⁻ and *sipA*⁻ *sopE*⁻ mutant are compared in strains SL1344 (B) and S1579/94 (C). Infection was for 15 minutes, with ruffles being identified using TRITC-phalloidin staining of actin. Results are the mean of three independent experiments ± standard error of the mean. Asterisk denote a significant difference when compared using a one-way ANOVA with a Bonferroni post-test at the level of $P<0.05$.

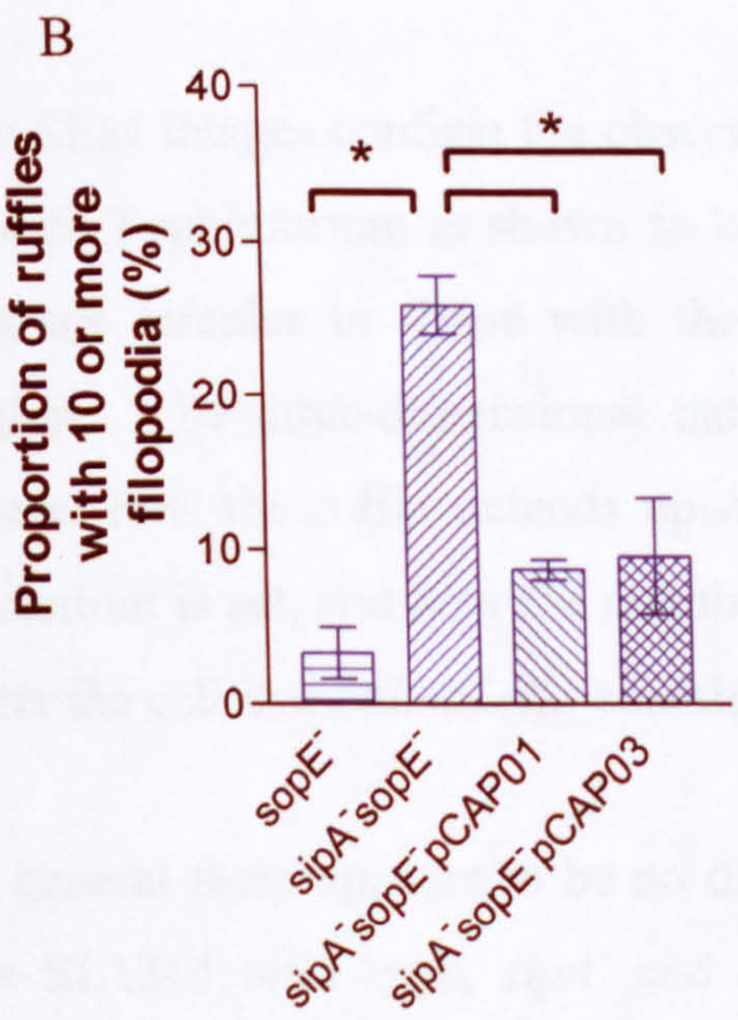

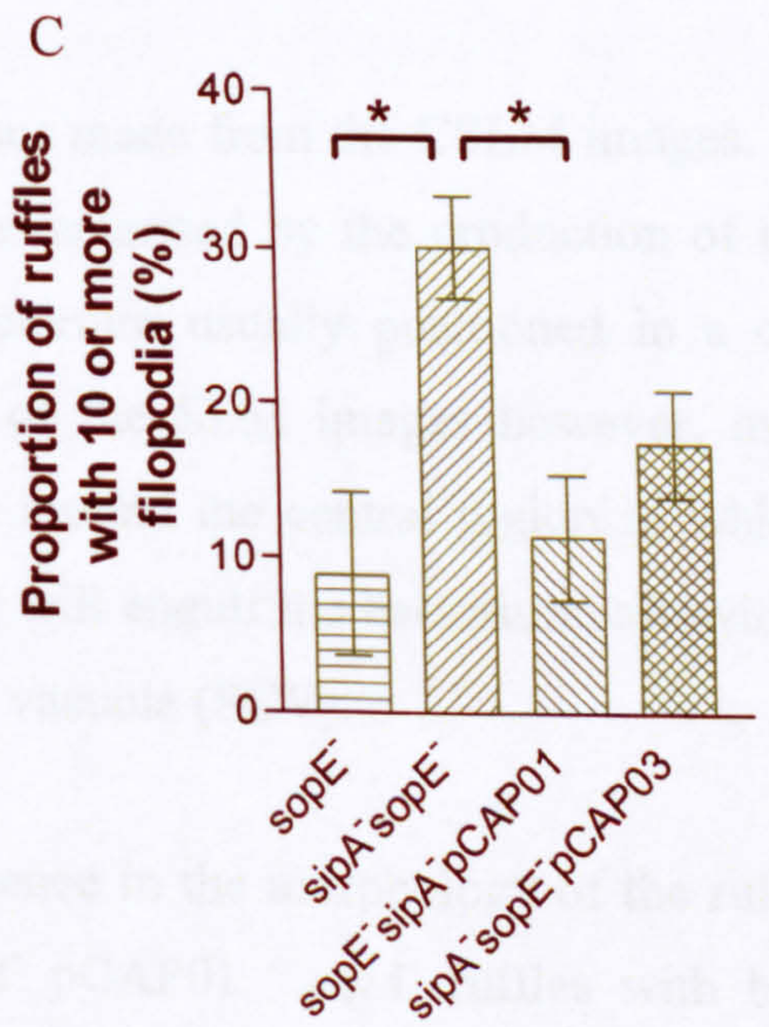

The proportion of ruffles with 10 or more filopodia was also measured (Figure 4.22). Again, no difference was found between all four wild type strains, eliminating the absence of SopE on its own as a cause for increased numbers of filopodia. Likewise, the absence of SipA in SL1344 and S1579/94 did not change the number of ruffles with large numbers of filopodia. However, absence of both SipA and SopE significantly increased the number of ruffles with ≥10 filopodia (3-10-fold increase) compared with the equivalent wild type or *sopE*⁻ mutant. Again, the phenotype of *sipA*⁻ *sopE*⁻ could be restored to the wild type phenotype with pCAP01 or pCAP03 (Figure 4.22), and indicates the 'spikiness' of the ruffles was increased when SipA and SopE were absent together.

The CLSM images of ruffles were obtained by imaging the actin of the cell, which had been labelled with a TRITC fluorophore. While this provides an insight into the nature of the ruffles, and their likely morphology, these images as actin representations of the ruffle can not provide accurate detail in regards to their ultrastructure, especially since actin may not necessarily be associated with all parts of the membrane. SEM was therefore performed on the apical membrane of MDCK cells that had been infected for 15 minutes with one of the serovar Typhimurium strains (Figure 4.23), to obtain greater information on the membrane appearance of the ruffles and associated projections.

The SEM images confirm the observations made from the CSLM images. Wild type *S.* Typhimurium is shown to be characterised by the production of ruffles that are circular in shape with the bacterium usually positioned in a central region. The three-dimensional nature of the SEM images however, make it clearer how the ruffle extends upwards around the central region in which the bacterium is sat, and how the membrane will engulf the bacterium, allowing it to enter the cell in a *Salmonella* containing vacuole (SCV).

In general there appears to be no difference in the morphology of the ruffles of the SL1344 wild type, *sipA*⁻ and *sipA*⁻ pCAP01. *sipA*⁻ ruffles with bacteria located near the periphery of the ruffle were observed in a few cases but poor image quality prevents a representative image being presented. SL1344 *sopE*⁻ and *sopE*⁻ pCAP03 ruffles also appear similar to those of the wild type, again

supporting the conclusions drawn from examining CLSM images. SL1344 *sipA*⁻ *sopE*⁻ produce wild type-like ruffles, but additionally there are ruffles with obvious finger-like protrusions extruding from them, an example of which is illustrated (Figure 4.23A). In this case it can clearly be seen that the bacterium is attached to the tip of the protrusion, and it is likely that it is being driven away from the ruffle centre, just as is seen with a *sipA*⁻ mutant in this strain, although the phenomenon appears more extreme with the additional absence of SopE.

The presence of pCAP01 in SL1344 *sipA*⁻ *sopE*⁻ leads to the ruffles behaving like those of the wild type, and therefore the *sopE*⁻ mutant it is equivalent to. However, pCAP03 fails to complement the double mutant, with a large number of ruffles possessing finger-like protrusions remaining. Since this strain should act in a similar manner to the *sipA*⁻ mutant, with bacteria being pushed to the edges of the ruffle, it may be that an altered concentration of SopE molecules in *sipA*⁻ *sopE*⁻ pCAP03 affects the signalling mechanisms and interactions that occur between bacteria and host, and are therefore insufficient to prevent the formation of filopodia and finger-like protrusions.

Only the ruffles of the wild type and *sipA*⁻ mutants (and *sipA*⁻ *sopE*⁻ mutant in S1579/94) were imaged from the other *S.* Typhimurium strains, since these are the most interesting ruffles regarding morphology. As mentioned, each wild type produces a circular ruffle with the bacterium located in the centre; this ruffle shape being maintained in S1579/94 *sipA*⁻, as had been the case for the *sipA*⁻ mutant of SL1344, the other SopE⁺ strain (Figure 4.23B). The *sipA*⁻ mutant of F98 and 12023 and the *sipA*⁻ *sopE*⁻ mutant of S1579/94 produced wild type-like ruffles and a proportion of ruffles with finger-like projections. In F98 (Figure 4.23C) and 12023 (Figure 4.23D) filopodia can also be identified in images, although this was not exclusive to these *sipA*⁻ *sopE*⁻ strains.

Figure 4.23 SEM images showing the morphology of representative membrane ruffles from MDCK cells infected for 15 minutes with wild type or effector mutants of *S.* Typhimurium strains SL1344 (A), S1579/94 (B), F98 (C) or 12023 (D). Scale bar 2μm.

A. SL1344

wt

sipA⁻

sipA⁻ pCAP01

sopE⁻

sopE⁻ pCAP03

sipA⁻ *sopE*⁻

sipA⁻ *sopE*⁻ pCAP01

sipA⁻*sopE*⁻ pCAP03

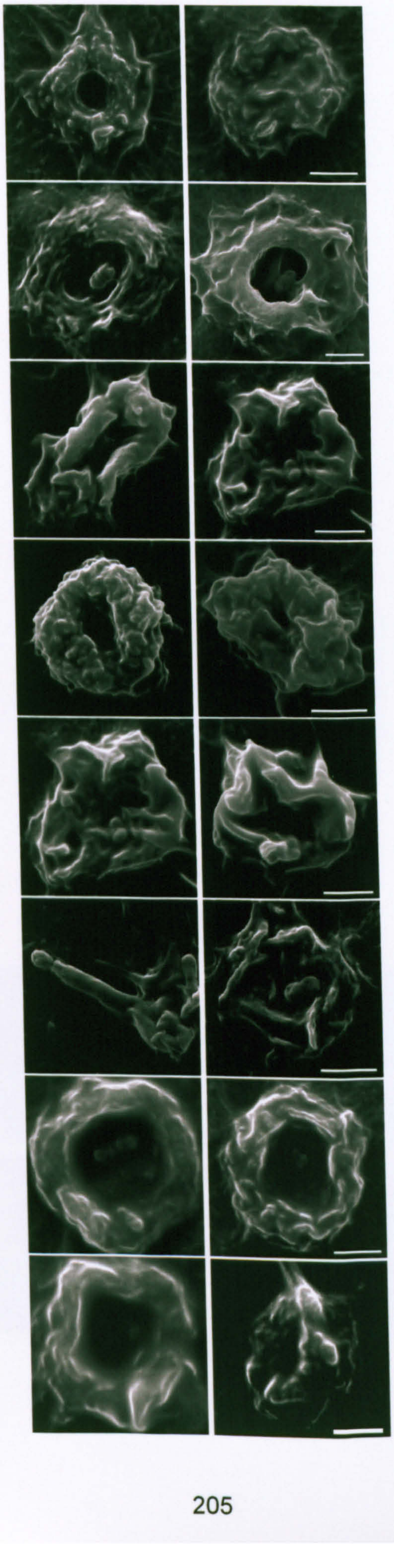

B. S1579/94

wt

sipA⁻

sopE⁻

sipA⁻ *sopE*⁻

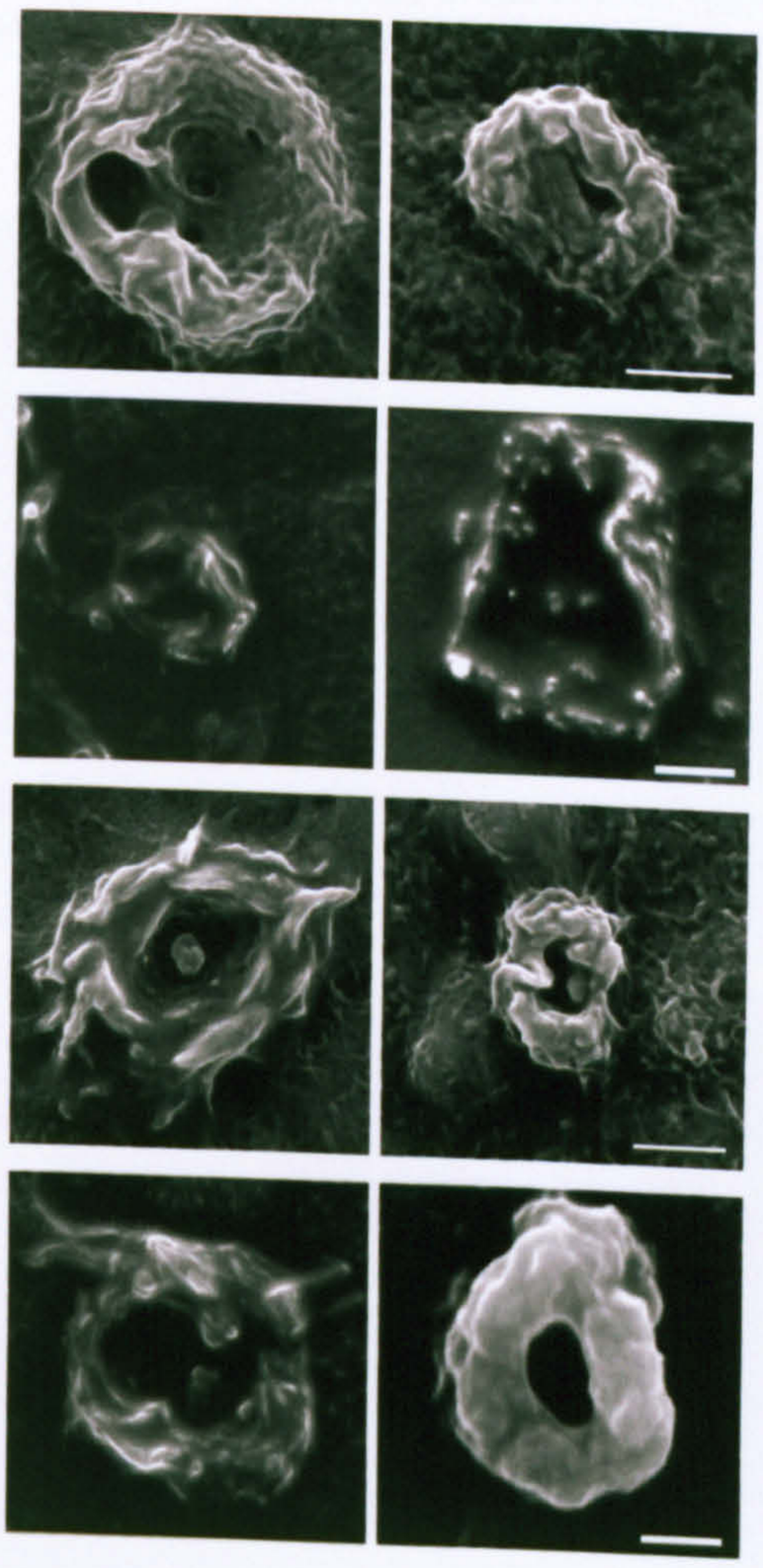

C. F98

D. 12023

wt

sipA⁻

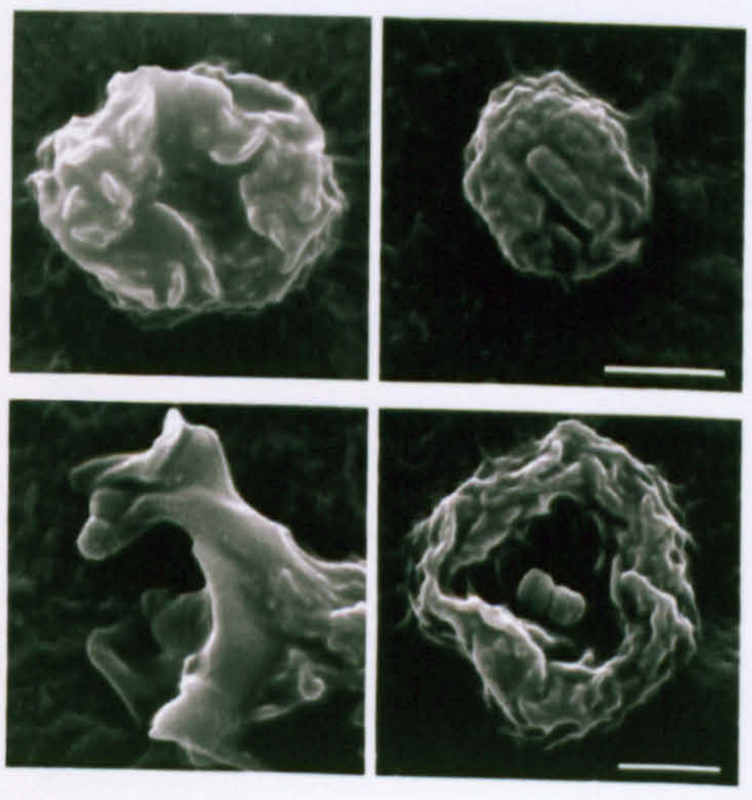

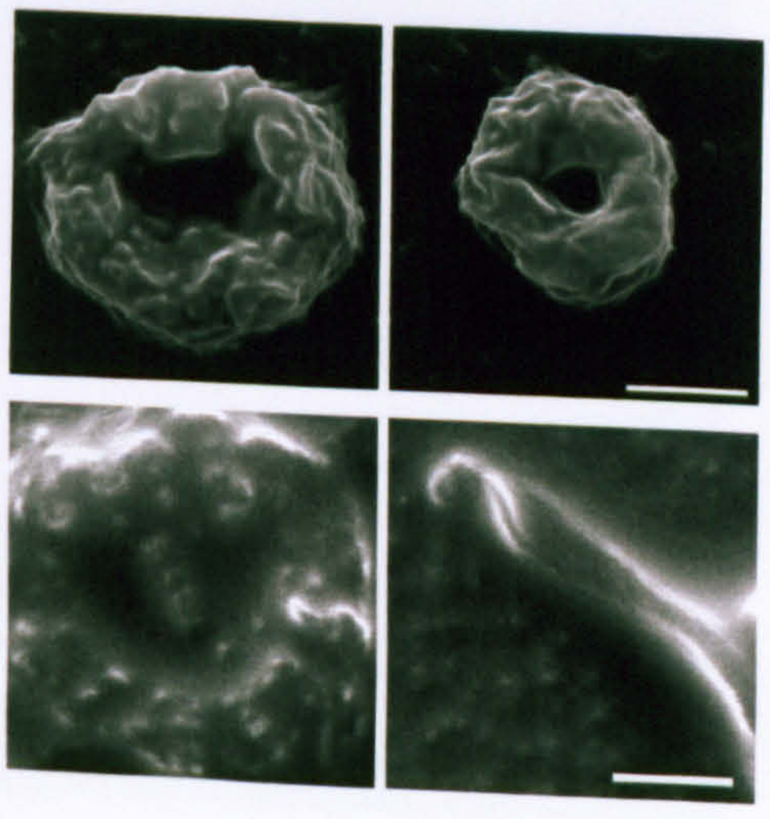

Figure 4.24 SEM and CSLM images of membrane ruffles induced by *sipA*⁻ *sopE*⁻ mutants of *S.* Typhimurium after a 15 minute infection of MDCK cells. A selection of images of membrane ruffles with finger-like protrusions is presented. SEM images (A) were of ruffles induced by F98 *sipA*⁻ *sopE*⁻ (panel a and b) and SL1344 *sipA*⁻ *sopE*⁻ mutants (panel c and d). Arrows in panel d indicate two areas where the bacterium is attached to the side of the finger-like protrusion. Scale bar 2μm. CSLM images (B) of ruffles induced by SL1344 *sipA*⁻ *sopE*⁻ mutants. Scale bar 10μm.

A.

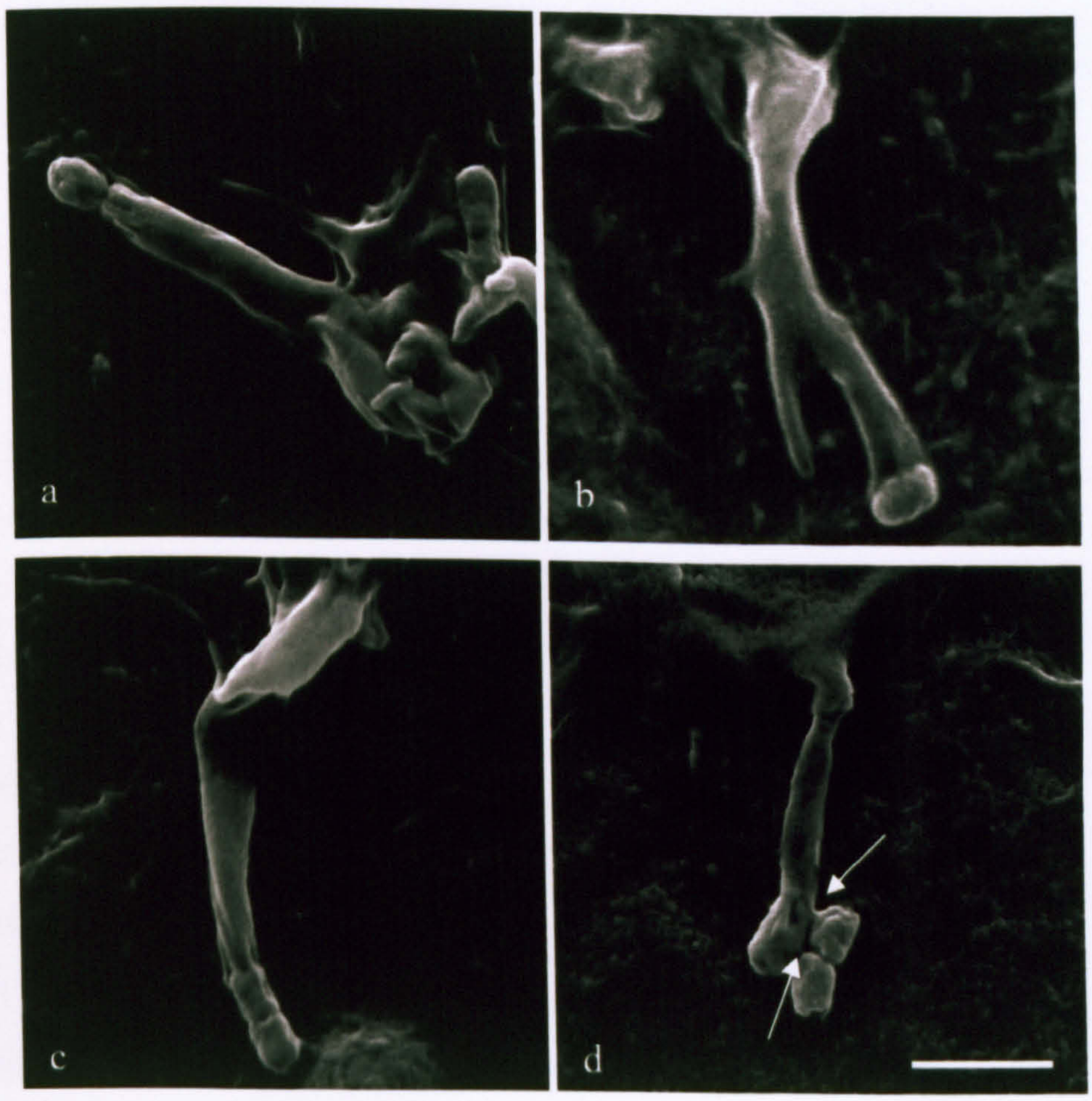

B.

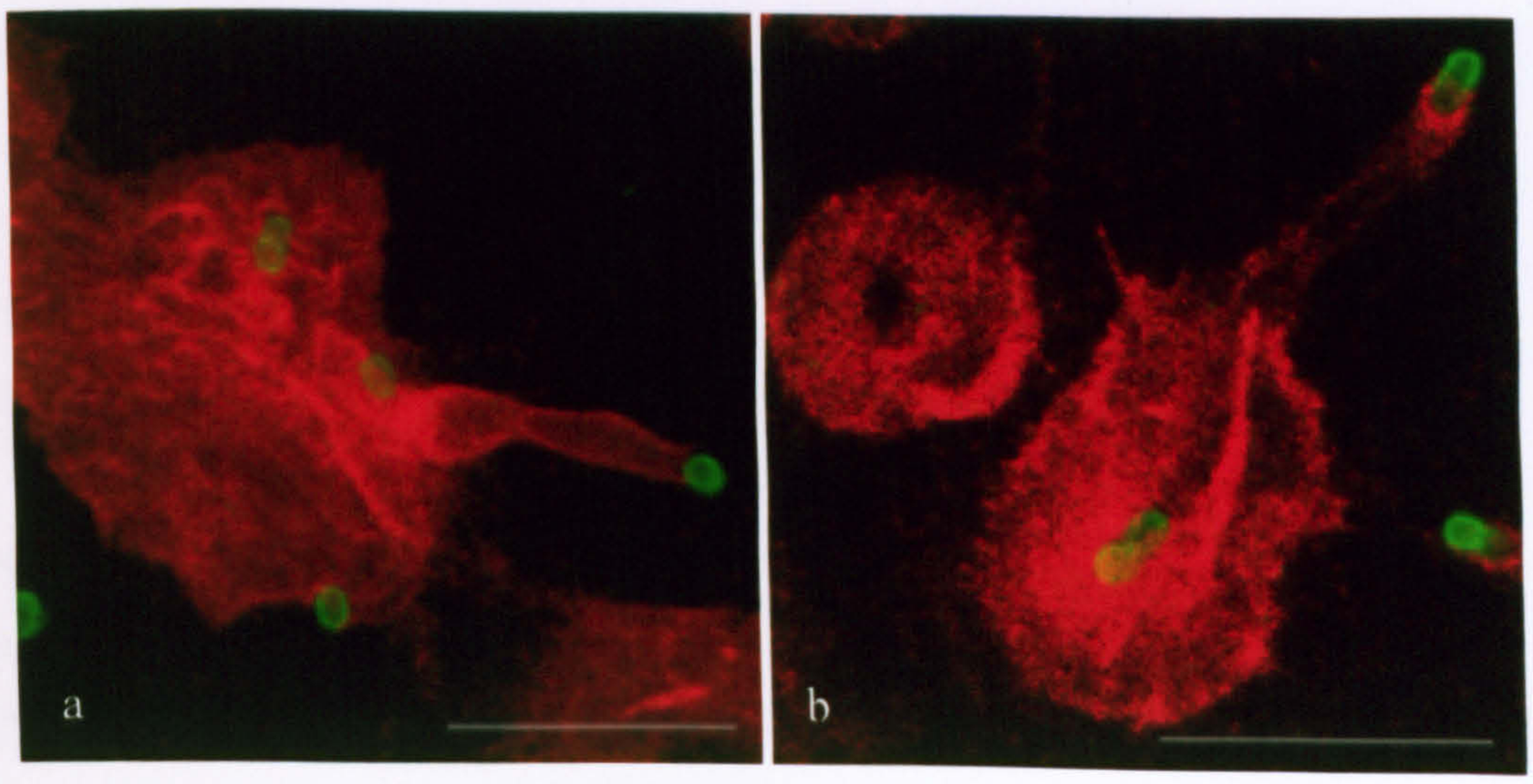

Figure 1.24 shows further examples of finger-like protrusions viewed by SEM and CSLM. The CSLM images (Figure 1.24B) show the finger-like protrusions are stained by TRITC-labelled phalloidin, indicating they are filled with actin, which extends up to the tip. However, they appear not to be entirely rigid, having a flexible nature, as indicated by the kink in the finger shown in Figure 1.24A, panel c. There is intimate contact between the bacterium and the tip of the finger-like protrusion, even in panel d where the bacterium is not located at the end of the finger but is attached to the side of the tip. In this case there appears to be two areas (highlighted by arrows) which tether the bacterium to the finger, although it is unclear what these tethering structures are. Figure 1.24A, panel c also indicates the host cell membrane at the tip of the protrusion may partly engulf the bacterium, and this impression is also given in Figure 1.24B panel b, since the bacterium seems to sit in a pocket of actin at the end of the finger. It is unclear whether the bacterium could potentially enter the host cell at the tip of the finger and then transverse through the finger into the cell.

Since the bacteria are often located on the end of the finger-like protrusions, the protrusion was believed to form adjacent to the bacterium, pushing it out from the ruffle it has induced, and this was later proved by time-lapse imaging (4.3.11). The intimate contact between bacteria and host cell membrane must keep the bacterium in place during this movement, although this is not always achieved since fingers may be found with no associated bacteria. The intimate contact between bacterium and host membrane in the protrusions appears to contrast with early events in ruffle induction where the bacterium has the ability to move across the ruffle surface toward the periphery and even detach, and perhaps indicates the mechanism involved with anchoring the bacterium to the centre of the ruffle, may be different from that which allows the bacterium to adhere.

Together the CLSM and SEM imaging show there are fundamental differences in the manner in which bacteria lacking either SipA and/or SopE interact with the ruffle they have induced, although the process of ruffle induction does not appear to be affected.

4.3.11. Use of time-lapse microscopy to analyse the kinetics of ruffle induction in each of the mutants

Phase-contrast time-lapse microscopy was employed to understand the sequence of events leading to the different ruffle morphologies observed by CLSM and SEM. Appendix III contains one movie for each wild type and mutant of the four *S.* Typhimurium strains to show the typical ruffling behaviour induced by these bacteria when interacting with MDCK I cells. Figure 4.25 shows phase-contrast stills of representative ruffles generated by the wild type and effector mutants of each strain, taken from movies generated by the time-lapse microscopy. These ruffle images replicate those presented in Figures 4.20 and 4.23. The wild type of each strain is shown to have circular ruffles with a centrally located bacterium. Stills from a time course of a SL1344 wild type ruffle illustrate the events occurring in the induction of wild type ruffles (Figure 4.26A). For a ruffle to be induced the bacterium must first adhere to the cell surface, as was first reported by Jones *et al.* in 1981, and which is shown at 0 seconds. Usually between 10 and 80 seconds after adherence the beginnings of a ruffle can be seen, which corresponds with the data of Schlumberger *et al.* (2005), who reported SipA and SopE delivery occurs 10-90 seconds after adherence. In this example it only takes 10 seconds before the ruffle starts to form (Figure 4.26A). The ruffle increases in size, with the bacterium remaining centrally located. Eventually a maximum size is achieved (at 110 seconds in Figure 4.25A), before the ruffle then starts to shrink, as the bacterium is brought into the cell (130 to 230 seconds in this case). What is not shown in this time course is that eventually the membrane ruffle completely dissipates so there is no record on the cell surface that the ruffle ever occurred.

Figure 4.25 Phase-contrast images of representative membrane ruffles generated in MDCK cells by the wild type and isogenic mutants of the four *S.* Typhimurium strains under study. Each image shows the maximum size achieved by the ruffle under observation. Images were taken from three individual experiments. Scale bar 5μm. Arrows indicate position of bacterium.

A. SL1344

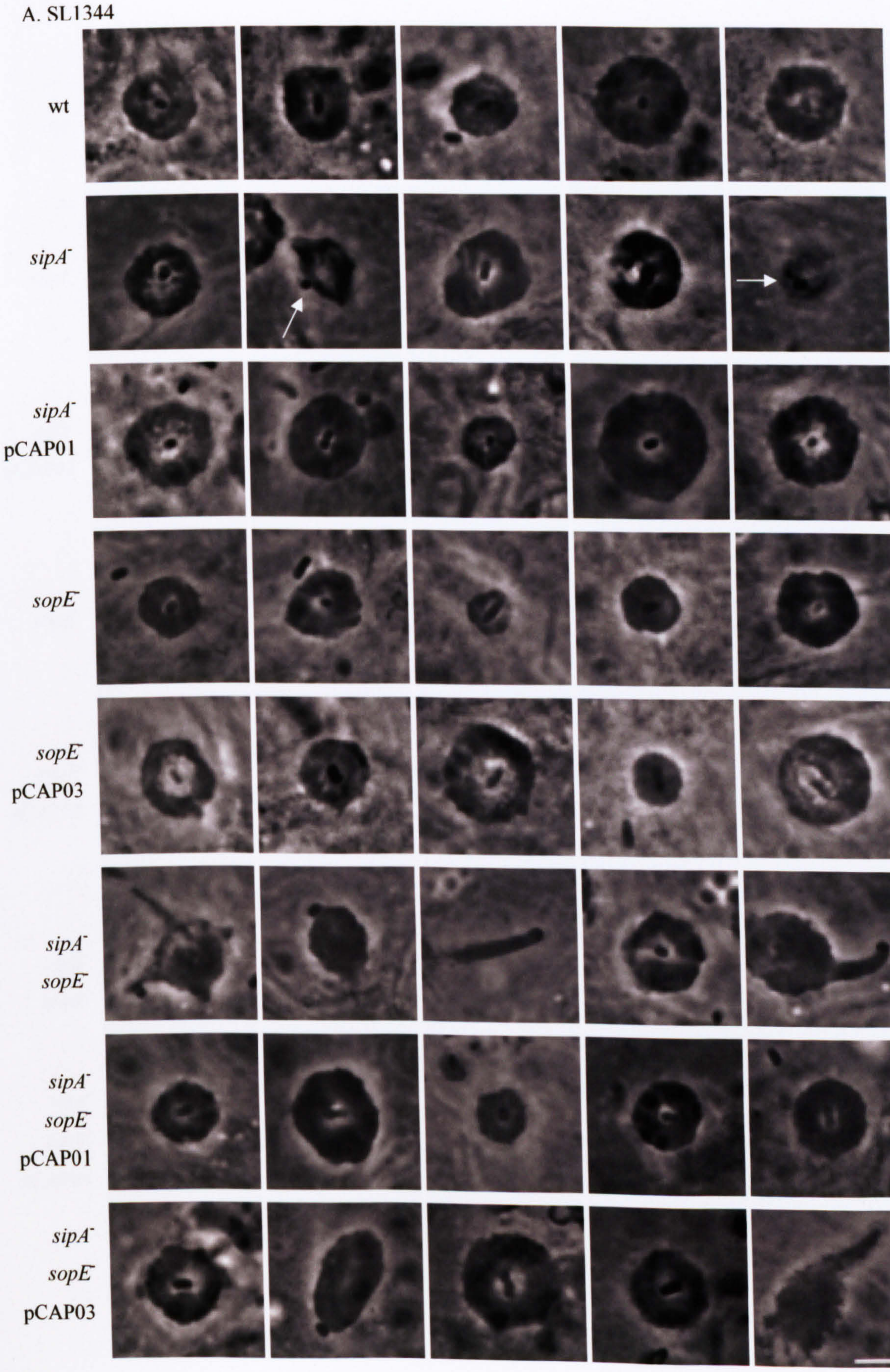

B. S1579/94

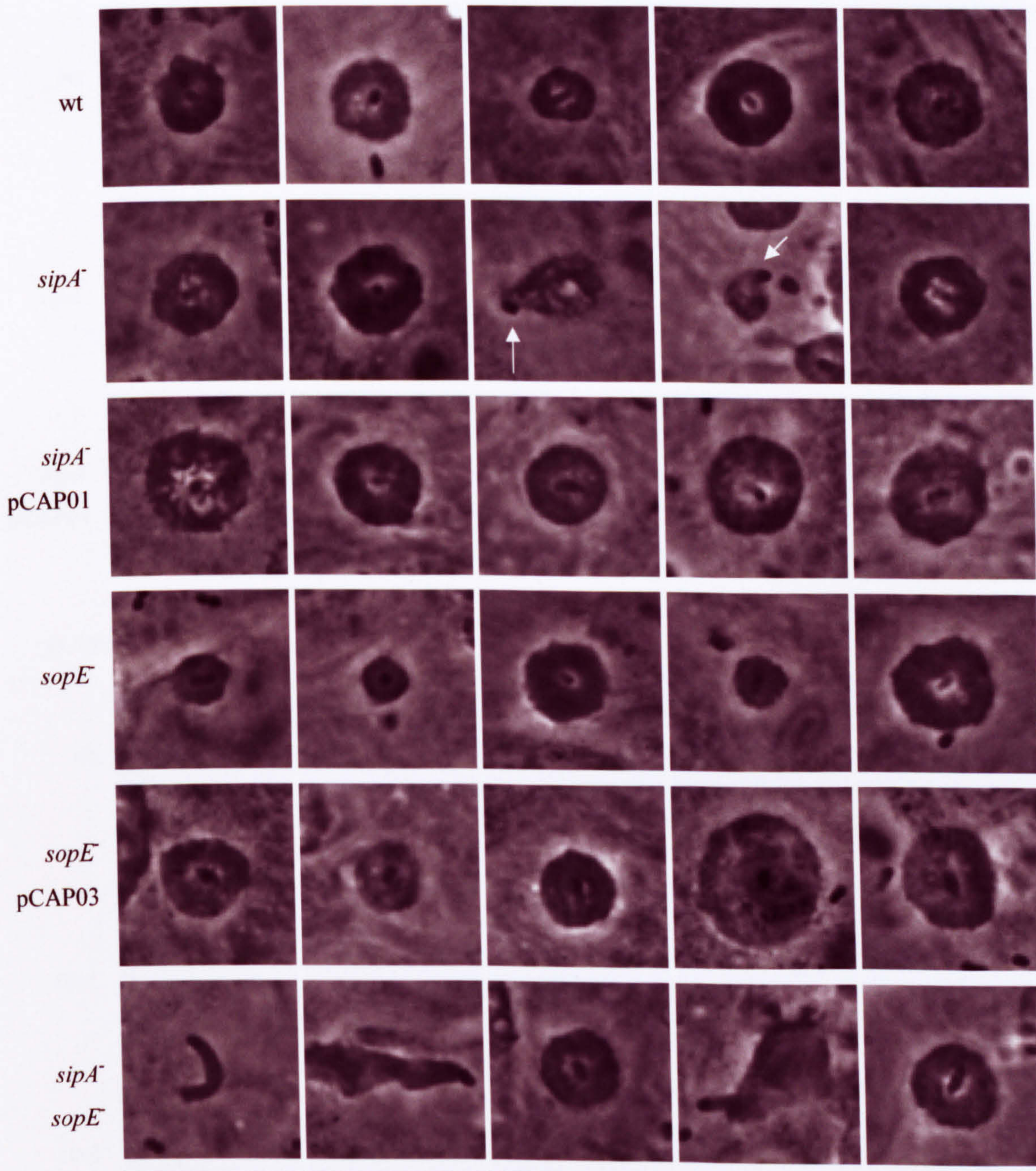
wt
sipA-
sipA-
pCAP01
sopE-
sopE-
pCAP03
sipA-
sopE-
sipA-
sopE-
pCAP01

C. F98

wt

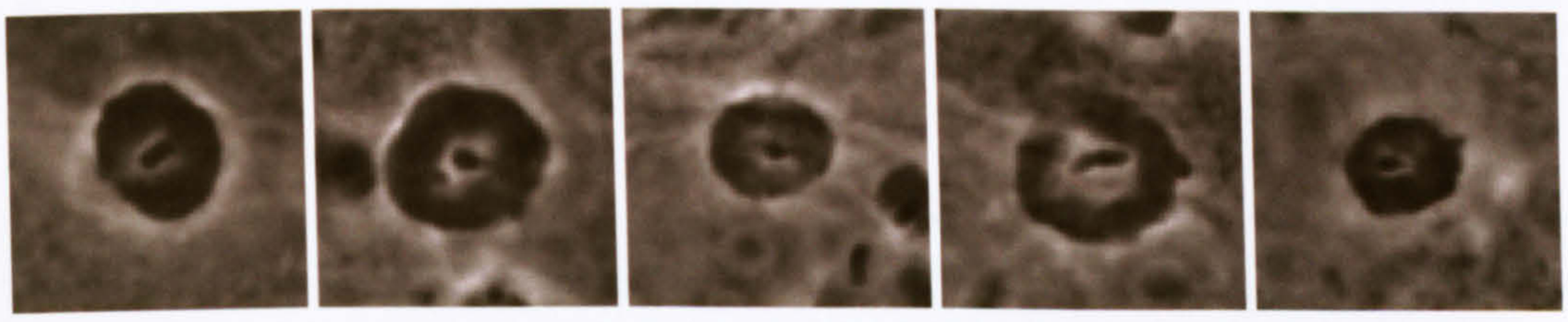

sipA⁻

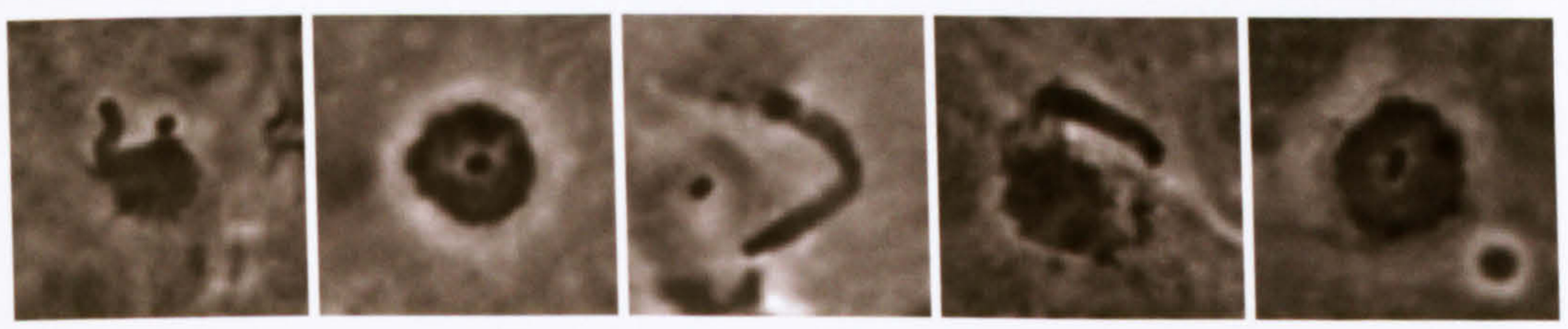

sipA⁻
pCAP01

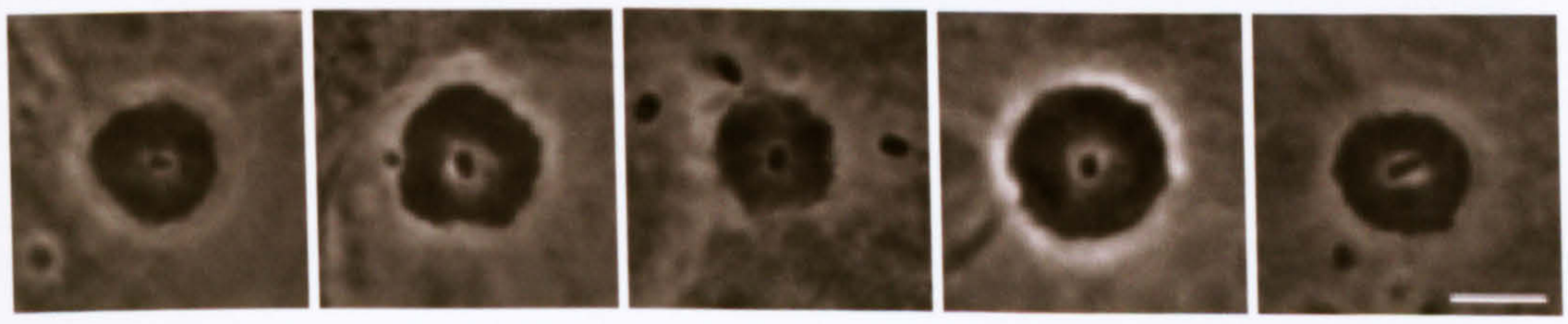

D. 12023

wt

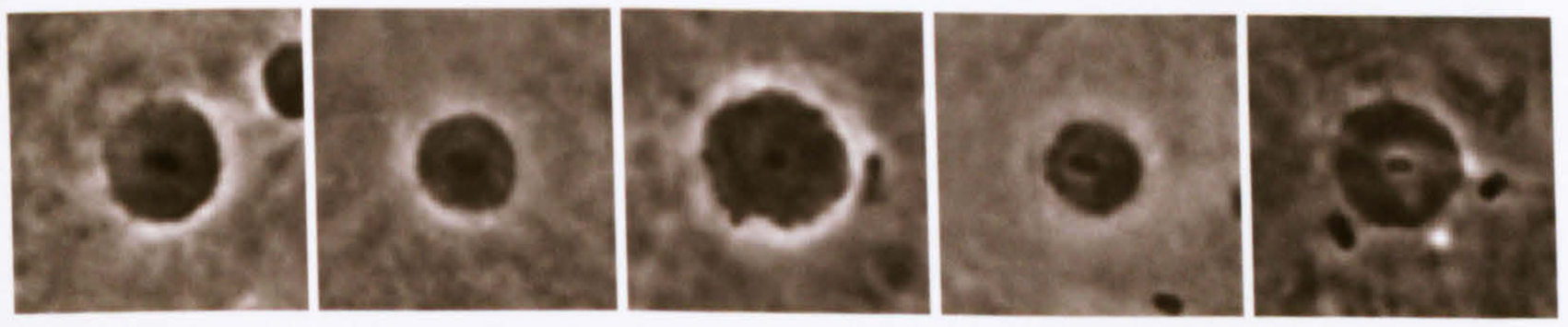

sipA⁻

sipA⁻
pCAP01

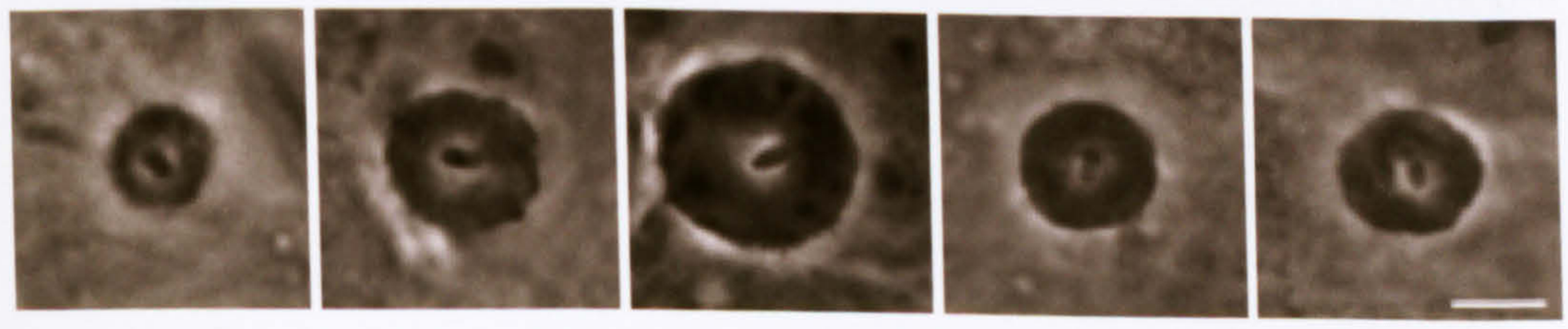

Figure 4.26 Use of time-lapse phase-contrast microscopy to examine membrane ruffle propagation and development. Phase-contrast images of the time course of a representative membrane ruffle generated in MDCK epithelial cells by *S.* Typhimurium SL1344 wild type (A) and its isogenic *sipA*⁻ (B) and *sipA*⁻ *sopE*⁻ (C) mutants is shown. Images were captured at 10 second intervals. Timestamps on each image indicate relative time compared to the first image in which this bacterium attached to cells (0s). Scale bar, 5μm. These images are derived from movies presented in Appendix III.

A. SL1344 wild type

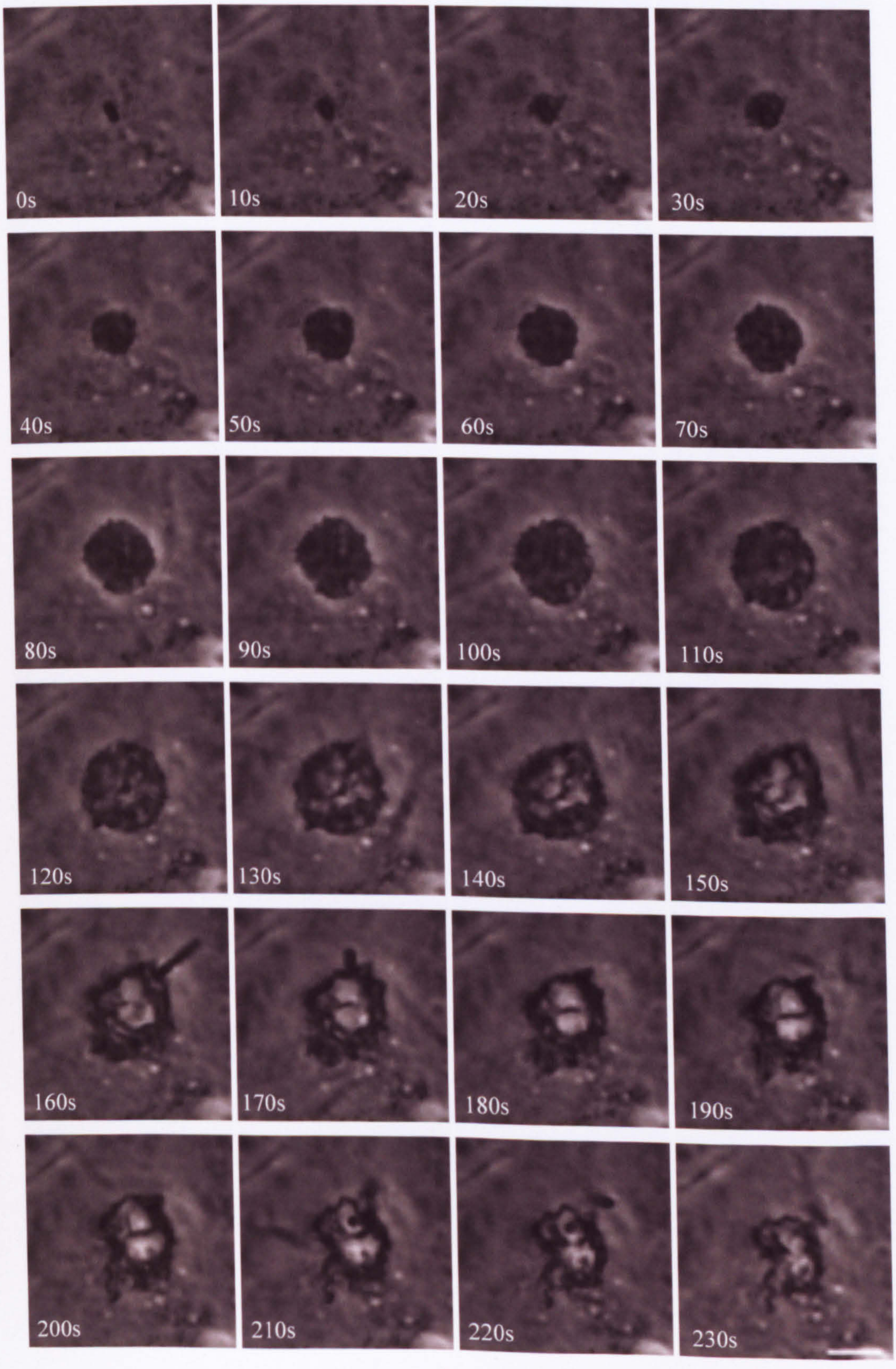

B. SL1344 *sipA*$^{-}$

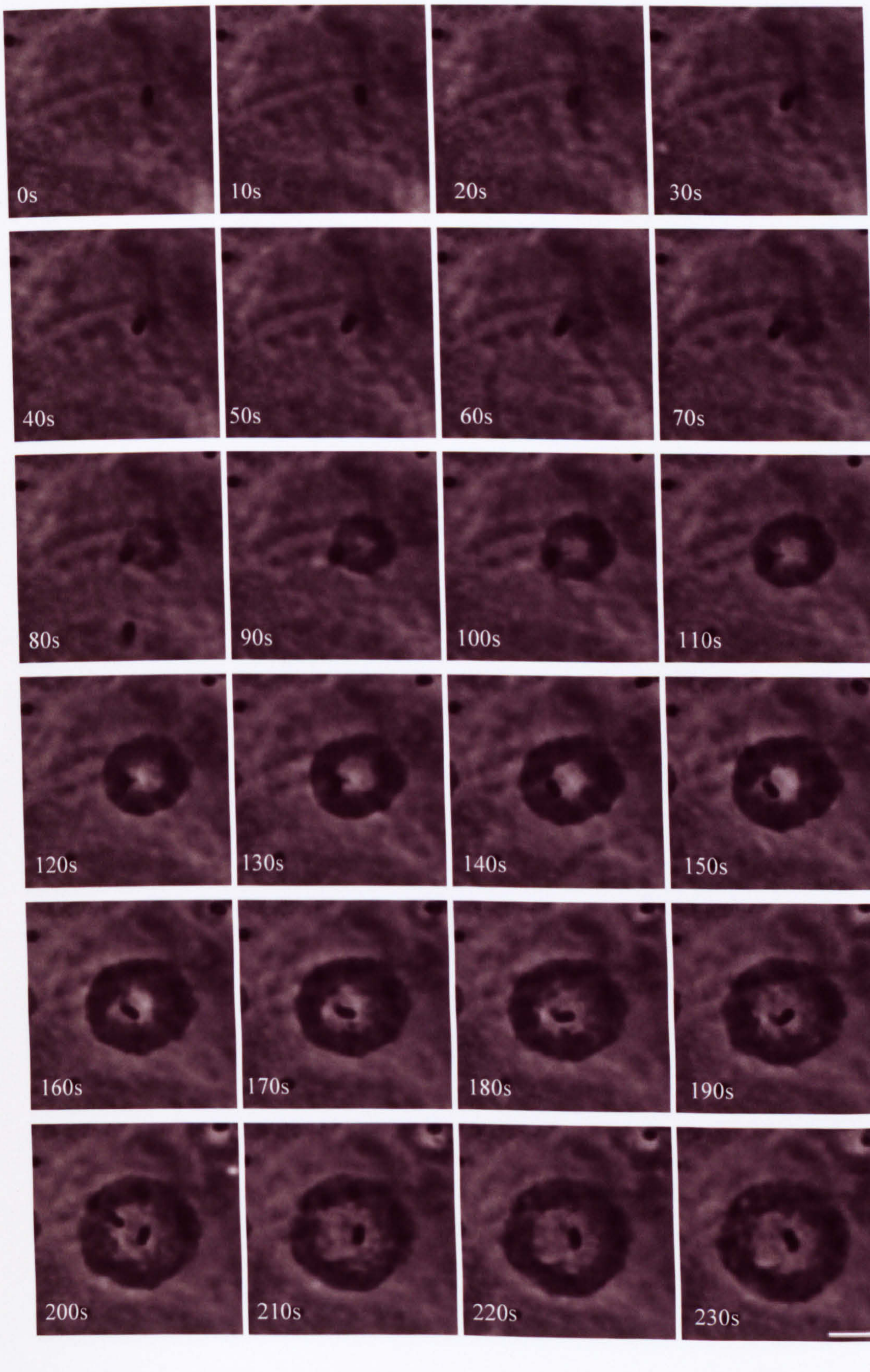

C. SL1344 *sipA*⁻ *sopE*⁻

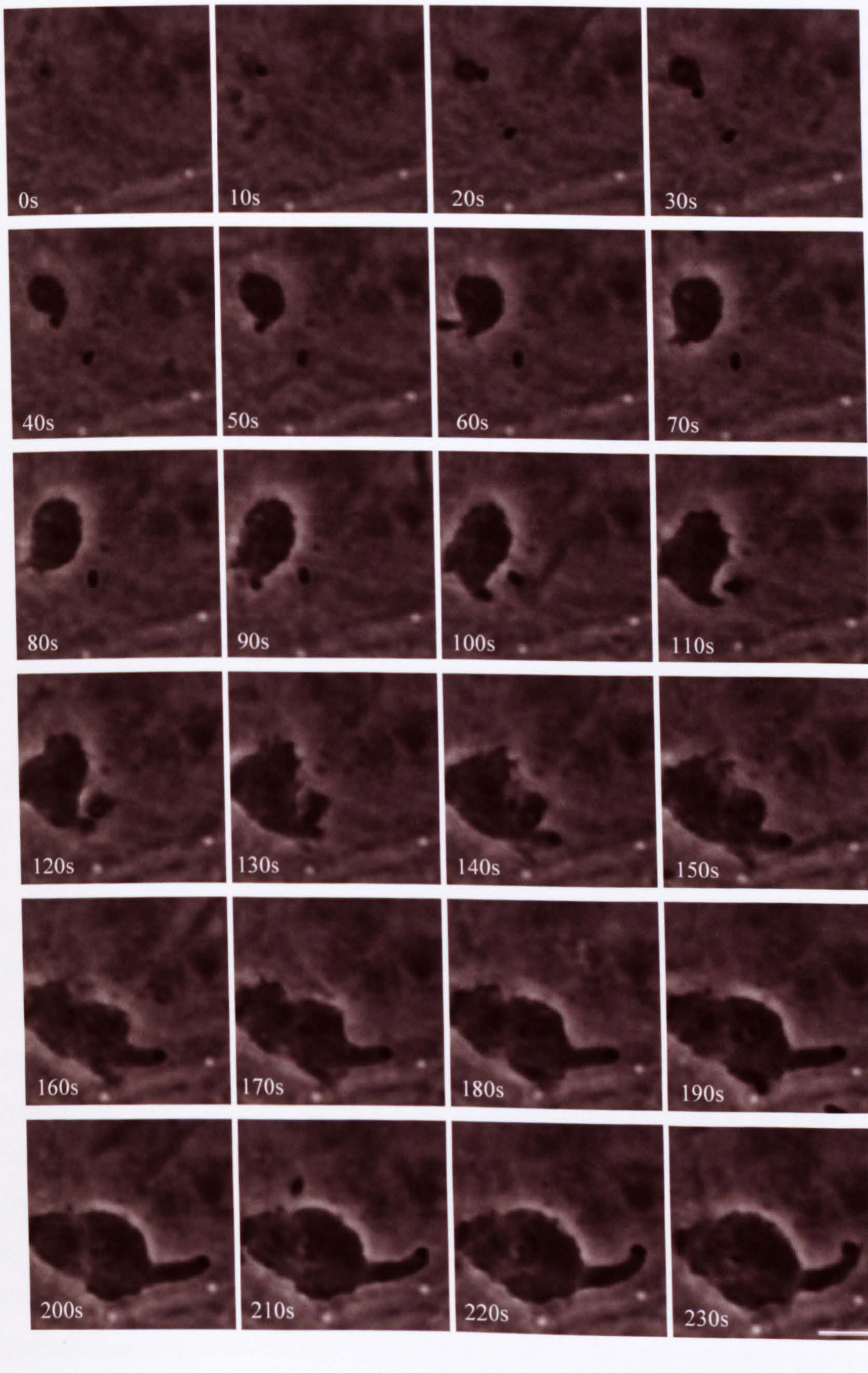

The events leading to the uptake of wild type bacteria by cells are identical to those of the majority of SL1344 and S1579/94 *sipA*⁻ bacteria. However, a small number of these bacteria (~10%) do not have a smooth transition into the host cell. As shown by the arrows in Figure 4.25A and B, some of the *sipA*⁻ bacteria are not in the centre of the ruffle, but are found at the edge. Figure 4.25B shows this appears to occur by the ruffle being initiated at one side of the bacterium, rather than around the entire bacterium as in the wild type. This leads to the *sipA*⁻ bacterium being pushed away from the original ruffle initiation point. Although the bacterium becomes located at the periphery of the ruffle, it can move back towards the centre (shown in frames 120 seconds to 170 seconds) where it is then possible for the bacterium to enter the cell (not shown). This behaviour repeats the observations reported by Jepson *et al.* (2001), and provides one explanation as to why at early time points these mutants have a reduced rate of invasion compared to the wild type, without the number of ruffles induced being affected. The behaviour of the mutant also highlights two key points. First the bacterium can perceive its location in relation to the ruffle, and secondly the central part of the ruffle is vital for the bacterium to enter the cell. How the bacterium realises it is not in the correct part of the ruffle for uptake is not clear, nor is it known how it is possible for it to move towards the centre. Perhaps inherent properties of the membrane, such as the presence of particular receptors or concentrations of specific lipids or proteins in the bilayer, drive the bacterium to be situated in the centre of the ruffle. The movement of the host cell membrane during ruffling may also help to move a bacterium towards the centre, and possibly also maintain it within this region.

The use of pCAP01 to complement the SL1344 and S1579/94 *sipA*⁻ mutants restores the wild type ruffling behaviour, indicating loss of SipA is the reason for this disruption in ruffling. Loss of SopE from SL1344 and S1579/94 did not appear to change the ruffling phenotype from that of the wild type, as is indicated by the ruffling behaviour of the F98 and 12023 wild types, which lack SopE. However, again it was noted that the ruffles of the SL1344 and S1579/94 *sopE*⁻ mutant appeared to be smaller than those of the wild type, an observation that had previously been made when examining ruffles using CLSM (Figure 4.15 and 4.20). The movies produced with time-lapse imaging provided the opportunity

to quantify this observation, since the maximum diameter achieved by each ruffle could be monitored, allowing a more accurate determination of average ruffle diameter. This is in comparison with CLSM experiments which provide a snap shot of ruffles at one particular time-point, and therefore ruffles at all stages of propagation.

Table 4.4 The absence of SopE affects the size of the ruffle induced. 30 randomly selected ruffles from phase-contrast time-lapse movies from three independent experiments were analysed for the maximum diameter they achieved. Data represents the means ± standard error of the mean. Asterisk denotes a significant difference when compared to SL1344 or S1579/94 wild type using a one-way ANOVA with Tukey post-test at the level of $P<0.05$.

	SL1344 wt	SL1344*sopE*⁻	S1579/94 wt	F98 wt	12023 wt
Mean diameter of ruffle (μm)	8.38 ± 0.378	* 5.97 ± 0.086	8.55 ± 0.703	* 6.17 ± 0.365	* 5.99 ± 0.283

The diameter of the ruffles induced by the wild types of F98 and 12023, which naturally lack SopE, is approximately 6μm which is significantly smaller than the ruffles induced by the SL1344 and S1579/94 wild types, which possess SopE (Table 4.4). From movies taken alongside those of all the wild types, the SL1344 *sopE*⁻ mutant was also shown to produce ruffles with a significantly smaller average diameter ($P<0.01$). This observation was subsequently replicated in S1579/94, where the *sopE*⁻ mutant produced ruffles with an average diameter of 5.71 ± 0.11μm, significantly smaller ($P=0.007$) than the average ruffle diameter of the wild type (7.87 ± 0.385μm). Thus, SopE does appear to affect ruffle size.

When *sipA* is deleted from a *sopE*⁻ strain i.e. F98 and 12023 wild types, and SL1344 and S1579/94 *sopE*⁻ mutants, wild type-like ruffles are seen but also the ruffles with dramatic changes to their morphology, as was revealed by CLSM and SEM. The time course stills of the SL1344 *sipA*⁻ *sopE*⁻ mutant (Figure 4.26C) shows how these finger-like protrusions are formed. Like the SL1344 or S1579/94 *sipA*⁻ mutants, the *sipA*⁻ *sopE*⁻ bacterium appears to initiate a ruffle at the side of the bacterium rather than around its whole periphery, and

consequentially the ruffle as it forms pushes the bacterium away from the centre. However, in the *sipA*⁻ *sopE*⁻ bacteria it appears the adherence of the host membrane to one site on the bacterial cell surface leads to the ruffle forming directly adjacent to the bacterium, and as the ruffle extends it pushes the bacterium out and away from the focus of the ruffle, producing a protrusion with the bacterium attached to the end. It appears that if the bacterium is associated with the host cell membrane at one of its poles then a finger-like protrusion is obtained, but if the attachment is along the length of the bacterium, a pedestal-like protrusion is observed. Both protrusions are dynamic, and have the ability to push the bacterium across the cell surface. On occasion when the protrusion leads the bacterium to come into contact with the cell surface, the bacteria is seen to detach and may then stimulate another ruffle or finger-like protrusion, which again may allow the bacterium to transverse further across the cell monolayer.

When the bacterium is attached to the ruffle protrusion and moved away from the centre of the ruffle it can not be taken up by the cell and explains why the invasion of the *sipA*⁻ *sopE*⁻ mutants is lower than the wild type. Why there may not be an additional invasion defect compared to the *sipA*⁻ mutant (Figure 4.19), considering it takes much longer for the *sipA*⁻ *sopE*⁻ mutant to reach the centre of a ruffle, is likely to be due to the fact that other bacteria may use the original ruffle centre to enter the cell (Francis *et al.*, 1992; Pattni *et al.*, 2001). pCAP01 and to a certain extent pCAP03 can restore the mutant to only producing wild type-like ruffles, indicating the absence of both effector proteins leads to the change in ruffle morphology. It is assumed that either lack of stimulation of certain cell signalling pathways or the loss of regulation of signalling cascades by these two proteins leads to the change in ruffle morphology, but is an area that requires further investigation.

To illustrate better, that loss of SipA with or without SopE leads to movement of the bacterium away from the centre of the ruffle, tracking software was used to monitor the location of a bacterium from when it adhered to the cell surface and induced a ruffle to its subsequent internalisation (Figure 4.27).

Figure 4.27 Use of tracking software to show how the positioning of the bacterium in relation to the ruffle it has induced is affected by loss of effector proteins. Volocity 4.0 software was used to mark the positions of ~20 bacteria in the chosen field of view in each 10 second frame of a 15 minute time course. The triangle represents the initial position of the bacterium, and each subsequent position is marked with a dot. Scale bar 10μm.

A. SL1344 wt

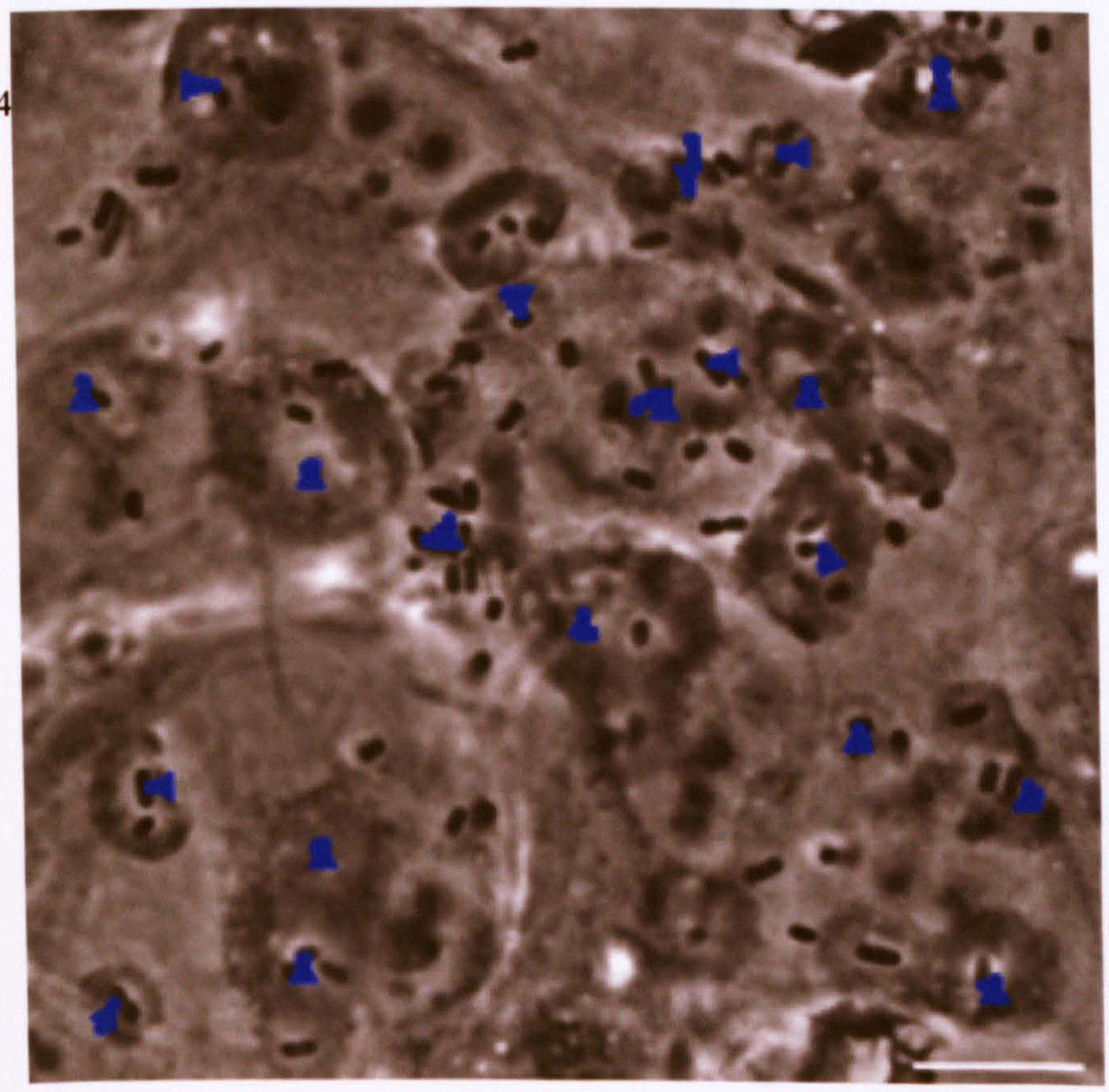

B. SL1344 *sipA*$^{-}$

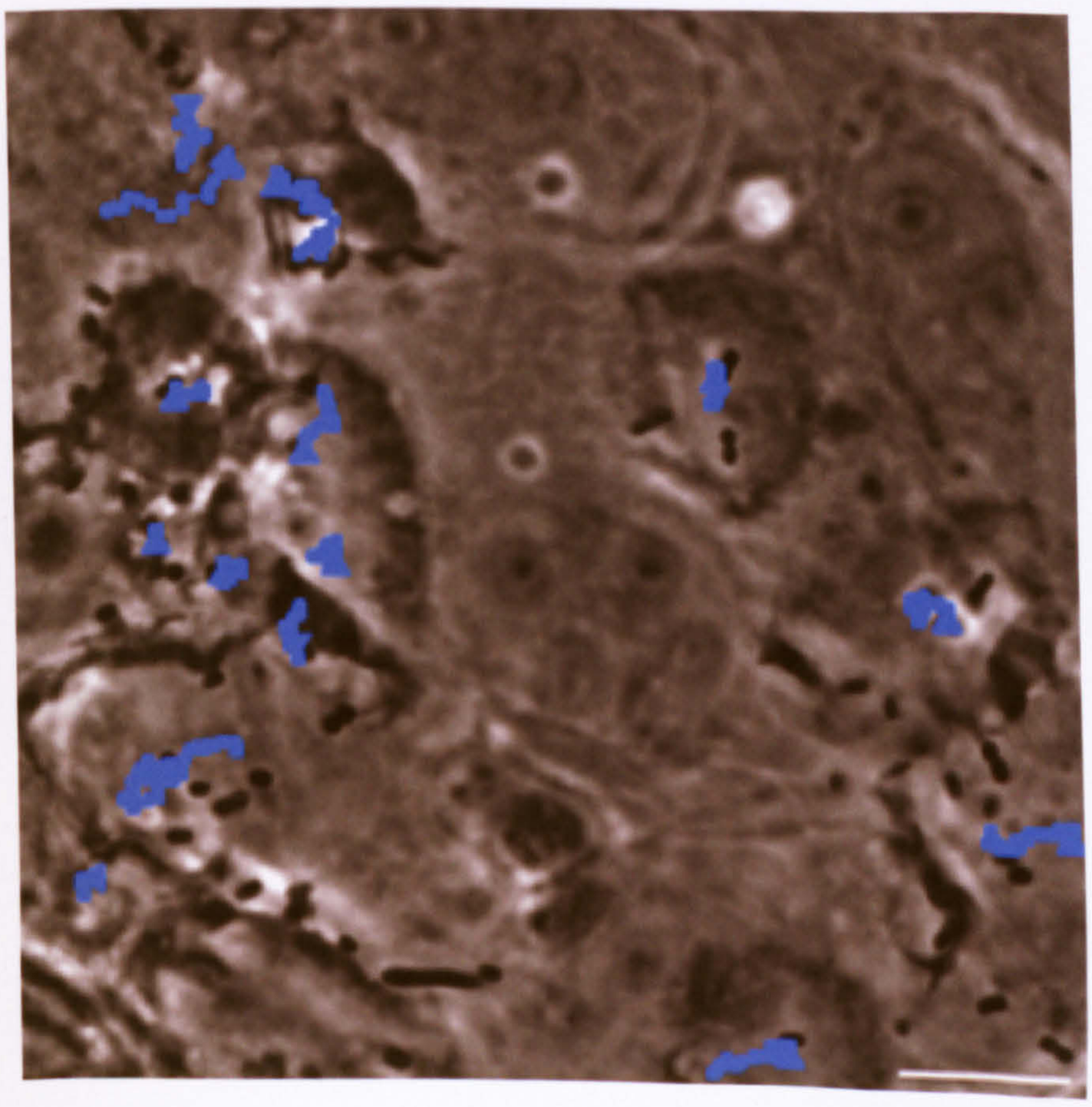

C. SL1344 *sopE*⁻

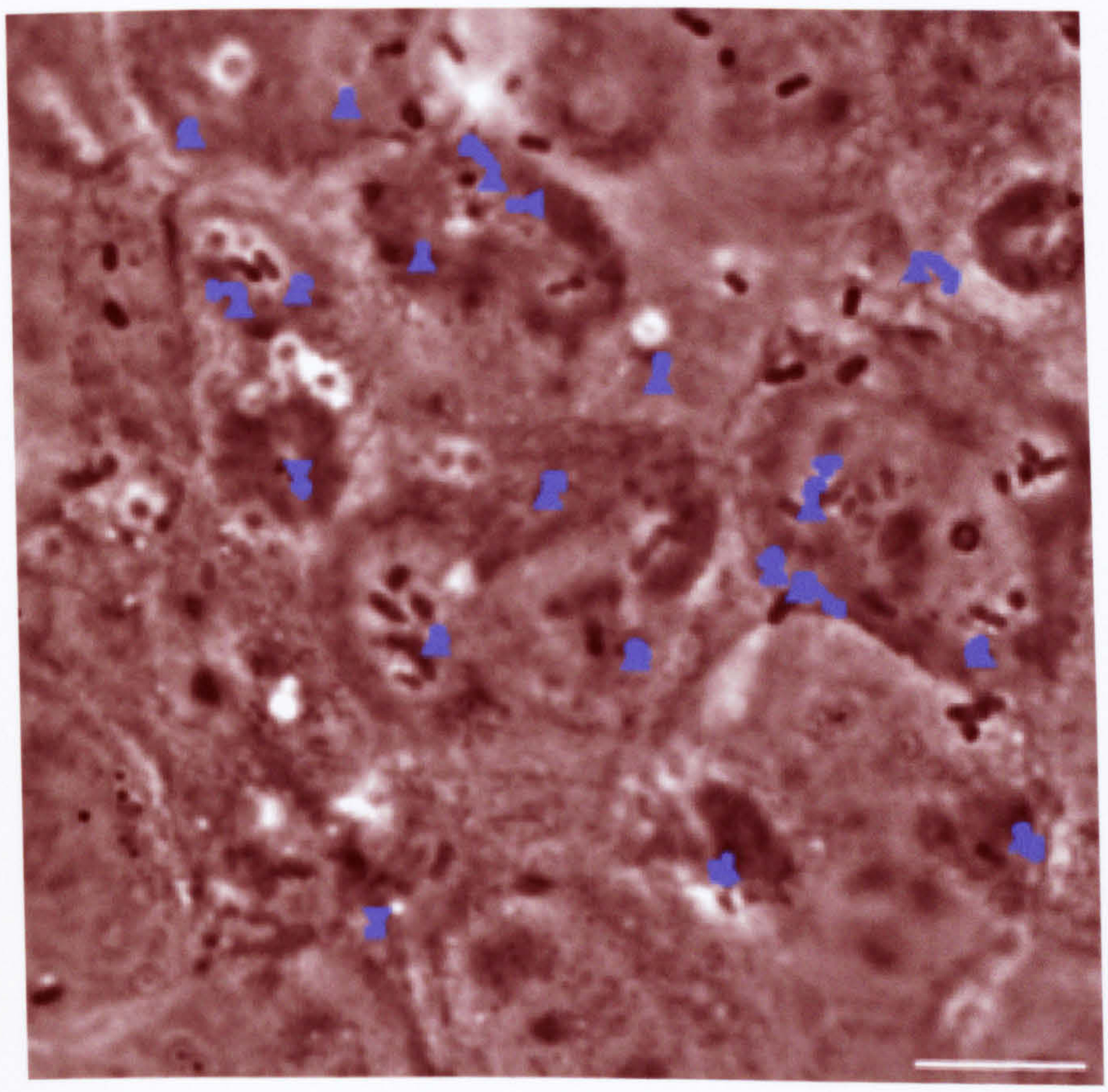

D. SL1344 *sipA*⁻ pCAP01

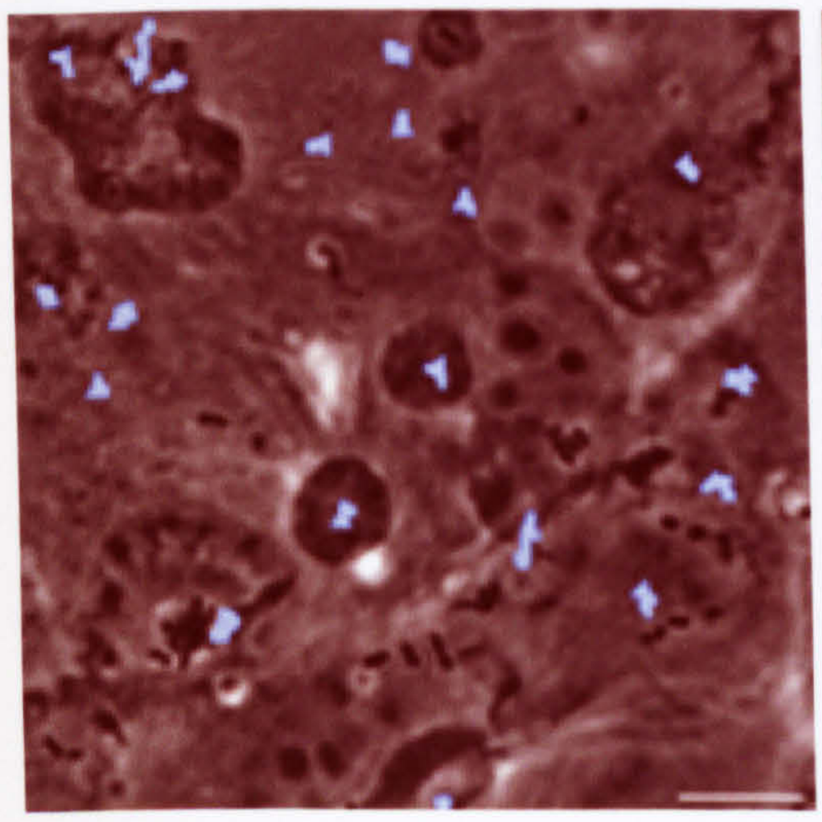

E. SL1344 *sopE*⁻ pCAP03

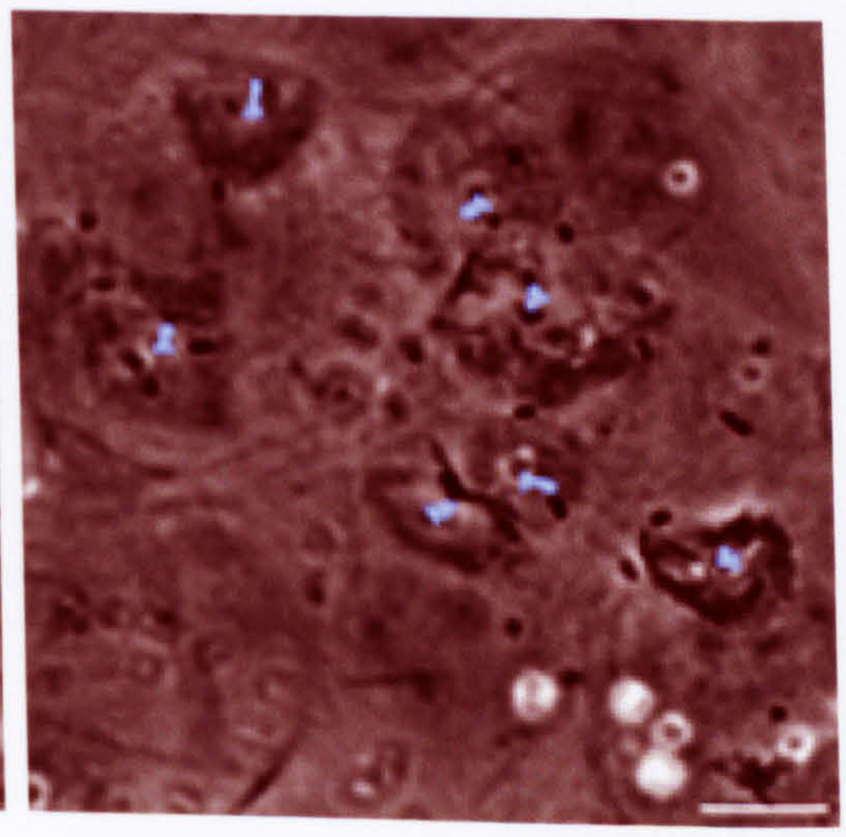

F. SL1344 *sipA*⁻ *sopE*⁻

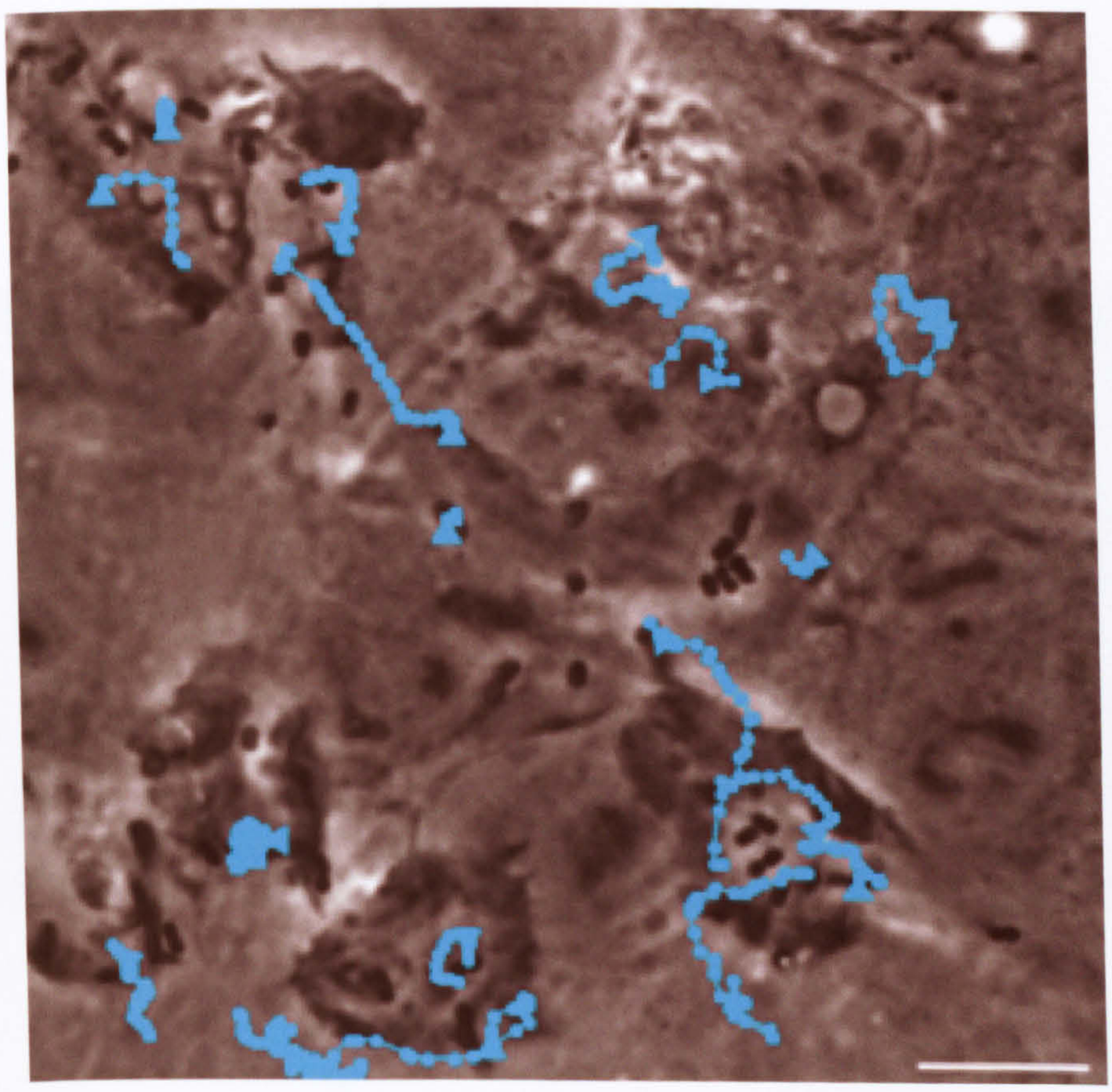

G. SL1344 *sipA*⁻ *sopE*⁻ pCAP01

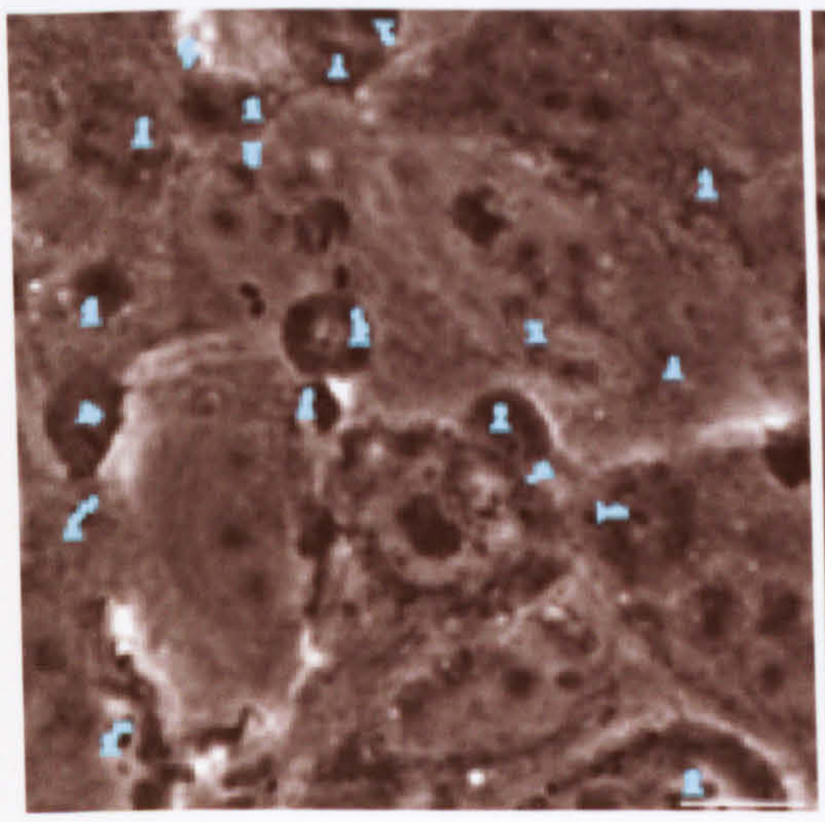

H. SL1344 *sipA*⁻ *sopE*⁻ pCAP03

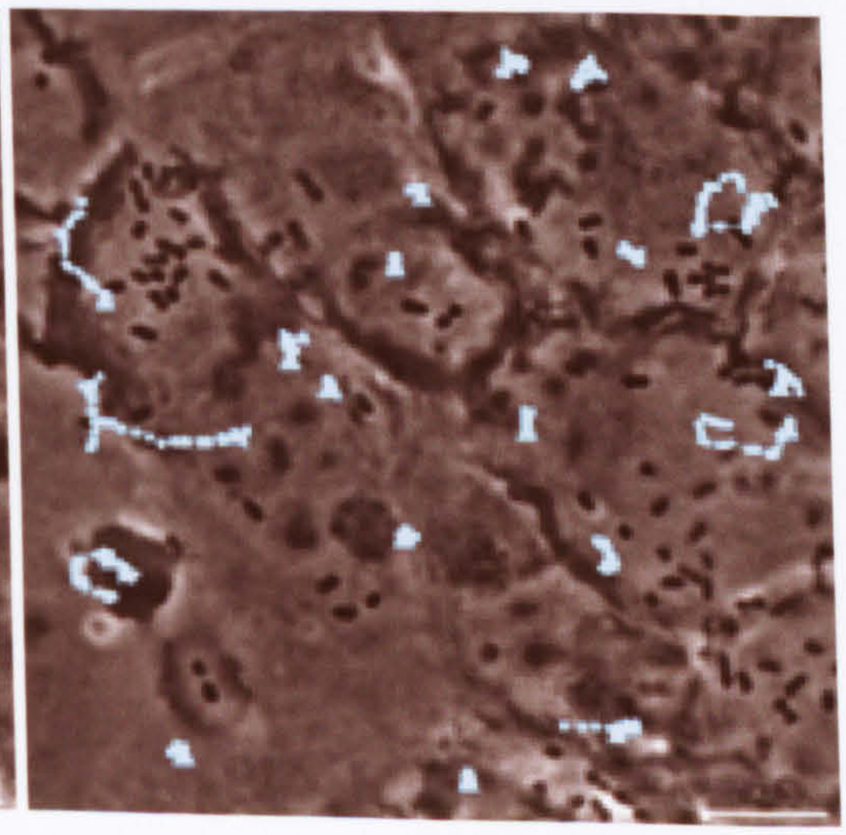

I. S1579/94 wild type

J. S1579/94 *sipA*$^-$

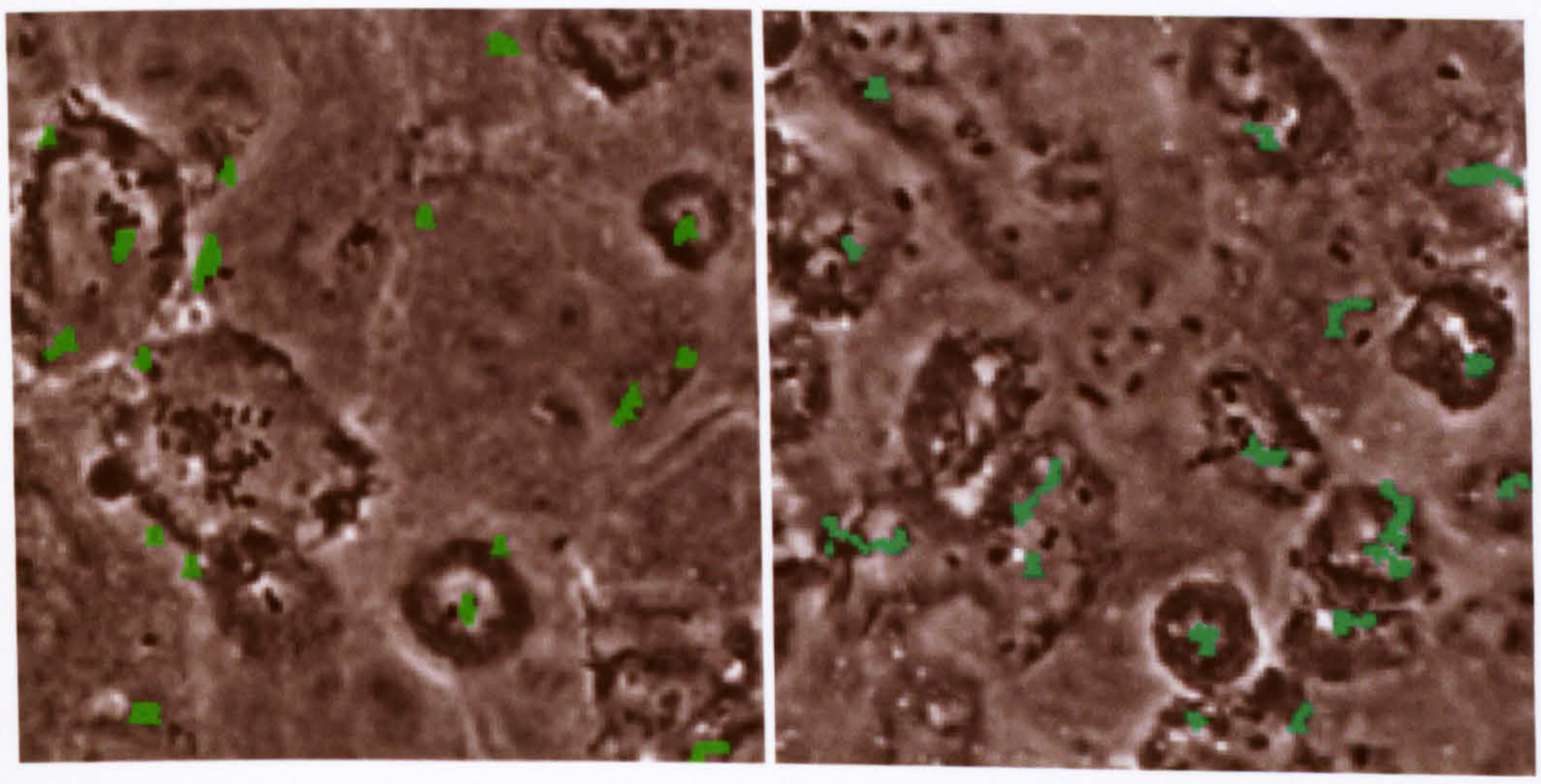

K. S1579/94 *sopE*$^-$

L. S1579/94 *sipA*$^-$ *sopE*$^-$

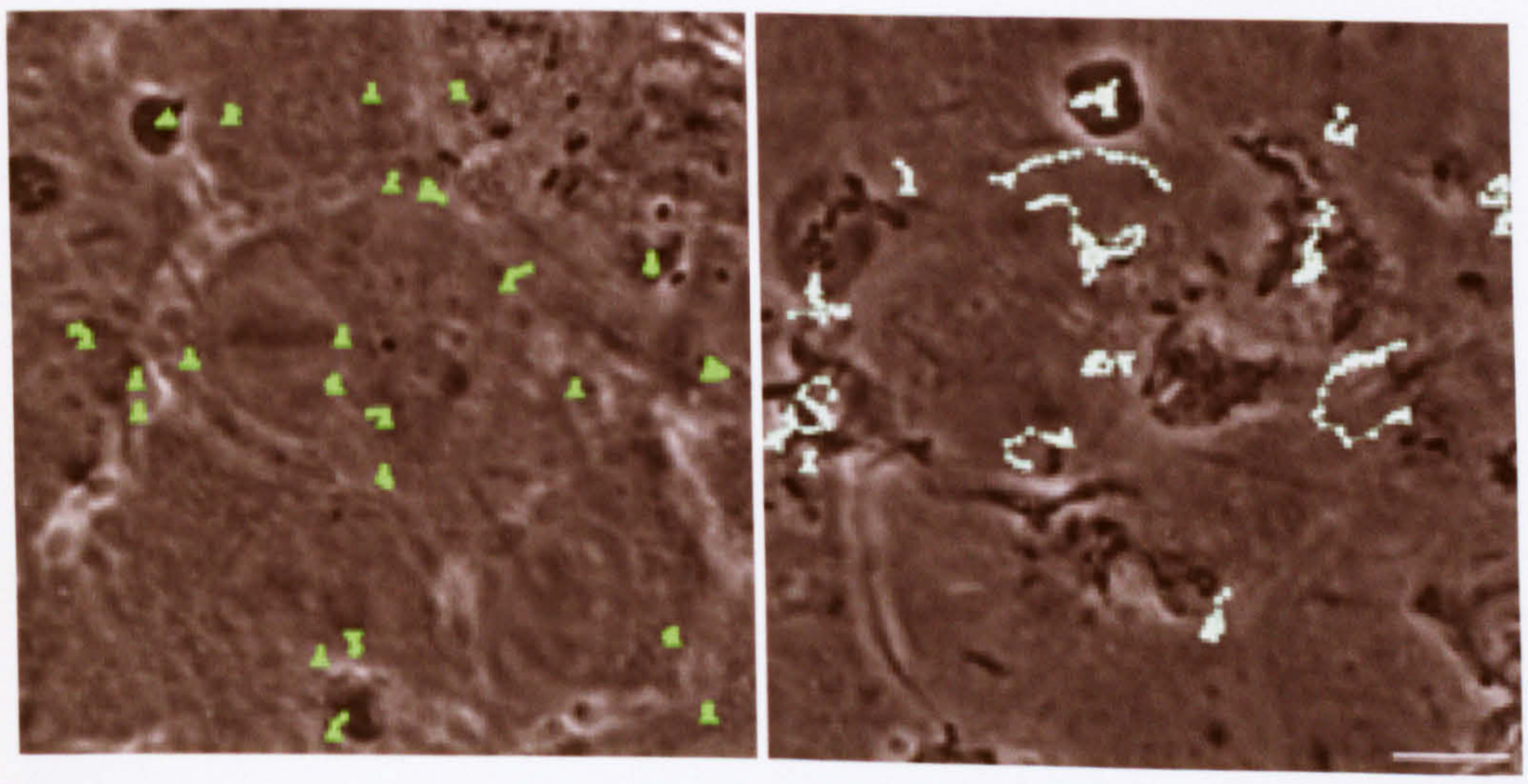

M. F98 wild type

N. F98 *sipA*$^-$

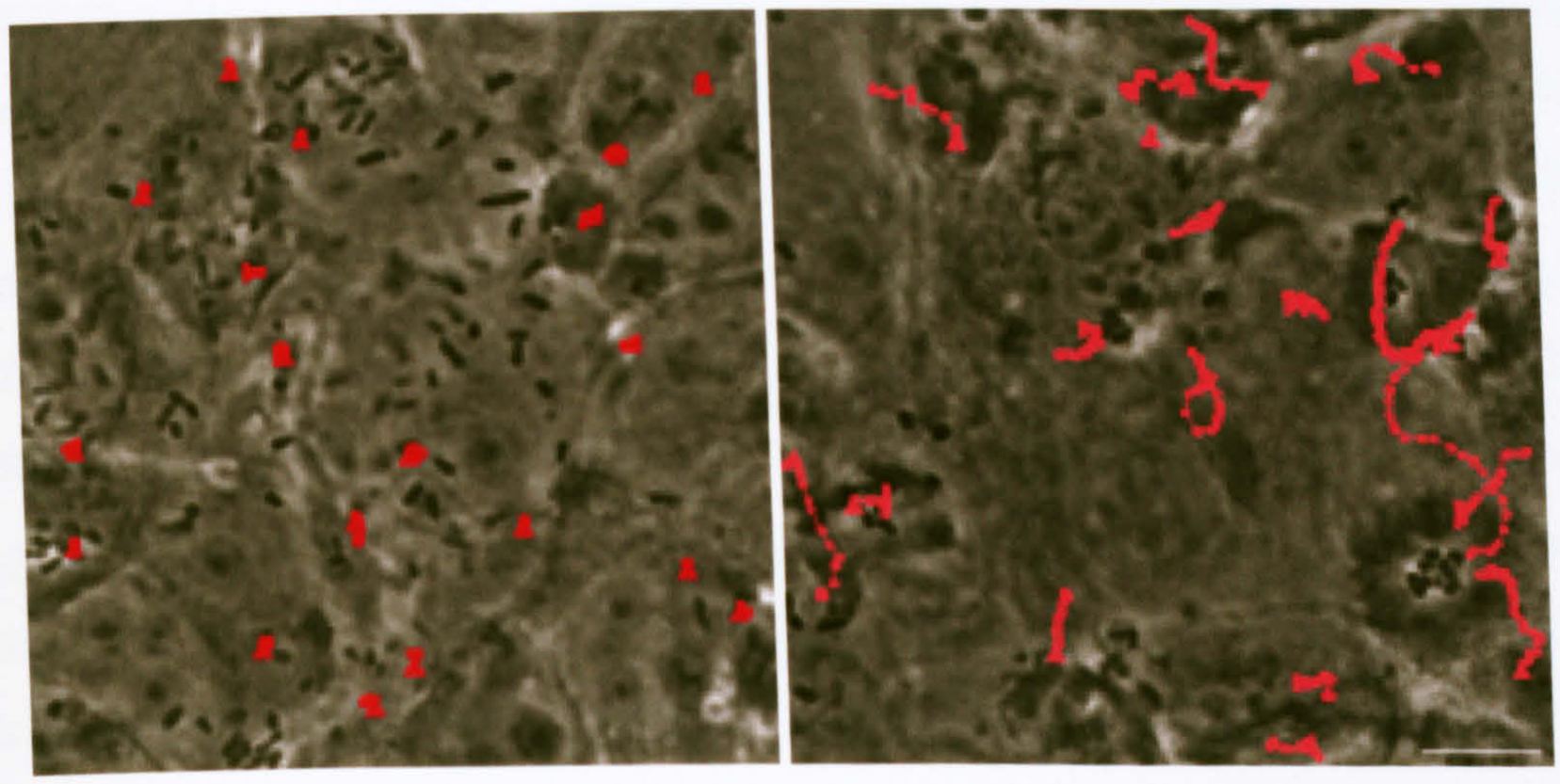

O. 12023 wild type

P. 12023 *sipA*$^-$

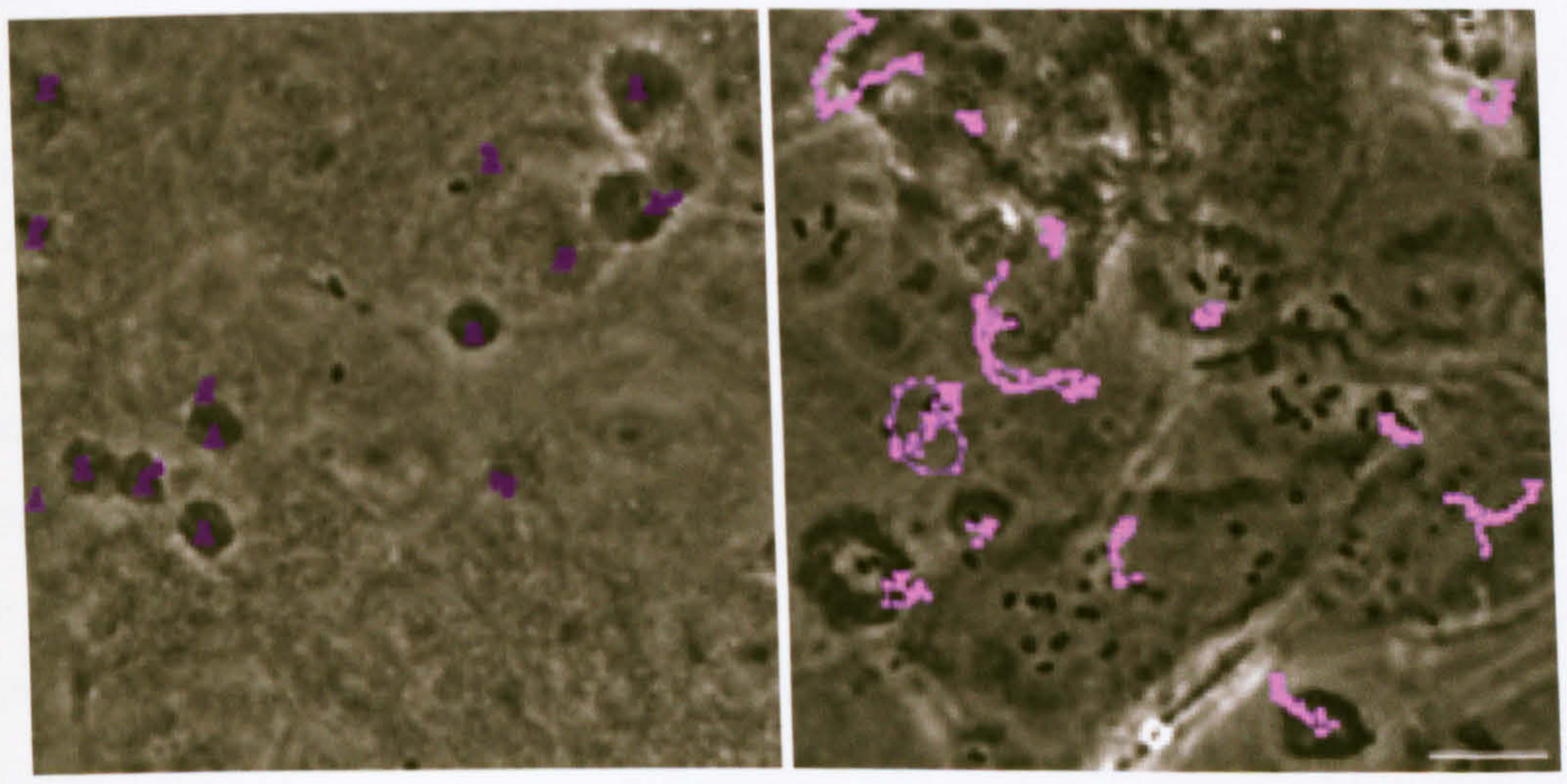

Since the position of SL1344 wild type bacteria (Figure 4.27A) in many of the movie frames does not change, when all the points are collated many overlap and this produces either a dot or a very short path on the cell surface. Thus, it is clear the position of wild type bacteria changes relatively little during the initiation and propagation of the ruffle. When the paths produced by the SL1344 *sipA*⁻ mutant (Figure 4.27B) are examined, it is found there are very few occasions when all the points overlap to produce a single dot. Instead paths are produced showing a small amount of movement by the bacterium away from the initial starting site, with a few slightly longer paths also being recorded. It was also noted while doing this analysis that those *sipA*⁻ bacteria that moved back to the central region of the ruffle often did not remain still in this area but continuously shifted position. This increased amount of movement in relation to wild type bacteria suggests that loss of SipA may somehow compromise the ability of the bacteria to maintain their position on the cell surface. SipA being the cause of this effect was proved by the ability of pCAP01, carrying the *sipA* gene, to restore the pattern back to one indicative of the wild type.

A loss of SopE from SL1344 and S1579/94 (Figure 4.27C and K respectively) has no effect on the positioning of the bacterium, with either no movement or very short paths being observed, just as had been described above for SL1344 wild type (Figure 4.27A).

When *sipA* and *sopE* are deleted from SL1344 (Figure 4.27F), there is a clear change in the behaviour of the bacteria with an increasing amount of movement being detected, characterised by longer path lengths. This shows that while the loss of SipA destabilises the interaction of the bacterium with the host cell membrane, allowing bacterial movement out from the ruffle centre, the additional loss of SopE further deteriorates the stability, allowing the bacterium to be moved much larger distances from the ruffle centre. The role of SipA and SopE in this behaviour is demonstrated by the ability of plasmids carrying these genes to restore a wild type pattern of movement, although it should be noted that in the presence of pCAP03, there are still a number of bacteria which exhibit movement characteristic of the *sipA*⁻ *sopE*⁻ mutant.

S. Typhimurium S1579/94, F98 and 12023 were also tracked (Figure 4.27). The phenotypes described for SL1344 were replicated in these strains, with wild type having very limited movement during the course of ruffle propagation, while the *sipA*⁻ *sopE*⁻ mutant showed a great deal of movement away from the ruffle focus. Thus, it would appear loss of SipA or SipA and SopE together causes a reduction in *Salmonella* invasion by increasing the proportion of bacteria that leave the centre of the ruffle, thereby increasing the time in which it takes to enter the cell, explaining why the effect is more severe at early time points. The change in morphology of the *sipA*⁻ *sopE*⁻ ruffles i.e. the production of the finger-like protrusions as a consequence of the loss of these effectors appears to be responsible for the movement of the bacterium from the ruffle centre and the subsequent decreased invasion.

While it was obvious from CLSM, SEM and time-lapse imaging that ruffle morphology and the size of the ruffles induced by *Salmonella* were affected by the presence or absence of specific effectors, and this could then be quantified by various counts, it was unknown whether SipA and SopE may have subtler effects on the kinetics of ruffle formation. Therefore, time-lapse images were used to study whether the kinetics of ruffle induction may be affected (Table 4.5 and 4.6).

When the wild type of each *S.* Typhimurium strain is compared it is found that the two strains lacking SopE, that is F98 and 12023, take significantly longer in inducing ruffle formation after adherence than both the SL1344 and S1579/94 wild types ($P<0.001$) (Table 4.5). This observation was repeated when comparing SL1344 wild type and its isogenic *sopE*⁻ mutant; *sopE*⁻ is significantly slower in its ability to form a ruffle after adherence compared to the wild type ($P<0.001$), and this defect can be restored by complementation with pCAP03 (Table 4.6). This indicates that not only does SopE play a role in determining the size of the ruffle but it also plays a part in determining the speed at which the ruffle is formed. This may fit with the role of SopE in activating signalling pathways required for stimulating actin polymerisation (Hardt *et al.*, 1998a; Zhou *et al.*, 2001; Patel and Galan, 2006).

Table 4.5 Comparisons of the time taken for membrane ruffle initiation after bacterial adherence. The time interval between bacterial binding to MDCK cells and induction of membrane ruffling was obtained from phase-contrast video microscopy. Data expressed as medians with the number of productive bacterial-cell interactions analysed (n), and the minimum (min.) and maximum (max.) time intervals measured. * denote a significant difference between a wild type and its isogenic *sipA*⁻ or *sipA*⁻ pCAP01, § denotes a significant difference compared to SL1344 wild type or S1579/94 wild type. Statistical differences were assessed by the Kruskal Wallis test; followed by Dunn's Multiple Comparison Test at a level of $P<0.05$.

		SL1344			S1579/94			F98			12023		
		Wild type	*sipA*⁻	*sipA*⁻ pCAP01	Wild type	*sipA*⁻	*sipA*⁻ pCAP01	Wild type	*sipA*⁻	*sipA*⁻ pCAP01	Wild type	*sipA*⁻	*sipA*⁻ pCAP01
	n	90	90	90	90	90	90	90	90	90	90	90	90
Ruffle induction time after adherence (s)	**Median**	**40**	**30**	**30**	**40**	**40**	**50**	**60§**	**50***	**30***	**70§**	**30***	**40***
	Min.	10	10	10	10	10	10	20	20	10	10	10	10
	Max.	290	480	380	310	280	210	270	180	90	320	140	130

Table 4.6 Comparisons of the time taken for membrane ruffle initiation after bacterial adherence for S. Typhimurium SL1344 wild type and its isogenic mutants. The time interval between bacterial binding to MDCK cells and induction of membrane ruffling was obtained from phase-contrast video microscopy. Data expressed as medians with the number of productive bacterial-cell interactions analysed (n), and the minimum (min.) and maximum (max.) time intervals measured. Asterisk denotes a significant difference from wild type. Statistical differences were assessed by the Kruskal Wallis test; followed by Dunn's Multiple Comparison Test at a level of $P<0.05$.

		SL1344							
		Wild type	*sipA*⁻	*sipA*⁻ pCAP01	*sopE*⁻	*sopE*⁻ pCAP03	*sipA*⁻ *sopE*⁻	*sipA*⁻ *sopE*⁻ pCAP01	*sipA*⁻ *sopE*⁻ pCAP03
Ruffle induction time after adherence (s)	n	90	90	90	90	90	90	90	60
	Median	**40**	**30**	**30**	**65***	**40**	**40**	**40**	**30**
	Min.	10	10	10	10	10	10	20	10
	Max.	290	480	380	330	270	140	210	100

In SL1344 and S1579/94, the wild type, *sipA*⁻ mutant and transcomplemented mutant do not differ from each other in the time it takes to induce a ruffle after adherence to the cell surface (Table 4.5 and 4.6). SipA having no affect on how quickly a ruffle is created would fit with its role managing and directing the actin polymerisation that has been stimulated by other effector molecules, rather than having a direct role in stimulating actin polymerisation. When F98 wild type, *sipA*⁻ and *sipA*⁻ pCAP01 are compared, a statistical difference is found between wild type and both *sipA*⁻ and *sipA*⁻ pCAP01, since the latter both take less time to produce a ruffle than wild type. The same trend is observed for 12023, and when SL1344 *sopE*⁻ is compared to SL1344 *sipA*⁻ *sopE*⁻ (Table 1.5). It is unclear why deletion of *sipA* from a *sopE*⁻ strain should produce a faster ruffle induction time. Since pCAP01 fails to return the ruffle induction time to wild type levels this may indicate it is not related to loss of SipA but is related to some other property of the strain.

The various types of microscopy that have been used in this study have shown that absence of SipA leads to reduced invasion of *Salmonella*, at early time points in all four strains of *S.* Typhimurium examined. Since the ruffle induction time is not affected, and the number of ruffles induced remains the same as wild type, this phenotype is likely to be the consequence of *sipA*⁻ mutants on some occasions being detached from the centre of the ruffle they have induced and pushed to its periphery, so that by the time they have moved back to the centre of the ruffle for invasion it takes a greater time for them to enter the host cell from the time of ruffle induction. The loss of SipA in a SopE⁻ background leads to a greater movement of the bacterium away from the centre of the ruffle due to a dramatic change in ruffle morphology that is characterised by increased numbers of filopodia and production of protrusions responsible for pushing the bacteria outside the zone of ruffling. In SL1344, S1579/94 and F98 this leads to a reduction in invasion, illustrating the importance of both SipA and SopE in invasion.

4.3.12. Examining the effects of loss of SipA and/or SopE from *Salmonella* on polarised MDCK II epithelial barrier integrity

Transepithelial electrical resistance (TER) serves as an instantaneous measure of the integrity of an epithelial layer and particularly the permeability of tight junctions. Infection of polarised cultured cell monolayers with *Salmonella* elicits a decrease in TER and disrupts the architecture of intercellular junctions (Finlay *et al.*, 1988; Finlay and Falkow, 1990; Jepson *et al.*, 1995; Jepson *et al.*, 2000). This behaviour is TTSS-1 dependent (Jepson *et al.*, 1996; Tafazoli *et al.*, 2003) with SopE, SopE2, SopB, and SipA all being implicated in the disruption of epithelial monolayer integrity (Raffatellu *et al.*, 2005; Boyle *et al.*, 2006). However, the roles of these effector proteins on tight junctions and monolayer integrity have only been examined after prolonged infection e.g. one to four hours after initiation of infection (Raffatellu *et al.*, 2005; Boyle *et al.*, 2006). Since it was previously shown that changes in TER and the F-actin distribution of MDCK II monolayers occurs as early as 15 minutes post-infection (Jepson *et al.*, 1995; Jepson *et al.*, 1996; Jepson *et al.*, 2000), polarised MDCK II monolayers were challenged with the SL1344 *sipA*$^-$, *sopE*$^-$ and *sipA*$^-$ *sopE*$^-$ mutants and examined 15 and 60 minutes after infection to determine whether SipA and/or SopE are responsible for disruption of monolayer integrity at early time points.

The effects on the barrier function of MDCK II polarised monolayers during *Salmonella* infection was assessed by measuring TER. Over the course of one hour, the TER remained unchanged in uninfected cells (data not shown), but infection with SL1344 wild type caused a 20-30% reduction in TER by 15 minutes, which was reduced by a further 10% 30 minutes post-infection. By 60 minutes TER was reduced to 40% of its initial value (Figure 4.28). The *sipA*$^-$ and *sipA*$^-$ *sopE*$^-$ mutants behaved in a similar manner to the wild type (Figure 4.28A and C), however, the *sopE*$^-$ mutant was observed to reduce TER very slowly, so that by 60 minutes TER was only 15% less than at the start of the experiment. This observation could imply a novel role for SopE in the initial stages of infection; however, there is evidence to suggest otherwise. Firstly, while the reduction in TER caused by *sopE*$^-$ is statistically different to that

induced by wild type at 60 minutes it is not significantly different to the reduction caused by the transcomplemented mutant, *sopE*⁻ pCAP03. Since pCAP03 has so far been able to restore the phenotype of the *sopE*⁻ mutant in the invasion assays conducted, this suggests there may be an alternative reason for the failure of the *sopE*⁻ mutant to reduce TER. Additionally, if absence of SopE does reduce the ability of *S.* Typhimurium to disrupt the barrier function of the epithelial monolayer it would be expected that the *sipA*⁻ *sopE*⁻ mutant would behave in a similar manner since SopE and an additional effector protein are missing. This was not found, the *sipA*⁻ *sopE*⁻ mutant reduced TER to wild type levels. As it has previously been shown that loss of both SopE and SopE2 with either SipA or SopB is required to prevent loss of epithelial barrier function (Boyle *et al.*, 2006), this also suggests the absence of SopE alone can not induce the changes in TER observed. Finally, complementation of *sipA*⁻ *sopE*⁻ with pCAP01 did not produce the same phenotype as the *sopE*⁻ mutant despite *sipA*⁻ *sopE*⁻ pCAP01 effectively having the same genotype as *sopE*⁻, again suggesting SopE alone can not disrupt the monolayer.

Figure 4.28 TER of MDCK II polarised monolayers during infection with *S.* Typhimurium. TER was measured 0, 15, 30 and 60 minutes after the initiation of infection with strain SL1344 wild type or effector mutants: *sipA*⁻ (A), *sopE*⁻ (B) or *sipA*⁻ *sopE*⁻ (C). Results are the mean from three independent experiments ± sem. All strains were compared in the three experiments, thus the wild type is the same in each graph. Asterisk denotes a significant difference from wild type at that time point using a One-way ANOVA followed by a Bonferroni post test at the level of $P<0.05$.

A

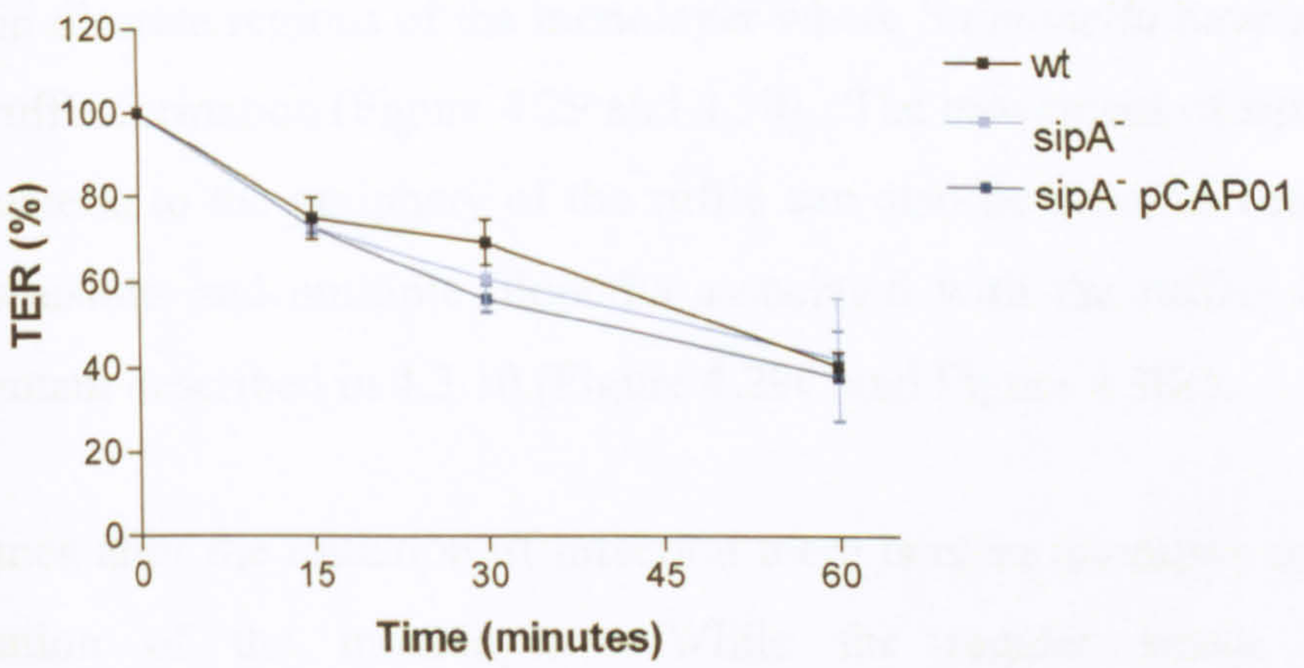

B

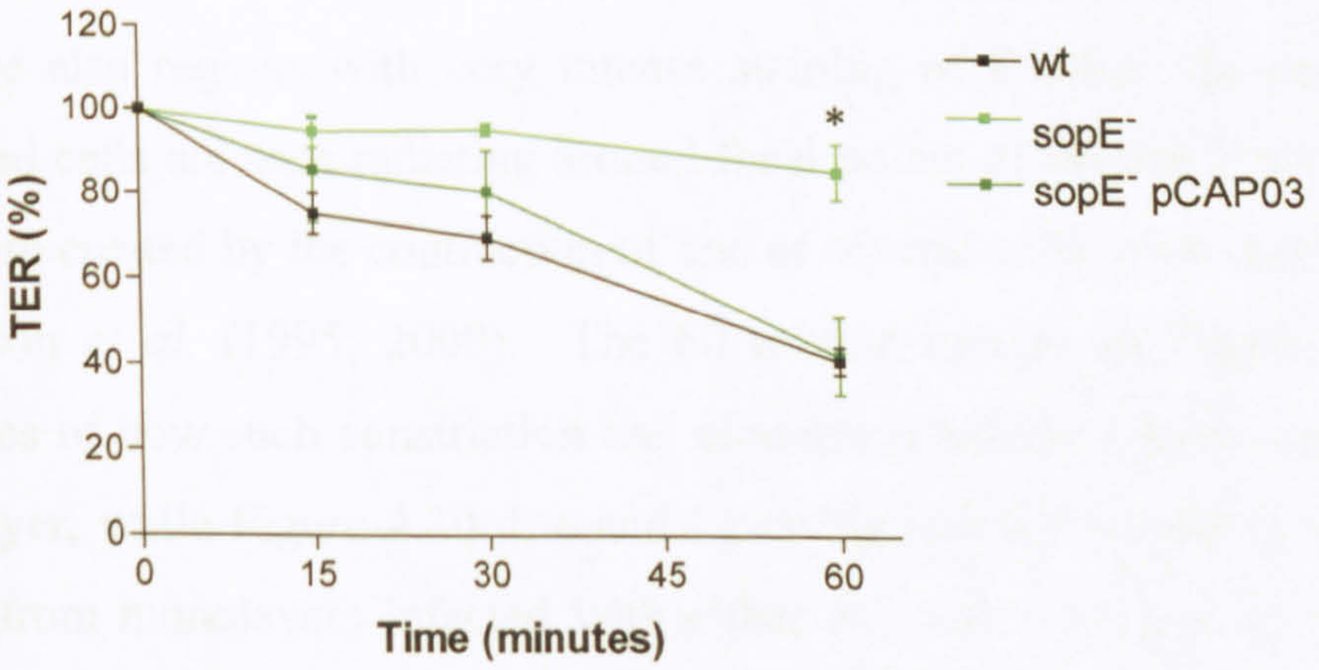

C

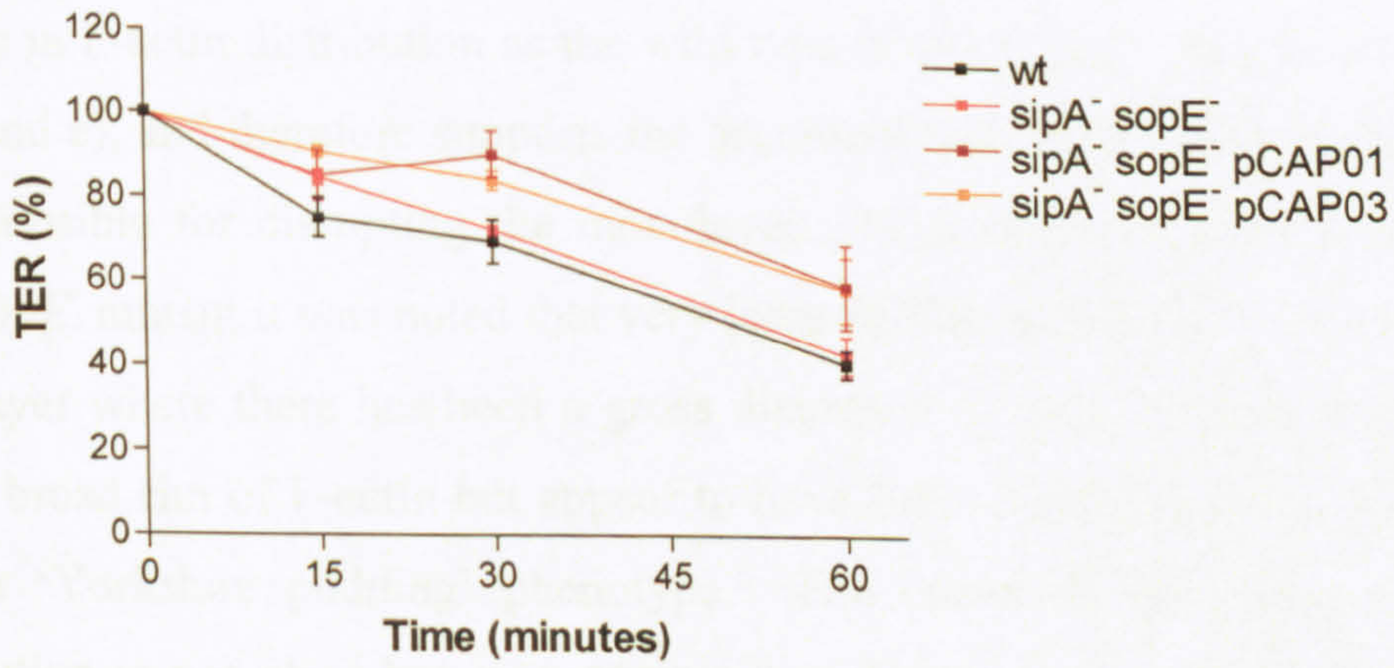

Alterations in the F-actin reorganisation of polarised monolayers during *Salmonella* infection was also examined by staining infected monolayers with TRITC-phalloidin. Confocal microscopy of the MDCK II monolayer after 15 minutes infection with the wild type or any of the mutants or transcomplemented mutants listed in Figure 4.28, reveals regular brush border and circumferential distribution of F-actin throughout the monolayer, with additional accumulation of F-actin in discrete regions of the monolayer where *Salmonella* have adhered and induce ruffle formation (Figure 4.29 and 4.30). The movement of *sipA*⁻ and *sipA*⁻ *sopE*⁻ bacteria to the periphery of the ruffle can also be seen, as can the finger-like protrusions and multiple filopodia associated with the ruffles of the *sipA*⁻ *sopE*⁻ mutant described in 4.3.10 (Figure 4.29C and Figure 4.30c).

60 minutes after the initiation of infection there is clear alteration in the F-actin organisation of the monolayer. While the regular brush border and circumferential distribution of F-actin can still be visualised in many of the cells, there are also regions with very intense staining of F-actin. In such regions, elongated cells are seen radiating around focal points of intense F-actin staining, which are created by the contraction of one or several cells, previously described by Jepson *et al.* (1995; 2000). The 60 minute images in Figure 4.29 show examples of how such constriction and elongation affects a large surface of the monolayer, while Figure 4.30 d, e and f provide specific examples of one such region from monolayers infected with either SL1344 wild type, *sopE*⁻ or *sipA*⁻ *sopE*⁻. The *sopE*⁻ mutant that failed to reduce TER appears to induce the same changes in F-actin distribution as the wild type (Figure 4.29A and B, and Figure 4.30d and e), and therefore supports the argument that SopE alone is unlikely to be responsible for disrupting the monolayer. In monolayers infected with the *sipA*⁻ *sopE*⁻ mutant it was noted that very large ruffles are found in regions of the monolayer where there has been a gross distortion of cells. These large ruffles have a broad rim of F-actin but appear to have little F-actin in the centre giving them a 'Yorkshire pudding' phenotype. The cause of this pattern of actin distribution is not clear but may represent a change in the signalling between *Salmonella* and epithelial cells due to absence of SopE and SipA.

Figure 4.29 TRITC-phalloidin staining of *S.* Typhimurium-infected MDCK II monolayers. Representative images of MDCK II polarised monolayers infected with SL1344 wt (A), *sopE*⁻ (B) *sipA*⁻ *sopE*⁻ (C) are shown after 15 and 60 minutes. The changes in the monolayer observed after infection with either wild type or *sopE*⁻ or *sipA*⁻ *sopE*⁻ illustrate the changes that are also seen with the *sipA*⁻ mutant and all the complemented mutants. Scale bar, 20μm.

A. SL1344 wild type

15 mins

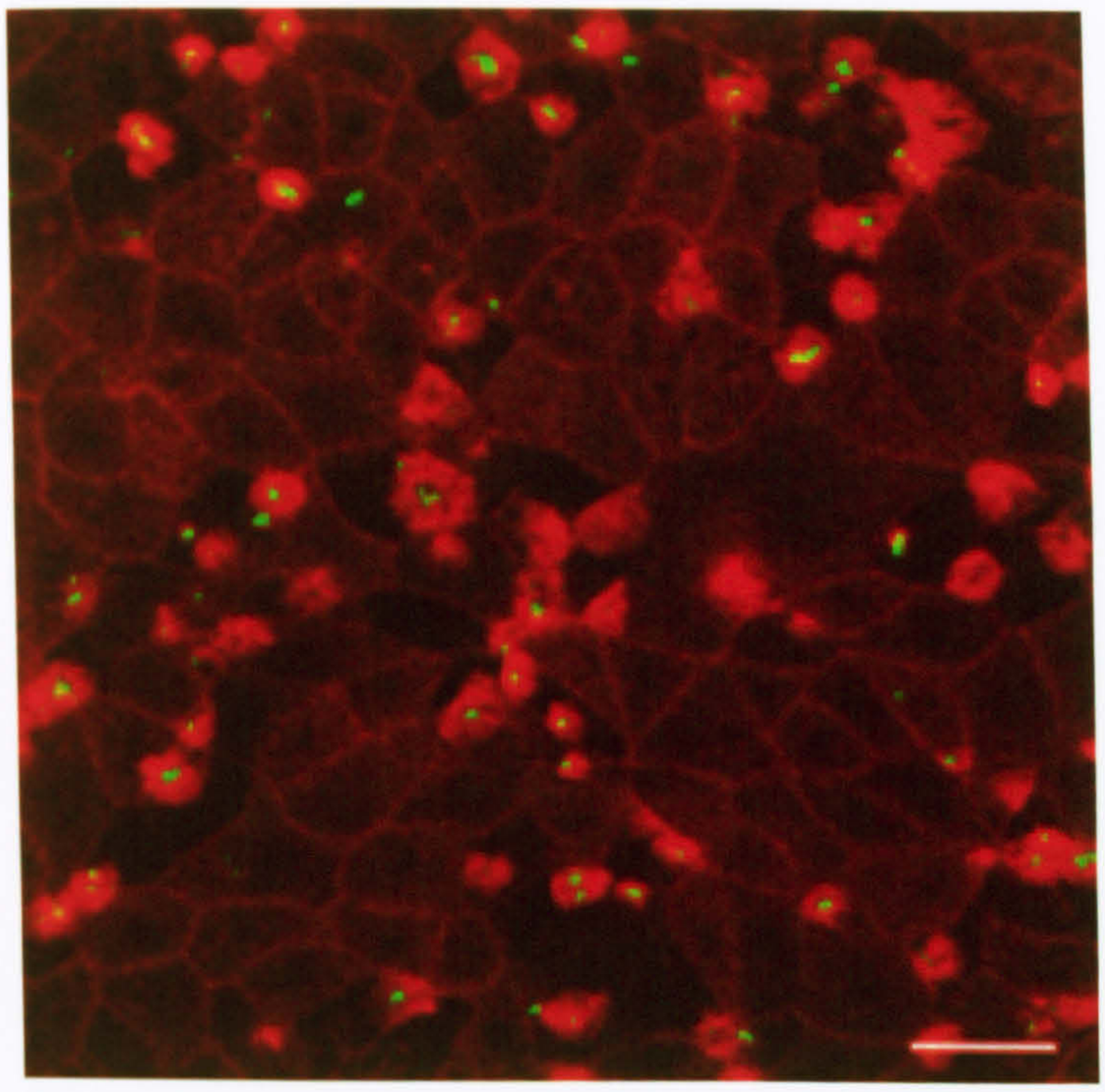

60 mins

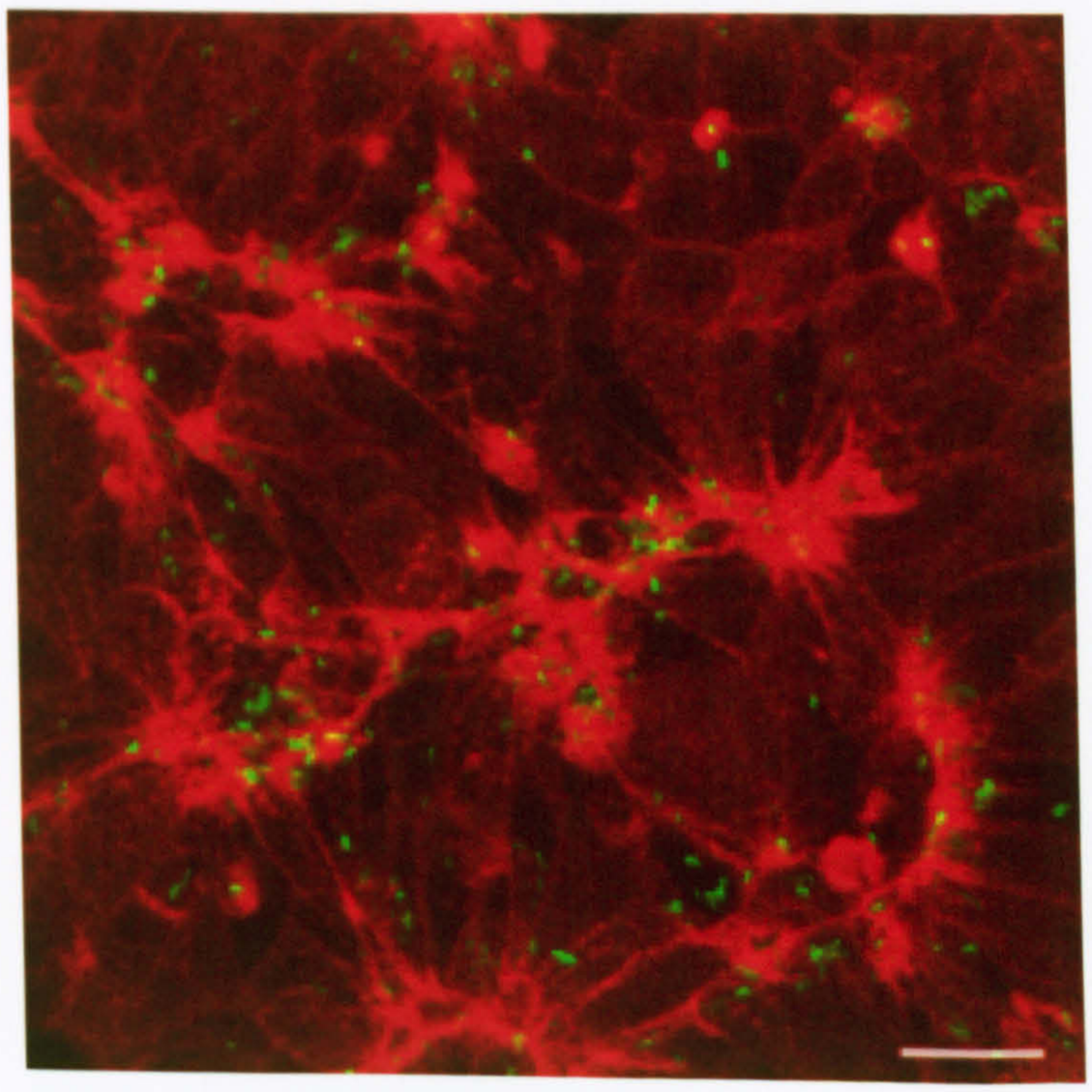

B. SL1344 *sopE*⁻

15 mins

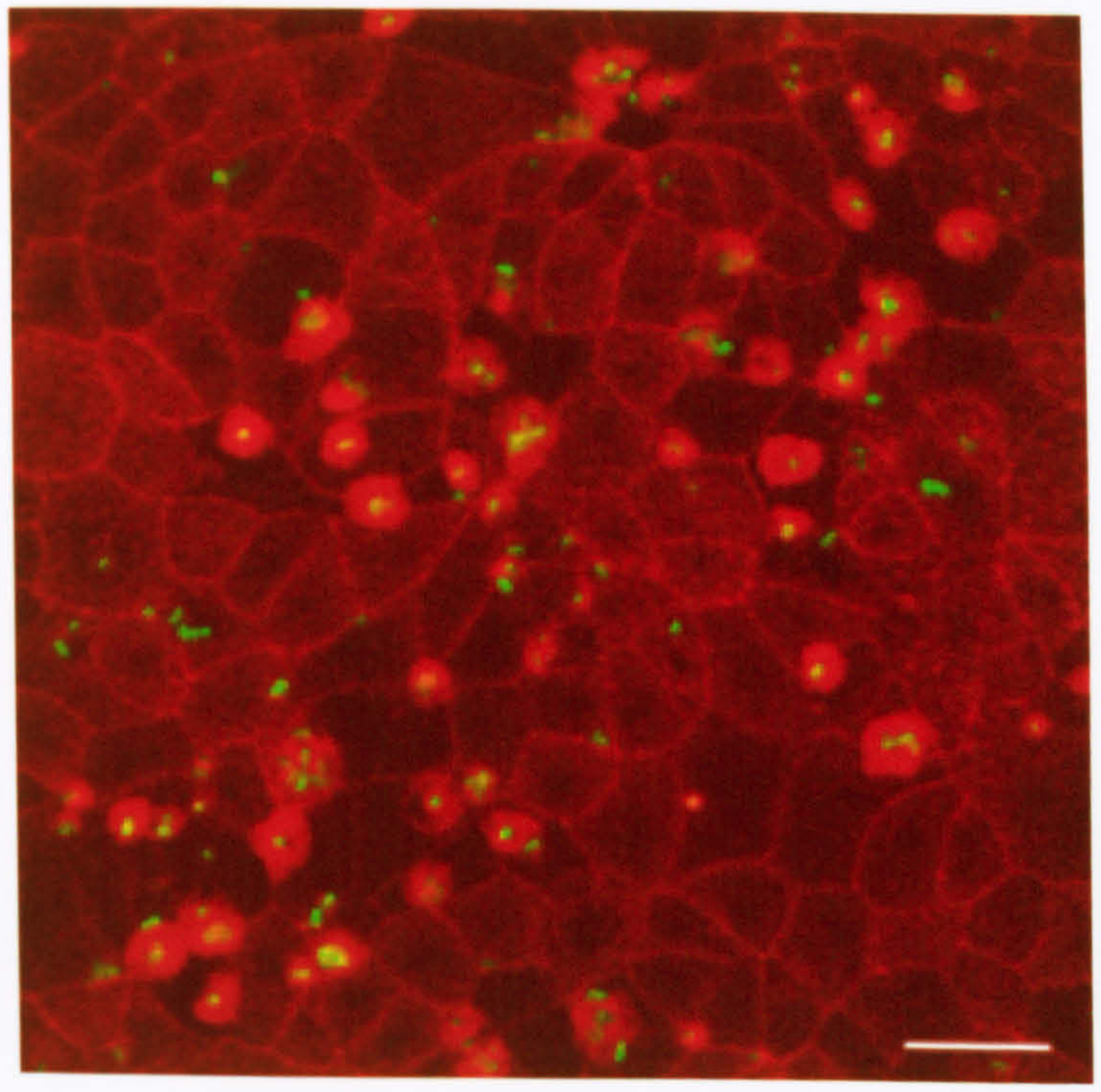

60 mins

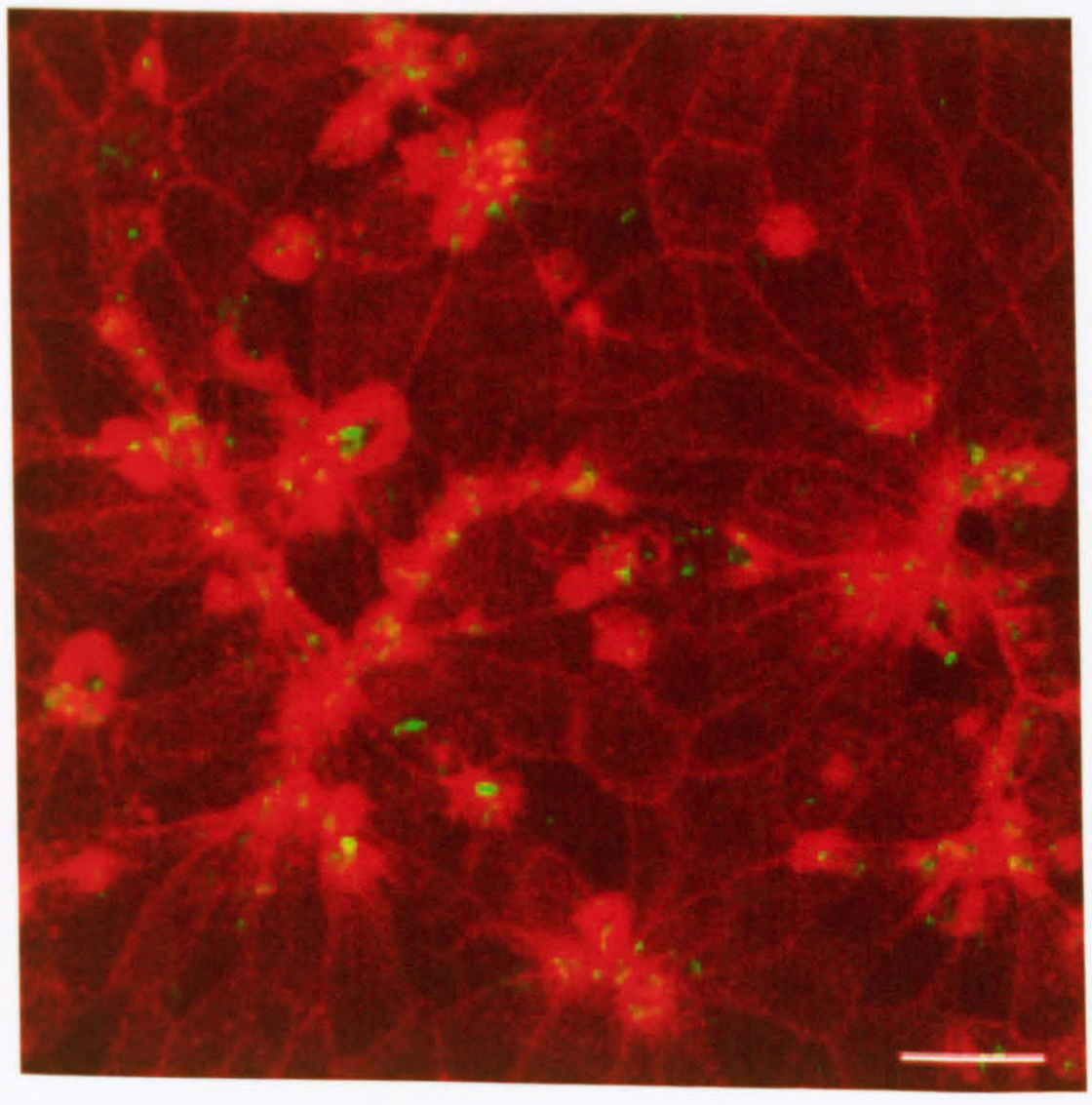

B. SL1344 *sopE*$^-$

15 mins

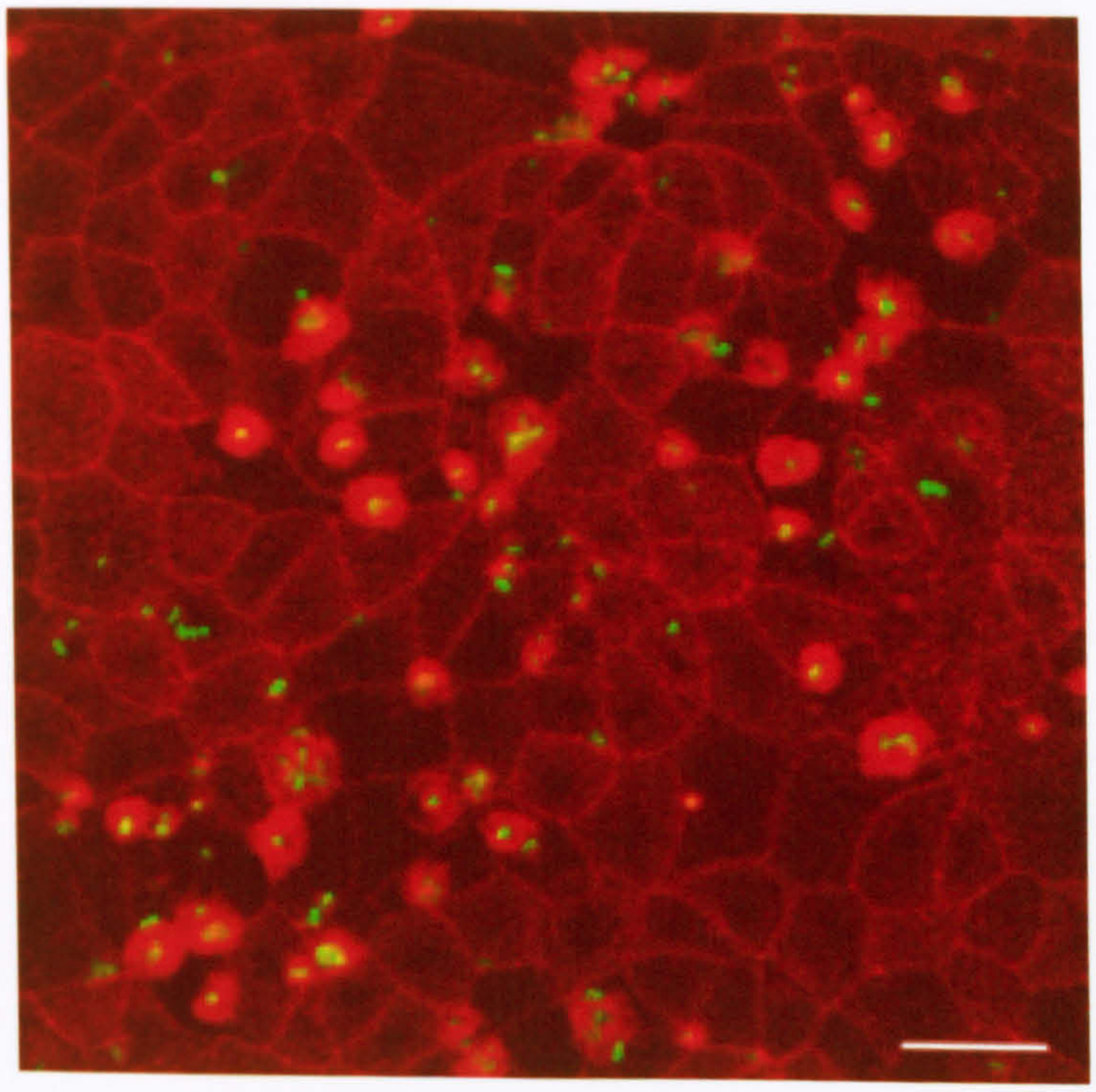

60 mins

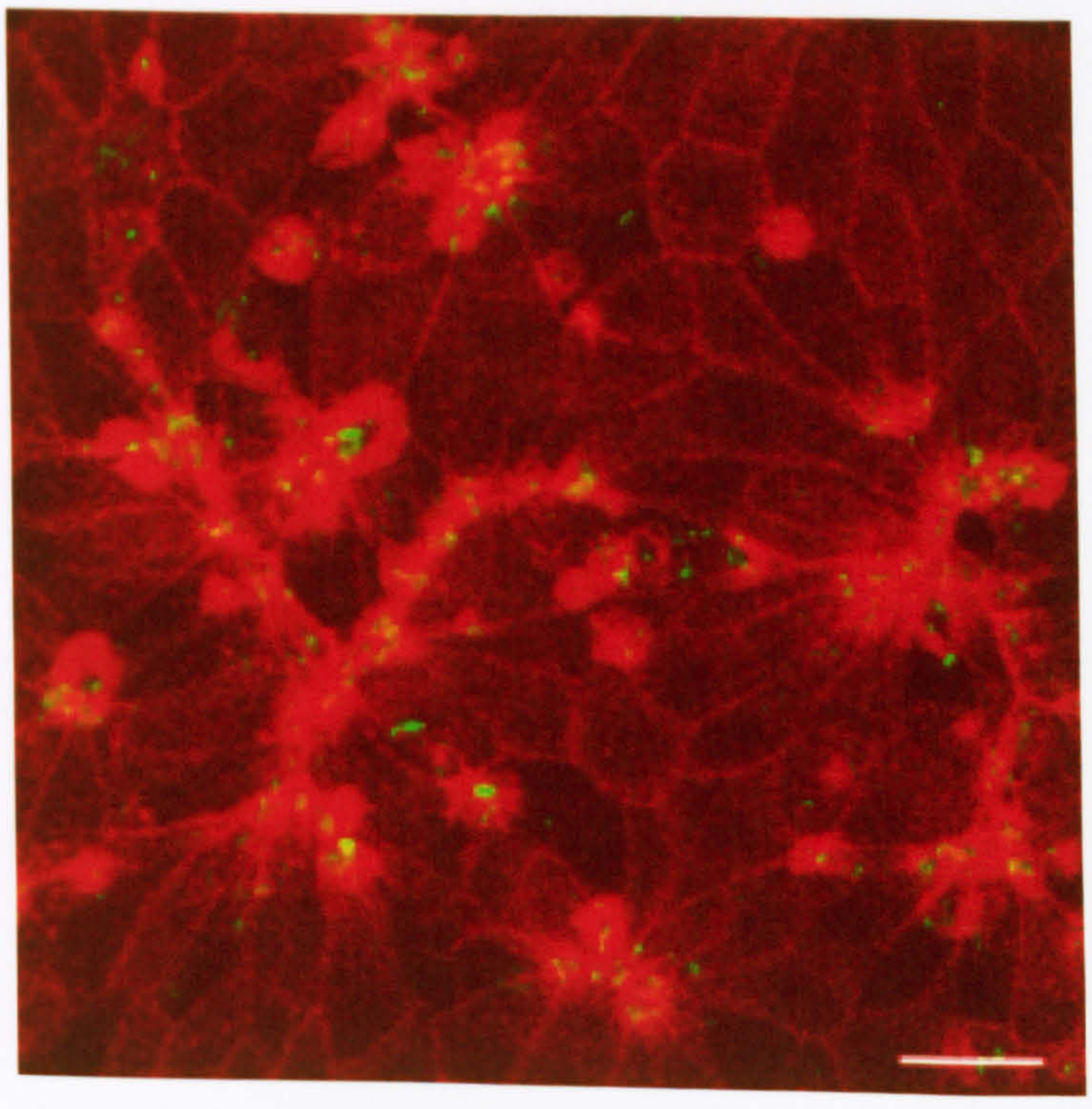

Figure 4.30 Images of TRITC-phalloidin stained MDCK II polarised monolayers showing the ruffles induced during infection for 15 or 60 minutes with SL1344 wt (a, d), *sopE*⁻ (b, e) *sipA*⁻ *sopE*⁻ (c, f). Arrows indicate bacteria located at ruffle periphery. Scale bar, 10μm.

15 mins

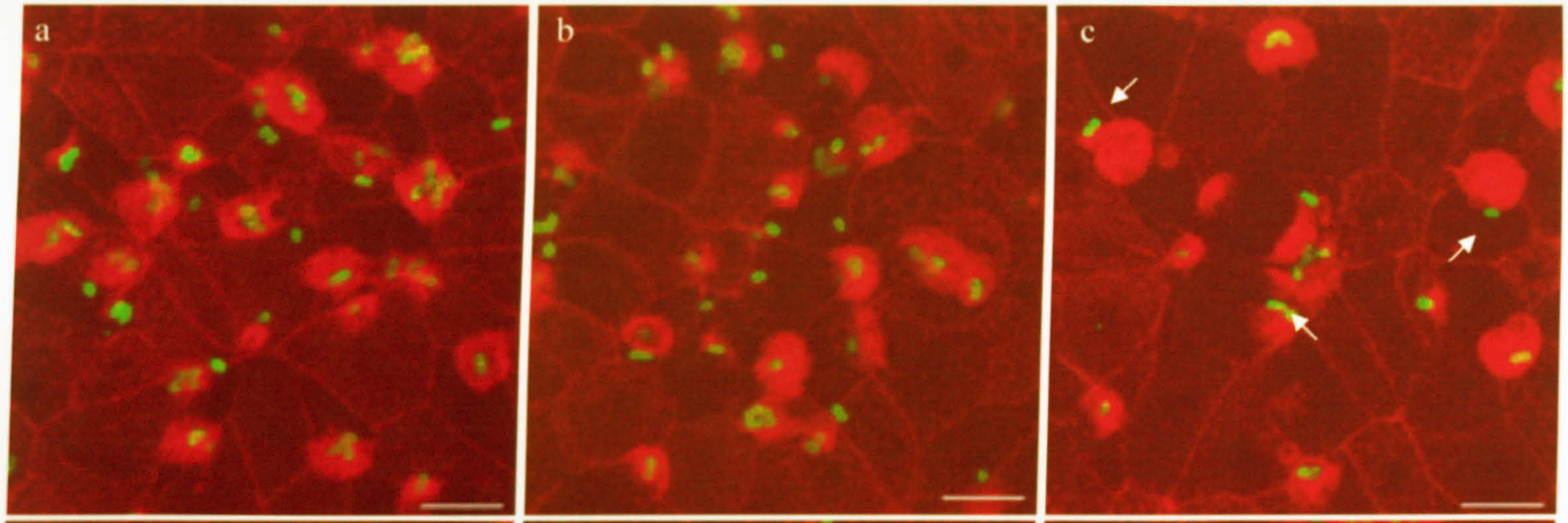

60 mins

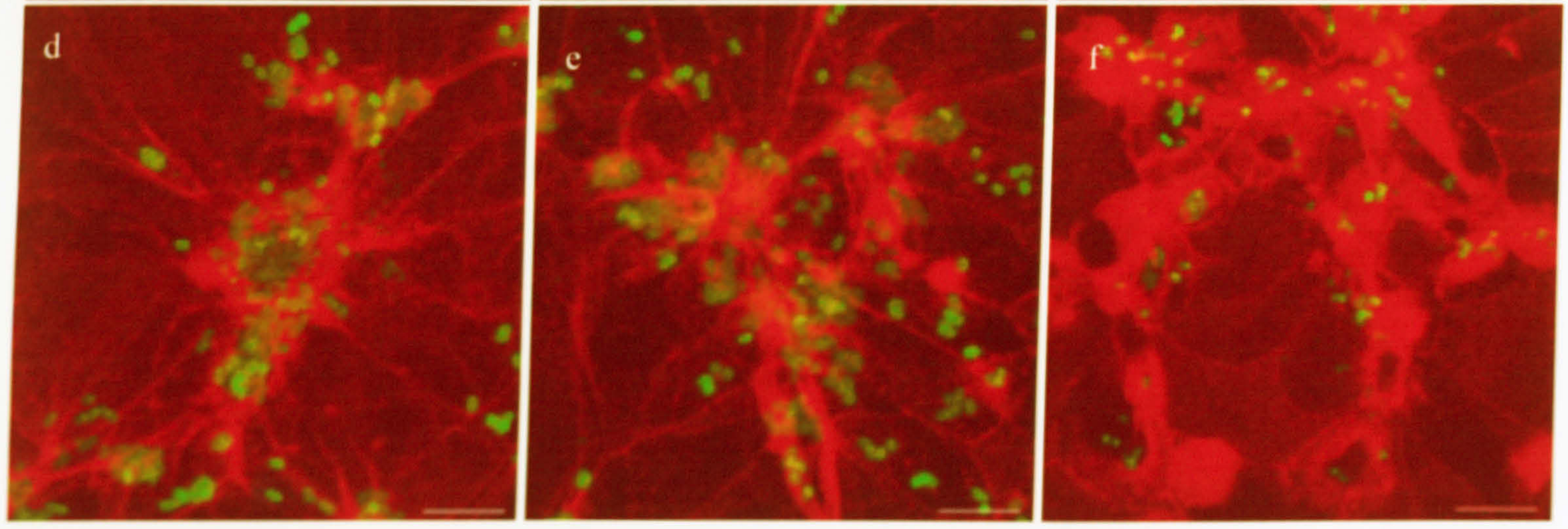

To gain a better understanding of how the monolayer becomes distorted during *Salmonella* invasion, MDCK cells that stably express GFP-actin were grown as a monolayer on coverslips, and time-lapse microscopy with phase-contrast and GFP images captured simultaneously was performed (Movies F1-3, Appendix III; Figure 4.31). Polarised monolayers grown on culture inserts, as used in Figure 4.29 and 4.30, could not be used because of the inherent problems of performing live-cell imaging through 'thick' samples.

As seen with CLSM, in resting cells there is a relatively high concentration of actin located at the periphery of the cell, corresponding to the cortical actin, with actin also distributed throughout the cell. Since the GFP-actin MDCK monolayer is relatively thin the distribution of actin throughout the cell and its exclusion from the nucleus can be observed (Figure 4.31). Observing the GFP-actin monolayer during the first 15 minutes of infection, there is relatively little change in cell shape throughout the monolayer. In regards to actin distribution, a similar pattern to that seen with CLSM is observed; discrete accumulations of actin occurring where a bacterium has adhered and induced ruffling, which are observed as bright spots of fluorescence in the GFP channel (Figure 4.31). In the ruffles induced by the SL1344 *sipA*$^{-}$ *sopE*$^{-}$ mutant, filopodia and finger-like protrusions are associated with some of the ruffles, as previously observed (Figure 4.15 and 4.20). These structures exhibit fluorescence, indicating actin runs throughout the structure and that actin polymerisation is likely to be the force that allows the fingers to be so dynamic (Figure 4.31C).

Figure 4.31 Using time-lapse microscopy to examine the recruitment of actin to the membrane ruffles induced by *S.* Typhimurium SL1344. Phase-contrast and the equivalent GFP image of representative membrane ruffling events generated in MDCK cells expressing GFP-actin by SL1344 wild type (A), *sipA*⁻ (B) and *sipA*⁻ *sopE*⁻ (C) are presented. Arrows point to membrane ruffles induced by the bacteria, the red arrow marks a finger-like protrusion. Scale bar 10μm.

Phase contrast channel GFP channel

A. SL1344 wild type

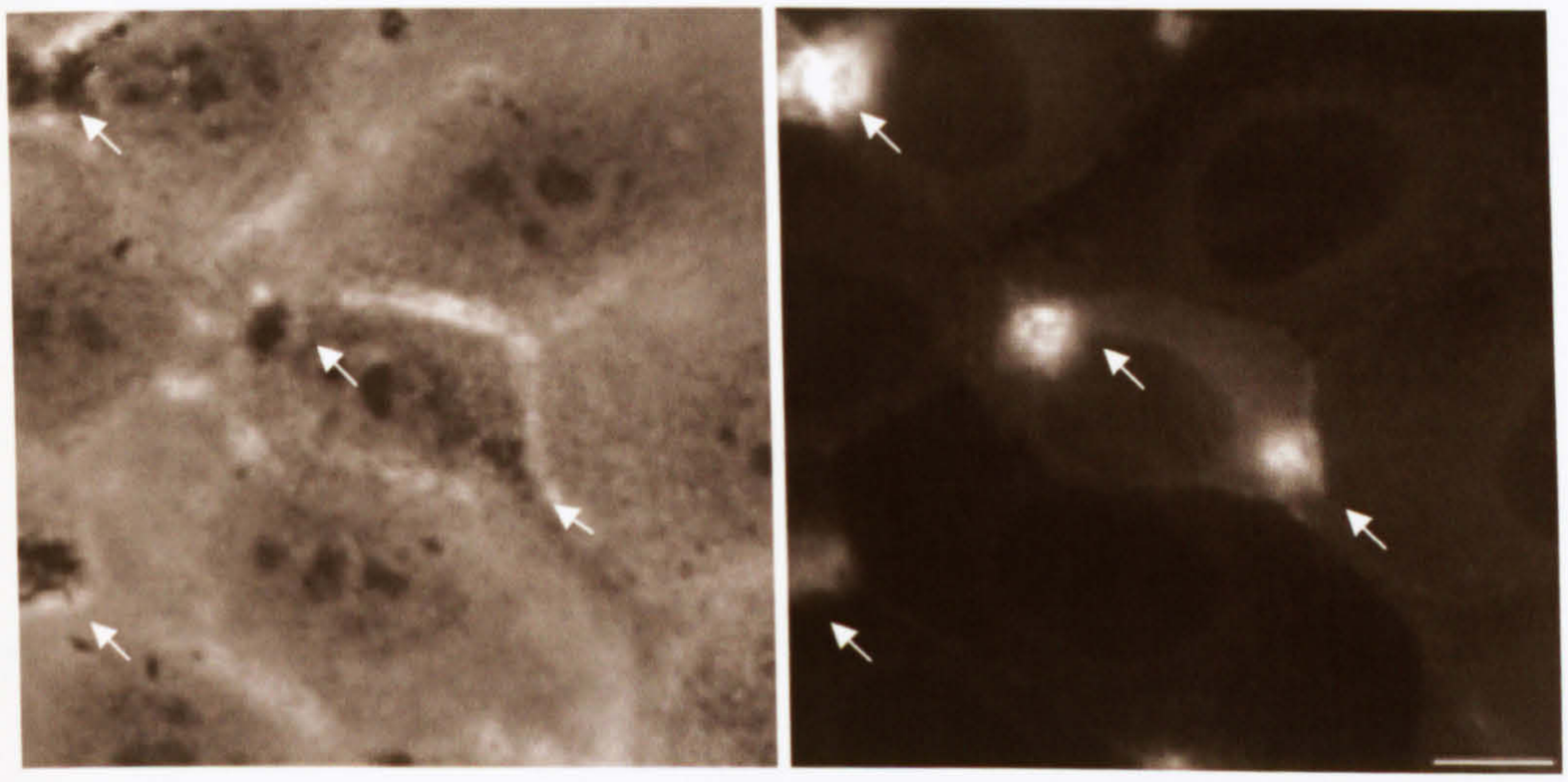

B. SL1344 *sipA*⁻

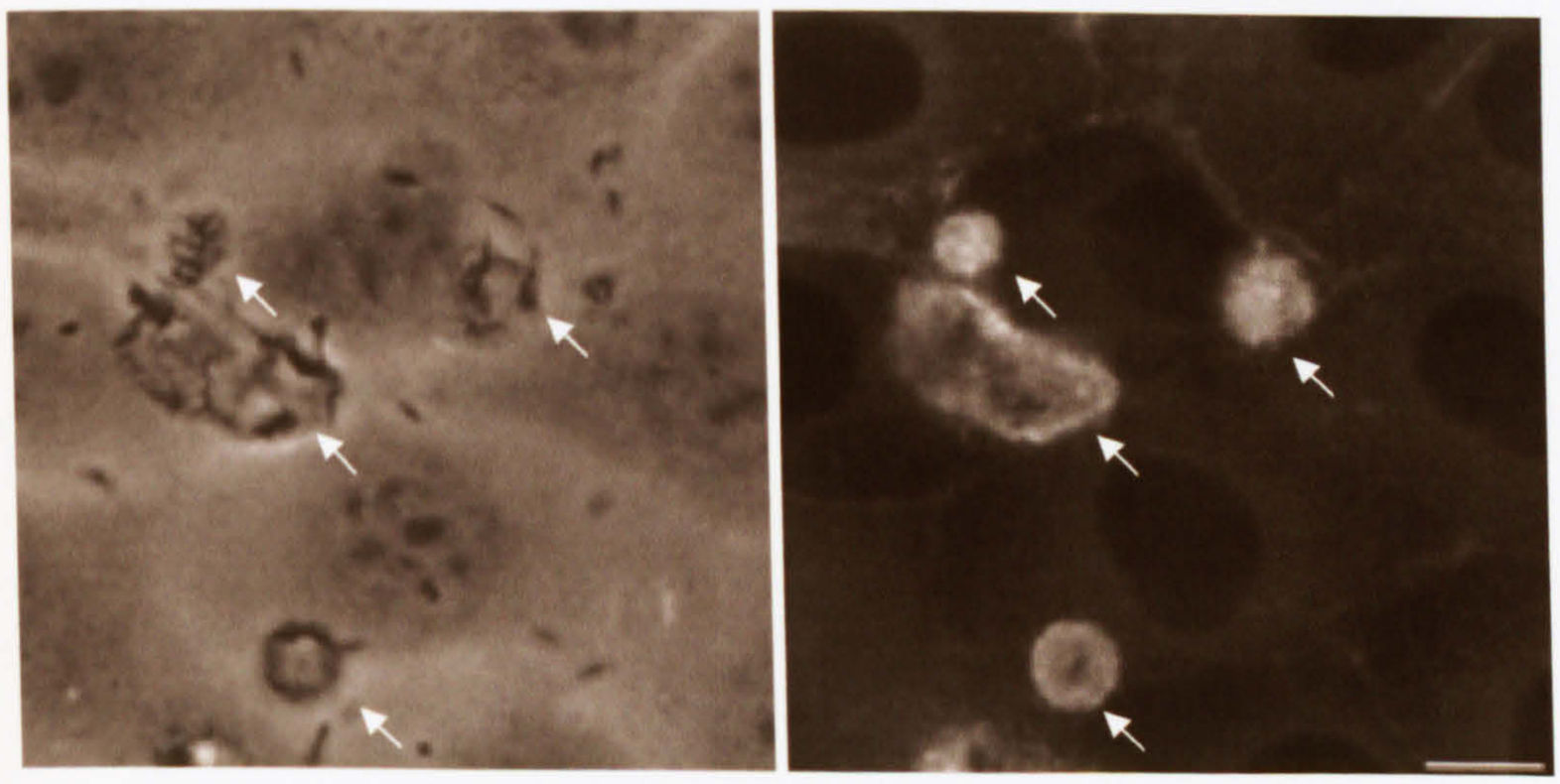

C. SL1344 *sipA*⁻ *sopE*⁻

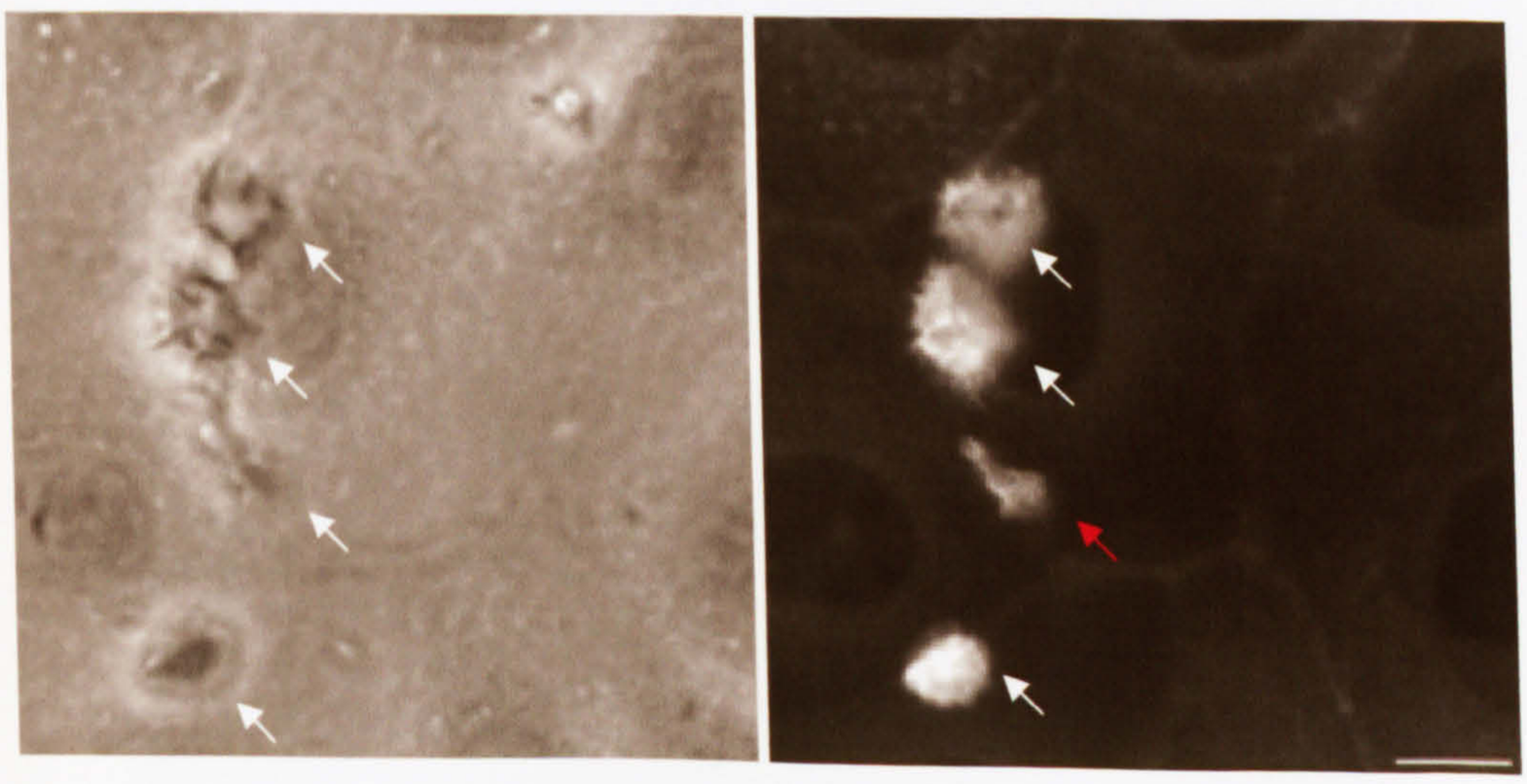

Figure 4.32 Changes in the shape and position of cells in a monolayer of MDCK GFP-actin cells during infection with *S.* Typhimurium SL1344 wild type for 60 minutes. The GFP channel of the same area of monolayer is shown at each time point. Ten cells were selected and a tracing made of their shape at each time point to show any changes that occurred. Although the images correspond to infection with the wild type, similar images were generated using any of the mutants. Scale bar, 100μm.

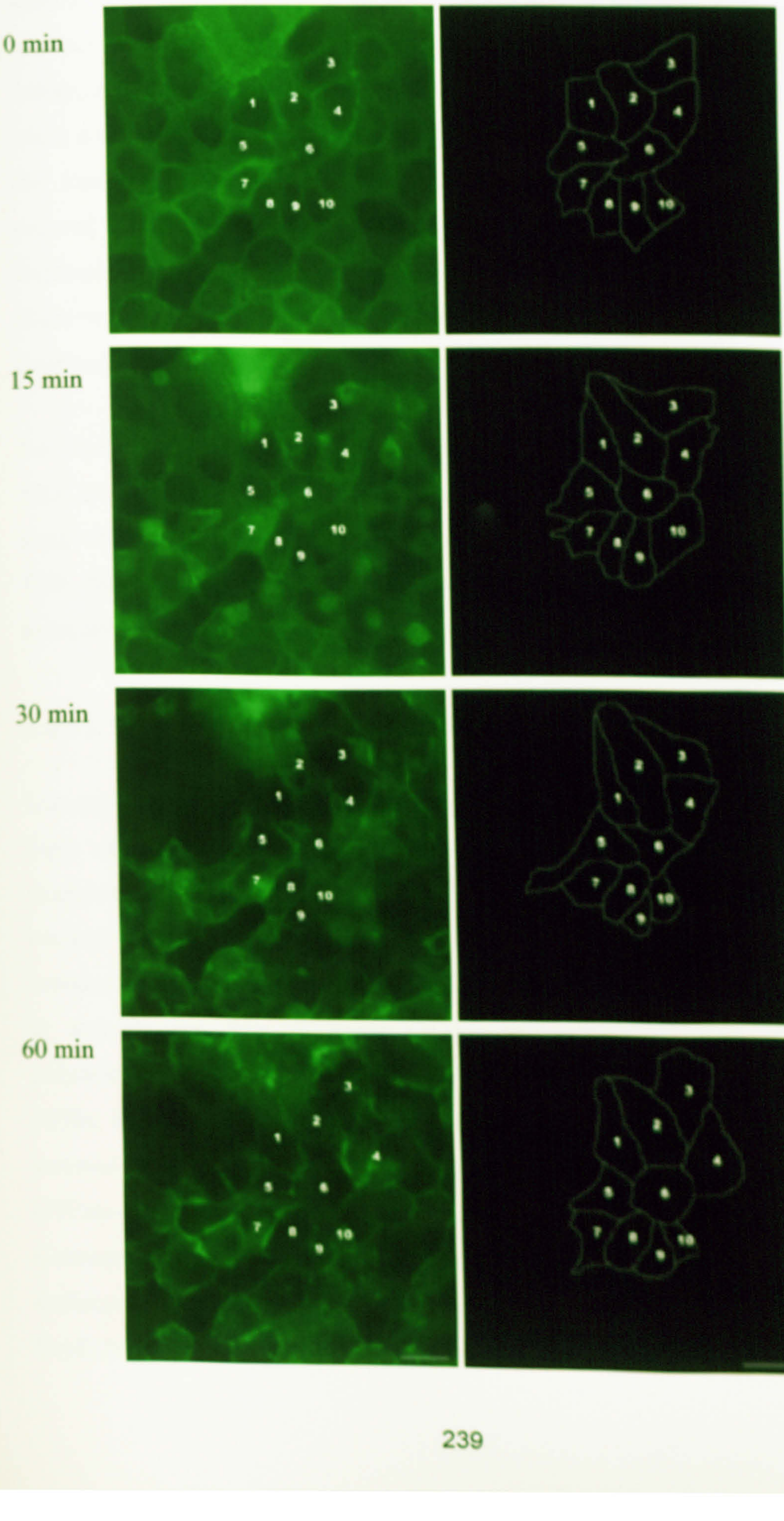

Fifteen minutes after infection is initiated, distortions in the monolayer start to be observed. For example in Figure 4.32, which monitors changes in the shape of cells during infection with *Salmonella* for 60 minutes, cells 1, 2 and 3 have started to elongate. As the infection proceeds, cells appear to move as cells contract causing adjacent cells to elongate. However, what has not been shown before, but is illustrated here, is how dynamic these changes in cell shape are; while a cell may contract initially, at later time points it may become elongated. For example in Figure 4.32, cell 5 becomes elongated at 30 minutes but is reduced in size by 60 minutes. This contraction and elongation of cells gives the impression that the cell monolayer is constantly shifting in position and illustrates that the interactions between *Salmonella* and epithelial cells are constantly being modulated.

No obvious differences were observed when comparing the changes in the MDCK monolayers by time-lapse microscopy induced by infection with *sipA*$^-$, *sopE*$^-$ and *sopE*$^-$ *sipA*$^-$ bacteria, and therefore support the conclusions from the TER data that SipA and/or SopE alone are not responsible for the loss of monolayer integrity at early time points.

4.3.13. Examining the effect of SptP in strain SL1344

One explanation for the dramatic change in the morphology of the ruffles when SipA and SopE are absent from a bacterium is that signalling pathways stimulated by the *Salmonella* effector proteins are altered. This may either be because certain signalling pathways are not stimulated or inhibited and/or because regulation of these host signalling pathways is affected. SopE is known to activate the Rho GTPases Cdc42 and Rac1, which stimulate actin polymerisation via the pathways that activate the Arp2/3 complex (Hardt *et al.*, 1998a; Stender *et al.*, 2000; Criss and Casanova, 2003). SptP, another effector secreted by TTSS-1, acts as an antagonist to SopE and SopE2, terminating Rho GTPase-stimulated actin polymerisation (Fu and Galan, 1998, 1999). Consequentially, F-actin depolymerises and the ruffle dissipates. If a, so far, undiscovered role of SipA is to help regulate the signalling events stimulated by SopE, it could be proposed that absence of SipA in a SopE$^-$ background leads to

uncontrolled signalling so that structures such as filopodia and finger-like protrusions are produced. In a *sptP*⁻ mutant, where the signalling pathways initiating ruffling will not be switched off immediately, there may be a point where the interaction between SipA and SopE becomes uncoupled, especially since SopE concentrations will eventually decline as it is sent for degradation (Kubori and Galan, 2003) while SipA persists (Brawn *et al.*, 2007). Thus, a similar dramatic change in ruffle morphology may be produced. To test this proposal the phenotype of a *sptP* deletion mutant was investigated.

A P22 lysate from a SL1344 *sptP* deletion mutant, created using the λ red system, was provided by Professor J. Hinton (Institute of Food Research, Norwich). This was subsequently used to introduce the *sptP* deletion into the SL1344 chromosome. PCR was performed using primers SptP5'pcr and SptP3'pcr (Table 4.3) to check kanamycin resistant transductants for absence of SptP. The wild type produced a PCR product of 2.1kb, while the *sptP*⁻ mutant produced a product of ~1.8kb.

Upon obtaining a SL1344 *sptP*⁻ mutant, its ability to induce ruffling in and to invade MDCK strain I cells was measured (Figure 4.33). The lack of difference between the wild type and the *sptP*⁻ mutant corresponds with the results of previous studies which found no role for SptP in the early interaction of *Salmonella* with the host (Kaniga *et al.*, 1996). Indeed the bacterium enters the cell before SptP acts to terminate ruffling so it was expected that loss of SptP would not affect ruffle induction or invasion.

Figure 4.33 Comparing the ability of SL1344 wild type and its isogenic *sptP*⁻ mutant to induce ruffles (A) and invade (B) MDCK cells. Infection was for 15 minutes, with the ability to induce ruffle formation being measured using TRITC-phalloidin staining of actin, and the ability to enter cells being measured using differential staining of adhered bacteria. Results are the mean of four independent experiments ± sem.

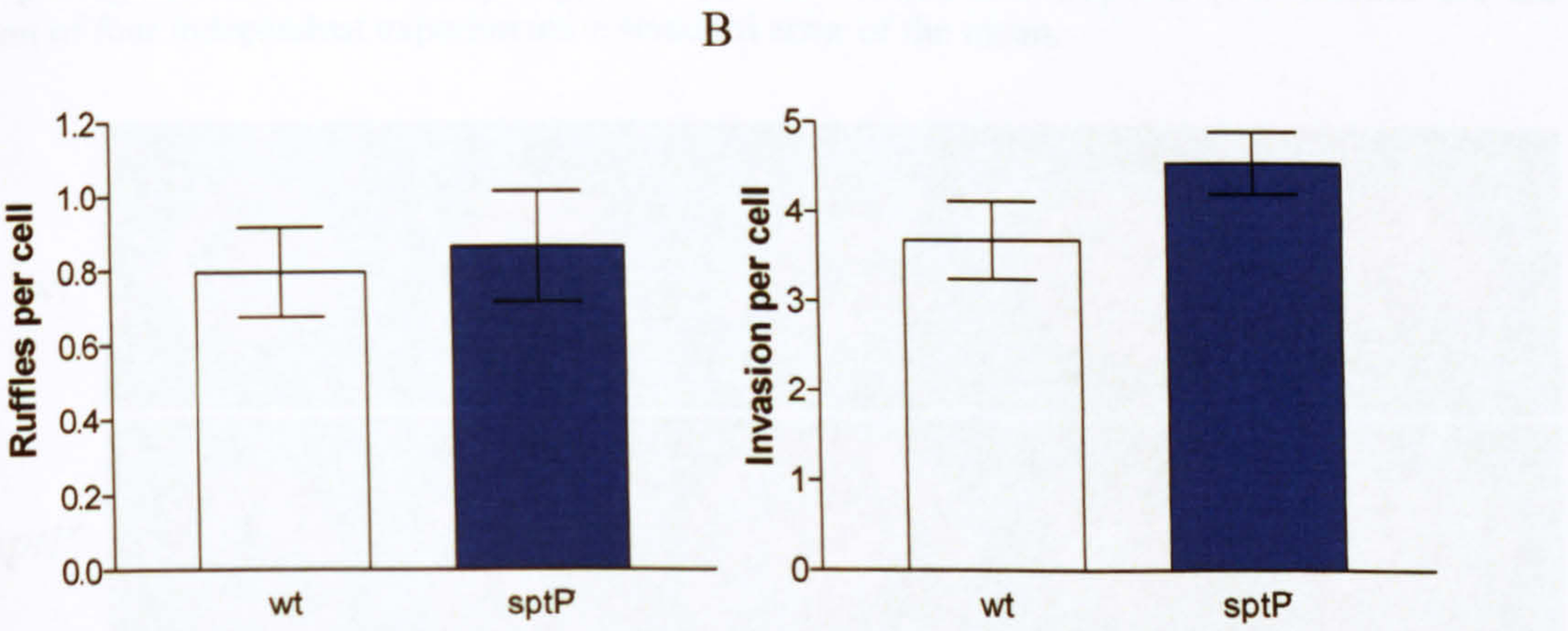

CLSM indicated that the ruffles of the *sptP*⁻ mutant had a similar morphology to those of the wild type (Figure 4.34A), being circular in shape with the bacterium located in the centre of the ruffle. However, the comparison was quantified by scoring the ruffles for the presence of bacteria and certain morphological structures i.e. presence of finger-like protrusions and filopodia, which had been present in the *sipA*⁻ *sopE*⁻ ruffles.

0.9% of wild type and 0.3% of *sptP*⁻ ruffles lacked an associated bacterium and indicates *sptP*⁻ bacteria are not affected in their interaction with the host cell membrane unlike *sipA*⁻ and *sipA*⁻ *sopE*⁻ bacteria. ≤1% of SL1344 wild type and *sptP*⁻ mutant had ruffles with finger-like protrusions associated with them, indicating this phenotype is rarely associated with ruffles of these bacteria (Figure 4.34B). It is possible in this instance the 'finger-like protrusions' are not those associated with *sipA*⁻ *sopE*⁻ ruffles but instead are artefacts, perhaps of multiple filopodia projecting from adjacent positions on the membrane, or cell debris. The mean proportion of ruffles with 10 or more filopodia is 11% for both wild type and *sptP*⁻, which corresponds to the proportion found on ruffles of the wild type, *sipA*⁻ and *sopE*⁻ single mutants of SL1344 (Figure 4.22). This ruffle morphology data therefore indicates the ruffles of *sptP*⁻ are very similar to wild type and do not resemble the ruffles of the SL1344 *sipA*⁻ *sopE*⁻ mutant.

Figure 4.34 Comparing the morphology of ruffles induced by SL1344 wild type and *sptP*⁻. CLSM images of SL1344 wild type and *sptP*⁻ ruffles are depicted in A. Each image shows a representative selection of TRITC-phalloidin-stained ruffles from MDCK cells infected for 15 minutes. Bacteria are stained with FITC. Each image is presented as a projected series of optical sessions showing membrane ruffles in their entirety. Scale bar 10μm. Ruffles were scored for morphological features including finger-like protrusions (B) and filopodia (C). Results are the mean of four independent experiments ± standard error of the mean.

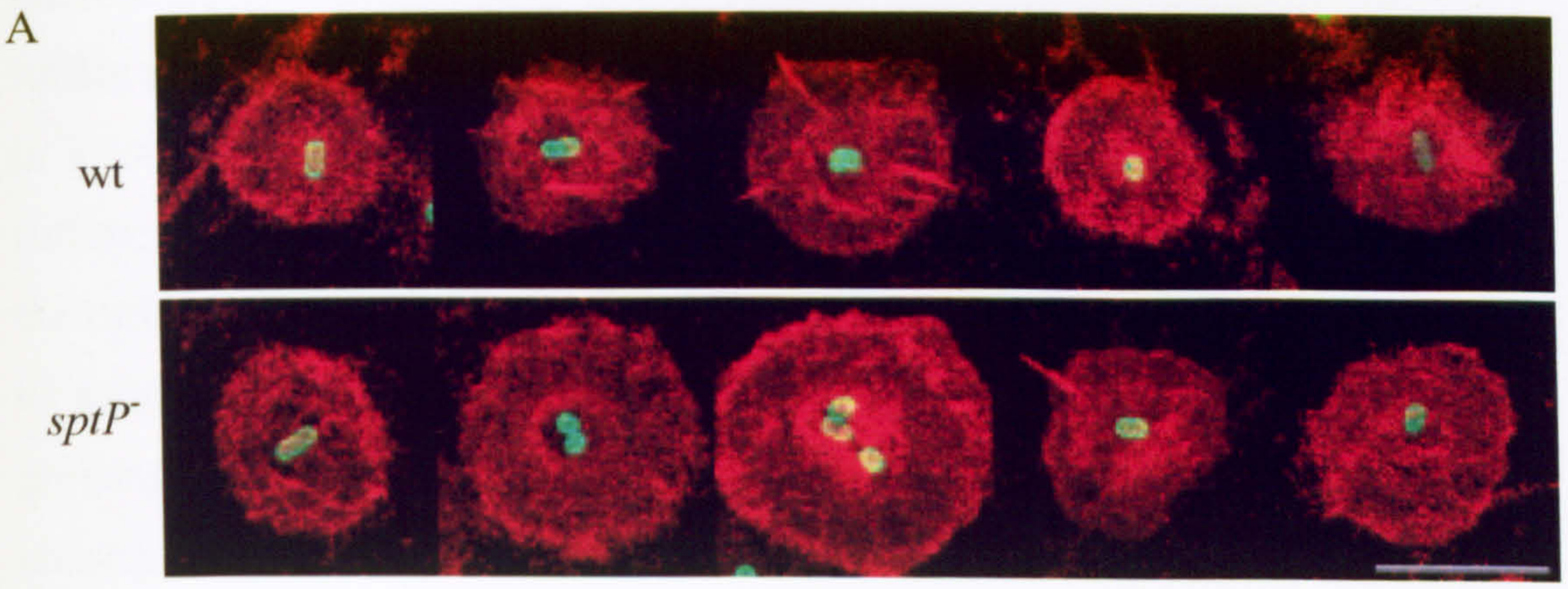

Figure 4.35 Use of time-lapse phase-contrast microscopy to examine membrane ruffle propagation and development. Phase-contrast images of representative membrane ruffles generated in MDCK epithelial cells by *S.* Typhimurium SL1344 wild type and *sptP*⁻ are shown. Scale bar 5μm.

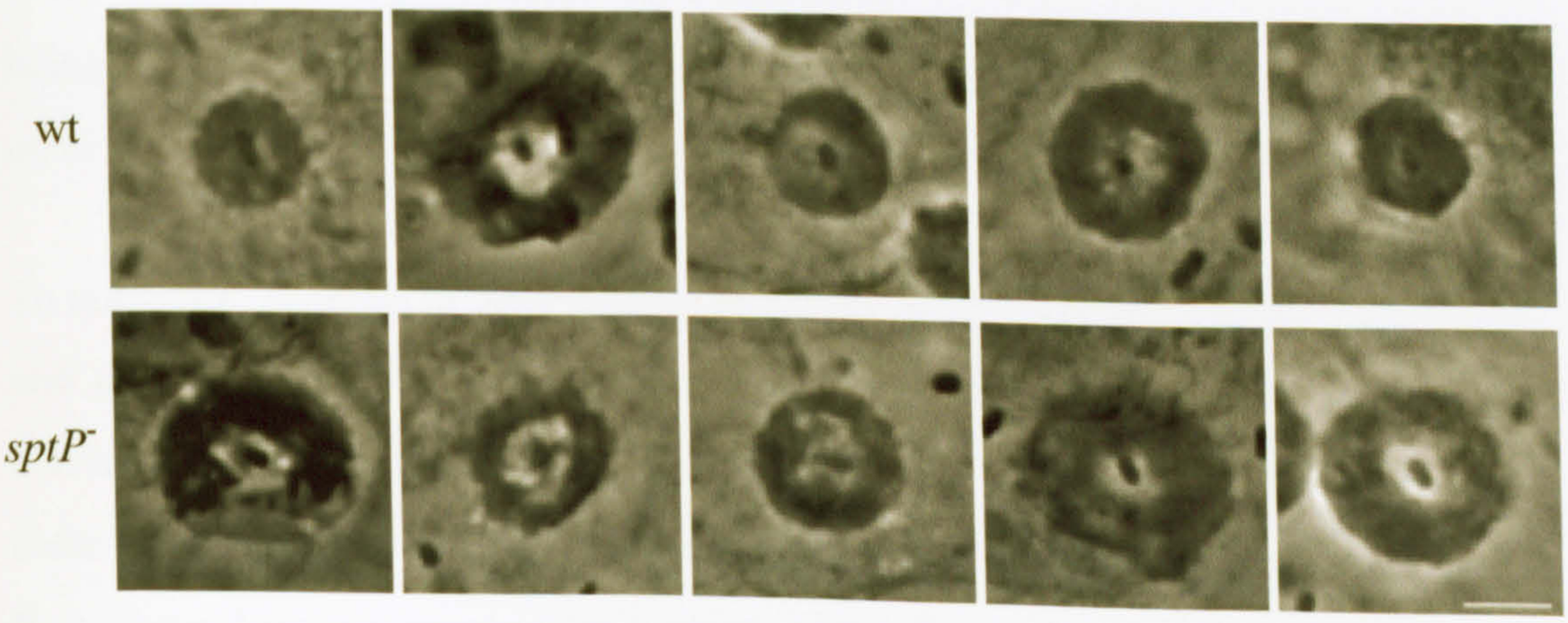

Since CLSM images only represent one point in time, it is possible that any change in ruffle morphology may not be elucidated by this technique. Therefore, phase-contrast time-lapse imaging was also used. Figure 4.35 shows representative ruffles induced by wild type and *sptP*⁻ when using this form of microscopy (a representative movie of each is located in Appendix III). The ruffles are similar to those depicted by CLSM, with a bacterium placed centrally in a roughly circular ruffle. No additional structures were associated with the ruffles; the only difference compared to the wild type was the apparent size of the ruffles. If SptP is absent, Rho GTPases, and therefore the pathways leading to actin polymerisation, will remain activated allowing the ruffle to continue growing in size, until host GAPs act to switch off the Rho GTPases. A consequence of this delay in terminating actin polymerisation would be the production of larger ruffles by the *sptP*⁻ mutant. Comparing the mean diameter of ruffles induced by the wild type and the *sptP*⁻ mutant found no difference; mean diameter of 8.86 ± 0.382 μm for the wild type compared to 9.55 ± 0.253 μm for the *sptP*⁻ mutant. However, it is important to note that only ruffles sufficiently separated from other ruffles can be used in this analysis to enable accurate calculation of the maximum diameter. It was felt a proportion of the *sptP*⁻ ruffles, which included many with the largest diameter, were excluded in the measurements because their large size meant they often merged with neighbouring ruffles and could not be measured. Therefore, a bigger difference between wild type and *sptP*⁻ ruffles may exist. It is interesting to contrast the effect loss of different effector proteins has on the size of the ruffles induced; loss of SopE leading to the production of small ruffles, while loss of SptP leads to the creation of larger ruffles. This illustrates the importance for *Salmonella* of being able to both switch on and switch off host Rho GTPases to induce its uptake.

To conclude, absence of SptP has no effect on the ability of *Salmonella* to initiate and propagate ruffles, and therefore has no immediate role in invasion, which confirms previously published data (Kaniga *et al.*, 1996). It was also shown that there is no dramatic change in the morphology of ruffles induced by *sptP*⁻, and thus, there does not seem to be a point where the interaction between SipA and SopE becomes uncoupled in this mutant and so did not provide any further

information as to how these effectors may interact to stimulate *Salmonella* invasion.

4.3.14. Examining the relationship between SipA and SopE2

Since SopE, SopE2 and SopB have all been shown to stimulate actin reorganisation via Rho GTPases (Hardt *et al.*, 1998a; Stender *et al.*, 2000; Zhou *et al.*, 2001; Patel and Galan, 2006), it was decided to investigate the effect of loss of SipA in the absence of SopE2 or SopB, to determine whether a similar phenotype as that described for a *sipA*⁻ *sopE*⁻ mutant is obtained. SopE2 is a homolog of SopE, having 69% similarity at the amino acid level to SopE and performing the same role i.e. a GEF for Rho GTPases (Bakshi *et al.*, 2000; Stender *et al.*, 2000). If the interaction between SipA and SopE2 was similar to the interaction between SipA and SopE it may hint at the pathways that are affected to cause this phenotype, since while SopE activates both Cdc42 and Rac1, SopE2 only activates Cdc42 (Hardt *et al.*, 1998a; Stender *et al.*, 2000).

The P22 lysate from a *sopE2* deletion mutant, created using the λ red system, was provided by Professor J. Hinton (Institute of Food Research, Norwich). P22 transduction was used to insert the *sopE2* deletion into the SL1344 wild type and SL1344 *sipA*⁻ mutant chromosome to produce SL1344 *sopE2*⁻ and *sipA*⁻ *sopE2*⁻ mutants respectively. Transductants were selected for resistance to kanamycin, and then checked for deletion of the *sopE2* gene by PCR using primers 5'pcr-sopE2 and 3'pcr-sopE2 (Table 4.3). The wild type produced a PCR product of 843bp, while the *sopE2* deletion mutants produced a product of ~1.2kb.

The *sipA*⁻ *sopE2*⁻ mutant was complemented for loss of SipA with pCAP01, which carries the *sipA* gene. A plasmid carrying the *sopE2* gene (pCAP02) was created in order to complement the loss of SopE2 in the *sopE2*⁻ and *sipA*⁻ *sopE2*⁻ mutants. To create pCAP02, the *sopE2* gene plus ~500bp up- and downstream of the gene were amplified from SL1344 wild type DNA in a PCR using primers 5'xhoIsopE2 and 3'sopE2hindIII (Table 4.3), to produce a PCR product with a 5' *Xho*I restriction site and a 3'*Hin*dIII recognition site. This PCR product and plasmid pACYC177 were cut with *Xho*I and *Hin*dIII. A 520bp fragment

containing part of the kanamycin resistance cassette was removed from pACYC177 during this restriction digest, and into this site the PCR product was ligated. *E. coli* DH5α was electroporated in the presence of the ligation reaction and colonies screened for a carbenicillin resistant, kanamycin sensitive phenotype, which indicated the presence of a plasmid which may contain the *sopE2* gene. Clones were analysed for the presence of the *sopE2* gene using a restriction digest with *Xho*I and *Hin*dIII. Digestion of correctly orientated *sopE2* generated two DNA bands of 3.4kb and 1.5kb, respectively. The presence of the *sopE2* gene was finally confirmed by two sequencing reactions performed by the MWG DNA sequencing service; one using the 5'pcr_sopE and 3'pcr_sopE primers, the second using the 5'xhoIsopE and 3'sopEhindIII primers. Electroporation was subsequently used to transform SL1344 *sopE2*$^-$ and *sipA*$^-$ *sopE2*$^-$ with plasmid pCAP02.

Once the SL1344 *sopE2* mutants had been created and complemented, the secreted proteins from each were collected and SDS-PAGE performed. A Western blot was then performed using anti-SipA, anti-SipC and anti-SopE2 antibodies to check the absence or presence of SopE2 matched the expected protein profile (Figure 4.36). P22 transduction was shown to have successfully introduced the *sopE2* mutation into SL1344.

Figure 4.36 Comparing the SopE2 profile of wild type, *sopE2*$^-$ and *sopE2*$^-$ pCAP02 serovar Typhimurium strain SL1344. Lane 1 corresponds to the wild type, lane 2 to the *sopE2*$^-$ mutant and 3 to *sopE2*$^-$ pCAP02. Culture supernatant proteins were prepared by precipitation with 10% Trichloroacetic acid, separated by SDS-PAGE, transferred to a nitrocellulose membrane, and probed with anti-SipA, anti-SipC, and anti-SopE2 monoclonal antibodies.

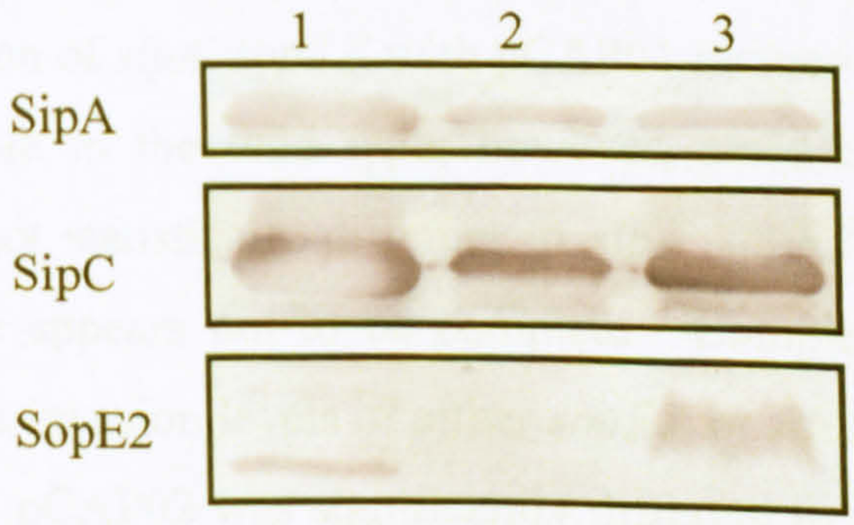

Once the mutants had been created they were examined for their ability to induce ruffles and invade MDCK cells. The average number of ruffles induced per cell was similar for the wild type, *sopE2*⁻ mutant and transcomplemented mutant (*sopE2*⁻ pCAP02) (Figure 4.37A). Deletion of *sipA* and *sopE2* together slightly reduced the mean number of ruffles, however, this was not statistically significant. Thus, as was observed with SopE, absence of SopE2 alone or with SipA does not affect the number of ruffles that can be induced.

After a 15 minute infection of MDCK cells a comparable number of wild type, *sopE2*⁻ and *sopE2*⁻ pCAP02 bacteria were internalised per cell (Figure 4.37B). It appears SopE2 is therefore less important for invasion than SopE, as the absence of SopE causes a 60% reduction in invasion compared to wild type (Figure 4.19), while there is only a 14% reduction in invasion when SopE2 is absent. Stender *et al.* (2000) reported a similar phenotype; a SL1344 *sopE2* single mutant having ~15% less invasion compared to its wild type, which made its invasion defect less pronounced than that of a *sopE* single mutant.

SL1344 *sipA*⁻ *sopE2*⁻ had 2.5-fold lower invasion than wild type, which was comparable to the invasion defect of the *sipA*⁻ *sopE*⁻ mutant. This suggests removal of SipA with either SopE or SopE2 has a similar effect on the interaction of the bacterium with its host cell. There is also a suggestion that the absence of SipA may be most important in determining the invasion of SL1344, since *sipA*⁻ *sopE2*⁻ has a similar invasion defect to *sipA*⁻ and *sipA*⁻ *sopE*⁻ despite the *sopE2* deletion having little effect on invasion by itself.

Complementation of *sipA*⁻ *sopE2*⁻ with pCAP01 increased invasion levels so they were comparable to the wild type; however, since invasion of *sipA*⁻ *sopE2*⁻ pCAP01 was not statistically different to *sipA*⁻ *sopE2*⁻, restoration of the wild type phenotype appears not to be complete. Complementation with pCAP02 failed to change invasion levels of either *sopE2*⁻ or *sipA*⁻ *sopE2*⁻, so that invasion of *sipA*⁻ *sopE2*⁻ pCAP02 was significantly different to wild type (Figure 4.37B). The plasmid expressing *sopE2* therefore appears to have similar problems to the *sopE* plasmid, pCAP03, in ensuring correct levels of the effector protein are expressed and secreted, to complement the mutant phenotype in regards to

invasion. The ability to induce ruffles does not appear to be affected. It would therefore be beneficial to trial the use of an alternative vector to provide conclusive evidence of the role of each effector in invasion, although the literature has so far supported the conclusions drawn from this work.

Figure 4.37 Examining the effect of SopE2 deletion from SL1344. The ability of SL1344 wild type and its isogenic *sopE2*⁻ and *sipA*⁻ *sopE2*⁻ mutants were compared in their ability to induce ruffles (A) and invade (B) MDCK cells. Infection was for 15 minutes, with the ability to induce ruffle formation being measured using TRITC-phalloidin staining of actin, and the ability to enter cells being measured using differential staining of adhered bacteria. Results measuring the number of ruffles are the mean of two independent experiments ± standard error of the mean, while the invasion results are the mean of four independent experiments ± sem. Asterisk denote a statistical difference when using a one way ANOVA with a Tukey post test at a level of $P<0.05$.

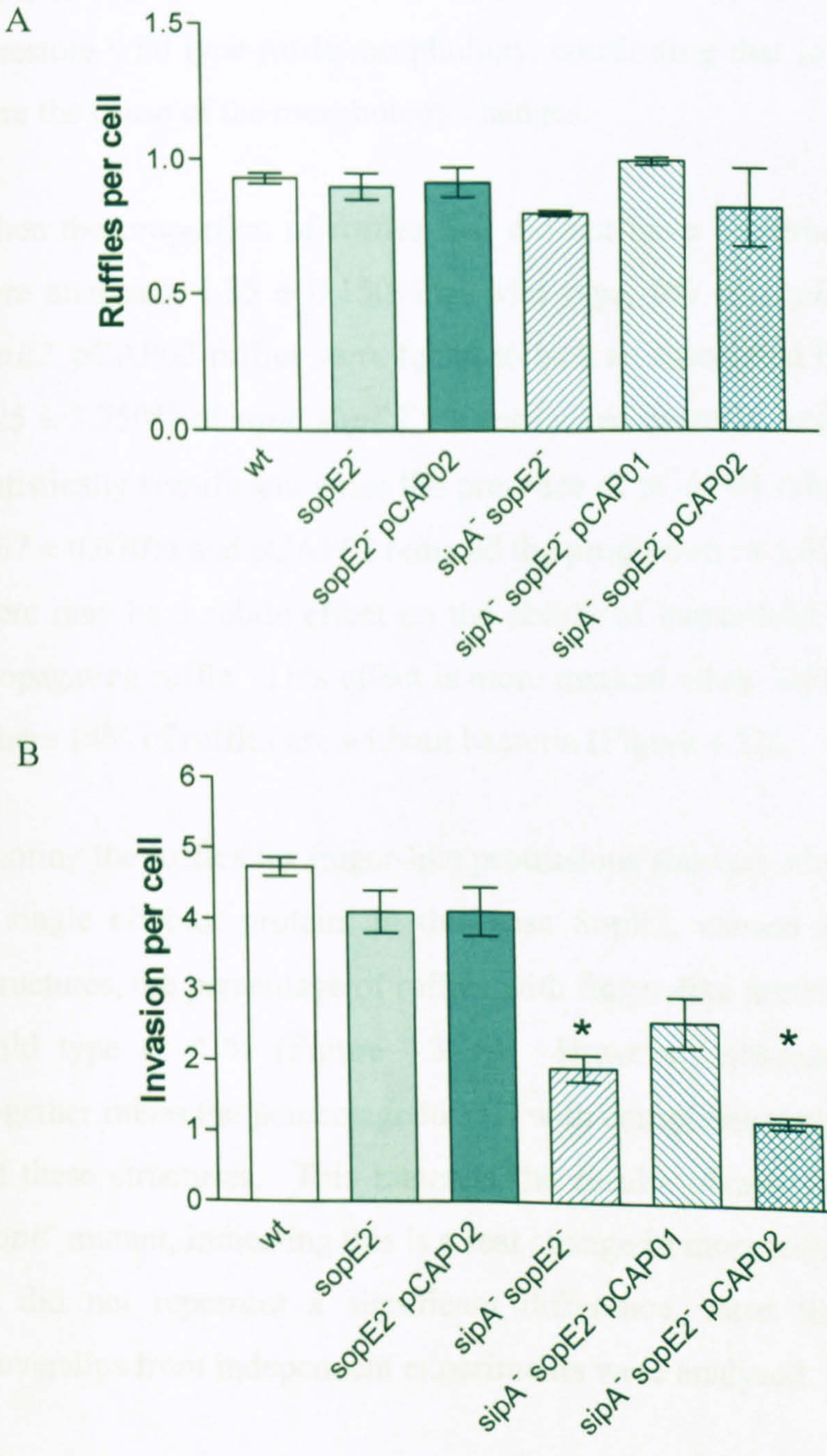

Having established that a *sipA*⁻ *sopE2*⁻ mutant has a similar invasion defect to a *sipA*⁻ *sopE*⁻ mutant, ruffle morphology was studied to determine whether there was also a similar change. CLSM images (Figure 4.38) indicated ruffles of the *sopE2*⁻ mutant had a similar morphology to those of the wild type and SL1344 *sopE2*⁻ pCAP02 i.e. smooth circular ruffles with bacteria located in the centre. However, unlike a single *sopE* mutant, the ruffles of the *sopE2* mutant did not appear to be smaller in size. A *sipA*⁻ *sopE2*⁻ mutant had ruffles that resembled those of the *sipA*⁻ *sopE*⁻ mutant, so while there were a proportion of ruffles resembling wild type ruffles, there were also a proportion of ruffles with finger-like protrusions and/or a high proportion of filopodia. While pCAP01 and pCAP02 were not able to restore invasion to wild type levels, they appeared able to restore wild type ruffle morphology, confirming that loss of SipA and SopE2 were the cause of the morphology changes.

When the proportion of ruffles that did not have bacteria associated with them were analysed, 1.35 ± 0.150% of wild type, 0% of *sopE2*⁻ and 0.7 ± 0.7% of *sopE2*⁻ pCAP02 ruffles were found to lack an associated bacterium. In contrast, 6.25 ± 3.750% of *sipA*⁻ *sopE2*⁻ ruffles lacked bacteria, and although this was not statistically significant, since the presence of pCAP01 returned the percentage to 0.67 ± 0.670% and pCAP02 reduced the proportion to 3.45 ± 1.850%, it indicates there may be a subtle effect on the ability of bacteria to remain attached to the propagating ruffle. This effect is more marked when SipA and SopE are absent, where 14% of ruffles are without bacteria (Figure 4.16).

Scoring the ruffles for finger-like protrusions showed once again that removal of a single effector protein, in this case SopE2, caused no production of these structures, the percentage of ruffles with finger-like protrusions being identical to wild type at <1% (Figure 4.39A). However, absence of SipA and SopE2 together raises the percentage to 5%, with complementation reducing the number of these structures. This matched the results obtained with the SL1344 *sipA*⁻ *sopE*⁻ mutant, indicating this is a real change in morphology, despite the fact here it did not represent a significant difference, most likely because only two coverslips from independent experiments were analysed.

Figure 4.38 CLSM images showing the morphology of membrane ruffles induced by wild type and *sopE2*⁻ mutants of *S.* Typhimurium SL1344. Each image shows a representative selection of ruffles from TRITC-phalloidin-stained MDCK cells infected for 15 minutes. Bacteria are stained with FITC. Each image is presented as a projected series of optical sessions showing membrane ruffles in their entirety. Scale bar 10μm

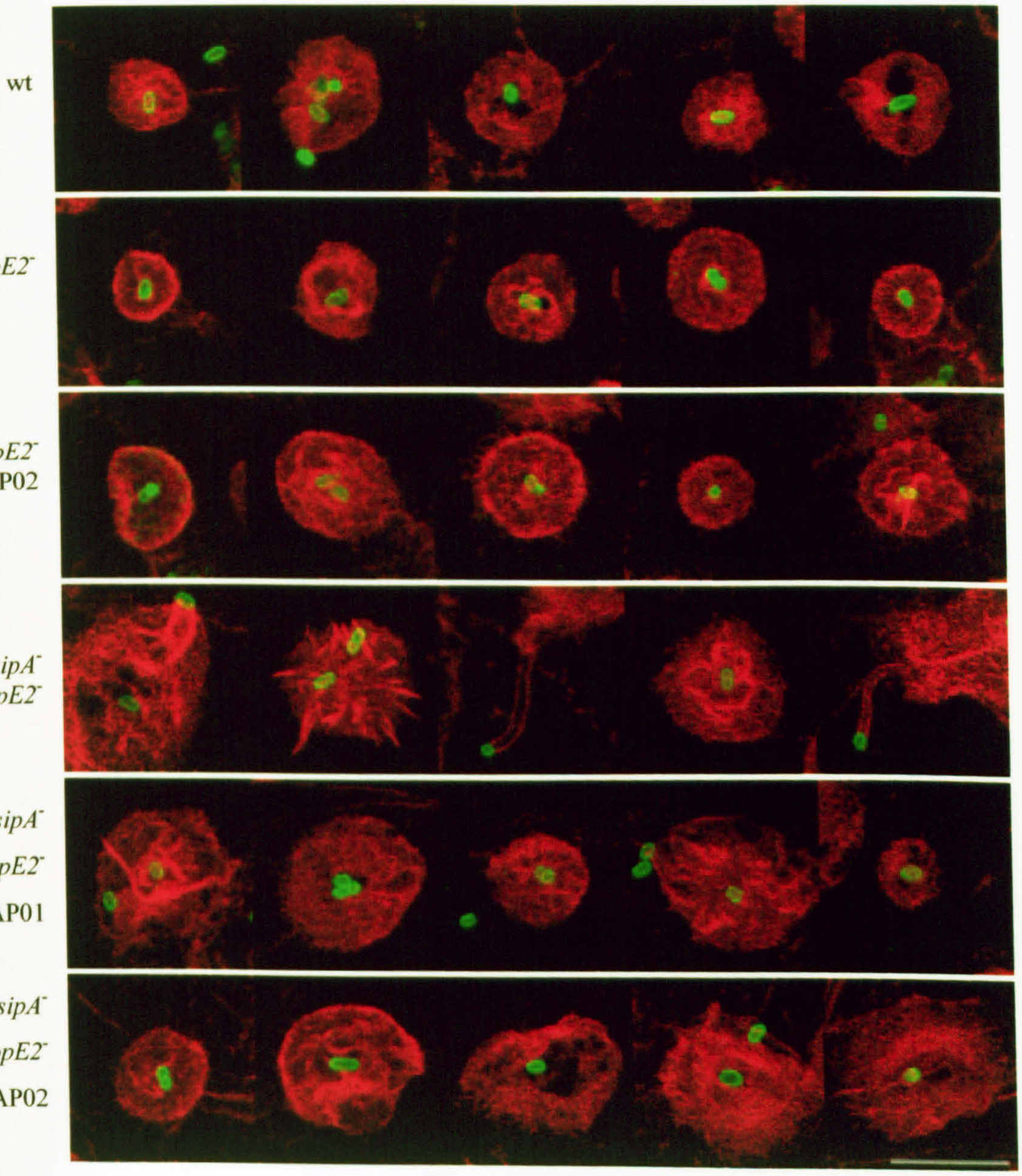

Figure 4.39 Quantifying morphology characteristics of ruffles induced by SL1344 wt and its isogenic *sopE2*⁻ and *sipA*⁻ *sopE2*⁻ mutants. The proportion of ruffles with finger-like protrusions (A) and with 10 or more filopodia (B) were measured. Infection was for 15 minutes, with ruffles being identified using TRITC-phalloidin staining of actin. Results are the mean of two independent experiments ± sem.

A

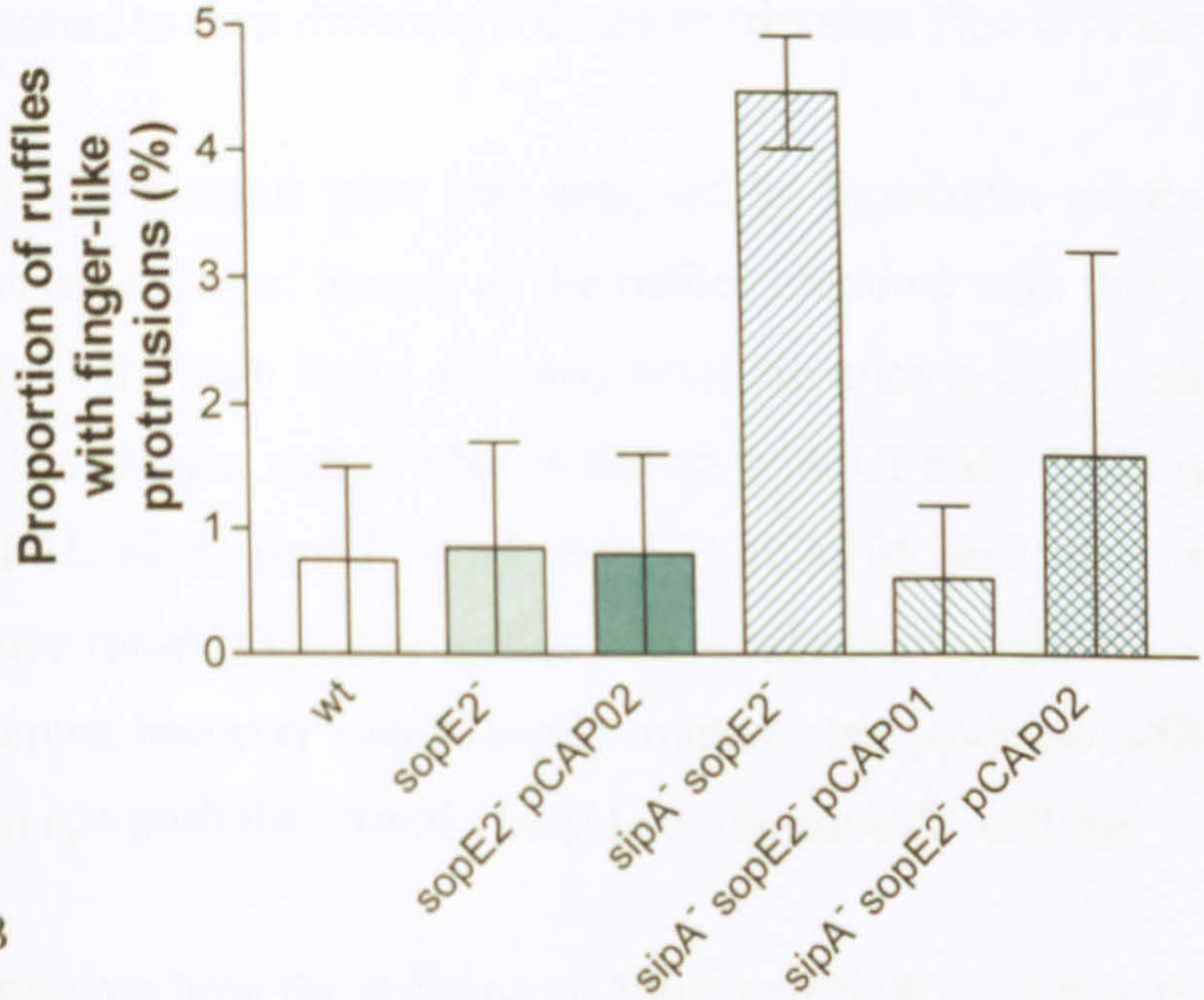

B

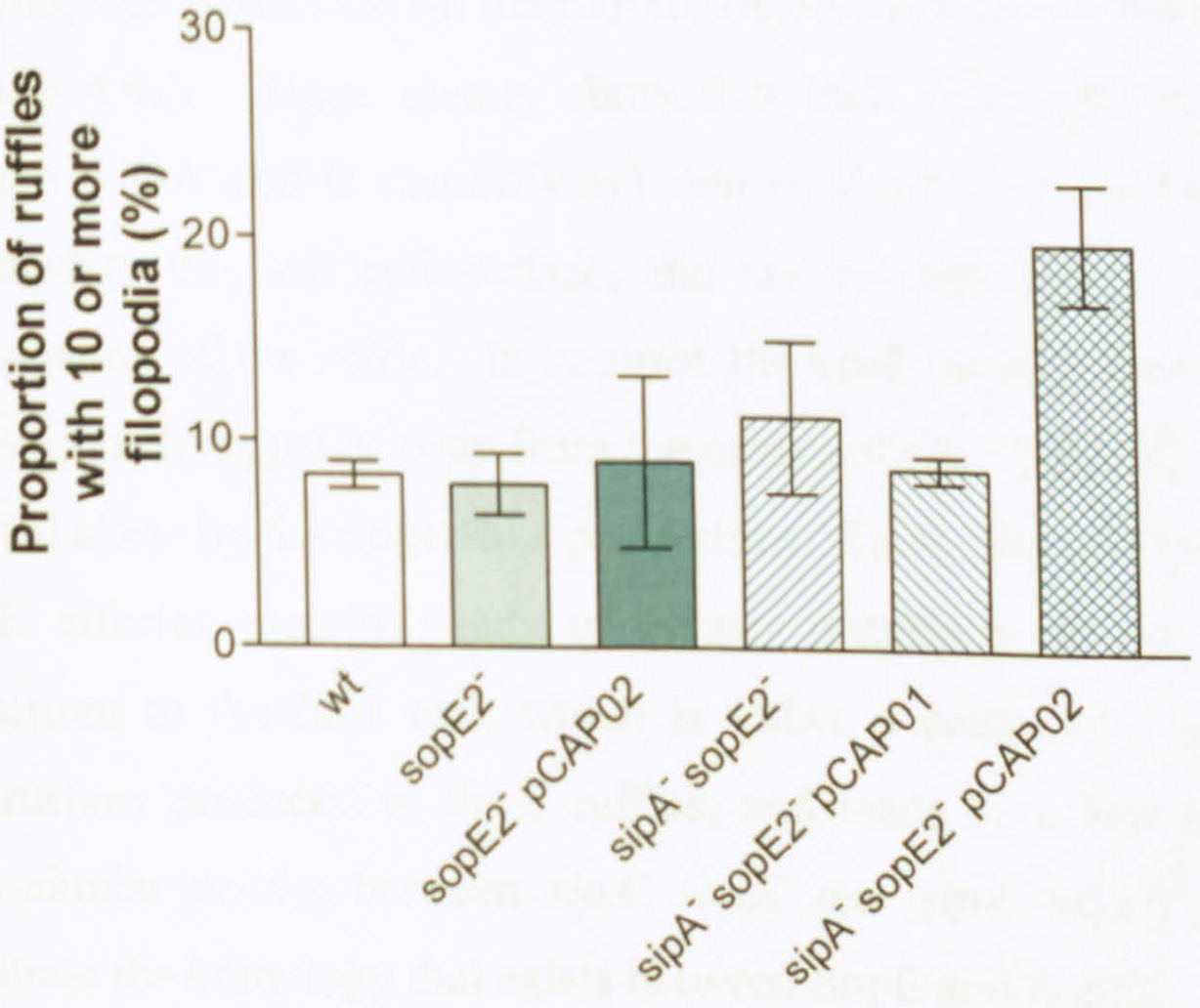

When examining the proportion of ruffles with 10 or more filopodia (Figure 4.39B), it was found that all the strains examined produced these ruffles at similar levels. This contrasts with the data from the SL1344 *sipA*⁻ *sopE*⁻ mutant where a quarter of all ruffles possessed 10 ≥ filopodia, an 8-fold increased compare to wild type (Figure 4.22). This indicates a potential difference in the signalling events that occur when either SopE or SopE2 is absent, and may correspond to their differing abilities to stimulate Rho GTPases.

The *sopE2* mutants were also analysed by time-lapse microscopy. Figure 4.40 shows examples of images of the ruffles obtained with this form of microscopy. A movie for each strain obtained from the microscopy is attached in Appendix III. The images repeat what is shown with CLSM. Wild type, *sopE2*⁻, *sopE2*⁻ pCAP02, *sipA*⁻ *sopE2*⁻, *sipA*⁻ *sopE2*⁻ pCAP01 and *sipA*⁻ *sopE2*⁻ pCAP03 all produce roughly circular ruffles of a similar size which have bacteria located in the centre; however a *sipA*⁻ *sopE2*⁻ mutant also produces ruffles with projections, which can push the bacteria outside of the zone of ruffling.

To measure how the deletion of SipA and SopE2 affects the positioning of the bacterium which may be a consequence of the change in ruffle morphology, tracking was performed on the movies obtained from the time-lapse microscopy (Figure 4.41). These clearly show that both wild type and *sopE2*⁻ bacteria (Figure 4.41A and B respectively) remain fixed in a position once they have attached to the host cell surface, and are not affected by the production and propagation of the ruffle. In contrast the *sipA*⁻ *sopE2*⁻ bacteria can be seen to travel quite long paths away from the centre of the ruffle, and in these cases it is pushed along by the finger-like protrusions. Thus, loss of SipA with either of the SopE effector proteins leads to greater instability in the attachment of the bacterium to the host cell, which is either a cause or a consequence of the protrusions produced in these ruffles, and leads to a less invasive phenotype. The similar results between *sipA*⁻ *sopE*⁻ and *sipA*⁻ *sopE2*⁻ bacteria serves to illustrate the homology that exists between SopE and SopE2.

Figure 4.40 Use of time-lapse phase-contrast microscopy to examine membrane ruffle propagation and development. Phase-contrast images of representative membrane ruffle generated in MDCK epithelial cells by *S.* Typhimurium SL1344 wild type and each of its isogenic *sopE2* mutants is shown. Scale bar, 5μm.

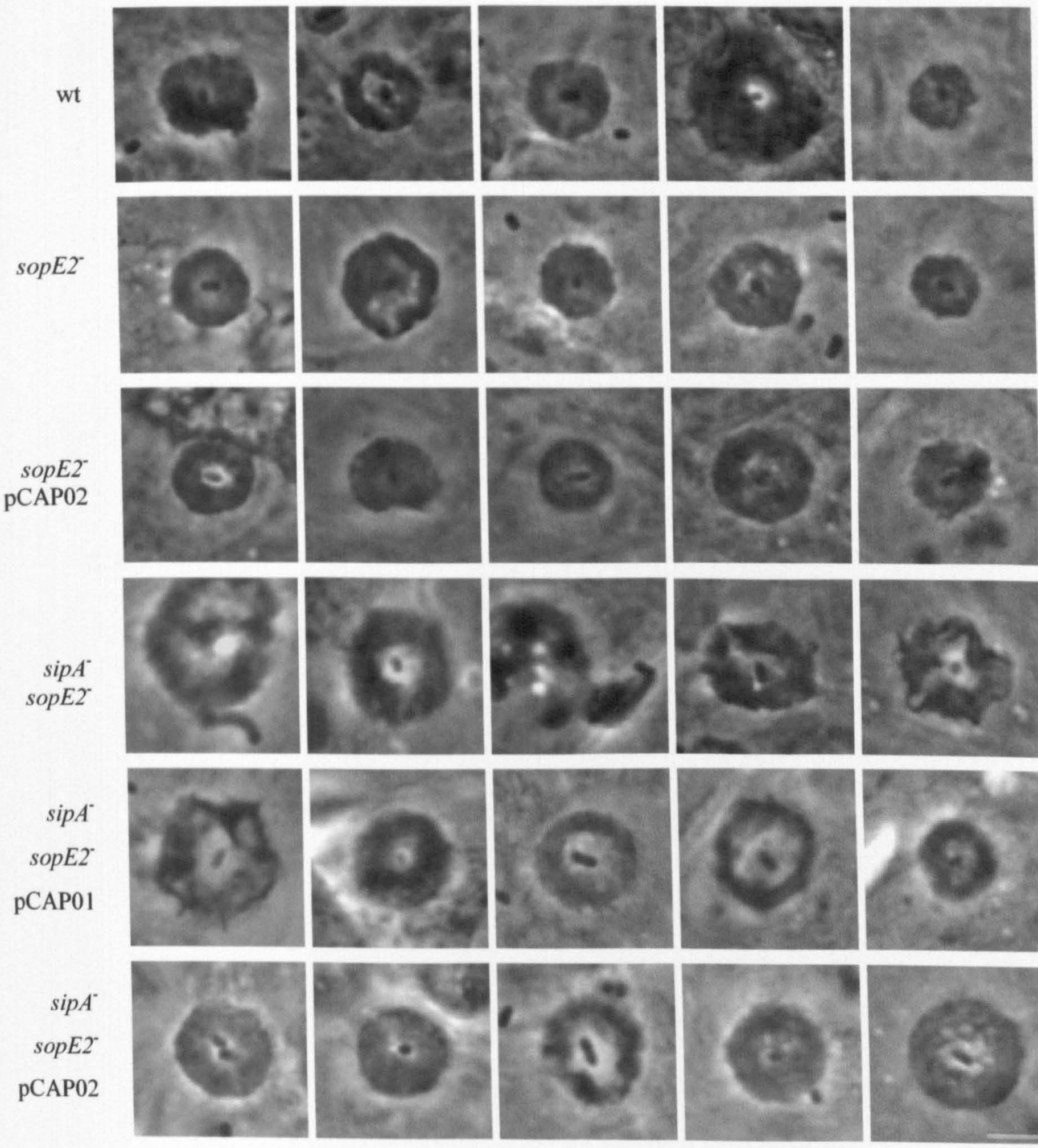

Figure 4.41 Use of tracking software to show how the positioning of the bacterium in relation to the ruffle it has induced is affected by loss of SopE2. Volocity 4.0 software was used to mark the positions of ~20 bacteria in the chosen field of view in each 10 second frame of a 15 minute time course. The triangle represents the initial position of the bacterium, and each subsequent position is marked with a dot. Scale bar 10μm.

A. SL1344 wt

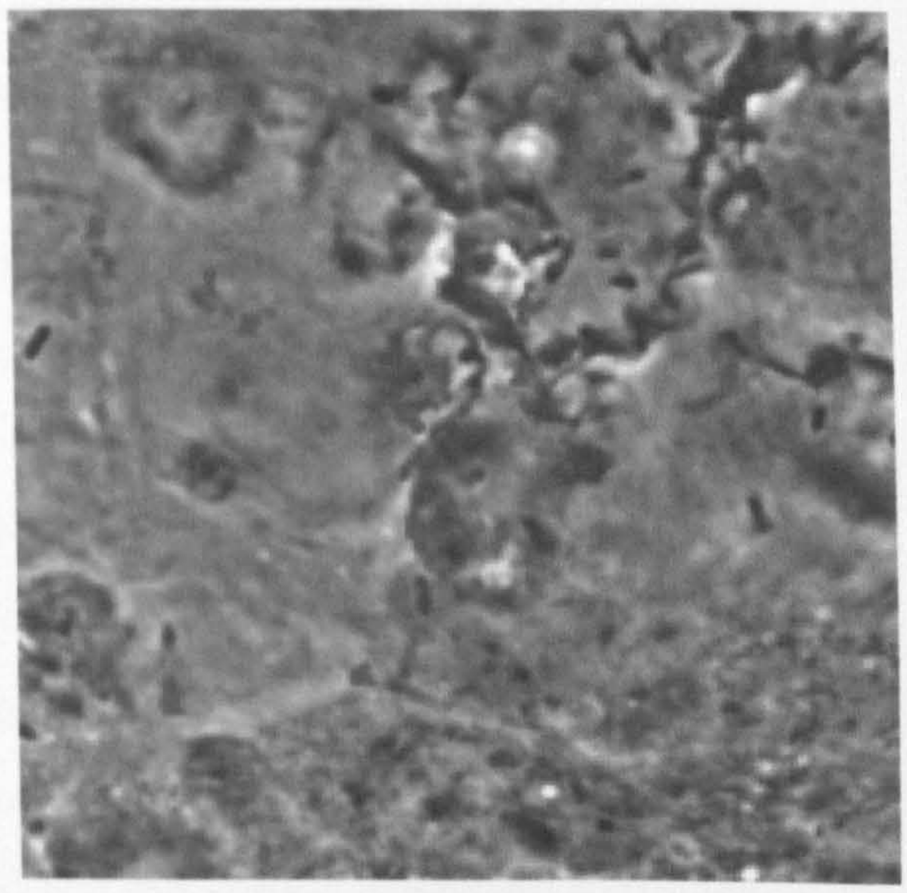

B. SL1344 *sopE2*$^{-}$

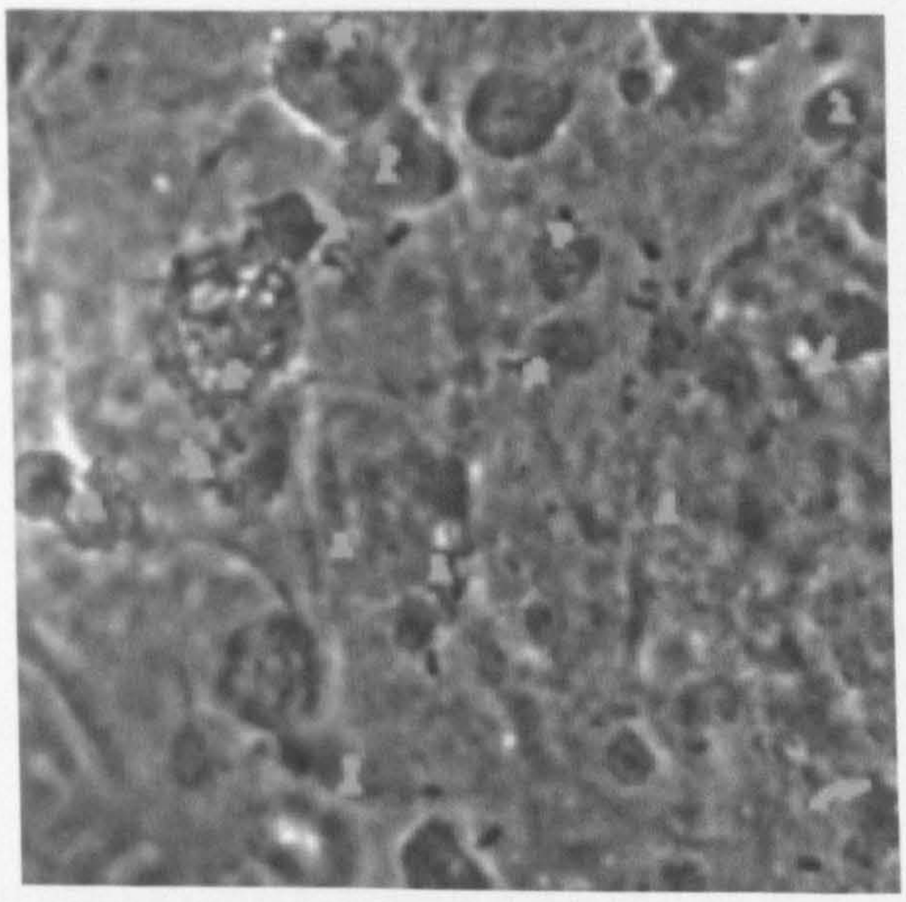

C. SL1344

sipA^{-}*sopE2*$^{-}$

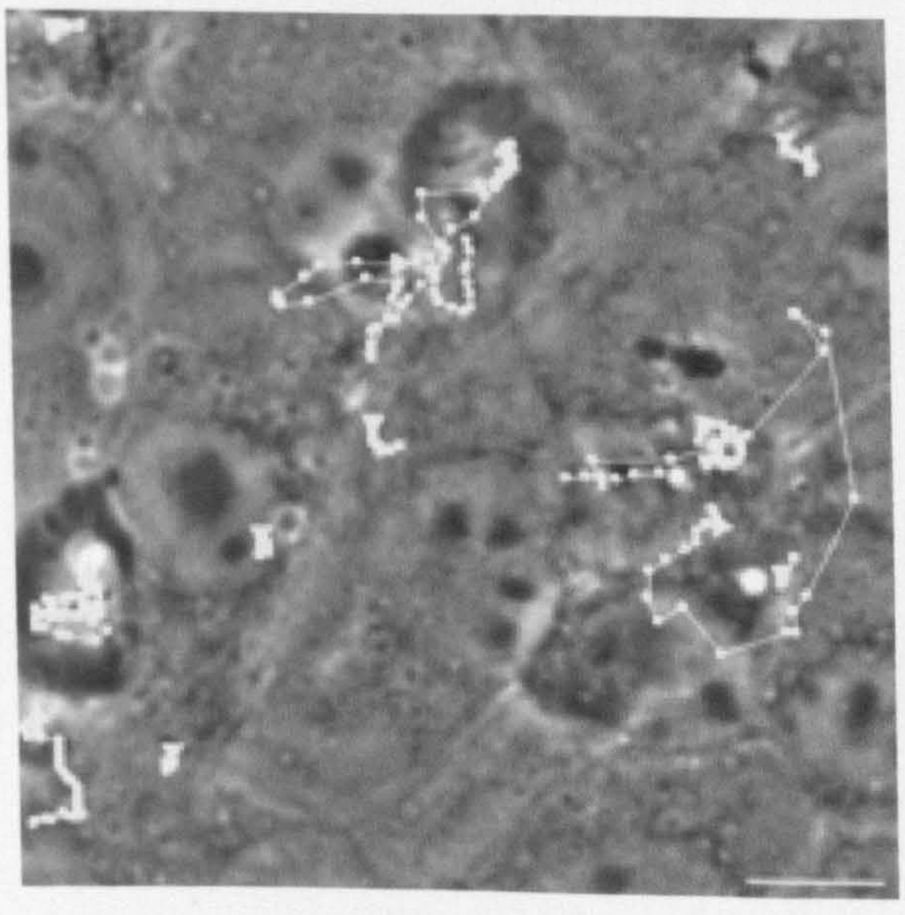

Measurements were made from the time-lapse microscopy of the average size of ruffles produced by the wild type and *sopE2*⁻ mutant and the average ruffle induction time after adherence. By eye, there did not appear to be a difference in the size of the ruffles induced by the wild type and *sopE2*⁻ mutant, and this was confirmed by measuring the maximum diameter achieved by thirty randomly selected ruffles from the phase-contrast time-lapse movies of three independent experiments. The mean diameter of wild type ruffles was 8.80 ± 0.411μm compared to 8.56 ± 0.488μm for the *sopE2*⁻ mutant.

A difference in behaviour between the *sopE*⁻ mutant and *sopE2*⁻ mutant, which may relate to the difference in their host cell signalling, was also evident when examining ruffle kinetics. The *sopE*⁻ mutant had been found to take significantly longer to induce ruffle formation after adhesion to the cell surface than wild type (Table 4.5 and 4.6) but the *sopE2*⁻ mutant induced ruffles in the same amount of time as the wild type (30 seconds) (Table 4.8). Bizarrely the transcomplemented mutant took significantly longer to induce ruffles. Perhaps the amounts of SopE2 expressed by this strain interfered with normal host cell functions and therefore ruffle initiation events. Alternatively, less SopE may have been secreted or had a lower concentration relative to SopE2, so the transcomplemented mutant behaves effectively like a *sopE*⁻ mutant, taking longer to induce ruffling. The *sipA*⁻ *sopE2*⁻ mutant behaved like the wild type, just as the *sipA*⁻ *sopE*⁻ mutant had.

Since a *sopE2*⁻ mutant has SopE stimulating host cell signalling and producing ruffles of wild type size, while a *sopE*⁻ mutant has SopE2 stimulating host signalling and producing small ruffles, it potentially indicates lack of Rac1 activation by SopE is the cause of these phenotypes; Cdc42 being activated by both SopE and SopE2 while only Rac1 is activated by SopE (Hardt *et al.*, 1998a; Friebel *et al.*, 2001; Stender *et al.*, 2000). Of course alternative protein/signalling pathways may also be affected, but this data indicates the advantage possessing both copies of the SopE protein has, leading to an increased amount of cross talk with the host to ensure the ruffle is created rapidly to allow invasion.

Table 4.7 Comparison of the kinetics of ruffle induction of SL1344 wild type and *sopE2*⁻ mutants using time-lapse microscopy. The time interval between bacterial binding to MDCK cells and induction of membrane ruffling was obtained from phase-contrast video microscopy. Data expressed as medians with the number of productive bacterial-cell interactions analysed (n), and the minimum (min.) and maximum (max.) time intervals measured. Asterisks denote a significant difference assessed by the Kruskal Wallis test; followed by Dunn's Multiple Comparison Test at a level of $P<0.05$.

		wild type	*sopE2*⁻	*sopE2*⁻ pCAP02	*sipA*⁻ *sopE2*⁻
Ruffle induction time after adherence (s)	n	90	90	90	83
	Median	**30**	**30**	**45***	**30**
	Min.	10	10	10	10
	Max.	170	250	380	140

4.3.15. Investigation into the relationship between SipA and SopB

While SopE and SopE2 are believed to be the main contributors to indirect actin polymerisation via activation of Rho GTPases, SopB (SigD) has also been shown to signal via these proteins (Zhou *et al.*, 2001; Patel and Galan, 2006). Therefore, an investigation into the effect of *sipA* deletion in SL1344 lacking SopB was begun.

Phage transduction was used to transfer the *sipA* deletion into SL1344 *sopB*⁻, provided by Dr O. Steele-Mortimer (Rocky Mountain Laboratory, U.S.A.). As before, a PCR using the 5'pcr-SipA and 3'pcr-SipA primers were used to check the loss of *sipA* from chloramphenicol resistant transformants; the wild type gene being amplified to produce a PCR product of 2.5kb while *sipA*⁻ *sopB*⁻ mutants produced a product of ~1kb, pertaining to the deletion of *sipA*. Once a suitable mutant was obtained it was examined alongside the *sopB*⁻ and *sopB*⁻ transcomplemented mutant in ruffling and invasion assays (Figure 4.42).

Figure 4.42 Comparing the ability of SL1344 wild type and its isogenic *sopB*⁻ mutant to induce ruffles (A) and invade (B) MDCK cells. Infection was for 15 minutes, with the ability to induce ruffle formation being measured using TRITC-phalloidin staining of actin, and the ability to enter cells being measured using differential staining of adhered bacteria. Results measuring the number of ruffles are the mean of three independent experiments ± sem.

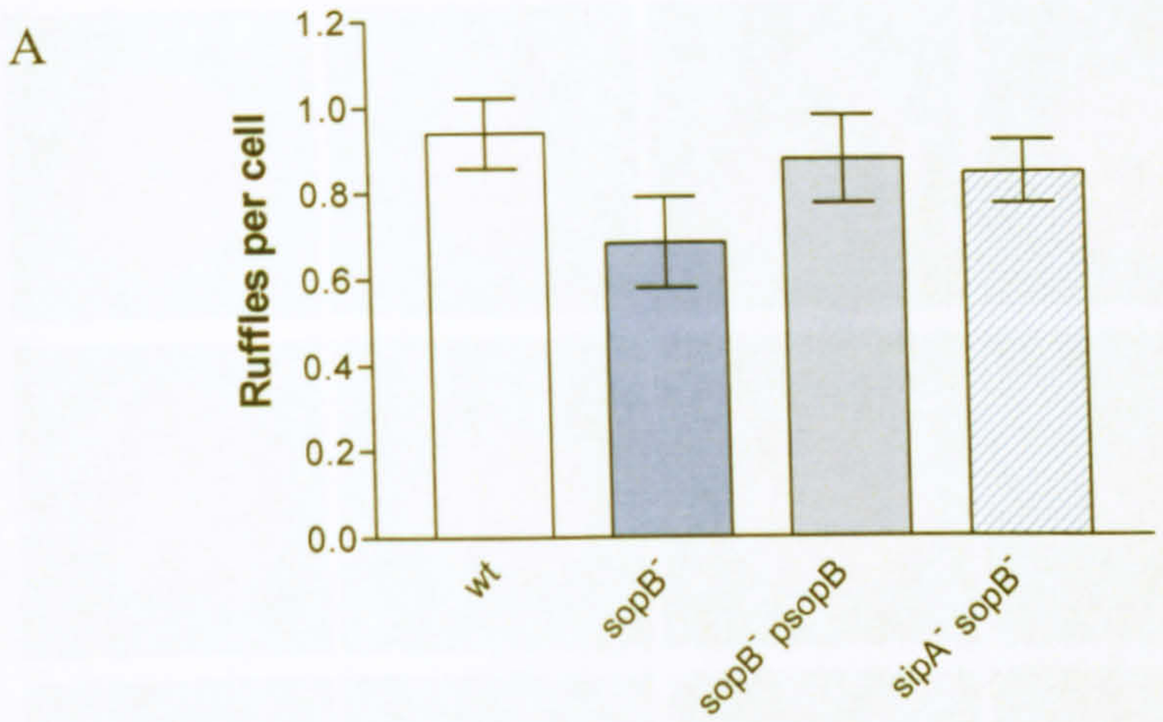

The ruffling and invasion ability of the *sopB*⁻ and *sipA*⁻ *sopB*⁻ mutants were found to be similar to wild type (Figure 4.42). These results confirm loss of a single effector protein or loss of SipA with either SopE, SopE2 or SopB does not affect the number of ruffles that can be generated by *Salmonella*, which is due to the redundancy these effectors share. In the invasion assay, similar numbers of wild type, *sopB*⁻, *sopB*⁻p*sopB* and *sipA*⁻ *sopB*⁻ bacteria were found per cell. Therefore, SopB appears from all the effectors studied here (SipA, SopE and SopE2) least important in invasion at relatively early time points. Additionally, of interest is the fact that absence of SipA and SopB does not lead to decreased invasion. This indicates the presence of SopE and SopE2 may be sufficient for invasion.

Figure 4.43 CLSM images showing the morphology of membrane ruffles induced by wild type and *sopB*⁻ mutants of *S.* Typhimurium SL1344. Each image shows a representative selection of ruffles from TRITC-phalloidin-stained MDCK cells infected for 15 minutes. Bacteria are stained with FITC. Each image is presented as a projected series of optical sessions showing membrane ruffles in their entirety. Scale bar 10μm.

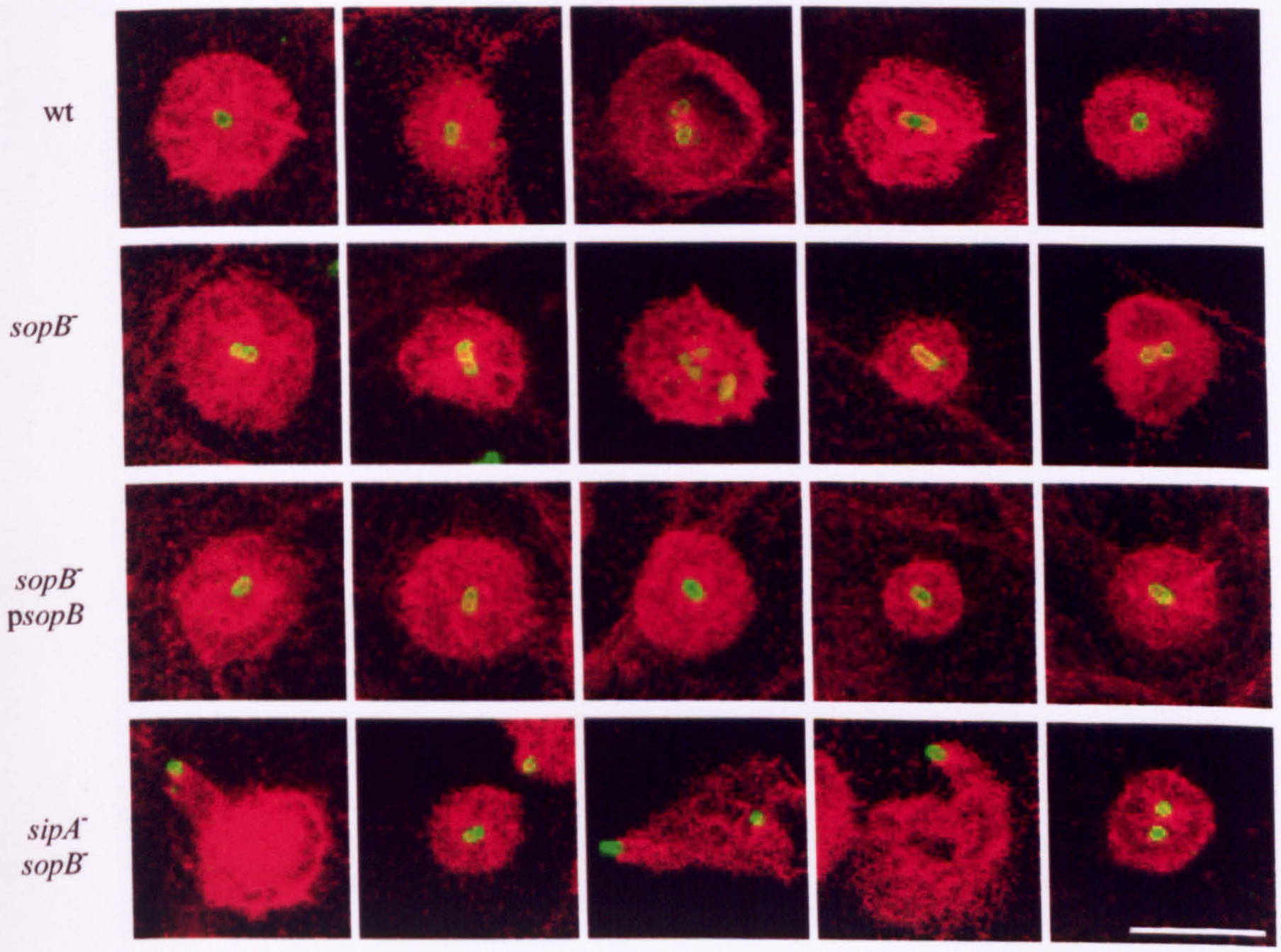

Figure 4.44 CLSM images showing actin accumulation around *Salmonella* containing vacuoles of *sopB*⁻ mutants. Panels A and C shows a selection of ruffles from TRITC-phalloidin-stained MDCK cells infected for 15 minutes with wild type (Panel a) or *sopB*⁻ (Panel c). Panels b (wild type) and d (*sopB*⁻) shows an overlay of the FITC-stained bacteria with the TRITC-phalloidin-stained MDCK cell. Each image is presented as a projected series of optical sessions showing membrane ruffles in their entirety. The white arrows mark SCVs surrounded by actin. Scale bar 30μm.

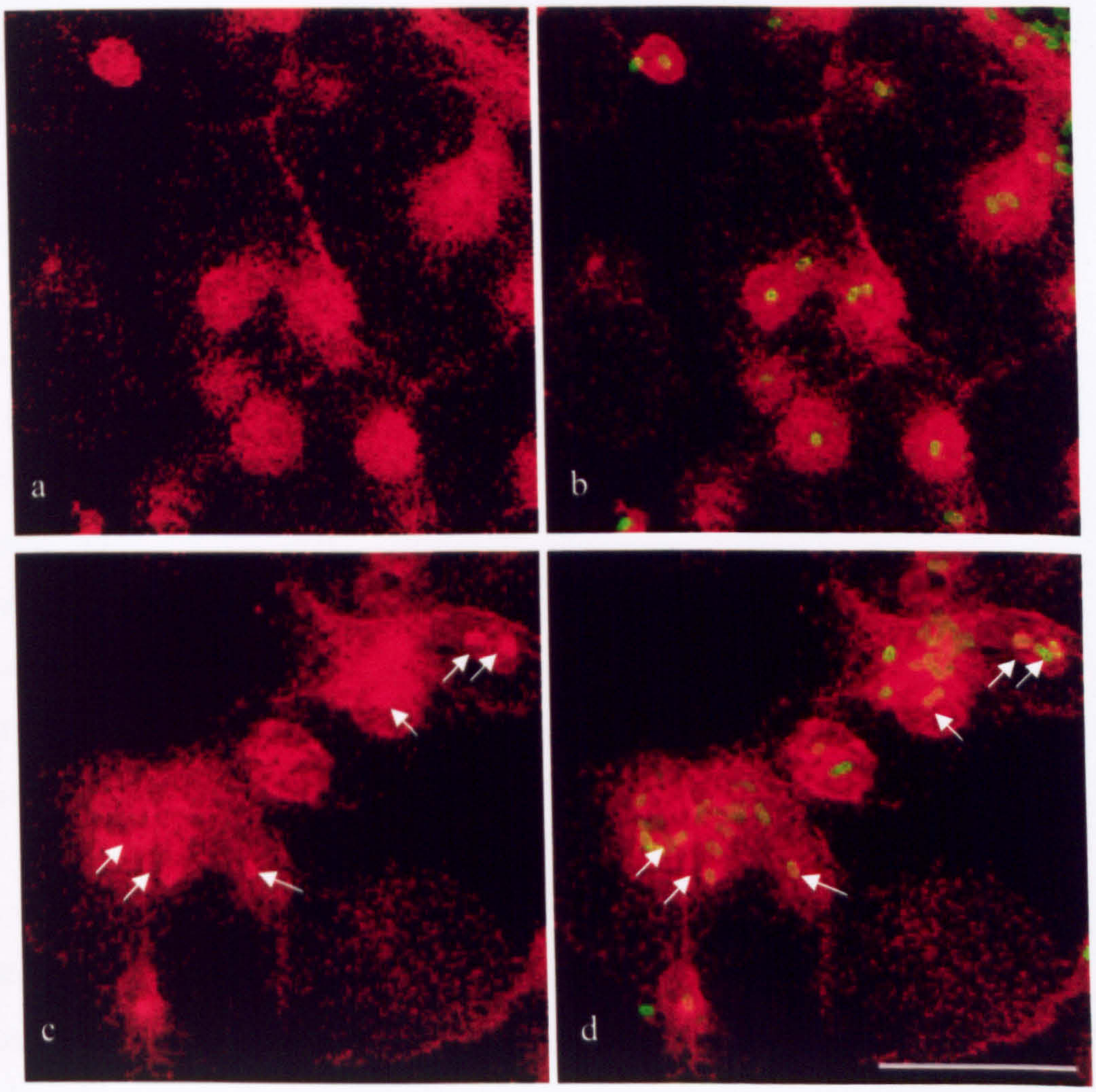

The morphology of the *sopB*⁻ mutant ruffles were like those of the wild type: circular ruffles with bacteria located in the centre (Figure 4.43). However, a ring of TRITC-phalloidin could be visualised around many of the *sopB*⁻ bacteria, which was not apparent with the wild type (Figure 1.40). This has been described before (Hernandez *et al.*, 2004), and represents accumulation of actin around the *Salmonella*-containing vacuoles (SCV). Expression of *sopB* from a plasmid removes the appearance of these rings, thus restoring the wild type phenotype, and showing SopB is responsible for the actin associated with the SCVs.

Loss of SipA and SopB leads to ruffles that possess protrusions like those found on *sipA*⁻ *sopE*⁻ and *sipA*⁻ *sopE2*⁻ ruffles. It therefore appears that removing SipA with one of the effectors known to stimulate Rho GTPases is responsible for this altered ruffle morphology. However, since the *sipA*⁻ *sopB*⁻ mutant does not exhibit reduced invasion, it suggests this altered behaviour in ruffling does not necessarily affect the ability of the bacterium to enter the cell. It would appear that SipA interacts with SopE, SopE2 and SopB in a way that has not previously been appreciated.

To establish whether the finger-like protrusions produced by the *sipA*⁻ *sopB*⁻ mutant were similar to those induced by the *sipA*⁻ *sopE*⁻ and *sipA*⁻ *sopE2*⁻ mutants, time-lapse microscopy was used to study how dynamic these structures were. Alongside the *sopB*⁻ and *sipA*⁻ *sopB*⁻ mutants, a SL1344 triple mutant lacking SipA, SopE and SopB (*sipA*⁻ *sopE*⁻ *sopB*⁻) that had been newly created, by transducing *sipA*⁻ *sopB*⁻ with the *sopE*⁻ mutation, was trialled. Appendix III provides a movie for each of these mutants to illustrate their ruffling behaviour (Movies B18-B21).

From Figure 4.45 it is clear that the observations made using confocal scanning laser microscopy (Figure 1.39) were valid. SL1344 wild type and *sopB*⁻ share similar ruffle morphology, while the ruffles of the *sipA*⁻ *sopB*⁻ mutant appear analogous to those observed with the *sipA*⁻ *sopE*⁻ and *sipA*⁻ *sopE2*⁻ mutants. The triple mutant SL1344 *sipA*⁻ *sopE*⁻ *sopB*⁻ had ruffles that were similar to those of the double mutants but there appear to be key differences. Namely the 'wild

type' ruffle formed prior to the production of a finger seemed more diffuse and rapidly disappeared leaving the finger-like protrusion moving the bacteria across the cell monolayer. A consequence of this behaviour was that all bacteria were moved away from their initial point of contact with the cell surface. This is best illustrated in Figure 4.45, where the positions of the bacteria are tracked through the time-course. The movement of the wild type and *sopB*⁻ mutant are minimal (Figure 1.42 A and B respectively), while absence of SipA and SopB together shows a larger number of the bacteria being moved away from where they initially adhered, and deletion of SipA, SopE and SopB leads to all the bacteria moving position during ruffling.

This initial work with the *sipA*⁻ *sopB*⁻ mutant and *sipA*⁻ *sopE*⁻ *sopB*⁻ mutant indicates removal of SipA with any of the effector proteins indirectly controlling actin reorganisation causes a disruption in the interaction with host cell signalling pathways, and that as further effector proteins are removed the phenotype becomes more extreme, suggesting a considerable effect on the ability of that bacterium to induce ruffling and invade.

Figure 4.45 Use of time-lapse phase-contrast microscopy to examine the membrane ruffle propagation and development of *sopB*⁻ mutants. Phase-contrast images of representative membrane ruffle generated in MDCK epithelial cells by *S.* Typhimurium SL1344 wild type, *sopB*⁻, *sipA*⁻ *sopB*⁻ *and sipA*⁻ *sopE*⁻ *sopB*⁻ mutants is shown. Images are taken from one sole experiment performed with these strains. Scale bar 5μm.

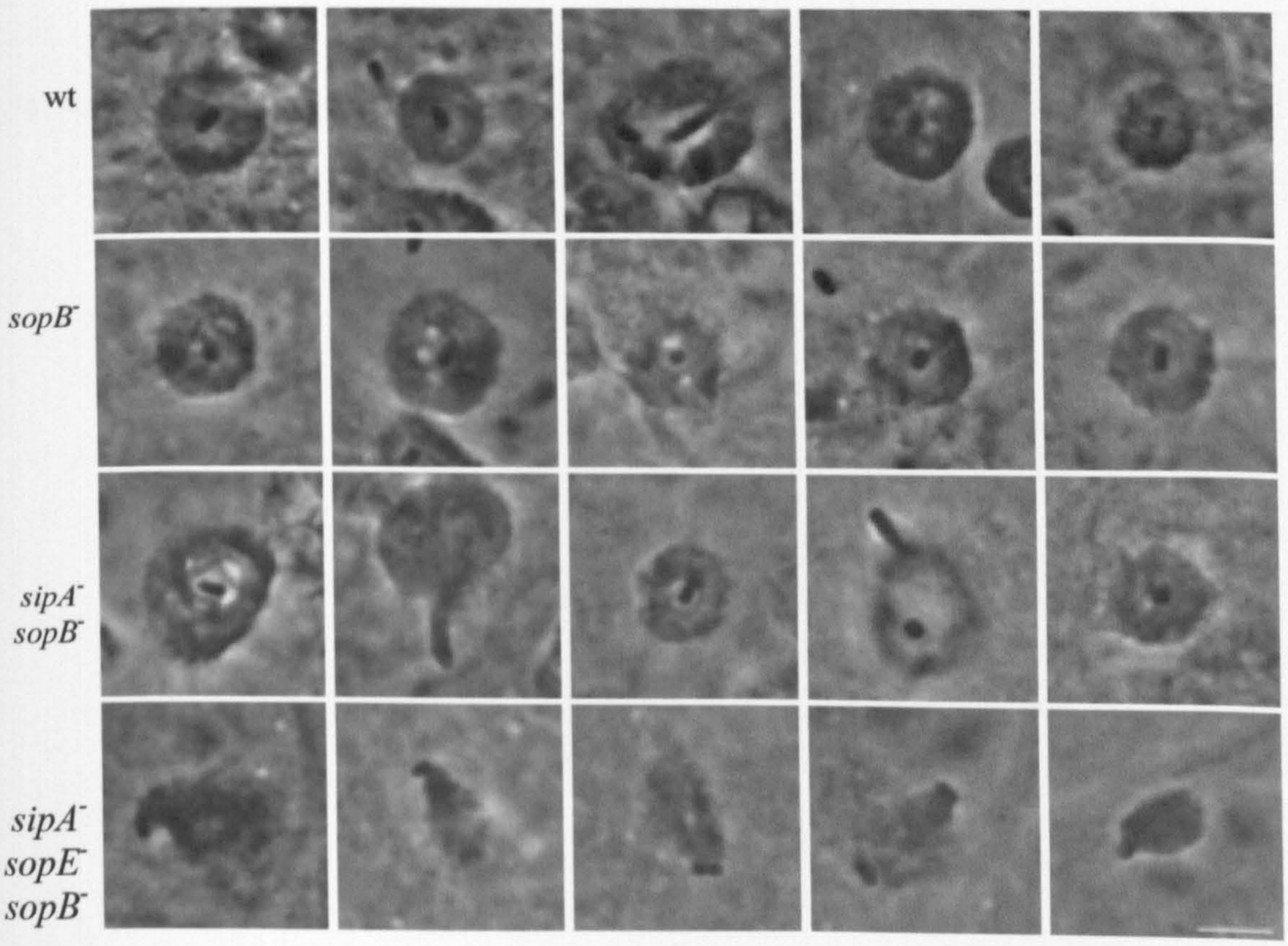

Figure 4.46 Use of tracking software to show how the positioning of the bacterium in relation to the ruffle it has induced is affected by loss of SopB. Volocity 4.0 software was used to mark the positions of ~20 bacteria in the chosen field of view in each 10 second frame of a 15 minute time course. The triangle represents the initial position of the bacterium, and each subsequent position is marked with a dot. Scale bar 10μm.

A. SL1344 wild type

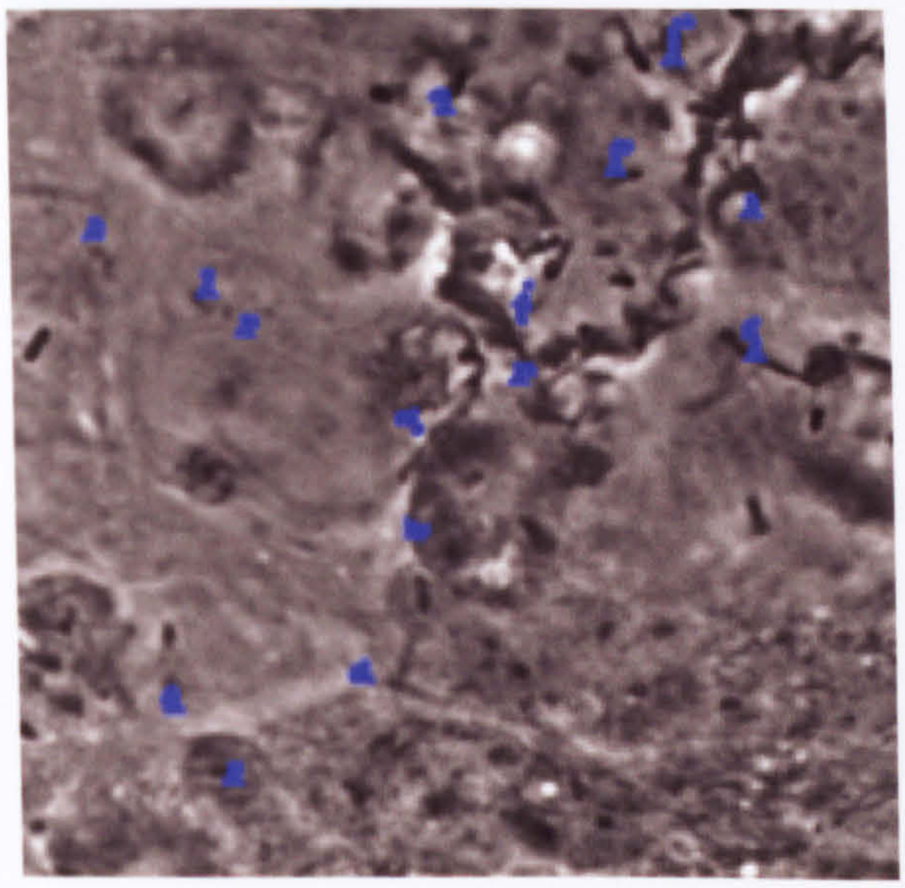

B. SL1344 *sopB*⁻

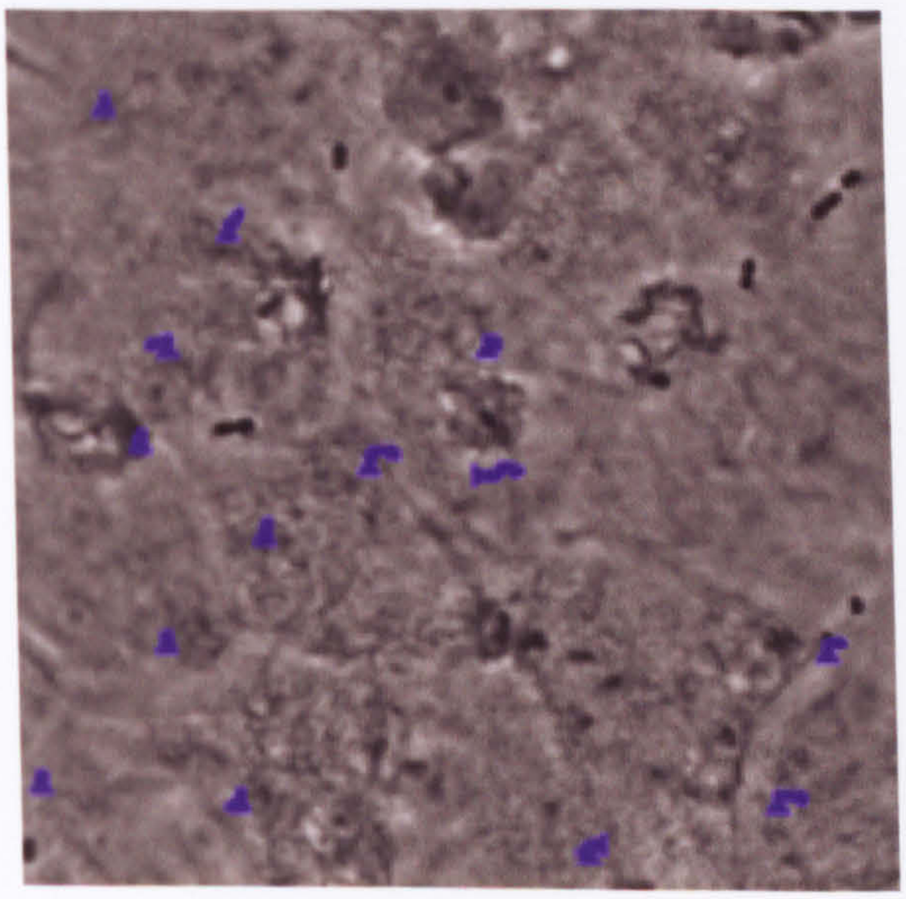

C. SL1344 *sipA*⁻ *sopB*⁻

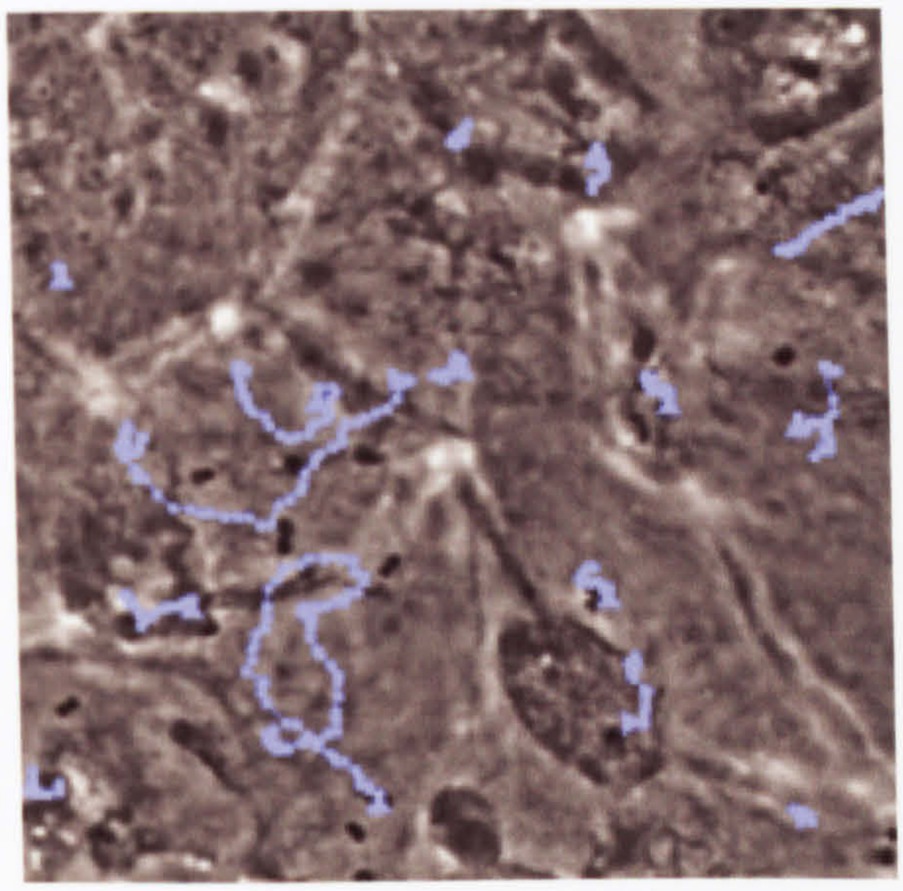

D. SL1344 *sipA*⁻ *sopE*⁻ *sopB*⁻

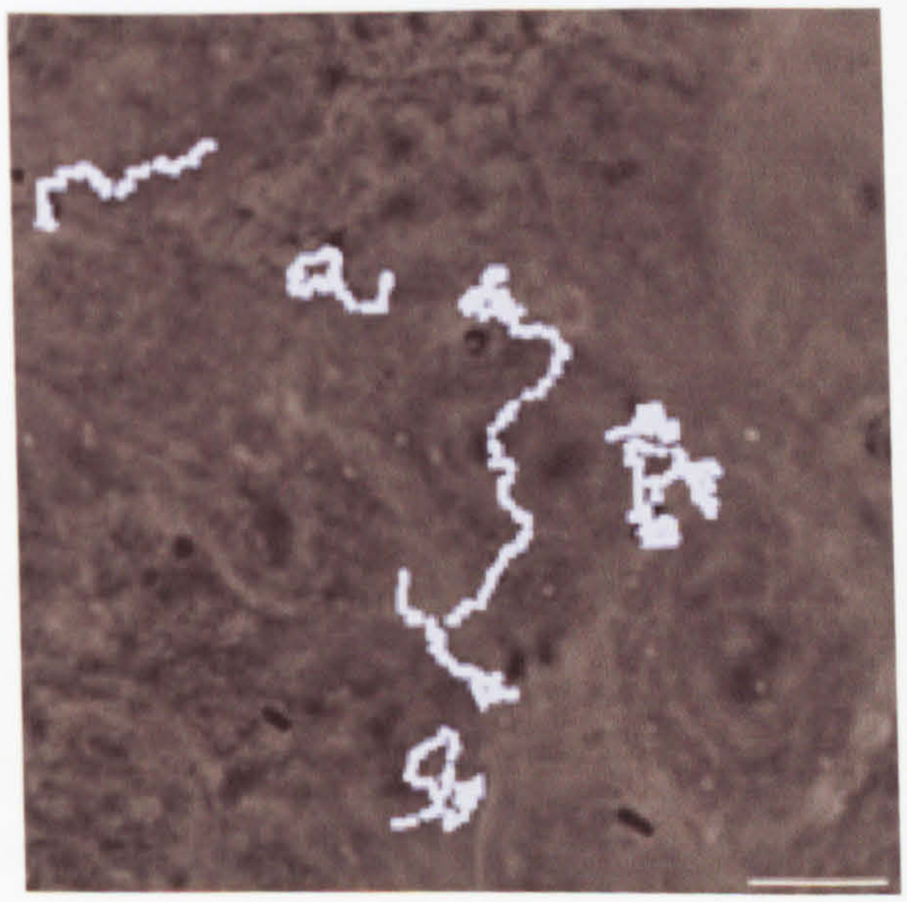

4.4. Discussion

The original studies examining the role of SipA in *Salmonella* pathogenesis (Kaniga *et al.*, 1995b; Hueck *et al.*, 1995), had determined that while this protein was encoded in *Salmonella* Pathogenicity Island 1 (SPI-1), where other proteins important for *Salmonella* invasion were also encoded (Galan and Curtiss III, 1989; Ginocchio *et al.*, 1992; Groisman and Ochman, 1993; Altmeyer *et al.*, 1993; Kaniga *et al.*, 1994; Collazo *et al.*, 1995), and it was secreted through TTSS-1 and translocated into the host cell, SipA did not have a role in invasion. Subsequent studies which reduced the length of infection time (Zhou *et al.*, 1999a; Jepson *et al.*, 2001; Higashide *et al.*, 2002), coupled with an increasing understanding of the structure and biochemistry of this protein (Mitra *et al.*, 2000; Galkin *et al.*, 2002; Lilic *et al.*, 2003), revealed that in fact SipA is involved with allowing *Salmonella* to gain access to the host cell.

The role of SipA in invasion has always been attributed to its direct interaction with F-actin, and further interactions with host and bacterial proteins to produce long bundles of F-actin suitable for supporting the membrane protrusions used to bring the adhered bacterium into the cell (McGhie *et al.*, 2001, 2004; Zhou *et al.*, 1999a; Zhou *et al.*, 1999b). However, Jepson *et al.* (2001) hypothesised that SipA may accelerate entry of *Salmonella* into cells by a mechanism distinct from, or secondary to, the membrane ruffles. Their data had shown the ability of *Salmonella* to form membrane ruffles was not affected by the absence of SipA, but loss of SipA reduced the ability of the bacterium to enter the ruffle. At this time it had also been shown that absence of SopE and SopE2 together abolished the ability of *S.* Typhimurium to induce the actin rearrangements required for entry without completely eliminating invasion (Stender *et al.*, 2000), potentially supporting a secondary mechanism of invasion, in which SipA could have a role. While it was later shown that SopB/SigD had the ability to stimulate actin rearrangements required for invasion, and it was SopB with SopE and SopE2 that were essential for invasion (Zhou *et al.*, 2001), it still did not explain the reduced ability of *sipA* mutants to enter the ruffles, nor exclude the possibility for a secondary uptake mechanism. This has been studied here.

To determine additional roles for SipA during invasion it was investigated whether the role of SipA is the same in all strains of *Salmonella enterica* serovar Typhimurium. An obvious difference in the behaviour of a *sipA* mutant in one strain compared to the behaviour of *sipA* mutants in other strains may yield clues to an additional role for SipA. Since SopE is encoded within the genome of a bacteriophage and present in only a small proportion of *S.* Typhimurium strains (Hardt *et al.*, 1998b; Mirold *et al*, 1999), one of which includes SL1344 used in all the work determining the role of SipA, it seemed logical to examine strains that lacked SopE, particularly since the redundancy of effector proteins can hide some phenotypes. To this end, naturally *sopE*$^-$ strains F98 and 12023 were chosen to be studied alongside SL1344 and S1579/94 that possessed SopE. SL1344 was included in order to compare the data obtained with that published in the literature.

The initial experiments examined the behaviour of the *sipA*$^-$ mutants after a 15 minute infection of MDCK cells. As Jepson *et al.* (2001) reported, the number of ruffles induced in this time period did not differ between the wild type and *sipA*$^-$ mutant in SL1344, and this behaviour was found to be the same in the other strains of serovar Typhimurium. Indeed, video microscopy revealed the time taken between adherence to the cell surface and initiation of ruffling was identical between the *sipA*$^-$ mutant and SopE$^+$ wild type, indicating the potential for the same number of ruffles to be produced in the same time period.

When confocal, scanning electron and phase-contrast microscopy were all used to compare the ruffles of a wild type and its isogenic *sipA*$^-$ mutant, these ruffles, apart from the changes in morphology seen with the *sipA*$^-$ *sopE*$^-$ mutants (discussed later), appear similar to wild type - they are produced by localised changes in the membrane and, as CLSM and time-lapse microscopy of GFP-actin MDCK cells reveals, filled with F-actin. This replicates the data of Jepson *et al.* (2001) whose data contrasted with the previous reports of a *sipA* mutant producing diffuse rather than localised actin rearrangements (Zhou *et al.*, 1999a). Reasons for the different observations have been hypothesised to be due to difference in the infection protocol or the microscopy techniques used, since Jepson *et al.* (2001) observed the same effects in HeLa cells, the cell line used by

Zhou *et al.* (1999a). The actin rearrangements being 'diffuse rather than localised' may potentially be a consequence of the ability of *sipA*⁻ bacteria to detach from the ruffles they have induced and initiate another ruffle in the immediate vicinity. The merging of these ruffles would produce a large area of F-actin that may give the impression of the ruffles not being localised. The ruffles may also not have been considered localised by Zhou *et al.* (1999a) because the bacteria are often located at the periphery of ruffles or are completely absent. Indeed a second report by one of the original authors (Higashide *et al.*, 2002) shows images where the ruffles of the *sipA* mutant do appear to be localised, although they show by confocal optical z-sections there is less F-actin associated with these ruffles, thus the terminology used in the original paper may account for the difference in reports, with diffuse referring to the amount of F-actin present. The amount of F-actin associated with ruffles in this study was not measured, and therefore, it is impossible to comment on whether this effect is also found in MDCK cells, however, it would appear sensible given that SipA is involved with preventing the depolymerisation of F-actin.

The 15 minute invasion data showed that in strains SL1344, S1579/94 and F98 absence of SipA significantly reduces invasion. Since the same effect was found between strains with $SopE^+$ and $SopE^-$ genotypes, this indicates the invasion defect is not dependent on the presence/absence of SopE. It is widely accepted that SipA exerts its affect at relatively early time points in invasion i.e. <30 minutes (Zhou *et al.*, 1999a), although in one study the effect was shown to be limited to time points ≤15 minutes (Jepson *et al.*, 2001). *sipA*⁻ mutants of SL1344, S1579/94 and F98 were shown here to have reduced invasion after 5 and 15 minute length infections. Since Jepson *et al.* (2001) had not found a SL1344 *sipA*⁻ mutant to have an invasion defect in comparison to the wild type after an infection length of 15 minutes it was decided to investigate why a difference was found here. Multiplicity of infection and the strain of MDCK cells used in the invasion protocol were tested for their effects on the invasion of the wild type and *sipA*⁻ mutant, and found to be unimportant. Furthermore, use of the SL1344 wild type and *sipA*⁻ mutant from the Jepson *et al.* (2001) paper failed to replicate the results published in the paper, reproducing the results of the

SL1344 wild type and *sipA*⁻ mutant used in this study. It can only be assumed there is some fundamental difference in the invasion protocol used between the studies for these different results; perhaps a property of the cell line used has changed through passage or the density of cells analysed for invasion is different.

Other reports stated the invasion defect of a SL1344 *sipA*⁻ mutant was seen until 20 minutes (Higashide *et al.*, 2002) or 30 minutes (Zhou *et al.*, 1999a). The data presented here for SL1344, corresponds with these reports since at 30 and 60 minutes no statistical difference was observed in invasion between wild type and *sipA*⁻. However, while there is no statistical difference there is still an obvious reduction in *sipA*⁻ invasion and this is much greater than previously reported (Zhou *et al.*, 1999a). Recent data from Raffatellu *et al.* (2005) using complementation of a *sipA sopABDE2* mutant of strain 14028 with different effector proteins showed SipA enhanced the invasion of the mutant 6-fold in non-polarised HT-29 cells after an hour long infection, but there was no increase in non-polarised or polarised T84 cells. This indicates the invasion data generated using cultured cell lines is partly dependent on the cells used in the assay, and the importance of different effectors will alter according to the properties of the cells. This may explain why with SL1344 invasion of MDCK strain I cells a larger defect in *sipA*⁻ invasion is observed after 30 and 60 minutes of invasion than has been previously reported in other cell lines (Hueck *et al.*, 1995; Kaniga *et al.*, 1995a; Kaniga *et al.*, 1995b; Zhou *et al.*, 1999a). This difference not being found statistically different may also reflect the rigorous statistical testing applied. S1579/94 and F98 *sipA* mutants exhibited reduced invasion at 30 and 60 minutes, although only in S1579/94 is this difference considered statistically different, indicating that essentially SL1344, S1579/94 and F98 strains of *S.* Typhimurium act similarly.

S. Typhimurium strain 12023 differs in its invasion properties compared to the other strains examined. The *sipA*⁻ mutant of strain 12023 after 15 minutes had invasion levels similar to the wild type which could indicate that in some strains of *S.* Typhimurium there may be differences in the importance of specific effector proteins. However, since this *Salmonella* strain was severely hampered in its invasion of MDCK cells regardless of the *sipA*⁻ mutation, it suggests that

there may be other properties of this strain masking the effect of SipA. A further, more extensive study of *Salmonella* strains may therefore provide additional information in regards to whether effector proteins have the same role and importance in each.

The reduced invasion of *sipA*⁻ bacteria was demonstrated to be caused by a significant time lag of entrance into cells by these bacteria compared with wild type bacteria, or for the bacteria not to enter at all (Jepson *et al.*, 2001). The time lag was caused by *sipA*⁻ bacteria being thrown to the periphery of the ruffles they induced and then having to move back to the centre for uptake, or where the bacteria had detached from the ruffle periphery, having to produce a new ruffle for its uptake. This behaviour was also observed for the *sipA*⁻ mutants of SL1344 and S1579/94 included in this study. However, in F98 and 12023, a much more dramatic phenotype was observed, for not only were the bacteria cast to the edge of the ruffle but they were pushed beyond the ruffle boundary on a highly dynamic membrane protrusion. The ruffles were also associated with an increased number of filopodia. The absence of SopE with SipA being the cause of this behaviour was supported by observing a similar response in cells to SL1344 and S1579/94 *sipA*⁻ *sopE*⁻ mutants. When the bacterium is attached to the ruffle protrusion and moved away from the centre of the ruffle it can not be taken up by the cell and explains why the invasion of the *sipA*⁻ *sopE*⁻ mutants is lower than the wild type. Why there may not be an additional invasion defect compared to the *sipA*⁻ mutant considering it takes longer for the *sipA*⁻ *sopE*⁻ mutant to reach the centre of a ruffle, is likely to be due to the fact that other bacteria may use the original ruffle centre to enter the cell (noted here; Francis *et al.*, 1992; Pattni *et al.*, 2001).

The SL1344 *sipA*⁻, *sopE*⁻ and *sipA*⁻ *sopE*⁻ mutants were also examined for their ability to disrupt the integrity of MDCK II monolayers after 15 and 60 minute infection lengths. The reduction in TER and changes in F-actin distribution across the monolayer, that occur as early as 15 minutes post-infection but are more pronounced after 60 minutes infection, associated with wild type infection (here; (Jepson *et al.*, 1995; Jepson *et al.*, 1996; Jepson *et al.*, 2000), were also observed for each of the mutants. From this data it would appear SipA and SopE

are therefore not required for disruption of the monolayer. However, given the redundancy of *Salmonella* effector proteins it may be that the effects of SipA and SopE are masked due to the presence of other effectors with similar roles e.g. SipC, SopE2 and SopB. Therefore, SipA and SopE may be important, as has been reported by Boyle *et al.* (2006). One difference however, that was noted between the interaction of wild type SL1344 and *sipA*⁻ *sopE*⁻, was that 60 minutes after infection was initiated SL1344 *sipA*⁻ *sopE*⁻ produced ruffles in the vicinity of gross cellular distortion which were very large and have a 'Yorkshire pudding' phenotype. The cause of this change in ruffling and actin distribution is not clear but may represent a change in the signalling between *Salmonella* and epithelial cells due to absence of SopE and SipA, and requires further attention.

Since SopE2 is 70% homologous to SopE and performs a similar role in host cells (Bakshi *et al.*, 2000; Stender *et al.*, 2000), it was investigated whether the absence of SipA and SopE2 together led to the same changes in ruffle morphology, or whether the interaction between SipA and SopE was exclusive. Like the *sipA*⁻ *sopE*⁻ mutant, the *sipA*⁻ *sopE2*⁻ mutant had decreased invasion compared to the wild type, and a cause or consequence of this was the production of ruffles with finger-like protrusions. Notable though, was the lack of an increase in ruffles with 10 or greater filopodia in the *sipA*⁻ *sopE2*⁻ mutant, indicating there may be some difference in the invasion of this mutant compared to the *sipA*⁻ *sopE*⁻ mutant. Since SopE and SopE2 both stimulate Rho GTPases to cause actin reorganisation (Hardt *et al.*, 1998a, Stender *et al.*, 2000; Friebel *et al.*, 2001; Patel and Galan, 2006), it was decided to investigate whether loss of SipA in the absence of SopB, another effector protein which stimulates Rho GTPases (Zhou *et al.*, 2001; Patel and Galan, 2006), produced the same phenotype. The *sipA*⁻ *sopB*⁻ mutant did not have reduced invasion compared to wild type but finger-like protrusions were associated with the ruffles it induced. This indicates altered signalling through the Rho GTPases may produce the change in ruffle morphology, but this change may not be related to the invasion defect.

Plasmid complementation of each of the mutants was used to test whether the changes in phenotype observed were due to absence of the particular gene under

consideration. While restoration of the change in ruffle morphology was often successfully achieved with plasmid complementation, restoration of invasion to wild type levels was not. Complementation of a mutant by expressing a functional copy of the deleted gene from a plasmid has often been found not to fully complement the mutant phenotype due to the pleiotropic effects plasmid maintenance or copy number artefacts may have on the bacterium (Abromaitis *et al.*, 2005; Birnbaum and Bailey, 1991; Knodler *et al.*, 2005). Thus, the failure here to fully complement the mutant phenotype is likely to reflect difference in expression of an effector gene from a plasmid rather than a chromosomal location.

Problems with restoring the wild type phenotype to mutants were particularly experienced with pCAP02 and pCAP03, expressing SopE2 and SopE, respectively. A similar problem in complementing *sopE* and *sopE2* mutants with plasmid copies of these genes was reported by Hapfelmeier *et al.* (2004). This may indicate the quantity of effector proteins is crucial to efficient invasion, and in this case may indicate use of the pACYC177 vector has either led to under or over expression of these proteins, and is why the complementation is not complete in any of the complemented mutants. To conclusively prove the role of each effector protein in invasion, it would be helpful to express the effector genes from alternative vectors and re-assess the contribution of each effector. In the case of the double mutant it is also important to express SipA and SopE alongside each other, to show the presence of both does complement the phenotype.

Evidently the work presented here has identified a consequence of losing SipA with other effector proteins but no data has been gathered to determine what leads to the differences, therefore only hypotheses can be drawn. Since the proportion of ruffles exhibiting finger-like protrusions was accompanied by an increase in the number of ruffles with large numbers of filopodia, for the *sopE*$^-$ *sipA*$^-$ mutant, it infers signalling events inside the host cell are altered compared to when wild type *Salmonella* infects. The altered signalling is likely to revolve around pathways stimulated by Rho GTPases since SopE, SopE2 and SopB stimulate host Rho GTPase-dependent actin rearrangements to create the ruffles

driving *Salmonella* internalisation. Cdc42 and Rac1 (Hardt *et al.*, 1998a; Friebel *et al.*, 2001), and more recently RhoG (Patel and Galan, 2006), are the Rho GTPases that have been implicated with these actin rearrangements, each stimulating specific actin reorganisations e.g. Cdc42 creating filopodia, Rac1 causing lamellipodia and membrane ruffles (Ridley *et al.*, 1992; Nobes & Hall, 1995), while RhoG appears to elicit membrane ruffles, lamellipodia, filopodia, and microvilli (Gauthier-Rouviere *et al.*, 1998). The level of activation of each of these Rho GTPases will be carefully regulated to provide the characteristic membrane ruffle that allows *Salmonella* uptake. It is therefore rational to assume changes in the regulation of these Rho GTPases lead to the change in morphology that was observed with the ruffles induced by *sipA⁻ sopE⁻* mutants.

In a *sipA⁻ sopE⁻* mutant, SopE2 and SopB will be responsible for promoting actin reorganisation, both of which activate RhoG and Cdc42 (Stender *et al.*, 2000; Friebel *et al.*, 2001; Patel and Galan, 2006). Both are involved with filopodia formation, and therefore, increased signalling via these Rho GTPases could explain the more 'spiky' ruffles produced by the *sipA⁻ sopE⁻* mutant. This phenotype would also remain if the recent hypothesis that Cdc42 is limited to nuclear responses (Patel and Galan, 2006) proves true, since RhoG can stimulate filopodia formation (Gauthier-Rouviere *et al*, 1998). The membrane protrusions that are also associated with the *sipA⁻ sopE⁻* mutant ruffles would probably be the result of RhoG-directed actin polymerisation in this instance, since broader extensions of the membrane ruffle are associated with this Rho GTPase, and not Cdc42; although of course it may be possible that other Rho GTPases not identified in this process, play a role.

Deletion of SipA with SopE2 or SopB also produced the dynamic membrane protrusions observed with the *sipA⁻ sopE⁻* mutant. In both the *sipA⁻ sopE2⁻* and *sipA⁻ sopB⁻* mutants it would be assumed that Cdc42, Rac1 and RhoG would be stimulated, since SopE activates Cdc42 and Rac1 (Hardt *et al.*, 1998a), and is assumed to activate RhoG (Patel and Galan, 2006), while SopB leads to the activation of Rac1 and RhoG (Patel and Galan, 2006). Since all three of the Rho GTPases are stimulated in these cases, and two of the Rho GTPases were stimulated in the *sipA⁻ sopE⁻* mutants, it indicates the protrusions are not a

consequence of the inability to stimulate one or more of the Rho GTPases. Therefore, it suggests the finger-like protrusions are the response to signalling events which have become unregulated and/or a consequence of other activities required for the interaction of bacteria and host cell being altered.

While we appear to know how *Salmonella* manipulates Rho GTPases to induce uptake, events downstream of the Rho GTPases that lead to actin polymerisation, and how these may be regulated by bacterial proteins, have not been well characterised. There is the possibility that *Salmonella* effector proteins could regulate the actions of each other, either directly or through host cell proteins, to alter the levels to which a particular Rho GTPase is activated, and therefore, the nature of the ruffle that is formed. If this was the case, the absence of specific or absence of combinations of particular effector proteins may lead to greater signalling through particular pathways with a reduction in others. A consequence of this could for example be greater production of filopodia or the membrane protrusions observed here. The concept of one effector protein regulating the responses to another effector protein is familiar in *Salmonella*, with SptP antagonising the actions of SopE and SopE2. The loss of SptP was investigated briefly here and while there were no finger-like protrusions produced by the *sptP*$^-$ mutant, there appeared to be unregulated ruffling, indicating the potential for the formation of superfluous structures such as additional filopodia and the finger-like protrusions seen with the ruffles of *sipA*$^-$ *sopE*$^-$, *sipA*$^-$ *sopE2*$^-$ and *sipA*$^-$ *sopB*$^-$ mutants.

To support the hypothesis that regulation of signalling events goes awry during infection with the double mutants studied here, it would be wise to complete the study into the ruffle morphology of effector mutants lacking combinations of the SipA, SopE, SopE2 and SopB effector proteins to find clues as to which parts of the host cell signalling pathways are affected. As yet is it unknown whether the lack of SipA alongside the absence of another effector molecule is the cause of the ruffle morphology, or whether the absence of any two of the effectors listed could produce the same response. A quick investigation with a *sipA*$^-$ *sopE*$^-$ *sopB*$^-$ mutant indicated this mutant still produced the membrane protrusions but there was a difference in the ruffling with a more diffuse circular membrane ruffle

being created initially, which quickly disappeared as the bacteria moved across the surface on their membrane protrusion, a behaviour resembling the movement of *Listeria* on the actin tails they create (Dabiri *et al.*, 1990). It would be interesting to know if this behaviour was seen with each triple mutant, and whether the quadruple mutant abrogates this phenotype.

Since it is assumed there must be some change in signalling and we know Rho GTPases act as the interface between bacterial and host proteins, the role of the Rho GTPases needs to be investigated. The selective inhibition of Cdc42, Rac1 and RhoG through the transfection of cells with either RNAi constructs or plasmids expressing dominant negative forms of the Rho GTPases could initially be used to determine if any is involved with driving the creation of finger-like protrusions, and if the same Rho GTPase is involved with filopodia creation. Dissecting the proteins associated with the filopodia would also be a useful exercise to determine whether the filopodia observed are homologous to the filopodia produced by the host in normal circumstances. This may be done by looking for proteins such as vasodilator-stimulated phosphoprotein (VASP) and fascin, which are associated with host filopodia, and potentially TEM and SEM studies could be performed to examine the morphology, and in particular the actin network, within these structures. Together, these initial experiments may provide the direction of further investigations to dissect better the bacteria-host cross talk that occurs during invasion and the role of each protein.

A second, or secondary, cause of the finger-like protrusions observed may be due to behaviour of bacteria at the host cell membrane. The *sipA*$^-$ mutants shift to the periphery of ruffles, causing a time lag before their entrance into host cells (Jepson *et al.*, 2001). This lack of ability on the part of the bacterium to remain located in the centre of the ruffle potentially indicates that SipA has a role in anchoring the bacterium to the cell surface. In the *sipA*$^-$ *sopE*$^-$, *sipA*$^-$ *sopE2*$^-$ and *sipA*$^-$ *sopB*$^-$ mutants it may be possible that lack of another effector protein, alongside the absence of SipA, further destabilises the bacterium so it is cast out further from the ruffle ('loses its grip'). Alternatively, unregulated actin polymerisation due to loss of the second effector may exist and the movement of the bacterium to the periphery, channels this into a finger-like protrusion. A

better understanding of the events allowing adherence of *Salmonella* to the cell surface, and the interactions that occur via TTSS-1, is needed to decide whether SipA could have an anchoring role.

Linked with the virulence of *Salmonella* are their flagella. Flagella are used to move the bacterium from the gut lumen, through the mucus layer to the epithelium, where the flagella are subsequently lost during adherence to the cell surface. One concept that has not been tested is whether loss of flagella does not occur correctly in the double mutants, perhaps because of loss of certain signalling events. If the *Salmonella* was adhered to the cell but still possessed all or part of its flagella it could possibly have the ability to pull itself along the membrane producing the type of protrusions that were observed. Use of a double mutant that lacks flagella could eliminate this hypothesis.

While the difference in the ruffles of *sipA*$^-$ *sopE*$^-$, *sipA*$^-$ *sopE2*$^-$ and *sipA*$^-$ *sopB*$^-$ mutants has been discussed, there was also found to be a difference in ruffles induced by a *sopE*$^-$ mutant. The ruffles were found to be smaller and also to take slightly longer to be initiated once the bacterium was adhered to the surface. Since SopE is known to act as a GEF for a variety of Rho GTPases (Hardt *et al.*, 1998a), and one of the consequences of Rho GTPase stimulation is actin polymerisation, the smaller ruffle size of *sopE*$^-$ strains suggests SopE provides an additional input of actin polymerisation to that stimulated by SopE2 and SopB. Potentially, this extra actin polymerisation could increase *Salmonella* uptake since the *sopE*$^-$ mutant of SL1344 was found to have significantly reduced invasion after 15 minutes compared to wild type, replicating the data of previous reports (Hardt *et al.*, 1998b), and strain 12023, which naturally lacks SopE, has very low invasion. However, in S1579/94, loss of SopE does not reduce invasion and wild type F98 which naturally lacks SopE invades MDCK cells in numbers identical to SL1344 and S1579/94 wild types which possess SopE. However, the level of invasion of each *S.* Typhimurium strain may be different, and if F98 possessed SopE it may have greater invasion than SL1344 and S1579/94, and likewise the invasion of 12023 may be improved. The insertion of a plasmid carrying *sopE* into F98 and 12023 wild types could show whether SopE does indeed enhance invasion and support the hypothesis made by Friebel *et al.*

(2001) that possession of the *sopE* gene increases the pathogenic potential of a *Salmonella* strain.

The increase in time it takes for a *sopE*$^-$ bacterium to initiate a ruffle after adherence may not be explained by the ability of SopE to stimulate actin polymerisation though. In a *sipA*$^-$ *sopE*$^-$ mutant, SopE2 and SopB are capable of inducing actin rearrangements and therefore it would not be expected that a delay would occur in a ruffle being produced. Indeed in a *sopE2* mutant ruffle induction time is identical to the wild type. However, SopE2 appears to have a relatively minor impact in invasion (Figure 1.35B; Stender *et al.*, 2000), indicating that it is of less importance in SL1344 than SopE and therefore may be expected not to affect ruffle induction time. The observed increase in ruffle induction time by *sopE*$^-$ *Salmonella* may therefore indicate that either there is some form of temporal regulation to the ruffle production process that relies on SopE-stimulated actin rearrangements proceeding first, or the lack of extra Rho GTPase stimulation slows down ruffle initiation. The selective inhibition of Cdc42, Rac1 and RhoG and the impact it has on ruffle induction times may help to dissect these events and the contribution of SopE to these processes.

To conclude, the hypothesis that the role of SipA in invasion may vary between *Salmonella* strains has been examined by investigating the effect of SipA deletion in four serovar Typhimurium strains, including those that possess or lack SopE. *sipA* null mutants have been compared to their wild types with respect to the number, morphology and dynamics of the membrane ruffles they induce, and their ability to invade cultured epithelial cells, using confocal and electron microscopy and live cell imaging. These studies have confirmed that SipA has no obvious effect on the number of ruffles formed during infection and reveal that it optimises entry of most strains into MDCK cells, with the extent of the invasion defect associated with SipA deletion not appearing to vary much between Typhimurium strains, at least in the invasion assay employed here. The SipA$^-$ SopE$^-$ *Salmonella* strains examined to date have been found to induce ruffles with markedly different morphology compared to that previously described for wild type and *sipA* null mutants, including the presence of multiple finger-like protrusions and numerous filopodia, both structures being highly

dynamic when examined by live cell imaging. Such structures have also been found associated with the ruffles of *sipA*⁻ *sopE2*⁻, *sipA*⁻ *sopB*⁻ and *sipA*⁻ *sopE2*⁻ *sopB*⁻ bacteria. In describing a novel role for SipA in membrane ruffling, the data may reveal SipA is more important in *Salmonella* invasion than previously thought; in particular, SipA may play a key role in induction of invasion-competent membrane ruffles, particularly where another effector protein is absent.

Chapter Five

Discussion

The studies presented in this thesis were aimed at investigating the molecular mechanisms through which *Salmonella enterica* serovar Typhimurium regulates and induces its uptake into epithelial cells. Such information enhances our knowledge of the interactions that occur between bacteria and their hosts, particularly the way in which bacteria manipulate their hosts, and may have the potential to provide advances in the diagnosis, treatment, and prevention of bacterial diseases, particularly relevant in this instance as *Salmonella enterica* are important zoonotic pathogens.

Genes involved with invasion, including those encoded by *Salmonella* Pathogenicity Island 1 (SPI-1), are stringently controlled to ensure expression is timed to the point of infection most productive for invasion. *Salmonella* has been shown to produce the signalling molecule autoinducer-2 (AI-2) (Surette and Bassler, 1998, 1999) synthesised by LuxS (Surette *et al.*, 1999; Schauder *et al.*, 2001), which is used by other bacterial species to co-ordinate gene expression with population density (Hammer and Bassler, 2003; Henke and Bassler, 2004a, c); a behaviour known as quorum sensing. Since *Vibrio* spp. have been shown to regulate type three secretion in response to quorum sensing using AI-1, CAI-1 and AI-2 molecules (Henke & Bassler, 2004a, b), and enteropathogenic and enterohaemorrhagic *E. coli* use AI-3 to regulate expression of virulence genes (Sperandio *et al.*, 1999; Sperandio *et al.*, 2002; Sperandio *et al.*, 2003), *Salmonella* could potentially use quorum sensing to regulate genes required for invasion. The expression of virulence determinants only when large numbers of *Salmonella* are present would enable a concerted attack on the host to be made, allowing host defences to be overwhelmed and a successful infection initiated (De Kievit *et al.*, 2001). Alternatively, since a large number of Gram-negative and Gram-positive bacteria have been shown to possess the *luxS* gene (Surette *et al.*, 1999), the potential exists for enteropathogens such as *Salmonella* to detect the AI-2 produced by the commensal flora of the gastrointestinal tract, and use

this as a marker of the appropriate environment in which to express those genes required for host colonisation (Kaper and Sperandio, 2005).

Prior to 2007, only the genes of the *luxS* regulated (*lsr*) operon were found to be regulated by *luxS* in *Salmonella* (Taga *et al.*, 2001; Taga *et al.*, 2003), and therefore there was no indication that quorum sensing was involved in invasion gene regulation. These genes had been identified by screening the *Salmonella* chromosome for genes with differential expression in a *luxS* mutant using transposon reporter fusions (Taga *et al.*, 2001). Use of microarrays, which allows study of individual gene expression across the genome, subsequently revealed 5% of genes were altered in SL1344 *luxS*⁻ compared to the parental strain SL1344, with *luxS* affecting transcription of genes involved in many aspects of bacterial physiology including general transport and metabolism, pathogenicity islands, surface structures, gene regulation and energy production (Dr C. M. A. Khan, personal communication). As it appeared there were likely to be other genes regulated by *luxS*, in addition to the *lsr* operon, this provided an impetus for investigating whether quorum sensing was used by *Salmonella* to regulate virulence.

Since the virulence of *Salmonella enterica* depends upon their ability to enter and survive in host cells, the question of whether *luxS* affected the ability of *S.* Typhimurium to invade epithelial cells was addressed. No difference was found between *S.* Typhimurium SL1344 wild type and its isogenic *luxS*⁻ mutant with respect to the number and morphology of the membrane ruffles induced or their ability to invade several epithelial cell lines. However, initially studies indicated the dynamics of the ruffling process was subtly altered in the *luxS*⁻ mutant, so that ruffles were induced in a shorter time period after adhesion (40 seconds as opposed to 60 seconds for wild type). It was hypothesised that quorum sensing may therefore reduce the speed at which *Salmonella* enters cells. A reason for such behaviour is not clear.

To determine whether the effect on ruffling dynamics was a consequence of absence of LuxS and possible changes in *Salmonella* metabolism or due to quorum sensing, it was decided to study a transcomplemented mutant and the

effect of treatment of the *luxS*⁻ mutant with synthetic AI-2. Only the former was studied since in comparing the wild type, the *luxS*⁻ mutant and transcomplemented mutant (*luxS*⁻ p*luxS*), no difference was observed in ruffle kinetics. This difference from the initial observations appears to be associated with the use of a different consignment of cells, and therefore suggests this ability to induce ruffles in a shorter time period after adhesion is not a consistent phenotype of the *luxS*⁻ mutant. This also highlights a limitation of the work presented in this thesis and many of the *in vitro* studies conducted examining the interactions of bacteria with host cells, namely that one particular cell line is often chosen for the work and thus the presence or absence of possible phenotypes between the wild type and mutant may not be detected. It also explains why there may be discrepancies in the role described for a particular protein. For example, contradictory data have been reported regarding the role of SipA (studied in the second part of this thesis) in membrane ruffle formation; Zhou *et al.* (1999a) found a *sipA*⁻ mutant less effective than wild type in inducing actin cytoskeleton rearrangements, while Jepson *et al.* (2001) reported no difference. Since the former study was conducted in HeLa cells and the latter in MDCK cells this may account for the difference, especially since there have already been descriptions that the importance of various *Salmonella* effector proteins in invasion appears to be different between cell lines (Raffatellu *et al.*, 2005). As MDCK cells also partially polarise and differences in mechanisms of *Salmonella* invasion have been shown between polarised and non-polarised cells, including those of the same cell line (Shi and Casanova, 2004; Raffatellu *et al.*, 2005), this also explains a reason for different results.

Such inconsistencies in the data derived from cultured cell models demonstrates a requirement for testing observations and hypotheses about molecular mechanisms of *Salmonella* invasion in several models, including those that allow complex environments such as exists in the gut, to be simulated (Hurley and McCormick, 2003). Three separate cultured cell lines (MDCK, HeLa and Caco-2) were used to examine the number of ruffles induced and the level of invasion of wild type and *luxS*⁻ here, and since similar results were obtained from each, only MDCK cells were used in studying ruffle dynamics. However, it may be important to assess the ruffle dynamics in HeLa, Caco-2 and other cell lines since

there appears to be a property of certain cells which can reveal a subtle difference between the wild type and the *luxS* mutant. Indeed, there has recently been a report that a *luxS* mutant is impaired in its ability to invade HEp-2 cells (Choi *et al.*, 2007), although in these experiments a 60 minute infection length was used and therefore the results are not directly comparable to those reported here. However, the results of Choi *et al.* do indicate that it may be important to investigate the effect of *luxS* on invasion over longer time periods in different cell types. Future work examining the role of quorum sensing in *Salmonella* invasion should also include the use of the HEp-2 cell line, not only to validate the results of Choi *et al.* but because a property of these cells may amplify differences between wild type and the *luxS* mutant, making it easier to determine possible effects of *luxS* on bacterial phenotype. Use of multiple cultured cell lines and indeed possible *in vivo* work should also be extended to the work presented here examining the role of SipA, since the role of various effector proteins may be altered depending on the availability of particular host proteins. Moreover, it would provide validation of the work presented here.

In addition to using more than one model in which to test hypotheses about the molecular mechanisms used by *Salmonella* during pathogenesis, work in this thesis has also indicated that the effects in more than one strain of *Salmonella* should be examined. Analysis of the role of SipA in the invasion of epithelial cells had previously only been conducted in *S.* Typhimurium strain SL1344 (Kaniga *et al*, 1995b; Hueck *et al.*, 1995; Zhou *et al.*, 1999a; Jepson *et al.*, 2001; Higashide *et al.*, 2002), and therefore it was decided to investigate whether SipA exhibits the same role in other strains of serovar Typhimurium, particularly since it is known the majority of *Salmonella* strains lack the *sopE* gene (Hardt *et al.*, 1998b; Mirold *et al.*, 1999), which as an effector that stimulates actin reorganisation (Hardt *et al.*, 1998a; Zhou *et al.*, 2001) may influence the role of SipA which binds actin. S1579/94 was compared alongside SL1344 to represent strains that possess SopE, while strains F98 and 12023 represented the majority of serovar Typhimurium strains which naturally lack SopE. One of the first observations made in this study was that not all *Salmonella* strains behave similarly; the 12023 wild type induced less ruffles and had a lower rate of invasion compared to the wild types of other strains, and its isogenic *sipA*⁻

mutant did not exhibit a prominent defect in invasion. Additionally, while absence of *sopE* was important for invasion of SL1344, it appeared not to be so important for S1579/94. This indicates the regulation and/or mechanisms of invasion may be different between *Salmonella* strains, and indicates the findings using one strain should not necessarily be relied upon to represent all strains of a particular serovar or species. This information suggests that in addition to examining the role of *luxS* in *Salmonella* invasion in further *in vitro* and *in vivo* models, another area of future work could be to compare absence of *luxS* in different serovar Typhimurium strains.

In the future it would be interesting to identify why 12023 is different to the other strains studied. This work could begin by examining the expression of SPI-1 genes which are required for invasion (Galan and Curtis III, 1989; Ginocchio *et al.*, 1992; Groisman and Ochman, 1993; Altmeyer *et al.*, 1993; Kaniga *et al.*, 1994). Flow cytometry was successfully used here to measure the expression of a single copy *prgH* promoter-*gfp*$^+$ fusion inserted into the *Salmonella* chromosome, and thus provide comparison of *prgH* gene expression between wild type and *luxS*$^-$ mutant SL1344. This technique, with changes to the promoter placed upstream of the *gfp*$^+$ gene, could be applied to studying expression of a variety of SPI-1 genes or effector protein genes outside this region of the chromosome, allowing comparison between the serovar Typhimurium strains, and potentially the ability to identify differences responsible for the altered behaviour of 12023 observed in the assays used here. These effector protein promoter-*gfp*$^+$ constructions could also be used in *luxS*$^-$ mutants to expand the work started here and published by Choi *et al.* (2007), investigating whether LuxS affects expression of SPI-1 genes, and therefore the invasion process.

Since the behaviour of strain 12023, which lacks a copy of the *sopE* gene, was different to the behaviour of the other strains examined, including other *sopE*$^-$ strains, it appears the presence or absence of SopE does not determine the role of SipA in regards to the dynamics and number of membrane ruffles induced or the ability to invade cultured epithelial cells. However, SopE does appear to interact with SipA in determining the morphology of the ruffles induced, since all the

SipA⁻ SopE⁻ *Salmonella* strains examined induced ruffles with markedly different morphology compared to that previously described for wild type and *sipA* null mutants, including the presence of multiple dynamic finger-like protrusions and numerous dynamic filopodia. This work was subsequently extended to examine the effect of absence of SipA in SL1344 *sopE2*⁻ and SL1344 *sopB*⁻ bacteria, where similar changes in ruffle morphology were observed. Since *sopE*⁻ *sopE2*⁻ and *sopE*⁻ *sopB*⁻ *S.* Typhimurium have not been shown to exhibit these same changes in ruffle morphology (Zhou *et al.*, 2001), this indicates a novel role for SipA in producing invasion-competent ruffles. It also reveals there is a further level of complexity in creating membrane ruffles that has not been appreciated, and that there is still much to understand regarding the interactions between effector proteins and host cell signalling pathways stimulated during invasion.

How SipA interacts with each of the effector proteins SopE, SopE2 and SopB to achieve the creation of invasion-competent ruffles still needs to be elucidated, which will form one of the strands of future work. Such work could involve creating the triple mutants; *sipA*⁻ *sopE*⁻ *sopE2*⁻, *sipA*⁻ *sopE*⁻ *sopB*⁻, and *sipA*⁻ *sopE2*⁻ *sopB*⁻, and the quadruple mutant *sipA*⁻ *sopE2*⁻ *sopE2*⁻ *sopB*⁻ in each of the strains of *Salmonella* studied here. Characterisation of the ruffle morphology induced by each of these mutants in each serovar Typhimurium strain would hopefully provide information on the ability of each effector protein to stimulate membrane ruffle formation alone, determine whether the role of each effector protein is similar in all strains of *Salmonella*, and possibly whether SipA interacts with SopE, SopE2 and SopB in the same manner and/or whether the interaction with one is more important. Initial examination of a SL1344 *sipA*⁻ *sopE*⁻ *sopB*⁻ mutant was made here, showing the production of finger-like protrusions, but it appears without the creation of focal accumulations of F-actin associated with invasion of the wild type. This indicates SopE2, while able to stimulate actin polymerisation, is not able to maintain localised actin polymerisation. Thus the role of SipA in the creation of invasion-competent ruffles may represent the ability to maintain actin polymerisation at the site where the bacterium has adhered and which may or may not involve maintaining other effector proteins in this region.

An alternative approach that is now being used to determine the role of individual effector proteins in *Salmonella* virulence is the deletion of all known effectors with a role in invasion and subsequent complementation of the mutant with one or more of the effectors (Raffatellu *et al.*, 2005). Such an approach prevents effector protein redundancy masking the effect of an individual protein. This method could also prove useful in proving the additional importance of SipA in ruffle production described here, and in determining the effectors it may interact with. However, since this method is dependent on plasmid complementation there is a risk that non-physiologically relevant concentrations of one or more of the effector proteins may lead to or prevent interactions either between effector proteins or effector proteins and host cell proteins leading to misinterpretation of the events occurring during invasion. This data may therefore need to be treated with care, although plasmid complementation is often a problem with any study trying to tease out the change in phenotype exhibited by a mutant, and indeed in some of the work here it was not felt possible to draw definite conclusions from the results because plasmids, particularly the SopE plasmid (pCAP03), did not restore the phenotype of the parent strain. If time had permitted an alternative vector would have been trialled from which to express the effector genes to improve the reliability of the data. The double and triple mutants would also have been complemented with a plasmid expressing each of the deleted genes to prove the deletion of all was responsible for the changes in phenotype observed.

While a description of a phenotype induced by *sipA*⁻ *sopE*⁻, *sipA*⁻ *sopE2*⁻ and *sipA*⁻ *sopB*⁻ mutants has been made, no work has yet been completed to provide an explanation of this phenotype. Elucidating the nature of the finger-like protrusions and filopodia that are stimulated by the *sipA*⁻ *sopE*⁻, *sipA*⁻ *sopE2*⁻ and *sipA*⁻ *sopB*⁻ mutants may aid understanding of the events that lead to their production, and consequentially the events that occur to produce the ruffles induced by wild type *Salmonella*. Since the fingers and filopodia associated with *sipA*⁻ *sopE*⁻, *sipA*⁻ *sopE2*⁻ and *sipA*⁻ *sopB*⁻ ruffles are filled with actin; it indicates these structures are similar to the filopodia produced by the host itself, and are produced in response to Rho GTPase stimulation. Since the stimulation of Rho GTPases by SopE, SopE2 and SopB (Hardt *et al.*, 1998a; Rudolph *et al.*, 1999;

Stender *et al.*, 2000; Patel and Galan, 2006) in wild type bacteria do not usually produce such large numbers of filopodia or these finger-like projections, it suggests there is some change in the signalling pathways downstream of the Rho GTPases. One method of elucidating the changes in host cell signalling would be to inhibit individual Rho GTPases, either through use of a dominant negative mutant or siRNA, and infecting the cells with one of the *sipA*⁻ double mutants. If inhibition of a particular Rho GTPase blocks creation of filopodia/fingers then downstream pathways of this Rho GTPase can be investigated for their contribution to the phenotype.

Since several Rho GTPases can be stimulated during *Salmonella* infection (Friebel *et al.*, 2001; Patel and Galan, 2006), and the downstream pathways they regulate may overlap, inhibition of Rho GTPases to decipher the pathway or proteins SipA may interact with to induce wild type ruffling events may not be successful. Therefore, other cellular pathways could be examined, particularly those determining whether lamellipodia or filopodia-like membrane structures are created. Membrane ruffles induced by *Salmonella* are created through Arp2/3–mediated actin polymerisation (Criss and Casanova, 2003), which creates a short and highly branched actin network, often associated with lamellipodia. Filopodia on the other hand are produced by vasodilator-stimulated phosphoprotein (VASP) acting in concert with actin-bundling proteins such as fascin. Investigation of pathways which regulate VASP, for example, may therefore yield clues to how *Salmonella* usually manipulates host cell signalling and the role of SipA in this process.

Another approach previously used to elucidate the role of SopE, SopE2 and SopB, is to transfect cells with the protein of interest and examine cell morphology and/or physiology using microscopy (Hardt *et al.*, 1998a; Stender *et al.*, 2000; Zhou *et al.*, 2001). Such an approach may be possible with SipA; use of fluorescently labelled SipA in particular may allow determination of the sites SipA is recruited to, and comparison with cells co-transfected with SipA and SopE/SopE2/SopB may potentially provide information as to whether the localisation of SipA is affected by effector proteins and the pathways they stimulate and/or whether SipA is involved with restricting effector proteins

within a specific domain of the cell. It may also be interesting to produce a *Salmonella* mutant which possesses a SipA protein that is targeted to a site in the host cell that will not be adjacent to adherent *Salmonella*, to determine what phenotype occurs. Would for instance actin polymerisation still occur at the site of bacterial adherence or would it move to the site where SipA is located?

The mechanisms by which SipA achieves invasion-competent ruffles need also to be considered in the context of the additional pathogenic effects *Salmonella* has upon the host. It has become apparent that the effector proteins secreted by TTSS-1 not only allow uptake of the bacterium into the cells but are responsible for aspects of pathogenesis which include disruption of tight junctions (Jepson *et al.*, 1996), apoptosis and fluid secretion (Bertelsen *et al.*, 2004). Although infection of an epithelial monolayer with *S.* Typhimurium was shown as early as 1988 to elicit disruption of tight junctions (Finlay *et al.*, 1988), only recently have attempts been made to determine which effectors are critical for this process. SipA, SopE, SopE2 and SopB have been implicated in tight junction disruption by examining polarised monolayers of cultured cells after an infection of >1 hours (Raffatellu *et al.*, 2005; Boyle *et al.*, 2006). However, since it was previously shown that effects on TER and the F-actin distribution of MDCK II monolayers occurs as early as 15 minutes post-infection with *S.* Typhimurium (Jepson *et al.*, 1996; Jepson *et al.*, 2000), it was examined here whether SipA and/or SopE are important in the initial changes to the integrity of the monolayer by examining the effects on TER and the F-actin distribution of MDCK II monolayers, 15 and 60 minutes after infection initiation. By comparing the SL1344 wild type with its isogenic *sipA*$^-$, *sopE*$^-$ and *sipA*$^-$ *sopE*$^-$ mutants, it appears the presence of SipA, SopE or both proteins together does not play a role in disruption of monolayer integrity. However, given the redundancy of the effector proteins required for invasion this does not mean SipA and SopE do not have a role. Comparison of the *sipA*$^-$, *sopE*$^-$, *sopE2*$^-$ and *sopB*$^-$ single, double, triple and quadruple effector mutants should therefore be performed to determine more accurately the role of each effector. Since SipA has been identified as only being required at early time points in invasion (here, Zhou *et al.*, 1999a; Jepson *et al.*, 2001), such a study would also involve examining the changes in the monolayer at a range of time points since it is possible that particular effectors

have roles at different times. Again absence of one or more of the effector proteins discussed here from different strains of *Salmonella* would ensure a similar process is conducted by all *S.* Typhimurium strains.

It is evident from this work that there are still many questions regarding the role of *Salmonella* effector proteins in invasion and their interactions with the host cell. The use of microscopy techniques is likely to be an important tool in providing some of the answers. The use of microscopy has a relatively long history in *Salmonella* research, from the first descriptions of how *Salmonella* induces its uptake in epithelial cells (Francis *et al.*, 1992; Francis *et al.*, 1993; Takeuchi, 1967), to the subsequent elucidation of the roles of effector proteins in creating the ruffles required for uptake (Hardt *et al.*, 1998a; Zhou *et al.*, 1999a; Stender *et al.*, 2000; Jepson *et al.*, 2001; Zhou *et al.*, 2001). Since Jepson *et al.* (2001) were able to determine why a *sipA*⁻ mutant was defective for invasion at only early time points using microscopy and here it has been shown a level of interaction between SipA and SopE/SopE2/SopB that has not been recognised previously exists, it is clear imaging cellular processes in living cells can frequently reveal facets of bacterial interactions with host cells that would be impossible to determine by other methods, and indicates microscopy has a further part to play in explaining the events that occur during invasion. Since *sipA*⁻ double mutants had never been examined by microscopy and thus one of the roles of SipA was only identified now, it may be worth screening all mutants using microscopy to determine their effects on invasion and ensure all possible roles are discovered.

In summary this thesis has examined the role of LuxS and SipA in the ability of *Salmonella* to induce its uptake into epithelial cells using a range of microscopy techniques. While LuxS does not appear to have a consistent role in invasion, a novel role for SipA in the production of invasion-competent ruffles was discovered in some strains of *Salmonella enterica* serovar Typhimurium.

Appendix I

Publications

Papers

Perrett, C. A. & M. A. Jepson (2007). Chapter 12: Applications of Cell Imaging in *Salmonella* Research. In Salmonella: Methods and Protocols (Methods in Molecular Biology). Volume 394. Schatten, H. and Eisenstark, A (Eds). Humana Press, pp 235-273.

Conference Abstracts

Perrett, C. A. & M. A. Jepson. Analysing the interplay between *Salmonella* effector proteins. 2nd ASM Conference on *Salmonella*: From Pathogenesis to Therapeutics, September 2006. (Oral presentation)

Appendix II

Preparation of solutions

Bacterial culture media

Luria-Bertani (Miller) Broth

The following are added to 900ml of distilled water:

Difco tryptone	10g
Beta Lab yeast extract	5g
NaCl	10g

Volume made up to 1litre with distilled water, and pH adjusted to pH7.

Sterilised by autoclaving.

SOC media

The following are added to 900ml of distilled water:

Bacto tryptone	20g
Beta Lab yeast extract	5g
NaCl	0.584g
KCl	0.186g
1M $MgCl_2$	10ml
1M $MgSO_4$	10ml
1M glucose	20ml

Volume adjusted to 1litre with distilled water and sterilised by autoclaving.

SOB media

The following added to 900ml of distilled water:

Bacto tryptone	20g
Beta Lab yeast extract	5g
NaCl	0.584g
KCl	0.186g
1M $MgCl_2$	10ml
1M $MgSO_4$	10ml

Volume adjusted to 1litre with distilled water and sterilised by autoclaving.

Antibiotics

Antibiotic	Stock concentration (mg/ml)	Working concentration (µg/ml)
Carbenicillin	100	100
Chloramphenicol	25	15
Kanamycin	10	100
Nalidixic acid	7.5	15
Tetracycline	10	15

Agarose gel electrophoresis buffers

10x Tris-Borate-EDTA (TBE) buffer

Tris base	107.8g
Boric acid	55g
Disodium EDTA.$2H_2O$	7.44g

Made up to 1litre in distilled water. Diluted 1:10 for use in making agarose gels, and in DNA electrophoresis.

SDS-PAGE electrophoresis buffers

2x SDS-PAGE sample buffer

0.5ml Tris-Cl pH6.8	2.5ml
10%(w/v) SDS	4.0ml
100% glycerol	2.0ml
β-mercaptoethanol	1.0ml
1% bromophenol blue	0.5ml

10x SDS-PAGE running buffer

Tris	30g
Glycine	144g
10% SDS	100ml

Made up to 1litre in distilled water.

Coomassie blue staining solution

Water	208mls
Methanol	208mls
Acetic acid	84mls
Coomassie blue	0.5g

Western Blot buffers

10x Transfer Buffer

Tris	30.3g
Glycine	144.4g

Made to 1litre in distilled water. Stored at 4°C.

1x Transfer Buffer

10x stock	100ml
Methanol	200ml

Made to 1litre in distilled water. Stored at 4°C.

Cell culture solutions

MDCK media

Eagles Minimum Essential Media (EMEM)	500mls
Foetal calf serum (FCS)	50mls
MEM non-essential amino acid solution (100x)	5ml
GlutaMAX	5ml
Kanamycin	5ml

HeLa media

Dulbecco's modified Eagles medium (DMEM)	500ml
Foetal calf serum (FCS)	50mls
GlutaMAX	5ml
Penicillin/Streptomycin solution	5ml

Caco-2 media

Dulbecco's modified Eagles medium (DMEM)	500ml
Foetal calf serum (FCS)	50mls
MEM non-essential amino acid solution (100x)	5ml
GlutaMAX	5ml
Gentamicin	5ml

Modified Krebs buffer

NaCl	8.006g
KCl	0.402g
$MgSO_4$	0.244g
KH_2PO_4	0.041g
NaH_2PO_4	0.041g
Glucose	1.802g
Tris	1.211g

Volume was made up to 950ml with distilled water and pH was adjusted to pH 7.7 at room temperature with 0.5M HCl. The volume was subsequently made up to 1litre with distilled water and the media made sterile by autoclaving. Stored at 4°C. For use in experiments, 1M $CaCl_2$ solution was added to the Krebs buffer to a final volume of 5% (v/v), and the solution warmed to 37°C.

Appendix III

Video microscopy data

Time-lapse phase-contrast microscopy was employed to study the interaction of *S.* Typhimurium with MDCK strain I cells. Movies showing the development of membrane ruffles are presented on the two CDs which accompany this thesis. The movies were generated using Improvision Openlab 4.0.3 software. The files have been converted into AVI files which are compatible with Windows Media Player.

CD One: Video microscopy data for Chapter Three

Movies showing the development of ruffles depicted in Chapter Three are located in the folder Chapter Three on CD One. Unless stated, the field of view is 100μm x 100μm and the total time of each movie represents 20 minutes of the experiment. The size of the AVI file is given in brackets.

Movie A1: *S.* Typhimurium SL1344 wild type. The entire field of view is shown in this movie (1344μm x 1024μm). (109MB)

Movie A2: *S.* Typhimurium SL1344 wild type (22.1MB)

Movie A3: *S.* Typhimurium SL1344 *luxS*⁻ (22.4MB)

Movie A4: *S.* Typhimurium SL1344 *luxS*⁻: propagation of a single ruffle. Data presented in Figure 3.5. Length of movie represents 12 minutes of the experiment (828KB)

Movie A5: *S.* Typhimurium SL1344 *luxS*⁻ p*luxS* (the transcomplemented mutant) (27.5MB)

CD Two: Video microscopy data for Chapter Four

Movies showing the development of ruffles depicted in Chapter Four are presented in folder Chapter Four on CD Two. Unless stated, the total time of each movie represents 10 minutes of the experiment. The size of the AVI file is given in brackets.

The following AVI files are presented in Folder Chapter Four, Folder 1. SL1344:

Movie B1: *S.* Typhimurium SL1344 wild type (10.4MB)

Movie B2: *S.* Typhimurium SL1344 wild type single ruffle. Data from this movie is presented in Figure 4.25A and represents 230 seconds of the experiment (398KB)

Movie B3: *S.* Typhimurium SL1344 *sipA*$^-$ (10.4MB)

Movie B4: *S.* Typhimurium SL1344 *sipA*$^-$ single ruffle. Data from this movie is presented in Figure 4.25B and represents 230 seconds of the experiment (414KB)

Movie B5: *S.* Typhimurium SL1344 *sipA*$^-$ pCAP01 (10.4MB)

Movie B6: *S.* Typhimurium SL1344 *sopE*$^-$ (10.4MB)

Movie B7: *S.* Typhimurium SL1344 *sopE*$^-$ pCAP03 (10.4MB)

Movie B8: *S.* Typhimurium SL1344 *sipA*$^-$ *sopE*$^-$ (10.4MB)

Movie B9: *S.* Typhimurium SL1344 *sipA*$^-$ *sopE*$^-$ single ruffle. Data from this movie is presented in Figure 4.25C and represents 230 seconds of the experiment (430KB)

Movie B10: *S.* Typhimurium SL1344 *sipA*$^-$ *sopE*$^-$ pCAP01 (10.4MB)

Movie B11: *S.* Typhimurium SL1344 *sipA*$^-$ *sopE*$^-$ pCAP03 (10.4MB)

Movie B12: *S.* Typhimurium SL1344 *sptP*$^-$ (10.4MB)

Movie B13: *S.* Typhimurium SL1344 *sopE2*$^-$ (10.4MB)

Movie B14: *S.* Typhimurium SL1344 *sopE2*$^-$ pCAP02 (10.4MB)

Movie B15: *S.* Typhimurium SL1344 *sipA*$^-$ *sopE2*$^-$ (10.4MB)

Movie B16: *S.* Typhimurium SL1344 *sipA*$^-$ *sopE2*$^-$ pCAP01 (10.4MB)

Movie B17: *S.* Typhimurium SL1344 *sipA*⁻ *sopE2*⁻ pCAP02 (10.3MB)

Movie B18: *S.* Typhimurium SL1344 *sopB*⁻ (10.4MB)

Movie B19: *S.* Typhimurium SL1344 *sipA*⁻ *sopB*⁻ (10.3MB)

Movie B20: *S.* Typhimurium SL1344 *sipA*⁻ *sopE*⁻ *sopB*⁻ (10.3MB)

Movie B21: *S.* Typhimurium SL1344 *sipA*⁻ *sopE*⁻ *sopB*⁻ extended time course. The total time of this movie represents 30 minutes of the experiment (32.2MB)

The following AVI files are presented in Chapter Four, Folder 2. S1579/94:

Movie C1: *S.* Typhimurium S1579/94 wild type (10.4MB)

Movie C2: *S.* Typhimurium S1579/94 *sipA*⁻ (10.4MB)

Movie C3: *S.* Typhimurium S1579/94 *sipA*⁻ pCAP01 (10.4MB)

Movie C4: *S.* Typhimurium S1579/94 *sopE*⁻ (10.4MB)

Movie C5: *S.* Typhimurium S1579/94 *sopE*⁻ pCAP03 (10.4MB)

Movie C6: *S.* Typhimurium S1579/94 *sipA*⁻ *sopE*⁻ (10.4MB)

The following AVI files are presented in Folder Chapter Four, Folder 3. F98:

Movie D1: *S.* Typhimurium F98 wild type (9.44MB)

Movie D2: *S.* Typhimurium F98 *sipA*⁻ (10.4MB)

Movie D3: *S.* Typhimurium F98 *sipA*⁻. This movie depicts the filopodia associated with the ruffles produced by *sipA*⁻ *sopE*⁻ mutants (3.56MB)

Movie D4: *S.* Typhimurium F98 *sipA*⁻ pCAP01 (10.5MB)

The following AVI files are presented in Folder Chapter Four, Folder 4. 12023:

Movie E1: *S.* Typhimurium 12023 wild type (10.3MB)

Movie E2: *S.* Typhimurium 12023 *sipA*⁻ (10.8MB)

Movie E3: *S.* Typhimurium 12023 *sipA*⁻ pCAP01 (10.4MB)

Time-lapse microscopy was performed with MDCK cells stably expressing GFP-actin. In these experiments, images were taken simultaneously in the bright channel (A) and the GFP channel (B) at 30 second intervals to minimise photobleaching. The following AVI files are presented on CD Two in Chapter 4, Folder 5. GFP-actin MDCK cells.

The total time of the following movies represents 20 minutes of the experiment unless otherwise stated. Data is presented in Figure 4.31. The size of the AVI file is given in brackets.

Movie F1-A: *S.* Typhimurium SL1344 wild type; bright channel (14MB)

Movie F1-B: *S.* Typhimurium SL1344 wild type; GFP channel (14MB)

Movie F2-A: *S.* Typhimurium SL1344 *sipA*$^-$; bright channel (10 minutes of the experiment shown) (6MB)

Movie F2-B: *S.* Typhimurium SL1344 *sipA*$^-$; GFP channel (10 minutes of the experiment shown) (6MB)

Movie F3-A: *S.* Typhimurium S1579/94 *sipA*$^-$ *sopE*$^-$; bright channel (13.2MB)

Movie F3-B: *S.* Typhimurium S1579/94 *sipA*$^-$ *sopE*$^-$; GFP channel (13.2MB)

The total time of the following movies represents 60 minutes of the experiment.

Movie F4-A: *S.* Typhimurium SL1344 wild type; bright channel. Data presented in Figure 4.32 (55.7MB)

Movie F4-B: *S.* Typhimurium SL1344 wild type; GFP channel. Data presented in Figure 4.32 (51.2MB)

References

(1994) Chapter 4: How cells are studied. In *Molecular Biology of the Cell*. Alberts, B., Bray, D., Lewis, J., Raff, M., Roberts, K. and Watson, J.D. (eds). New York & London: Garland Science/Taylor & Francis Group, pp. 139-194.

(2000) WHO positional paper on Typhoid Vaccines. *World Health Organisation Weekly Epidemiological Record* **75**: 257-264.

(2004a) Chapter 17: Cytoskeleton In *Essential Cell Biology*. Alberts, B., Johnson, A., Lewis, J., Raff, M., Bray, D., Hopkin, K., Roberts, K. and Walter, P. (eds). New York & London: Garland Science/Taylor & Francis Group.

(2004b) Chapter 18: Cell Motility and Shape I:Microfilaments. In *Molecular Cell Biology*. Lodish, H., Berk, A., Matsudaira, P., Kaiser, C.A., Krieger, M., Scott, M.P., Zipursky, L. and Darnell, J. (eds). New York: W. H. Freeman and Company, pp. 751-794.

(2005) Centers for Disease Control and Prevention (CDC) Bacterial Foodborne and Diarrheal Disease National Case Surveillance Annual Report. *http://www.cdc.gov/foodborneoutbreaks/documents/fbsurvsumm2005.pdf*.

(2006) United States of America Department of Agriculture Economic Research Service (ERS) Foodborne Illness Cost Calculator. *http://www.ers.usda.gov/data/foodborneillness/*.

Abromaitis, S., Faucher, S., Beland, M., Curtiss, R., and Daigle, F. (2005) The presence of the tet gene from cloning vectors impairs Salmonella survival in macrophages. *Fems Microbiology Letters* **242**: 305-312.

Ahmer, B.M.M. (2004) Cell-to-cell signalling in Escherichia coli and Salmonella enterica. *Molecular Microbiology* **52**: 933-945.

Altier, C., Suyemoto, M., and Lawhon, S.D. (2000) Regulation of Salmonella enterica serovar typhimurium invasion genes by csrA. *Infection and Immunity* **68**: 6790-6797.

Altier, C. (2005) Genetic and environmental control of Salmonella invasion. *Journal of Microbiology* **43**: 85-92.

Altmeyer, R.M., McNern, J.K., Bossio, J.C., Rosenshine, I., Finlay, B.B., and Galan, J.E. (1993) Cloning and Molecular Characterization of a Gene Involved in Salmonella Adherence and Invasion of Cultured Epithelial-Cells. *Molecular Microbiology* **7**: 89-98.

Anderson, J.M. (2001) Molecular structure of tight junctions and their role in epithelial transport. *News in Physiological Sciences* **16**: 126-130.

Audia, J.P., Webb, C.C., and Foster, J.W. (2001) Breaking through the acid barrier: An orchestrated response to proton stress by enteric bacteria. *International Journal of Medical Microbiology* **291**: 97-106.

Bajaj, V., Hwang, C., and Lee, C.A. (1995) hilA is a novel ompR/toxR family member that activates the expression of Salmonella typhimurium invasion genes. *Molecular Microbiology* **18**: 715-727.

Bajaj, V., Lucas, R.L., Hwang, C., and Lee, C.A. (1996) Co-ordinate regulation of Salmonella typhimurium invasion genes by environmental and regulatory factors is mediated by control of hilA expression. *Molecular Microbiology* **22**: 703-714.

Bakshi, C.S., Singh, V.P., Wood, M.W., Jones, P.W., Wallis, T.S., and Galyov, E.E. (2000) Identification of SopE2, a Salmonella secreted protein which is highly homologous to SopE and involved in bacterial invasion of epithelial cells. *Journal of Bacteriology* **182**: 2341-2344.

Barker, G., and Simmons, N.L. (1981) Identification of 2 Strains of Cultured Canine Renal Epithelial-Cells (Mdck Cells) Which Display Entirely Different Physiological-Properties. *Quarterly Journal of Experimental Physiology and Cognate Medical Sciences* **66**: 61-72.

Barrow, P.A., Huggins, M.B., Lovell, M.A., and Simpson, J.M. (1987) Observations on the Pathogenesis of Experimental Salmonella-Typhimurium Infection in Chickens. *Research in Veterinary Science* **42**: 194-199.

Barrow, P.A., Huggins, M.B., and Lovell, M.A. (1994) Host-Specificity of Salmonella Infection in Chickens and Mice Is Expressed in-Vivo Primarily at the Level of the Reticuloendothelial System. *Infection and Immunity* **62**: 4602-4610.

Bassler, B.L., Wright, M., and Silverman, M.R. (1994) Multiple Signaling Systems Controlling Expression of Luminescence in Vibrio-Harveyi - Sequence and Function of Genes Encoding a 2nd Sensory Pathway. *Molecular Microbiology* **13**: 273-286.

Bassler, B.L., Greenberg, E.P., and Stevens, A.M. (1997) Cross-species induction of luminescence in the quorum-sensing bacterium Vibrio harveyi. *Journal of Bacteriology* **179**: 4043-4045.

Bassler, B.L. (1999) How bacteria talk to each other: regulation of gene expression by quorum sensing. *Current Opinion in Microbiology* **2**: 582-587.

Bassler, B.L., and Losick, R. (2006) Bacterially speaking. *Cell* **125**: 237-246.

Baumler, A.J., and Heffron, F. (1995) Identification and Sequence-Analysis of Lpfabcde, a Putative Fimbrial Operon of Salmonella-Typhimurium. *Journal of Bacteriology* **177**: 2087-2097.

Bertelsen, L.S., Eckmann, L., Paesold, G., Marcus, S.L., Finlay, B.B., and Barrett, K.E. (2001) Modulation of chloride secretory-responses of intestinal epithelial cells by the Salmonella effector SopB. *Faseb Journal* **15**: A825-A825.

Bertelsen, L.S., Paesold, G., Marcus, S.L., Finlay, B.B., Eckmann, L., and Barrett, K.E. (2004) Modulation of chloride secretory responses and barrier function of intestinal epithelial cells by the Salmonella effector protein SigD. *American Journal of Physiology-Cell Physiology* **287**: C939-C948.

Beuzon, C.R., Meresse, S., Unsworth, K.E., Ruiz-Albert, J., Garvis, S., Waterman, S.R., Ryder, T.A., Boucrot, E., and Holden, D.W. (2000)

Salmonella maintains the integrity of its intracellular vacuole through the action of SifA. *Embo Journal* **19**: 3235-3249.

Birnbaum, S., and Bailey, J.E. (1991) Plasmid Presence Changes the Relative Levels of Many Host-Cell Proteins and Ribosome Components in Recombinant Escherichia-Coli. *Biotechnology and Bioengineering* **37**: 736-745.

Bishop, A.L., and Hall, A. (2000) Rho GTPases and their effector proteins. *Biochemical Journal* **348**: 241-255.

Bodey, G.P., Fainstein, V., and Guerrant, R. (1986) Infections of the Gastrointestinal-Tract in the Immunocompromised Patient. *Annual Review of Medicine* **37**: 271-281.

Bos, J.L., Rehmann, H., and Wittinghofer, A. (2007) GEFs and GAPs: Critical elements in the control of small G proteins. *Cell* **129**: 865-877.

Bourdet-Sicard, R., and Van Nhieu, G.T. (1999) Actin reorganization by SipA and Salmonella invasion of epithelial cells. *Trends in Microbiology* **7**: 309-310.

Boyle, E.C., Brown, N.F., and Finlay, B.B. (2006) Salmonella enterica serovar Typhimurium effectors SopB, SopE, SopE2 and SipA disrupt tight junction structure and function. *Cellular Microbiology* **8**: 1946-1957.

Braga, V.M.M. (2002) Cell-cell adhesion and signalling. *Current Opinion in Cell Biology* **14**: 546-556.

Brawn, L.C., Hayward, R.D., and Koronakis, V. (2007) Salmonella SPI1 Effector SipA Persists after Entry and Cooperates with a SPI2 Effector to regulate Phagosome Maturation and Intracellular Replication. *Cell Host & Microbe* **1**: 63-75.

Brenner, F.W., Villar, R.G., Angulo, F.J., Tauxe, R., and Swaminathan, B. (2000) Salmonella nomenclature - Guest commentary. *Journal of Clinical Microbiology* **38**: 2465-2467.

Bronstein, P.A., Miao, E.A., and Miller, S.I. (2000) InvB is a type III secretion chaperone specific for SspA. *Journal of Bacteriology* **182**: 6638-6644.

Buchwald, G., Friebel, A., Galan, J.E., Hardt, W.D., Wittinghofer, A., and Scheffzek, K. (2002) Structural basis for the reversible activation of a Rho protein by the bacterial toxin SopE. *Embo Journal* **21**: 3286-3295.

Cain, R.J., Hayward, R.D., and Koronakis, V. (2004) The target cell plasma membrane is a critical interface for Salmonella cell entry effector-host interplay. *Molecular Microbiology* **54**: 887-904.

Cao, J.G., and Meighen, E.A. (1989) Purification and Structural Identification of an Autoinducer for the Luminescence System of Vibrio-Harveyi. *Journal of Biological Chemistry* **264**: 21670-21676.

Carter, P.B., and Collins, F.M. (1974) Growth of Typhoid and Paratyphoid Bacilli in Intravenously Infected Mice. *Infection and Immunity* **10**: 816-822.

Catron, D.M., Sylvester, M.D., Lange, Y., Kadekoppala, M., Jones, B.D., Monack, D.M., Falkow, S., and Haldar, K. (2002) The Salmonella-containing vacuole is a major site of intracellular cholesterol accumulation and recruits the GPI-anchored protein CD55. *Cellular Microbiology* 4: 315-328.

Chakravortty, D., Hansen-Wester, I., and Hensel, M. (2002) Salmonella pathogenicity island 2 mediates protection of intracellular Salmonella from reactive nitrogen intermediates. *Journal of Experimental Medicine* **195**: 1155-1166.

Chen, L.M., Hobbie, S., and Galan, J.E. (1996a) Requirement of CDC42 for Salmonella-induced cytoskeletal and nuclear responses. *Science* **274**: 2115-2118.

Chen, L.M., Kaniga, K., and Galan, J.E. (1996b) Salmonella spp are cytotoxic for cultured macrophages. *Molecular Microbiology* **21**: 1101-1115.

Chen, L.M., Bagrodia, S., Cerione, R.A., and Galan, J.E. (1999) Requirement of p21-activated kinase (PAK) for Salmonella typhimurium-induced nuclear responses. *Journal of Experimental Medicine* **189**: 1479-1488.

Chen, X., Schauder, S., Potier, N., Van Dorsselaer, A., Pelczer, I., Bassler, B.L., and Hughson, F.M. (2002) Structural identification of a bacterial quorum-sensing signal containing boron. *Nature* **415**: 545-549.

Choi, J., Shin, D., and Ryu, S. (2007) Implication of quorum sensing in *Salmonella* virulence: the *luxS* gene is necessary for expression of genes in pathogenicity island 1. *Infection and Immunity* **published online ahead of print.**

Clark, M.A., Jepson, M.A., Simmons, N.L., and Hirst, B.H. (1994) Preferential Interaction of Salmonella-Typhimurium with Mouse Peyers Patch M-Cells. *Research in Microbiology* **145**: 543-552.

Clark, M.A., Reed, K.A., Lodge, J., Stephen, J., Hirst, B.H., and Jepson, M.A. (1996) Invasion of murine intestinal M cells by Salmonella typhimurium inv mutants severely deficient for invasion of cultured cells. *Infection and Immunity* **64**: 4363-4368.

Clark, M.A., Hirst, B.H., and Jepson, M.A. (1998) Inoculum composition and Salmonella pathogenicity island 1 regulate M-cell invasion and epithelial destruction by Salmonella typhimurium. *Infection and Immunity* **66**: 724-731.

Collazo, C.M., Zierler, M.K., and Galan, J.E. (1995) Functional-Analysis of the Salmonella-Typhimurium Invasion Genes Invi and Invj and Identification of a Target of the Protein Secretion Apparatus Encoded in the Inv Locus. *Molecular Microbiology* **15**: 25-38.

Collazo, C.M., and Galan, J.E. (1997) The invasion-associated type III system of Salmonella typhimurium directs the translocation of Sip proteins into the host cell. *Molecular Microbiology* **24**: 747-756.

Collier-Hyams, L.S., Zeng, H., Sun, J., Tomlinson, A.D., Bao, Z.Q., Chen, H., Madara, J.L., Orth, K., and Neish, A.S. (2002) Salmonella AvrA effector

inhibits the key proinflammatory, anti-apoptotic NF-kappa B pathway. *Journal of Immunology* **169**: 2846-2850.

Collins, F.M. (1972) Salmonellosis in Orally Infected Specific Pathogen-Free C57b1 Mice. *Infection and Immunity* **5**: 191-&.

Cossart, P., and Sansonetti, P.J. (2004) Bacterial invasion: The paradigms of enteroinvasive pathogens. *Science* **304**: 242-248.

Criss, A.K., Ahlgren, D.M., Jou, T.S., McCormick, B.A., and Casanova, J.E. (2001a) The GTPase Rac1 selectively regulates Salmonella invasion at the apical plasma membrane of polarized epithelial cells. *Journal of Cell Science* **114**: 1331-1341.

Criss, A.K., Silva, M., Casanova, J.E., and McCormick, B.A. (2001b) Regulation of Salmonella-induced neutrophil transmigration by epithelial ADP-ribosylation factor 6. *Journal of Biological Chemistry* **276**: 48431-48439.

Criss, A.K., and Casanova, J.E. (2003) Coordinate regulation of Salmonella enterica serovar Typhimurium invasion of epithelial cells by the arp2/3 complex and rho GTPases. *Infection and Immunity* **71**: 2885-2891.

Crump, J.A., Luby, S.P., and Mintz, E.D. (2004) The global burden of typhoid fever. *Bulletin of the World Health Organization* **82**: 346-353.

Dabiri, G.A., Sanger, J.M., Portnoy, D.A., and Southwick, F.S. (1990) Listeria-Monocytogenes Moves Rapidly through the Host-Cell Cytoplasm by Inducing Directional Actin Assembly. *Proceedings of the National Academy of Sciences of the United States of America* **87**: 6068-6072.

Dai, S.P., Sarmiere, P.D., Wiggan, O., Bamburg, J.R., and Zhou, D.G. (2004) Efficient Salmonella entry requires activity cycles of host ADF and cofilin. *Cellular Microbiology* **6**: 459-471.

Darwin, K.H., and Miller, V.L. (1999) Molecular basis of the interaction of Salmonella with the intestinal mucosa. *Clinical Microbiology Reviews* **12**: 405-+.

Darwin, K.H., and Miller, V.L. (2000) The putative invasion protein chaperone SicA acts together with InvF to activate the expression of Salmonella typhimurium virulence genes. *Molecular Microbiology* **35**: 949-959.

Darwin, K.H., and Miller, V.L. (2001) Type III secretion chaperone-dependent regulation: activation of virulence genes by SicA and InvF in Salmonella typhimurium. *Embo Journal* **20**: 1850-1862.

Datsenko, K.A., and Wanner, B.L. (2000) One-step inactivation of chromosomal genes in Escherichia coli K-12 using PCR products. *Proceedings of the National Academy of Sciences of the United States of America* **97**: 6640-6645.

Davies, D.G., Parsek, M.R., Pearson, J.P., Iglewski, B.H., Costerton, J.W., and Greenberg, E.P. (1998) The involvement of cell-to-cell signals in the development of a bacterial biofilm. *Science* **280**: 295-298.

De Kievit, T.R., Gillis, R., Marx, S., Brown, C., and Iglewski, B.H. (2001) Quorum-sensing genes in Pseudomonas aeruginosa biofilms: Their role

and expression patterns. *Applied and Environmental Microbiology* **67**: 1865-1873.

De la Cruz, E.M., Mandinova, A., Steinmetz, M.O., Stoffler, D., Aebi, U., and Pollard, T.D. (2000) Polymerization and structure of nucleotide-free actin filaments. *Journal of Molecular Biology* **295**: 517-526.

Deeks, M.J., and Hussey, P.J. (2005) Arp2/3 and scar: Plants move to the fore. *Nature Reviews Molecular Cell Biology* **6**: 954-964.

Deiwick, J., Salcedo, S.P., Boucrot, E., Gilliland, S.M., Henry, T., Petermann, N., Waterman, S.R., and Gorvel, J.P. (2006) The translocated Salmonella effector proteins SseF and SseG interact and are required to establish an intracellular replication niche. *Infection and Immunity* **74**: 6965-6972.

Deleu, S., Choi, K., Reece, J.M., and Shears, S.B. (2006) Pathogenicity of Salmonella: SopE-mediated membrane ruffling is independent of inositol phosphate signals. *Febs Letters* **580**: 1709-1715.

Derzelle, S., Duchaud, E., Kunst, F., Danchin, A., and Bertin, P. (2002) Identification, characterization, and regulation of a cluster of genes involved in carbapenem biosynthesis in Photorhabdus luminescens. *Applied and Environmental Microbiology* **68**: 3780-3789.

DesMarais, V., Macaluso, F., Condeelis, J., and Bailly, M. (2004) Synergistic interaction between the Arp2/3 complex and cofilin drives stimulated lamellipod extension. *Journal of Cell Science* **117**: 3499-3510.

Dibb-Fuller, M.P., Allen-Vercoe, E., Thorns, C.J., and Woodward, M.J. (1999) Fimbriae- and flagella-mediated association with and invasion of cultured epithelial cells by Salmonella enteritidis. *Microbiology-Sgm* **145**: 1023-1031.

Eberhard, A., Burlingame, A.L., Eberhard, C., Kenyon, G.L., Nealson, K.H., and Oppenheimer, N.J. (1981) Structural Identification of Autoinducer of Photobacterium-Fischeri Luciferase. *Biochemistry* **20**: 2444-2449.

Edsall, G., Gaines, S., Landy, M., Tigertt, W.D., Sprinz, H., Trapani, R.J., Mandel, A.D., and Benenson, A.S. (1960) Studies on Infection and Immunity in Experimental Typhoid Fever .1. Typhoid Fever in Chimpanzees Orally Infected with Salmonella Typhosa. *Journal of Experimental Medicine* **112**: 143-&.

Ellermeier, C.D., and Slauch, J.M. (2003) RtsA and RtsB coordinately regulate expression of the invasion and flagellar genes in Salmonella enterica serovar typhimurium. *Journal of Bacteriology* **185**: 5096-5108.

Ellermeier, C.D., and Slauch, J.M. (2004) RtsA coordinately regulates DsbA and the Salmonella pathogenicity island 1 type III secretion system. *Journal of Bacteriology* **186**: 68-79.

Ellermeier, C.D., Ellermeier, J.R., and Slauch, J.M. (2005) HilD, HilC and RtsA constitute a feed forward loop that controls expression of the SPI1 type three secretion system regulator hilA in Salmonella enterica serovar Typhimurium. *Molecular Microbiology* **57**: 691-705.

Ellermeier, J.R., and Slauch, J.M. (2007) Adaptation to the host environment: regulation of the SPI1 type III secretion system in Salmonella enterica serovar Typhimurium. *Current Opinion in Microbiology* **10**: 24-29.

Elsinghorst, E.A. (1994) Measurement of Invasion by Gentamicin Resistance. In *Bacterial Pathogenesis, Pt B*. Vol. 236, pp. 405-420.

Engebrecht, J., Nealson, K., and Silverman, M. (1983) Bacterial Bioluminescence - Isolation and Genetic-Analysis of Functions from Vibrio Fischeri. *Cell* **32**: 773-781.

Engebrecht, J., and Silverman, M. (1984) Identification of Genes and Gene-Products Necessary for Bacterial Bioluminescence. *Proceedings of the National Academy of Sciences of the United States of America-Biological Sciences* **81**: 4154-4158.

Fierer, J., and Guiney, D.G. (2001) Diverse virulence traits underlying different clinical outcomes of Salmonella infection. *Journal of Clinical Investigation* **107**: 775-780.

Finlay, B.B., and Falkow, S. (1988) Comparison of the Invasion Strategies Used by Salmonella-Cholerae-Suis, Shigella-Flexneri and Yersinia-Enterocolitica to Enter Cultured Animal-Cells - Endosome Acidification Is Not Required for Bacterial Invasion or Intracellular Replication. *Biochimie* **70**: 1089-1099.

Finlay, B.B., Gumbiner, B., and Falkow, S. (1988) Penetration of Salmonella through a Polarized Madin-Darby Canine Kidney Epithelial-Cell Monolayer. *Journal of Cell Biology* **107**: 221-230.

Finlay, B.B., and Falkow, S. (1990) Salmonella Interactions with Polarized Human Intestinal Caco-2 Epithelial-Cells. *Journal of Infectious Diseases* **162**: 1096-1106.

Finlay, B.B., Ruschkowski, S., and Dedhar, S. (1991) Cytoskeletal Rearrangements Accompanying Salmonella Entry into Epithelial-Cells. *Journal of Cell Science* **99**: 283-&.

Fortune, D.R., Suyemoto, M., and Altier, C. (2006) Identification of CsrC and characterization of its role in epithelial cell invasion in Salmonella enterica serovar Typhimurium. *Infection and Immunity* **74**: 331-339.

Foster, J.W. (1991) Salmonella Acid Shock Proteins Are Required for the Adaptive Acid Tolerance Response. *Journal of Bacteriology* **173**: 6896-6902.

Francis, C.L., Starnbach, M.N., and Falkow, S. (1992) Morphological and Cytoskeletal Changes in Epithelial-Cells Occur Immediately Upon Interaction with Salmonella-Typhimurium Grown under Low-Oxygen Conditions. *Molecular Microbiology* **6**: 3077-3087.

Francis, C.L., Ryan, T.A., Jones, B.D., Smith, S.J., and Falkow, S. (1993) Ruffles Induced by Salmonella and Other Stimuli Direct Macropinocytosis of Bacteria. *Nature* **364**: 639-642.

Freeman, J.A., and Bassler, B.L. (1999) Sequence and function of LuxU: a two-component phosphorelay protein that regulates quorum sensing in Vibrio harveyi. *Journal of Bacteriology* **181**: 899-906.

Freeman, J.A., Lilley, B.N., and Bassler, B.L. (2000) A genetic analysis of the functions of LuxN: a two-component hybrid sensor kinase that regulates quorum sensing in Vibrio harveyi. *Molecular Microbiology* **35**: 139-149.

Friebel, A., Ilchmann, H., Aelpfelbacher, M., Ehrbar, K., Machleidt, W., and Hardt, W.D. (2001) SopE and SopE2 from Salmonella typhimurium activate different sets of RhoGTPases of the host cell. *Journal of Biological Chemistry* **276**: 34035-34040.

Friis, L.M., Pin, C., Pearson, B.M., and Wells, J.M. (2005) In vitro cell culture methods for investigating Campylobacter invasion mechanisms (vol 61, pg 145, 2005). *Journal of Microbiological Methods* **63**: 104-104.

Frost, A.J., Bland, A.P., and Wallis, T.S. (1997) The early dynamic response of the calf ileal epithelium to Salmonella typhimurium. *Veterinary Pathology* **34**: 369-386.

Fu, Y.X., and Galan, J.E. (1998) The Salmonella typhimurium tyrosine phosphatase SptP is translocated into host cells and disrupts the actin cytoskeleton. *Molecular Microbiology* **27**: 359-368.

Fu, Y.X., and Galan, J.E. (1999) A Salmonella protein antagonizes Rac-1 and Cdc42 to mediate host-cell recovery after bacterial invasion. *Nature* **401**: 293-297.

Galan, J.E., and Curtiss, R. (1989) Cloning and Molecular Characterization of Genes Whose Products Allow Salmonella-Typhimurium to Penetrate Tissue-Culture Cells. *Proceedings of the National Academy of Sciences of the United States of America* **86**: 6383-6387.

Galan, J.E. (1996) Molecular genetic bases of Salmonella entry into host cells. *Molecular Microbiology* **20**: 263-271.

Galan, J.E., and Zhou, D. (2000) Striking a balance: Modulation of the actin cytoskeleton by Salmonella. *Proceedings of the National Academy of Sciences of the United States of America* **97**: 8754-8761.

Galan, J.E. (2001) Salmonella interactions with host cells: Type III secretion at work. *Annual Review of Cell and Developmental Biology* **17**: 53-86.

Galkin, V.E., Orlova, A., VanLoock, M.S., Zhou, D.G., Galan, J.E., and Egelman, E.H. (2002) The bacterial protein SipA polymerizes G-actin and mimics muscle nebulin. *Nature Structural Biology* **9**: 518-521.

Gallois, A., Klein, J.R., Allen, L.A.H., Jones, B.D., and Nauseef, W.M. (2001) Salmonella pathogenicity island 2-encoded type III secretion system mediates exclusion of NADPH oxidase assembly from the phagosomal membrane. *Journal of Immunology* **166**: 5741-5748.

Galyov, E.E., Wood, M.W., Rosqvist, R., Mullan, P.B., Watson, P.R., Hedges, S., and Wallis, T.S. (1997) A secreted effector protein of Salmonella dublin is translocated into eukaryotic cells and mediates inflammation

and fluid secretion in infected ileal mucosa. *Molecular Microbiology* **25**: 903-912.

Gauthier-Rouviere, C., Vignal, E., Meriane, M., Roux, P., Montcourier, P., and Fort, P. (1998) RhoG GTPase controls a pathway that independently activates Rac1 and Cdc42Hs. *Molecular Biology of the Cell* **9**: 1379-1394.

Gebert, A. (1997) The role of M cells in the protection of mucosal membranes. *Histochemistry and Cell Biology* **108**: 455-470.

Gebert, A., and Preiss, G. (1998) A simple method for the acquisition of high-quality digital images from analog scanning electron microscopes. *Journal of Microscopy-Oxford* **191**: 297-302.

Gewirtz, A.T., Siber, A.M., Madara, J.L., and McCormick, B.A. (1999) Orchestration of neutrophil movement by intestinal epithelial cells in response to Salmonella typhimurium can be uncoupled from bacterial internalization. *Infection and Immunity* **67**: 608-617.

Gewirtz, A.T., Navas, T.A., Lyons, S., Godowski, P.J., and Madara, J.L. (2001a) Cutting edge: Bacterial flagellin activates basolaterally expressed TLR5 to induce epithelial proinflammatory gene expression. *Journal of Immunology* **167**: 1882-1885.

Gewirtz, A.T., Simon, P.O., Schmitt, C.K., Taylor, L.J., Hagedorn, C.H., O'Brien, A.D., Neish, A.S., and Madara, J.L. (2001b) Salmonella typhimurium translocates flagellin across intestinal epithelia, inducing a proinflammatory response. *Journal of Clinical Investigation* **107**: 99-109.

Giannella, R., Broitman, S.A., and Zamcheck, N. (1971) Salmonella Enteritis .1. Role of Reduced Gastric Secretion in Pathogenesis. *American Journal of Digestive Diseases* **16**: 1000-1006.

Giannella, R., Washingt.O, Gemski, P., and Formal, S.B. (1973) Invasion of Hela-Cells by Salmonella-Typhimurium - Model for Study of Invasiveness of Salmonella. *Journal of Infectious Diseases* **128**: 69-75.

Ginocchio, C., Pace, J., and Galan, J.E. (1992) Identification and Molecular Characterization of a Salmonella-Typhimurium Gene Involved in Triggering the Internalization of Salmonellae into Cultured Epithelial-Cells. *Proceedings of the National Academy of Sciences of the United States of America* **89**: 5976-5980.

Groisman, E.A., and Ochman, H. (1993) Cognate Gene Clusters Govern Invasion of Host Epithelial-Cells by Salmonella-Typhimurium and Shigella-Flexneri. *Embo Journal* **12**: 3779-3787.

Groisman, E.A., and Ochman, H. (1997) How Salmonella became a pathogen. *Trends in Microbiology* **5**: 343-349.

Hammer, B.K., and Bassler, B.L. (2003) Quorum sensing controls biofilm formation in Vibrio cholerae. *Molecular Microbiology* **50**: 101-114.

Hapfelmeier, S., Ehrbar, K., Stecher, B., Barthel, M., Kremer, M., and Hardt, W.D. (2004) Role of the Salmonella pathogenicity island 1 effector proteins SipA, SopB, SopE, and SopE2 in Salmonella enterica subspecies

1 serovar typhimurium colitis in streptomycin-pretreated mice. *Infection and Immunity* **72**: 795-809.

Haraga, A., and Miller, S.I. (2003) A Salmonella enterica serovar typhimurium translocated leucine-rich repeat effector protein inhibits NF-kappa B-dependent gene expression. *Infection and Immunity* **71**: 4052-4058.

Hardt, W.D., Chen, L.M., Schuebel, K.E., Bustelo, X.R., and Galan, J.E. (1998a) S-typhimurium encodes an activator of Rho GTPases that induces membrane ruffling and nuclear responses in host cells. *Cell* **93**: 815-826.

Hardt, W.D., Urlaub, H., and Galan, J.E. (1998b) A substrate of the centisome 63 type III protein secretion system of Salmonella typhimurium is encoded by a cryptic bacteriophage. *Proceedings of the National Academy of Sciences of the United States of America* **95**: 2574-2579.

Harrison, R.E., Brumell, J.H., Khandani, A., Bucci, C., Scott, C.C., Jiang, X.J., Finlay, B.B., and Grinstein, S.L. (2004) Salmonella impairs RILP recruitment to Rab7 during maturation of invasion vacuoles. *Molecular Biology of the Cell* **15**: 3146-3154.

Hashim, S., Mukherjee, K., Raje, M., Basu, S.K., and Mukhopadhyay, A. (2000) Live Salmonella modulate expression of Rab proteins to persist in a specialized compartment and escape transport to lysosomes. *Journal of Biological Chemistry* **275**: 16281-16288.

Hautefort, I., Proenca, M.J., and Hinton, J.C.D. (2003) Single-copy green fluorescent protein gene fusions allow accurate measurement of Salmonella gene expression in vitro and during infection of mammalian cells. *Applied and Environmental Microbiology* **69**: 7480-7491.

Hayward, R.D., and Koronakis, V. (1999) Direct nucleation and bundling of actin by the SipC protein of invasive Salmonella. *Embo Journal* **18**: 4926-4934.

Hayward, R.D., and Koronakis, V. (2002) Direct modulation of the host cell cytoskeleton by Salmonella actin-binding proteins. *Trends in Cell Biology* **12**: 15-20.

Henke, J.M., and Bassler, B.L. (2004a) Quorum sensing regulates type III secretion in Vibrio harveyi and Vibrio parahaemolyticus. *Journal of Bacteriology* **186**: 3794-3805.

Henke, J.M., and Bassler, B.L. (2004b) Bacterial social engagements. *Trends in Cell Biology* **14**: 648-656.

Henke, J.M., and Bassler, B.L. (2004c) Three parallel quorum-sensing systems regulate gene expression in Vibrio harveyi. *Journal of Bacteriology* **186**: 6902-6914.

Hensel, M. (2004) Evolution of pathogenicity islands of Salmonella enterica. *International Journal of Medical Microbiology* **294**: 95-102.

Hernandez, L.D., Heuffer, K., Wenk, M.R., and Galan, J.E. (2004) Salmonella modulates vesicular traffic by altering phosphoinositide metabolism. *Science* **304**: 1805-1807.

Hersh, D., Monack, D.M., Smith, M.R., Ghori, N., Falkow, S., and Zychlinsky, A. (1999) The Salmonella invasin SipB induces macrophage apoptosis by binding to caspase-1. *Proceedings of the National Academy of Sciences of the United States of America* **96**: 2396-2401.

Higashide, W., Dai, S.P., Hombs, V.P., and Zhou, D.G. (2002) Involvement of SipA in modulating actin dynamics during Salmonella invasion into cultured epithelial cells. *Cellular Microbiology* **4**: 357-365.

Hobbie, S., Chen, L.M., Davis, R.J., and Galan, J.E. (1997) Involvement of mitogen-activated protein kinase pathways in the nuclear responses and cytokine production induced by Salmonella typhimurium in cultured intestinal epithelial cells. *Journal of Immunology* **159**: 5550-5559.

Hobert, M.E., Sands, K.A., Mrsny, R.J., and Madara, J.L. (2002) Cdc42 and Rac1 regulate late events in Salmonella typhimurium-induced interleukin-8 secretion from polarized epithelial cells. *Journal of Biological Chemistry* **277**: 51025-51032.

Hong, K.H., and Miller, V.L. (1998) Identification of a novel Salmonella invasion locus homologous to Shigella ipgDE. *Journal of Bacteriology* **180**: 1793-1802.

Hopkins, S.A., Niedergang, F., Corthesy-Theulaz, I.E., and Kraehenbuhl, J.P. (2000) A recombinant Salmonella typhimurium vaccine strain is taken up and survives within murine Peyer's patch dendritic cells. *Cellular Microbiology* **2**: 59-68.

Huang, F.C., Werne, A., Li, Q., Galyov, E.E., Walker, W.A., and Cherayil, B.J. (2004) Cooperative interactions between flagellin and SopE2 in the epithelial interleukin-8 response to Salmonella enterica serovar typhimurium infection. *Infection and Immunity* **72**: 5052-5062.

Hueck, C.J., Hantman, M.J., Bajaj, V., Johnston, C., Lee, C.A., and Miller, S.I. (1995) Salmonella-Typhimurium Secreted Invasion Determinants Are Homologous to Shigella Ipa Proteins. *Molecular Microbiology* **18**: 479-490.

Hueck, C.J. (1998) Type III protein secretion systems in bacterial pathogens of animals and plants. *Microbiology and Molecular Biology Reviews* **62**: 379-+.

Humphreys, S., Rowley, G., Stevenson, A., Anjum, M.F., Woodward, M.J., Gilbert, S., Kormanec, J., and Roberts, M. (2004) Role of the two-component regulator CpxAR in the virulence of Salmonella entetica serotype typhimurium. *Infection and Immunity* **72**: 4654-4661.

Hurley, B.P., and McCormick, B.A. (2003) Translating tissue culture results into animal models: the case of Salmonella typhimurium. *Trends in Microbiology* **11**: 562-569.

Ikeda, J.S., Schmitt, C.K., Darnell, S.C., Watson, P.R., Bispham, J., Wallis, T.S., Weinstein, D.L., Metcalf, E.S., Adams, P., O'Connor, C.D., and O'Brien, A.D. (2001) Flagellar phase variation of Salmonella enterica serovar typhimurium contributes to virulence in the murine typhoid infection

model but does not influence Salmonella-induced enteropathogenesis. *Infection and Immunity* **69**: 3021-3030.

Jepson, M.A., Collaresbuzato, C.B., Clark, M.A., Hirst, B.H., and Simmons, N.L. (1995) Rapid Disruption of Epithelial Barrier Function by Salmonella-Typhimurium Is Associated with Structural Modification of Intercellular-Junctions. *Infection and Immunity* **63**: 356-359.

Jepson, M.A., Lang, T.F., Reed, K.A., and Simmons, N.L. (1996) Evidence for a vapid, direct effect on epithelial monolayer integrity and transepithelial transport is response to Salmonella invasion. *Pflugers Archiv-European Journal of Physiology* **432**: 225-233.

Jepson, M.A., and Clark, M.A. (1998) Studying M cells and their role in infection. *Trends in Microbiology* **6**: 359-365.

Jepson, M.A., Schlecht, H.B., and Collares-Buzato, C.B. (2000) Localization of dysfunctional tight junctions in Salmonella enterica serovar Typhimurium-infected epithelial layers. *Infection and Immunity* **68**: 7202-7208.

Jepson, M.A., and Clark, M.A. (2001) The role of M cells in Salmonella infection. *Microbes and Infection* **3**: 1183-1190.

Jepson, M.A., Kenny, B., and Leard, A.D. (2001) Role of sipA in the early stages of Salmonella typhimurium entry into epithelial cells. *Cellular Microbiology* **3**: 417-426.

Jones, B.D., Lee, C.A., and Falkow, S. (1992) Invasion by Salmonella-Typhimurium Is Affected by the Direction of Flagellar Rotation. *Infection and Immunity* **60**: 2475-2480.

Jones, B.D., and Falkow, S. (1994) Identification and Characterization of a Salmonella-Typhimurium Oxygen-Regulated Gene Required for Bacterial Internalization. *Infection and Immunity* **62**: 3745-3752.

Jones, B.D., Ghori, N., and Falkow, S. (1994) Salmonella-Typhimurium Initiates Murine Infection by Penetrating and Destroying the Specialized Epithelial M-Cells of the Peyers-Patches. *Journal of Experimental Medicine* **180**: 15-23.

Jones, G.W., Richardson, L.A., and Uhlman, D. (1981) The Invasion of Hela-Cells by Salmonella-Typhimurium - Reversible and Irreversible Bacterial Attachment and the Role of Bacterial Motility. *Journal of General Microbiology* **127**: 351-360.

Jones, M.A., Wood, M.W., Mullan, P.B., Watson, P.R., Wallis, T.S., and Galyov, E.E. (1998) Secreted effector proteins of Salmonella dublin act in concert to induce enteritis. *Infection and Immunity* **66**: 5799-5804.

Kaniga, K., Bossio, J.C., and Galan, J.E. (1994) The Salmonella-Typhimurium Invasion Genes Invf and Invg Encode Homologs of the Arac and Puld Family of Proteins. *Molecular Microbiology* **13**: 555-568.

Kaniga, K., Trollinger, D., and Galan, J.E. (1995a) Identification of 2 Targets of the Type-III Protein Secretion System Encoded by the Inv and Spa Loci

of Salmonella-Typhimurium That Have Homology to the Shigella Ipad and Ipaa Proteins. *Journal of Bacteriology* **177**: 7078-7085.

Kaniga, K., Tucker, S., Trollinger, D., and Galan, J.E. (1995b) Homologs of the Shigella IpaB and IpaC Invasins Are Required for Salmonella-Typhimurium Entry into Cultured Epithelial-Cells. *Journal of Bacteriology* **177**: 3965-3971.

Kaniga, K., Uralil, J., Bliska, J.B., and Galan, J.E. (1996) A secreted protein tyrosine phosphatase with modular effector domains in the bacterial pathogen Salmonella typhimurium. *Molecular Microbiology* **21**: 633-641.

Kaper, J.B., and Sperandio, V. (2005) Bacterial cell-to-cell signaling in the gastrointestinal tract. *Infection and Immunity* **73**: 3197-3209.

Kaplan, H.B., and Greenberg, E.P. (1985) Diffusion of Autoinducer Is Involved in Regulation of the Vibrio-Fischeri Luminescence System. *Journal of Bacteriology* **163**: 1210-1214.

Khoramian-Falsafi, T., Harayama, S., Kutsukake, K., and Pechere, J.C. (1990) Effect of Motility and Chemotaxis on the Invasion of Salmonella-Typhimurium into Hela-Cells. *Microbial Pathogenesis* **9**: 47-53.

Kiama, S.G., Dreher, D., Cochand, L., Kok, M., Obregon, C., Nicod, L., and Gehr, P. (2006) Host cell responses of Salmonella typhimurium infected human dendritic cells. *Immunology and Cell Biology* **84**: 475-481.

Kimbrough, T.G., and Miller, S.I. (2000) Contribution of Salmonella typhimurium type III secretion components to needle complex formation. *Proceedings of the National Academy of Sciences of the United States of America* **97**: 11008-11013.

Kleerebezem, M., Quadri, L.E.N., Kuipers, O.P., and deVos, W.M. (1997) Quorum sensing by peptide pheromones and two-component signal-transduction systems in Gram-positive bacteria. *Molecular Microbiology* **24**: 895-904.

Knodler, L.A., Vallance, B.A., Hensel, M., Jackel, D., Finlay, B.B., and Steele-Mortimer, O. (2003) Salmonella type III effectors PipB and PipB2 are targeted to detergent-resistant microdomains on internal host cell membranes. *Molecular Microbiology* **49**: 685-704.

Knodler, L.A., Finlay, B.B., and Steele-Mortimer, O. (2005) The Salmonella effector protein SopB protects epithelial cells from apoptosis by sustained activation of Akt. *Journal of Biological Chemistry* **280**: 9058-9064.

Kohler, H., Sakaguchi, T., Hurley, B.P., Kase, B.J., Reinecker, H.C., and McCormick, B.A. (2007) Salmonella enterica serovar Typhimurium regulates intercellular junction proteins and facilitates transepithelial neutrophil and bacterial passage. *American Journal of Physiology-Gastrointestinal and Liver Physiology* **293**: G178-G187.

Kubori, T., Matsushima, Y., Nakamura, D., Uralil, J., Lara-Tejero, M., Sukhan, A., Galan, J.E., and Aizawa, S. (1998) Supramolecular structure of the Salmonella typhimurium type III protein secretion system. *Science* **280**: 602-605.

Kubori, T., Sukhan, A., Aizawa, S.I., and Galan, J.E. (2000) Molecular characterization and assembly of the needle complex of the Salmonella typhimurium type III protein secretion system. *Proceedings of the National Academy of Sciences of the United States of America* **97**: 10225-10230.

Kubori, T., and Galan, J.E. (2003) Temporal regulation of Salmonella virulence effector function by proteasome-dependent protein degradation. *Cell* **115**: 333-342.

Kusters, J.G., Mulderskremers, G., Vandoornik, C.E.M., and Vanderzeijst, B.A.M. (1993) Effects of Multiplicity of Infection, Bacterial Protein-Synthesis, and Growth-Phase on Adhesion to and Invasion of Human Cell-Lines by Salmonella-Typhimurium. *Infection and Immunity* **61**: 5013-5020.

La Ragione, R.M., Cooley, W.A., Velge, P., Jepson, M.A., and Woodward, M.J. (2003) Membrane ruffling and invasion of human and avian cell lines is reduced for aflagellate mutants of Salmonella enterica serotype Enteritidis. *International Journal of Medical Microbiology* **293**: 261-272.

Lee, C.A., and Falkow, S. (1990) The Ability of Salmonella to Enter Mammalian-Cells Is Affected by Bacterial-Growth State. *Proceedings of the National Academy of Sciences of the United States of America* **87**: 4304-4308.

Lee, C.A., Silva, M., Siber, A.M., Kelly, A.J., Galyov, E., and McCormick, B.A. (2000) A secreted Salmonella protein induces a proinflammatory response in epithelial cells, which promotes neutrophil migration. *Proceedings of the National Academy of Sciences of the United States of America* **97**: 12283-12288.

Lee, I.S., Lin, J.S., Hall, H.K., Bearson, B., and Foster, J.W. (1995) The Stationary-Phase Sigma-Factor Sigma(S) (Rpos) Is Required for a Sustained Acid Tolerance Response in Virulent Salmonella-Typhimurium. *Molecular Microbiology* **17**: 155-167.

Lenz, D.H., Mok, K.C., Lilley, B.N., Kulkarni, R.V., Wingreen, N.S., and Bassler, B.L. (2004) The small RNA chaperone Hfq and multiple small RNAs control quorum sensing in Vibrio harveyi and Vibrio cholerae. *Cell* **118**: 69-82.

Lilic, A., and Stebbins, C.E. (2004) Re-structuring the host cell: up close with Salmonella's molecular machinery. *Microbes and Infection* **6**: 1205-1211.

Lilic, M., Galkin, V.E., Orlova, A., VanLoock, M.S., Egelman, E.H., and Stebbins, C.E. (2003) Salmonella SipA polymerizes actin by stapling filaments with nonglobular protein arms. *Science* **301**: 1918-1921.

Lilic, M., Vujanac, M., and Stebbins, C.E. (2006) A common structural motif in the binding of virulence factors to bacterial secretion chaperones. *Molecular Cell* **21**: 653-664.

Lilley, B.N., and Bassler, B.L. (2000) Regulation of quorum sensing in Vibrio harveyi by LuxO and Sigma-54. *Molecular Microbiology* **36**: 940-954.

Lin, S.L., Le, T.X., and Cowen, D.S. (2003) SptP, a Salmonella typhimurium type III-secreted protein, inhibits the mitogen-activated protein kinase pathway by inhibiting Raf activation. *Cellular Microbiology* **5**: 267-275.

Lundberg, U., Vinatzer, U., Berdnik, D., von Gabain, A., and Baccarini, M. (1999) Growth phase-regulated induction of Salmonella-induced macrophage apoptosis correlates with transient expression of SPI-1 genes. *Journal of Bacteriology* **181**: 3433-3437.

Ly, K.T., and Casanova, J.E. (2007) Mechanisms of *Salmonella* entry into host cells. *Cell Microbiology* **9**: 2103-2111.

Mansson, L.E., Melican, K., Boekel, J., Sandoval, R.M., Hautefort, I., Tanner, G.A., Molitoris, B.A., and Richter-Dahlfors, A. (2007) Real-time studies of the progression of bacterial infections and immediate tissue responses in live animals. *Cellular Microbiology* **9**: 413-424.

Marcus, S.L., Brumell, J.H., Pfeifer, C.G., and Finlay, B.B. (2000) Salmonella pathogenicity islands: big virulence in small packages. *Microbes and Infection* **2**: 145-156.

Marcus, S.L., Wenk, M.R., Steele-Mortimer, O., and Finlay, B.B. (2001) A synaptojanin-homologous region of Salmonella typhimurium SigD is essential for inositol phosphatase activity and Akt activation. *Febs Letters* **494**: 201-207.

Marlovits, T.C., Kubori, T., Lara-Tejero, M., Thomas, D., Unger, V.M., and Galan, J.E. (2006) Assembly of the inner rod determines needle length in the type III secretion injectisome. *Nature* **441**: 637-640.

Mason, D., Mallo, G.V., Terebiznik, M.R., Payrastre, B., Finlay, B.B., Brumell, J.H., Rameh, L., and Grinstein, S. (2007) Alteration of epithelial structure and function associated with PtdIns(4,5)P-2 degradation by a bacterial phosphatase. *Journal of General Physiology* **129**: 267-283.

Mastroeni, P., Ugrinovic, S., Chandra, A., MacLennan, C., Doffinger, R., and Kumararatne, D. (2003) Resistance and susceptibility to Salmonella infections: lessons from mice and patients with immunodeficiencies. *Reviews in Medical Microbiology* **14**: 53-62.

McCormick, B.A., Colgan, S.P., Delparcher, C., Miller, S.I., and Madara, J.L. (1993) Salmonella-Typhimurium Attachment to Human Intestinal Epithelial Monolayers - Transcellular Signaling to Subepithelial Neutrophils. *Journal of Cell Biology* **123**: 895-907.

McCormick, B.A., Hofman, P.M., Kim, J., Carnes, D.K., Miller, S.I., and Madara, J.L. (1995a) Surface Attachment of Salmonella-Typhimurium to Intestinal Epithelia Imprints the Subepithelial Matrix with Gradients Chemotactic for Neutrophils. *Journal of Cell Biology* **131**: 1599-1608.

McCormick, B.A., Miller, S.I., Carnes, D., and Madara, J.L. (1995b) Transepithelial Signaling to Neutrophils by Salmonellae - a Novel Virulence Mechanism for Gastroenteritis. *Infection and Immunity* **63**: 2302-2309.

McCormick, B.A., Parkos, C.A., Colgan, S.P., Carnes, D.K., and Madara, J.L. (1998) Apical secretion of a pathogen-elicited epithelial chemoattractant

activity in response to surface colonization of intestinal epithelia by Salmonella typhimurium. *Journal of Immunology* **160**: 455-466.

McCormick, B.A. (2007) Bacterial-induced hepoxilin A(3) secretion as a pro-inflammatory mediator. *Febs Journal* **274**: 3513-3518.

McDaniel, T.K., Jarvis, K.G., Donnenberg, M.S., and Kaper, J.B. (1995) A Genetic-Locus of Enterocyte Effacement Conserved among Diverse Enterobacterial Pathogens. *Proceedings of the National Academy of Sciences of the United States of America* **92**: 1664-1668.

McGhie, E.J., Hayward, R.D., and Koronakis, V. (2001) Cooperation between actin-binding proteins of invasive Salmonella: SipA potentiates SipC nucleation and bundling of actin. *Embo Journal* **20**: 2131-2139.

McGhie, E.J., Hayward, R.D., and Koronakis, V. (2004) Control of actin turnover by a Salmonella invasion protein. *Molecular Cell* **13**: 497-510.

Mead, P.S., Slutsker, L., Dietz, V., McCaig, L.F., Bresee, J.S., Shapiro, C., Griffin, P.M., and Tauxe, R.V. (1999) Food-related illness and death in the United States. *Emerging Infectious Diseases* **5**: 607-625.

Michael, B., Smith, J.N., Swift, S., Heffron, F., and Ahmer, B.M.M. (2001) SdiA of Salmonella enterica is a LuxR homolog that detects mixed microbial communities. *Journal of Bacteriology* **183**: 5733-5742.

Miki, H., Yamaguchi, H., Suetsugu, S., and Takenawa, T. (2000) IRSp53 is an essential intermediate between Rac and WAVE in the regulation of membrane ruffling. *Nature* **408**: 732-735.

Miller, M.B., Skorupski, K., Lenz, D.H., Taylor, R.K., and Bassler, B.L. (2002) Parallel quorum sensing systems converge to regulate virulence in Vibrio cholerae. *Cell* **110**: 303-314.

Miller, S.T., Xavier, K.B., Campagna, S.R., Taga, M.E., Semmelhack, M.F., Bassler, B.L., and Hughson, F.M. (2004) Salmonella typhimurium recognizes a chemically distinct form of the bacterial quorum-sensing signal AI-2. *Molecular Cell* **15**: 677-687.

Mills, D.M., Bajaj, V., and Lee, C.A. (1995) A 40 Kb Chromosomal Fragment Encoding Salmonella-Typhimurium Invasion Genes Is Absent from the Corresponding Region of the Escherichia-Coli K-12 Chromosome. *Molecular Microbiology* **15**: 749-759.

Mills, S.D., and Finlay, B.B. (1994) Comparison of Salmonella-Typhi and Salmonella-Typhimurium Invasion, Intracellular Growth and Localization in Cultured Human Epithelial-Cells. *Microbial Pathogenesis* **17**: 409-423.

Mirold, S., Rabsch, W., Rohde, M., Stender, S., Tschape, H., Russmann, H., Igwe, E., and Hardt, W.D. (1999) Isolation of a temperate bacteriophage encoding the type III effector protein SopE from an epidemic Salmonella typhimurium strain. *Proceedings of the National Academy of Sciences of the United States of America* **96**: 9845-9850.

Mirold, S., Ehrbar, K., Weissmuller, A., Prager, R., Tschape, H., Russmann, H., and Hardt, W.D. (2001a) Salmonella host cell invasion emerged by

acquisition of a mosaic of separate genetic elements, including Salmonella pathogenicity island 1 (SPI1), SPI5, and sopE2. *Journal of Bacteriology* **183**: 2348-2358.

Mirold, S., Rabsch, W., Tschape, H., and Hardt, W.D. (2001b) Transfer of the Salmonella type III effector sopE between unrelated phage families. *Journal of Molecular Biology* **312**: 7-16.

Mitra, K., Zhou, D.G., and Galan, J.E. (2000) Biophysical characterization of SipA, an actin-binding protein from Salmonella enterica. *Febs Letters* **482**: 81-84.

Monack, D.M., Raupach, B., Hromockyj, A.E., and Falkow, S. (1996) Salmonella typhimurium invasion induces apoptosis in infected macrophages. *Proceedings of the National Academy of Sciences of the United States of America* **93**: 9833-9838.

Mrsny, R.J., Gewirtz, A.T., Siccardi, D., Savidge, T., Hurley, B.P., Madara, J.L., and McCormick, B.A. (2004) Identification of hepoxilin A(3) in inflammatory events: A required role in neutrophil migration across intestinal epithelia. *Proceedings of the National Academy of Sciences of the United States of America* **101**: 7421-7426.

Murli, S., Watson, R.O., and Galan, J.E. (2001) Role of tyrosine kinases and the tyrosine phosphatase SptP in the interaction of Salmonella with host cells. *Cellular Microbiology* **3**: 795-810.

Nakayama, S., Kushiro, A., Asahara, T., Tanaka, R., Hu, L., Kopecko, D.J., and Watanabe, H. (2003) Activation of hilA expression at low pH requires the signal sensor CpxA, but not the cognate response regulator CpxR, in Salmonella enterica serovar Typhimurium. *Microbiology-Sgm* **149**: 2809-2817.

Nobes, C.D., and Hall, A. (1995) Rho, Rac, and Cdc42 Gtpases Regulate the Assembly of Multimolecular Focal Complexes Associated with Actin Stress Fibers, Lamellipodia, and Filopodia. *Cell* **81**: 53-62.

Norris, F.A., Wilson, M.P., Wallis, T.S., Galyov, E.E., and Majerus, P.W. (1998) SopB, a protein required for virulence of Salmonella dublin, is an inositol phosphate phosphatase. *Proceedings of the National Academy of Sciences of the United States of America* **95**: 14057-14059.

Ozbudak, E.M., Thattai, M., Kurtser, I., Grossman, A.D., and van Oudenaarden, A. (2002) Regulation of noise in the expression of a single gene. *Nature Genetics* **31**: 69-73.

Pang, T., Bhutta, Z.A., Finlay, B.B., and Altwegg, M. (1995) Typhoid-Fever and Other Salmonellosis - a Continuing Challenge. *Trends in Microbiology* **3**: 253-255.

Pardon, P., Sanchis, R., Marly, J., Lantier, F., Guilloteau, L., Buzonigatel, D., Oswald, I.P., Pepin, M., Kaeffer, B., Berthon, P., and Popoff, M.Y. (1990) Experimental Ovine Salmonellosis (Salmonella-Abortusovis) - Pathogenesis and Vaccination. *Research in Microbiology* **141**: 945-953.

Patel, J.C., Rossanese, O.W., and Galan, J.E. (2005) The functional interface between Salmonella and its host cell: opportunities for therapeutic intervention. *Trends in Pharmacological Sciences* **26**: 564-570.

Patel, J.C., and Galan, J.E. (2006) Differential activation and function of Rho GTPases during Salmonella-host cell interactions. *Journal of Cell Biology* **175**: 453-463.

Paterson, H.F., Self, A.J., Garrett, M.D., Just, I., Aktories, K., and Hall, A. (1990) Microinjection of Recombinant-P21rho Induces Rapid Changes in Cell Morphology. *Journal of Cell Biology* **111**: 1001-1007.

Pattni, K., Jepson, M., Stenmark, H., and Banting, G. (2001) A PtdIns(3)P-specific probe cycles on and off host cell membranes during Salmonella invasion of mammalian cells. *Current Biology* **11**: 1636-1642.

Perrett, C.A., and Jepson, M.A. (2007) Chapter 12: Applications of Cell Imaging in *Salmonella* Research In *Salmonella: Methods and Protocols (Methods in Molecular Biology)*. Vol. 394. Schatten, H. and Eisenstark, A. (eds): Humana Press, pp. 235-272.

Plano, G.V., Day, J.B., and Ferracci, F. (2001) Type III export: new uses for an old pathway. *Molecular Microbiology* **40**: 284-293.

Pollard, T.D., and Borisy, G.G. (2003) Cellular motility driven by assembly and disassembly of actin filaments. *Cell* **112**: 453-465.

Popoff, M.Y., Bockemuhl, J., and Gheesling, L.L. (2004) Supplement 2002 (no. 46) to the Kauffmann-White scheme. *Research in Microbiology* **155**: 568-570.

Raffatellu, M., Wilson, R.P., Chessa, D., Andrews-Polymenis, H., Tran, Q.T., Lawhon, S., Khare, S., Adams, L.G., and Baumler, A.J. (2005) SipA, SopA, SopB, SopD, and SopE2 contribute to Salmonella enterica serotype Typhimurium invasion of epithelial cells. *Infection and Immunity* **73**: 146-154.

Ramboarina, S., Fernandes, P.J., Daniell, S., Islam, S., Simpson, P., Frankel, G., Booy, F., Donnenberg, M.S., and Matthews, S. (2005) Structure of the bundle-forming pilus from enteropathogenic Escherichia coli. *Journal of Biological Chemistry* **280**: 40252-40260.

Ramsden, A.E., Holden, D.W., and Mota, L.J. (2007a) Membrane dynamics and spatial distribution of Salmonella-containing vacuoles. *Trends in Microbiology* **15**: 516-524.

Ramsden, A.E., Mota, L.J., Munter, S., Shorte, S.L., and Holden, D.W. (2007b) The SPI-2 type III secretion system restricts motility of Salmonella-containing vacuoles. *Cellular Microbiology* **9**: 2517-2529.

Rathman, M., Barker, L.P., and Falkow, S. (1997) The unique trafficking pattern of Salmonella typhimurium-containing phagosomes in murine macrophages is independent of the mechanism of bacterial entry. *Infection and Immunity* **65**: 1475-1485.

Reed, K.A., Booth, T.A., Hirst, B.H., and Jepson, M.A. (1996) Promotion of Salmonella typhimurium adherence and membrane ruffling in MDCK epithelia by staurosporine. *Fems Microbiology Letters* **145**: 233-238.

Reed, K.A., Clark, M.A., Booth, T.A., Hueck, C.J., Miller, S.I., Hirst, B.H., and Jepson, M.A. (1998) Cell-contact-stimulated formation of filamentous appendages by Salmonella typhimurium does not depend on the type III secretion system encoded by Salmonella pathogenicity island 1. *Infection and Immunity* **66**: 2007-2017.

Reis, B.P., Zhang, S.P., Tsolis, R.M., Baumler, A.J., Adams, L.G., and Santos, R.L. (2003) The attenuated sopB mutant of Salmonella enterica serovar Typhimurium has the same tissue distribution and host chemokine response as the wild type in bovine Peyer's patches. *Veterinary Microbiology* **97**: 269-277.

Rescigno, M., Urbano, M., Valzasina, B., Francolini, M., Rotta, G., Bonasio, R., Granucci, F., Kraehenbuhl, J.P., and Ricciardi-Castagnoli, P. (2001) Dendritic cells express tight junction proteins and penetrate gut epithelial monolayers to sample bacteria. *Nature Immunology* **2**: 361-367.

Ridley, A.J., and Hall, A. (1992) Distinct Patterns of Actin Organization Regulated by the Small Gtp-Binding Proteins Rac and Rho. *Cold Spring Harbor Symposia on Quantitative Biology* **57**: 661-671.

Rudolph, M.G., Weise, C., Mirold, S., Hillenbrand, B., Bader, B., Wittinghofer, A., and Hardt, W.D. (1999) Biochemical analysis of SopE from Salmonella typhimurium, a highly efficient guanosine nucleotide exchange factor for RhoGTPases. *Journal of Biological Chemistry* **274**: 30501-30509.

Rychlik, I., and Barrow, P.A. (2005) Salmonella stress management and its relevance to behaviour during intestinal colonisation and infection. *Fems Microbiology Reviews* **29**: 1021-1040.

Salcedo, S.P., and Holden, D.W. (2003) SseG, a virulence protein that targets Salmonella to the Golgi network. *Embo Journal* **22**: 5003-5014.

Sato, S.B., and Toyama, S. (1994) Interference with the Endosomal Acidification by a Monoclonal-Antibody Directed toward the 116 (100)-Kd Subunit of the Vacuolar-Type Proton Pump. *Journal of Cell Biology* **127**: 39-53.

Schauder, S., Shokat, K., Surette, M.G., and Bassler, B.L. (2001) The LuxS family of bacterial autoinducers: biosynthesis of a novel quorum-sensing signal molecule. *Molecular Microbiology* **41**: 463-476.

Schechter, L.M., and Lee, C.A. (2001) AraC/XylS family members, HilC and HilD, directly bind and derepress the Salmonella typhimurium hilA promoter. *Molecular Microbiology* **40**: 1289-1299.

Schlumberger, M.C., Muller, A.J., Ehrbar, K., Winnen, B., Duss, I., Stecher, B., and Hardt, W.D. (2005) Real-time imaging of type III secretion: Salmonella SipA injection into host cells. *Proceedings of the National Academy of Sciences of the United States of America* **102**: 12548-12553.

Schlumberger, M.C., Kappeli, R., Wetter, M., Muller, A.J., Misselwitz, B., Dilling, S., Kremer, M., and Hardt, W.D. (2007) Two newly idenitified

SipA domains (F1,F2) steer effector protein localization and contribute to *Salmonella* host cell manipulation. *Molecular Microbiology* **65**: 741-760.

Scholz, O., Thiel, A., Hillen, W., and Niederweis, M. (2000) Quantitative analysis of gene expression with an improved green fluorescent protein. *European Journal of Biochemistry* **267**: 1565-1570.

Shea, J.E., Hensel, M., Gleeson, C., and Holden, D.W. (1996) Identification of a virulence locus encoding a second type III secretion system in Salmonella typhimurium. *Proceedings of the National Academy of Sciences of the United States of America* **93**: 2593-2597.

Shelobolina, E.S., Sullivan, S.A., O'Neill, K.R., Nevin, K.P., and Lovley, D.R. (2004) Isolation, characterization, and U(VI)-reducing potential of a facultatively anaerobic, acid-resistant bacterium from Low-pH, nitrate- and U(VI)-contaminated subsurface sediment and description of Salmonella subterranea sp nov. *Applied and Environmental Microbiology* **70**: 2959-2965.

Shi, J., and Casanova, J.E. (2004) Activation of racl by the Salmonella effector SopE triggers formation of an IRSp53/WAVE2 complex: WAVE2 but not IRSp53 is necessary for bacterial internalization. *Molecular Biology of the Cell* **15**: 149A-149A.

Shi, J., Scita, G., and Casanova, J.E. (2005) WAVE2 signaling mediates invasion of polarized epithelial cells by Salmonella typhimurium. *Journal of Biological Chemistry* **280**: 29849-29855.

Shi, J., and Casanova, J.E. (2006) Invasion of host cells by Salmonella typhimurium requires focal adhesion kinase and p130Cas. *Molecular Biology of the Cell* **17**: 4698-4708.

Silva, M., Song, C., Nadeau, W.J., Matthews, J.B., and McCormick, B.A. (2004) Salmonella typhimurium SipA-induced neutrophil transepithelial migration: involvement of a PKC-alpha-dependent signal transduction pathway. *American Journal of Physiology-Gastrointestinal and Liver Physiology* **286**: G1024-G1031.

Small, P.L.C., Isberg, R.R., and Falkow, S. (1987) Comparison of the Ability of Enteroinvasive Escherichia-Coli, Salmonella-Typhimurium, Yersinia-Pseudotuberculosis, and Yersinia-Enterocolitica to Enter and Replicate within Hep-2 Cells. *Infection and Immunity* **55**: 1674-1679.

Soncini, F.C., and Groisman, E.A. (1996) Two-component regulatory systems can interact to process multiple environmental signals. *Journal of Bacteriology* **178**: 6796-6801.

Soncini, F.C., Vescovi, E.G., Solomon, F., and Groisman, E.A. (1996) Molecular basis of the magnesium deprivation response in Salmonella typhimurium: Identification of PhoP-regulated genes. *Journal of Bacteriology* **178**: 5092-5099.

Soto, G.E., and Hultgren, S.J. (1999) Bacterial adhesins: Common themes and variations in architecture and assembly. *Journal of Bacteriology* **181**: 1059-1071.

Sperandio, V., Mellies, J.L., Nguyen, W., Shin, S., and Kaper, J.B. (1999) Quorum sensing controls expression of the type III secretion gene transcription and protein secretion in enterohemorrhagic and enteropathogenic Escherichia coli. *Proceedings of the National Academy of Sciences of the United States of America* **96**: 15196-15201.

Sperandio, V., Torres, A.G., Giron, J.A., and Kaper, J.B. (2001) Quorum sensing is a global regulatory mechanism in enterohemorrhagic Escherichia coli O157 : H7. *Journal of Bacteriology* **183**: 5187-5197.

Sperandio, V., Torres, A.G., and Kaper, J.B. (2002) Quorum sensing Escherichia coli regulators B and C (QseBC): a novel two-component regulatory system involved in the regulation of flagella and motility by quorum sensing in E-coli. *Molecular Microbiology* **43**: 809-821.

Sperandio, V., Torres, A.G., Jarvis, B., Nataro, J.P., and Kaper, J.B. (2003) Bacteria-host communication: The language of hormones. *Proceedings of the National Academy of Sciences of the United States of America* **100**: 8951-8956.

Stebbins, C.E., and Galan, J.E. (2000) Modulation of host signaling by a bacterial mimic: structure of the Salmonella effector SptP bound to Rac1. *Molecular Cell* **6**: 1449-1460.

Steele-Mortimer, O., Meresse, S., Gorvel, J.P., Toh, B.H., and Finlay, B.B. (1999) Biogenesis of Salmonella typhimurium-containing vacuoles in epithelial cells involves interactions with the early endocytic pathway. *Cellular Microbiology* **1**: 33-49.

Steele-Mortimer, O., Knodler, L.A., Marcus, S.L., Scheid, M.P., Goh, B., Pfeifer, C.G., Duronio, V., and Finlay, B.B. (2000) Activation of Akt/protein kinase B in epithelial cells by the Salmonella typhimurium effector SigD. *Journal of Biological Chemistry* **275**: 37718-37724.

Stein, M.A., Leung, K.Y., Zwick, M., GarciadelPortillo, F., and Finlay, B.B. (1996) Identification of a Salmonella virulence gene required for formation of filamentous structures containing lysosomal membrane glycoproteins within epithelial cells. *Molecular Microbiology* **20**: 151-164.

Stender, S., Friebel, A., Linder, S., Rohde, M., Mirold, S., and Hardt, W.D. (2000) Identification of SopE2 from Salmonella typhimurium, a conserved guanine nucleotide exchange factor for Cdc42 of the host cell. *Molecular Microbiology* **36**: 1206-1221.

Stradal, T.E.B., and Scita, G. (2006) Protein complexes regulating Arp2/3-mediated actin assembly. *Current Opinion in Cell Biology* **18**: 4-10.

Sukhan, A., Kubori, T., Wilson, J., and Galan, J.E. (2001) Genetic analysis of assembly of the Salmonella enterica serovar typhimurium type III secretion-associated needle complex. *Journal of Bacteriology* **183**: 1159-1167.

Surette, M.G., and Bassler, B.L. (1998) Quorum sensing in Escherichia coli and Salmonella typhimurium. *Proceedings of the National Academy of Sciences of the United States of America* **95**: 7046-7050.

Surette, M.G., and Bassler, B.L. (1999) Regulation of autoinducer production in Salmonella typhimurium. *Molecular Microbiology* **31**: 585-595.

Surette, M.G., Miller, M.B., and Bassler, B.L. (1999) Quorum sensing in Escherichia coli, Salmonella typhimurium, and Vibrio harveyi: A new family of genes responsible for autoinducer production. *Proceedings of the National Academy of Sciences of the United States of America* **96**: 1639-1644.

Swanson, J.A., and Baer, S.C. (1995) Phagocytosis by Zippers and Triggers. *Trends in Cell Biology* **5**: 89-93.

Tafazoli, F., Magnusson, K.E., and Zheng, L.M. (2003) Disruption of epithelial barrier integrity by Salmonella enterica serovar typhimurium requires geranylgeranylated proteins. *Infection and Immunity* **71**: 872-881.

Taga, M.E., Semmelhack, J.L., and Bassler, B.L. (2001) The LuxS-dependent autoinducer Al-2 controls the expression of an ABC transporter that functions in Al-2 uptake in Salmonella typhimurium. *Molecular Microbiology* **42**: 777-793.

Taga, M.E., Miller, S.T., and Bassler, B.L. (2003) Lsr-mediated transport and processing of Al-2 in Salmonella typhimurium. *Molecular Microbiology* **50**: 1411-1427.

Takeuchi, A. (1967) Electron Microscope Studies of Experimental Salmonella Infection .I. Penetration into Intestinal Epithelium by Salmonella Typhimurium. *American Journal of Pathology* **50**: 109-&.

Taylor, J., Lovell, R., and McCall, A.M. (1953) Discussion of the epidemiology and treatment of Salmonella infections in man and animals with special reference to *Salmonella* dublin. *Proceedings of the Royal Society of Medicine* **46**: 445-449.

Terebiznik, M.R., Vieira, O.V., Marcus, S.L., Slade, A., Yip, C.M., Trimble, W.S., Meyer, T., Finlay, B.B., and Grinstein, S. (2002) Elimination of host cell PtdIns(4,5)P-2 by bacterial SigD promotes membrane fission during invasion by Salmonella. *Nature Cell Biology* **4**: 766-773.

Tsolis, R.M., Adams, L.G., Ficht, T.A., and Baumler, A.J. (1999a) Contribution of Salmonella typhimurium virulence factors to diarrheal disease in calves. *Infection and Immunity* **67**: 4879-4885.

Tsolis, R.M., Townsend, S.M., Miao, E.A., Miller, S.I., Ficht, T.A., Adams, L.G., and Baumler, A.J. (1999b) Identification of a putative Salmonella enterica serotype typhimurium host range factor with homology to IpaH and YopM by signature-tagged mutagenesis. *Infection and Immunity* **67**: 6385-6393.

Unsworth, K.E., Way, M., McNiven, M., Machesky, L., and Holden, D.W. (2004) Analysis of the mechanisms of Salmonella-induced actin assembly during invasion of host cells and intracellular replication. *Cellular Microbiology* **6**: 1041-1055.

Uzzau, S., Brown, D.J., Wallis, T., Rubino, S., Leori, G., Bernard, S., Casadesus, J., Platt, D.J., and Olsen, J.E. (2000) Host adapted serotypes of Salmonella enterica. *Epidemiology and Infection* **125**: 229-255.

van Asten, A., and van Dijk, J.E. (2005) Distribution of "classic" virulence factors among Salmonella spp. *Fems Immunology and Medical Microbiology* **44**: 251-259.

Van Asten, F., Hendriks, H., Koninkx, J., Van der Zeijst, B.A.M., and Gaastra, W. (2000) Inactivation of the flagellin gene of Salmonella enterica serotype Enteritidis strongly reduces invasion into differentiated Caco-2 cells. *Fems Microbiology Letters* **185**: 175-179.

van der Woude, M.W., and Baumler, A.J. (2004) Phase and antigenic variation in bacteria. *Clinical Microbiology Reviews* **17**: 581-+.

Vazquez-Torres, A., and Fang, F.C. (2000) Cellular routes of invasion by enteropathogens. *Current Opinion in Microbiology* **3**: 54-59.

Vazquez-Torres, A., Xu, Y.S., Jones-Carson, J., Holden, D.W., Lucia, S.M., Dinauer, M.C., Mastroeni, P., and Fang, F.C. (2000) Salmonella pathogenicity island 2-dependent evasion of the phagocyte NADPH oxidase. *Science* **287**: 1655-1658.

Vendeville, A., Winzer, K., Heurlier, K., Tang, C.M., and Hardie, K.R. (2005) Making 'sense' of metabolism: Autoinducer-2, LuxS and pathogenic bacteria. *Nature Reviews Microbiology* **3**: 383-396.

Verdu, E., Viani, F., Armstrong, D., Fraser, R., Siegrist, H.H., Pignatelli, B., Idstrom, J.P., Cederberg, C., Blum, A.L., and Fried, M. (1994) Effect of Omeprazole on Intragastric Bacterial Counts, Nitrates, Nitrites, and N-Nitroso Compounds. *Gut* **35**: 455-460.

Vernikos, G.S., and Parkhill, J. (2006) Interpolated variable order motifs for identification of horizontally acquired DNA: revisiting the Salmonella pathogenicity islands. *Bioinformatics* **22**: 2196-2203.

Vetter, I.R., and Wittinghofer, A. (2001) Signal transduction - The guanine nucleotide-binding switch in three dimensions. *Science* **294**: 1299-1304.

Wallis, T.S., Starkey, W.G., Stephen, J., Haddon, S.J., Osborne, M.P., and Candy, D.C.A. (1986) The Nature and Role of Mucosal Damage in Relation to Salmonella-Typhimurium-Induced Fluid Secretion in the Rabbit Ileum. *Journal of Medical Microbiology* **22**: 39-49.

Walters, M., Sircili, M.P., and Sperandio, V. (2006) AI-3 synthesis is not dependent on luxS in Escherichia coli. *Journal of Bacteriology* **188**: 5668-5681.

Wang, X.D., Deboer, P.A.J., and Rothfield, L.I. (1991) A Factor That Positively Regulates Cell-Division by Activating Transcription of the Major Cluster of Essential Cell-Division Genes of Escherichia-Coli. *Embo Journal* **10**: 3363-3372.

Waterman, S.R., and Small, P.L.C. (1998) Acid-sensitive enteric pathogens are protected from killing under extremely acidic conditions of pH 2.5 when they are inoculated onto certain solid food sources. *Applied and Environmental Microbiology* **64**: 3882-3886.

Watson, P.R., Paulin, S.M., Bland, A.P., Jones, P.W., and Wallis, T.S. (1995) Characterization of Intestinal Invasion by Salmonella-Typhimurium and

Salmonella-Dublin and Effect of a Mutation in the Invh Gene. *Infection and Immunity* **63**: 2743-2754.

Welch, M.D., and Mullins, R.D. (2002) Cellular control of actin nucleation. *Annual Review of Cell and Developmental Biology* **18**: 247-288.

Wendland, M., and Bumann, D. (2002) Optimization of GFP levels for analyzing Salmonella gene expression during an infection. *Febs Letters* **521**: 105-108.

Wheeler, J.G., Sethi, D., Cowden, J.M., Wall, P.G., Rodrigues, L.C., Tompkins, D.S., Hudson, M.J., and Roderick, P.J. (1999) Study of infectious intestinal disease in England: rates in the community, presenting to general practice, and reported to national surveillance. *British Medical Journal* **318**: 1046-1050.

Williams, C., Galyov, E.E., and Bagby, S. (2004) Solution structure, backbone dynamics, and interaction with Cdc42 of Salmonella guanine nucleotide exchange factor SopE2. *Biochemistry* **43**: 11998-12008.

Winzer, K., Hardie, K.R., Burgess, N., Doherty, N., Kirke, D., Holden, M.T.G., Linforth, R., Cornell, K.A., Taylor, A.J., Hill, P.J., and Williams, P. (2002) LuxS: its role in central metabolism and the in vitro synthesis of 4-hydroxy-5-methyl-3(2H)-furanone. *Microbiology-Sgm* **148**: 909-922.

Wood, M.W., Rosqvist, R., Mullan, P.B., Edwards, M.H., and Galyov, E.E. (1996) SopE, a secreted protein of Salmonella dublin, is translocated into the target eukaryotic cell via a sip-dependent mechanism and promotes bacterial entry. *Molecular Microbiology* **22**: 327-338.

Wood, M.W., Jones, M.A., Watson, P.R., Hedges, S., Wallis, T.S., and Galyov, E.E. (1998) Identification of a pathogenicity island required for Salmonella enteropathogenicity. *Molecular Microbiology* **29**: 883-891.

Xavier, K.B., and Bassler, B.L. (2003) LuxS quorum sensing: more than just a numbers game. *Current Opinion in Microbiology* **6**: 191-197.

Xavier, K.B., and Bassler, B.L. (2005) Regulation of uptake and processing of the quorum-sensing autoinducer AI-2 in Escherichia coli. *Journal of Bacteriology* **187**: 238-248.

Xavier, K.B., Miller, S.T., Lu, W.Y., Kim, J.H., Rabinowitz, J., Pelczer, I., Semmelhack, M.F., and Bassler, B.L. (2007) Phosphorylation and processing of the quorum-sensing molecule autoinducer-2 in enteric bacteria. *Acs Chemical Biology* **2**: 128-136.

Zhang, S.P., Santos, R.L., Tsolis, R.M., Stender, S., Hardt, W.D., Baumler, A.J., and Adams, L.G. (2002) The Salmonella enterica serotype typhimurium effector proteins SipA, SopA, SopB, SopD, and SopE2 act in concert to induce diarrhea in calves. *Infection and Immunity* **70**: 3843-3855.

Zhang, Y., Higashide, W.M., McCormick, B.A., Chen, J., and Zhou, D.G. (2006) The inflammation-associated Salmonella SopA is a HECT-like E3 ubiquitin ligase. *Molecular Microbiology* **62**: 786-793.

Zhou, D., Mooseker, M.S., and Galan, J.E. (1999a) Role of the S-typhimurium actin-binding protein SipA in bacterial internalization. *Science* **283**: 2092-2095.

Zhou, D.G., Mooseker, M.S., and Galan, J.E. (1999b) An invasion-associated Salmonella protein modulates the actin-bundling activity of plastin. *Proceedings of the National Academy of Sciences of the United States of America* **96**: 10176-10181.

Zhou, D.G., Chen, L.M., Hernandez, L., Shears, S.B., and Galan, J.E. (2001) A Salmonella inositol polyphosphatase acts in conjunction with other bacterial effectors to promote host cell actin cytoskeleton rearrangements and bacterial internalization. *Molecular Microbiology* **39**: 248-259.

Zigmond, S.H. (2004) Beginning and ending an actin filament: Control at the barbed end. In *Current Topics in Developmental Biology, Vol 63*. Vol. 63, pp. 145-188.